Developing a refined tephrostratigraphy for Scotland, and constraining abrupt climatic oscillations of the Last Glacial-Interglacial Transition (ca 16-8 ka BP) using high resolution tephrochronologies

Rhys Gregory Owen Timms

Centre for Quaternary Research,
Department of Geography,
Royal Holloway,
University of London

Thesis submitted for the degree of Doctor of Philosophy
at the University of London

September, 2016

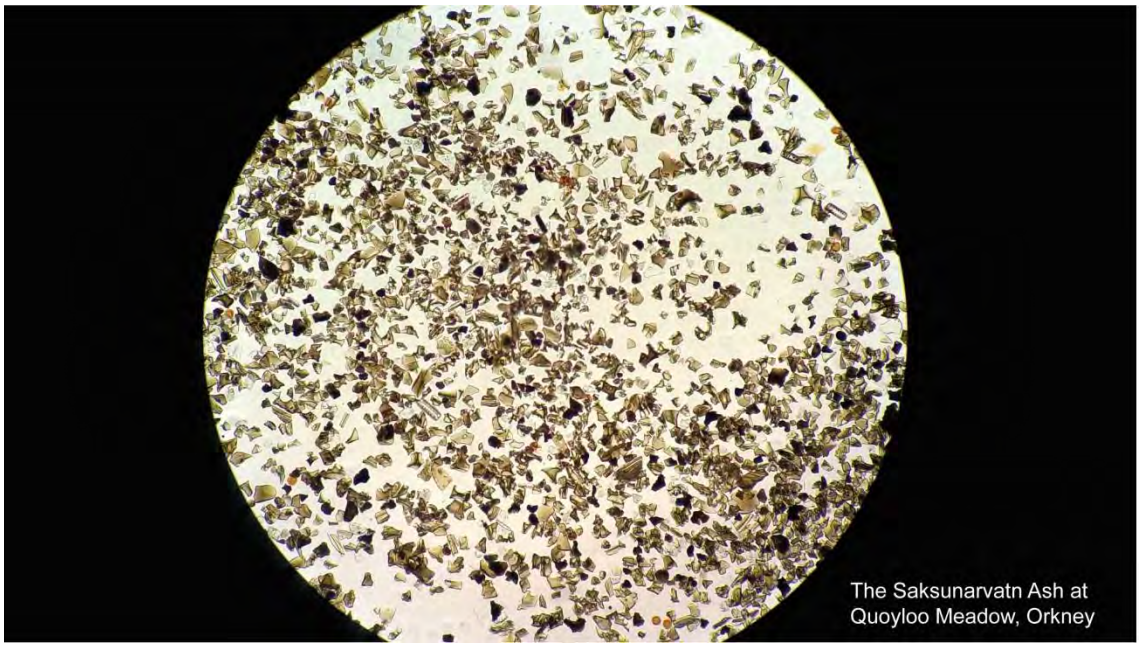

We come from the land of the ice and snow,
from the midnight sun where the hot-springs blow[1]…

[1]Page, J and Plant, R (1970) 'Immigrant Song' *Led Zeppelin III*. Atlantic Records

Declaration

This thesis presents the results of original research undertaken by the author, none of the results, illustrations or text are based on published or unpublished work of others, except where specified and acknowledged.

Signature: 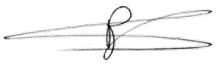 Date: 22/09/2016

Abstract

Understanding the abrupt climatic oscillations that characterised the Last Glacial to Interglacial Transition (LGIT, ca. 16-8 ka) requires an ability to precisely correlate the archives within which such transitions are recorded. One way in which to scrutinise the timing of abrupt events in the LGIT is tephrochronology, a technique which exploits the isochronous potential of tephra horizons derived from the geologically 'instantaneous' settlement of volcanic ash. In NW Europe, macro- and crypto-tephra layers of varying age and provenance have become increasing utilised as a means to correlate palaeoclimate records, and to test the spatial and temporal synchronicity of key climatic transitions.

At present, however, tephrostratigraphies in NW Europe are limited by: 1) the number of horizons that have robust chronological constraint, and 2) our abilities to trace these tephras across multiple sites. As a result, the potential of generating continental-scale tephra lattices is greatly restricted, and a spatial disparity in the number and type of tephras has emerged. It is hypothesised that part of this disparity may relate to the resolution at which sequences are studied and the inconsistent manner in which methodologies are applied. In order to test this hypothesis, five terrestrial basins from western Scotland were examined in detail for tephra content. Four of the sites were examined contiguously at high resolutions, whilst the fifth was examined using traditional 'scan and resample' strategies. Three new tephras for the LGIT are identified, and several existing tephras previously unknown in the British Isles were also detected. The results from this tephrostratigraphic study suggest that the series of eruptive episodes impacting Northern Britain through the LGIT is richer than appreciated hitherto. Results also indicate that tephras may have been missed in previous tephrostratigraphic investigations due to: 1) incomplete stratigraphic refinement, 2) a propensity to focus on tephras of greatest concentration, and 3) a conflation of horizons.

Using the high-resolution site-tephrostratigraphies, a composite tephrochronological age model was developed. The purpose of this exercise was to establish whether age models constructed exclusively from tephra horizons could provide a viable means to constrain abrupt climatic oscillations in sites which traditionally are difficult to date e.g. carbonate basins. The resulting age model achieves centennial-decadal scale precision through the early Holocene, and is used to accurately constrain the first record incidence of the 10.3 ka event in the British Isles. This study emphasises the importance of contiguous high resolution refinement, and demonstrates that this approach is essential if the true tephrostratigraphic complexity of NW Europe is to be fully understood, and if tephras are to be used successfully in constraining abrupt climatic events.

Publications arising from this study

Timms, R.G.O., Matthews, I.P., Palmer, A.P., Candy, I. and Abel, L (2016) 'A high-resolution tephrostratigraphy from Quoyloo Meadow, Orkney, Scotland: Implications for the tephrostratigraphy of NW Europe during the Last Glacial-Interglacial Transition' *Quaternary Geochronology*

Acknowledgements

I would like to express my utmost thanks and gratitude to many people, whose assistance, patience and encouragement has greatly assisted in the completion of this thesis.

First and foremost I would like to thank my supervisors Dr I. Matthews, Dr A. Palmer and Prof I. Candy for their constant guidance and support over the past four years. I would further like to thank all of the staff within the Geography department, who have made Royal Holloway such a great institution to study. Specific thanks must go to, Prof J. Lowe, Dr A. MacLeod, Dr S. Blockley, Dr C. Mayers, Dr C. Gallant, Dr M. Perez, Dr M. Hardiman, Ms E. Turton, Ms R. Christie, Mr I. Valcarcel, Ms J. Kynaston, Mr M. Kelsey, Mrs K. Flowers and Mr R. Aung for all of their assistance with this project.

In particular I would like to thank Dr C. Hayward at the Tephra Analysis Unit (TAU), located at the School of Geosciences University of Edinburgh, for the many hours of guidance on the microprobe, and for the ferociously strong coffee that often accompanied such endeavours.

I would also like to thank four cohorts of MSc Quaternary Science students for their interest, free labour, and memorable trips up to Scotland. Thanks also to the Geography and Earth Science PhD, and post-doctoral students who have made this such a great experience. In particular I would like to thank Ash Abrook for the Veltins, Jacob Bendle for the group of doom, Dorothy Weston for the tephra chat, Jenni Sherriff for her role as PhD oracle, Steph Walker for the geochronology 'bants', Anna Bird for the guilt cake, and Paul Lincoln for a lifetimes supply of van based anecdotes.

A special note of thanks must go to Dr N. Moar, Ms K. Thompson (SNH), Mr A. Leitch (RSPB), Major M. Macrae, and Orkney Brewery for information and permission on gaining access the sites examined in this thesis. Further thanks must go to Prof. K Edwards, Dr J. Bunting, Dr M. Farrell, and Dr J. Larsen for openly sharing unpublished data.

I would finally like to thank Holly who has made this final year that much more enjoyable, and to my long time suffering parents, thank-you for your unrelenting support, encouragement, and tins of fish.

Contents

List of Figures

Chapter 4. Methodology

Chapter 5. Quoyloo Meadow Results

Chapter 6. Crudale Meadow Results

Chapter 10. A Revised Tephrostratigraphy for Scotland

Chapter 11. Site Age Models and Tephrochronological Refinement

Chapter 12. Tephro-stratigraphical and -chronological Applications

List of Tables

1. Introduction

1.1 Quaternary environmental change

Synonymous with the term 'Ice Age', the Quaternary Period (the past 2.6 Ma) can be considered the culmination of a global climatic deterioration that typified the Late Cenozoic era, and which heralded an intensification in the frequency and magnitude of cold and warm climatic events (Ruddiman and Raymo 1988; Zachos et al. 2001). This climatic cyclicity is thought to have been governed primarily by changes in the orbital cycles of precession (19 and 23 ka), obliquity (41 ka) and eccentricity (100 ka) i.e. the Milankovitch hypothesis (Hays et al. 1976; Imbrie and Imbrie 1979; Ruddiman et al. 1986; Imbre et al. 1993; Maslin and Ridgwell 2005). As a result of this, approximately fifty glacial/interglacial cycles have occurred during the Quaternary (Lisiecki and Raymo 2005). However, superimposed on these long term variations are many more, centennial and decadal scale 'sub-Milankovitch' events (e.g. Bond et al. 1999; Genty et al. 2003; Steffensen et al. 2008).

These short-lived abrupt transitions are well documented in ice-core, marine and terrestrial archives (e.g. Bond et al. 1993; Mayewski et al. 2004; Alley and Ágústsdóttir 2005; Rohling and Pälike 2005; Rasmussen et al. 2006; 2007; 2014), and have received increasing attention because they are frequently considered as potential analogues for future abrupt climatic events over the next 100-500 years (e.g. Vellinga and Wood 2002; 2008; Hulme 2003). Understanding the impact of these 'events' on environmental systems, and the natural resilience of the climate system is fundamental if future challenges are to be mitigated successfully (IPCC 2007). Integral to this understanding is the development of an appreciation of the timing and phasing of abrupt climatic oscillations, which may only be achieved if past events are studied with refined chronological precision.

One of the best intervals in which to study these abrupt transitions is between the Last Glacial Maximum (LGM) and the current Interglacial; a period of climatic warming known as the 'Last Termination' or the 'Last Glacial to Interglacial Transition' (LGIT) (Björck et al. 1998; Walker et al. 1999; Walker et al. 2012; Figure 1.1). Numerous abrupt events are recorded throughout this period, and archives are typically well preserved and frequently of high resolution (Lowe and Walker 2015). These attributes means that this interval provides an excellent opportunity to examine climatic drivers and environmental responders at a resolution and precision unmatched elsewhere in the Quaternary (e.g. Blunier and Brook 2001; Magney 2004; Alley and Ágústsdóttir 2005; Barton 2009; Wanner et al. 2011).

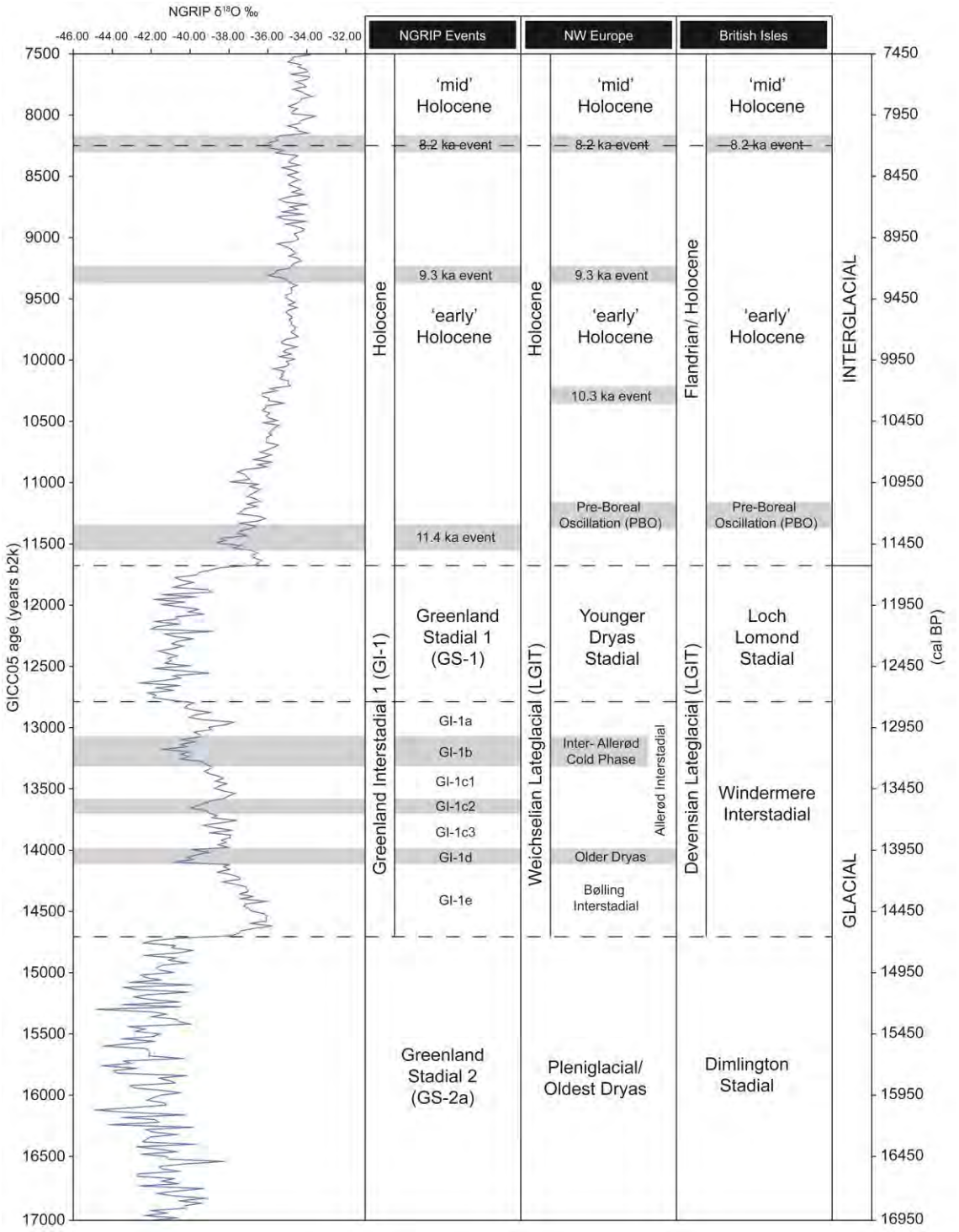

Figure 1.1 Lateglacial or Last Glacial to Interglacial Transition (LGIT) event stratigraphy for Greenland, NW Europe, and the British Isles. The Greenland event stratigraphy is divided into Stadials (GS: cold phase), and Interstadials (GI: warm phase), with comparable, but not necessarily synchronous phases identified in European climate archives (Lowe et al. 2001; Walker et al. 2001). GI-1 is divided into a seven subunits, with (GI-1d, GI-1c2, GI1b) reflecting short lived cold events punctuating an otherwise comparatively warm interval (GI-1e, GI-1c3, GI-1c1, GI-1a). Within the context of the early Holocene a number of similar revertence episodes are also identified, most notably the 11.4 ka event, 9.3 ka event, and the 8.2 ka event (Hammer et al. 1986; von Grafenstein 1999; Alley and Ágústsdóttir 2005; Rasmussen et al. 2007). It is the identification of these revertence episodes within the Greenland ice core records, which have recently been used to propose a formal subdivision of the Holocene (Walker et al. 2012).

Currently, however, there are a number of limitations with using palaeoclimatic events as analogues for future abrupt transitions. Fundamental to understanding what drives abrupt events, and how sensitive different parts of the Earth system are to their impact is our ability to generate independent age determinations for these events in a variety of different archives. In doing so this helps facilitate the testing of: 1) the synchroneity/asychroniety of these events across regional/hemispheric/global scales; 2) whether there are lags in climatic response between different regions, and; 3) the response time of biological and geomorphic systems to these abrupt events. Whilst radiocarbon dating has allowed some of these ideas to be investigated, the absence of suitable material in some archives, and problems associated with the radiocarbon calibration curve restrict the widespread application of this technique (Lowe et al. 2015). In recent years the development of tephrochronology (the use of volcanic ash horizons as means of absolute correlation between records) has improved the precision by which LGIT records are constrained, and hence enabled a more robust testing of climatic synchroneity/asychroniety and environmental response.

1.2. Synchronising records of the Last Termination and early Holocene

The adoption of the Greenland ice core records as a regional stratotype for NW Europe has heralded a shift in the way palaeoenvironmental studies focused on the LGIT are conducted (Lowe et al. 2001, 2008a, 2015; Figure 1.1). The high-resolution isotopic record of these archives has allowed a number of abrupt climatic events to be studied in detail. These investigations have illustrated that, during the Last Termination, climatic shifts between cold and warm regimes operated at decadal, and in some instances sub-decadal timescales (Dansgaard et al. 1993; Taylor et al. 1993; Rasmussen et al. 2006; Steffensen et al. 2008). However, a key issue that remains prominent is whether these abrupt events and the accompanying environmental response was regionally synchronous within terrestrial, marine, and cryospheric archives, or whether there were significant 'leads' and 'lags' between them (Lowe et al. 2008a). Testing this remains fundamental to Quaternary investigations, and of utmost importance to climate models which are reliant on empirical data sets for simulating future climatic scenarios (IPCC 2007). These answers at present remain elusive, as more ‘traditional’ climate archives (lake sediments, peat bogs etc.) have not yet attained the level of stratigraphic resolution or chronological precision to rival the Greenland ice-core records. As a result, meaningful comparisons between records, or to the regional stratotype have been limited (Lowe et al. 2008a).

Crucially, however, a number of methodological advances have emerged which are bringing this elusive goal closer. These developments have either arisen in parallel with the ice core records, or have been more widely adopted since the establishment of the regional stratotype. These advancements and innovations include: 1) refinements to the IntCal calibration curve (e.g. Reimer et al. 2013); 2) the adoption of Bayesian age modelling techniques (e.g. Bronk Ramsey 1995, 2008, 2009; Blockley et al. 2004, 2007; 2008; Blaauw 2010); 3) the development of high precision varve chronologies (e.g. Brauer et al; 1999; Palmer et al. 2010); 4) the construction of tephrochronological frameworks or lattices (e.g. Blockley et al. 2014; Lowe et al. 2015), and; 5) the development of protocols by which all of these techniques can be applied i.e. the INTIMATE approach (Lowe et al. 2008a).

1.3 The 'INTIMATE approach'

The INTegrating Ice-core Marine, and TErrestrial records Working Group (INTIMATE) has examined and advocated methodologies by which the degree of regional climate synchronicity can be reliably tested. A key aspect of this work was the establishment of the Greenland ice core records as a regional stratotype for the Last Termination in NW Europe. Historically this period was subdivided on the basis of climate events inferred from palaeoenvironmental records (e.g. Iversen 1954; Mangerud et al. 1974 Figure 1.1). This is problematic because bio- and litho-zones are time-transgressive, whereas chrono-zones are not (Walker 1995; Björck et al. 1998). Such a legacy has resulted in an assumed climate synchronicity, and the development of the "coherent myth" in regards to palaeoenvironmental studies in NW Europe and elsewhere (Björck et al. 1998; Lowe et al. 2001; Wunsch 2006; Lowe et al. 2008a; Blaauw 2012).

As a means to rectify this, and to prevent further erroneous practices, the INTIMATE group, in addition to the establishment of the Greenland stratotype, proposed a series of protocols and recommendations by which palaeoenvironmental questions can be objectively posed (Lowe et al. 2008a). These are:

1) Palaeoenvironmental interpretations should be based on independent and (preferably) quantified proxy data.
2) Site records should be defined using a local stratigraphic terminology.
3) The timing and duration of palaeoenvironmental events should be based on independently generated chronologies.
4) Palaeoenvironmental reconstructions and chronologies that emerge, should then be compared with an independent regional stratotype, and the degree of

compatibility with the stratotype sequence assessed, taking account of any dating uncertainties.

Following these protocols, and utilising the advancements in geochronological control noted above, studies in recent years have been able to illustrate: 1) the dynamic spatial variability of climatic transitions (Lane et al. 2013); 2) the phasing of environmental response to abrupt climate change (Lane et al. 2012a); and 3) the complex interplay between climate and human dispersal, details that would have otherwise remained obscured by the broader uncertainties of traditional radiometric dating techniques (Lowe et al. 2012; Barton et al. 2015). Particularly important in all of these studies has been the employment of tephras as time-parallel marker horizons. These have enabled spatially disparate climate records to be linked with a precision unmatched by other geochronological techniques, and hence secured tephrochronology as an invaluable technique in testing climatic synchronicity (Alloway et al. 2007; Lowe 2011; Davies et al. 2012; Davies 2015).

1.4 Study rationale

Despite the establishment of a regional stratotype in NW Europe, the methodological advances, and the recommendations of the INTIMATE group, there is still a propensity to 'tune' or 'wiggle-match' between records (e.g. Marshall et al. 2002; Lang et al. 2010; Whittington et al. 2015 Figure 1.2). This has perpetuated the notion of an assumed climatic synchronicity, and accentuates an inherent limitation of the INTIMATE approach. Many techniques seen as advancements in recent years (see section 1.3) are only applicable to sites which either: 1) exhibit an abundance of datable radiocarbon material, or; 2) are annually laminated. The exception to this of course is tephra, but it is only within the last few years that the benefits of this approach have begun to emerge.

Rasmussen et al. (2014b) note that significant advances have been made in tephrochronology, and specifically refinements in: 1) the geochemical fingerprinting of tephras; 2) the dating of tephra horizons; 3) the detection of volcanic signals in the Greenland ice core records; 4) the extension of dispersal 'footprints', and; 5) the construction of regional tephra databases. Whilst this is a substantial advancement of a technique which in the context of the LGIT was only conceptualised twenty years ago, many of these developments have yet to be fully adopted by the wider palaeoenvironmental community. Greater efforts are needed to illustrate the potential of tephra, and the applicability of the technique beyond sequences that have already

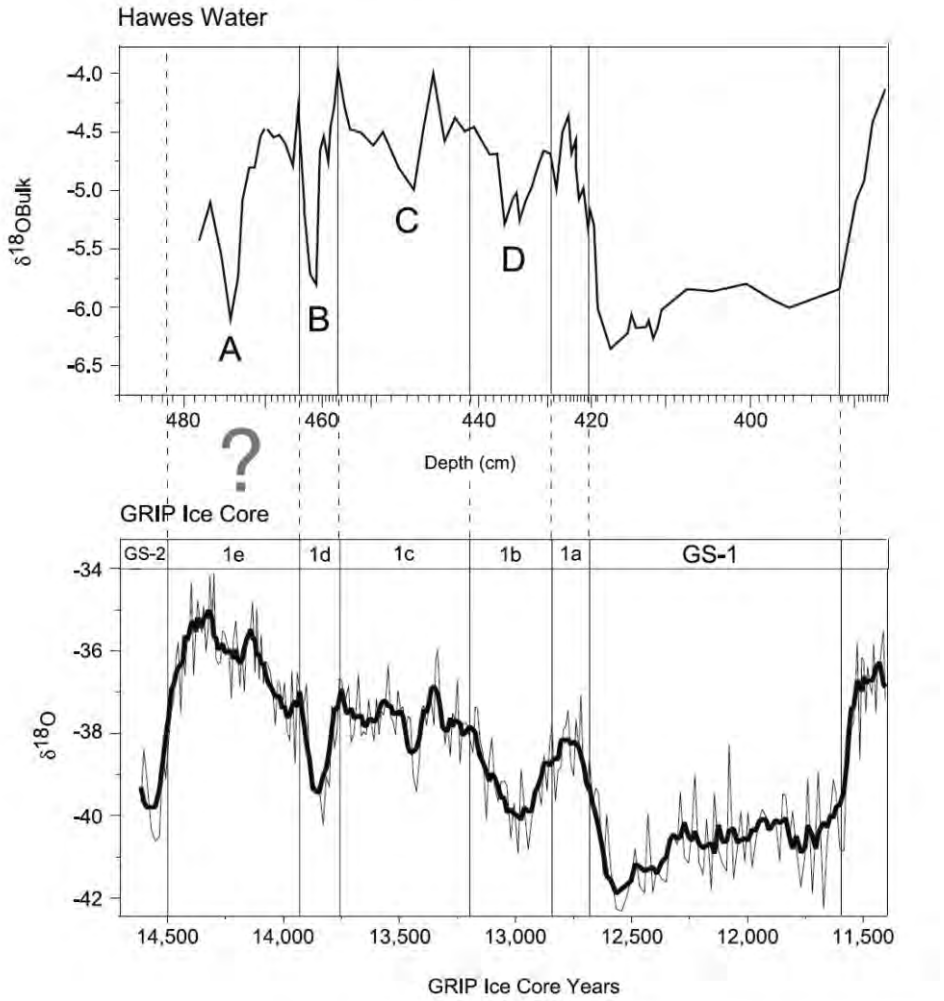

Figure 1.2 An example of a NW European palaeoenvironmental record being 'tuned' or 'wiggle-matched' to the GRIP ice core record on the basis of aligning peaks and troughs in $\delta^{18}O$ values. This process assumes climatic synchronicity as opposed to testing it. It is essential that independent age control be developed for sequences, and then compared to Greenland using a chronological approach. Figure from Marshall et al. (2002).

been the focus of intense study, and which also already possess robust chronological frameworks e.g. Kråkenes (Birks et al. 1996; Bakke et al. 2009; Lohne et al. 2014), Meerfelder Maar (Brauer et al. 1999; Lane et al. 2013) etc. At present the most significant tephra studies for NW Europe have derived from these well resolved sites (e.g. see section 1.3), but what is also evident from these and other studies is that there is a significant disparity in the distribution of tephras across NW Europe. It is hypothesised that part of this disparity may have arisen from low resolution sampling strategies, and a tendency of studies to focus on intervals containing the most concentrated tephra horizons. Historically this approach was justified by methodological limitations, but improvements to tephra shard extraction and characterisation techniques now permit the analysis of horizons which are less concentrated, and which are populated by smaller shards (e.g. Hayward 2012). At present therefore the number of tephra links that can be made across Europe is limited,

and further refinement and expansion of the European tephrostratigraphic framework is needed to fully maximise the promise of tephrochronology (Lowe et al. 2015). By applying new techniques in well studied regions it is hoped that regional disparities can be reduced, new tephra links can be made, and greater opportunities for constraining abrupt climatic events established. Fundamental to this study will therefore be the routine application of high resolution techniques, and the methodical analysis of major and minor peaks in tephra concentration. It is expected that this approach will provide a greater degree of tephrostratigraphical control, and mitigate issues associated with low resolution or select interval refinement strategies. Consequently it is hoped that tephra disparity in Europe can be reduced, and the overall number of tephra 'linkages' increased, an essential requisite for testing climatic synchronicity.

Northern Britain is one such region ideally suited for the further development and expansion of tephra frameworks. Application of higher resolution strategies at select intervals has already yielded positive results in establishing new links (e.g. MacLeod 2008; Matthews et al. 2011; MacLeod et al. 2015), and the region is also positioned in proximity to the North Atlantic which makes it a key location in recording the abrupt climatic oscillations that typified the LGIT (e.g. Brooks et al. 2012; 2016; Whittington et al. 2015; Candy et al. 2016).

1.5 Study site locations

Palaeolacustrine records from Scotland have long been used in the reconstruction of Quaternary climates (e.g. Pennington et al. 1972; Sissons 1974; Gray and Lowe 1977; Lowe et al. 1999), and it is thought that as many as 150 records spanning the LGIT and early Holocene may have now been investigated (Figure 1.3; John Lowe pers. comm. 2014). These sites largely represent infilled or partially infilled basins, which began accumulating sediments after the retreat of the Late Devensian Ice Sheet. These limnic or mire sequences can be typically distinguished by four major lithostratigraphic units: 1) a minerogenic unit at the base, representing the cold, unstable climate immediately following the retreat of the Late Devensian Ice Sheet i.e. the Dimlington Stadial (GS-2); 2) an organic-rich (gyttja/lake mud) or carbonate-rich sediment, deposited during the Windermere Interstadial (Bølling-Allerød, GI-1); 3) a minerogenic unit representing the climatic deterioration of the Loch Lomond Stadial (Younger Dryas, GS-1); and 4) a transition into organic-rich or carbonate-rich deposits of the Holocene (Lowe and Walker 2015, p. 156). These major lithostratigraphic units are occasionally punctuated by subtle, climatically driven lithostratigraphic variations, for example those representing the short-lived 'Older Dryas' (GI-1d) and Gerzensee (GI-1b) colder spells

Figure 1.3 Distribution of the LGIT and early Holocene age sites in Scotland. Seventy-seven locations are illustrated here, but as many as one hundred and fifty may have been investigated (John Lowe pers. comm. 2014). The labelled sites are published tephra sites and the locations highlighted in red are the basins that will be examined in this thesis. These sites are located in areas where little previous tephra work has been conducted (see Chapter 3).

within the Windermere (Bølling-Allerød, GI-1) Interstadial (Figure 1.1). One of the major advantages of studying the LGIT in lacustrine sequences is that they frequently offer the potential of reconstructing environmental change through a wide range of proxies (i.e. pollen, chironomids, stable isotopes, diatoms, biomarkers). Consequently, any high-resolution chronologies that are generated can be used to underpin high-resolution palaeoclimatic reconstructions.

Five sites were chosen for investigation in this study, Quoyloo Meadow, Crudale Meadow, Spretta Meadow, Tanera Mòr and Little Lochans (Figure 1.3). These basins are positioned in areas that have been relatively understudied in terms of tephrostratigraphic investigations, but are key locales for the further development of both: 1) high resolution palaeoenvironmental data on accordance to these localities proximity to the North Atlantic, and; 2) the regions are likely to provide new tephrostratigraphic links to the Nordic countries, Ireland and NW Europe as a whole. Further details on this rationale is given in Chapter 3.

1.6 Aims and objectives

1.6.1 Aims

This study aims to establish whether tephrochronology can be used to develop robust and independent age controls on palaeoenvironmental records independent from any existing chronology, and whether the precision of these age models can be used to reliably constrain abrupt climatic oscillations of the LGIT and early Holocene. This study therefore shall focus on sites which, as well as addressing the primary aim, also:

1) Enable the Scottish tephrostratigraphic record to be extended, both in a geographic context, and hopefully also in regard to the suite of tephras that can be identified.
2) Intersect with previously examined locations, to establish whether higher resolution sampling and chemical characterisation techniques can impact on the number and chemical type of tephras identified.

1.6.2 Objectives

To facilitate the aims, a number of objectives need to be achieved:

- To develop and implement refined protocols for the sampling and extraction of cryptotephra horizons.

- To conduct higher resolution chemical analyses of tephras than has previously been undertaken in the British Isles.
- Extend and refine the current tephrostratigraphic framework for Scotland, and highlight potential areas of uncertainty.
- Establish the tephrostratigraphic relationship of purely 'British' tephras, (i.e. those which have only been found in the British Isles) with their more 'European' counterparts.
- Adhere to INTIMATE protocols, and use the isochronous potential of tephra horizons to construct independent age-depth models for the studied sequences.
- Establish whether composite age modelling can help to increase precision and reduce age uncertainties for both palaeolacustrine records and poorly dated tephra horizons.

1.8 Thesis structure

This thesis is divided into thirteen chapters (not including references or appendices). **Chapter 2** provides an outline of the principles and methodological considerations behind tephrostratigraphy and tephrochronology, with a specific emphasis on cryptotephras and their application in NW Europe. **Chapter 3** delivers greater detail on the rationale behind the study sites, and also provides essential background information on these locations. **Chapter 4** introduces the key methods and approaches utilised in this thesis. **Chapters 5-9** present the main litho- and tephro-stratigraphic results from the five study sites. **Chapter 10** evaluates tephrostratigraphic data produced in this thesis and considers how the sampling approach may significantly affect the results from similarly aged sequences in Scotland and the rest of Europe. A tephrostratigraphic framework for Scotland is presented, and key questions concerning tephra studies in NW Europe are addressed. **Chapter 11** deals with the main chronological issues surrounding tephras in NW Europe and further develops a series of refined age models for existing sequences, and for the sites examined in this thesis. In the final sections of the chapter an updated and refined series of ages for tephras characterising Scottish and NW European tephrostratigraphies are presented. **Chapter 12** considers the tephrostratigraphical and tephrochronological advances made in this thesis. Using Quoyloo Meadow as a case study, a number of climate proxies are developed, and these are used to answer whether tephra-derived chronologies can be used to constrain abrupt climatic oscillations of the LGIT. **Chapter 13** summarises the main conclusions of this work and discusses directions for future research.

Chapter 2. Tephrostratigraphy and Tephrochronology

2.1 Introduction and chapter structure

As outlined in the previous chapter, tephrochronology offers one of the best opportunities to accurately constrain abrupt climatic events during the LGIT and early Holocene. This chapter provides a comprehensive review of cryptotephrochronology in the context of palaeoenvironmental lacustrine records, and the application of the technique in the British Isles and NW Europe. It is, however, beyond the scope of this project to consider tephrochronology in its entirety, readers wishing to delve deeper should refer to comprehensive reviews provided by Alloway et al. (2007), Lowe (2011), and Davies (2015).

This chapter is divided into four main sections: 1) general definitions and principles are introduced; 2) specific methodologies applicable to distal cryptotephrochronology are reviewed; 3) source regions for tephras impacting the British Isles and NW Europe are considered; and; 4) a review on the development and application of tephrochronology in the British Isles and NW Europe is given. This latter section also highlights the current issues facing the application of tephrochronology in NW Europe, and how this thesis may help resolve some of those issues.

2.2 Tephrochronology: origins and definitions

Understanding the dynamism of the Quaternary period, and how climatic oscillations manifest temporally and spatially, requires the accurate and precise dating of palaeoenvironmental records. As studies have striven towards a better understanding of the complex interplay between climate and environment, there has been an inherent need to improve the way in which climate records are correlated, and their synchronicity tested. One method that has become central to this involves the identification, characterisation, and dating of layers resulting from volcanic eruptions; tephrochronology.

Tephrochronology is a discipline which exhibits a complicated and often misused nomenclature; it is thus prudent to outline terms which may appear confusing for those not familiar with the discipline (Table 2.1). The term ***tephra*** comes from the Greek τέφρα meaning ‘ashes’, and its (re)occurrence within the literature derives from the work of Sigurður Þórarinsson (1944), who introduced it as a collective term to describe volcanic clastic ejecta, regardless of type, size or shape. It is thus inclusive of all grain sizes, ranging from very fine ash (dust) (<0.06 mm), medium ash (0.06-0.5 mm), coarse ash (0.5-2.0 mm), lapillus or lapilli (2.0-64.0 mm) to blocks or bombs (>64.0

mm) (Lowe and Hunt 2001). In his seminal paper, Þórarinsson (1944) identified the potential of tephra layers in Iceland to act as isochronous marker horizons, and discussed how they could be utilised in deciphering rates of change within many areas of environmental and archaeological science. He proposed that ***tephrochronology*** be used as an international term to describe the geological chronology derived from the 'measuring, interconnecting, and dating of volcanic ash layers'. ***Tephrochronology*** (*sensu stricto*) is therefore a term referring to tephra layers as isochrons or time-parallel marker horizons, not a term to date tephra horizons. The process of determining a numerical age for an individual tephra, or to multiple tephras within a relative sequence i.e. a ***tephrostratigraphy*** is termed ***tephrochronometry***. Through time, however, ***tephrochronology*** (*sensu lato*) has also become an umbrella term used interchangeably when referring to all associated tephra terminology, despite efforts to suggest an alternative e.g. ***tephra studies*** or ***tephrology*** (Self and Sparks 1981; Froggatt and Lowe 1990).

Table 2.1 Summary of common tephra nomenclature.

Term	Definition
Tephra	All volcanic ejecta regardless of type, size or shape; from the Greek τέφρα meaning 'ashes'
(Crypto-) Tephrochronology	The chronological relationship (absolute) between tephra layers, and their use as time synchronous marker horizons. **Tephrochronology** may also be used interchangeably with all aspects of tephra research and application
(Crypto-) Tephrostratigraphy	The stratigraphic relationship between tephra layers and their relative ages
Tephrochronometry	The process of obtaining a numerical age for a tephra layer
Macrotephra	The study of visible tephra horizons
Cryptotephra	Tephra layer (glass component) not visible to the naked eye; from the Greek 'κρυπτός' meaning 'secret' or 'hidden'
Microtephra	Alternative term for Cryptotephra, same definition as above
Tephra studies & Tephology	Alternative terms proposed to encompass all tephra related nomenclature and as an appropriate title for the field of tephra studies (not in common use)
Tephric	'Related to' or 'of tephra'

Over the past three decades, a new sub-discipline of tephrochronology has emerged. This has turned away from the traditional study of proximal deposits and visible ***macrotephras***, to one that is typified by the identification, extraction and characterisation of tephra layers that are invisible to the naked eye (e.g. Dugmore 1989; Turney et al. 1997). This field initially grew out of NW Europe, and the term ***microtephra*** was used to describe the occurrence of these horizons, a term validated by their microscopic properties (Turney et al. 1997). However, some argued that this

terminology lacked clarity, suggesting it was ambiguous of whether the term made reference to the size of the constituent particles, or the thickness of the deposit (Lowe and Hunt 2001). As a result the term ***cryptotephra*** was proposed (Lowe and Hunt 2001); crypto coming from the Greek κρυπτός meaning 'secret' or 'hidden'; and therefore reflecting the concealed nature of these deposits. Subsequently ***cryptotephrostratigraphy*** and ***cryptotephrochronology*** have emerged as terms to describe the 'hidden' sequences of tephra and their application as dating tools in distal environments.

2.3 Principles of distal-tephrochronology

The main principles of tephrochronology relate to three prominent themes: 1) that the dispersal and settlement of volcanic ash is rapid (with respect to geological timescales); 2) that tephra layers represent isochronous events that are not reworked or modified by post depositional processes, and; 3) that tephras are uniformly distributed across the landscape or in the very least pervasive throughout the region encompassed by the ash plume (Boygle 1999; Pyne-O'Donnell 2011). In this section these principles are considered in the context of distal-tephrochronology; the section follows a chronological narrative through eruption, dispersal and settlement, sources of error and measures to mitigate those errors are considered.

2.3.1 Tephra generation and dispersal

Tephra is formed by brittle fragmentation during the most energetic phases of magmatic and phreatomagmatic eruptions. In the former, it is the expansion of gases within the magma itself which causes fracturing, whilst in the latter the process is driven by the interaction of external water sources and the rapid expansion of super-heated steam (Zimanowski et al. 2003; Francis and Oppenheimer 2004). The principles of thermodynamics dictate that fracture is dependent upon the internal strain rate of the material in question, the higher the strain rate the smaller the resulting particle size (Yew and Taylor 1994; Jordan et al. 2014). Particles derived from this process are driven upwards within an eruption column that is it defined by two major phases; the gas-thrust stage, and an upper convective region (Figure 2.1; Sparks 1986). An eruption column will continue to rise until the density of the plume reaches equilibrium with that of the surrounding atmosphere, a point determined by the respective temperature of both plume and atmosphere (Francis and Oppenheimer 2004). At this point the plume will begin to spread laterally, a phenomenon that has been likened to an opening umbrella (Alloway et al. 2007). It is thus principally the eruption intensity,

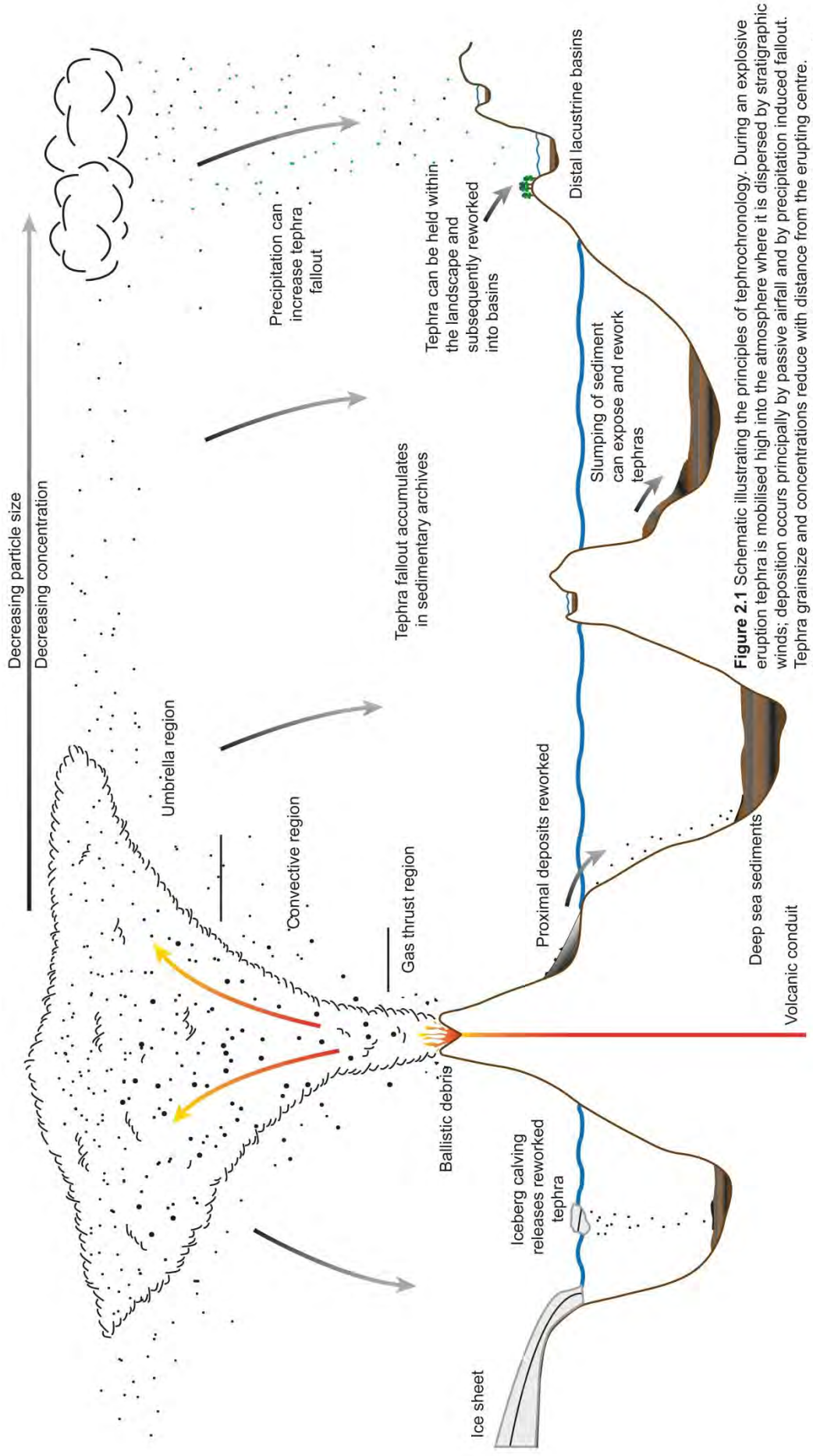

Figure 2.1 Schematic illustrating the principles of tephrochronology. During an explosive eruption tephra is mobilised high into the atmosphere where it is dispersed by stratigraphic winds; deposition occurs principally by passive airfall and by precipitation induced fallout. Tephra grainsize and concentrations reduce with distance from the erupting centre. Deposition within sedimentary archives e.g. Ice sheets, marine sediments and lacustrine sediments is relatively rapid thereby forming isochronous marker horizons across spatially disparate records. Reworking of tephra can occur in all depositional environments.

and the temperature of erupted material that will determine the height of an eruption column.

Settling velocities of entrained tephra particles will be highly dependent upon grain-size or aggregated grain-size i.e. where particles are fused together (Lacasse 2001; Taddeucci et al. 2011); the largest of those fragments will follow ballistic trajectories and will be little affected by plume dynamics. Thus proximal deposits, i.e. those close to an eruption centre, will typically contain larger or aggregated grains (Taddeucci et al. 2011; Stevenson et al. 2012), and exhibit a greater variety of erupted material i.e. being composed of heavier lithic fragments, crystal bearing lithics, and loose crystals (Larsen and Eríksson 2008; Lowe 2011). For distal-tephrochronologists it is those particles occupying the intermediate and fine size ranges which are of utmost interest. Fine particles (<100 μm) may be mobilised to high altitudes and subsequently transported great distances if their densities can be supported by atmospheric winds (Lacasse 2001). In distal settings, downwind from the eruption centre, tephra deposits therefore tend to be composed of smaller lighter pumice fragments and vitreous glass shards, undergoing a reduction in grain size and thickness with distance from the erupting centre (Stevenson et al. 2015).

2.3.2 Understanding distal-tephra dispersal

Cryptotephra studies focused on historic and pre-historic eruptions have frequently represented tephra dispersal maps as broad conical shaped envelopes, especially in north-west Europe (e.g. Davies et al. 2010; Figure 2.2). With such schematic representations of fallout, it could be assumed that fine-grained volcanic ash is almost ubiquitously distributed across the entire landscape; unfortunately for cryptotephrochronologists this is not the case, and such diagrams are misleading. The occurrence of ash layers in depositional environments is neither homogenous, certain, nor as simplistic as such diagrams would allude to. Wastegård and Davies (2009), on reviewing tephra distributions over Europe in the last 1000 years, concluded that dispersal is often multidirectional, sporadic and difficult to predict. In recent years, however, a greater insight has come from the study of contemporary eruptions, Davies et al. (2010); Stevenson et al. (2012) examining the Eyjafjöll 2010 eruption, and Stevenson et al. (2013) in their review of the Grímsvötn 2011 eruption, emphasised the critical role that short lived weather patterns play in the distribution of tephras. These studies have illustrated that dispersal follows complex trajectories made even more intricate by different phases of the eruption coinciding with differing weather patterns, all factors which may create scattered and patchy patterns of deposition. Synoptic conditions, wind strength, and precipitation rates are also considered significant

controlling factors in the rate and volume of tephra deposition (Pyne-O'Donnell 2011; Lowe 2011). Quantifying the influence of all of these variables is difficult, however, it has certainly been noted that intense periods of rainfall accompanying eruptions have caused greater rates of deposition through wash-out processes, than would otherwise result from dry-air deposition (Lowe 2011; Pyne-O'Donnell 2011; Stevenson et al. 2012).

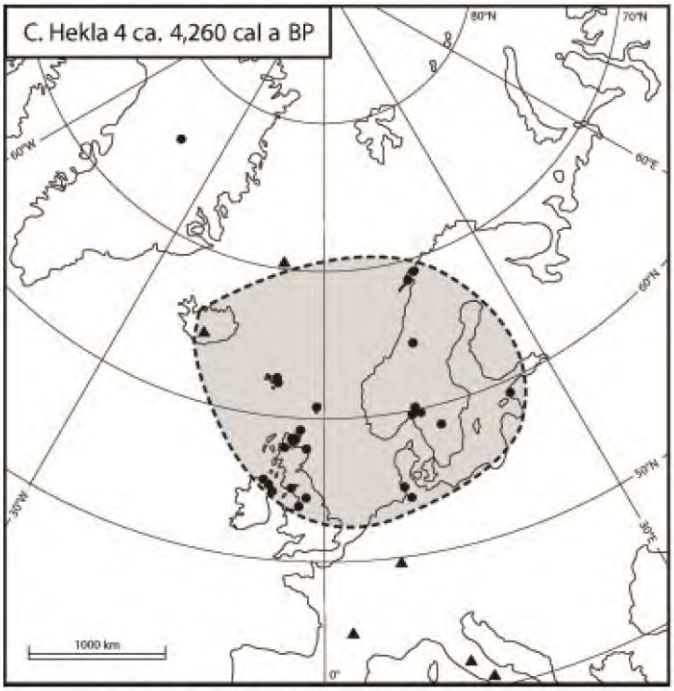

Figure 2.2 Map illustrating the inaccurate representation of tephra dispersal in association with the Hekla 4 eruption. From Davies et al. (2010).

It is important to note that these relatively short term atmospheric and weather phenomena would be further modulated by the seasons, and by the longer term climatic regime (e.g. stadial/ interstadial) (Sigurdsson 1990; Lacasse 2001; Pyne-O' Donnell 2011). Large eruptions recorded during the Pleistocene glacial phases such as the Vedde Ash appear to exhibit much greater dispersal radii when compared to Holocene equivalents, a discrepancy which is unlikely to have resulted from eruption dynamics alone (Lacasse 2001). It has been suggested that an increase in atmospheric density caused by a cooler climate may have predominated through glacial phases, thus raising the neutral buoyancy height of an eruption column, and allowing any erupting plume to attain greater altitudes (Sparks 1986 Sigurdsson 1990; Lacasse 2001). Such factors may help explain dispersal differences between eruptions of similar magnitude during these differing periods (Lacasse 2001), although for NW Europe it is believed that such factors are negligible.

2.3.3 Taphonomic considerations of distal-tephra

It is clear that the distribution and deposition of volcanic ash in distal environments is highly dependent on the residing climatic, atmospheric and weather regimes (section 2.3.2). To add yet further intricacies, site specific or local catchment factors can also have significant bearing on the deposition, accumulation and preservation of ash layers within sedimentary archives. These factors are important to consider, as any uncertainty arising from these processes will have connotations for the robustness of correlations, and for the validity of isochron placement (Boygle 1999; Pyne-O'Donnell 2011). It is beyond the scope of this thesis to review the entire discipline of distal-tephra taphonomy; focus here is directed towards lacustrine basins. Readers should look toward the work of Ruddiman and Glover (1972); Brendryen 2010; 2011; Griggs et al. (2014a,b) for taphonomic factors dominant in marine settings, whilst Payne and Gehrels 2010; Watson et al. (2015) tackle such problems in peat sequences.

Mangerud et al. (1984) was amongst the earliest studies to comment upon tephra taphonomy and the spatial variability exhibited by distal-tephra beds. The study, which named and chemically characterised the Vedde Ash, also noted the positive relationship between the thickness of the ash bed and the proximity of the horizons to basin inlet channels. Given the apparent efficiency at which ash had been mobilised into the basins, Mangerud hypothesised that a correlation may exist between ash bed thickness (volume) and the size of the surrounding catchment, further suggesting, and subsequently confirming, that streamflow had a significant influence on the concentration of tephra to be found within lake basins (Figure 2.3).

This spatial disparity in macrotephra horizons has also been noted in the U.K. at Loch Ashik in Scotland. Davies et al. 2001 and Pyne-O'Donnell (2005; 2011) commented on how the visible distribution of the Vedde Ash was remarkably constrained within the relatively small basin, and unlike in Mangerud et al. (1984), approximately 40 m away from the main inlet area where no visible ash was evident at all. The authors suggest the spatially constrained nature of the deposit was caused by palaeo-inlet channels, variable basin morphometry, and a delivery of shards by storm events or rapid snow melts flushing the denser 'heavier' basaltic shards along with coarser grained sediments into the deepest parts of the basin (Pyne-O'Donnell 2011). Subsequent work by Pyne-O'Donnell (2005; 2011) demonstrated how this distributional unevenness also impacted the field of cryptotephrostratigraphy. An extensive study into taphonomic process at three small Lochans in western Scotland including Loch Ashik, identified significant spatial variability for three tephras deposited during the LGIT; the Penifiler Tephra, the Vedde Ash and the Ashik Tephra. Catchment size, basin

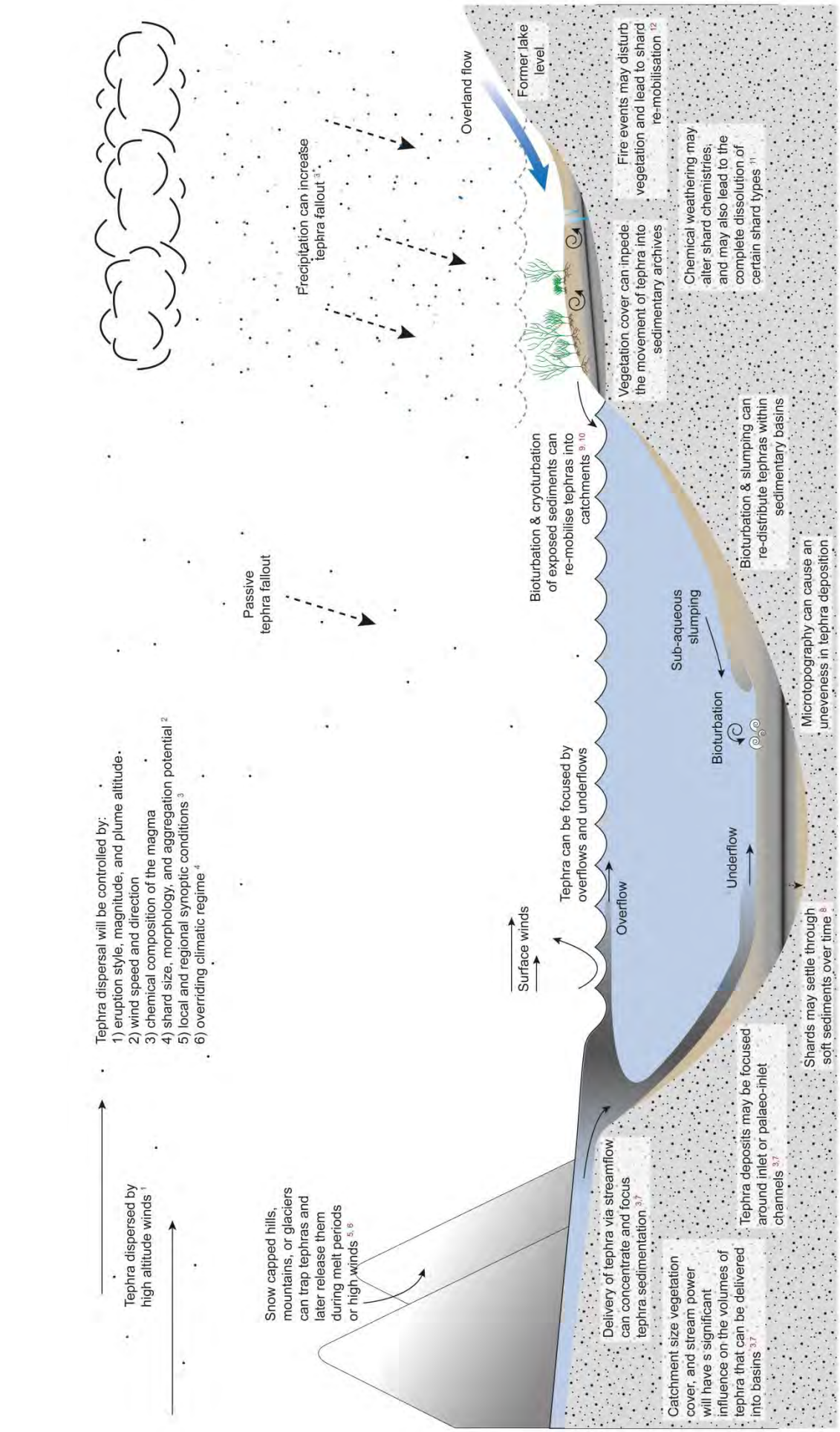

Figure 2.3 Schematic diagram illustrating the major taphonomic factors influencing tephra accumulation and preservation within lacustrine sequences. Key references: 1. Lacasse (2001); 2. Stevenson et al. (2012); 3. Pyne-O'Donnell (2011); 4. Sigurdsson (1990); 5. Davies et al. (2007); 6. Bergman et al. (2004);7. Mangerud et al. 1984; 8. Anderson et al. (1984); 9. Boygle (1999); 10. Kirkbride and Dugmore 2005; 11. Pollard et al. (2003); 12. Swindles et al. (2013).

morphometry, the position of inlet (palaeo-) channels, and landscape changes through time were determined to be four of the most important physical factors to influence tephra distributions within these sequences. But perhaps the most significant find was that the position of the depositional hypocentre was not constant, and that it had clearly varied though time. The lateglacial horizons could be correlated to the proximity of the (palaeo-) inlet channels as shown by Mangerud et al. (1984), but the Holocene ash layers in their highest concentrations occurred much closer to the centre of the lakes. It was hypothesised that the climatic amelioration of the early Holocene resulted in a reduction in lake levels, thereby focusing and restricting tephra deposition to the central, deeper parts of the basins (Pyne-O' Donnell 2011).

This theory also raises some important questions concerning the exposure of tephra-bearing lake sediments to erosive forces if lake levels are reduced (Figure 2.3). The net effect of this is that tephras held within the sediments may subsequently be remobilised into the catchment. This process of remobilisation is not only applicable at exposed basin margins, but also to areas within the greater catchment e.g. peatlands, soils and other basins higher up in the system (Boygle 1999); snow beds may also act as a trap for tephra shards as suggested by Davies et al. (2007). A remobilisation of shards from any of these sources may potentially give a false signal of an eruption, or mask a younger layer with a diffuse spread of tephra when redeposited within a lake (see section 2.3.4). Identifying these reworked deposits in lacustrine sequences can be difficult, though it has been suggested that cryptotephras that are formed entirely from primary fallout are marked by a discrete horizon of glass shards indicative of a rapid input of ash (Davies 2015). However, this is not always the case and will be discussed further in section 2.3.4. In some cases a physical alteration to the tephra shards may indicate reworking. Rounding of particles can occur, and in more proximal locations the glassy coating of fresh crystals may be lost (Wilcox and Naeser 1992; Leahy 1997). However, in distal environments loose crystals are rare and the process of sieving during shard extraction may also cause a rounding of grains.

What is clearly evident is that there are a multitude of physical factors affecting tephra distributions within lake basins, a sentiment that has repeatedly been expressed in the literature when dealing with various proxies associated with palaeoclimatic reconstructions (e.g. Bonny 1978; Pennington 1979; Bradbury 1996; Edwards and Whittington 2000). These studies *inter alia* have demonstrated sediment accumulation in lakes can be influenced by focussing, slumping, bioturbation, reworking, and bottom-profile variations (Figure 2.3), inherently impacting upon the distribution and preservation of the accompanying proxies. Despite these findings it remains typical for

distal-tephra studies, as it is typical for many palaeoenvironmental disciplines working with terrestrial records, to identify the longest stratigraphic sequence, and to extract a single contiguous core from which to reconstruct the environmental history. It is perhaps not surprising therefore that there is a growing body of evidence to suggest that the single core approach can be equally detrimental to the recovery of a full tephrostratigraphic sequence (e.g. Boygle 1999; Pyne-O'Donnell 2011). There is however, a caveat on this interpretation that a single core will not be representative of the entire tephra suite; and one which relates to sampling resolution. This theme is considered further in section 2.4.1.

2.3.4 Defining the isochron

One of the fundamental principles of tephrochronology is that the dispersal and settlement of volcanic ash is rapid (with respect to geological timescales). However, defining the primary input and hence the position of the isochron is not always clear. As discussed above, there are many taphonomic considerations and these can influence the way in which a shard distribution profile manifests in lacustrine sequences. Figure 2.4 provides a series of hypothetical shard distributions, and suggests the likely mechanisms responsible.

It is typical in distal-tephra studies to assign the isochron to the peak in shard concentration (Lowe 2011). Distinctive tephra peaks like those exhibited in Figure 2.4 (A-D) & (F-G) can therefore be considered the most reliable when constructing age models and dealing with palaeoenvironmental indicators. However, assigning an isochron for scenarios B&H and C&I requires the operator to distinguish between the mechanisms of deposition and/ or re-working/ down-working. In situations where there is a significant degree of doubt in the depositional history, thin-section analysis of the sedimentary matrix may provide enough evidence to determine the primary mode of deposition and whether any re-working/ down-working has occurred (e.g. Griggs et al. 2014; Lane et al. 2015). For scenarios (F-G) morphological analyses of the glass shards may help identify the concentration of each respective population, although identifying whether multiple populations exist can only be reliably tested with a thorough chemical analysis of the combined horizon.

Understanding the taphonomic factors and placing the isochron can be challenging in distal-tephra studies. However, careful interpretation of the results can provide inferences about the stability of the local landscape, the effectiveness of erosive processes, and importantly a visual clue of when landscape degradation may have commenced. For example, a pulsed input reflected as a 'peak and tail' in the tephrostratigraphy may signify a period of rapid re-sedimentation; perhaps signalling an

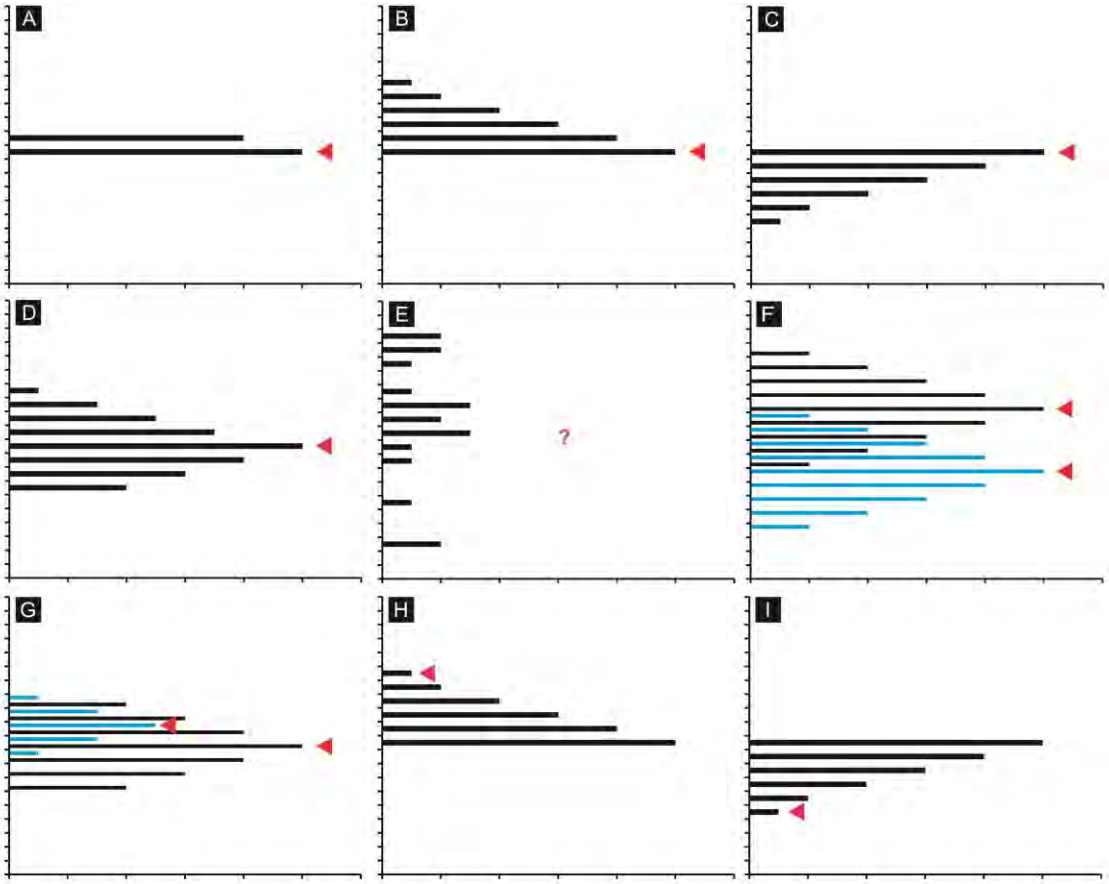

Figure 2.4 Schematic diagram illustrating several hypothetical shard distribution profiles; the red arrow denotes the position of the isochron.
A) Rapid primary input; in distal environments this is most commonly caused by airfall, but may also be represented by a rapid influx of re-worked material (see section 2.3.3).
B) Secondary input, or a reworking of the isochron can form a 'peak and tail' distribution
C) Vertical migration of shards downcore can also create a 'peak and tail' distribution. In this instance the tail is caused by bio-/cryoturbation. In unconsolidated sediments shards may also filter through voids (Davies et al. 2007).
D) A profile exhibiting elements from B & C; perhaps the most common distribution of distal-tephras in lacustrine sequences.
E) A distribution of shards that exhibits no clear isochron. Such a distribution may be derived from multiple input events i.e. a number of closely spaced eruptions, a gradual reworking of tephra bearing sediments (see section 2.3.3), or extensive bio-/cryoturbation within the basin.
F) Two closely spaced eruptions possessing overlapping distribution profiles. Diagnostic physical or chemical characteristics may be needed to separate and quantify the individual populations.
G) Two closely spaced eruptions, but one being masked by the other. This distribution does not necessarily reflect the size of the eruptions in question but merely how each is manifest in the sequence examined.
H) In this instance the isochron is not represented by the maximum shard concentrations; instead significant down-working has taken place. This has been observed in soft sediments where a large tephra input can result in density-induced placement e.g. Williams Lake (Anderson et al. 1985).
I) In this instance the isochron is not represented by the maximum shard concentrations, instead the isochron is placed at the onset of deposition, this may occur due to snow trapping large quantities of tephra within the catchment and releasing this only when large scale melting occurs e.g. Getvaltjärnen (Davies et al. 2007).

abrupt geomorphic change (Figure 2.4 B-C & H-I). This would contrast to a 'background' signal where reworking and re-deposition would produce a profile of constant values, and thereby signal a gradual reworking of the landscape (Figure 2.4 E; Boygle 1999; Lowe 2011).

It is important to note that the premise of isochron placement occurring with peak concentration is only considered good practice with silicic shards. There is some suggestion that for basaltic populations the first occurrence of shards is what defines the isochron (Pyne-O'Donnell 2005; 2011). This is thought to primarily reflect their greater densities which in turn makes them less susceptible to taphonomic processes. (Pyne-O'Donnell 2005; 2011). Basaltic distributions may therefore look like any of those in Figure 2.4 with the exception of the isochron being placed at the bottom of the stratigraphic pile. Whether this is an acceptable practice remains open to debate, in reality there is no universal scheme or checklist when assigning the isochron to tephra layers in distal settings. Each horizon must be considered in its own right and in light of accompanying bio-/litho-stratigraphic information. However, it is fundamental that the chosen position of the isochron is clearly reported, and that this information is accompanied by shard count profiles. Providing this data enables the re-interpretation of a sequence, which is especially important if new information arises for a site, or new techniques for stratigraphic refinement are developed.

2.3.5 Distal-tephra preservation in lacustrine sequences

Glass is prone to two types of aqueous attack. In neutral to acidic environments, where the pH <9 the main mechanism is ionic exchange, this leads to the formation of a leached layer on the glass surface, which is often referred to as a 'gel layer' or 'hydration rim' (Pollard et al. 2003; Blockley et al. 2005). In alkaline or basic conditions where the pH >9 the main process is dissolution, this leads to the complete dissolution of the glass in some circumstances (Pollard et al. 2003; Blockley et al. 2005). In reality both of these processes can operate together, and are controlled by the local pH, glass composition and surface area (Pollard et al. 2003). Chemical tests have allowed for a 'robustness' index to be produced for LGIT and Holocene tephras (Pollard et al. 2003), but, in essence, rhyolitic glass exhibits a greater chemical stability than andesitic basaltic glasses (Pollard et al. 2003). This fact may have some bearing on why silicic glasses dominate the tephrostratigraphies of NW Europe, despite the primary volcanism in Iceland being basaltic in composition (Thordarson and Höskuldsson 2008).

2.3.6 Principles of distal-tephrochronology: section summary

In these first two sections of this chapter, the general principles concerning tephrochronology and distal-tephrochronology have been introduced. The technique offers a means to precisely link spatially disparate climate and archaeological archives, by utilising the isochronous marker horizon that forms when tephra is deposited into sedimentary environments. However, as with many geochronological techniques there are fundamental limitations and caveats to data interpretation.

2.4 Methodological considerations in distal-tephrochronology

This section details the varying methods employed in distal-tephrochronology. For the specific methods employed within this research see Chapter 4.

2.4.1 Sampling and refinement strategies

Integral to distal-tephrochronology is the resolution at which potentially tephra-bearing horizons are examined. At present, no method can successfully detect cryptotephras within host substrates, quantify these, and return robust chemical analyses with the same rigour as conventional destructive laboratory techniques (Gehrels et al. 2008; Davies 2015; (see section 2.4.2). However, such methodologies are demanding in time and labour, which inherently limits the volume of material that can be realistically examined in typical tephrostratigraphic studies (Davies 2015). As a compromise, the most common approach that is adopted in distal-terrestrial sequences is the 'scan and resample' or 'rangefinder' technique (e.g. Pilcher and Hall 1992; Langdon and Barber 2004; Lane et al. 2014; Davies 2015). The strategy is illustrated schematically in Figure 2.5. In this example 5-10 cm scan samples provide a preliminary concentration value, and are used to establish the approximate depth of peak shard concentration. Once a peak is identified, higher resolution refinement is conducted. In terrestrial sites this is usually at 1 cm (e.g. Lane et al. 2014), but in some instances 0.5 cm (Macleod 2008; Matthews et al. 2011) and 0.1 cm (Pyne-O'Donnell 2011) resolutions have been applied.

As with many disciplines the resolution of refinement will dictate the level of detail that can be established, and, in this context, potentially the number of tephras that can be identified. Studies at Loch Laggan (MacLeod 2008) and Abernethy Forest (Matthews et al. 2011) have demonstrated that targeted and contiguous high resolution sampling can provide a more coherent, and more complex narrative to the history of volcanic events deposited during the Scottish Lateglacial and early Holocene than has been

appreciated hitherto. It is seldom the case, however, that tephra is the only consideration when resolving palaeoenvironmental or archaeological sequences, thus for many studies identifying 'key tephras' (see section 2.8) is sufficient to provide a broad chronological or stratigraphical context. Conversely, incomplete refinement has implications for studies wishing to understand tephra dispersal patterns, taphonomic factors, and further limits the number of tephrostratigraphic links that can be made between sites (see section 2.8).

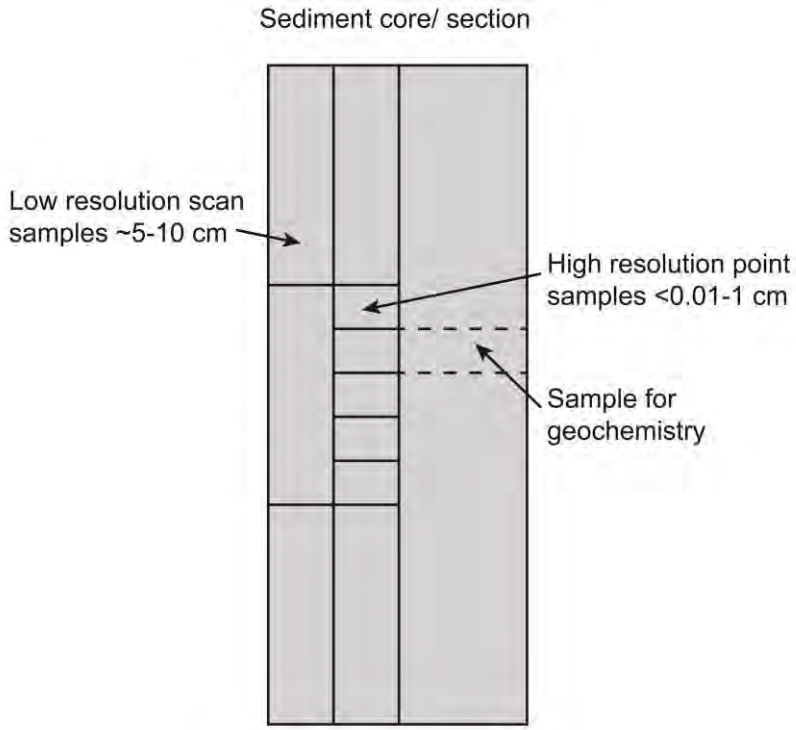

Figure 2.5 Schematic representation of the 'scan and resample' or 'rangefinder' sampling strategy.

Studies have repeatedly demonstrated the variable nature of tephra deposits within terrestrial settings, and how tephra concentrations and hence shard profiles may vary between cores or sections taken from the same site (e.g. Boygle 1999; Pyne-O'Donnell 2011; Watson et al. 2015). There is therefore an inherent uncertainty that peak shard characterisation as defined by scan sampling is truly representative of the entire suite of tephras preserved within a stratigraphic sequence. By peak sampling tephras for geochemical analyses this problem of intra-site variability is further exacerbated and risks generalising regional tephrostratigraphies in favour for larger more stratigraphically dominant tephras.

2.4.2 Extraction methods

Numerous techniques have been devised to detect cryptotephra within terrestrial sedimentary archives. These methods can be categorised as either destructive (i.e.

host sediments are removed and/ or destroyed) or non-destructive, which typically refer to indirect remote scanning methods which exploit a distinctive characteristic of the tephra horizon (e.g. magnetic properties).

2.4.2.1 Destructive techniques

Technique: Ashing.
For: Highly organic sediments e.g. peat.
A simple inexpensive method which removes organic substrates through incineration; the application does not require any specialist equipment, and is suitable for any chemical composition of tephra. However, heating above 350°C is suggested to alter shard chemistry, primarily though the uptake of potassium (Pilcher and Hall 1992; Dugmore and Larsen in prep: cited in Dugmore et al. 1995; Larsen 2013); and can be observed under the microscope as sintering anomalies on shard surfaces (van den Bogaard and Schmincke 2002). The procedure is therefore not recommended for samples destined for Electron Probe Microanalysis (EPMA) or other chemical determinations.
Key references: Dugmore (1989); Pilcher and Hall (1992).

Technique: Acid digestion.
For: Highly organic sediments e.g. peat.
This method utilises a series of strong acids to dissolve organic matter within tephra samples. The technique has been used for both the quantification of shard concentrations, and geochemical preparations. Several studies have, however, published findings on the chemical alteration of glass shards in acid and alkaline environments, including the complete dissolution of more fragile glasses (e.g. Pollard et al. 2003; Blockley et al. 2005). Recent work by Roland et al. (2015) suggests that in some circumstances acid digestion does not affect shard geochemistry. However, this experiment has only been conducted on relatively robust rhyolitic glasses derived from Hekla, and not the more susceptible rhyolitic and basaltic glasses as determined by Pollard et al. (2003) e.g. Katla and Grímsvötn glass. As tephra correlations are principally based on a measurement of major and minor elemental ratios, it is intrinsic that chemical alteration of shards be avoided in the laboratory.
Key references: Dugmore et al. (1995); Pollard et al. (2003); Blockley et al. (2005); Roland et al. (2015).

Technique: Alkali treatment.
For: Lacustrine sequences possessing high volumes of biogenic silica e.g. diatoms.

By using sodium hydroxide (NaOH) biogenic silica can be preferentially dissolved from sediment sequences. The technique is designed to be implemented in samples which possess high levels of these silicic 'mimics' (e.g. Rose et al 1996; see section 4.6). Due to the optical characteristics, and similar chemical structure to tephra, these mimics can often survive acid digestion and density separation techniques; and therefore interfere with the successful identification of tephra horizons. However, studies have shown that shards exposed to harsh alkaline conditions can be severely chemically altered, and in some cases dissolve entirely; basic populations' i.e. basaltic tephras are most susceptible in these instances (Pollard et al. 2003; Blockley et al. 2005). As with many chemical pre-treatments the potential for shard degradation is too great to allow the technique to be used in studies where subtle chemical variations are required for tephra correlations (Blockley et al. 2005).
Key reference: Rose et al. (1996).

Technique: Density Separation.
For: Suitable for all substrates.
Liquids of specific and variable density are used to physically separate and concentrate tephra shards from host substrates. Heavy liquids such as sodium polytungstate are inert, and can be used without chemical alteration to the shard structure. This technique is one of the few extraction methods that can be used universally for both the quantification and chemical preparatory stages of tephra analyses. The technique is however, limited when dealing with certain substrates. In minerogenic sequences, successful extraction is biased towards more silicic tephras, as the specific density of more basic shard populations coincides with densities of many mineral components e.g. quartz (Blockley et al. 2005). This makes the technique less suitable for separating basaltic shards from minerogenic-rich sediments unless a thorough stepped floatation procedure is carried out, or the 'heavy residues' i.e. those left from silicic extractions are subject to magnetic separation (see below). This dilemma is a particular problem for studies focussing upon lacustrine records.
Key references: Eden et al. (1992); Merkt et al. (1993); Turney (1998b); Blockley et al. (2005).

Technique: Magnetic separation.
For: Suitable for all substrates.
The technique exploits the known magnetic properties of more basic tephras to separate these from their host sediments (Froggatt and Gosson 1982). To optimise results, exposure to high temperatures in excess of 450°C is required to enhance the magnetic potential of the shard population (Mackie et al. 2002). Owing to the bias

inherent with density separation methods, this technique, used in conjunction with the former, offer the best opportunity to extract the entire eruptive suite of tephras likely to be identified in NW European lacustrine records; and is further essential in identifying whether certain silicic populations exhibit a bi-modality e.g. Vedde Ash and the Penifiler tephra (e.g. Mangerud et al. 1984; Pyne-O'Donnell 2007); both being important in these cases owing to the repeating chemical signature of the more silicic component associated with these tephras.

Key references: Mackie et al. (2002); Griggs et al. (2014)

Technique: Microwave digestion.

For: Currently only tested on peat.

Developed as an alternative to acid digestion, it has many benefits over the former, in that it requires lower volumes of reagents and less processing time. However, the technique demands specialist equipment and still requires the use of strong acids. As a result, provisional findings suggest that shards still exhibit chemical alteration following extraction; it is an approach therefore that reduces processing time, but is one that is unsuitable for tephras that need chemical characterisation.

Key reference: Payne and Blackford (2005).

Technique: Resin impregnation.

For: Any loose or consolidated sediment.

Although technically not a tephra extraction technique, the process of sediment dehydration and epoxy resin impregnation is a destructive method by which tephra can be examined. Impregnated blocks or polished thin sections are suitable for a host of none-destructive scanning techniques e.g. polarising and fluorescence microscopy, X-ray fluorescence (XRF), scanning electron microscopy with/without elemental analysis (SEM); inherently yielding information concerning tephra composition variability, alteration features, tephra taphonomy, and grain size distribution within host substrates (e.g. Wulf et al. 2004; De Vleeschouwer et al. 2008).

Creating resin blocks is however only suitable on samples where no further quantitative proxy work is required; whist duplicate cores may be used such demand on material and specialist equipment may limit application.

Key references: Wulf et al. (2004); De Vleeschouwer et al. (2008).

Technique: Slide mounts.

For: suitable for all substrates.

The process is extremely simple, taking 'raw' sediment and mounting it on a slide for optical examination. Whilst incredibly rapid, the downside is that there is no refinement

stage, thus depending on shard concentrations there may be a large volume of material to sift through.
Key reference: Griffiths (2001).

2.4.2.2 Non-destructive techniques

Technique: Continuously imaging flow cytometer.
For: Any sediment.
The method requires sample extraction following standard destructive protocols, and is a counting assistant only. The technique is limited by the size and diversity of the imagining library in which it compares analysed materials, as a consequence the shards counts are below what can be achieved by an experienced operator on a polarising light microscope.
Key reference: D'Anjou (2014).

Technique: Light reflectance and luminescence properties.
For: Currently only tested on peat.
Volcanic glass is detected via the properties of its light reflectance/luminescence against the background values emitted by the host substrate. The main limitation is the substrate and the concentration of the tephra horizon.
Key reference: Caseldine et al. (1999).

Technique: Magnetic susceptibility.
For: Any sediment.
The technique capitalises upon the magnetic susceptibility signal of tephras, and more specifically that of the mineral suite. The technique is cheap and effective, and large core sections can be scanned rapidly. However, its ability to detect cryptotephras is questionable and the technique is prone to false positives as other minerogenic sediments can create a positive reading. In that sense the technique is best applied in highly organic substrates.
Key references: Bunting (1994); Van den Bogaard et al. (1994); Nowaczyk (2001).

Technique: X-ray diffraction.
For: Only tested in marine sequences.
An exploratory method to determine the presence of tephras in marine sequences; the approach is relatively rapid but requires expensive specialist equipment. How well this technique performs with very low shard concentrations typical of terrestrial sites has yet to be demonstrated.

Key reference: Andrews et al. (2006).

Technique: X-ray fluorescence (XRF).
For: Lacustrine and organic rich sediments.
Core scanning is rapid and can provide bulk compositional information. However, the method is limited to the detection of major and minor elements and thus does not distinguish glass over mineral assemblages.
Key reference: Lowe et al. (1980).

Technique: X-radiography.
For: Lacustrine and organic rich sediments.
A scanning technique which provides an image relating to density changes within a sediment matrix, from which tephra horizons may be detected. However, not all horizons are of sufficient density to be detected on X-radiographs.
Key reference: Dugmore and Newton (1998).

2.4.3 Characterising distal tephras: geochemical techniques

Tephra studies rely on the precise and accurate characterisation of tephra layers. This can be conducted by several means, but is essentially governed by the distance of the deposit from the eruptive source. In proximal locations primary characterisation follows standard lithological techniques, i.e. grain-size, colour, bed thickness etc. with petrological analysis of the mineral suite also employed (e.g. Wulf et al. 2004). These techniques can be extended into the distal environment if the horizon remains visible, but preferential density sorting of the lithic and mineral/crystal suite can often result in distal tephra layers exhibiting 'mineral poor' assemblages that prevent classification by this method (Alloway et al. 2007; Pollard et al. 2006).

Whilst it is possible to characterise distally travelled tephras by mineral assemblage (e.g. Jouannic et al. 2015), the difficulties and unreliability of this approach have seen chemical determinations of individual glass shards grow in precedence as a technique (e.g. Hunt and Hill 1993; Turney et al. 2004). The glass or vitreous phase is considered synonymous with that of the eruptive melt, and is unlikely to be contaminated by conduit recycling i.e. the inclusion of xenocrysts and xenoliths in the same way lithic and crystal fractions may be. Because of this, the glass phase potentially provides a unique chemical signature or 'fingerprint' that can be identified in both proximal and distal settings. This allows distal-tephra deposits to be traced and linked to the proximal environment and to specific volcanic centres.

Geochemical characterisation or 'fingerprinting' of tephra horizons is therefore amongst the most important processes in tephrochronology; however, the process remains one of the most challenging, especially in distal environments where shard sizes are typically <100 μm. To deal with such small shard sizes the most commonly employed technique for chemical determinations is the Electron Probe Microanalyser (EPMA), which can be used to target individual glass shards (Lowe 2011). Typically ten elements (Si, Al, Ti, Fe, Mn, Mg, Ca, Na, K, and P) are analysed and recorded as routine, but some systems have the capacity to additionally record S, F, and Cl (Hayward 2012). The X-rays produced by these elements can be recorded in one of two ways; either by Energy-Dispersive Spectrometry (EDS) or Wavelength-Dispersive Spectrometry (WDS) (see Coulter et al. 2010). The former is often advocated for its speed of analysis, as all X-ray energies produced from the sample are analysed simultaneously and converted to an electrical charge which is related to the energy of the analysed element (Reed 2005).The latter uses spectrometer crystals to diffract the X-rays generated by the sample, which are in turn counted one element at a time in a gas filled chamber (Coulter et al. 2010). There are, however, a number of well documented issues associated with each respective system (e.g. Hunt and Hill 1993; Spray and Rae 1995; Morgan and London 1996; Hunt and Hill 2001; Coulter et al. 2010). The use of either therefore involves a certain level of compromise, and a significant problem relating to both systems is Na loss through sample heating (Hayward 2012). Whilst procedures and methods have adapted correspondingly, some of the approaches limit the size of the sample that can be analysed (Hunt and Hill 2001); in distal tephrochronology, limits on shards size are a considerable hindrance, and a major scientific bias. Recent work by Hayward (2012) however, has developed new protocols enabling the routine use of narrower diameter beams (5 μm and 3 μm) without Na loss. This development in methodology allows for greater analytical precision on smaller samples, and reduces the associated bias, both fundamental concerns in this study, and distal cryptotephrochronology as a discipline.

An emerging problem associated with major elemental analyses of glass shards is that volcanic systems have the tendency to produce deposits of a similar or matching geochemical signature e.g. the Katla system in Iceland which during the LGIT is purported to have produced at least four eruptions of indistinguishable chemistry (Lane et al. 2012b; Tomlinson et al. 2012a). This has led to issues of stratigraphic discrimination in the distal environment where one of these tephras has been identified but without firm stratigraphical control (e.g. Mithen et al. 2015). As a result some studies have turned toward trace and rare-earth elements (REEs) as a means to add additional 'robustness' to correlations (Pearce et al. 2007; Lowe 2011). For distal

shards two principle methods exist; Laser Ablation Inductively Coupled Plasma Mass Spectrometry (LA-ICP-MS) and Secondary Ion Mass Spectrometry (SIMS). The former has gained ground over its rival especially in NW Europe in recent years, due primarily to improvements in spot size, machine sensitivity and its comparative speed and cost (e.g. Pearce et al. 2007; 2011; Tomlinson et al. 2010). The SIMS by comparison is much more expensive, and analyses take considerably longer; however, the system is less destructive to the sample glass due to the Ion Probe using 'sputtering' (where only a small fraction of the sample surface is ionized) as opposed to laser ablation which is considerably more destructive during the analytical process (Lowe 2011). This makes the SIMS more usable when dealing with smaller and thinner samples, such as those recovered from ice core records (Lowe 2011). Nonetheless both systems have been shown to produce comparable outputs (Horn et al. 1997; Morishita et al. 2005; Hardiman 2012). Single shard analyses by these methods allow for the characterisation of around 30 trace elements, which provide an insight into magmatic processes, and have been used successfully to assist in discriminating between tephras not distinguishable by major element analyses alone (e.g. Pearce et al. 2007; Kuehn et al. 2009; Davies et al. 2012; Bramham-Law et al. 2013). However, the success rate at which trace elements can discriminate between ashes is unclear. This has caused some to question the justification of pursuing such an approach, especially as, in most magmatic systems, major and trace elements follow systematic pathways (Pollard et al. 2006).

2.4.4 Understanding and exploring geochemical data

2.4.4.1 Data quality

When collecting data by any of the aforementioned analytical techniques it is considered good practice to run a series of internal and external standards to ensure that conditions of the machine are kept constant (Hunt and Hill 1996; Jochum et al. 2005). Variations in these measurements, which are taken before, during, and after sample analysis, can indicate whether system calibrations have drifted and hence whether sample totals are likely to be affected.

2.4.4.2 Outliers

On occasion non-vitreous material may be analysed in error. Crystalline minerogenic materials or biogenic amorphous silicates can be especially difficult to identify and filter out during sample preparation. This is due to similar morphological properties and the inability to implement some diagnostic 'tests' during sample preparation (see section 4.6). However, in most circumstances these objects are easily distinguished post

analysis by their compositional totals. Quartz grains and biogenic silica for example often exhibit SiO_2 totals in excess of 90 % wt, whereas common minerogenic grains such as sodium and potassium feldspars can be distinguished more readily by their high Al_2O_3 (ca. 18 % wt) and K_2O (ca. 17 % wt) values (Pollard et al. 2006), and the near absence of FeO or TiO_2 (Hunt and Hill 1993). Such compositional totals are well outside the typical ranges of volcanic glasses and are discarded from interpretative phases, based on this premise of 'goodness of fit' with data generated within the study and from elsewhere. Erroneous measurements may also arise from crystal contamination within glass shards; these melt inclusions (microlites) can be detected during the course of analyses by examining the targeted shard in transmitted and reflected light. However, not all analytical facilities possess this capability, and inclusions under the glass surface may be difficult to identify regardless. On occasion therefore, these inclusions may be inadvertently analysed, but due to their feldspathic composition, resulting Na_2O and K_2O totals will likely be elevated above 'normal' values, and thus can be easily excluded based on their 'goodness of fit' with other glass chemical data.

2.4.4.3 Analytical totals

Major element analyses derived from EPMA measurements are reported as percentage sample weight for each measured elemental oxide. In theory totals should therefore reach 100%, however, due to several of factors this is seldom the case. Erroneous analytical totals may be caused by:

1) Glass water content; H_2O is not detectable by EPMA as hydrogen cannot generate X-Rays (Hunt and Hill 1993), although it is possible to measure its content by other means (e.g. Harms and Schmincke 2000; Hayward 2012). In a study of the Laacher See Tephra, Harms and Schmincke (2000) established that water content may be as high as 5.7 %, and is highly dependent on a magma body's ability to degas. Water content may also be increased above a shard's 'original' value by hydration processes in the post depositional environment (Hunt and Hill 1993; see section 2.3.5). However, some have argued that the influence of hydration should be minimal for sectioned polished shards, as this process exposes the 'dry-core' for analysis (Pollard et al. 2006).
2) Poorly-polished or poorly carbon-coated samples during EPMA measurements may lead to a charging of the sample surface and the generation of erroneous results (Hunt and Hill 1993; Hall and Hayward 2014). Intersection of a melt inclusion as discussed above may also on occasion yield low analytical totals (Pollard et al. 2006).

3) Charging and heating within the sample during electron bombardment can cause a depletion/ migration of certain elements and especially the mobile alkalis. This has the effect of lowering alkali totals and giving apparently higher concentrations of other elements, such as Si and Al (Morgan and London 1996; Hayward 2012).
4) Standard analyses do not include elements such as S, F, P and Cl although some systems are beginning to (Hayward 2012). Lower analytical totals may therefore reflect the non-analysis of these elements in older systems.

To account for these variabilities and to standardise comparisons between data sets it has been advocated that all analytical totals are normalised to 100 % (Froggatt 1992). This proposition is based on the notion that low totals are a consequence of water content, derived in principle not by magmatic processes but by alteration in the depositional environment. Thus it was argued that normalising the data removes this environmental bias; however, as shown, this is not the only factor for consideration when dealing with low totals, and a variety of other studies have maintained that normalisation masks the quality of the data (e.g. Hunt and Hill 1993; Pollard et al. 2006; Pearce et al. 2014). Hunt and Hill (1993) suggest that no manipulation of raw data should occur, instead a process of 'filtering' should take precedence, with totals expressing values lower than 95 % being rejected from correlations. This arbitrary figure has been an issue of contention amongst geochemists and tephrochronologists with some advocating that both lower (92 %) and higher (98 %) totals should be the cut-off (Hunt and Hill 1993; Matthews 2008). In reality there is unlikely to be a 'correct' approach; however, in Europe it has become standard practice to implement the 95 % cut off, whilst elsewhere in the world normalisation is more prevalent (e.g. Shane 2000; Westgate et al. 2001).

2.4.4.4 The unit sum problem

Both major and trace element data are expressed as a percentage, or as parts per million (ppm). In essence, therefore, a concentration expressed as a percentage involves not only the concentration of the particular element, but also the sum of the concentrations of all other elements (Pollard et al. 2006), for example:

$$wt\%\ SiO_2 = \frac{wt\ [SiO_2]}{\Sigma\ \text{wt all oxides}} \times 100$$

The result is that if the concentration of any one element changes then the percentage abundance of all other elements must also change. Therefore each element is constrained by the sum of the elements that have gone before it. This introduces a negative bias when using bi-plots as any increase along the dominant x-axis will lead to a decrease of any element plotted along the y-axis (Rollinson 1993). This has particular significance for tephra studies, as first order correlations are often made visually using bi-plots (Pollard et al. 2006).

2.4.5 Correlating tephra layers

Once chemical data sets have been filtered, a number of comparative methods are employed to test potential correlations with known eruptions, and to assign a volcanic provenance. Despite being a fundamental aspect of tephrochronology, there is no standardised or agreed method by which this is undertaken, and a variety of qualitative and statistical means are normally used.

2.4.5.1 Harker diagrams, bi-plots and ternary diagrams

Amongst the most common methodologies is to compare data sets visually through graphical means (Davies 2015). Oxide-oxide bi-plots (Harker diagrams) and tri-plots (ternary diagrams) provide a means to visually exploring the data and provides: i) an insight into the compositional range and structure of the data; ii) the detection of outliers, and; iii) an assessment of the chemical similarity of the data with that of differing tephras horizons.

It is possible to generate 45 separate x-y plots from 10 major elements and many more if trace elements data sets are available. In these instances an overlap in the distribution of data may signal a potential correlation (Figure 2.6). However, the usefulness of each of the major and trace elements in distinguishing between tephras is dependent on: i) the number of analyses; ii) the quality of the acquired and reference data sets; iii) whether the data is normalised or not; iv) whether a reference data set occupies the full compositional range of a tephra layer; v) the volcanic region in question; and, vi) the chemical similarity between volcanic systems (this can be an issue for some Icelandic systems Jakobsson et al. (2008)). An overlapping dataset between two or more samples may therefore be indicative of a correlation; however, other lines of evidence must also be considered e.g. stratigraphic superposition and associated chronological data. These additional factors are extremely important when making robust correlations, and may aid correlation where chemical data alone is insufficient.

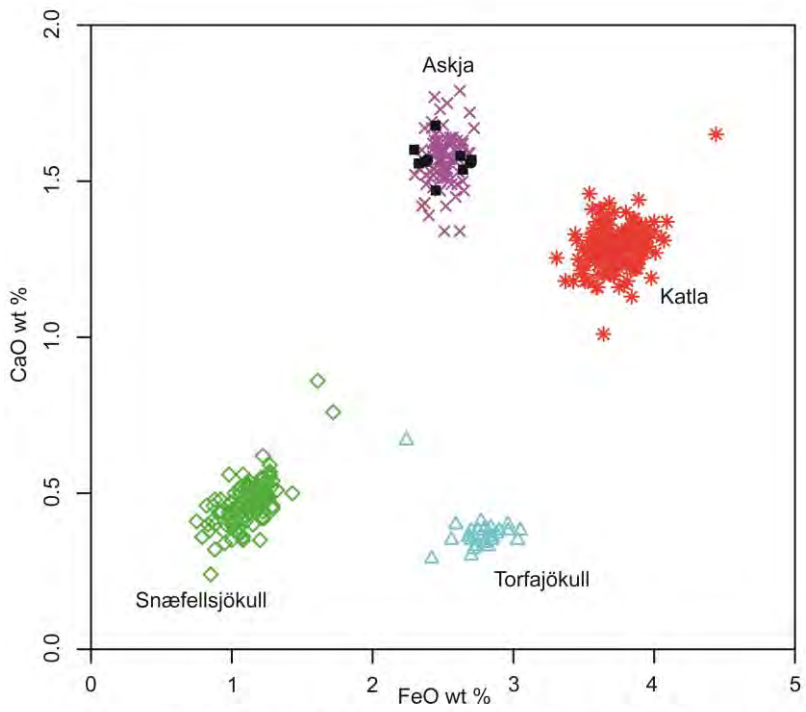

Figure 2.6 A bi-plot diagram of FeO vs CaO. In this instance the sample data set is represented by black squares, and shows a likely correlation to the Askja volcanic field.

Studies have suggested that the visual comparison of data does not allow for the full compositional range of elements to be considered together (Pollard et al. 2006). Whilst Pollard et al. (2006) have argued tri-plots are better than bi-plots, due to the fact that more elements are taken into account during comparative stages, their use in fact further manipulates and transforms the data (Matthews 2008). Each element in a tri-plot is expressed as a percentage of the new sum, meaning that the data is further distorted by a second round of averaging. Rollinson (1993) highlights that elements with the smallest variation can have the greatest variation after this process, and further illustrates the potential limitations caused by the unit-sum problem in geochemical correlations.

2.4.5.2 Statistical methodologies

As a means to provide a quantitative measure of correlations and to test the validity of graphical correlations, various statistical methods can and have been employed in tephrostratigraphic studies. Tests include: statistical distance analysis, cluster analysis, t-test comparisons of means, similarity coefficients, as well as Principal Component Analysis (PCA), Discriminant Function Analysis (DFA) and Kernel Density Estimates (KDE) (Lowe et al. 2011; Bronk Ramsey et al. 2015a). Some of these methods such as cluster analysis and t-tests only consider mean values, which is potentially misleading if data sets are heterogeneous, i.e. containing more than one population. PCA, DFA, and

KDE are used to compare the overall distribution of the data, and such techniques can be used alongside standard bi-plots to quantify similarities between data sets (e.g. Andrews et al. 2002; Lowe et al. 2011; Bronk Ramsey et al. 2015a). Whilst such statistical and multivariate techniques provide a quantified value of correlation, outputs are still dependent on the quality of inputted data, and cannot quantify precision or accuracy within the dataset.

2.4.6 Tephrochronometry: dating tephra layers

Tephrochronometry is the process by which a numerical age for a tephra is obtained; this may be achieved by the following means:

***Method*:** Direct dating of the tephra.
***Techniques*:** Historically written accounts, Fission-track dating, Argon isotopes (^{40}Ar-^{39}Ar)
***For*:** Tephra horizons which have occurred in historical time, or horizons which exhibit mineral assemblages that can be directly dated.

Historically written accounts of volcanic eruptions were one of the earliest means by which an age could be assigned to a tephra layer; in Iceland this technique has enabled the dating of > 100 eruptions from the last nine centuries (Alloway et al. 2007). However, this approach has been limited by the accuracy of written accounts, and is constrained to regions proximal to volcanic centres. A more widely applied technique and crucially one which can be applied to older tephras is to use primary minerals such as zircon, hornblende, K-feldspar, biotite, and quartz to directly date a tephra deposit (Lowe 2011). These minerals may constitute a component of the ash bed, or be held within the lithic or glass suites as mineral inclusions (Lowe 2011). However, as with historical records, the greater the distance from volcanic source the less applicable these techniques are. This is primarily due to 'distance settling' and the poor representation of mineral fractions in far field localities (Lowe 2011).
Applied references: e.g. Þórarinsson (1944), van den Bogaard (1995).

***Method*:** Indirect dating of the host sediment.
Techniques: Radiocarbon, incremental records, luminescence, U-series, electron spin resonance, ^{210}Pb, ^{137}Cs, ^{3}He and ^{21}Ne surface exposure dating
***For*:** Tephra horizons held within a sedimentary unit and not directly datable.

Indirect dating is by far the most widely applied methodology in developing numerical ages for distal tephra horizons (Alloway et al. 2007; Lowe 2011). The potential techniques are numerous, and reflect the many methods used in geochronology. However, emphasis here is placed on radiocarbon and incremental methods, as these have particular relevance in the context of NW Europe. Radiocarbon dating since its advent in the late 1950s has become one of the primary methods for tephra age determination (Alloway et al. 2007). However, in order for this approach to be applicable, it requires that: 1) the hosting sedimentary unit contains enough datable material e.g. wood, leaves, shells etc. and 2) this material is coincidental with a tephra horizon. Whilst much success has been had in constraining tephras by this approach in NW Europe (e.g. Lohne et al. 2013), these requirements can be a limiting factor in the context of the LGIT. (e.g. Loch Ashik: Pyne-O'Donnell 2007). The poor preservation of macrofossils in some circumstances means that tephra ages may result in very large age ranges (e.g. the Abernethy Tephra: Matthews et al. 2011; Bronk Ramsey et al. 2015b) or because of a lack of datable material, remain undated entirely (e.g. the Breakish Tephra: Pyne-O' Donnell 2007).

An alternative method which has demonstrated to be particularly valuable for producing very precise age estimates is the incremental approach. Tracing tephras to annually laminated records for example ice cores or varved lake sequences has refined the age estimates of many tephras in NW Europe (e.g. Abbot and Davies 2012; Brauer et al. 1999; Lane et al. 2015; Ott et al. 2016). However, it is seldom that an incremental chronology is continuous, meaning that such sequences are often left 'floating' without a firm chronological 'anchor'. Whilst the relative age of two or more tephras can be identified in this manner (e.g. Ott et al. 2016), for a sequence to be of utmost value, the annually laminated sequence must be anchored in time. As a result all subsequent tephra age estimates will be dependent on the robustness of this 'anchoring' (e.g. Ott et al. 2016).

Applied references: e.g. Matthews et al. (2011), Brauer et al. (1999), Ott et al. (2016).

***Method*:** Stratigraphical or geochemical correlation of the tephra to a horizon with an existing age range.

***Techniques*:** Physical properties (colour, texture, grain-size etc.); Geochemical methods (EPMA, LA-ICP-MS, SIMS etc.).

***For*:** Tephras which cannot be dated by direct or indirect methods.

In many instances it may not be possible to date a tephra by either direct or indirect means, or obtain an age that is better than that already published. In such circumstances correlation to a tephra of known age is desirable, and stratigraphical or geochemical means are likely to prove the most viable means to do so. Correlation by this method must employ the principles of superposition and hence understand the context of the tephra in question. Failure to do so can lead to an erroneous correlation and hence the misallocation of age.

Applied references: e.g. Brooks et al. (2012), Timms et al. (2016).

***Method*:** Age depth modelling.

***Techniques*:** Various statistical approaches (see below).

For: Tephras which cannot be dated by direct or indirect methods.

Depositional age modelling has become critical in advancing tephrochronometry in recent years. Whilst a variety of differing approaches to age modelling can be undertaken e.g. linear interpolation, splines, linear and polynominal regression models (e.g. Bennett 1994; Bennett and Fuller 2002; Telford et al. 2004; Blaauw 2010), several studies have highlighted the inherent limitations and simplifications of such approaches (e.g. Telford et al. 2004; Blaauw 2010), whilst others have advocated and shown that Bayesian methods can produce very reliable models (e.g. Blockley et al. 2004; Blaauw and Christen, 2005; Bronk Ramsey, 2008). In NW Europe significant advances have been made with developing tephra frameworks or lattices (see section 2.7), underpinned with sites dated by Bayesian-based models and the internationally agreed ^{14}C calibration curves (e.g. Blockley et al. 2004; 2008a; 2008b; Reimer et al. 2004; 2009; 2013; Bronk Ramsey 2008; 2009; Bronk Ramsey et al. 2015b).

While Bayesian-based models have been used to assign modelled ages to tephras within individual sequences (e.g. Matthews et al. 2011), collective chronological information concerning individual tephra horizons from several sites can be combined in a regional Bayesian model. This process was adopted by Bronk Ramsey et al. (2015b) for tephras in the RESET tephra lattice (see section 2.7). The output of this combined model is a best age estimate range for each tephra isochron. These ages may then be transferred to any site in which the associated tephra is traced, and has significant impact on those sequences which exhibit poor chronological control, or in marine sites where such age estimates are used to circumvent reservoir off-sets (e.g. Thornally et al. 2011).

Applied references: e.g. Bronk Ramsey et al. (2015b).

2.4.7 Methodological considerations: section summary

In the third section of this chapter methodological approaches to distal-tephrochronology have been introduced and reviewed. The section is best summarised by a quote from Tryon et al. (2008: 655) who state that "correlations between tephra deposits are best considered testable hypotheses, subject to continual revision with expanded datasets…the strongest correlations are those that show concordance between multiple independent datasets, including stratigraphic, fossil, chronological, and geochemical evidence".

2.5 Source regions of tephra in the Britain Isles and NW Europe

2.5.1 Volcanic provinces

During the course of the late Pleistocene and early Holocene, several volcanic provinces generated and dispersed tephra across NW Europe. For the British Isles tephrostratigraphic records are dominated by tephra derived from Iceland, but for the rest of NW Europe several other volcanic provinces provide key tephrostratigraphic markers. These include the Massif Central in France, the Eifel district in Germany, and the Campanian region of Italy.

2.5.2 Iceland

Volcanism in Iceland is unusual in that it is a product of both mid-ocean rifting and mantle hot spot volcanism (Ingólfsson et al. 2008). Late Quaternary volcanism in Iceland has been confined to several neovolcanic zones, which collectively cover ~30,000 km^3, and appear as distinct 15–50 km-wide belts of active faulting and volcanism (Thordarson and Larsen 2007). Of these neovolcanic zones approximately Forty-two volcanic systems have been identified within Iceland and its insular shelf (Jakobsson et al. 2008; Thordarson and Höskuldsson 2008). Twenty-eight terrestrial volcanic systems are considered to have been active during the Holocene, and a further three are considered to have been active during the late Pleistocene (Jakobsson et al. 2008; Figure 2.7 and Table 2.2). A volcanic system can be defined as a spatial grouping of eruption sites which possess a common characteristic relating to tectonics, petrology or geochemistry (Jakobsson 1979a). In their simplest form, the volcanic systems of Iceland consist of a central volcano and an accompanying fissure swarm, which may or may not host a crustal magma chamber. Basic and more evolved magmas can be erupted from a central volcano, but only basic (basaltic) lava is emitted from fissure sites (Larsen and Eiríksson 2008). In total, twenty systems are known to feature a fissure swarm, and twenty-three central volcanoes have been identified

across nineteen of the volcanic systems (Thordarson and Larsen 2007; Thordarson and Höskuldsson 2008).

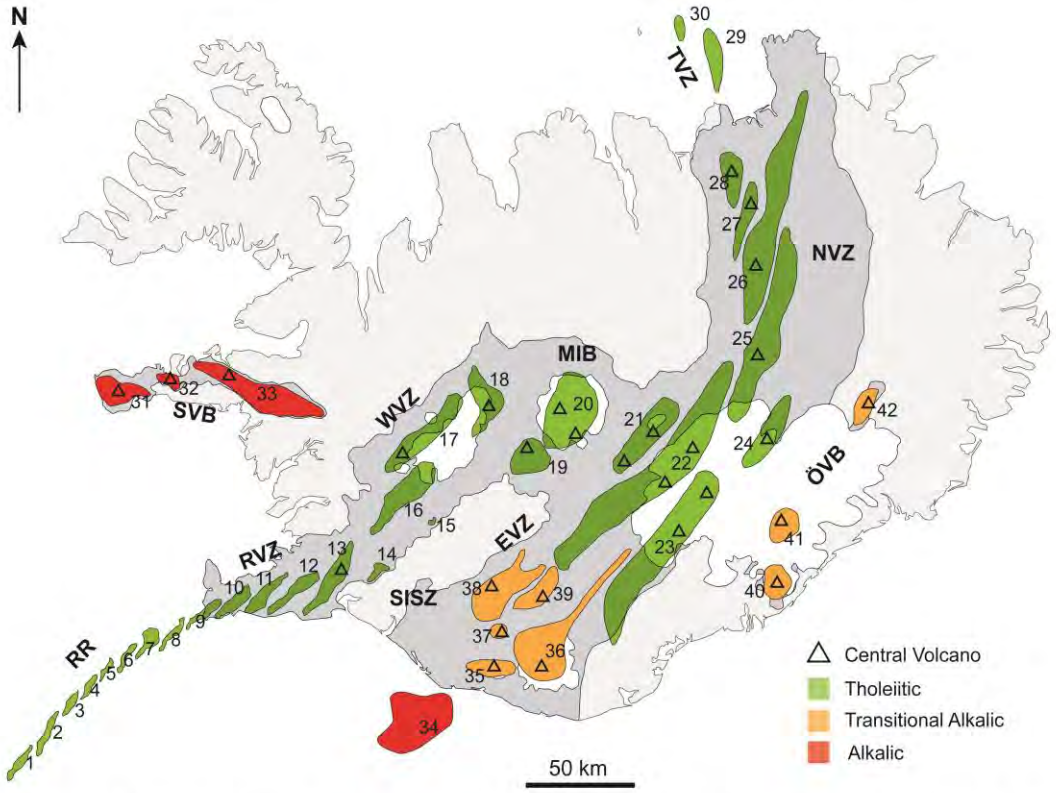

Figure 2.7 Active volcanic zones and systems in Iceland, abbreviations are as follows: **RR**, Reykjanes Ridge; **RVB**, Reykjanes Volcanic Belt; **SISZ**, South Iceland Seismic Zone; **WVZ**, Western Volcanic Zone; **MIB**, Mid-Iceland Belt, **EVZ**, Eastern Volcanic Zone; **NVB**, Northern Volcanic Zone, **TFZ**, Tjörnes Fracture Zone; **SVB**, Snæfellsnes Volcanic Belt; **ÖVB**, Öræfi Volcanic Belt. Numbers refer to active systems (see Table 2.2). Adapted from Jakobsson et al. (2008), Thordarson and Höskuldsson (2008).

Each of the volcanic systems in Iceland possess a distinct geochemical suite, this allows tephras to be distinguished from one another, and also enables the source system to be identified. In the distal environment this information is essential, as it allows an understanding of the tephrostratigraphic superposition, and allows robust correlations to be made across spatially disparate sites. However, similarities in the geochemical signature do exist between tephras and between systems, and this can make the task of correlating horizons difficult if geochemical datasets are small and stratigraphic information is lacking or uncertain. These themes are discussed further in section 2.8, but the similarities in the geochemical signatures relate to the three major petrological provinces that define Icelandic volcanism. These are: the tholeiitic series, the transitional alkalic series, and the alkalic series (Jakobsson 1979a,b; Jakobsson et al. 2008; Figure 2.7; Table 2.2). All three series are capable of producing tephra ranging from basalts through to rhyolites, with the style of volcanism as equally diverse

(e.g. Thorarinsson and Sæmundsson 1977; Thordarson and Larsen 2007; Thordarson and Höskuldsson 2008).

Table 2.2 Forty-two volcanic systems were thought to be active during the late Pleistocene and Holocene both onshore and offshore, the numbers listed correlated to those in Figure 2.7. The major producers of basaltic tephra in Iceland are the following 7 volcanic systems: Reykjanes, Svartsengi, Vestmannaeyjar, Katla, Kverkfjöll, Bárðarbunga-Veiðivötn, and Grímsvötn. Central volcanoes on 7 volcanic systems are the major producers of silicic volcanism, those are: Eyjafjallajökull, Katla, Hekla, Torfajökull, Askja, Öræfajökull, and Snæfellsjökull. In addition several volcanic systems have produced minor amounts of tephra, including: Fremrinámur, Krafla, and Ljósufjöll (Modified from Jakobsson et al. 2008; Larsen and Eríksson 2008; Thordarson and Höskuldsson 2008).

N. O	Volcanic Zone	Name	System Type	Central Volcano(s)	Comments
1	RR	Steinahóll	Tholeiitic		Submarine
2	RR	Gullhóll	Tholeiitic		Submarine
3	RR	Stóri-Brandur	Tholeiitic		Submarine
4	RR	Eldeyjarbodi	Tholeiitic		Submarine
5	RR	Grjóthryggur	Tholeiitic		Submarine
6	RR	Langagrunn	Tholeiitic		Submarine
7	RR	Geirfuglasker	Tholeiitic		Submarine, two islets
8	RR	Eldey	Tholeiitic		Submarine, one island, one islet
9	RVZ	Reykjanes	Tholeiitic		Partly submarine
10	RVZ	Svartsengi			
11	RVZ	Krísuvík	Tholeiitic		
12	RVZ	Brennisteinsfjöll	Tholeiitic		
13	WVZ	Hengill	Tholeiitic	Hengill	Includes Hrómundartindur
14	WVZ	Grímsnes	Tholeiitic		
15	WVZ	Geysir	Tholeiitic		
16	WVZ	Skjaldbreidur	Tholeiitic		
17	WVZ	Prestahnúkur	Tholeiitic	Prestahnúkur	
18	WVZ	Hveravellir	Tholeiitic	Hveravellir	
19	MIB	Kerlingarfjöll	Tholeiitic	Kerlingarfjöll	Last active during late Pleistocene
20		Hofsjökull	Tholeiitic	Hofsjökull/ Arnarfell	
21	MIB	Tungnafellsjökull	Tholeiitic	Tungnafellsjökull/ Hágöngur/ Vonarskard	
22	EVZ	Bárðarbunga-Veiðivötn	Tholeiitic	Bárðarbunga/ Hamarinn	Includes Veiðivötn and Tungnaárörræfi
23	EVZ	Grímsvötn	Tholeiitic	Grímsvötn/ Thórdarhyrna	Includes Skaftárörræfi
24	NVZ	Kverkfjöll	Tholeiitic	Kverkfjöll	Includes Fjallgardar
25	NVZ	Askja	Tholeiitic	Askja	Includes Dyngjufjöll
26	NVZ	Fremrinámur	Tholeiitic		Includes Heidarspordur

27	NVZ	Krafla	Tholeiitic	Krafla	
28	NVZ	Þeistareykir	Tholeiitic	Þeistareykir	
29	TVZ	Tjörnesgrunn	Tholeiitic		Submarine, two islands
30	TVZ	Skjálfandadjúp	Tholeiitic		Submarine
31	SVB	Snæfellsjökull	Alkalic	Snæfellsjökull	
32	SVB	Lýsuhyrna (Helgrindur/ Lýsuskarð)	Alkalic		
33	SVB	Ljósufjöll	Alkalic	Ljósufjöll	
34	EVZ	Vestmannaeyjar	Alkalic		Partly submarine
35	EVZ	Eyjafjallajökull	Transitional Alkalic	Eyjafjallajökull	
36	EVZ	Katla	Transitional Alkalic	Mýrdalsjökull	
37	EVZ	Tindfjallajökull	Transitional Alkalic	Tindfjallajökull	
38	EVZ	Hekla	Transitional Alkalic	Hekla	Includes Vatnafjöll
39	EVZ	Torfajökull	Transitional Alkalic	Torfajökull	Includes Raudfossafjöll
40	ÖVB	Öræfajökull	Transitional Alkalic	Öræfajökull	
41	ÖVB	Esjufjöll	Transitional Alkalic	Snæhetta	Last active during late Pleistocene
42	ÖVB	Snæfell	Transitional Alkalic	Snæfell	Last active during Mid-Late Pleistocene

For the production of far travelled distal tephra, eruptions need to be explosive, and in Iceland two main styles dominate Plinian/Subplinian (magmatic ‘dry’ eruptions), and Phreatoplinian, Surtseyan (phreatomagmatic ‘wet’ explosions) (Thordarson and Larsen 2007). During the LGIT the wasting and retreat of the Icelandic glaciers produced an abundance of meltwater and elevated ground water levels, this series of events produced favourable conditions for explosive phreatomagmatic volcanism (Larsen and Eiríksson 2008); and as further pressures were released from the system via continued glacial unloading, an increase in explosive volcanism is noted to have occurred (Slater et al. 1998; Sigvaldason 2002; Carrivick et al. 2009; Sigmundsson et al. 2010). Despite this abundance of explosive volcanism through the LGIT there is almost no evidence for proximal deposits in Iceland at this time (Björck et al. 1992; Haflidason et al. 2000; Norðdahl et al. 2008; Gudmundsdóttir et al. 2016). Most soils in Iceland are less than 11,500 years old and this is thought to reflect the extensive ice cover that persisted in many areas of Iceland well into the Holocene, and also as a result of sea level changes during the Pre-Boreal (Ingólfsson et al. 1995; Larsen and Eriksson 2008, 2013). With the exception of the Skagi Peninsula, in the north of Iceland, much of the country did not offer good preservation potential for eruptive material (Björck et al. 1992; Norðdahl et al. 2008; Larsen and Eriksson 2013). As a result almost the entire eruptive history of

the late Pleistocene is known only from what can be identified within the distal record (Haflidason et al. 2000). The earliest confirmed tephra horizons that are found both in proximal and distal locations are the Vedde Ash (12,102-11,914 cal. yrs BP), the Askja-S/10ka (10,956-10,716 cal. yrs BP) and the Saksunarvatn Ash (10,257-10,056 cal. yrs BP); from Katla, Askja and Grímsvötn respectively (e.g. Mangerud et al. 1984; Hjort et al. 1985; Mangerud et al. 1986; Björck et al. 1992; Sigvaldason 2002; Lane et al. 2012b; Bronk Ramsey et al. 2015b). The distal tephra record for the LGIT is illustrated in Figure 2.8 and Table 2.3; it is evident that the most active or at least the most explosive centres during this period were Katla, Hekla, Torfajökull, Askja, Grímsvötn, and Snæfellsjökull.

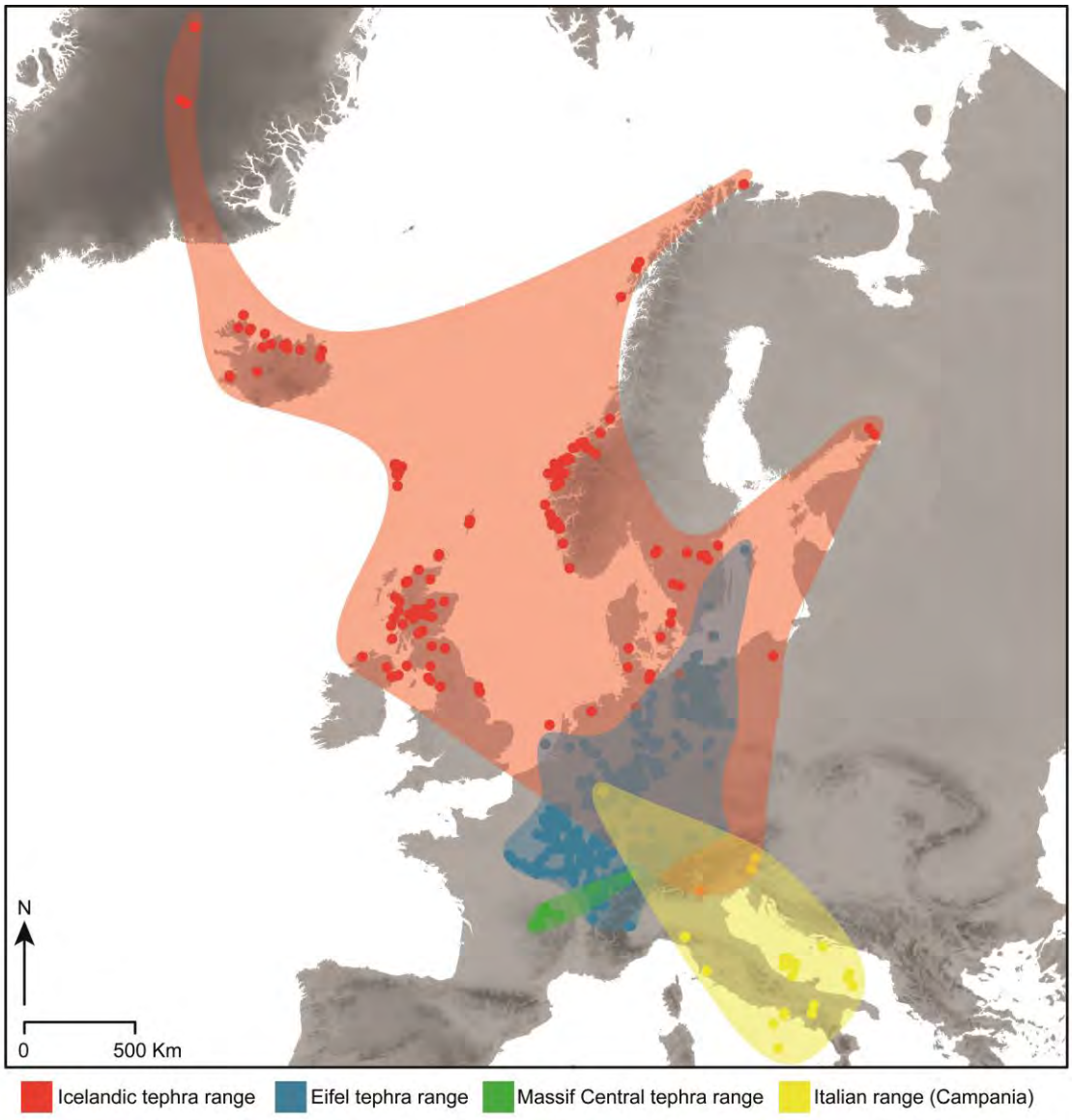

Figure 2.8 Tephra distributions from the four main volcanic provenances to have influence on NW Europe during the LGIT. Only terrestrial and ice-core sites are plotted due to uncertainties concerning ice berg rafting in the North Atlantic. The Icelandic dispersal envelop is largely dominated by the Vedde Ash and the Saksunarvatn Ash. The Eifel tephra range is dominated by the dispersal of the Laacher See Tephra, whilst for the Italian tephra range the Neapolitan Yellow Tuff dominates.

Table 2.3 Tephras erupting from Iceland during the LGIT, column 2 (En = Environment in which the tephras are found) T = Terrestrial, M = Marine, I = Ice core. Source region abbreviations KOL = Kolbeinsey Ridge or other primitive volcanoes such as Hrossaborg in Askja from the NVZ (Kristjánsdóttir et al. 2007); TFZ = Tjörnes Fracture Zone. Recent work by Alison MacLeod and Siwan Davies on the Sluggan tephras has put doubt their Icelandic provenance, with a local geological outcrop being proposed as their origin (MacLeod and Davies 2016).

Tephra	En	Source	Age	Composition	Reference
Torfajökull 8.2ka	T	Torfajökull	ca. 8200 kyrs	Rhyolitic	Ian Matthews pers. comm. 2015
G1	M		ca. 8200 kyrs	Basaltic	Thornally et al. 2011
Suðuroy	T/ M	Katla	8070 ± 90 cal. yrs BP	Rhyolitic	Wastegård 2002
K1a	M	Katla	ca. 8400 kyrs	Basaltic	Thornally et al. 2011
K1b	M	Katla	ca. 8400 kyrs	Basaltic	Thornally et al. 2012
V1-2269	M	Katla?	9122-8751 2σ/ 9048-8828 1σ cal. yrs BP	Rhyolitic	Kristjánsdóttir et al. 2007
2322/1209.5	M	Grímsvötn	9120-8845 cal. yrs BP	Basaltic	Jennings et al. 2014
SSn (Svinavatn)	T	Snæfellsjökull?	9450 ± 50 cal. yrs BP	Rhyolitic	Boygle 1999
QUB 606	T	Snæfellsjökull?	ca. 9500 cal. yrs BP	Rhyolitic	Pilcher et al. 2005
GRIP 1465.58m	I	Unknown	9600 ± 76 GICC05 yrs b2k	Basaltic	Grönvold et al. 1995
An Druim	T	Torfajökull	9560 ± 40 cal. yrs BP	Rhyolitic	Ranner et al. 2005
Breakish	T	Askja?	Unknown	Rhyolitic	Pyne-O'Donnell 2007
Høvdarhagi	T	Torfajökull	9850-9600 cal. yrs BP	Rhyolitic	Lind and Wastegård 2011
Skopun	T	Katla	9850-9600 cal. yrs BP	Intermediate	Lind and Wastegård 2011
G2 2269	M	Grímsvötn	10,051-9770 cal. yrs BP	Basaltic	Jennings et al. 2014

2322/1605.5	M	Grímsvötn	10,130-9848 cal. yrs BP	Basaltic	Jennings et al. 2014
Grims 2322-1617.5	M	Grímsvötn	10,151-9866 cal. yrs BP	Basaltic	Jennings et al. 2014
G3 2269	M	Grímsvötn	10,191-9901 cal. yrs BP	Basaltic	Jennings et al. 2014
Fosen	T	Unknown	ca. 10,200 cal. yrs BP	Rhyolitic	Lind et al. 2013
10-1P 36	M	Katla	ca. 10,300 kyrs	Rhyolitic	Thornally et al. 2011
Grims 2322-1719.5	M	Grímsvötn	10,302-10,035 cal. yrs BP	Basaltic	Jennings et al. 2014
L-274	T	Mixed	10,225 ± 100 cal. yrs BP	Rhyolitic	Lind and Wastegård 2011
Saksunarvatn	T/ M/I	Grímsvötn	10,176 ± 49 cal. yrs BP	Basaltic	Mangerud et al. 1986
2322/1749.5	M	Grímsvötn	10,372-10,104 cal. yrs BP	Basaltic	Jennings et al. 2014
Grims 2322-1797.5	M	Grímsvötn	10,489-10,249 cal. yrs BP	Basaltic	Jennings et al. 2014
Högtorpsmossen	T	Unknown	10,298 ± 108 cal. yrs BP	Rhyolitic	Björck and Wastegård 1999
Ashik	T	Grímsvötn/ Torfajökull	10,400 ± 300 cal. yrs BP	Basaltic/Rhyolitic	Pyne-O'Donnell 2007
V2-2269	M	Katla?	10,632-10,237 2σ/ 10,526-10,318 cal. yrs BP	Rhyolitic	Kristjánsdóttir et al. 2007
Hovsdalur	T	Snæfellsjökull	10,475 ± 175 cal. yrs BP	Rhyolitic	Wastegård 2002
KOL1-2269	M	KOL/Iceland	10,869-10,379 2σ/ 10,672-10,461 1σ cal. yrs BP	Basaltic	Kristjánsdóttir et al. 2007
L-3574	T	Mixed	ca. 10,800 cal. yrs BP	Basaltic/ Intermediate/ Rhyolitic	Dugmore and Newton 1998
Askja-S/10ka	T/ M	Askja	10,830 ± 57 cal. yrs BP	Rhyolitic	Sigvaldason 2002; Davies et al. 2003

V3-2269	M	Katla?	11,005-10,587 cal. yrs BP	Rhyolitic	Kristjánsdóttir et al. 2007
1-THOL-1 /Tv-3	T	Bárðarbunga-Veiðivötn	11,015 ± 225 cal. yrs BP	Basaltic/Rhyolitic	Björck et al. 1992
Sandoy B	T	Bárðarbunga-Veiðivötn	11,230 ± 42 cal. yrs BP	Basaltic	Lind and Wastegård 2011
KOL2-2269	M	KOL/Iceland	11,353-10,905 2σ/ 11,230-10,999 1σ cal. yrs BP	Basaltic	Kristjánsdóttir et al. 2007
Sandoy A	T	Bárðarbunga-Veiðivötn	11,330 ± 42 cal. yrs BP	Basaltic	Lind and Wastegård 2011
KOL3-2269	M	KOL/Iceland	11,462-10,1995 2σ/ 11,284-11,078 1σ cal. yrs BP	Basaltic	Kristjánsdóttir et al. 2007
Hässeldalen	T	Snæfellsjökull	11,388 ± 156 cal. yrs BP	Rhyolitic	Davies et al. 2003
Abernethy (AF555)	T	Katla	11,462 ± 122 cal. yrs BP	Rhyolitic	Matthews et al. 2011
Vedde	T/ M/I	Katla	12,023 ± 43 cal. yrs BP	Basaltic/ Intermediate/ Rhyolitic	Mangerud et al. 1984; Lane et al. 2012b
LAS-1	T	Iceland?	Unknown: estimated (10.8-11.0 ^{14}C yrs BP)	Rhyolitic	Davies 2003
Vallensgård Mose	T	Iceland?	Unknown	Rhyolitic	Turney et al. 2006
MD99-2275 (3412)	M	Bárðarbunga-Veiðivötn	ca. 12,165 cal. yrs BP	Basaltic	Søndergaard 2005; Gudmundsdóttir et al. 2012
MD99-2275 (3417)	M	Katla	ca. 12,210 cal. yrs BP	Basaltic	Søndergaard 2005; Gudmundsdóttir et al. 2012
NGRIP 1508.26m	I	Katla	12,248 ± 117 GICC05 yrs b2k	Rhyolitic	Mortensen et al. 2005
NGRIP 1511.34m	I	Unknown	12,360 ± 120 GICC05 yrs b2k	Rhyolitic	Mortensen et al. 2005
NAAZ1	M	Katla/ Grímsvötn/	12400 ± 500 cal. yrs BP	Basaltic/Rhyolitic	Ruddiman and Glover 1972

		Bárðarbunga-Veiðivötn			
1-THOL-2/ Tv-1	T/I	Grímsvötn	12,646 ± 65 b2k	Basaltic	Mortensen et al. 2005
MD99-2275 (3468)	M	Grímsvötn	ca. 12,667 cal. yrs BP	Basaltic	Søndergaard 2005; Gudmundsdóttir et al. 2012
K2	M	Grímsvötn/Katla	ca. 12,600 kyrs	Basaltic	Thornally et al. 2011
15-4P 472	M	Katla	ca. 12,800 kyrs	Basaltic	Thornally et al. 2011
Sluggan B	T	Unknown	12800 ± 500 cal. yrs BP	Rhyolitic	Lowe et al. 2004
Roddans Port A	T	Unknown	Unknown	Rhyolitic	Turney et al. 2006
MD99-2275 (3505)	M	Bárðarbunga-Veiðivötn	ca. 12,999 cal. yrs BP	Basaltic	Søndergaard 2005; Gudmundsdóttir et al. 2012
NGRIP 1531.92m	I	Hekla?	13,030 ± 140 GICC05 yrs b2k	Intermediate	Mortensen et al. 2005
IA2	M	Katla	13,150± 146 b2k	Rhyolitic	Bond et al. 2001
10-1P 144	M	Grímsvötn	ca. 13,400 kyrs	Basaltic	Thornally et al. 2011
MD99-2275 (3553)	M	TFZ KOL	ca. 13,429 cal. yrs BP	Basaltic	Søndergaard 2005; Gudmundsdóttir et al. 2012
NGRIP 1553.85m	I	Askja	13,580 ± 156 GICC05 yrs b2k	Rhyolitic	Mortensen et al. 2005
R1	M	Katla	ca. 13,600 kyrs	Rhyolitic	Thornally et al. 2011
Penifiler Tephra	T	Unknown/Katla	13,939 ± 66 cal. yrs BP	Basaltic/Rhyolitic	Pyne-O'Donnell 2007
Roddans Port B	T	Unknown	Unknown	Rhyolitic	Turney et al. 2006
K3	M	Katla	ca. 14,000 kyrs	Basaltic	Thornally et al. 2011
NGRIP 1573.00m	I	Katla	14,020 ± 167 GICC05 yrs b2k	Basaltic	Mortensen et al. 2005
Borrobol Tephra	T	Unknown	14,098 ± 47 cal. yrs BP	Rhyolitic	Turney et al. 1997

15-4P 504	M	Katla	ca. 14,100 kyrs	Basaltic	Thornally et al. 2011
KOL-GS-2	M	KOL/Iceland	13,400 ^{14}C yrs BP	Basaltic/Rhyolitic	Eríksson et al. 2000
GS-2/BAS-1	M	Iceland	13,400 ^{14}C yrs BP	Basaltic	Hafliðason et al. 2000
GS-2/BAS-2	M	Iceland	13,400 ^{14}C yrs BP	Basaltic	Hafliðason et al. 2000
GS-2/BAS-3	M	Iceland	13,400 ^{14}C yrs BP	Basaltic	Hafliðason et al. 2000
GS-2/BAS-4	M	Iceland	14,000 ^{14}C yrs BP	Basaltic	Hafliðason et al. 2000
NGRIP 1579.15m	I	Hekla	14,175 ± 172 GICC05 yrs b2k	Basaltic	Mortensen et al. 2005
MD99-2275 (3660)	M	Bárðarbunga-Veiðivötn/ Krafla	ca. 14,389 cal. yrs BP	Basaltic	Søndergaard 2005; Gudmundsdóttir et al. 2012
Sluggan A	T	Unknown	14,500 ± 500 cal. yrs BP	Rhyolitic	Lowe et al. 2004
NGRIP 1595.1m	I	Bárðarbunga-Veiðivötn	14,500 ± 180 GICC05 yrs b2k	Basaltic	Mortensen et al. 2005
MD99-2275 (3678) & MD99-2271 (802)	M	Unknown	ca. 14,550 cal. yrs BP	Basaltic/Rhyolitic	Søndergaard 2005; Gudmundsdóttir et al. 2011; 2012
G2	M	Grímsvötn	ca. 14,600 kyrs	Basaltic	Thornally et al. 2011
10-1P 192	M	Katla	ca. 14,700 kyrs	Rhyolitic	Thornally et al. 2011
G3	M	Grímsvötn	ca. 15,000 kyrs	Basaltic	Thornally et al. 2011
Dimna Ash	T	Katla	15,100 ± 300 cal. yrs BP	Rhyolitic	Koren et al. 2008
NGRIP 1619.58m	I	Hekla	15,298 ± 105 b2k	Intermediate	Mortensen et al. 2005
NGRIP 1628.25	I	Unknown	15,685 ± 113 b2k	Rhyolitic	Mortensen et al. 2005

2.5.3 Massif Central (France)

The Massif Central is an intra-plate volcanic province located in modern day southern France (Nowell et al. 2006). The Chaîne des Puys contains approximately 80 volcanic centres including basaltic scoria cones, maars and domes which began forming ca. 200 ka years ago (Jordan et al. 2016). There is evidence to suggest that the system has been relatively active through the late Pleistocene and early Holocene, producing numerous eruptions of a trachy-basaltic/ trachy-andesitic composition from the Chaîne des Puys volcanic field (Juvigne 1992; Juvigne et al. 1996; Vernet et al. 1998; Vernet et al. 2000; Miallier et al. 2004; Table 2.4). However, very little research focused on tracing these eruptions in distal settings, and therefore most ashes can only be used as local stratigraphic markers (Figure 2.8). Recent work by Vannière et al. (2004) and Jouannic et al. (2015), however, have been able to improve the superposition of some tephras from the Massif Central, by identifying their presence within sequences that also contain the Laacher See Tephra (see below) and the Vedde Ash. There is therefore much scope for integrating the Massif Central tephras into European-wide tephra frameworks or lattices, but a greater effort is needed in regards to geochemical characterisation and the reporting of the data.

Table 2.4 Tephras erupted from the Massif Central during the LGIT, ages from the RESET database (c14.arch.ox.ac.uk/reset/).

Source	Eruption	Age μ ± σ (cal. yrs BP)	Reference
Chaîne des Puys	La Vache-Lassolas	8822 ± 175	Juvigne 1992
Chaîne des Puys	Vasset-Killian	9525 ± 495	Juvigne et al. 1996
Chaîne des Puys	Pariou	9530 ± 495	Miallier et al. 2004
Chaîne des Puys	Chopine (Taphanel)	9860 ± 260	Juvigne 1992
Chaîne des Puys	Puy de Dome	11,195 ± 405	Juvigne 1992
Chaîne des Puys	T4 Godivelle	12,660 ± 195	Juvigne et al. 1996
Chaîne des Puys	T5 Godivelle	12,660 ± 115	Juvigne et al. 1996
Chaîne des Puys	La Moutade Tephra	13,235 ± 115	Vernet et al. 1998
Chaîne des Puys	Puy de la Nugère	13,270 ± 65	Juvigne et al. 1996
Chaîne des Puys	Les Roches Tephra	13,875 ± 175	Vernet et al. 2000

2.5.4 Eifel district (Germany)

The Eifel district, like the Massif Central, is an intra-plate volcanic province located in western Germany (Nowell et al. 2006). Quaternary volcanism in the region is likely a product of asthenosphere upwelling (Shaw and Woodland 2012), derived either from a

low velocity mantle plume, or more passive mantle movements (Goes et al. 1999; Granet et al. 1995). During the course of the Late Pleistocene the Eifel district was the origin of a large Phreatoplinian eruption from which the Laacher See Tephra (LST), dated to 12,979-12,889 cal. yrs BP is derived (Bronk Ramsey et al. 2015b; Table 2.5). The eruption distributed ash over much of central Europe in several phases, which trend on an North-South axis (e.g. van den Bogaard and Schmincke 1985; Turney et al. 2006; Figure 2.8). The horizon possesses a distinctive phonolitic chemistry, that contrasts markedly with other Northern European volcanic systems. It is therefore an important marker horizon for testing the synchronicity of climate and environmental transitions at the end of the Lateglacial Interstadial. Recent work by Lane et al. (2012) and Housley et al. (2013), however, suggests that there may have been a precursor event to the LST with a similar chemical signature to one of the known LST phases; this may make tephrostratigraphic correlations more tentative in future studies. A second tephra is also known from the Eifel district during the course of the LGIT, but is markedly less useful as an isochron, being substantially more spatially constrained than the LST. The eruption is dated to 11,400-10,907 cal. yrs BP and produced the Ulmener Maar Tephra (UMT) (Zolitschka et al. 1995; Bronk Ramsey et al. 2015b).

Table 2.5 Tephras erupted from the Eifel district during the LGIT, ages from Bronk Ramsey et al (2015b).

Source	Eruption	Age μ ± σ (cal. yrs BP)	Reference
Ulmener Maar	Ulmener Maar Tephra (UMT)	11,096 ± 117	Zolitschka et al. 1995
Laacher See	Laacher See Tephra (LST)	12,937 ± 23	van den Bogaard and Schmincke 1985

2.5.5 Italian volcanic region

The 'Italian' volcanic region consists of a number of volcanic districts, including the: Tuscan province, Roman Province, Campanian Province, and the Aeolian and Sicilian Districts (Wulf et al. 2004). Whilst a major contributor to the Mediterranean tephrostratigraphy, eruptions from these Italian zones are typically distributed eastwards and rarely northwards. As a result it is uncommon to find Italian tephras of any extent in NW Europe. There are exceptions, however, and these eruptions have principally stemmed from the Campanian Province or Campanian Volcanic Zone (CVZ). The CVZ was particularly active during the LGIT and several tephra layers of a trachyte to phonolite composition are known have been generated through this period (Wulf et al. 2004). Amongst the largest is the Neapolitan Yellow Tuff (NYT; 14,588-13,884 cal. yrs BP; Bronk Ramsey et al. 2015b), a product of a caldera forming eruption at Phlegraean Fields (Lane et al. 2015). The NYT can be distinguished from

other horizons generated in this district, by the tephra's bi-modal composition and its straddling of the phono-trachyte boundary (Tomlinson et al. 2012b; Lane et al. 2015). The tephra has recently been identified within the varved sequence at Meerfelder Maar in Germany (Figure 2.8); a significant find which greatly expands the distribution of this tephra, but also provides a tephrostratigraphic link between northern and southern Europe.

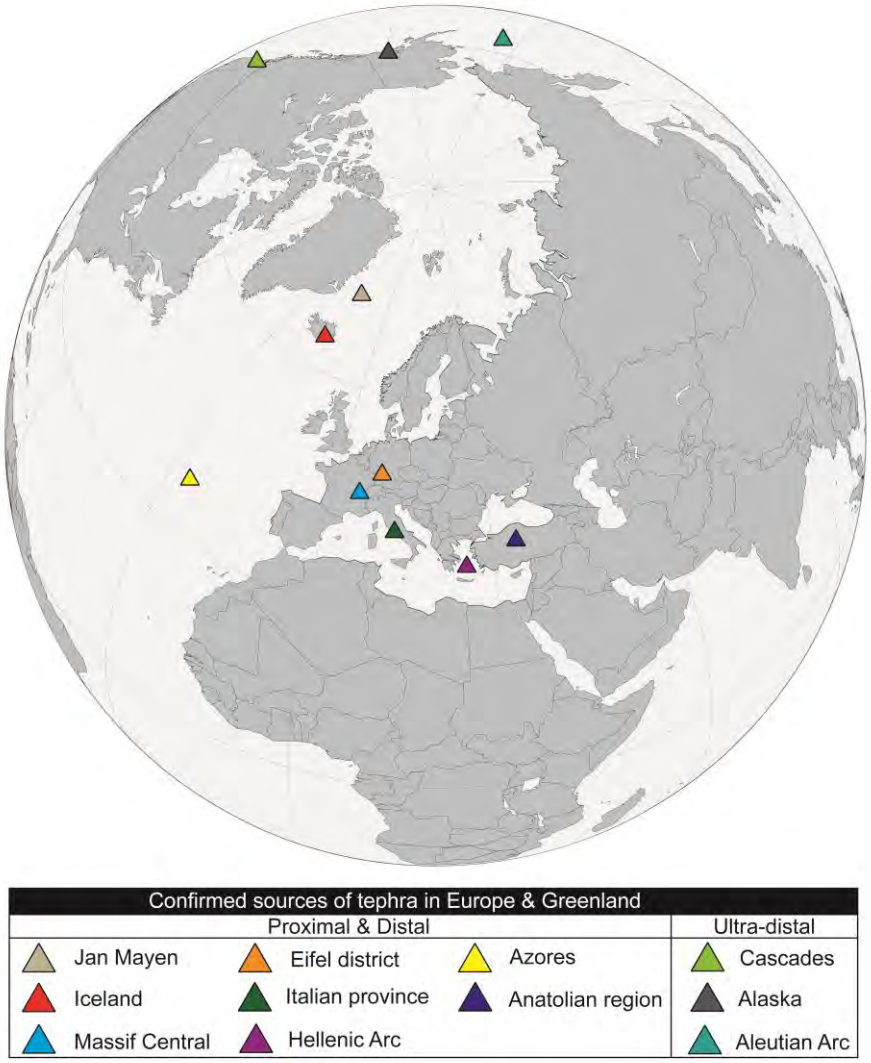

Figure 2.9 Proximal, distal and ultra-distal volcanic regions that have distributed tephra over Europe and Greenland during the Late Pleistocene and Holocene. For NW Europe during the LGIT, Iceland, the Massif Central and the Eifel district are of most importance.

2.5.6 Additional provinces

Outside the temporal remit of this study it is worth noting that several other provinces have distributed ash over the British Isles (Figure 2.9). In the late Holocene (<3000 cal. yrs BP) a number of layers with trachytic compositions have been identified within peat sequences in Ireland (Hall and Pilcher 2002; Chambers et al. 2004; Hall and Mauquoy 2005; Reilly 2006). The source region for these tephra was originally suggested as Jan

Mayen, an isolated volcanic island in the Greenland Sea (Lacasse and Garbe-Schönberg 2001; Chambers et al. 2004). However, more recently Johansson et al. (2016) have argued that the more likely source of these tephras is that of the Azores, a chain of islands situated on the mid-Atlantic ridge (Moore 1990; Cole et al. 1995; Reilly and Mitchell 2014).

Other notable tephra discoveries in the British Isles include the White River Ash from the Bona-Churchill massif, Alaska (Jensen et al. 2014). This has particular significance for distal-tephra studies, illustrating that it is possible to successfully identify shards which have travelled more than 7000 km from source, and is made perhaps even more significant by the relatively moderate sized eruption that produced the ash layer. Such ultra-distal tephras as they have been termed are currently best represented on the very fringes of NW Europe. Marine records from the Greenland Sea, Greenland Ice core records and archaeological sites from Greenland's western coastline have yielded tephras from the Aleutians, Cascades and a series of tephras as yet uncorrelated to centres in the Pacific (Jennings et al. 2014; Bourne et al. 2015; Blockley et al. 2015). Hitherto, ultra-distal tephras have yet to be identified in deposits of LGIT age in Europe, however, the possibility of this occurring should not be overlooked when making correlations.

2.6 Development of distal-tephra studies in the British Isles and NW Europe: an overview

Following Sigurður Þórarinsson's (1944) pioneering work in Iceland and his suggestion that tephras may be traced to the distal environment, several workers from the 1950s onwards began to pursue this goal. Studies were initially focused on visible and non-visible deposits within Scandinavian peat bogs e.g. Persson (1971), with the discipline later evolving into the marine realm, and terrestrial lacustrine sequences e.g. Ruddiman and Glover (1972); Sigurdsson (1982); Mangerud et al. (1984); Kvamme et al. (1989). By the late 1980s several Icelandic macrotephra layers had been found within the marine setting e.g. Kvamme et al. (1989), and two separate visible horizons of LGIT age had been identified within terrestrial lacustrine sediments: the Vedde Ash in Norway (Mangerud et al. 1984; *inter alia*), and the Saksunarvatn Ash in the Faroe Islands (Mangerud et al. 1986; *inter alia*). At the same time, work in France and Germany had begun to trace eruptions from the Chaine des Puys and the Eifel to the distal environment (e.g. Juvigne 1982; van den Bogaard and Schmincke 1985).

For the British Isles, Persson (1971) had remarked that there was potential to trace Icelandic tephras beyond the Nordic countries and noted that the Shetland Isles and Scotland in particular would be good candidates to investigate. The first evidence of an Icelandic tephra in proximity to the British Isles came from Long et al. (1986), and Long and Morten (1987) who identified the Vedde Ash within Younger Dryas aged sediments on the continental shelf around Scotland. This discovery was soon complemented by the identification of a Hekla cryptotephra layer in Holocene sediments from Caithness, Scotland (Dugmore 1989). Dugmore's discovery facilitated a rapid expansion in both the number of tephra studies, and consequently the number of tephra layers identified within the British Isles, factors encouraged by the possibility of at least 12 eruptions that were thought to have dispersed ash away from Iceland during the Holocene (Dugmore 1989). The majority of these studies were focused on organic sequences within the British Isles (e.g. Dugmore and Newton 1992; Pilcher and Hall 1992; Blackford et al. 1992; Hall et al. 1993; Dugmore et al. 1995, 1996 *inter alia*), although notable tephra studies also took place across NW Europe (e.g. van den Bogaard et al. 1994). For terrestrial records of LGIT age, this early surge in cryptotephra studies yielded very little in terms of sites or horizons. Only four studies reported the occurrence of an Icelandic tephra from the period. The Saksunarvatn Ash was discovered in Shetland, northern Germany, Orkney and western Norway (Bennett et al. 1992; Merkt et al. 1993; Bunting 1994, and Birks et al. 1996). Elsewhere in Europe the Laacher See's distribution was being mapped to areas outside of Germany (e.g. Juvigne et al. 1995).

By 1997 just three LGIT aged tephras were known to be found distally in NW European terrestrial records: the Laacher See Tephra, the Vedde Ash, and the Saksunarvatn Ash, with only the latter two having any distribution across the British Isles (Figure 2.10). This relative paucity of tephras in LGIT sequences compared to mid-late Holocene records (e.g. Dugmore et al. 1995; Pilcher and Hall 1996; Pilcher et al. 1996) was likely related to glass extraction methodologies, as the 'ashing' or chemical digestion techniques utilised to separate cryptotephras from organic sediments proved ineffective at extracting cryptotephras held within minerogenic substrates (see section 2.4.2). An important innovation came with the adoption of the density separation technique (Eden et al. 1992; Lowe and Turney 1997; Turney et al. 1997; Turney 1998a,b; Figure 2.10). Turney's work at Borrobol, Scotland yielded two cryptotephras within highly minerogenic substrates; the well-established Vedde Ash, and a tephra at that time which was unique to the study site, the Borrobol Tephra (Turney et al. 1997). This identification of a previously undocumented ash layer in LGIT deposits led to an increase in the frequency studies in Britain and Europe, and within a few years a more

detailed picture of Late Pleistocene volcanism had begun to emerge (Figure 2.10). At the same time new tephras were being identified across Europe, exciting new work in Greenland began to identify ash layers within the GRIP and GISP2 ice core records, including the established Vedde and Saksunarvatn Ashes, but also tantalising previously unrecognised basaltic and silicic horizons (Grönvold et al. 1995; Zielinski et al. 1997).

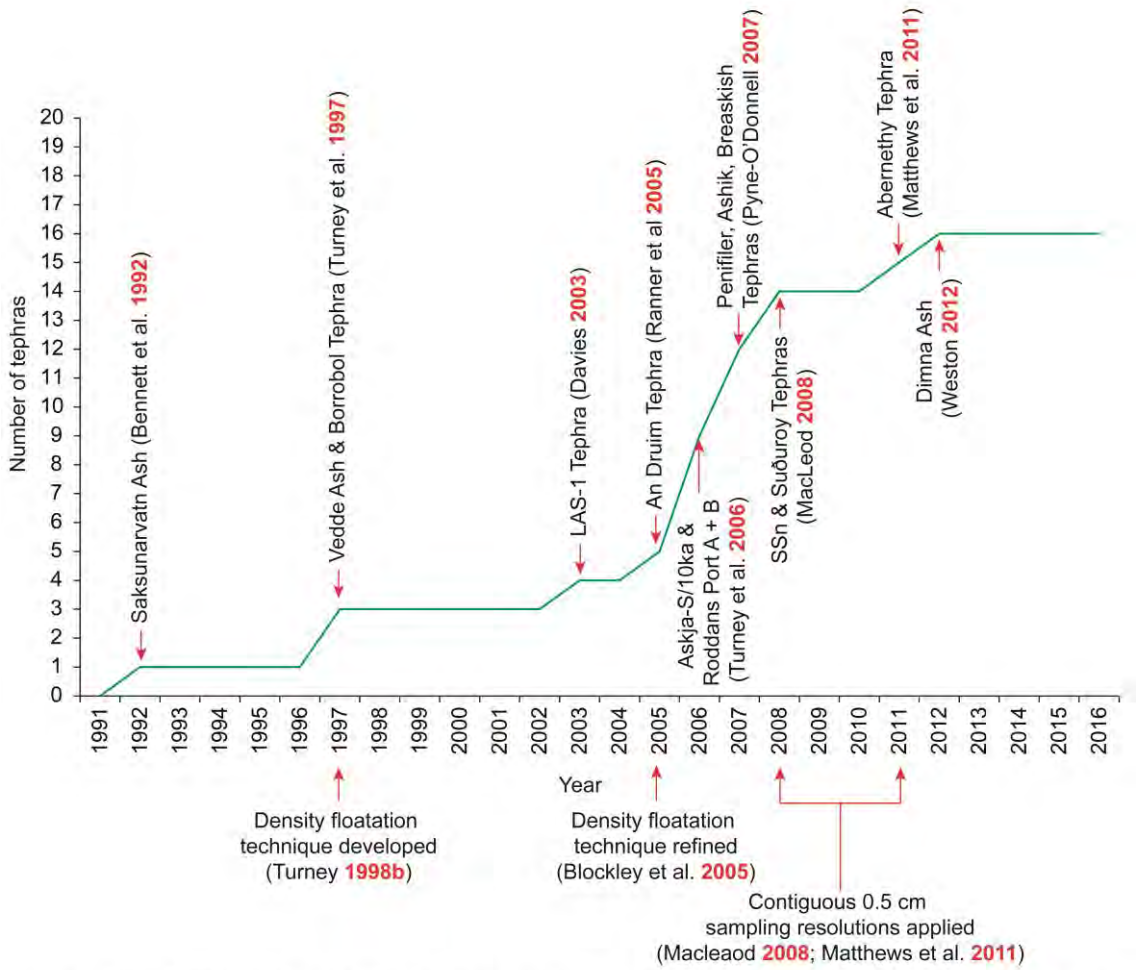

Figure 2.10 LGIT aged tephra discoveries in the British Isles. Large increases in the number of tephras can be seen to coincide with modifications to extraction and sampling techniques.

In the late 1990s Haflidason et al. (2000) conducted an extensive review of tephrostratigraphic studies in NW Europe, and concluded that over 100 tephra layers had been deposited within sedimentary sequences of the last 15,000 years. It was subsequently shown that this number was a significant underestimate of the true number of erupted events. Successive studies concerning the frequency of Icelandic eruptions have highlighted that, in the historical period alone (last 1100 years), more than 200 eruptions from active centres have occurred (Thordarson and Larsen 2007; Larsen and Eiríksson 2008; 2013). For the pre-historic period, the number is inherently more difficult to ascertain due to the poor preservation potential in the proximal

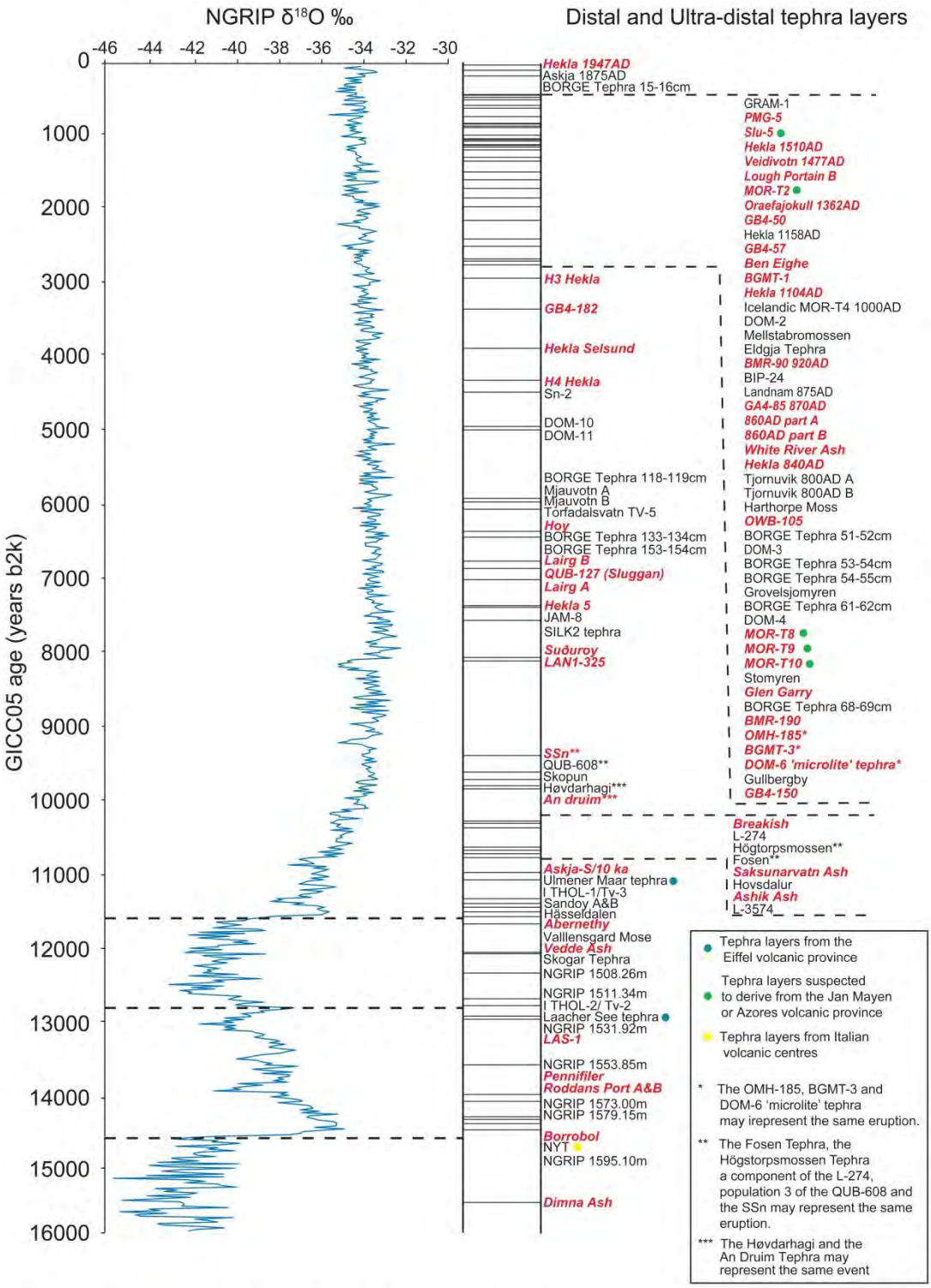

Figure 2.11 A synthesis of distal tephra layers identified across northwest Europe over the last 16,000 cal. yrs BP, plotted against the NGRIP Oxygen isotope signal and the GICC05 ice core chronology (Rasmussen et al. 2006). In total, 114 layers have been detected in terrestrial and Ice core sequences: 105 from Iceland, 2 from the Eifel province, 1 from Italian centres, 5 from the Jan Mayen or Azores province, and 1 Ultra-distal from Alaska (White River Ash). A total of 56 ash layers have been detected in the British Isles, these are represented in red bold italics. The Sluggan tephras are excluded from this figure due to their local geological origin (MacLeod and Davies 2016). Figure modified from Matthews (2008).

environment, although Óladóttir et al. (2005) suggest that Katla alone may have produced over 172 basaltic and 10 silicic layers during the last 8400 years. If the eruptive frequency of other centres in Iceland is comparable, then there is the potential for many hundreds of eruptions to be identified within proximal and distal records. It is likely however, that, whilst eruption frequencies may have been high, the magnitude and hence transport capabilities were not sufficient to distribute all of these tephras to the distal environment. Nonetheless this possibility of repeated volcanic events from the same system at relatively close intervals does raise an important issue relating to stratigraphic and geochemical discrimination, a problem that has become more prominent in recent years and one that is discussed further in section 2.8.2.

A total of 114 tephras are now identified in the distal environment across Europe and Greenland during the last 16,000 kyrs, with 61 of those characterising LGIT deposits (Figure 2.11). For the British Isles in particular, 57 tephra horizons have been identified in the last 16,000 kyrs, with 16 tephras occurring through LGIT (ca. 16-8 kyrs).

2.7 Tephra lattices and frameworks

With the rapidity of developments that took place in Europe during the 1990s and early 2000s it quickly became apparent that a formalised stratigraphy was required to order and delimit the increasing number of layers, and to ensure that the isochronous potential of each marker horizon was fully utilised. Whilst in theory tephras could offer time parallel marker horizons between sites, in reality a large proportion of the tephras identified across NW Europe during this time were spatially limited, poorly defined and lacked chronological certainty (Lowe et al. 2001; Turney et al. 2004; Lawson et al. 2012). Lowe et al. (2001) and Turney et al. (2004) *inter alia* noted the possibilities of tephrochronology in assisting palaeoenvironmental questions if they could be fully integrated within the wider palaeoclimate community. The resulting INTIMATE initiative spearheaded the use of tephra in NW Europe as a means to constrain abrupt climatic oscillations of the LGIT and further spawned a number of other projects with similar objectives (Davies 2015; Lowe et al. 2015) for example:

RESET: Response of Humans to Abrupt Environmental Transitions
TRACE: Tephra Constraints on Rapid Climatic Events
SMART: Synchronising Marine and Ice-core Records using Tephrochronology

The shared aim of these projects was the construction of tephra ‘frameworks’ or ‘lattices’ i.e. a network of sites interlinked by common tephras. The schematic of the

RESET tephra lattice in Figure 2.12 illustrates that frameworks are principally composed of a number of sites linked, firstly, at the local 'sub-cell' level by locally important tephras, and then in turn to regional cells by more ubiquitous 'key' tephra horizons (Figure 2.12). The term 'key' tephra or 'key marker horizon' had existed in the literature long before the advent of tephra frameworks, and can be used to describe those tephras with: 1) the most widespread distributions; 2) the most secure stratigraphic relationship; and 3) the most reliable ages (Dugmore and Newton 2012; Lowe et al. 2015). In the context of Figure 2.12, key tephras include the Vedde Ash, and Campanian Ignimbrite (Lowe et al. 2015).

The purpose of these tephra frameworks are to further refine the isochronous potential of tephra horizons, and to use the improved ages to address key challenges of the palaeoclimate community. Such challenges include: 1) to improve the precision by which past climatic/environmental changes can be reconstructed; 2) to improve the accuracy by which the inferred environmental changes can be dated; and 3) to provide well constrained and quantifiable palaeoclimate data to the modelling community (Lowe et al. 2001). A main argument and goal of INTIMATE has been the necessity to test the spatial and temporal synchroneity of climate events through independent chronologies, rather than assume synchroneity by aligning records to a regional chronology (e.g. Bjorck et al. 1998; Lowe et al. 2001; Turney et al. 2004; Chapter 1). As a consequence tephra lattices must therefore contain the following: 1) sequences of tephras ubiquitous or frequent across a study region; 2) horizons which can be reliably correlated based on distinctive chemical characteristics; 3) tephras which are positioned at key stratigraphic/ climato-stratigraphic intervals and boundaries; and 4) tephras which have quantifiable ages associated with them, or which have the capacity to be quantified (Lowe et al. 2015; Timms et al. 2016). Providing these criteria are met, then tephra lattices offer an opportunity to test the asynchronous nature of abrupt climate change with a greater degree of chronological control and finesse than has previously been achievable (e.g. Lane et al. 2012a; 2013; Lowe et al. 2012; 2015; Barton et al. 2015; Bronk Ramsey et al. 2015b).

In addition to testing palaeoenvironmental questions, tephra lattices have further facilitated a greater 'tephra connectivity' between regions. A good example comes from Lane et al. (2011) in their study of Lake Bled (Figure 2.12). Prior to the discovery of the Italian Pomici Principali and the Icelandic Vedde Ash within the record, these tephras possessed an uncertain stratigraphical and chronological relationship. Both had been identified mid-way through the Younger Dryas, but had never recognised in the same sequence. In Lake Bled these tephras were found to be stratigraphically

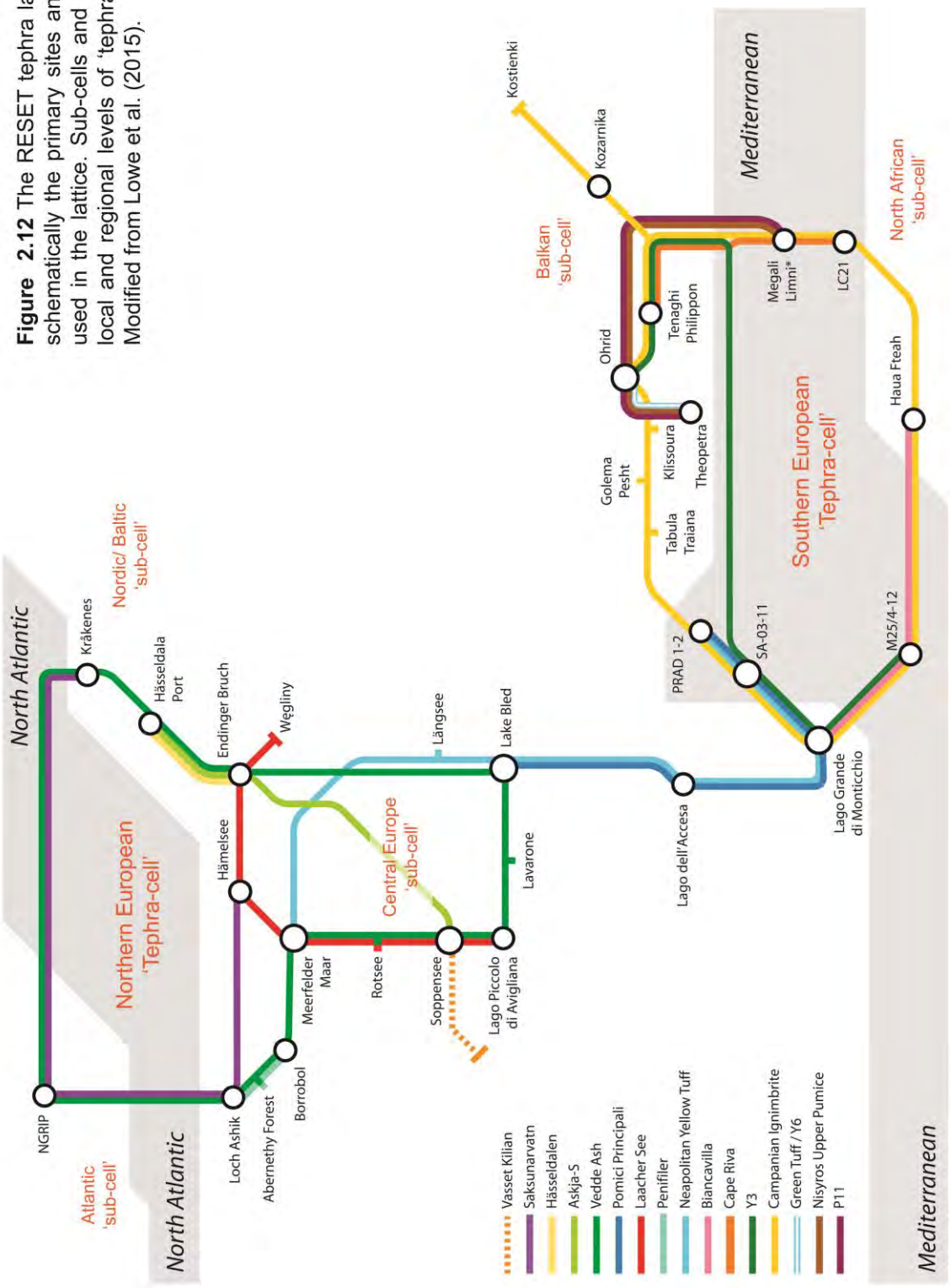

Figure 2.12 The RESET tephra lattice, showing schematically the primary sites and key tephras used in the lattice. Sub-cells and Cells illustrate local and regional levels of 'tephra-connectivity'. Modified from Lowe et al. (2015).

distinct, with the Vedde Ash being deposited just prior to the Pomici Principali (Lane et al. 2011a). The significance of this finding means that all sequences containing the Pomici Principali can now be confidently aligned to any climate archive that contains the Vedde Ash, including the Greenland ice core records (Lowe et al. 2015). More recently the discovery of the Italian Neapolitan Yellow Tuff in Meerfelder Maar Germany has also significantly widened the scope of linking southern and northern European tephra cells (Lane et al. 2015; Lowe et al. 2015; Figure 2.12).

At present, however, Lake Bled and Meerfelder Maar are two relatively rare sites in Europe, in that they are able to link the northern and southern Europe tephra cells within the wider European lattice (Lowe et al. 2015; Figure 2.12). This notion of 'key sites' and 'key marker horizons' is an important concept, and one which currently limits the application of tephra frameworks in Europe and elsewhere. This theme is considered below, but it is evident that there is an emerging hierarchy in Europe, both in terms of the 'usefulness' of individual tephra horizons, and the 'role' of the sites in which they are found.

2.8 Distal-tephrochronological challenges in NW Europe

2.8.1 Tephra usefulness, spatial disparity, and tephra site hierarchies

Figure 2.13 and Table 2.6 summarises the total number of tephras that are found across the Northern European Tephra-cell (Figure 2.12) and ranks them based on their frequency of occurrence (it should be noted that not all of these are illustrated in Figure 2.12). The top nine tephras in the list can be regarded as key marker horizons due to their wide distributions and well constrained age. However, both the Penifiler and Borrobol possess matching major elemental signatures which can cause problems for stratigraphic discrimination (see section 2.8.2). Therefore only the top seven tephras (excluding the Penifiler) in Table 2.6 can be considered reliable isochrons and 'key' marker horizons in NW Europe during the LGIT. The fifty-seven other tephra horizons either possess a much more limited distribution, or, in the case of forty of these tephras (ca. 63%), have only been identified at single site. Whilst this is a significant revelation, perhaps more significant statistic is that ca. 81% of those tephras cannot be used to make country to country linkages (Figure 2.13). The exact reasoning behind this spatial disparity and lack of 'connectivity' is unclear, but may relate to a whole host of parameters involving the transport and delivery of shards, the preservation potential of the depositional environment, and the way in which tephrostratigraphic sequences have been resolved (see sections 2.4.1-2.4.2).

Table 2.6 Frequency of tephra horizons preserved in NW European terrestrial and Ice Core records during the LGIT.

Tephra	Total number of sites	Tephra	Total number of sites
Laacher See	603+	1-THOL-1 /Tv-3	1
Vedde	121+	Sandoy B	1
Saksunarvatn	40+	Sandoy A	1
NYT	23+	NGRIP 1508.26m	1
Askja-S/10ka	20	NGRIP 1511.34m	1
Penifiler Tephra	16	1-THOL-2/ Tv-1	1
Hässeldalen	13	LAS-1	1
Borrobol Tephra	12	Vallensgård Mose	1
Ulmener Maar	9	Roddans Port A	1
T4 Godivelle	6	NGRIP 1531.92m	1
Puy de la Nugère	6	NGRIP 1553.85m	1
T5 Godivelle	5	Roddans Port B	1
Suðuroy	4	NGRIP 1573.00m	1
Ashik	4	NGRIP 1595.1m	1
Chopine (Taphanel)	4	NGRIP 1619.58m	1
La Moutade Tephra	3	NGRIP 1628.25	1
Les Roches Tephra	3	La Vache-Lassolas	1
Abernethy	2	Pariou	1
Vasset-Killian	2	Puy de Dome	1
Dimna Ash	2	NGRIP 1579.15m	1
SSn (Svinavatn)	2	GISP2 1586.49	1
An Druim	2	GISP2 1586.76	1
Fosen	2	QUB 608	1
QUB 606	1	LAN1-325	1
GRIP 1465.58m	1	SSB 534-512	1
Breakish	1	Tøvelde-198	1
Høvdarhagi	1	T573	1
Skopun	1	HBG_T1414	1
L-274	1	T1130	1
Högtorpsmossen	1	T1137	1
Hovsdalur	1	WE T642/655	1
L-3574	1	WE T727	1

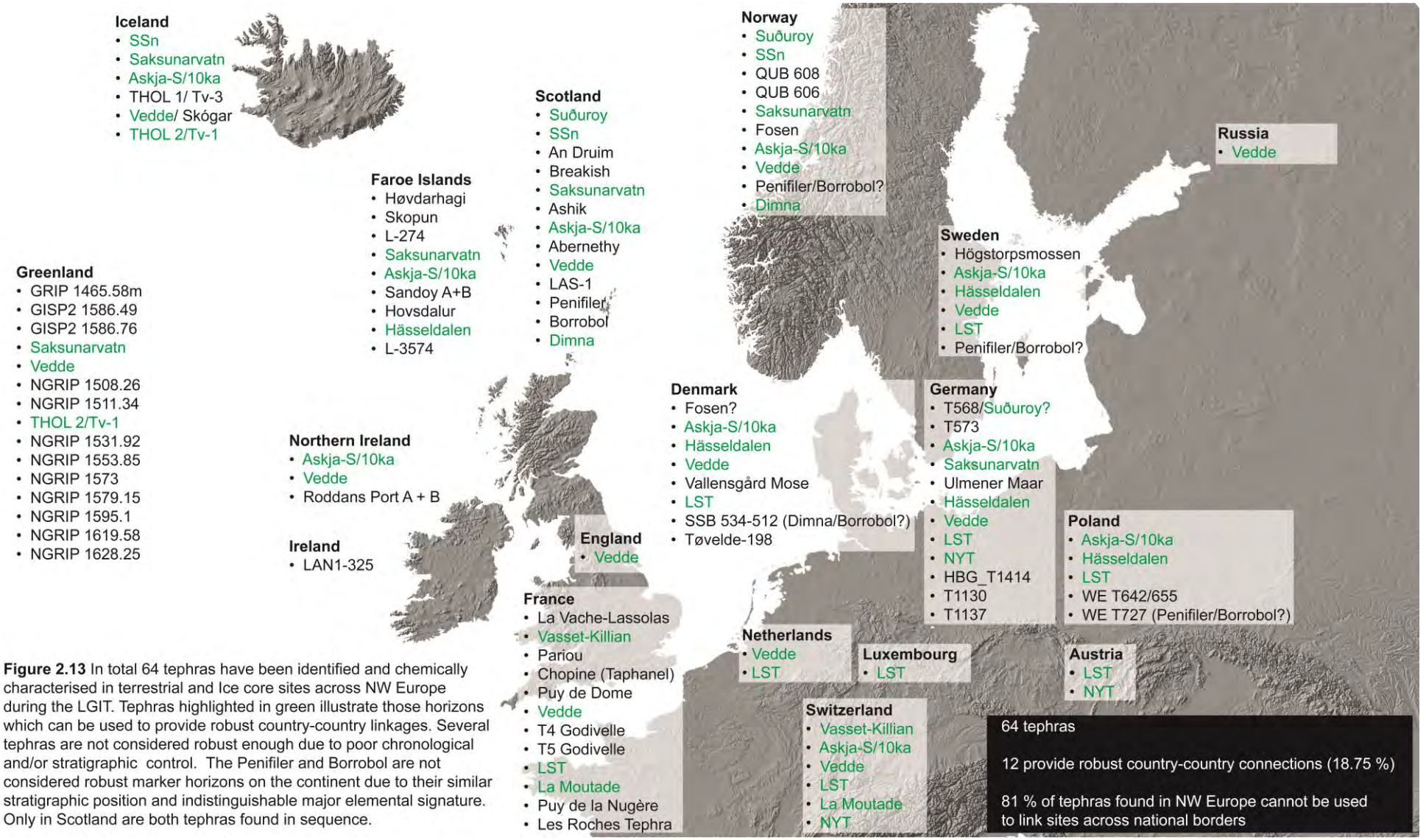

Figure 2.13 In total 64 tephras have been identified and chemically characterised in terrestrial and Ice core sites across NW Europe during the LGIT. Tephras highlighted in green illustrate those horizons which can be used to provide robust country-country linkages. Several tephras are not considered robust enough due to poor chronological and/or stratigraphic control. The Penifiler and Borrobol are not considered robust marker horizons on the continent due to their similar stratigraphic position and indistinguishable major elemental signature. Only in Scotland are both tephras found in sequence.

What is evident in Figure 2.13 and Table 2.6 is that the tephras which have the greatest frequency of occurrence, and hence those that make the key branches within NW European lattices, are those tephras which have been known for longest i.e. the Laacher See Tephra, the Vedde Ash, and the Saksunarvatn Ash. The cause of this is likely two-fold: firstly these eruptions are amongst the largest events that are known to have occurred during the late Pleistocene, and are thus some of the few examples that can be identified without the need of specialist separation equipment (e.g. Mangerud et al. 1984; Mangerud et al. 1986; Bennett et al. 1992; Bunting et al. 1994 van den Bogaard 1995). Secondly, and as a consequence of the first point, these tephras have been known about for at least 3 decades; studies have therefore undertaken selective analysis in order to trace them (e.g. Wastegård 2000a; Bramham-Law et al. 2013). This means their representation within the tephra framework is over emphasised in relation to other, more 'minor' horizons. Given the recent work following the contemporary eruptions of Eyjafjöll and Grímsvötn in Iceland (Davies et al. 2010; Stevenson et al. 2012; 2013), it is evident that even relatively small-moderate sized eruptions can have much greater dispersal radii than has previously been recognised in the palaeo-tephra record. It is fair to state therefore, that the 'key marker horizons' such as the Vedde etc. are in part only considered 'key' as a consequence of their selective study within palaeoclimate and tephrostratigraphic records. It is this notion of selective sampling and targeted tephra studies which may have contributed to the apparent disparity in tephrostratigraphic records across NW Europe. Recent work from MacLeod et al. (2015) has demonstrated that the number of tephras identified and characterised in some sites and especially those that were the focus of early studies may be under-estimated (e.g. Turney et al. 1997; Lowe et al. 2008b). This is probably partly because of the incomplete tephrostratigraphic refinement of early studies and the overall inconsistent manner in which tephrostratigraphic studies have been conducted.

At present therefore most tephras identified across Europe when viewed from a regional 'connectivity' perspective have limited 'usefulness'; this phenomenon can be described as the ***primary tephra hierarchy*** in NW Europe. Alongside this, a ***secondary tephra hierarchy*** has started to emerge, and one which relates to the role each tephra site has within a lattice. Typically tephra records fit into one of three roles: 1) ***linking sites*** that contain tephras derived from multiple centres, and which are able to link differing tephra cells together e.g. Lake Bled and Meerfelder Maar (Lane et al 2011b; 2015); 2) ***chronological reference sites*** that provide a high level of dating precision to specific horizons, which can then be transferred to the rest of the lattice e.g. NRGIP (Mortensen et al. 2005), Kråkenes, Norway (Lohne et al. 2013) or; 3) ***palaeoclimatic sites*** which possess key climatic information at geographically

important locations e.g. Loch Ashik, Scotland (Brooks et al. 2012). In some rare circumstances sites may exist which incorporate elements from all three e.g. Meerfelder Maar, Germany (Lane et al. 2015), Soppensee, Switzerland (Hajdas 1993; Lane et al. 2012c), and Grande di Monticchio, Italy (Wulf et al. 2004; 2008; 2012).

Whilst the emergence of tephra and tephra-site hierarchies should not be viewed as a negative development, more can be done to minimise the disparity between records. Part of this problem relates to the way in which sequences are resolved and the over-emphasis placed on certain 'key' horizons. However, such an objective will only be achievable with more thorough and more methodical approaches to tephrostratigraphic refinement than is currently undertaken as the norm (see section 2.4.1).

2.8.2 Repeating chemical signatures and tephrostratigraphic superposition

Another increasing problem in European tephrostratigraphic sequences is the issue of repeating chemical signatures. It has been demonstrated that a number of tephras erupted from the same volcanic system during the LGIT possess indistinguishable major and trace element compositions (e.g. Pyne-O'Donnell et al. 2008; Lane et al. 2012b; Tomlinson et al. 2012a; Lind and Wastegård 2011; Lind et al. 2013; 2016 Table 2.7). One of the main challenges now facing researchers is being able to reliably differentiate between eruptions produced from the same system. Whilst independent age control can assist, this approach is not always viable, and errors associated with age control may be greater than the age range between potential candidates, i.e. the Borrobol and Penifiler Tephras (Table 2.7). This has meant that the stratigraphic superposition of tephras, i.e. the consecutive ordering of horizons, is becoming more intrinsic to the process of correlation, yet this remains an issue of contention in NW Europe.

Without a competent record of tephra superposition, studies must consider other lines of stratigraphic evidence (e.g. lithostratigraphical: Pyne-O'Donnell 2007; biostratigraphical: Kelly et al. 2016; or archaeological information: Mithen et al. 2015) before making tephrostratigraphic correlations. The Scottish lateglacial is one key example where a relatively ubiquitous lithostratigraphy, i.e. the 'tripartite' sequence, can be used as a temporal guide (Lowe and Walker 2015, p. 156; see Chapter 1), and has been used to distinguish the Penifiler Tephra from the Borrobol Tephra at several sites in Scotland (e.g. Pyne-O'Donnell 2007; Pyne-O'Donnell et al. 2008). However, whilst the tripartite sequence may be considered diagnostic in Scotland, the lithostratigraphical representation of the same period within the rest of the British Isles can be markedly different (e.g. Palmer et al. 2015). The use of external stratigraphic

information in tephra correlations also creates a scenario of circular reasoning, whereby the stratigraphic inference is used to correlate a tephra, with that tephra then being used to date the sequence. Tephra correlations must therefore be principally guided by an absolute chronology (if possible), geochemical characteristics, and tephrostratigraphic superposition, and only litho-, biostratigraphical or archaeological information as a last, tentative resort. Where any such guides are absent from a record, studies that exhibit one or more of the tephras as shown in Table 2.7 may be left with a 'floating' tephrostratigraphy, i.e. one that cannot be firmly anchored in time (e.g. Mithen et al. 2015; Housley et al. 2015).

Table 2.7 Tephras which possess indistinguishable major trace elemental signatures. In the case of the Katla tephras these are also indistinguishable based on trace elemental analyses. The Borrobol-type tephras all exhibit a chemical signature that has yet been traced to a source region. The SSn and the QUB have been tentatively correlated to Snæfellsjökull, but for the other tephras in the group Snæfellsjökull, Torfajökull, Hekla, and Öræfajökull have all been refuted as potential candidates (Lind et al. 2013).

Tephra	Age	Composition	Reference
Torfajökull			
An Druim	9671-9490 cal. yrs BP	Rhyolitic	Ranner et al. 2005
Høvdarhagi	9850-9600 cal. yrs BP	Rhyolitic	Lind and Wastegård 2011
Ashik	10,400 ± 300 cal. yrs BP	Basaltic/ Rhyolitic	Pyne-O'Donnell 2007
Snæfellsjökull			
Hovsdalur	10,695-10,285 cal. yrs BP	Rhyolitic	Wastegård 2002
Hässeldalen	11,543-11,232 cal. yrs BP	Rhyolitic	Davies et al. 2003
Katla			
Suðuroy	8070 ± 90 cal. yrs BP	Rhyolitic	Wastegård 2002
Abernethy (AF555)	11,721-10,716 cal. yrs BP	Rhyolitic	Matthews et al. 2011
Vedde	12,102-11,914 cal. yrs BP	Basaltic/ Intermediate/ Rhyolitic	Mangerud et al. 1984; Lane et al. 2012b
Dimna Ash	15,400-14,850 cal. yrs BP	Rhyolitic	Koren et al. 2008
Snæfellsjökull/Unknown (Borrobol-type tephras)			
SSn (Svinavatn)	9450 ± 50 cal. yrs BP	Rhyolitic	Boygle 1999
QUB 606	ca. 9500 cal. yrs BP	Rhyolitic	Pilcher et al. 2005
Fosen	ca. 10,200 cal. yrs BP	Rhyolitic	Lind et al. 2013
L-274	10,325-10,125 cal. yrs BP	Rhyolitic	Lind and Wastegård 2011
Högtorpsmossen	10,556-9931 yr cal. yrs BP	Rhyolitic	Björck and Wastegård 1999
Penifiler Tephra	14,063-13,808 cal. yrs BP	Basaltic/ Rhyolitic	Pyne-O'Donnell 2007
Borrobol Tephra	14,190-14,003 cal. yrs BP	Rhyolitic	Turney et al. 1997

It is worth noting, however, that part of this problem of repeating signatures may lie with the poor stratigraphical and chronological control that exists for certain horizons. Lind et al. (2013) highlight this issue with the Fosen Tephra, dated to ca. 10,200 cal. yrs BP, a horizon identified at Grønlia Fen in Norway. It was noted that the Fosen, a tephra 'unique' to the study site, possessed a chemical and stratigraphical similarity to five other tephras deposited during the early Holocene: the Högstorpsmossen ca. 10,200 cal. yrs BP (Björck and Wastegård 1999); a component of L-274, dated to ca. 10,200 cal. yrs BP (Lind and Wastegård 2011); population 3 of the QUB-608, dated to ca. 9500 cal. yrs BP (Pilcher et al. 2005); and the SSn, dated to ca. 7300 cal. yrs BP (Boygle 1999). Lind et al. (2013) highlight the strong possibility that these individual horizons may in fact be the same layer, but a more robust conclusion is prevented from being made by the poor age controls characterising the aforementioned tephras at their respective sites. A similar scenario is true for two other tephras in Table 2.7, the An Druim and Høvdarhagi tephras, both thought to be from the Torfajökull volcanic centre, and both possessing very similar age estimates (Ranner et al. 2005; Lind and Wastegård 2011; Kelly et al. 2016). Lind and Wastegård (2011) argue for their separation based on a bi-modal chemical characteristic that is absent from the An Druim tephra; however, given the spatial dynamics of ash clouds it is plausible that shards possessing a narrower chemical range were deposited in Scotland compared to a wider range being delivered to the Faroe Islands (Stevenson et al. 2012; 2013). This hypothesis remains equivocal without additional data, but it is possible that some complexity associated with the NW European tephrostratigraphic record may be reduced with a re-evaluation, and an amalgamation of tephra horizons if sufficient data arises to do so.

2.8.3 Taphonomy and resolution of refinement

One of the least understood factors concerning distal-tephrochronology is the way in which a tephra layer manifests within a sedimentological archive, and how this might change with time. Studies by Mangerud et al. 1984, Boygle (1999), Davies (2001), Pyne-O'Donnell (2011), and Bertrand et al. (2014) amongst others have all illustrated that tephra dispersal and accumulation is seldom homogenous in lacustrine environments and that the depositional foci of a lake may change with time (see section 2.3.3). This has inherent consequences for isochron placement, and for distinguishing between primary horizons, i.e. those that are derived directly from an eruption, and secondary horizons, i.e. those which are reworked (see section 2.3.4). A technique which has shown significant promise in this regard is X-ray microtomography (Griggs et al. 2014b), but as yet its application remains limited to macrotephra

horizons. Thus the principal recommendation from taphonomic studies is that multiple sequences should be examined to gain a reliable insight into isochron placement, a sentiment that has been reiterated by numerous studies from other depositional environments e.g. Dugmore and Newton (2012), Reide and Thastrup (2013), Griggs et al. (2014a), Streeter and Dugmore 2014, and Watson et al. (2015).

What Boygle (1999), Pyne-O'Donnell (2011), and Dugmore and Newton (2012) have also highlighted is that it is unlikely that any one archive, i.e. a single core from within a lake or a single lake/ depositional body, will exhibit the full range of tephras known to have been deposited within a region. Thus in order to fully understand the complete tephrostratigraphy of an area it could be argued that both a multi-core and a multi-site approach must be adopted. Following these recommendations, new sites with extensive multi-core surveys must be added to a regional tephrostratigraphy until it can be confidently claimed that no new tephras will be found by adding more profiles (Dugmore and Newton 2012).

What these studies have perhaps failed to consider is the amount of tephrostratigraphic information that can be gathered from individual cores if modifications to the standardised sampling and chemical characterisation procedures are made. Studies at Loch Laggan (MacLeod 2008) and Abernethy Forest (Matthews et al. 2011) have demonstrated that targeted and contiguous high resolution sampling, i.e. at 1cm or higher, can provide a more coherent, and more complex narrative to the history of volcanic events deposited during the Scottish Lateglacial and early Holocene than has been appreciated hitherto.

2.9 Chapter summary

This chapter has: 1) presented the fundamental principles behind tephrochronology; 2) introduced key methodological concepts of the discipline; and 3) outlined the major developments in the application of the technique in NW Europe. From this review it is evident that the development of distal-tephrochronology, and its application in NW European palaeoclimate sequences, has in no doubt been paradigm shifting. A wealth of knowledge regarding the asynchronous nature of palaeoclimatic transitions is beginning to emerge, with tephra firmly established as an invaluable contributor to this understanding. However, as with many techniques, a preliminary surge in interest driven by great promise and potential is eventually surpassed by a realisation that the technique or approach has a number of inherent limitations. The technique subsequently undergoes a second 'maturing' phase, whereby the realistic possibilities

of the technique are brought into focus. Distal-tephrochronology in the context of NW Europe is now entering into this latter phase; a number of limitations and caveats in the technique have been illustrated in the latter sections of this chapter, with such issues beginning to constrain what can be achieved following existing tephra methodologies. Some of the key concerns highlighted are: 1) issues of tephrostratigraphic disparity between neighbouring locales; 2) problems associated with geochemical distinguishment and repeatability of chemical signatures; 3) uncertainties with tephrostratigraphic superposition; and 4) queries over the number of tephras identified within sites, and the level of level of stratigraphic refinement needed to identify those.

Outlined in the ensuing Chapter are details on the tephrostratigraphic framework of the British Isles, and how the challenges identified in the latter sections of this Chapter relate specifically to this geographical region.

Chapter 3. Study Rationale and Site Locations

3.1 Introduction and chapter structure

The aim of this chapter is to provide a regional context for the rest of the thesis, and to introduce the selected study sites. The chapter is divided into three main sections with the following structure: 1) a brief overview of the British LGIT tephrostratigraphic framework with an emphasises of local intra-disparity of identified tephras; 2) an introduction of the study sites and a description of relevant background information, and; 3) a reiteration of the aims and objectives of the thesis.

3.2 The current LGIT tephrostratigraphic framework for the British Isles

In the British Isles, the current LGIT tephrostratigraphic framework is composed of sixteen tephra isochrons distributed across thirty-six individual sites Figure 3.1. In total forty-seven locations have been examined for tephras through this interval, although evidently not all of these have yielded tephra (e.g. Wastegård et al. 2000a), or have had their findings validated by geochemical characterisation (e.g. Williams et al. 2007). It is worth noting also, that a proportion of these sites fall into the category of 'grey-literature' e.g. unpublished dissertations, thus in many instances this work remains incomplete. A full list of sites and the tephras they exhibit are presented in Table 3.1.

Figure 3.1 (opposite) Distribution of the main LGIT age tephras across the British Isles. 34 sites are shown, although the total number of sites investigated is believed to be 47. Circle charts represent a palaeoenvironmental or archaeological site with each coloured segment representing a different tephra horizon and geochemically characterised. Question marks are placed in the centre of a coloured section where either uncertainty surrounds the tephra correlation or where the tephra correlation has been made purely by stratigraphic superposition. Question marks placed on boundaries between two coloured sections represent uncertainty in the correlation due to an overlapping major element signature and/or stratigraphic placement. **Dallican Water**: Bennett et al. (1992); **Loch of Benston**: Bondevik et al. (2005); **Quoyloo Meadow** & **Crudale Meadow**: Bunting (1994); **Lochan an Druim**: Ranner et al. (2005); **Borrobol**: Turney et al. (1997; Pyne-O'Donnell et al. (2008; Lind et al. (2016); **Summer Isles**: Roberts (1997); Wastegård et al. (2000); Weston (2012); Callicott (2013); **Druim Loch**: Pyne-O'Donnell (2007); Pyne-O'Donnell et al. (2008) Pyne-O'Donnell (2011); **Loch Ashik**: Davies et al. (2001); Pyne-O'Donnell (2007); Pyne-O'Donnell et al. (2008); Pyne-O'Donnell (2011); **Kennethmont**: Turney (1998); **Abernethy Forest**: Matthews et al. (2011); **Loch Etteridge**: Lowe et al. (2008b); MacLeod et al. (2015); **Loch Laggan** (MacLeod 2008); **Inverlair**: Kelly et al. (2016); **Glen Turret**: (**Bank**) MacLeod et al. (2015); **Mishnish** (Davies 2003); **Loch an t-Suidhe**: Roberts (1999); Davies (2003); Pyne-O'Donnell (2007); Pyne-O'Donnell et al. (2008); Pyne-O'Donnell (2011); **Pulpit Hill**: Lincoln (2011); **Tirinie**: Candy et al (2016); **Menteith:** Grosvesnor (2009); **Tynaspirit West**: Roberts (1997); Turney et al. (1997); Pyne-O'Donnell (2007); **Muir Park Reservoir**: Roberts (1997); Cooper (1999) Brooks et al. (2016); **Rubha Port an t-Seilich**: Mithen et al. (2015); **Howburn Farm**: Housley et al. (2015); **Whitrig Bog**: Turney (1998); Pyne-O'Donnell et al. (2008); **Halsenna Moor**: Lane (2004); **Flixton Island**: Darvill (2011); Palmer et al. (2015); **Gransmoor**: Wastegård et al. (2000a); **Llyn Gwernan**: Woodcock (2003); **Traeth Mawr**: Williams (2001); Woodcock (2003); Williams et al. (2007); **Lough Nadourcan**: Turney et al. 2006; **Roddans Port**: Turney et al. 2006; **Long Lough**: Turney et al. 2006; **Loughanascaddy Crannog**: Matthews (2008)

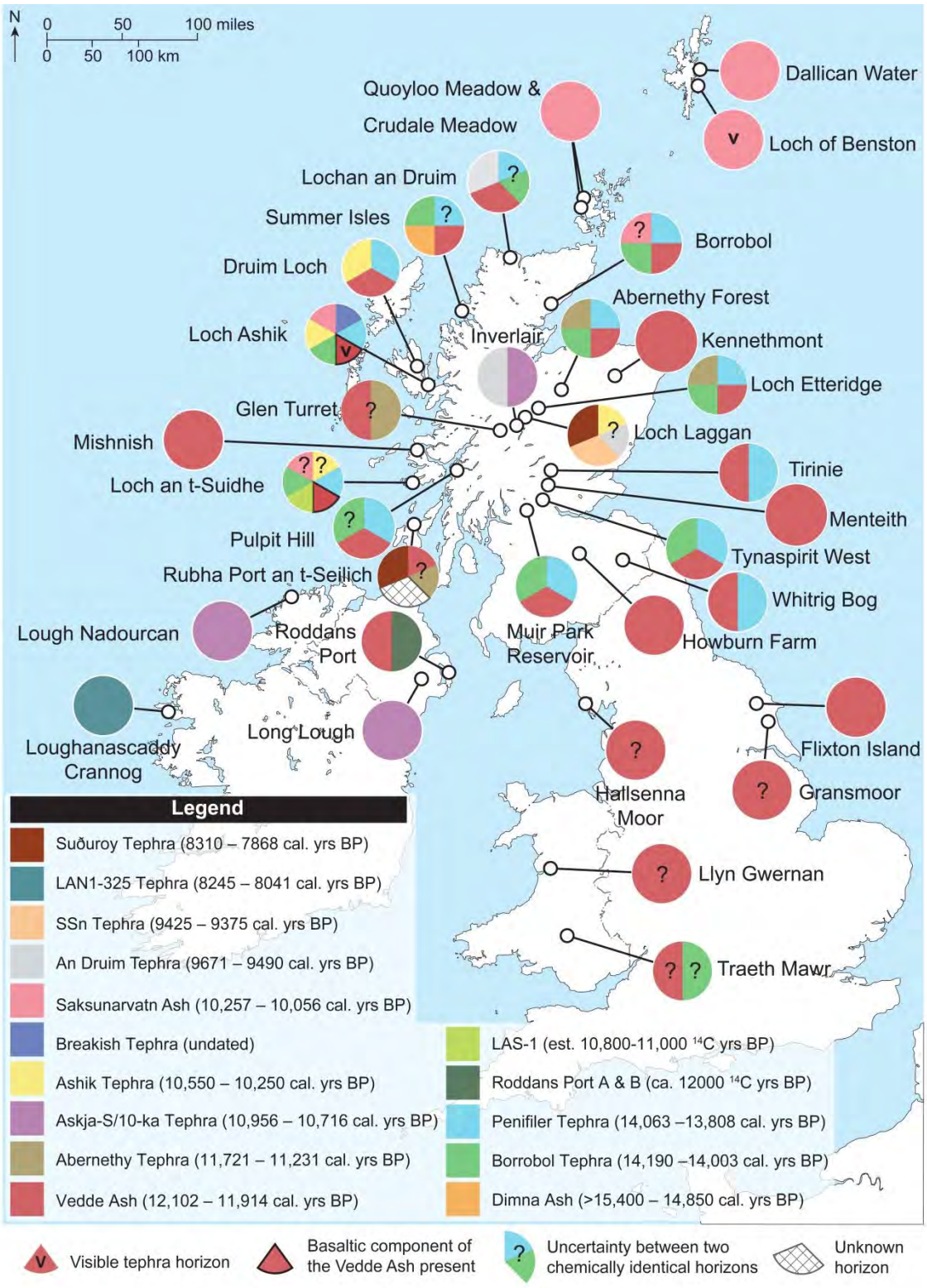

Figure 3.1 (caption opposite)

Table 3.1 LGIT aged tephra sites in the British Isles. In total 47 sites have been examined to date with 36 of those yielding tephras. At present sixteen tephra isochrones are recognised across the British Isles during the LGIT, but as many as 64 may characterise European ice and terrestrial records (see section 2.8).

Region	Site	Tephras	Latitude	Longitude	References
Scotland					
1	Dallican Water	Saksunarvatn	60.39167	-1.1	Bennett et al. 1992
2	Loch of Benston	Saksunarvatn (visible)	60.26451	-1.16278	Bondevik et al. 2005
3	Quoyloo Meadow	Saksunarvatn	59.06642	-3.30933	Bunting 1994
4	Crudale Meadow	Saksunarvatn	59.0159	-3.32853	Bunting 1994
5	Lochan An Druim	An Druim, Vedde, Borrobol/Penifiler	58.475	-4.685556	Ranner et al. 2005
6	Tanera Mor (TM2 97')	Vedde. Penifiler, Borrobol	58.0142	-5.41313	Roberts 1997; Wastegård et al. 2000a
7	Tanera Mor 2	Ashik?, Vedde, Penifiler, Borrobol, Dimna	58.00288	-5.40098	Weston 2012
8	Eilean Fada Mor	Three peaks of tephra - resemble 'Borrobol type', (no geochemistry)	58.01368	-5.4332	Callicott 2013
9	Borrobol	Saksunarvatn (no geochemistry) Vedde, Penifiler, Borrobol	58.15	-3.83333	Turney et al. 1997; Turney 1998a; Pyne O'Donnell 2007; Pyne O'Donnell et al. 2008; Lind et al. 2016
10	Druim Loch	Ashik, Vedde, Penifiler	57.38333	-6.16667	Dadswell 2002; Pyne O'Donnell 2004; Pyne O'Donnell 2007; Pyne O'Donnell et al. 2008
11	Loch Ashik	Breakish, Saksunarvatn, Ashik, Vedde (visible), Penifiler, Borrobol	57.23333	-5.81667	Davies et al 2001; Davies 2003; Matthews 2002; Pyne O'Donnell 2004; Pyne O'Donnell 2007; Pyne O'Donnell et al 2008; Pyne O'Donnell 2011; Brooks et al. 2012

12	Kennethmont	Vedde	57.3506	-2.76798	Roberts 1997; Turney 1998a; Wastegård et al. 2000a
13	Abernethy Forest	Looked for Saksunarvatn (not found), AF555, Vedde, Penifiler, Borrobol	57.23333	-3.7	Matthews et al. 2011
14	Loch Laggan East	Suðuroy, SSn, An Druim/Ashik?	56.97067	-4.41669	MacLeod 2008
15	Glen Turret Fan	AF555/Vedde? (no geochemistry)	56.99254	-4.72689	MacLeod et al. 2015
16	Mishnish	Vedde	56.61667	-6.13333	Davies 2003; Mackie et al. 2002
17	Loch Torr a'Beithe	ongoing	56.88874	-5.86417	Weston PhD data (ongoing)
18	Loch a'Beithe	ongoing	56.88874	-5.86417	Weston PhD data (ongoing)
19	Inverlair	An Druim/Ashik, Askja-S/10Ka	56.86468	-4.70945	Kelly 2010
20	Loch Etteridge	AF555?, Vedde, Penifiler, Borrobol	57.01009	-4.15819	Albert 2007; Hardiman 2007; Lowe et al. 2008b; MacLeod et al. 2015
22	Larig Mor 1	?	56.79784	-5.11453	Harding 2013
23	Larig Mor 2	?	56.76845	-5.11476	Harding 2013
24	Drumochter	?	56.84172	-4.24081	Harding 2013
25	Feagour Channel	?	56.98306	-4.35337	Harding 2013
26	Loch an t'Suidhe	Saksunarvatn? (no geochemistry), Ashik (no geochemistry), Vedde(b), LAS-1 (limited to two cores), Penifiler, Borrobol	56.31253	-6.25369	Roberts 1999; Davies 2003; Pyne O'Donnell 2004; Pyne O'Donnell 2007; Pyne O'Donnell et al. 2008; Pyne O'Donnell 2011
27	Pulpit Hill	Ashik?, AF555?, Vedde, Penifiler, Borrobol?	56.40562	-5.48374	Lincoln 2011
28	Tirinie	Vedde, Penifiler	56.78752	-3.81517	Candy et al. 2016
29	Tynaspirit West	Vedde, Penifiler, Borrobol	56.21667	-4.13333	Roberts 1997; Turney et al. 1997; Pyne O'Donnell 2007; Pyne O'Donnell et al. 2008
30	Lake of Menteith	Vedde	56.17272	-4.29358	Grosvenor 2009

31	Muir Park Reservior	Vedde, Penifiler, Borrobol	56.1	-4.41667	Roberts 1997; Cooper 1999; Lowe and Roberts 2003
32	Islay	No tephra found			Roberts 1997
33	Rubha Port an t-Seilich	Suðuroy, mixed horizon (Borrobol/Hasseldalen), basal Katla type (AF555, Vedde)	55.83122	-6.10468	Mithin et al. 2015
34	Whitrig Bog	Vedde, Penifiler, Borrobol	55.60715	-2.60281	Turney et al 1997; Pyne O'Donnell 2008
35	Howburn Farm	Vedde	55.67278	-3.48361	Housley et al. 2014; Tipping et al. 2016
England					
36	Haweswater	looked for Vedde = 0	54.18254	-2.80161	Wastegård et al. 2000a
37	St. Bees Head	looked for Vedde = 0, Dimlington Stadial tephra?	54.48781	-3.5989	Wastegård et al. 2000a; Lane 2004
38	Hallsenna Moor	Vedde (no geochem)	54.39046	-3.44377	Lane 2004
39	Gransmoor	looked for Vedde <10 (no geochem)	54.02076	-0.30526	Wastegård et al. 2000a
40	Star Carr	Vedde	54.21659	-0.42048	Darville 2011; Palmer et al. 2015
Wales					
41	Llyn Gwernan	No tephra	52.72597	3.920119	Woodcock 2003
42	Traeth Mawr	Vedde (no geochem)	54.92984	-3.48563	Williams 2001; Woodcock 2003; Williams et al. 2007
N. Ireland					
43	Sluggan Moss	Vedde (no geochem)	54.76611	-6.29194	Cooper 1999
44	Lough Nadourcan	Askja-S/10ka	55.05	-7.9	Turney et al. 2006
45	Long Lough	Askja-S/10ka	54.43333	-5.91667	Turney et al. 2006
46	Roddans Port	Vedde, Roddans Port A+B	54.51667	-5.5	Turney et al. 2006
Ireland					
47	Loughanascaddy crannog (Achill Island)	LAN1-325			Matthews 2008

Of the sixteen tephra isochrones known to occur in the British Isles through the LGIT, only six of these can be reliably traced to European sequences (Table 3.2). As discussed in Chapter 2, the Northern European tephra 'cell' is host to some significant disparities in the quantity and identity of cryptotephra layers, with many tephras restricted to single sites, or countries based on current data. At present, therefore, the number of tephra-linkages that can be made across this region currently limits the effectiveness of this tephra framework. A good example of this is the early Holocene Hässeldalen Tephra, which is an important marker horizon for constraining the PBO in Europe. The tephra has been identified at thirteen sites on the European mainland (e.g. Davies et al. 2003; Wohlfarth et al. 2006), but as yet there are no reliably confirmed cases of this tephra within records from the British Isles.

Table 3.2 Traceability of tephras across the British Isles. Sixteen tephra isochrons have been identified in LGIT aged sites from the British Isles. However, only six of these can be reliably identified in European sequences.

Tephra	Scotland	England	Wales	Ireland (including N. Ireland)	Europe
Suðuroy	x				x
LAN1-325				x	
SSn	x				x
An Druim	x				
Saksunarvatn	x				x
Breakish	x				
Ashik	x				
Askja-S/10ka	x			x	x
Abernethy	x				?
Vedde	x	x	?	x	x
LAS-1	x				
Roddans Port A				x	
Roddans Port B				x	
Penifiler	x				?
Borrobol	x		?		?
Dimna	x				x

This disparity of tephra distributions also seems to be evident within the confines of the British Isles. Of the sixteen tephra isochrones, only eight of these can be confidently traced across multiple sites (An Druim Tephra, Saksunarvatn Ash, Ashik Tephra, Askja-S/10ka Tephra, Abernethy Tephra, Vedde Ash, Penifiler Tephra, Borrobol Tephra; Figure 3.1). Figure 3.1 also illustrates the regional difference that has emerged in the number of tephras identified in the north, central, and southern regions of the British Isles. Following this existing model of tephra distribution, a study conducted in Scotland might expect to find on average, 2.5 tephra layers per site, whilst in England, Wales and Ireland (including N. Ireland) 1 tephra layer per site might be expected. The Scottish sector clearly possesses a greater number and variety of tephras, including the only occurrences of macrotephra and basaltic tephra layers in the British Isles (Bennett et al. 1992; Bunting 1994; Davies et al. 2001; Bondevik et al. 2005; Pyne O'Donnell 2007; 2011; Whittington et al. 2015). However, it is interesting to note that, despite the number of studies that have been conducted in Scotland, there appears to be a very definite difference in the suite of tephras identified when compared to those in Ireland (Figure 3.1). In Scotland during the Windermere Interstadial, tephrostratigraphic records typically identify the Borrobol and/ or Penifiler Tephras (e.g. Pyne-O'Donnell et al. 2008; Matthews et al. 2011). Whereas in Irish sequences the Roddans Port Tephras seem more applicable (Turney et al. 2006). In the early Holocene this difference is also noted, with Irish sequences characterised more definitely by the Askja-S/10ka Tephra, whilst in Scotland other ash layers are much more ubiquitous for example the Ashik Tephra (Pyne-O'Donnell 2007), with the Askja-S/10 only have been recently confirmed (Kelly et al. 2016). Admittedly the amount of data between the two locales is disproportionate, but it does nonetheless highlight an important discrepancy, and one which should be investigated.

3.3 Study site rationale

It is evident that there are two categories of 'discrepancy' in the context of the British Isles tephra framework: 1) inter-disparity between the British Isles and Europe and 2) intra-disparity, i.e. within regions of the British Isles. Given the wealth of research that has previously been undertaken in Scotland, and the regularity in which certain tephras are now 'routinely' identified (Table 3.1), this area represents a good testing ground for the implementation of new approaches and modified techniques (see Chapter 4 for methods).

Figure 3.2 highlights Northern Britain divided into several tephrostratigraphic sectors. Listed within these divisions are key points on why the sector may be relevant in the

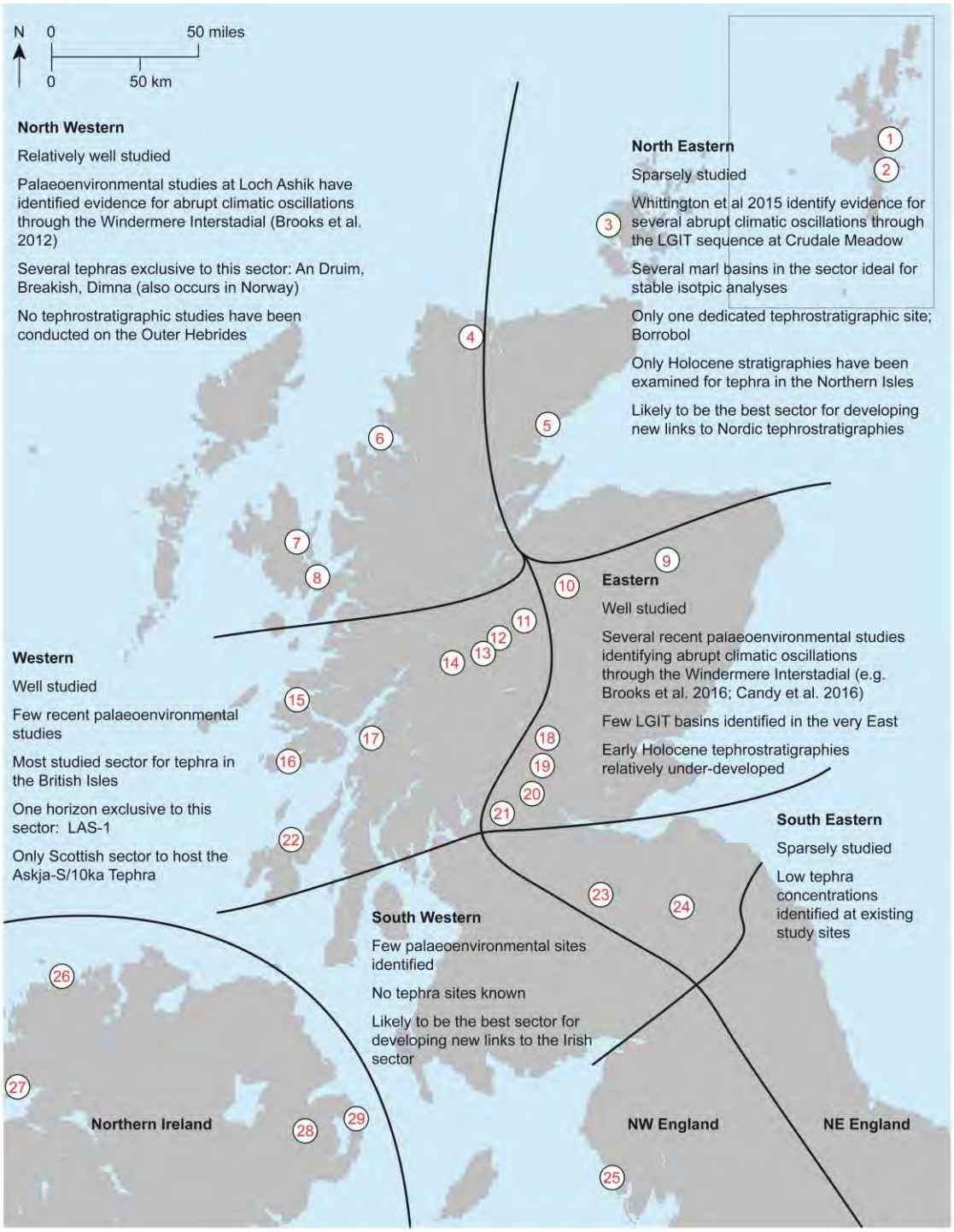

Figure 3.2 Tephrostratigraphic sectors of Northern Britain. In each sector several parameters are listed which provide a rationale for their study. It was decided in the context of this thesis that the North Eastern, North Western and South Western sectors would be investigated. 1) Dallican Water: Bennett et al. (1992); 2) Loch of Benston: Bondevik et al. (2005); 3) Quoyloo Meadow, Crudale Meadow Bunting (1994); 4) Lochan an Druim: Ranner et al. (2005); 5) Borrobol: Turney et al. (1997); Pyne-O'Donnell et al. (2008); Lind et al. (2016); 5) Tanera Mór: Roberts (1997); Wastegård et al. (2000a); Weston (2012); Eilen Fada Mór: Callicott (2013); 7) Druim Loch: Pyne-O'Donnell (2007); Pyne-O'Donnell et al. (2008) Pyne-O'Donnell (2011); 8) Loch Ashik: Davies et al. (2001); Pyne-O'Donnell (2007); Pyne-O'Donnell et al. (2008); Pyne-O'Donnell (2011); 9) Kennethmont: Turney (1998); 10) Abernethy Forest: Matthews et al. (2011); 11) Loch Etteridge: Lowe et al. (2008b); MacLeod et al. (2015); 12) Loch Laggan (MacLeod 2008); 13) Inverlair: Kelly et al. (2016); 14) Glen Turret: (Bank) MacLeod et al. (2015); 15) Mishnish (Davies 2003); 16) Loch an t-Suidhe: Roberts (1999); Davies (2003); Pyne-O'Donnell (2007); Pyne-O'Donnell et al. (2008); Pyne-O'Donnell (2011); 17) Pulpit Hill: Lincoln (2011); 18) Tirinie: Candy et al. (2016); 19) Menteith: Grosvesnor (2009); 20) Tynaspirit West: Roberts (1997); Turney et al. (1997); Pyne-O'Donnell (2007); 21) Muir Park Reservoir: Roberts (1997); Cooper (1999) Brooks et al. (2016); 22) Rubha Port an t-Seilich: Mithen et al. (2015); 23) Howburn Farm: Housley et al. (2015); 24) Whitrig Bog: Turney (1998); Pyne-O'Donnell et al. (2008); 25) Halsenna Moor: Lane (2004); 26) Lough Nadourcan: Turney et al. 2006; 27) Loughanascaddy Crannog: Matthews (2008); 28) Long Lough: Turney et al. (2006); 29) Roddans Port: Turney et al. (2006).

context of this thesis. On this premise the North Eastern, North Western and South Western sectors have been chosen for further study. These areas likely offer the best opportunities to further develop tephrostratigraphic links to Nordic, European and Irish tephrostratigraphies, as well as occurring in key regions for palaeoenvironmental study.

3.4 The north eastern sector

The North Eastern sector of Scotland (Figure 3.2) has a relative abundance of carbonate basins, which, as demonstrated by Whittington et al. (2015), exhibit great potential in developing high resolution quantifiable palaeoclimatic information. Few tephrostratigraphic studies have been conducted in carbonate basins, and so little is known as to whether the relatively high pH substrates will negatively affect tephra preservation (Pollard et al. 2003). However, the region lies in relative proximity to the Icelandic volcanic province, and is strongly influenced by the dominant westerly air movements that characterise the North Atlantic. As a result it is likely that this region will have been exposed to all but the most localised tephra forming eruptions derived from Icelandic province (e.g. Lacasse, 2001; Davies et al. 2010; Swindles et al. 2011; Stevenson et al. 2012, 2013).

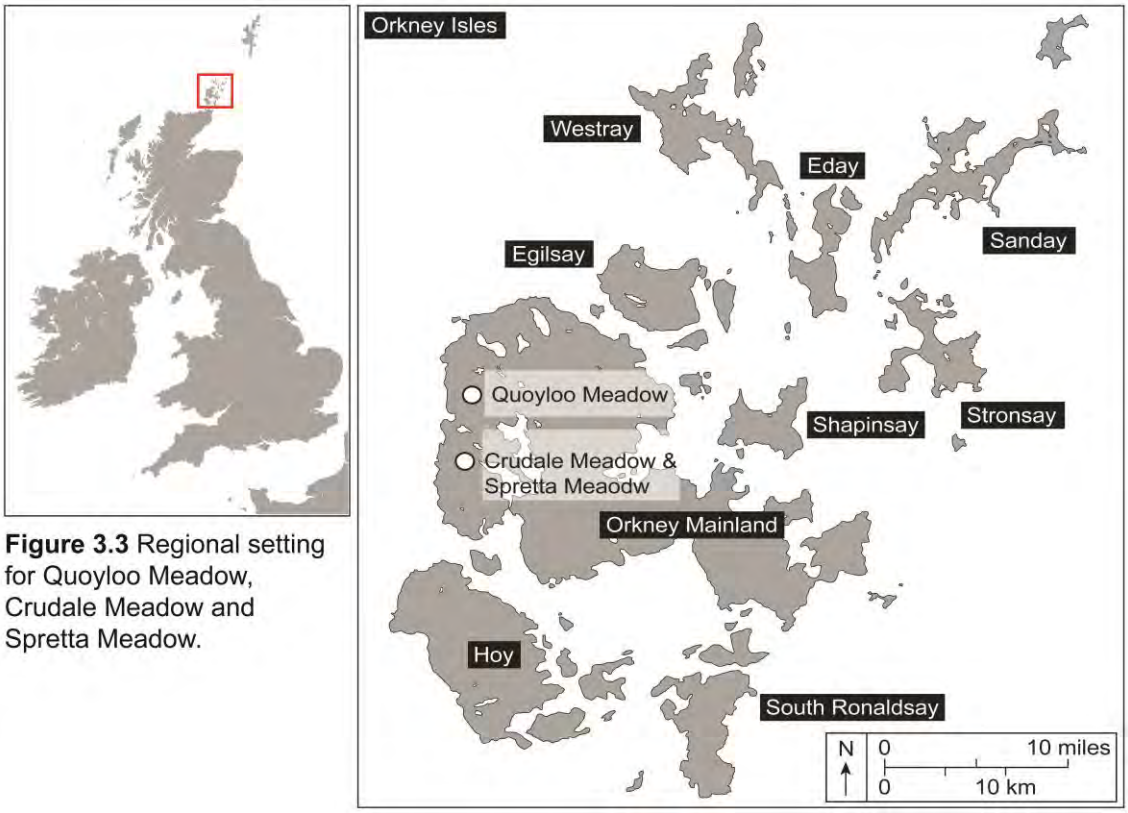

Figure 3.3 Regional setting for Quoyloo Meadow, Crudale Meadow and Spretta Meadow.

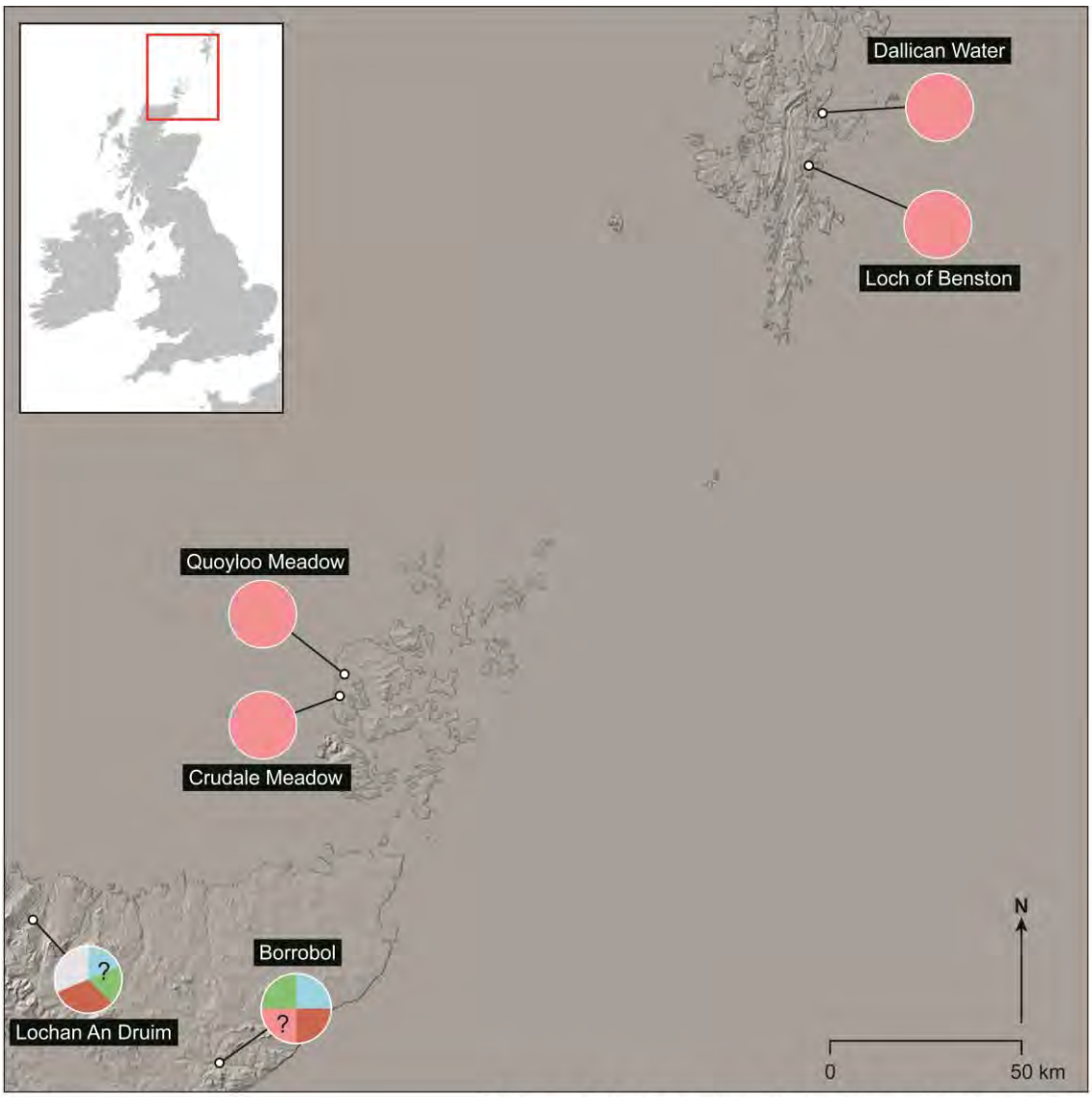

Figure 3.4 Distribution of sites in the North Eastern Sector of Scotland that have been examined for LGIT aged tephras. At Lochan An Druim a tephra exhibiting Borrobol-type chemistries was identified within Windermere interstadial sediments, however the site age model gives a much younger age than would be expected for both the Borrobol and Penifiler Tephras (Ranner et al 2005; Lind et al 2016). At Borrobol brown shards identified at the top of the examined sequence by Turney (1998) were assigned to the Saksunarvatn Ash by the premise of superposition, but this has never been confirmed with chemical analyses. Hitherto the only LGIT aged tephra identified in the Northern Isles is the Saksunarvatn Ash.

It was decided that three basins on Orkney Mainland would be investigated as part of this project (Figure 3.3); two previously examined carbonate basins, Quoyloo Meadow and Crudale Meadow (Moar 1969a; Bunting 1994; Whittington et al. 2015), and one previously unexamined non-carbonate site, Spretta Meadow (Jane Bunting pers. comm. 2013). The former were chosen for the possibility of developing high resolution

palaeoclimatic data, and it was hoped that the latter would act as a control against possible degradation and dissolution of tephras identified in the carbonate basins.

3.4.1 North eastern sector: regional tephrostratigraphic context

The regions of Caithness and Sutherland at the northern tip of Scotland, and the outlying Orcadian and Shetland archipelagos, are amongst the first regions in Scotland to have yielded tephras of LGIT age. Five sites in particular compose the tephrostratigraphy of this sector (Figure 3.4), and are outlined below.

3.4.1.1 Shetland and Orkney

The earliest discovery of an LGIT aged tephra from the British Isles was by Bennett et al. (1992) from Dallican Water, Shetland (60.387425 -1.096608; Figure 3.4), where the Saksunarvatn Ash was identified amongst early-Holocene lake muds (Figure 3.5 C). The horizon was quantified as tephra-like objects per 50 non-organic objects, and it is unlikely that the counts presented in the study are fully representative of the total concentration of tephra. Bennett et al. (1992) also note that there was a continuous record of tephra throughout the sediment sequence, suggesting that either reworking was prolific at the site, or that several unidentified eruptions are also preserved within the sequence (Figure 3.4). The discovery of the Saksunarvatn Ash on Shetland was soon complemented by the identification of the same ash layer in two carbonate rich sequences from Orkney Mainland; Quoyloo Meadow (59.066417 -3.309333) and Crudale Meadow (59.015897 -3.328533) (Bunting 1994; Figure 3.4 and 3.5 A, B). Almost no additional tephra work has been conducted across the Northern Isles with the exception of a more recent study conducted at Loch of Benston, Shetland (Figure 3.4), where Bondevik et al. (2005) identified a visible tephra horizon pertaining to the Saksunarvatn Ash. The noteworthiness of this discovery was however, missed in the original manuscript, as the horizon was never reported as a macroscopic tephra (Jan Mangerud pers. comm. 2015). Note this horizon is not shown in Figure 3.4 as no quantitative counts have been conducted at the site.

3.4.1.2 Caithness and Sutherland

The first dedicated LGIT aged cryptotephra study of the region, and for the British Isles, came from the work of Turney et al. (1997) and Turney (1998) at Borrobol, near Helmsdale (58.15 -3.83; Figure 3.4). The pioneering study identified two tephras, one within Loch Lomond Stadial silts and clays, and a second horizon much lower in the stratigraphy, occupying a position akin to the early phases of the Windermere Interstadial (Turney et al. 1997; Figure 3.5 G). Chemical analyses of the tephra peaks confirmed that the former correlated to the well-known Vedde Ash horizon, whilst the

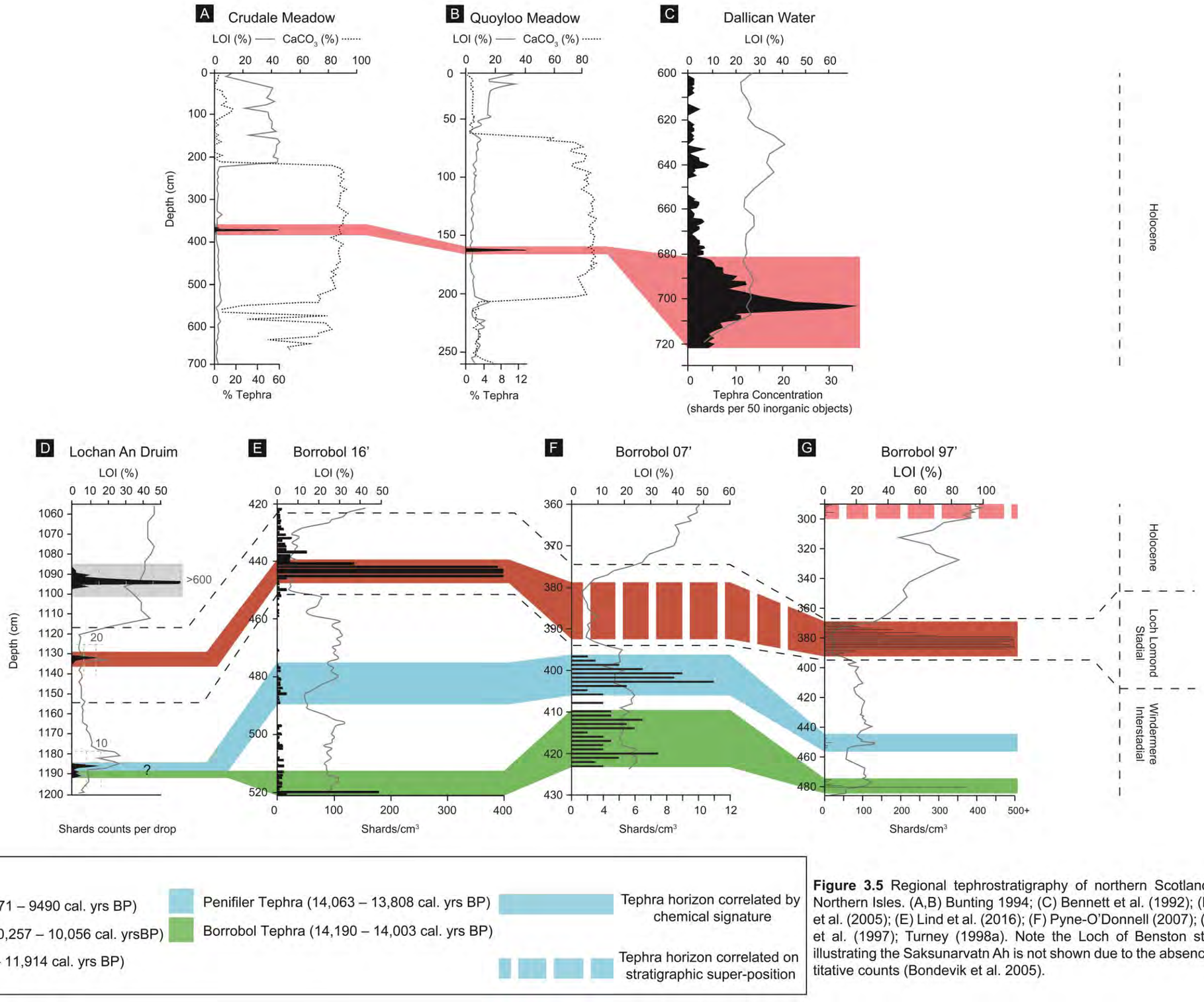

Figure 3.5 Regional tephrostratigraphy of northern Scotland and the Northern Isles. (A,B) Bunting 1994; (C) Bennett et al. (1992); (D) Ranner et al. (2005); (E) Lind et al. (2016); (F) Pyne-O'Donnell (2007); (G) Turney et al. (1997); Turney (1998a). Note the Loch of Benston stratigraphy illustrating the Saksunarvatn Ah is not shown due to the absence of quantitative counts (Bondevik et al. 2005).

second, lower peak possessed a chemical signature which at the time of discovery was unique. The tephra was termed the Borrobol, and the discovery of both horizons led to a surge in interest, and the identification of many more cryptotephra layers across northern Europe (see section 2.6).

In light of the discovery of the Penifiler Tephra, a horizon which bears a indistinguishable chemical signature to that of the Borrobol Tephra, and which is also contained with Windermere Interstadial aged sediments, the site at Borrobol has been the subject of renewed investigation (Pyne-O'Donnell 2007; Pyne-O'Donnell et al. 2008; Lind et al. 2016; Figure 3.5 E-G). Work by Pyne-O'Donnell (2007) on a separate sequence to that of Turney et al. (1997), and Turney (1998a) identified three peaks within the Interstadial sediments (Figure 3.5 F). Correlation was made to the Borrobol and the Penifiler, however, the low totals exhibited in this study contrast markedly to the work originally produced by Turney et al. (1997) and Turney (1998a) (Figure 3.5 G). Thus caution must be exhibited in interpreting the significance of any such peak. Nonetheless a re-evaluation of the original Borrobol sequence by Pyne-O'Donnell et al. (2008), and subsequently on new material by Lind et al. (2016) has gone towards confirming the presence of both the Borrobol and Penifiler Tephra's at the site (Figure 3.5 E G).

It should also be noted that Turney (1998) identified the presence of brown shards toward the top of the examined sequence at Borrobol, and ascribed these to the Saksunarvatn Ash on the premise of superposition. Chemical analysis of this horizon has never been undertaken, and such correlations thus remain tentative (Figure 3.5 G).

Further to the west, in Sutherland, the most northerly LGIT aged tephra site in mainland Britain can be found. Lochan An Druim (58.475 -4.685556; Figure 3.5 D) was investigated by Ranner (2005) and Ranner et al. (2005). Four peaks were identified within the scanned stratigraphy and resolved to 1 cm before three of these were selected for chemical characterisation (Figure 3.5 D). Within Windermere Interstadial deposits a basal tephra with a 'Borrobol-type' chemical signature was identified. An interpolated age based on a polynomial regression model dates the horizon at ca. 13,610 cal years BP, slightly younger than both the Borrobol and Penifiler Tephras. This date is misleadingly precise, and it is likely this tephra can be correlated with the Penifiler Tephra, although a definitive correlation remains elusive (Pyne-O'Donnell et al. 2008; Lind et al. 2016). Mid way through the Loch Lomond Stadial deposits, the Vedde Ash is present, and above this in Holocene sediments a tephra correlating to the Torfajökull system was identified. Radiocarbon dates from the centimetre below the

tephra place the isochron at 9671-9490 cal. BP, which makes the tephra too young to be a correlative of the Ashik Tephra; it has therefore been named the An Druim Tephra (Ranner et al. 2005).

3.4.2 North eastern sector: the geology of Orkney

Given the recent findings, and subsequent warnings over geological contamination of tephra samples (MacLeod and Davies 2016). It is necessary to consider the base geology of Orkney Mainland. The basement complex of Orkney consists of Neoproterozoic granitic formations of the Moine Supergroup, with these in turn overlain by Devonian aged sandstones, the dominant rock type found across Orkney (Mykura et al. 1976). The oldest of such sandstones outcrop near Yesnaby (Figure 3.6) and consist of two units: the Qui Ayre formation, and the Harra Ebb formation. These in turn are overlain by mid-late Devonian sandstones which are more ubiquitous, and represented by two major groups, the Stromness Flags (Upper and Lower), and the Rousay Flags. Both instances of 'flags' consist of rhythmically bedded carbonate-rich siltstones and shales with subordinate fine-grained, thinly bedded sandstones (Mykura et al. 1976). The uppermost sandstone strata are known as the Eday Group, and are particularly noted for its fossiliferous horizons. In addition to the sedimentary deposits, over two hundred Permian-aged dykes and other volcanic intrusions are noted across Orkney, with several outcropping in the west of Orkney Mainland (Figure 3.6). Despite the presence of igneous geology, these are unlikely to cause problems due to their distinctive trachybasalt composition (Mykura et al. 1976), and the propensity of distal tephras to be of a more silicic or basaltic composition. The location of the three Orcadian study sites reported in this thesis are shown in Figure 3.6.

3.4.3 North eastern sector: glacial history and deposits of Orkney

The Orkney archipelago is of a critical locality for understanding the glacial history of Northern Scotland, and the neighbouring North Sea basin (e.g. Geikie 1877; Peach and Horne 1880). The glacial record is mainly preserved in glacial sediments restricted to lower ground where thicknesses typically range from 3-10m (Mykura et al.1976; Sutherland 1991). Some of the earliest studies commented upon shelly marine tills (Figure 3.7) and concluded ice must have migrated from the mainland, across sea beds to occupy Orkney (Peach and Horne 1880). Material within the glacial sediments is predominately local in origin, with most lithologies only being transported a matter of kilometres from source (Rae 1976). In the north and east, deposits are principally composed of sandstone and 'marls' from the Eday Beds, whilst further to the west the dominant lithologies originate from the Rousay and Stromness flagstones i.e. silts and mudstones (Mykura et al. 1976; Rae 1976). This spatial difference in deposits has

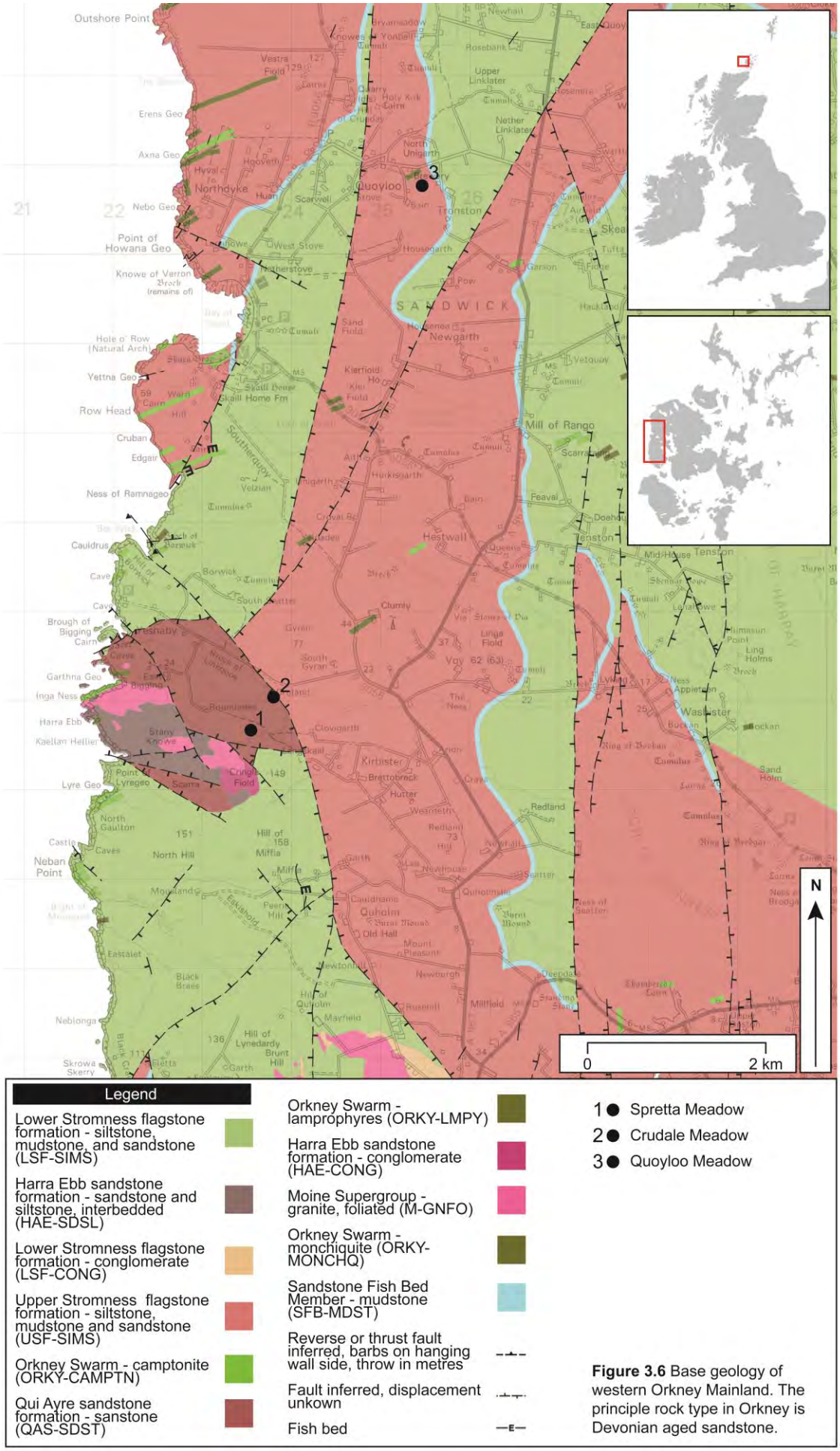

Figure 3.6 Base geology of western Orkney Mainland. The principle rock type in Orkney is Devonian aged sandstone.

been ascribed to the pattern of underlying geology, and the principal direction of ice flow (Rae 1976). Such ice movements across Orkney have been reconstructed from various lines of geomorphic evidence (e.g. Rae 1976). Glacial striae are amongst the more definitive lines of evidence, and orientation of these structures is most predominantly in a north-westerly direction (Figure 3.7), although occurrences have also been noted to orientate northwards, north-north-west, as well as west and south-west (Wilson et al. 1935; Mykura et al. 1976; Rae 1976; Figure 3.7). This evidence has been supplemented with the identification and provenancing of far travelled glacial erratics, which have origins in Sutherland, the Northern Highlands, the Grampians, and the Central Valley of Scotland (Sutherland 1991). However, some specimens which have been described from Sanday and Flotta, and most notably the Saville erratic appear to have a Scandinavian origin (Peach and Horne 1880; Wilson et al. 1935; Figure 3.7). It is considered that Scottish ice emerging from the Moray Firth was deflected across the archipelago as a result of a more dominant Scandinavian ice mass in the North Sea Basin. Whether or not, Scandinavian ice transversed the isles at any point remains open to debate, as associated erratics may have been re-entrained by Scottish ice left remnant from previous glaciations (Rae 1976; Sutherland 1991).

Whilst there is a general consensus concerning the direction of ice movement and the remnant glaciological features, there has been continued debate as to the timing of events, and more specifically when ice last crossed the archipelago (Ballantyne et al. 2007; Phillips et al. 2008). Up until relatively recently contrasting hypotheses existed, with some authors advocating an early or mid-Devensian age (MIS-4/ MIS-3) for the last advance of ice across Orkney, and thereby suggesting the archipelago remained ice free during the late-Devensian (MIS-2) (e.g. Rae 1976; Sutherland 1984; 1991; Bowen et al. 2002). However, it is now considered most probable that ice existed in the North Sea basin during the late-Devensian, and also highly likely that the BIIS was joined with the FIS until about 18.5-17 kyrs, at which point the BIIS and FIS ‘unzipped’ and rapid retreat ensued (e.g. Hall and Bent 1990; Sejrup et al. 1994; Hughes et al. 2011; Clark et al. 2012; Sejrup et al. 2015; Hughes et al. 2016; Sejrup et al. 2016).

For Orkney, this occupation by Late Devensian ice is supported most conclusively by the cosmogenic exposure dating of glacial erratics, and ice-moulded bedrock by Philips et al. (2008). The findings of which imply that deglaciation of the islands took place sometime after the LGM. Recent recalibration of these ages by Hughes et al. (2016) places the ‘most credible’ age of deglaciation at between 16-17 kyrs, although the islands appear not to have been entirely ice free until 15 kyrs, and are furthermore

Figure 3.7 Glaciological features of the Orkney archipelago compiled from the work of Peach and Horne (1880); Wilson et al. (1935); Rae (1976); and Sutherland (1991). The pattern of Dimlington ice retreat is based on the recalibrated ages of Phillips et al. (2008) by Hughes et al. (2016). Loch Lomond Stadial moraine features are from Ballantyne et al. (2007) and digitised by Bickerdike et al. (2016).

noted to have supported a separate ice mass to that of mainland Scotland through this period (Clark et al. 2012; Hughes et al. 2016; Figure 3.7). The final retreat of ice from Orkney left a series of basins across the Islands, which during the following Windermere Interstadial, Loch Lomond Stadial and Holocene gradually became infilled, and hence preserve the palaeoenvironmental history of the archipelago (e.g. Moar 1969a; Bunting 1994; Whittington et al. 2015). It is worth noting that there is evidence to suggest that the Island of Hoy in the southwest of the archipelago, played host to a small, locally nourished glaciers during the Loch Lomond Stadial (e.g. Charlesworth 1955; Rae 1976; Sutherland 1991; Ballantyne et al. 2007; Figure 3.7). It would seem that ice was restricted to this locale, and reflects the higher elevation of the island in comparison to the rest of the archipelago.

3.4.4 North eastern sector: Quoyloo Meadow

3.4.4.1 Site description

Located 2.5 km NE of the Prehistoric village of Skara Brae, Quoyloo Meadow (59.066417 -3.309333) occupies a topographic low within Upper and Lower Stromness Flagstones; a geologic group principally composed of interbedded mudstone, limestone, siltstone and sandstone formations (Mykura et al. 1976). At its maximum extent the basin is 0.6 km x 0.3 km, occupies an area of 0.1 km^2, and lies at an altitude of 30 m asl (Figure 3.8). The construction of a drainage network across the site for the provision of improved agricultural ground has altered the basin profile and channelised all natural inflows and outflows; the current catchment to basin area ratio is estimated at 12:1; however, it is likely the basin profile would have been larger prior to anthropogenic modification. A natural spring is focused off the hills to the west and at present is the only inflow to the basin. At the northern tip, an outflow undercuts a road before resurfacing from a culvert 150 m to the north east. The basin is currently colonised by a valley mire environment, but was previously occupied by an open water body during the LGIT (Bunting 1994).

3.4.4.2 Previous work

The site was originally investigated by Bunting (1994) who reported a 2.60 m core sequence, with the lower 1.40 m exhibiting a LGIT- early Holocene lithostratigraphic and pollen-stratigraphic succession (Figure 3.9). The lowermost litho- and biostratigraphic units i.e. QM-S1a and QM-P1a (Figure 3.9) are correlated to the Windermere Interstadial, although organic sedimentation appears limited within the sequence. Pollen concentrations are also low, and illustrate that a dwarf-shrub heathland predominated during this period. The sparsely vegetated landscape and the dominance of clastic sedimentation though the Windermere Interstadial, suggests that

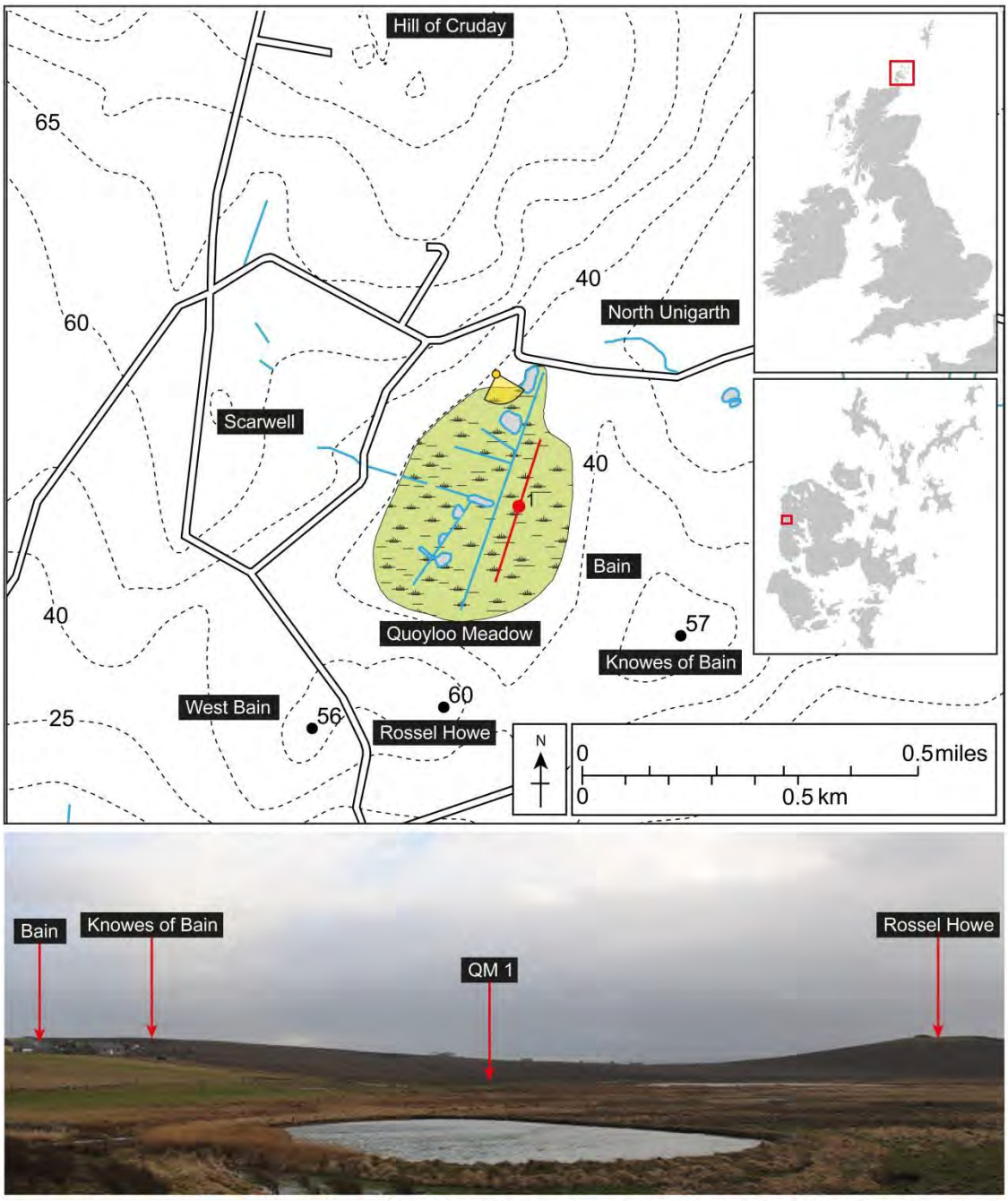

Figure 3.8 Topographic map of the Quoyloo Meadow basin. Note the position of the position of the transect and QM 1 core site. The catchment of the basin is estimated at 12:1. Contours in m (asl).

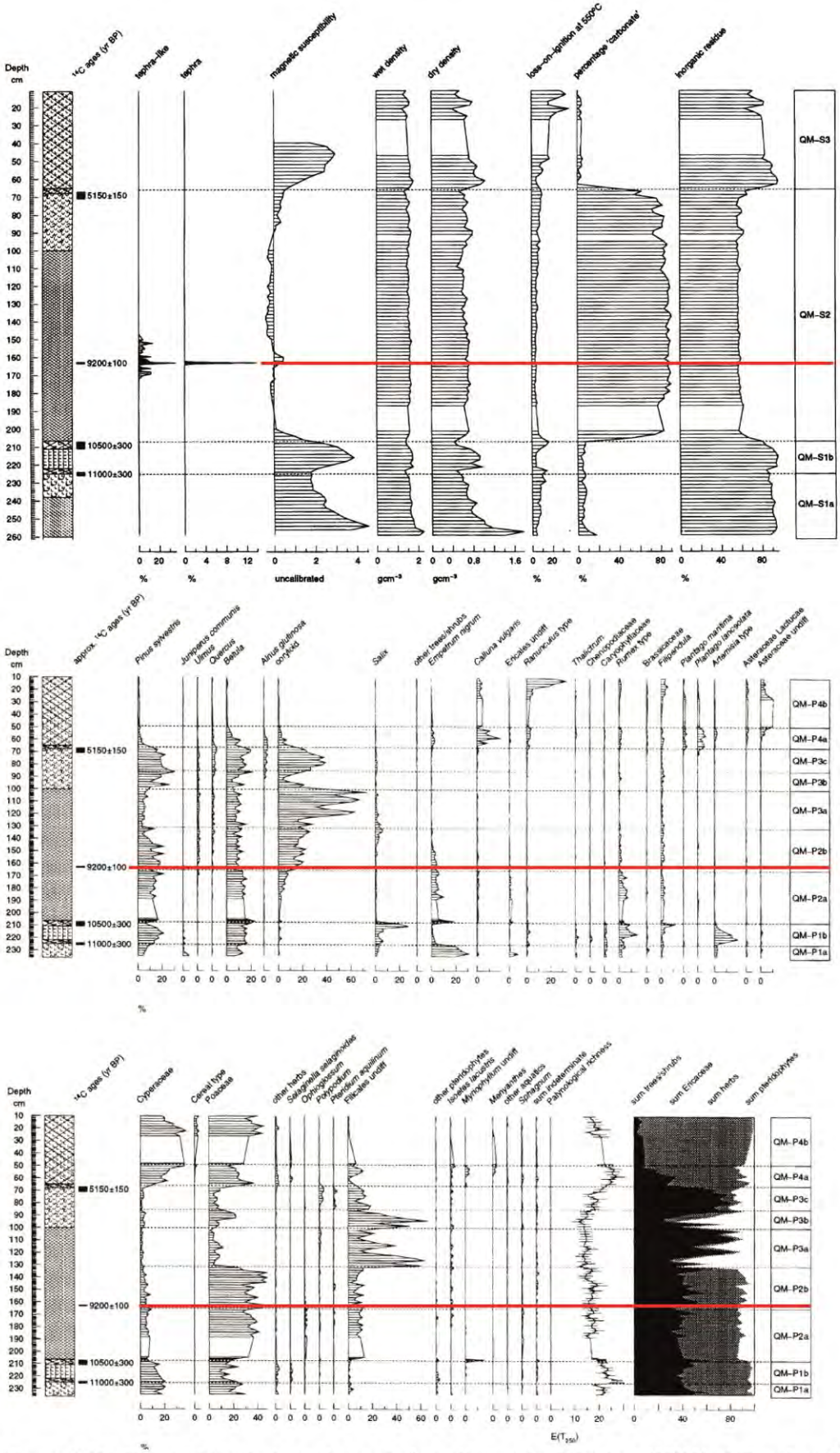

Figure 3.9 Litho- and biostratigraphic units from the work of Bunting (1994) at Quoyloo Meadow. Four lithostratigraphic units were identified, whilst 9 pollen zones were delineated. Note the position of the Saksunarvatn Ash in the sequence (red line). The data here suggests the basin began accumulating sediments some time during the Windermere Interstadial.

whilst climate had ameliorated, erosion of the landscape decreased but did not cease entirely (Bunting 1994; 1996). This unit is succeeded by QM-S1b and QM-P1b, which are characteristic of the climatic and landscape deterioration that accompanied the Loch Lomond Stadial; clastic sedimentation remains dominant whilst vegetation becomes sparser and more herb-dominated (Figure 3.9). This cold phase ended with the onset of marl sedimentation and the establishment of a tall herb grassland around the Quoyloo Meadow site (QM-S2 and QM-P2a), both indicators of a warming environment and a gradually stabilising landscape (Bunting 1994; 1996). A tephra horizon was also identified within this interval, and chemically correlated to the Saksunarvatn Ash (10,257-10,056 cal. BP), further confirming the early Holocene climatic correlation (Bunting 1994; Figure 3.9).

3.4.5 North eastern sector: Crudale Meadow

3.4.5.1 Site description

Crudale Meadow (59.015897 -3.328533) lies at an altitude of 6-8 m asl, is located approximately 0.3 km to the northeast of Spretta Meadow (see section 3.4.6), and about 1.6 km due west of the Loch of Stenness (Figure 3.10). The basin lies on a fault between early Devonian Qui Ayre sandstones, and the mid-late Devonian Upper Stromness Flagstones (Figure 3.6). The site is flanked on three sides by hills; to the north, Gyran (77 m); to the west, Breck of Linkquoy (42 m); and to the south, Billia Fiold (59 m). The latter acts as a natural barrier between Crudale Meadow and Spretta Meadow. In its current configuration the extent of the basin stretches 0.35 km x 0.2 km and occupies an area of 0.09 km^2, which provides the site with an estimated catchment to basin area of 26:1. A single outflow of the basin to the east is supplemented by two basin inflows, to the west the Burn of Cruland which drains a relatively low lying catchment to the west-northwest, and the Burn of Sowadee which drains a much larger area further to the south. The Burn of Sowadee first runs into Spretta Meadow (see section 3.4.6), and exits the basin at its eastern margin, from here it flows round the base of Billia Fiold, and enters into Crudale Meadow at the south-eastern corner as the Burn of Clovigarth (Figure 3.10). Presently the basin is dominated by a valley mire environment with some shallow open water areas.

3.4.5.2 Previous work

The site was originally investigated by Moar (1969a), who named the locale ‘Yesnaby’, and again by Bunting (1994) and Whittington et al. (2015), who refer to the site as ‘Crudale Meadow’ (Figure 3.10). The latter two studies are offset from the original core site by approximately 100 m. These are defined by slightly shorter stratigraphies (6.38 and 5.76 m respectively) compared to that obtained by Moar (7.20 m). A palynological

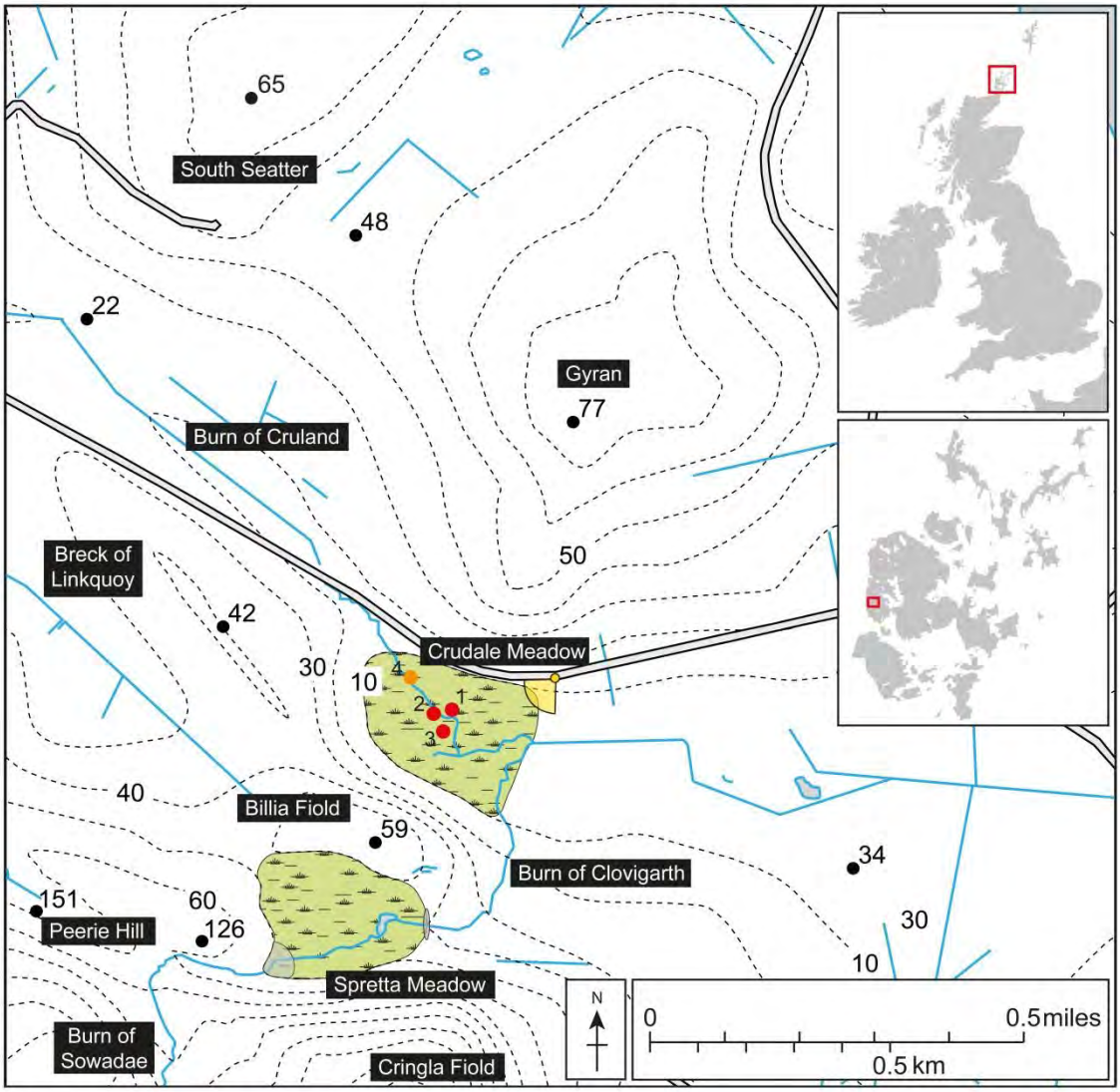

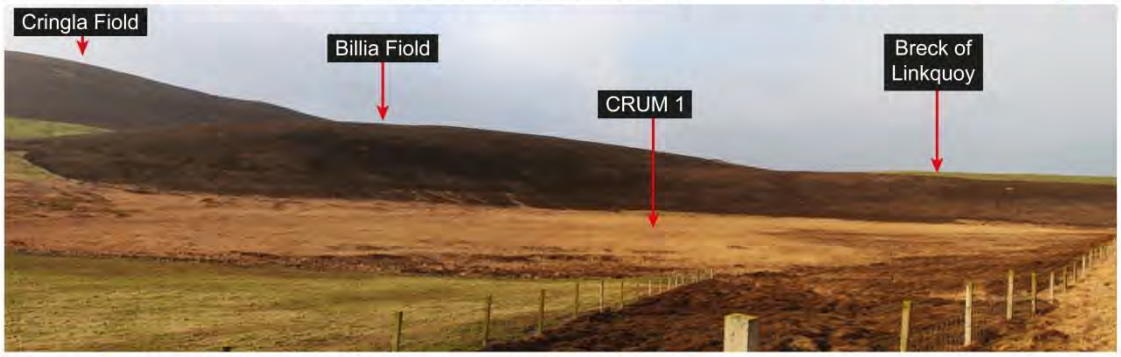

Legend

1 ● CRUM 1 & core site of Bunting (1994); Whittington et al. (2015)
2 ● CRUM 2
3 ● CRUM 3
4 ● 'Yesnaby' core site of Moar (1969)

Direction of inset photograph

Approximate extent of Spretta Meadow debris fan

Approximate extent of Spretta Meadow rock platform

Figure 3.10 Topographic map of the Crudale Meadow and adjoining Spretta Meadow basins. Note the position of the Yesnaby core (Moar 1969) in comparison to the Bunting (1994), Whittington et al. (2015) and CRUM 1 core from this study. The catchment of the basin is estimated at 26:1. Contours in m (asl).

assessment of the site, spanning the LGIT-present day, was the focus of Moar (1969a) and Bunting (1994), whereas the emphasis of Whittington et al. (2015) was exclusively on the LGIT and early Holocene. The lithostratigraphic results from all three studies are summarised in Table 3.3.

The stratigraphic information from these studies suggests that the basin does exhibit a classic 'tri-partite' succession of LGIT aged deposits; a pattern which can be widely recognised across Scotland (Lowe and Walker 2015). The biostratigraphic signature of the site is indicative of a similar narrative, with pollen and mollusc-inferred cold phases broadly coincidental with lithological changes (Whittington et al. 2015). In conjunction with these, a high resolution (1 cm) isotopic analyses has provided a an insight into potential mechanisms of change, as the authors argue that the isotopic signature reflects changes in air temperature. These oscillations are highlighted in Figure 3.11, and thought to reflect episodes of climatic deterioration and amelioration (Whittington et al. 2015). Between the base of the Whittington et al. (2015) sequence, thought to be representative of the early Windermere Interstadial (CRU-1), and CRU-4 (Loch Lomond Stadial), there are at least two pronounced reductions in $\delta^{18}O$, C1 and C2 (Figure 3.11). It is postulated that these oscillations coincide with GI-1d and GI-1b respectively (Whittington et al. 2015). Whilst a third event positioned between C1 and C2 (Figure 3.11) may represent a brief cold revertence phase within GI-1c (Whittington et al 2015). The Loch Lomond Stadial is clearly recorded in all palaeoenvironmental proxies (CRU-4/ C3), and is typified by the cessation of carbonate precipitation, and the total absence of Mollusca through the interval. Cold climate pollen taxa predominate, and concentrations are the lowest for the entire record (Moar 1969a; Bunting 1994; Whittington et al. 2015). The end of the Loch Lomond Stadial is typified by a rapid rise in $\delta^{18}O$ values, a relative increase of Molluscan numbers, and a significant decrease in clastic sedimentation, all of which signal climatic recovery and landscape stabilisation. However, this warming phase is truncated by a strong climatic oscillation (C4), with all proxies indicating a severe cooling event (Whittington et al. 2015). It is likely that this downturn is representative of the PBO (Whittington et al. 2015). Recovery from this climatic downturn is rapid, although it is punctuated by a minor oscillation reflected in the isotopic and palynological signature (C5). The authors suggest that a correlation to a cold episode reflected in some regional records including the ice-cores can be tentatively made, but state that, even with the Saksunarvatn Ash providing an isochronous marker, chronological uncertainties limited the robustness of these prospective correlations.

Table 3.3 Sedimentological description of core sequences examined from Crudale Meadow in Moar (1969a), Bunting (1994), and Whittington et al. (2015). Climatic zone codes: DS=Dimlington Stadial; WI= Windermere Interstadial; LLS=Loch Lomond Stadial; EH=early Holocene; H=Holocene.

Moar (1969)			Bunting (1994)			Whittington et al (2015)		
Depth (cm)	Sedimentological description	Climatic zone	Depth (cm)	Sedimentological description	Climatic zone	Depth (cm)	Sedimentological description	Climatic zone
0-77	Grey silty mud	H	0-23	Organic detritus with some sand and silt	H	0-194	Sedge peat	H
77-208	Brown fibrous peat	H	23-210	Organic detritus	H	194-201	Gyttja	H
208-480	Buff-coloured shell marl	EH/H	210-546	Marl with organic detritus and shell fragments grading downwards into organic lake mud and marl. Tephra centred on 386.5 cm	EH/H	201-202	Gyttja/marl transition	H
480-570	Blue-gray slightly shelly marl, containing a clay fraction; *Chara* oospores frequent	EH	546-570	Clay silt with occasional organic fragments grading downwards into clay rich organic detrital lake mud	LLS	202-499	Marl with shells	EH/H
570-580	Transition; Polytrichum alpinum leaves recovered at 575 cm; *Chara* oopspores frequent	EH	570-658	Carbonate-rich organic mud; below 596 cm carbonate-rich clay	WI	499-500	Gyttja	EH
580-600	Blue-grey clay	LLS	658-682	Clay with some carbonate and sand	DS	500-508	Grey clayey silt	LLS
600-655	Blue-grey, slightly shelly clay marl; one seed of *Emperrum nigrum* at 640 cm, leaf fragments of cf. *Dryas octopetala* and numerous oospores of *Chara*	WI				508-514	Grey clayey silt with organic inclusions	LLS
655-720	Faintly pink clay; stones struck as 720 cm	DS				514-523	Grey clayey silt	LLS
						523-537	Marl	WI

						537-559	Marl with shells	WI
						559-561.5	Grey clayey silt	WI (GI-1d)
						561.5-576	Marl with shells	WI

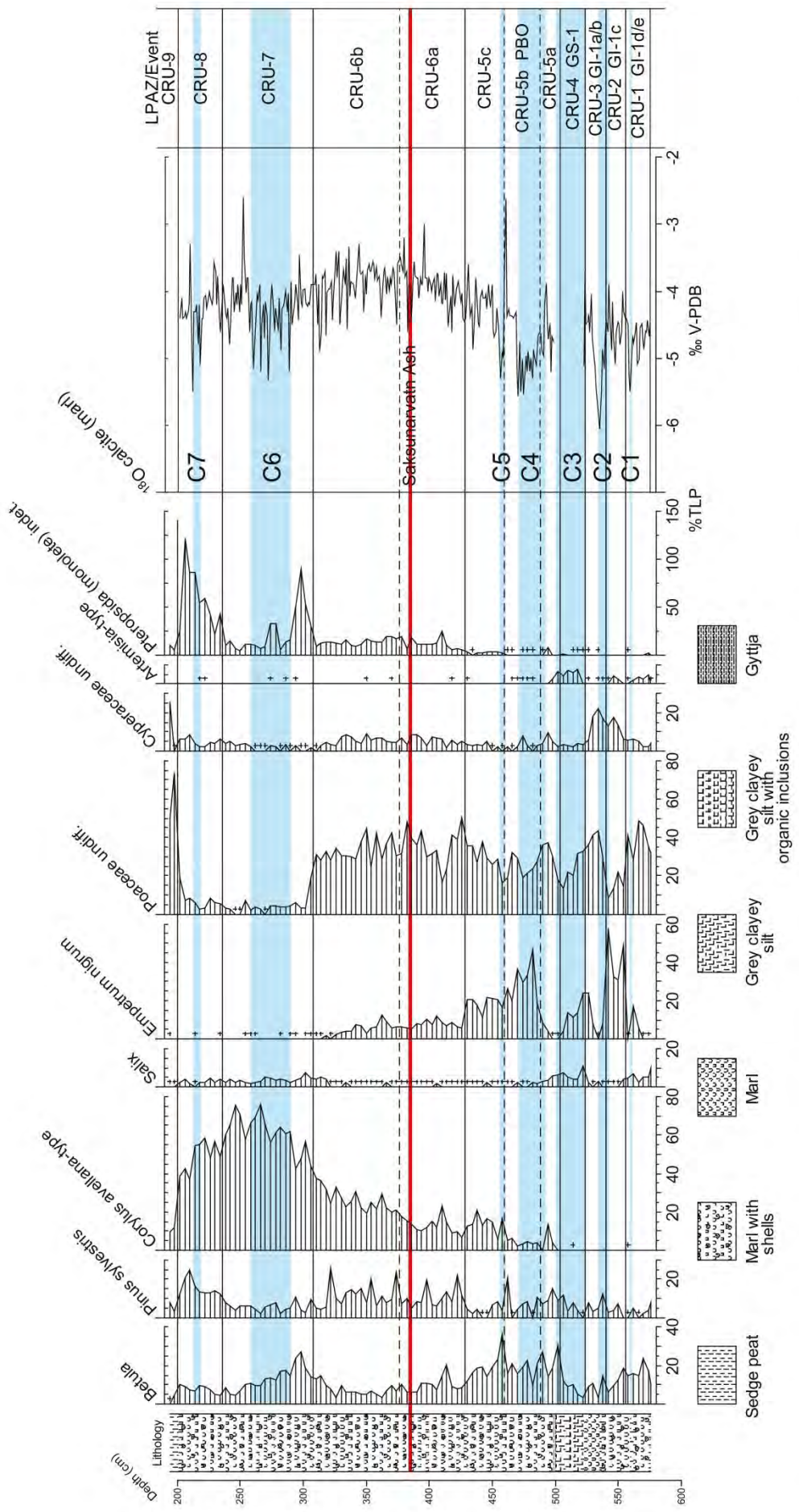

Figure 3.11 Selected pollen taxa displayed as percentage total land pollen, and isotope ($\delta^{18}O$ marl) data for Crudale Meadow. Inferred 'cold' (C) events are shaded blue and labelled. The position of the Saksunarvatn Ash is marked as red. Modified from Whittington et al. (2015).

Following this interval, all proxies show a progressive amelioration in climate through the early Holocene sediments, with this trend continuing until 3.30 m depth, at which point the isotopic record shows a progressive cooling trend, and is further punctuated by two notable minima; C6 and C7, tentatively correlated to the 9.3 and 8.2 ka events respectively. In comparison no such oscillations are detected within the biostratigraphic record, which conversely shows a progressive warming through this period. No explanation as to why this is the case is provided by Whittington et al. (2015), which perhaps raises the question of the validity of such climatic correlations. As a result a robust chronological model will be needed to test these hypotheses.

3.4.6 North eastern sector: Spretta Meadow

3.4.6.1 Site description

Spretta Meadow (59.012281 -3.332953) lies at an altitude of 42-44 m asl, and is located approximately 0.3 km to the southwest of Crudale Meadow (see section 3.4.5), and about 2.3 km due west of the Loch of Stenness (Figure 3.10). At present the site is covered with a semi-aquatic peat system and is constrained on three sides by hills: to the north Billia Fiold (59 m), to the west Peerie Hill (68 m) and to the south Cringla Fiold (149 m). These hills and the surrounding area exhibit a mixed geology but can be broadly classified as Devonian aged sandstones and Neoproterozoic granites (Figure 3.6). In its current configuration the basin stretches approximately 0.23 x 0.2 km, covers an area of 0.09 km^2, and possess an estimated catchment to basin ratio of 25:1. The site serves as the primary basin for the Burn of Sowadee, which drains the surrounding landscape and flows into the basin at the southwestern margin, where it flows over a small debris fan (Figure 3.12). The Burn runs through the basin and exits at the eastern margin, it is here that a rock platform lies across the flow of the exiting channel. This natural barrier has likely acted as a control on the maximum level of any lake that formed in the basin. From here the stream flows down into the adjoining basin, Crudale Meadow.

3.4.6.2 Previous work

Previous work on the site has been limited to the mid-late Holocene interval, and only in an exploratory context. An initial coring of the basin took place in September 2007 by Dr J. Bunting and M. Farrell as part of a PhD project tasked with understanding prehistoric communities' response to climatic and environmental change. A 3.5 m sequence from the centre of the basin was recovered (Figure 3.12), which yielded an upper unit of peat and a lower unit of dark brown gyttja (Figure 3.13). However, the study failed to identify or retrieve the basal sediments, and it was hypothesised that a longer sequence would exist at the site.

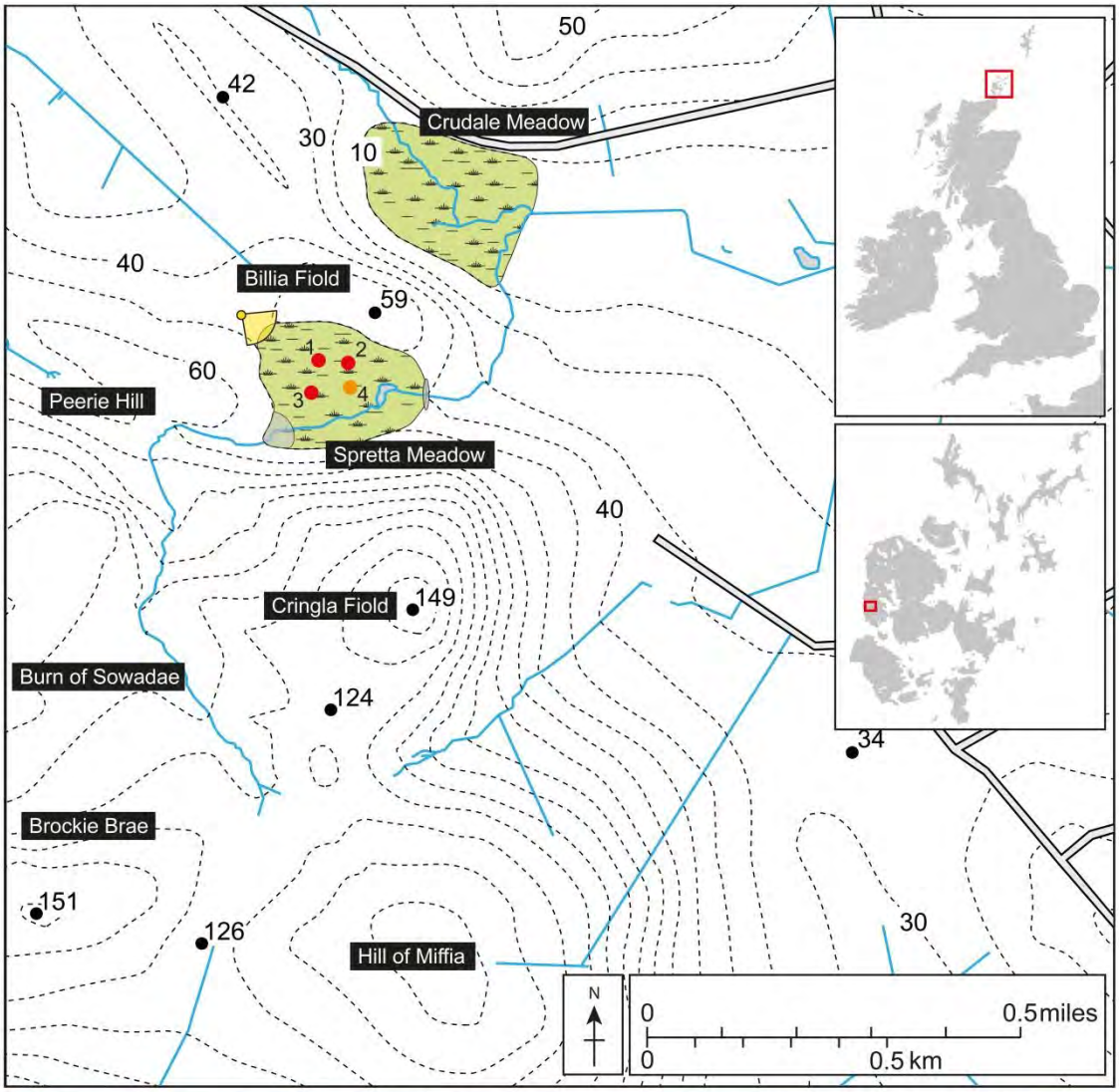

Legend

1 SPME1
2 SPME 2
3 SPME 3
4 Bunting Farrell core
Direction of inset photograph
Approximate extent of debris fan
Approximate extent of rock platform

Figure 3.12 Topographic map of the Spretta Meadow and adjoining Crudale Meadow basins. Note the position of the core sites and the position of the debris fan. The catchment of the basin is estimated at 25:1.

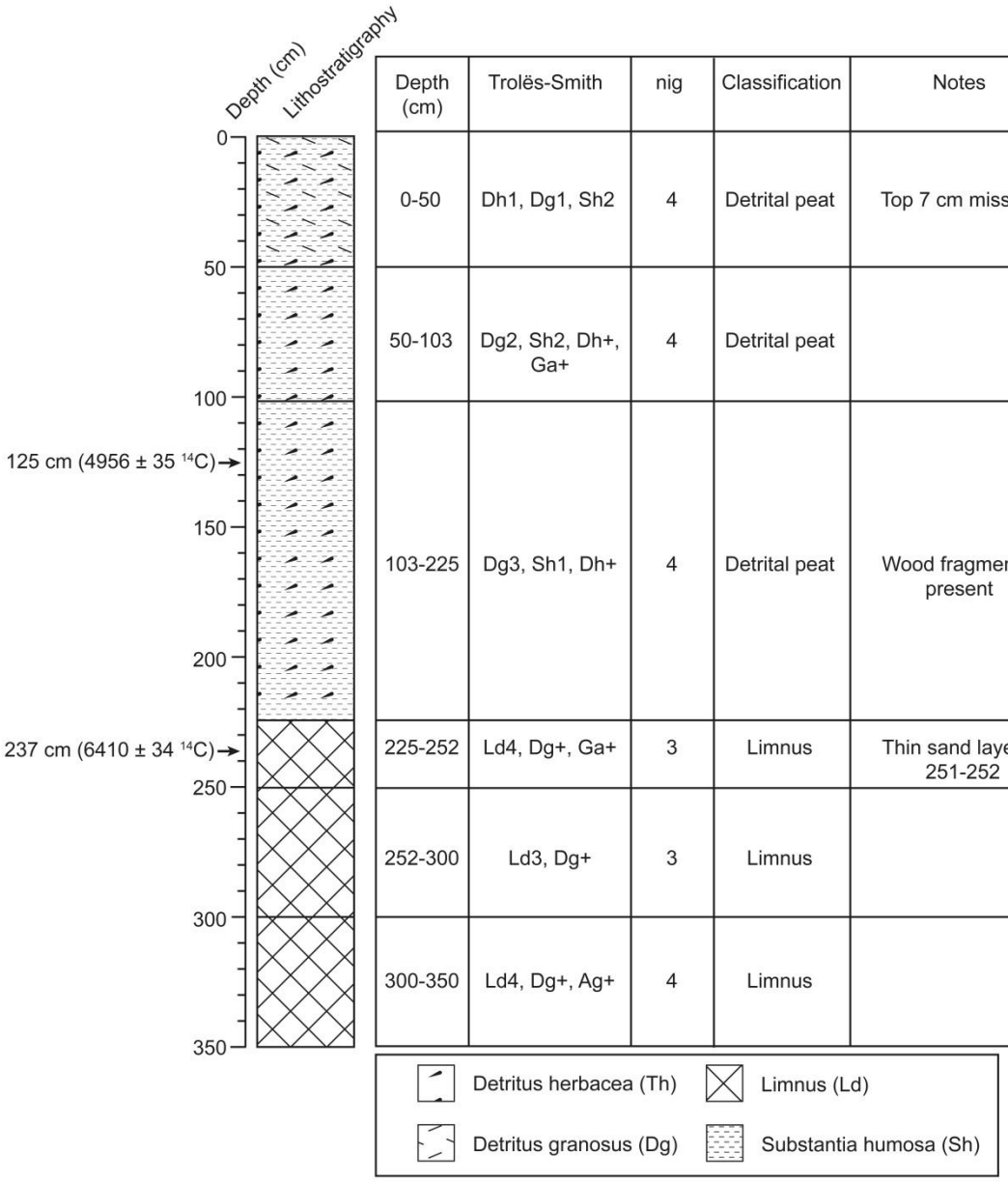

Depth (cm)	Trolës-Smith	nig	Classification	Notes
0-50	Dh1, Dg1, Sh2	4	Detrital peat	Top 7 cm missing
50-103	Dg2, Sh2, Dh+, Ga+	4	Detrital peat	
103-225	Dg3, Sh1, Dh+	4	Detrital peat	Wood fragments present
225-252	Ld4, Dg+, Ga+	3	Limnus	Thin sand layer at 251-252
252-300	Ld3, Dg+	3	Limnus	
300-350	Ld4, Dg+, Ag+	4	Limnus	

Figure 3.13 Spretta Meadow basin lithostratigraphy (Michelle Farrell pers. comm. 2013). The profile shows a transition from mid-Holocene lake muds to a detrital peat deposit. The age of the sequence is supported by two radiocarbon dates. See Figure 3.12 for core location.

3.5 The north western sector

The North Western sector (Figure 3.2) has had some of the most detailed tephrostratigraphic work conducted anywhere in NW Europe (e.g. Pyne-O'Donnell 2011). It thus represents a good locale for the testing of higher resolution sampling strategies, and the effects this many have on the number of tephras identified within a sequence (see Chapter 4.0 for methods). The area has also been recently identified by Brooks and Langdon (2014) as one of key regions in Europe, which require additional palaeoenvironmental data and especially quantifiable temperature data. It was decided

that a single basin from the island of Tanera Mòr, in the Summer Isles, would be investigated as part of this project (Figure 3.14) and forms part of a wider multi-island project designed to reconstruct the palaeoenvironmental history of the archipelago (John Lowe pers. comm. 2012).

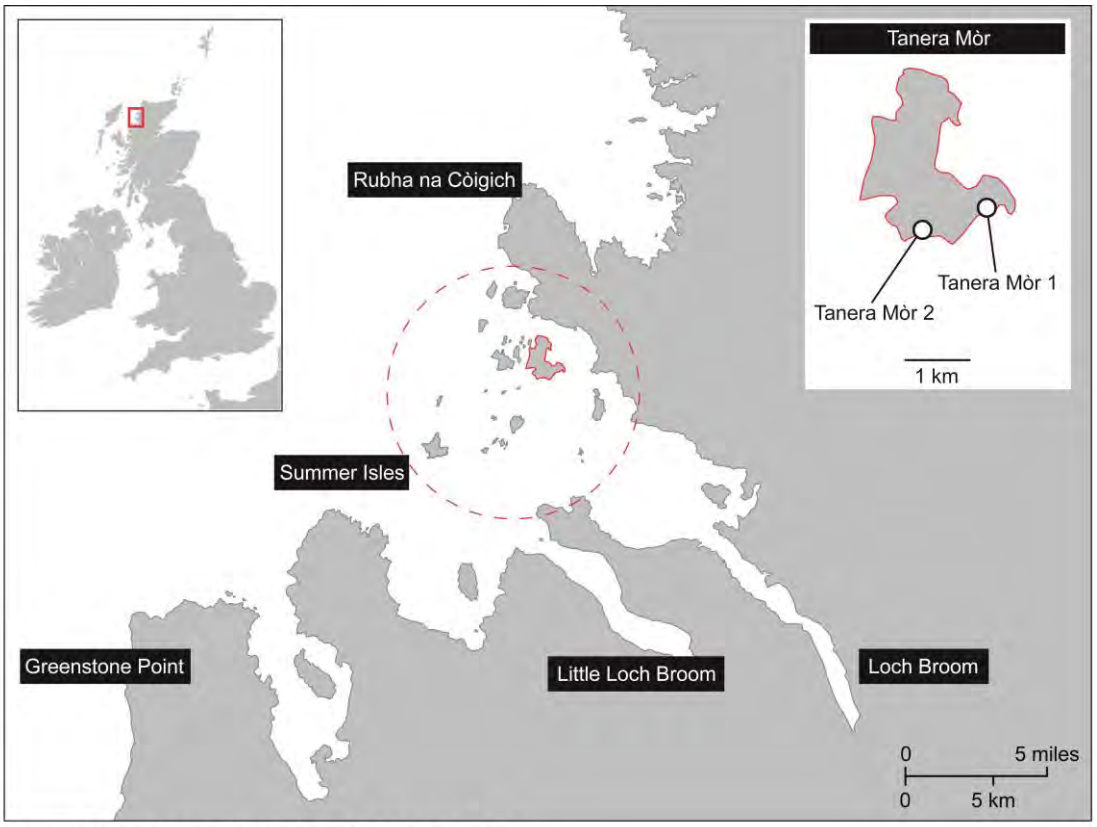

Figure 3.14 Regional context for Tanera Mòr

3.5.1 North western sector: regional tephrostratigraphic context

The North Western sector of Scotland has been the focus of several tephrostratigraphic studies (e.g. Roberts 1997; Davies et al. 2001; Pyne'O-Donnell 2005; 2007; 2011; Ranner et al. 2005; Weston 2012; Callicott 2013; Figure 3.15) On the Summer Isles, a number of Bachelors and Masters dissertations have been undertaken at Royal Holloway, University of London. Studies conducted prior to, and during the early phases of this research are presented below, with the more recent study conducted by Valentine (2015) being presented in Chapter 10 (section 10.3.3.1). The reason for this distinction is based on the emerging results of this study and the influence it had on the work of Valentine (2015).

3.5.1.1 Isle of Skye

Two sites have been studied on Skye as part of the regional tephrostratigraphic framework of Scotland: Loch Ashik (57.241231 -5.829669) and Druim Loch (57.397089 -6.1749). Both palaeolacustrine sequences have been studied in great detail using

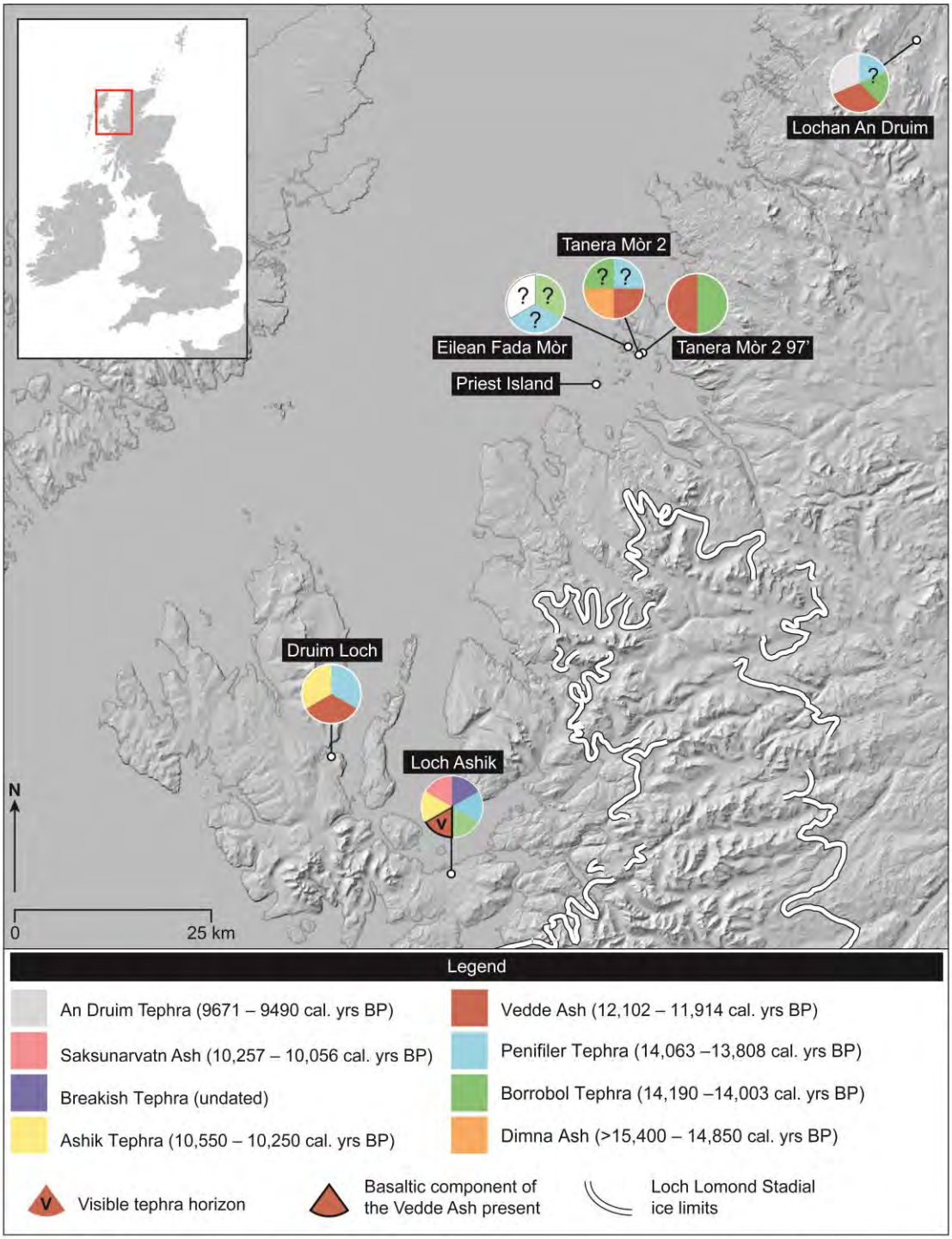

Figure 3.15 Distribution of sites in western Scotland that have been examined for LGIT aged tephras. Stratigraphic uncertainty concerns the finding of shards exhibiting a Borrobol-type morphology at Eilean Fada Mòr (Callicott 2013) and Tanera Mòr 2 (Weston 2012). At Lochan An Druim a tephra exhibiting Borrobol-type chemistries was identified within Windermere interstadial sediments, however the site age model gives a much younger age than would be expected for both the Borrobol and Penifiler tephra's (Ranner et al. 2005; Lind et al. 2016).

standardised scan and resample strategies (see section 2.4.1) (Pyne-O'Donnell 2005; 2011). Loch Ashik, on the south of Skye has been examined by several authors (Davies et al. 2001; Matthews 2002; Davies 2003; Pyne-O'Donnell 2005; Pyne-O'Donnell 2007; Pyne-O'Donnell et al. 2008; Pyne-O'Donnell 2011; Brooks et al. 2012) in part driven by the rare occurrence of a visible (macroscopic) ash layer identified at

the site by Davies et al. (2001). The six cores best representing the Loch Ashik sequence are shown in Figure 3.16, and what is clearly discernible is that not one core represents the 'complete' tephrostratigraphy of the site. This was one of the major conclusions of Pyne-O'Donnell (2005; 2011), who advocated that a multi-core approach should be undertaken to fully understand site tephrostratigraphies.

The basal tephra found across eighteen of the twenty cores extracted from Loch Ashik by Pyne-O'Donnell (2005; 2011) returned chemistries of 'Borrobol-type' affinity, however, the stratigraphic placing of this horizon, i.e. above an LOI downturn thought indicative of GI-1d, led Pyne-O'Donnell (2005; 2007) to conclude that this was a new tephra, distinct from the Borrobol Tephra which shares the same chemical signature (Turney et al. 1997). This was later independently confirmed at the site by the discovery of the Penifiler and Borrobol Tephras within a deeper core, extracted and analysed as part of Brooks et al. (2012; Figure 3.16 E). What is particularly significant about the finding of the Penifiler at Loch Ashik, and what has eluded authors at other sites, is the identification of a basaltic component (Pyne-O'Donnell 2005; Pyne-O'Donnell et al. 2008; Figure 3.16 D). This basaltic fraction, which correlates to the Katla system, was identified in three cores in conjunction with the rhyolitic fraction, but only in one were the concentrations deemed significant for chemical analysis (Figure 3.16 D). There is some suggestion therefore that the shards were relocated from the overlying Vedde Ash layer during coring, however, such conclusions remain equivocal (Pyne-O'Donnell 2005). The Vedde Ash was identified in the overlying stadial clays, and is noteworthy at Loch Ashik for two reasons: 1) it was, and remains, the only reported incidence of this tephra as a macroscopic ash layer in the British Isles (Davies et al. 2001); and 2) the horizon is represented by both rhyolitic and basaltic end members of the tephra, thus it is one of only two sites in the British Isles with the more basic fraction (Figure 3.16).

Within the sediments of the early Holocene a second new tephra for LGIT aged sequences was identified in the Loch Ashik basin by Pyne-O'Donnell (2005; 2007). The Ashik Tephra, as it was termed, has a bi-modal composition of rhyolitic shards thought to have derived from Torfajökull, and a basaltic component indicative of the Grímsvötn system. To date, however, the tephra remains limited in extent to sites in western and central Scotland (Pyne-O'Donnell 2007; MacLeod 2008). Two additional Holocene tephras have been chemically characterised at the site, the basaltic Saksunarvatn Ash from two cores (Figure 3.16 E), and a rhyolitic tephra possessing unusually high concentrations of TiO_2, FeO and CaO, identified in a single core from a neighbouring basin (Figure 3.16 A). Termed the Breakish Tephra, this layer

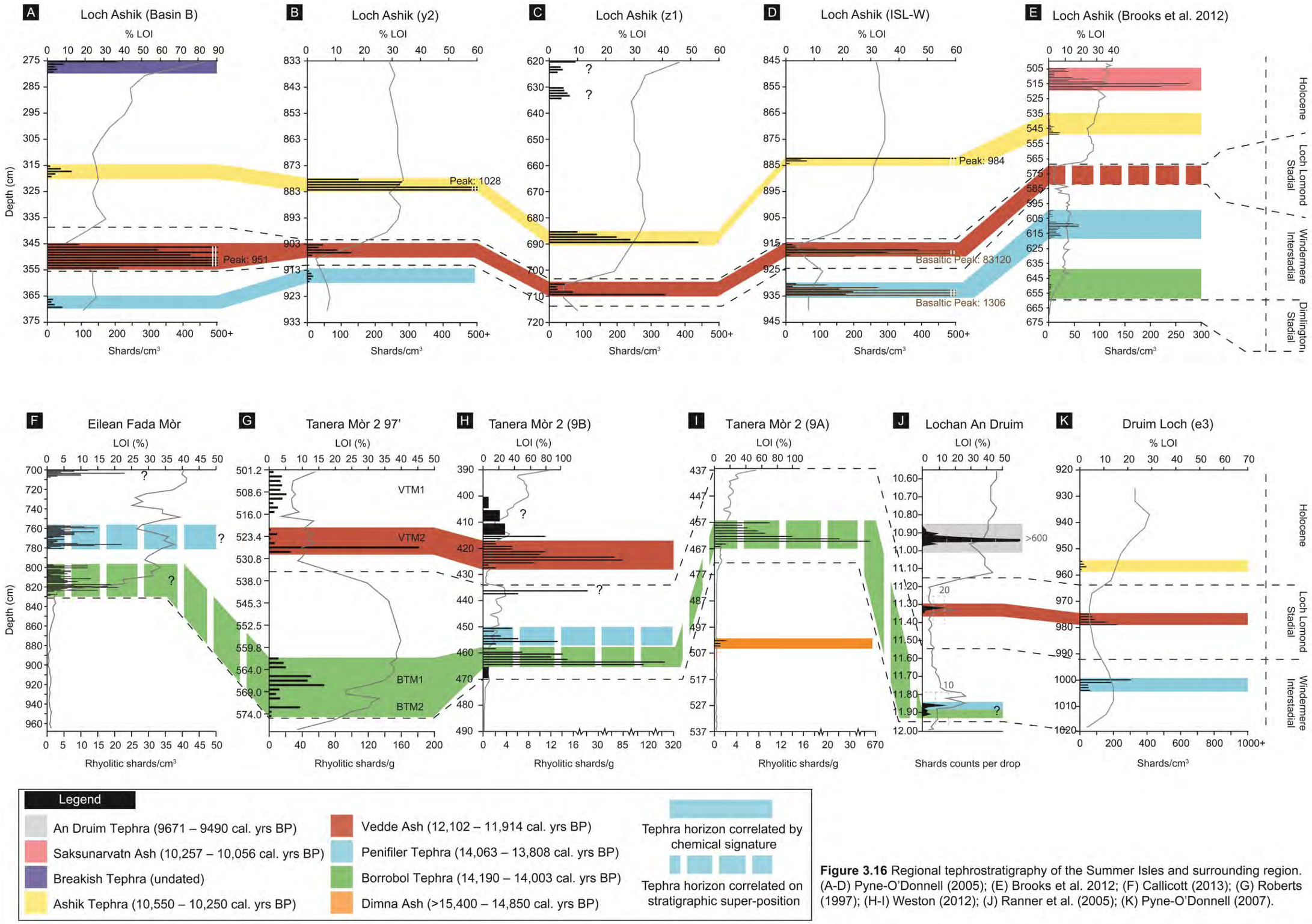

Figure 3.16 Regional tephrostratigraphy of the Summer Isles and surrounding region. (A-D) Pyne-O'Donnell (2005); (E) Brooks et al. 2012; (F) Callicott (2013); (G) Roberts (1997); (H-I) Weston (2012); (J) Ranner et al. (2005); (K) Pyne-O'Donnell (2007).

is unique for sequences in NW Europe during the LGIT, with the only known tephra exhibiting a similar chemical composition being the Glen Garry Tephra, a correlative too young to be credible (Lowe et al. 2016).

It is worth noting that several 'unknown' tephras were highlighted in the Loch Ashik sequence in addition to these chemically characterised horizons. These silicic tephras reside in cores above the Ashik Tephra, with an example presented in Figure 3.16 C. Pyne-O'Donnell (2005) attributes these to reworking; however, in light of recent developments with early Holocene tephras in Scotland and NW Europe (e.g. Lind and Wastegård 2011; Lind et al. 2013; MacLeod et al. 2015; Kelly et al. 2016), it is likely that these tephras may offer new tephrostratigraphic links and should be re-investigated.

A similar, but less extensive suit of tephras has been identified at Druim Loch as at Loch Ashik (Pyne-O'Donnell 2005; 2007; 2011). The rhyolitic component of the Penifiler Tephra, and the Vedde Ash were identified, along with both the rhyolitic and basaltic components of the Ashik Tephra (Figure 3.16 K).

3.5.1.2 Summer Isles

Three tephrostratigraphic studies in the Summer Isles have been undertaken by various authors prior to the results of this study being finalised. An initial examination of the archipelago was undertaken by Roberts (1997) in which a single basin, Tanera Mòr 2 referred to as TM2 '97 in this study, yielded tephras of LGIT age (Figure 3.16 G).

Four peaks were identified in the sequence using scan and resample strategies, and were initially classified by their morphological characteristics; BTM1 and BTM2 referring to 'Borrobol Tephra', and VTM1 and VTM2 referring to 'Vedde Tephra'. Only three of these were successfully analysed: BTM1 and 2 returned Borrobol-type chemistries and VTM2 correlated to the Vedde Ash (Roberts 1997; Roberts et al. 1998; Wastegård et al. 2000a). Roberts (1997) assigned both BTM peaks to the Borrobol Tephra, which at the time was the only known eruption bearing this chemical signature, but noted the horizon's stratigraphically diffuse profile (Roberts et al. 1998). A re-evaluation of tephra sites in Scotland by Pyne-O'Donnell et al. (2008) commented on the occurrence of a 'doubled-peaked' Borrobol in several records, and suggested TM2 97' fitted with this model. However, more recent work by Lind et al. (2016) has suggested this secondary peak i.e. BTM1 (Figure 3.16 G) may be more indicative of the Penifiler, although correlations remain ambiguous.

A reinvestigation of Tanera Mòr was conducted by Weston (2012) on two cores from TM2 (Figure 3.15), a different basin to that of Roberts (1997). Several peaks within the stratigraphy were identified using standard scan and resample strategies, and two horizons were successfully analysed (Figure 3.16). Correlations can be made with the sequence from Roberts (1997), chemically via the Vedde Ash, and stratigraphically using the morphological similarities of TM2 9A 464 and TM2 9B 463 with that of the Borrobol Tephra (BTM1 and 2) as identified in TM2 '97. However, the most significant finding of Weston (2012) was the discovery of a horizon below the hypothesised Borrobol Tephra. This horizon was successfully analysed and returned chemistries indistinct from the Dimna Ash, a tephra which has previously only been identified in Norway, and one that exhibits a minimum radiocarbon age of 15,400-14,850 cal. BP (Koren et al. 2008).

Work on the neighbouring Island of Eilean Fada Mòr (Figure 3.15) was conducted by Callicott (2013). Three groupings of tephra were identified within a composite stratigraphy, with each grouping exhibiting multiple peaks (Figure 3.16 F). An unclear lithostratigraphy has meant that tentative correlations can only be made on the basis of optical analysis. This reveals populations dominated by colourless blocky shards with an abundance of microlitic inclusions. Such morphologies are indicative of LGIT aged Borrobol-type deposits, and so possible correlations to the Borrobol and Penifiler could be made, however the uppermost horizon remains a mystery (Figure 3.16 F).

3.5.1.3 Sutherland

Lochan An Druim (58.475 -4.685556) is the most northerly site in mainland Britain to have yielded tephras of LGIT age (Ranner 2005; Ranner et al. 2005). The details of this tephrostratigraphy are given in section *3.4.1.2*.

3.5.2 North western sector: the geology of the Summer Isles

The study region is part of the Hebridean terrane, one of five geological terranes which comprise mainland Scotland (Trewin 2002). A gneissose Archaean to Palaeoproterozoic rock (the Lewisian Complex) forms the basement of the region. This is overlain by coarse Torridonian sandstone of Neoproterozoic age, which dominates the landscape and forms many of the local mountains e.g. Ben Mór Coigach, and Beinn Ghobhlach (Figure 3.17). In places carbonate marine shelf deposits of Cambro-Ordovician age also occur (Park et al. 2002). The Summer Isles in particular are composed of Neoproterozoic sandstones of the Aultbea and Applecross Formations (Figure 3.17). It seems unlikely therefore that geological contamination is a risk for tephra studies at the site (MacLeod and Davies 2016).

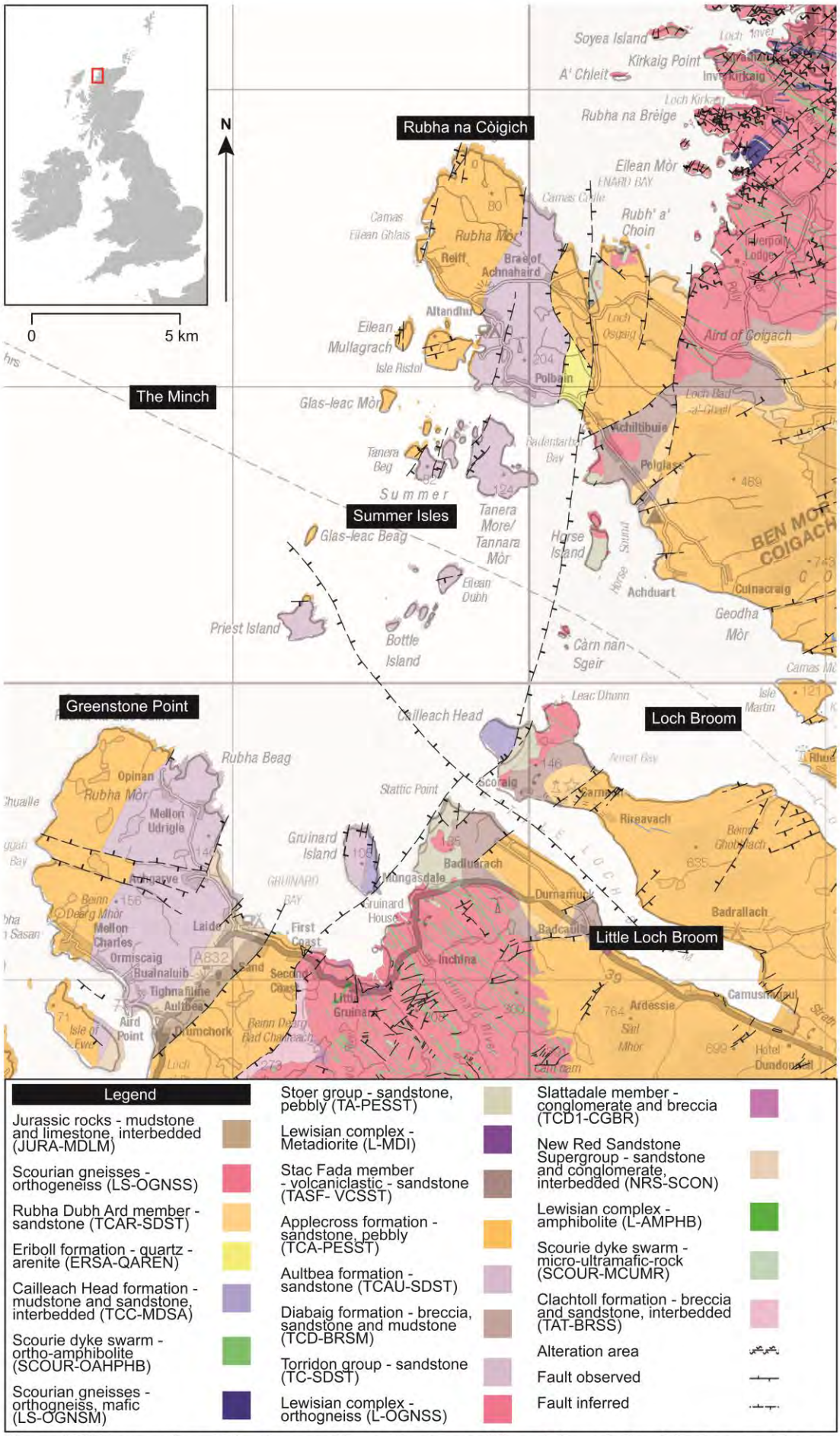

Figure 3.17 Base geology of the Summer Isles region. Tanera Mòr and the majority of the Summer Isles are composed of Neoproterozoic sandstones of the Aultbea and Applecross Formations (Trewin 2002).

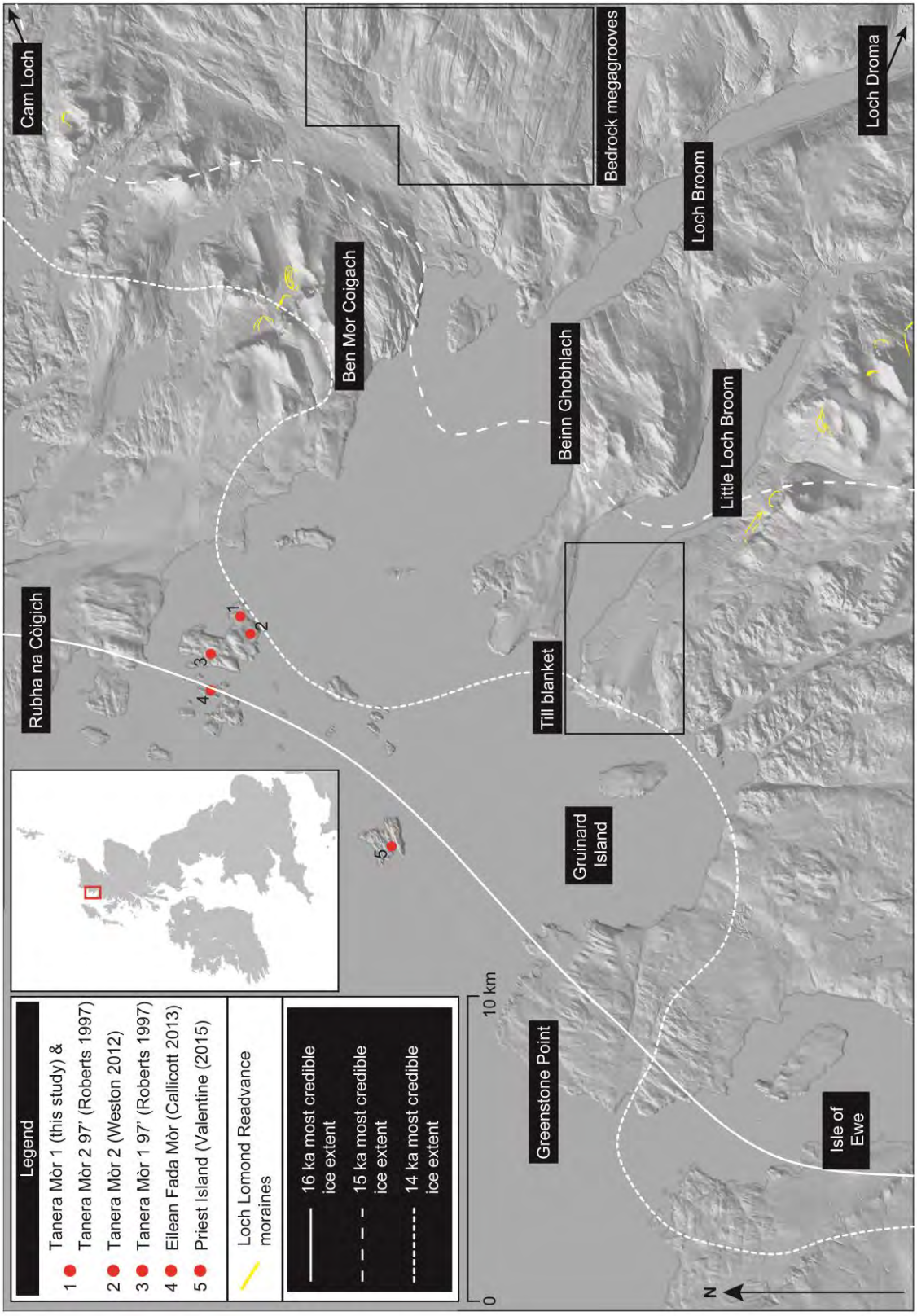

Figure 3.18 Glaciological features of the Summer Isles region as recognised in Bradwell et al. (2007), Stoker et al. (2009) and Bickerdike et al. (2016). The pattern of Dimlington ice retreat is based on the 'most credible' ice extent from Hughes et al. (2016).

3.5.3 North western sector: glacial history and deposits of the Summer Isles

The northwest of Scotland exhibits a classic fjord landscape, indicative of repeated and prolonged glacial incision (e.g. Stoker et al. 1994). In the Summer Isles region, the remnant topography shows a strong imprinting of glacial erosion (bedrock megagrooves), and streamlined subglacial deposits (till blankets) (Stoker et al. 2009; Figure 3.18). During the most recent glaciation, the area was host to the Minch palaeo-ice stream, which crossed the continental shelf and dominated the northwestern sector of the BIIS (Stoker and Bradwell 2005; Bradwell et al. 2007; Stoker et al. 2009). The deglaciation and rate of ice retreat in this sector, and in Scotland as a whole, is one that has proven controversial in recent years (e.g. Ballantyne and Stone 2012). The traditionally held view of complete deglaciation in Scotland during the Windermere Interstadial (e.g. Sissons 1977; Sutherland 1984) has been questioned by a number of authors in light of new geomorphological and cosmogenic-isotopic evidence (e.g. Everest and Kubik 2006; Golledge et al. 2007; Bradwell et al. 2008). Studies by Bradwell et al. (2008), Stoker et al. (2009) and Ballantyne et al. (2009) in the Summer Isles region have yielded results suggesting the pattern of ice recession was substantially more dynamic than previous hypotheses proposed, and crucially have provided much younger ages for deglaciation than existing radiocarbon chronologies at Loch Droma and Cam Loch would suggest (Kirk et al 1963; Pennington et al. 1972; Pennington, 1977). This led Bradwell et al. (2008), and Stoker et al. (2009) to conclude that substantial and dynamic ice caps persisted in the region in the Windermere Interstadial (ca. 14.0-13.0 kyrs).

This model has been challenged by Ballantyne and Stone (2012) who argue that if cosmogenic ages are recalibrated, and additional geomorphological, palynological, tephrostratigraphical and radiocarbon evidence is considered, than the Bradwell and Stoker model of deglaciation is highly improbable. Further recalibration of cosmogenic dates in the region has been conducted by Hughes et al. (2016) in their extensive review of the last Eurasian ice sheets. The time-slices produced as part of this study are shown in Figure 3.18 and 3.19, and agree more consistently with the greater regional evidence (see above), and traditionally held view of lowland and coastal deglaciation prior to, and during the early phases of the Windermere Interstadial.

During the Loch Lomond Readvance several small corrie glaciers formed in the higher areas surrounding the Summer Isles region (Figure 3.18) e.g. Ben Mór Coigach (Sissons 1977) Beinn Dearg Bheag and Beinn Dearg Mòr (Sissons 1977; Ballantyne 1987). Whilst the main Loch Lomond Stadial ice sheet stalled just to the south in the vicinity of Loch na Sheallag (Bennet 1991; Bickerdike et al. 2016).

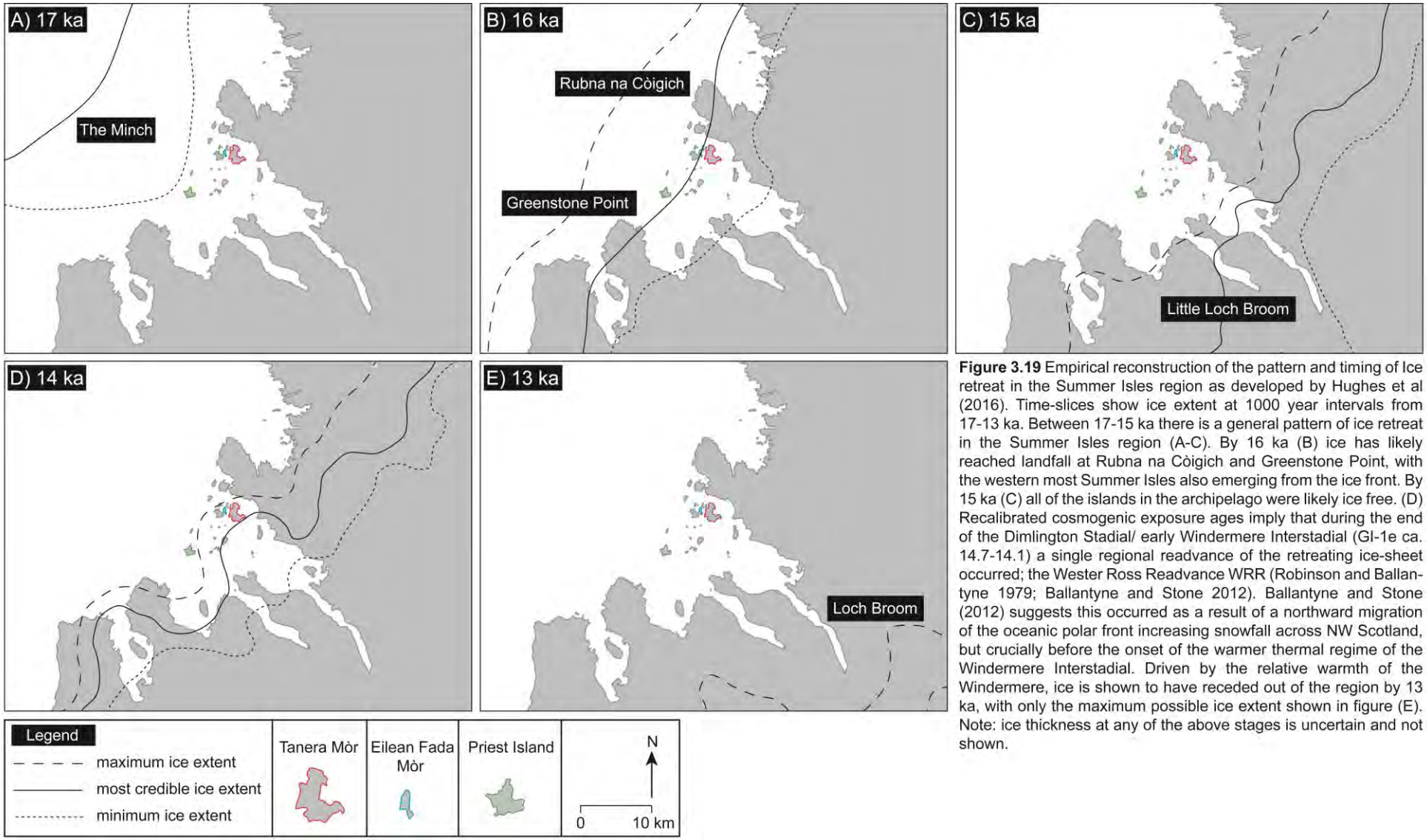

Figure 3.19 Empirical reconstruction of the pattern and timing of Ice retreat in the Summer Isles region as developed by Hughes et al (2016). Time-slices show ice extent at 1000 year intervals from 17-13 ka. Between 17-15 ka there is a general pattern of ice retreat in the Summer Isles region (A-C). By 16 ka (B) ice has likely reached landfall at Rubna na Còigich and Greenstone Point, with the western most Summer Isles also emerging from the ice front. By 15 ka (C) all of the islands in the archipelago were likely ice free. (D) Recalibrated cosmogenic exposure ages imply that during the end of the Dimlington Stadial/ early Windermere Interstadial (GI-1e ca. 14.7-14.1) a single regional readvance of the retreating ice-sheet occurred; the Wester Ross Readvance WRR (Robinson and Ballantyne 1979; Ballantyne and Stone 2012). Ballantyne and Stone (2012) suggests this occurred as a result of a northward migration of the oceanic polar front increasing snowfall across NW Scotland, but crucially before the onset of the warmer thermal regime of the Windermere Interstadial. Driven by the relative warmth of the Windermere, ice is shown to have receded out of the region by 13 ka, with only the maximum possible ice extent shown in figure (E). Note: ice thickness at any of the above stages is uncertain and not shown.

Figure 3.20 Topographic map of the Summer Isles illustrating the position of key sites mentioned in text.

3.5.4 North western sector: Tanera Mòr

3.5.4.1 Site description

The Summer Isles archipelago is located between the headlands of Rubha Còigeach and Greenstone Point, and lies within the Minch, a water body that separates the Western Isles from the NW Scottish mainland (Figure 3.20). The archipelago consists of four main islands: Tanera Mòr which is the largest (~3.04 km^2), along with Tanera Beg, Priest Island and Horse Island; numerous other small islands and skerries also occur within the area, for example Eilean Fada Mòr. Sites in the Summer Isles were initially surveyed between 1980-1986 by D. Shirley, and then again by a group from London Guildhall University in September 1994. It was from these cores that Roberts (1997) identified two sequences yielding LGIT aged deposits, one from Tanera Mor (TM2 97') and one from Eilean Fada Mor (EF1 97'), with only the former being examined for tephra. The islands were re-cored by a team from Royal Holloway in the summer of 2011, from which the studies of Weston (2012) and Callicott (2013) were derived. As part of Royal Holloway's investigation TM2 97' was re-examined and given the site coding of TM1 in this study (Figure 3.20). The basin (58.006156, -5.393478) is an infilled isolation basin lying at an altitude of 14 m O.D and covers an area of 7000 m^2; the catchment of the basin is considered to be minimal, with no observable inflows.

3.5.4.2 Previous work

A study of the basin by Roberts (1997) revealed a 6.36 m sequence, with the lower 1.59 m covering the LGIT (Figure 3.21). Nine lithological units were identified between 4.36-6.36 m, with a notable LOI oscillation occurring within the Windermere Interstadial at 5.65-5.70 m, and further oscillations associated with the Loch Lomond Stadial. No previous palaeoenvironmental work has been conducted on the basin, and the results from the previous tephrostratigraphic studies are summarised in section *3.5.1.2*.

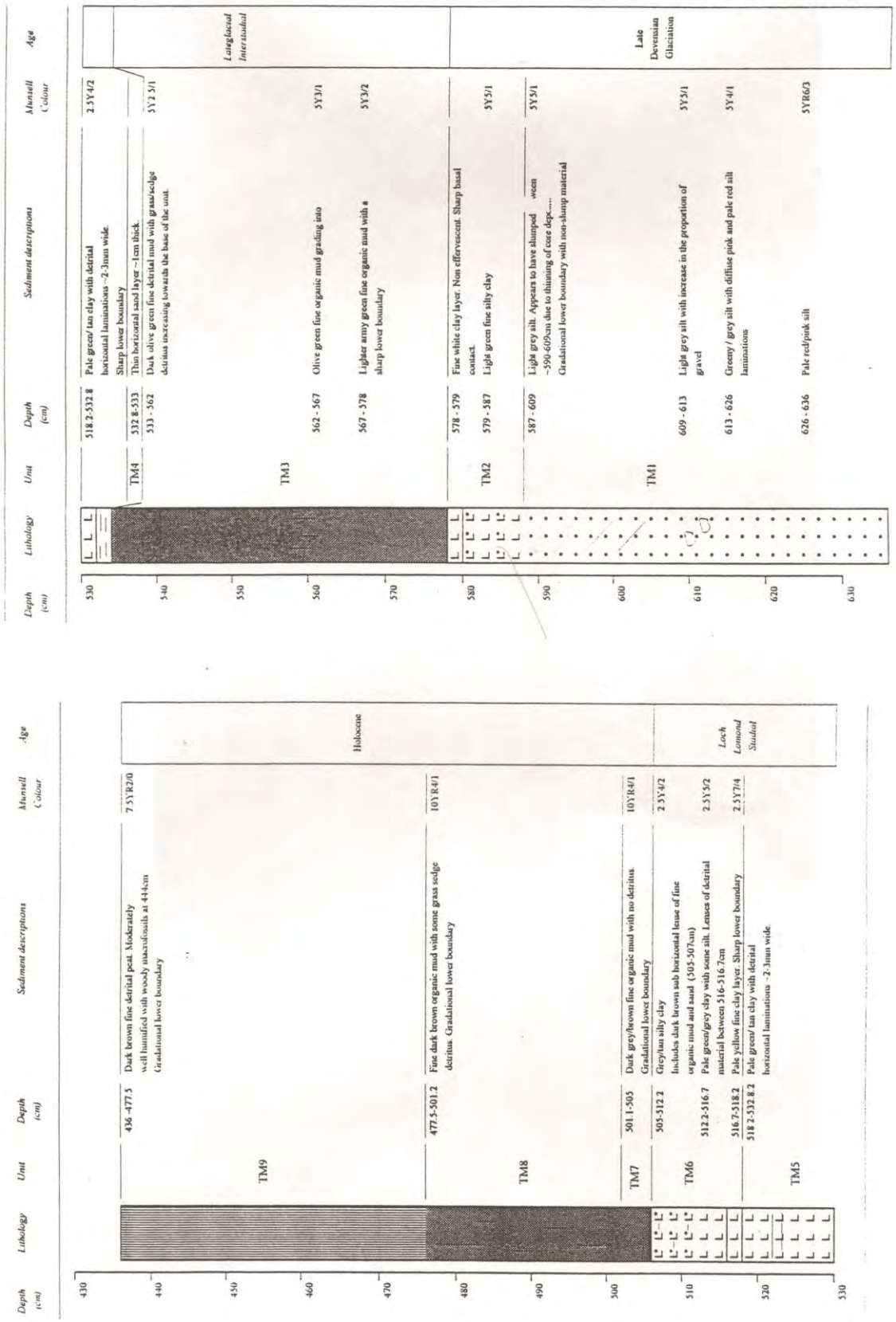

Figure 3.21 Core stratigraphy from TM2 97'(Roberts 1997). The sequence exemplifies a typical Scottish LGIT sedimentological profile.

3.6 The south western sector

The South Western sector of Scotland (Figure 3.2) is relatively understudied in both palaeoenvironmental and tephrostratigraphic contexts. This fact alone makes it an important locale to consider; however, it is the proximity to Northern Ireland which makes it particularly relevant here. As noted in section 3.2 there seems to be a strong regional disparity between Scotland and Ireland in terms of tephras, which henceforth requires further investigation. It was decided that the site of Little Lochans, located within the Stranraer isthmus would be examined as part of this project (Figure 3.22). The site has previously only been investigated by Moar (1969b), who conducted a regional palynological assessment of LGIT and early Holocene basins within the area.

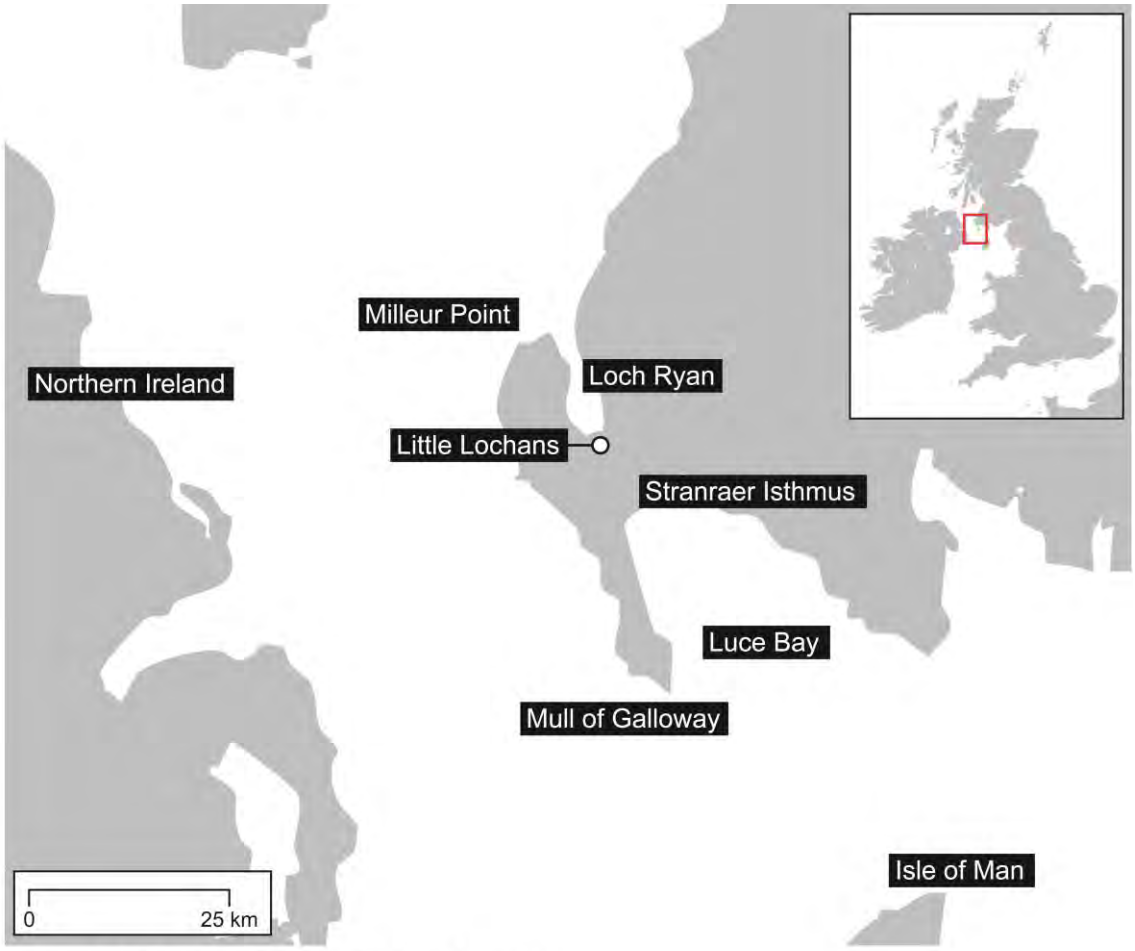

Figure 3.22 Regional context for Little Lochans

3.6.1 South western sector: regional tephrostratigraphic context

Whilst central and northern regions of Scotland have undergone extensive study into the distribution and preservation of tephras within lacustrine palaeoclimate records dating from the LGIT, the rest of the British Isles has not been examined in such detail. Figure 3.23 illustrates the distribution of sites in southern Scotland, northern

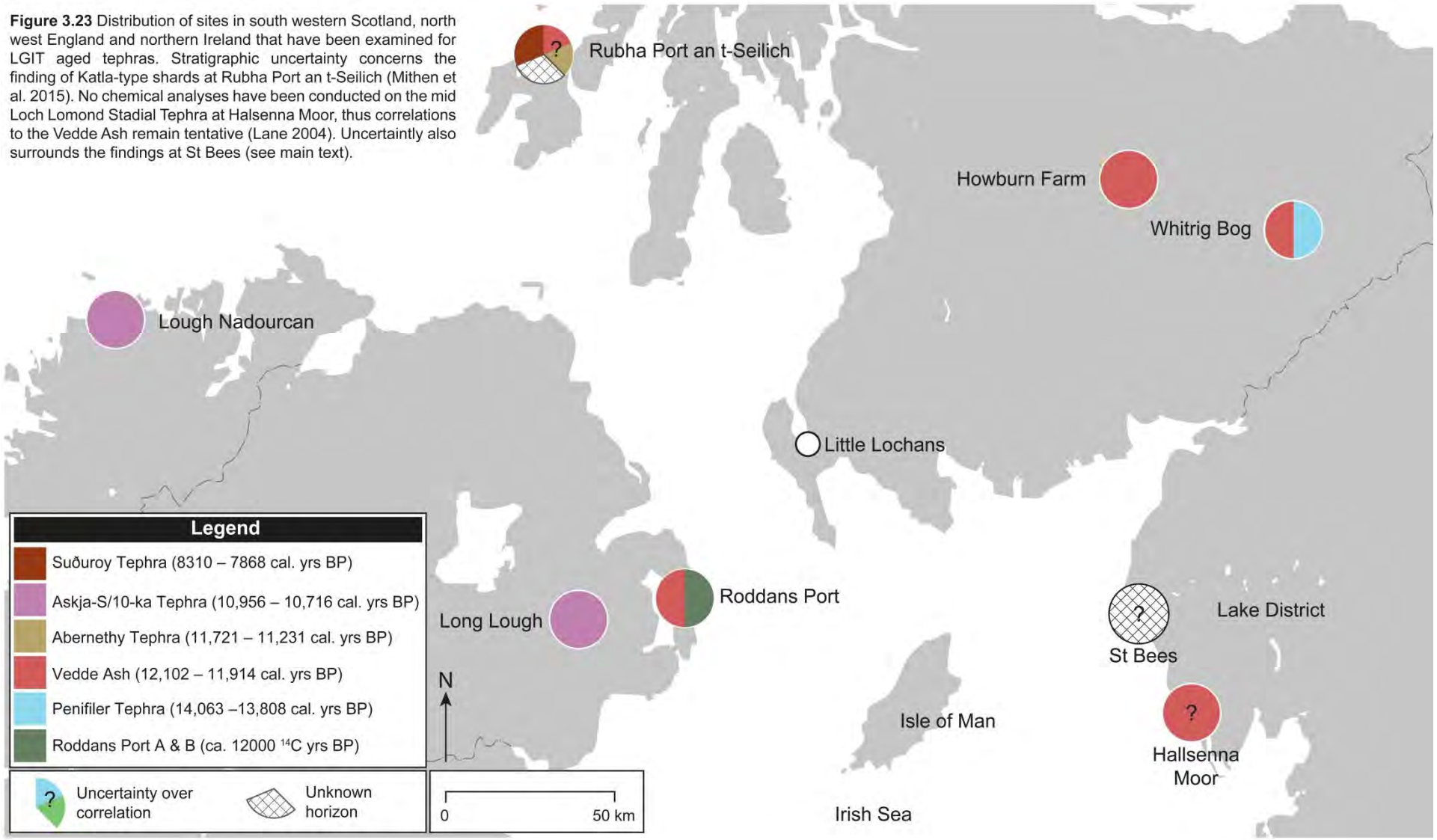

Figure 3.23 Distribution of sites in south western Scotland, north west England and northern Ireland that have been examined for LGIT aged tephras. Stratigraphic uncertainty concerns the finding of Katla-type shards at Rubha Port an t-Seilich (Mithen et al. 2015). No chemical analyses have been conducted on the mid Loch Lomond Stadial Tephra at Halsenna Moor, thus correlations to the Vedde Ash remain tentative (Lane 2004). Uncertaintly also surrounds the findings at St Bees (see main text).

Ireland and northern England, including locations where tephras have been searched for but not identified.

3.6.1.1 Southern Scotland

The tephrostratigraphy of southern Scotland is composed of three sites; Rubha Port an t-Seilich (55.831219, -6.104678), Howburn Farm (55.672778, -3.483611), and Whitrig Bog (55.60715, -2.602814) (Figure 3.23). Rubha Port an t-Seilich, an archaeological site, marks the most south-westerly location in Scotland to have returned tephras of LGIT age (Mithen et al. 2015). Two Katla-derived horizons were identified, which are separated by a tephra that bears some chemical affinity to the Borrobol-type tephras, and to tephras which are thought to derive from Snæfellsjökull (Mithen et al. 2015). Whilst it is commonly recognised that four tephras of Katla provenance have been identified in terrestrial sequences during the LGIT (Lane et al. 2012b), as many as twelve rhyolitic layers from Katla may have been identified in sedimentary environments around the North Atlantic margin during this period (Table 2.3). However, problems associated with stratigraphic discrimination, and poor age control, prevents reliable quantification of this number. A similar scenario is true for the Borrobol-type tephras and Snæfellsjökull-derived horizons, with as many as eight and two layers identified, respectively (Lind et al. 2013; 2016). With limited stratigraphic information and radiocarbon dates only constraining the upper portions of the profile, i.e. above the tephras, only tentative correlations can be made. The authors suggest a correlation to the Vedde and the Suðuroy for the two Katla horizons (Figure 3.24 J), but refrain from suggesting a correlative for the intersecting horizon.

Howburn Farm, like Rubha Port an t-Seilich is an archaeological site (Housley et al. 2014; Tipping et al. 2016). Relatively high concentrations of shards have been identified within the profile, but as yet only limited analyses have been undertaken. A secondary peak in shard concentration within a long and contiguous distribution of shards, has returned chemistries indicative of Katla rhyolites (Figure 3.24). An inference was made based upon sedimentological characteristics that the horizon identified was that of the Vedde Ash, but as noted above, caution must be exhibited where only single horizons characterise site tephrostratigraphies. Whitrig Bog marks the most southerly tephra-bearing site in Scotland and has been examined initially by Turney et al. (1997), and again by Pyne-O'Donnell et al. (2008). The results of the two studies are shown in Figure 3.24 (F,G) and show markedly different tephra concentrations and distribution profiles. Turney et al. (1997), guided by work elsewhere in Scotland, focused on two intervals of the Whitrig Bog stratigraphy that were thought to be representative of the early-Windermere Interstadial, and Loch

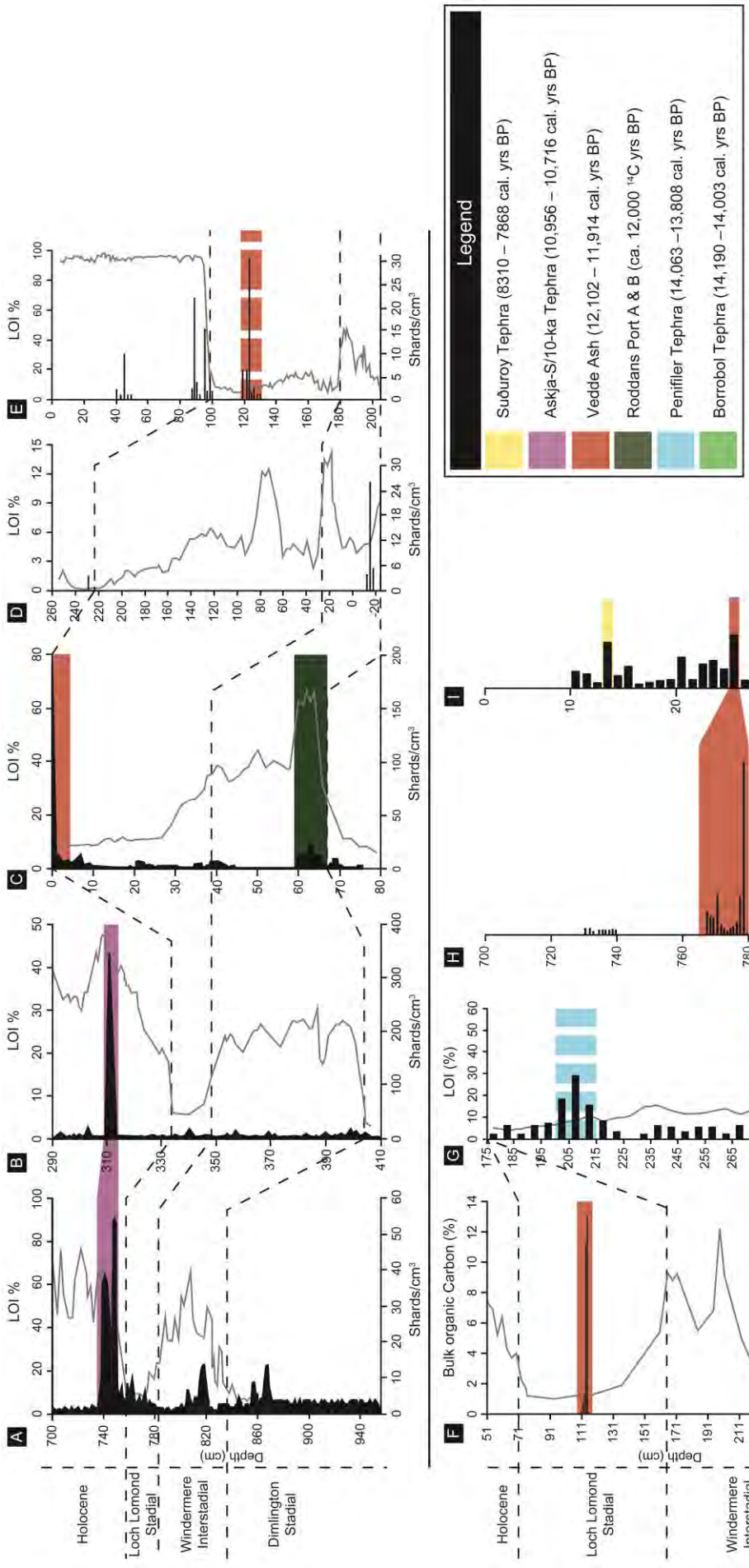

Figure 3.24 Regional tephrostratigraphy. (A) Lough Nadourcan (Turney et al. 2006); (B) Long Lough (Turney et al. 2006); (C) Roddans Port (Turney et al. 2006); (D) St Bees (Lane 2004); (E) Hallsenna Moor (Lane 2004); (F) Whitrig Bog (Turney et al. 1997); (G) Whitrig Bog (Pyne-O'Donnell et al. 2008); (H) Howburn Farm (Housley et al. 2014; Tipping et al. (2016); (I) Rubha Port an t-Seilich (Mithen et al. 2015). Solid colour bars represent correlations based on chemical analyses, stripped bars represent correlations based on stratigraphic superposition.

Lomond Stadial (Turney et al. 1997; Turney 1998a). The study identified two tephras, the Vedde Ash and the Borrobol Tephra. Subsequent work by Pyne-O'Donnell et al. (2008) identified an additional peak within mid-Interstadial sediments and is correlated to the Penifiler Tephra on the premise of superposition only. Caution must be exhibited with this interpretation as a consistent background of shards was detected throughout the profile (Figure 3.24 G).

3.6.1.2 North-west England

In England as a whole, very few sites have been examined for tephra horizons of LGIT age, and even fewer have had tephras identified. Hallsenna Moor (54.390464, -3.443772) was the first site in England to yield LGIT-age tephras. Low resolution (10 cm) scans of the sequence by Matthews (unpublished data) and Lane (2004) revealed the presence of tephra in all intervals covering the 2.0 m sequence. Three peaks revealed by Lane (2004) were refined to 1 cm resolution and are shown in Figure 3.24 (E). Both colourless and brown shards were identified throughout the profile but a failure to obtain chemical analyses has prohibited their chemical classification. It is probable, however, that the lowermost horizon (122-123 cm) relates to the Vedde Ash, as this tephra occurs mid-way through sediments linked to the Loch Lomond Stadial (Walker 2004; Lane 2004). Correlating the other tephras on the premise of superposition is, however, made more difficult by the occurrence of a depositional hiatus at the transition from the Loch Lomond Stadial - Holocene (Walker 2004), thus these tephras remain uncorrelated (Lane 2004). Work at neighbouring St Bees (54.487814, -3.5989) by Wastegård et al. (2000a) and Lane (2004) has been even less conclusive. Wastegård et al. (2000a) were unable to identify any shards within their selective analysis of the Loch Lomond Stadial sediments, and suggest that the sequence may not span the entirety of the stade. However, Lane (2004) was able to identify four distinctive intervals composed of colourless and brown shards (Figure 3.24). Unfortunately chemical analyses of the horizons has had limited success. Based on stratigraphic superposition, therefore, tephras at the base of the sequence have been tentatively correlated to a series of Basaltic tephras previously only identified in North Atlantic marine sites, and dated to ca. 13.4 - 23.5 ^{14}C kyrs (Haflidason et al. 2000; Lane 2004). Tephras within Loch Lomond Stadial aged deposits are considered re-worked, somewhat supporting the conclusions of Wastegård et al. (2000a), whilst those occupying the upper portion of the sequence remained uncorrelated (Lane 2004). Further to the east in the Lake District, analyses of Loch Lomond Stadial aged sediments at Haweswater (54.182539, -2.801606), and an undisclosed section of a sequence from Little Haweswater (54.185528, -2.798722) also failed to return any shards (Wastegård et al. 2000a; Ian Matthews pers. comm. 2016).

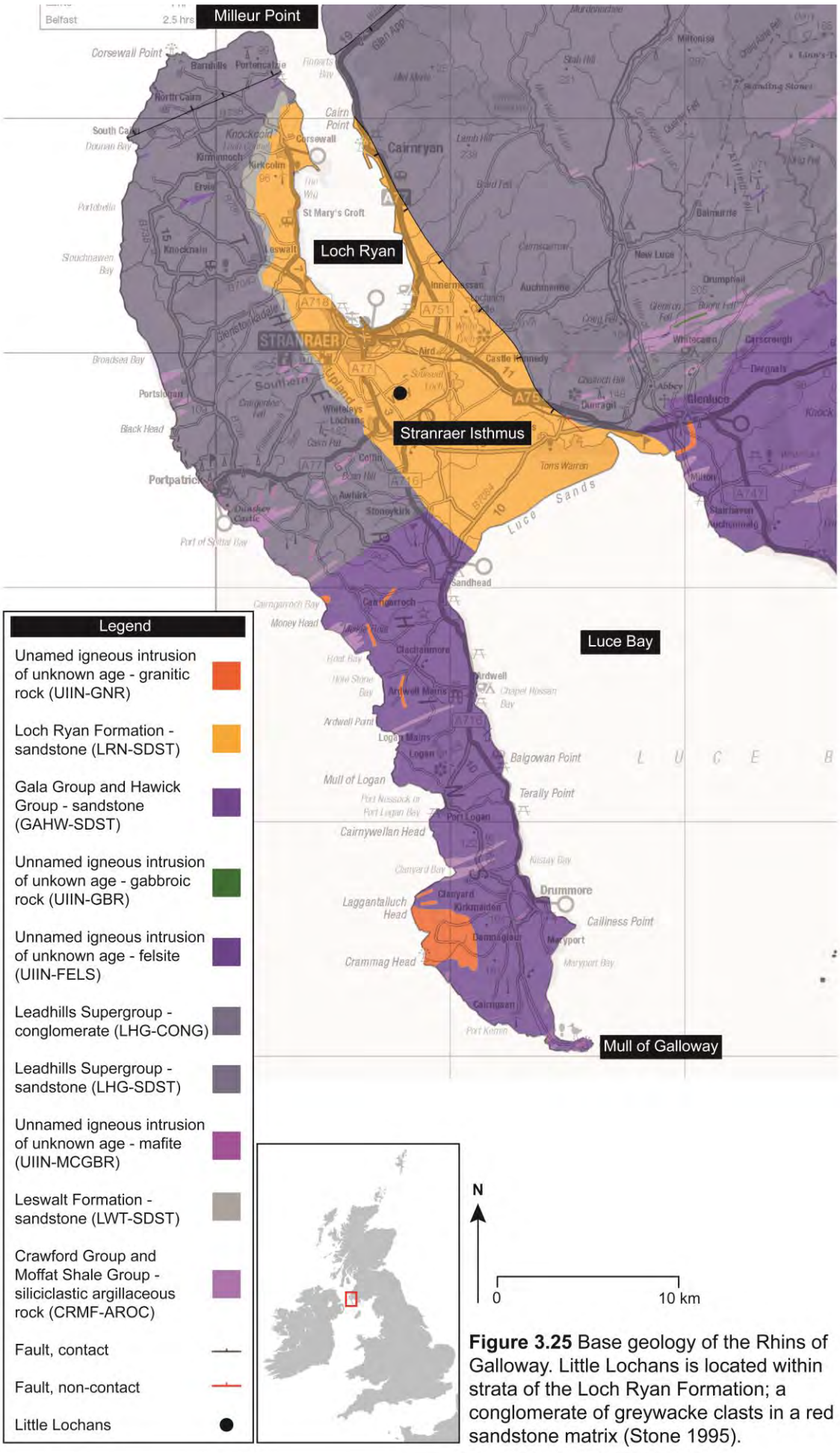

Figure 3.25 Base geology of the Rhins of Galloway. Little Lochans is located within strata of the Loch Ryan Formation; a conglomerate of greywacke clasts in a red sandstone matrix (Stone 1995).

3.6.1.3 Northern Ireland

In Northern Ireland, and indeed Ireland as a whole, there has been relative paucity of LGIT tephra studies when compared to Holocene investigation (e.g. Pilcher and Hall 1992; Swindles et al. 2011). One of the few conducted was by Turney et al. (2006) who identified and examined three sites. The results are presented in Figure 3.24 (A-C), and as illustrated, a consistent 'background' of tephra is observed throughout all profiles. Chemical analyses were conducted at selective 'peaks' within the individual stratigraphies, which revealed several different tephra horizons across the three sites. At Roddans Port (54.516667, -5.5) within the early Windermere Interstadial, a spread of tephra over approximately 6 cm was identified, with analyses of the peak returning a bi-modal rhyolitic population. The two populations have no definite provenance, and were termed the Roddans Port A & B Tephras, which to date remain unique to the study site (Turney et al. 2006). At the top of the sequence a tephra matching the chemical composition of the Vedde Ash was also identified; to date this remains the only confirmed occurrence of the Vedde Ash in Ireland. At Lough Nadourcan (55.05, -7.9), and Long Lough (54.433333, -5.916667) a tephra was identified in early Holocene sediments which correlates to the Askja-S/10ka Tephra. This was the first documented occurrence of the tephra within the British Isles, and despite it prominence in continental Europe (e.g. Davies et al. 2003; Wulf et al. 2016), and within Iceland (Sigvaldason 2002) the distribution of this tephra has remained limited in the British Isles until relatively recently (Kelly et al. 2016). It is worth noting that subsequent work at Lough Nadourcan (Watson et al. 2010) has failed to identify any tephra relating to LGIT-age deposits, suggesting unevenness in preservation at the site.

3.6.2 South western sector: the geology of the Rhins of Galloway

The South Western sector is part of the Southern Uplands, one of five geological terranes which comprise mainland Scotland (Trewin 2002; Stone 1995). The terrane is principally composed of Lower Palaeozoic strata, with the Rhins of Galloway forming the most south-westerly margin; the term Rhins comes from the Gaelic 'rinn' meaning a 'point or promontory' (Stone 1995). The Mull of Galloway marks the most southerly point of the Rhins, and from here the peninsular trends NNE for 45 km to Milleur Point, which marks the most northerly tip (Figure 3.25). The Stranraer isthmus is approximately 10 km wide, and forms a natural barrier between Loch Ryan to the north and Luce Bay to the south (Figure 3.25). This linking belt of land is formed of a coarse breccia called the Loch Ryan Formation, a conglomerate of greywacke clasts in a red sandstone matrix (Stone 1995). Whilst no igneous geology is described from the area, the Stranraer isthmus may have been exposed to glacially transported obsidian from

nearby Arran (MacLeod and Davies 2016). Thus caution should be applied on interpreting any tephrostratigraphic study in the region.

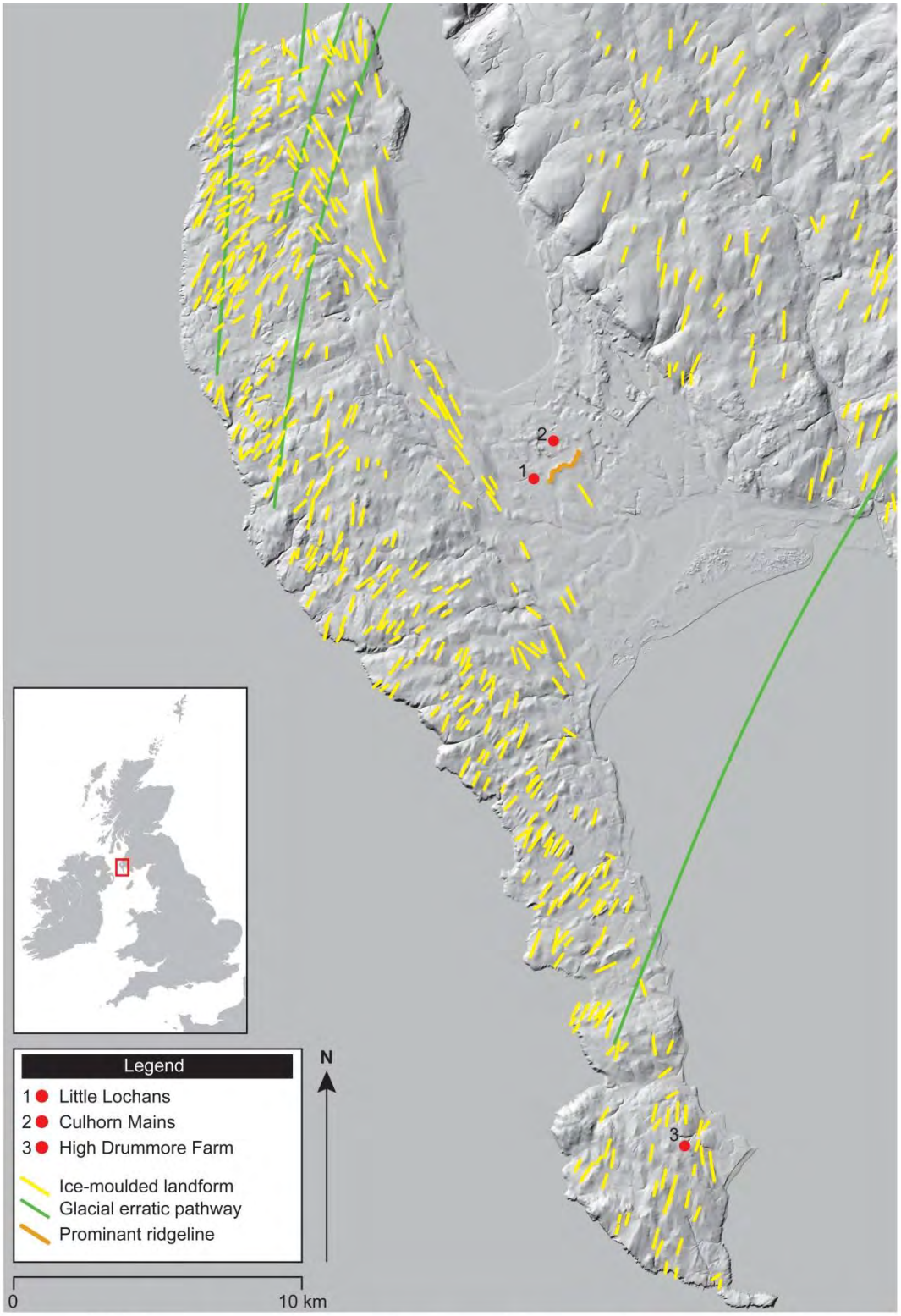

Figure 3.26 Glaciological features on the Rhins of Galloway. The area is noted for its ice moulded landforms. Sites containing sediments of the LGIT are shown in red. A prominent ridgeline near to the Little Lochans site has a debated origin, but likely represents a moranic deposit (Peacock and Everest 2010).

3.6.3 South western sector: glacial history and deposits of the Rhins of Galloway

The glacial history of the region, like many areas of the British Isles continues to be debated. Evidence for glacial activity comes from morphological and sedimentological evidence. The area in particular is noted for its streamlined landforms, and glacial microgranite erratics derived from nearby Ailsa Craig (Figure 3.26). Both lines of evidence have been used to imply major changes in the direction of ice movement across the region during the last glacial phase (Charlesworth 1927a;b; Hill and Prior 1968; Sutherland 1984; Salt and Evans 2004; Hughes et al. 2014). Of particular relevance to this study are the glacial sands and gravels overlying the Stranraer isthmus. These are some of the most extensive in south-west Scotland, with thicknesses of up to 43 m being recorded in certain places (Stone 1995). Kame mounds and kettle holes are numerous across the isthmus, and were deposited as ice receded from the landscape. Many of the kettle holes still exist as lochans, but a large proportion have become terrestrialised through the course of the LGIT and Holocene (e.g. Moar 1969b). Few dates exist in the region to constrain deglaciation, but the peninsular and the eastern Galloway Hills probably became ice free ca. 17-15 kyrs (Hughes et al. 2011; Clark et al. 2012; Ballantyne et al. 2013), and notably prior to the rapid warming and transition from Dimlington Stadial - Windermere Interstadial at ca. 14.7 kyrs (Brooks and Birks 2000; Brooks et al. 2012).

During the Loch Lomond Stadial small cirque glaciers developed in higher areas of the Southern Uplands (Cornish 1981; Ballantyne et al. 2013), and periglacial features have been noted throughout the Rhins district e.g. fossil frost wedges (Moar 1969b; Sissons 1974).

3.6.4 South western sector: Little Lochans

3.6.4.1 Site description

Little Lochans (54.880203, -4.9977) is a small infilled kettle-hole located within the Stranraer isthmus, about 3 km (2 miles) south-east from the centre of Stranraer. The basin lies at 16 m O.D. and is situated approximately 500 m west from the prominent NNE-SSW trending ridgeline described by Peacock and Everest (2010) and assumed part of Charlesworth's (1927 a;b) Lammermuir-Stranraer moraine. A number of other glaciological features can be observed in the surrounding landscape and are depicted in Figure 3.27; these are representative of the dead ice landscape that characterised the area following the last deglaciation. The basin was originally examined by Moar (1969a) who noted that the site has been drained for the improvement of pastoral land, causing a deflation of the peat surface which had then been further exacerbated by the

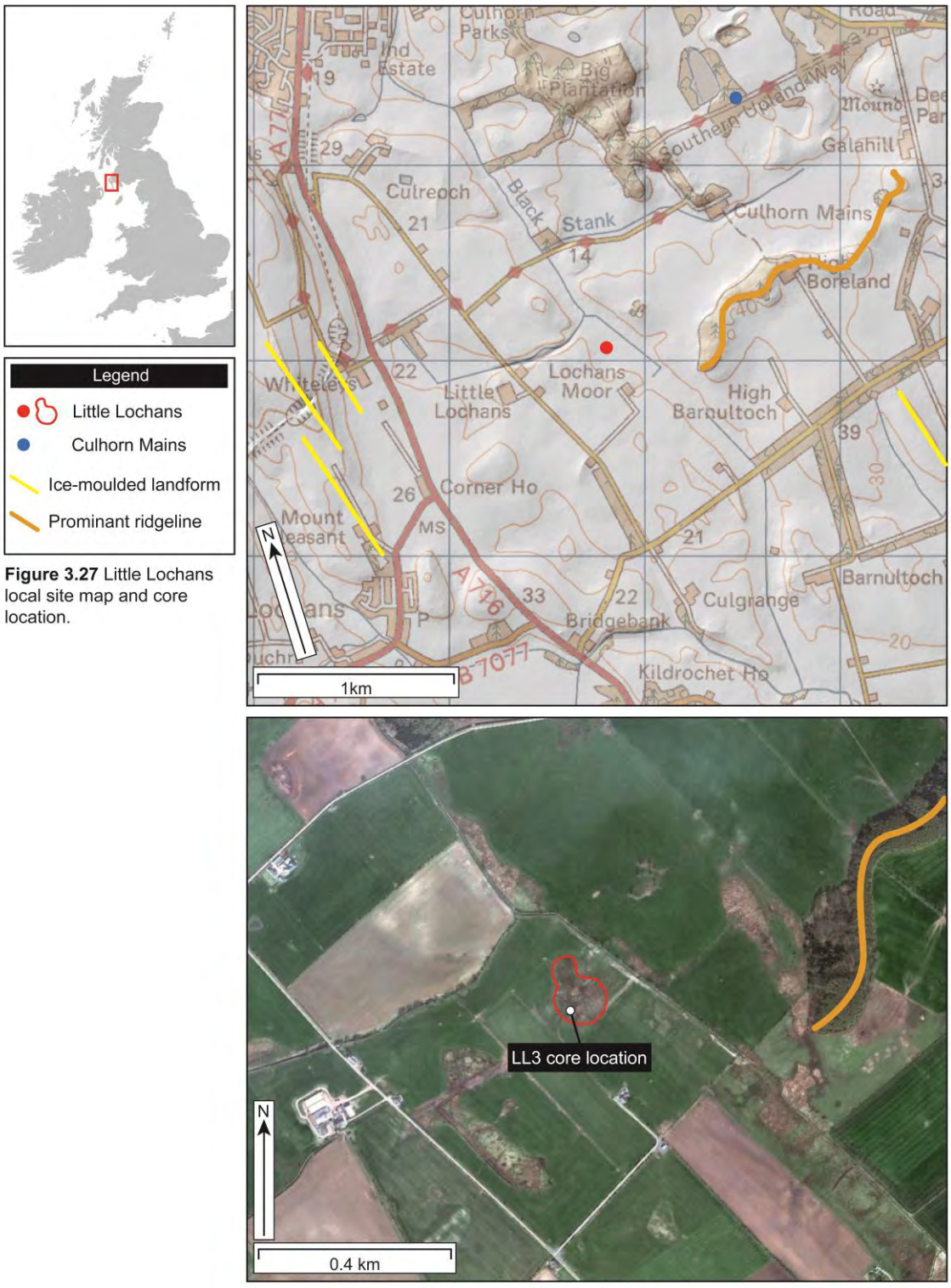

Figure 3.27 Little Lochans local site map and core location.

trampling of cattle. In the early 2000s high voltage power lines were installed through the site, likely causing further disturbance to the underlying sediments.

The catchment of the basin is considered to be minimal, with no observable inflows and a relatively subdued topography surrounding the site (Figure 3.27). Therefore it is likely that sediment accumulation has been derived predominantly from aeolian and overland

flow processes. A measurement of the site's spatial characteristics from aerial imagery suggests that the current perimeter of the site is ca. 450m, measuring 150 x 90 m, and covers an area of ca. 11,500 m^2.

3.6.4.2 Previous work

A study of the basin by Moar (1969b) revealed a 5.50 m sequence, with the lower 1.20 m depicting the classic tri-partite sequence indicative of Scottish LGIT aged deposits (Figure 3.28; Table 3.4). A lithological description shows basal silty-marls grading into purer marls, before a transition into fine detritus muds at 5.0 m. This unit ends abruptly at 4.80 m where it is replaced by a 0.3 m thick unit of clay. Above this the lithology transitions back into fine detritus muds. A palynological analysis shows the site being dominated by herbaceous taxa through all climatic zones e.g. *Gramineae*, *Cyperaceae*, *Rumex*, *Artemisia*; an assemblage that is typical of pioneer communities developing on skeletal soils. Woody taxa are present, but in much lower quantities, oscillations in *Betula* and *Salix* centred on 5.30 m and 4.90 m may be indicative of short lived climatic events but this is difficult to ascertain without higher sampling resolutions and a reporting of the pollen concentration data. A similar sequence is represented at Culhorn Mains (54.891928, -4.988242) leading Moar (1969a) to conclude that both profiles are indicative of the Late Devensian - Holocene transition, with the landscape around the Stranraer isthmus being predominantly treeless up until the early Holocene.

Table 3.4 Sedimentological description of the Little Lochans sequence examined in Moar (1969a).

Depth (cm)	Description
0-35	Disturbed layer
35-135	Dark humified peat
135-380	Dark-brown peat containing small fragments of wood and some *Sphagnum* leaves; fruits of *Betula* cf. *pubescens* and *Carex* utricles were scattered throughout this layer, and at 350-360 cm there were found seeds of *Menyanthes* and one mericarp of *Hydrocotyle vulgaris*.
380-430	Light-brown *Sphagnum* peat; *Betula* cf. *pubescens* fruits occurred at various levels; at 410 cm there were numerous *Carex* nutlets, *Pontentilla palustris* fruits and one stone of *Potamogeton polygonifolius*.
430-450	Dark fine detritus mud; included in this layer there was one seed of *Nymphaea alba*, a few fruits of *Betula pubescens* at 430 cm, one fruit of *Batrachium* type *Ranunculus* and oospores of *Chara*
450-460	Silty mud; nuts of *Myriophyllum* cf. *spicatum*; *Batrachium* type *Ranunculus* fruit, *Carex* nutlets, a few *Sphagnum* leaves and *Nitella* oospores were recovered from this layer.
460-480	Grey silty clay; in this layer there were seeds of *Juncus* spp. and a few leaves of *Polytrichum piliferum*.
480-500	Dark silty mud; a few *Sphagnum* leaves and *Chara* oospores were present.
500-550	Buff-coloured marl, silty near the base; *Carex* utricles, an achene of *Batrachium Ranunculus* and numerous oospores of *Chara* spp. were recovered; boulder clay at 550 cm.

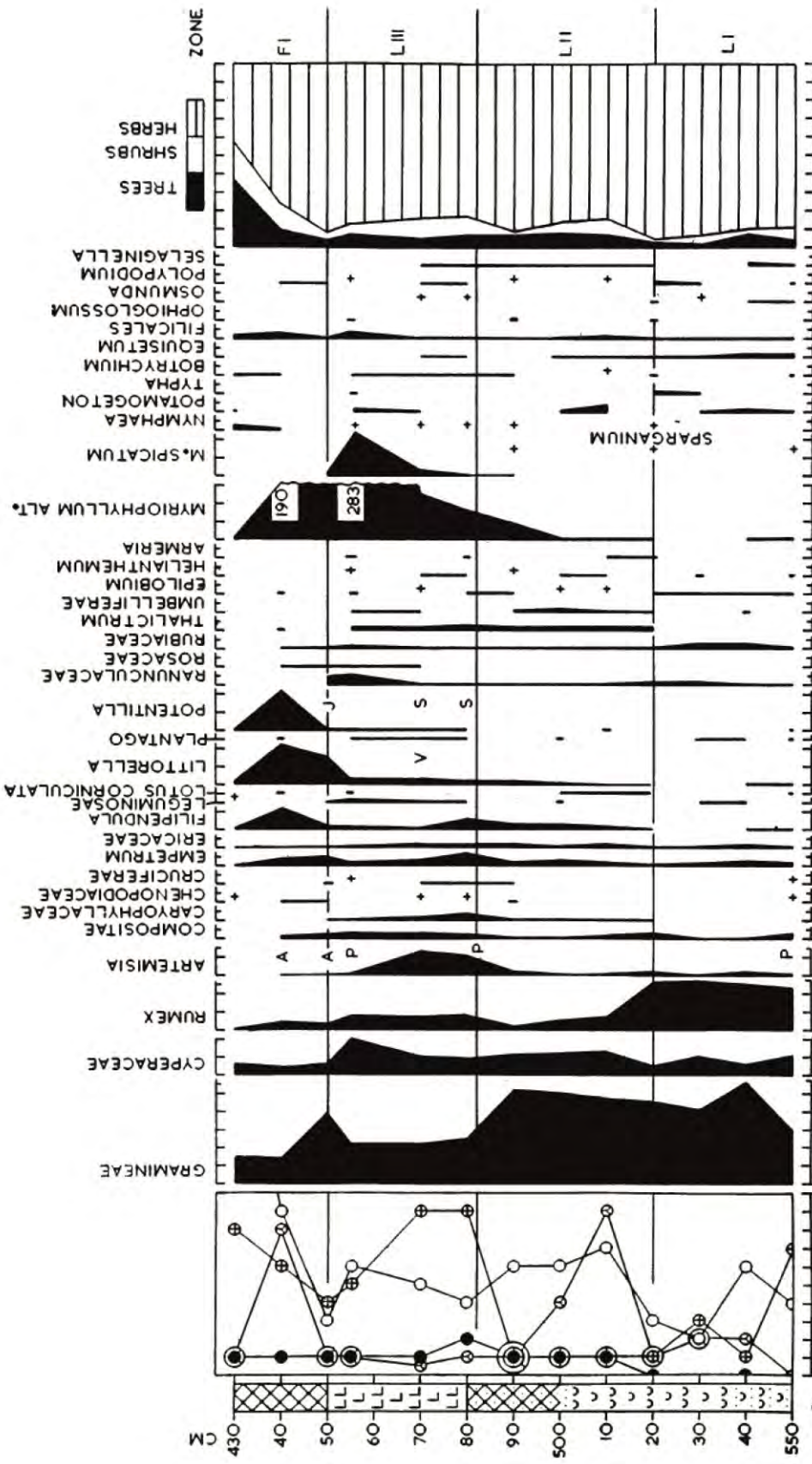

Figure 3.27 Lithological and palynological results from Moar (1969b). The site is indicative of a typical LGIT to early Holocene succession, and typified by herbaceous taxa through all climatic zones suggesting the landscape was largely treeless through this time.

3.7 Chapter summary

This chapter has provided the rationale, and background information of the sites selected for study in this project. It has been illustrated that a disparity exists between the regional tephrostratigraphies of the British Isles, as well as between the British Isles and the rest of Europe (for the latter see section 2.8.1). Three Scottish sectors were chosen for investigation due to their potential for: 1) developing new links to Nordic, European and Irish tephrostratigraphies, and; 2) acting as testing grounds for modified sampling and extraction techniques. Two of the chosen sectors i.e. the North Eastern and North Western have previously been shown to be sensitive to abrupt climatic oscillations of the LGIT (e.g. Brooks et al. 2012; Whittington et al. 2015). These are therefore good candidates for evaluating the potential of tephra horizons in constraining such events. All sites chosen overlap with previous tephrostratigraphic investigations, with three of the five basins having already been examined for LGIT age tephras (e.g. Bunting 1994; Roberts 1997; Whittington et al. 2015). As a result, modifications to sampling and extraction techniques can be reliably assessed.

Chapter 4. Methodology

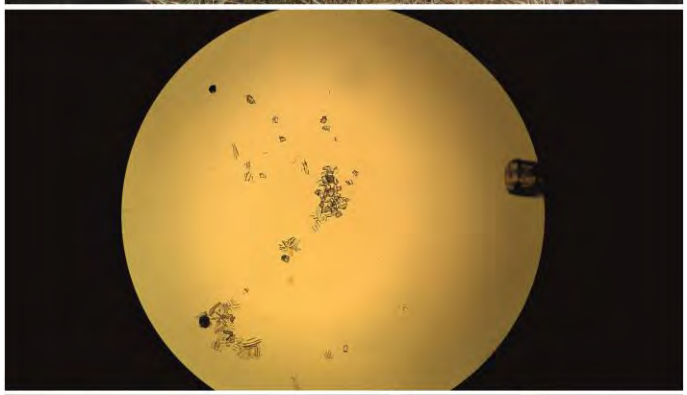

4.1 Introduction and chapter structure

This chapter provides details on the laboratory protocols and methods that were utilised during the course of this research. Site specific methodologies such as coring and surveying strategies are presented in the corresponding results chapters. Specific emphasis here is given to the refinement of tephra extraction methods, as notable modifications of the technique have occurred since Turney (1998b) and Blockley et al. (2005). In addition to these, a new scheme for the refinement of macrotephra using heavy liquids is proposed.

4.2 Laboratory protocols

4.2.1 Sediment storage

All core sequences used in this project were wrapped individually in plastic film, and kept in a cold storage facility at 4°C to prevent cross contamination and to minimise degradation of the substrate.

4.2.2 Contamination procedure

A principal objective of this study is to reliably quantify and characterise tephra horizons. It is vital therefore that strict and robust laboratory protocols are implemented to prevent the cross contamination between sampled horizons and other lab users. To ensure this, sub-sampling of sequences containing macro tephra horizons were conducted in isolation; and all tephra processing was conducted in a separate laboratory space to other tephra projects. These areas were cleaned with deionised water before and after use, and sub-sampling equipment was also washed thoroughly between samples. Sieve meshes were changed every 3-5 samples when processing material for tephra counts, and rinsed thoroughly with deionised water between each use. For geochemical analyses, sieve meshes were changed after every sample. To check for airborne contamination during the processing of macrotephra horizons, a 'blank' background sample was run alongside the processed batch. A centrifuge tube with a wide diameter funnel would be left open next to the sieving station with the surface of the funnel being periodically rinsed into the tube. Any residing residue would then be mounted and checked for the possibility of airborne tephra contamination; in all cases these 'blank' background samples returned a negative result, indicating that the lab protocols for reducing airborne tephra contamination were effective.

4.3 Sedimentological methods

4.3.1 Sediment description

Prior to sub-sampling, sedimentary core sequences were cleaned back horizontally with a scalpel; the freshly exposed surface of the cores were described in the laboratory using a modified sedimentary classification scheme of Troëls-Smith (1955) and given a colour value from the Munsell Soil Color system. Together these schemes provide a description of the physical constituents, the degree of decomposition, and the component parts, with the Munsell Soil Color system providing a standardised and universal colour coding.

4.3.2 Digital imaging

Sedimentary core sequences were photographed at ca. 10 cm resolution using a Canon DSLR camera mounted in a ridged copier stand. The individual photos were 'stitched' together using Adobe Photoshop CS2 to produce composite images; the output provides a visual accompaniment to the lithological description, and a historical record of the sequences before destructive laboratory techniques were conducted.

4.3.3 Loss on ignition (LOI)

LOI provides an approximation of organic content, and hence insight into biological productivity via the oxidising or 'ashing' of organic material at 500-550°C (Dean 1974; Bengtsson and Enell 1986; Heiri et al. 2001). Typically 40-60 % of the LOI can be attributed to the organic carbon content, with a variable proportion of chemically bound water, inorganic carbon, volatile salts and other compounds also contributing to this value (Dean 1974; Bengtsson and Enell 1986; Heiri et al. 2001). Samples of ca. 1 cm^3 were taken at contiguous 1 cm intervals through all cores examined in this study, with the ashed residues being retained for tephra quantification. The LOI procedure follows Bengtsson and Enell (1986), and can be summarised with the equation below:

$$\mathrm{LOI} = \frac{(\mathbf{a})}{(\mathbf{d})} \times 100$$

Where a = ashed weight and d = dry sample weight.

4.3.4 Calcimetry

Whilst the LOI procedure can also be used to estimate the carbonate content of sediments via a secondary phase of heating to 900-1000°C (Dean 1974; Bengtsson and Enell 1986; Heiri et al. 2001), heating to this temperature will have a detrimental

effect on glass preservation and chemistry (van den Bogaard and Schmincke 2002; Pollard et al. 2003). An alternative volumetric method for the measurement of carbonate within samples was thus employed. Subsamples of ca. 1 cm^3 were taken for calcimetry from stratigraphic units which displayed a reaction to 10 % hydrochloric acid (HCL) during the lithological description phase. A contiguous 1 cm sampling strategy was applied at Quoyloo Meadow (Abel 2015), and at Little Lochans, whilst a 2 cm sampling resolution was employed at Crudale Meadow (Table 4.1). Samples were dried and powdered using a pestle and mortar, and processed following the method of Gale and Hoare (1991). The technique uses a Bascomb calcimeter to measure the volume of carbon dioxide evolved during a reaction with a specified volume of hydrochloric acid. Calcium carbonate content is then quantified using the following equation:

$$CaC0_3 = \frac{\mathbf{VpC}}{\mathbf{MT}}$$

Where $\boldsymbol{V}$ = volume of CO_2 evolved during the reaction (cm^3); $\boldsymbol{p}$ = barometric pressure (mm Hg); $\boldsymbol{C}$ = constant; $\boldsymbol{M}$ = mass of the sample; and $\boldsymbol{T}$ = temperature (=°C+273.15)

Table 4.1 Sampling resolution for calcimetry samples used in this study.

Site	Core	Sample(s) (cm)	Resolution	Operator(s)
Quoyloo Meadow	QM1D	120-170	4cm intervals	Abel (2015)
	QM1E	160-210		
Little Lochans	LL3A	100-150	Contiguous 1cm intervals	Timms (this study)
	LL3B	130-180		
	LL3C	160-210		
	LL3D	200-250		
	LL3E	232-282		

4.3.5 Total organic carbon (TOC)

Whilst LOI is the most widely used method of establishing organic content in lacustrine sediments (Lowe and Walker 2015), more accurate measurements can be made, especially in carbonate sediments where the proportion of inorganic carbon liberated via the ashing process is likely to be elevated (Bengtsson and Enell 1986). Total organic carbon (TOC) content was determined via the titration method of Walkley and Black (1934) at two of the three carbonate sites. Samples of ca. 1 cm^3 were extracted from Quoyloo Meadow at a 4 cm resolution (Abel 2015) and at a contiguous 1 cm resolution from Little Lochans (Table 4.2). The following equation is used to calculate total organic carbon content following the standard laboratory procedure:

$$\% \text{ TOC} = \frac{[(10 - (\mathbf{Vt} \times \mathbf{Mf})) \times 0.3 \times 1.33]}{\mathbf{W}}$$

Where Vt = volume of ferrous ammonium sulphate solution (FAS) required in the sample titration; Mf = volume of FAS required in a blank titration; and W = weight of the sample.

Table 4.2 Sampling resolution for TOC samples used in this study.

Site	Core	Sample(s) (cm)	Resolution	Operator(s)
Quoyloo Meadow	QM1D	120-170	Contiguous 1cm intervals	Abel (2015)
	QM1E	160-210		
Crudale Meadow	CRUM1D	360-410	2cm intervals	Timms (this study)
	CRUM1E	400-450		
	CRUM1F	440-490		
	CRUM1G	480-530		
	CRUM1H	520-570		
	CRUM1I	560-610		
	CRUM1J	600-650		
	CRUM1K	620-670		
	CRUM1L	644-694		
Little Lochans	LL3A	100-150	Contiguous 1cm intervals	Timms (this study)
	LL3B	130-180		
	LL3C	160-210		
	LL3D	200-250		
	LL3E	232-282		

4.3.6 Magnetic susceptibility

Magnetic susceptibility is a non-destructive technique that can be used as an indicator of minerogenic flux (Dearing 1986). Magnetic susceptibility was conducted at a 1 cm resolution on all cores examined in this study. Measurements were carried out using a Bartington instruments MS2c core loop sensor, which provides a measure of volume specific magnetic susceptibility in $x10^{-5}$ SI units.

4.4 Palaeoenvironmental methods

4.4.1 $\delta^{18}O$ and $\delta^{13}C$ stable isotope analysis

The use of oxygen isotopes as a palaeoclimate indicator in calcareous lake systems is based on the observation that the $^{18}O/^{16}O$ ratio of precipitation and hence lake water depends on climate, and especially that of temperature. Carbon isotopes ($^{13}C/^{12}C$), however, cannot be interpreted in such a broad manner, and instead results tend to be

much more indicative of the local catchment, and basin specific factors (Siegenthaler and Eicher 1986).

Subsamples 0.5 cm thickness and of ca. 0.5 cm^3 volume were extracted contiguously from the Quoyloo Meadow sequence at depths which correspond to those taken for calcimetry and TOC (Table 4.3). Samples were placed into glass vials and treated with 0.5 % Sodium hexametaphosphate (SHMP) ($(NaPO_3)_6$) to disaggregate the sediment. Sieving was conducted at 63 µm with de-ionised water to remove detrital material and biogenic carbonate contamination, i.e. molluscs, ostracods etc. Sieved samples were air dried and treated with 10 % hydrogen peroxide (H_2O_2) to remove organic material, before being rinsed two times with de-ionised water and allowed to air dry. These samples were ground to a powder using an agate pestle and mortar and weighed using a Mettler Toledo XP6 microbalance. The mass of sediment ranged 500-1100 µg; however, samples exhibiting <10% $CaCO_3$ were weighed to ca. 1500 µg. $\delta^{18}O$ and $\delta^{13}C$ values were determined by analysing the CO_2 evolved from a reaction of the sample with Phosphoric acid (H_3PO_4) at 90°C using a VG PRISM series 2 mass spectrometer located in the Earth Science Department at Royal Holloway. Internal (RHBNC) and external (NBS19, LSVEC) standards were run to check for machine precision and drift.

Table 4.3 Sampling resolution of $\delta^{18}O$ and $\delta^{13}C$ isotope analyses from Quoyloo Meadow.

Site	Core	Sample(s) (cm)	Resolution	Operator(s)
Quoyloo Meadow	QM1D	155-170	Contiguous 0.5cm intervals	Abel (2015) Timms (this study)
	QM1E	160-191		

4.4.2 Pollen stratigraphy

Pollen samples for Quoyloo Meadow and Tanera Mor 1 were prepared following standard Royal Holloway protocols and spiked with *Lycopodium* spores to facilitate the calculation of pollen concentration. Counts were conducted by two collaborators (Table 4.4), with sample resolution also varying between sites and depths.

Table 4.4 Pollen sample resolutions from study sites

Site	Core	Sample(s) (cm)	Resolution	Operator
Quoyloo Meadow	QM1F	189.5-229.5	0.5cm intervals	Abrook (unpublished)
	QM1A 170-220 (duplicate)	177.5 - 192.5		
	QM1B 140-190 (duplicate)	159.5 – 183.5		
	QM1A 120-170 (duplicate)	128.5 - 156.5		
Tanera Mòr 1	TM1-BH9A	426-460	2cm intervals	Lowe (unpublished)
		466, 468, 476, 482, 484	undefined	
		492-524	2cm intervals	

4.4.3 Chironomid analysis

Chironomidae or non-biting midges are known to reflect ecological changes in lacustrine sequences via shifts in their species-abundance and population composition (Brooks 2006). However, it is their finite tolerance to temperature changes which has proven of most interest and use in Quaternary palaeoenvironmental studies. Fifteen samples were taken at a variable resolution through the Quoyloo Meadow sequence (Table 4.5). Samples of weight ranging 0.2-1.0 g were processed in order to attain the ca. 50 head capsules needed for a quantitative assessment of mean July air temperature, a number deemed statistically representative of the sample population (Brooks et al. 2007). Samples were prepared following the method of Brooks et al. (2007), and analysed at the Department of Life Sciences, Natural History Museum, London by Agnieszka Soszyńska-Maj and Steve Brooks.

Table 4.5 Chironomid sample resolution form Quoyloo Meadow

Site	Core	Sample(s) (cm)	Resolution	Operator
Quoyloo Meadow	QM1D	135, 147, 161, 164	Undefined	Soszyńska-Maj and Brooks (unpublished)
	QM1E	177, 185, 189, 191, 193, 197, 201, 205		
	QM1G	208, 220, 232		

4.5 Tephra sampling and extraction

4.5.1 Rationale for a contiguous high resolution approach

A fundamental aspect of cryptotephra research is establishing a sampling strategy with sufficient scope and resolution that the resulting tephrostratigraphy will meet the requirements of the project. As discussed in Chapter 2, the standardised scan and resample protocols, and the predisposition to focus on peak shard concentrations for

chemical characterisation have likely led to: 1) an underestimation of tephras preserved in stratigraphic sequences, and; 2) a spatial disparity in the distribution of tephras in NW Europe.

In order to test this hypothesis, it is necessary that a contiguous high resolution sampling strategy be adopted, it is also necessary that this work is complemented by a more systematic and thorough approach to the chemical characterisation of cryptotephra horizons than has been previously undertaken in NW European terrestrial sites.

4.5.2 Tephra sub-sampling strategy

Residues derived from contiguous 1 cm LOI measurements were retained for tephra quantification. In sequences where previous studies had identified tephra layers or where a macrotephra was recognised, the scan phase was negated. This strategy was applicable for all sites with the exception of Little Lochans where 5 cm scans were used to establish a first order shard concentration.

4.5.3 Modified density flotation method

Following the advent of cryptotephra studies in the early 1990s a multitude of strategies have been devised to identify ash horizons within differing substrates (see section 2.4.2). For minerogenic sequences such as lacustrine records, the density flotation technique is amongst the most widely accepted and utilised within the cryptotephra community (Lowe 2011; Davies 2015). The technique employs a stepped density separation using the inert heavy liquid sodium polytungstate (SPT) ($(Na_6\ (H_2W_{12}O_{40})\ H_2O)$). A modified version of the Blockley et al. (2005) method was implemented here, and the revised flowchart of the technique is outlined in Figure 4.1. A procedure for handling macrotephras was also devised during this project, which follows recommendations from Blockley et al. (2005); Gehrels et al. (2006) and Bourne (2012). The corresponding flowchart is presented in Figure 4.2. Modifications to the Blockley et al. (2005) method and their justification are outlined below:

1) The sieved size range is increased from 25-80 μm to 15-125 μm. In doing so shard concentrations are maximised, w is especially important in the distal setting where smaller shards are becoming increasingly viable for chemical analysis (Hayward 2012).

2) Blockley et al. (2005) suggests that dilute detergent can be used to assist in disaggregating organic materials. However, it has been recognised that detergent can

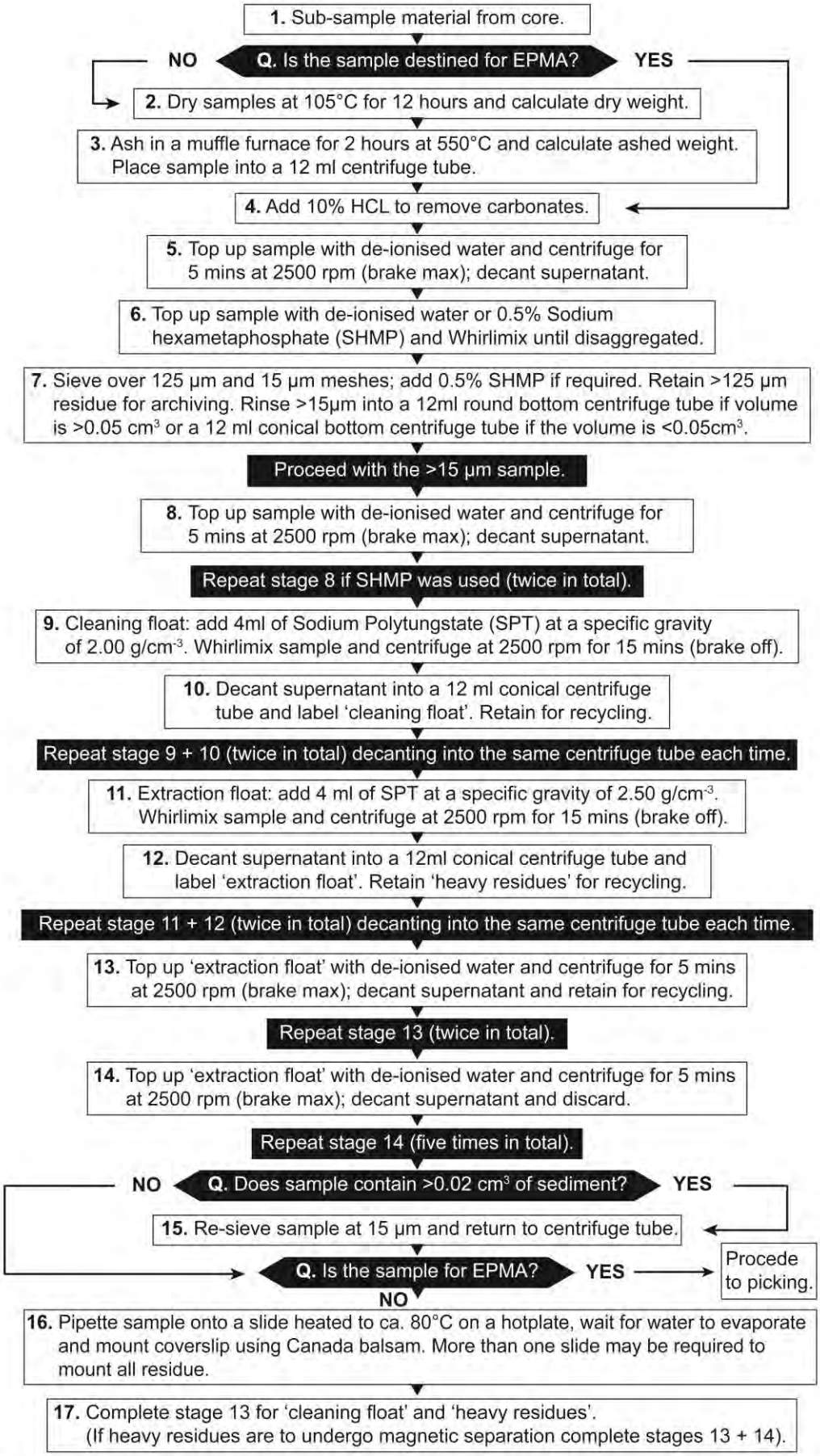

Figure 4.1 A revised extraction method for cryptotephras based on Blockley et al. (2005); this modified technique was developed and applied to all cryptotephra horizons examined during the course of this study.

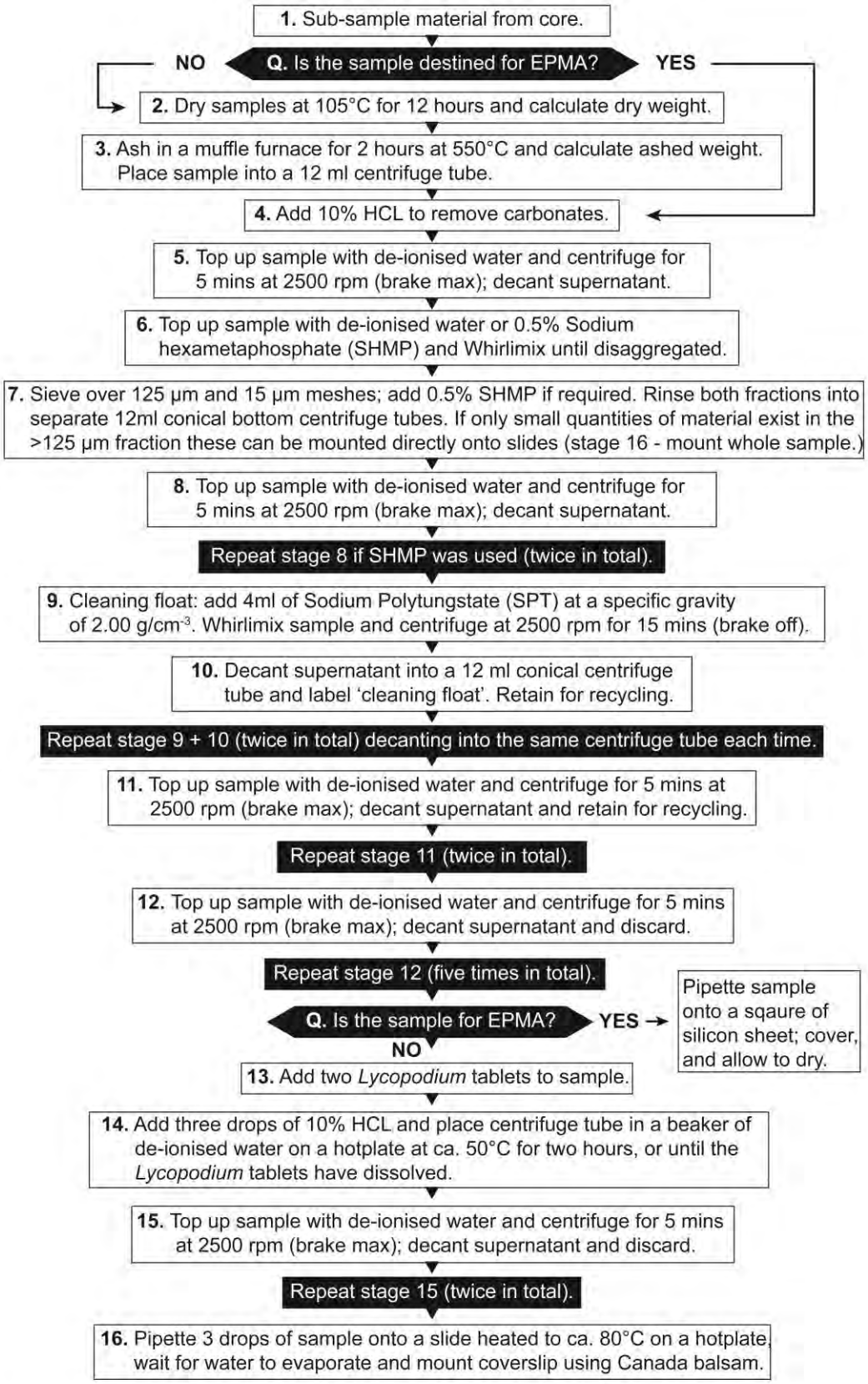

Figure 4.2 An extraction protocol for the extraction and refinement of macrotephra horizons, this technique was applied to all macrotephra horizons examined during the course of this study.

build up within the SPT used for cleaning and extraction. In some instances the SPT has been observed to froth and foam. In-house laboratory tests have shown no quantifiable difference in extraction performance; however, there is a possibility that the specific gravity of the liquid may be slightly altered. This concentrated detergent can also persist through the extraction procedure, and unless thoroughly rinsed out this residue can infringe upon optical microscopy and inhibit shard identification. Experimentation with dilute (0.5%) SHMP, a deflocculant, has proven successful as an alternative in this study, with no noticeable alteration to shard structure or chemistry observed.

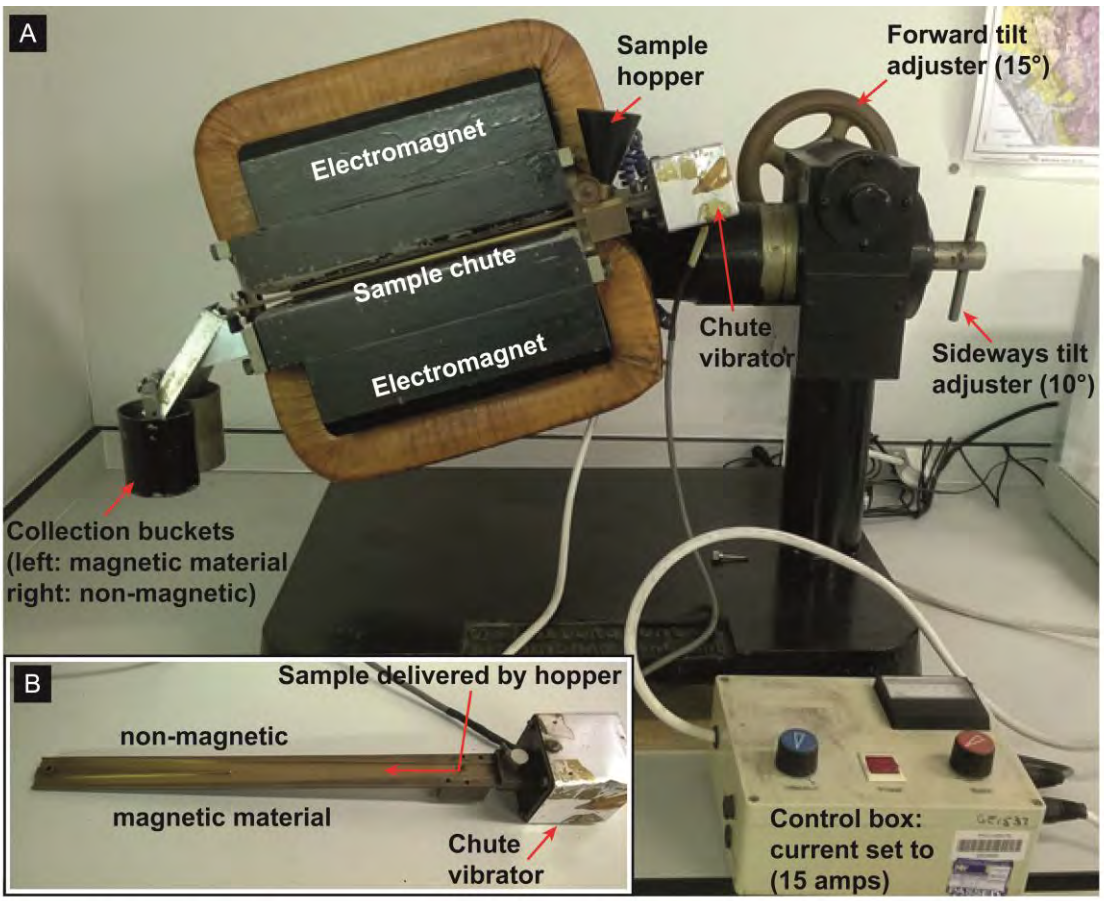

Figure 4.3 Frantz Magnetic Barrier Separator ™, and associated setup parameters used to separate basaltic material from host substrates in this study.

4.5.4 Magnetic separation

Magnetic separation was conducted on heavy residues resulting from the density floatation process (Figure 4.1). The technique follows that of Mackie et al. (2002) and uses a Frantz Magnetic Barrier Separator™ to extract basaltic glass from minerogenic substrates (Figure 4.3). Dried samples were heated in a furnace to 550°C to enhance the magnetic properties of the tephra shards (Mackie 2000). The Frantz was set with a forward tilt of 15°, a sideways tilt of 10°, and the electrical current was set at 15 amps; these were found to be the optimal conditions for extracting basaltic glass from an

Icelandic source in Scottish lacustrine sequences (Mackie et al. 2002). Due to time constraints only selected horizons were processed; these were focused on intervals that had already yielded silicic fractions. The specific depths for each sequence are reported in the relevant results chapter.

4.6 Tephra identification and quantification

4.6.1 Optical microscopy of tephra horizons

Tephra slides were examined using an Olympus CX-41 transmitted light microscope fitted with cross polarising filters and a Vernier stage. Magnification was provided by a 10x magnification eyepiece and two objectives (20x and 40x). Slides were transversed systematically from left to right, and counts were conducted at 20x magnification; the 40x objective was primarily used to examine morphological detail and to assist in distinguishing between genuine tephra shards, non-tephra objects, and 'tephra-like' particles, also termed 'mimics'. Shard numbers were recorded on a mechanical click counter.

Volcanic glass is primarily distinguished by morphology, and a number of diagnostic optical properties. In ideal circumstances the extraction and refinement process would remove all superfluous material, leaving just tephra shards to be examined and quantified. However, in reality this is not the case, and whilst the density separation process removes a high proportion of organic and minerogenic material from the mounted sample, a component still remains. Chemical treatments could be employed to remove these fractions, but doing so risks the chemical alteration of the shard structure, and in some cases has been shown to completely dissolve shards which possess more delicate and fragile compositions (e.g. Pollard et al. 2003; Blockley et al. 2005). As such, it is down to the skill of the operator to learn and refine those skills crucial in identifying cryptotephras.

4.6.2 Morphology

The morphology of tephra shards is highly variable, even within chemically homogenous populations, but shape, size, and surface characteristics can provide a means to distinguish shards against none tephra objects. Figure 4.4 illustrates some archetypal characteristics that are fundamental in identifying distinguishing tephra. As can be observed in Figure 4.4 shape can vary from spherical and smooth, to angular and blocky, or long and needle-like which largely depends on eruptive style and chemical composition (Lowe 2011; Jordan 2014). However, it is often internal

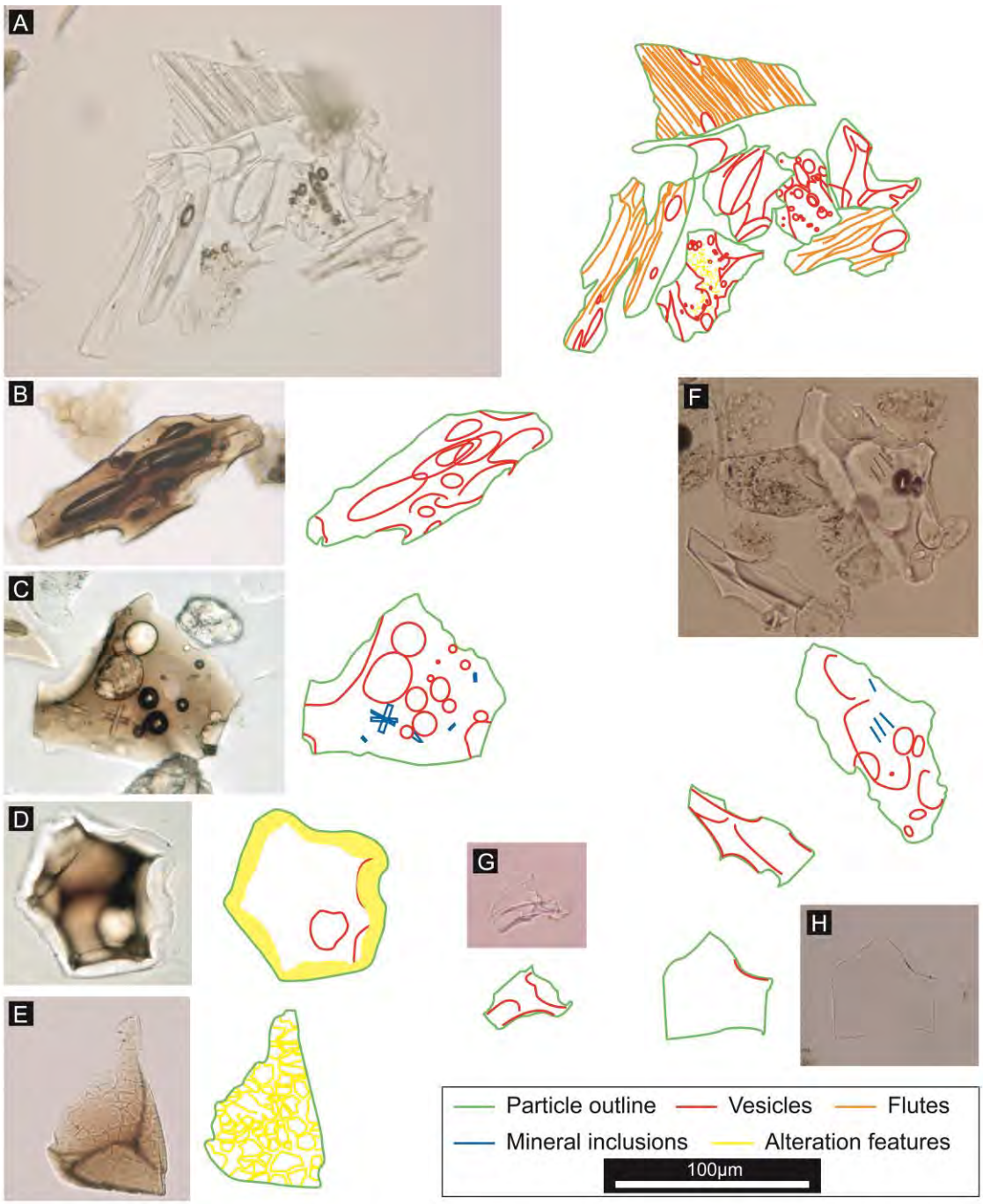

Figure 4.4 An example of some typical shard morphologies. (**A**) Shards from the Agnano Monte Spina eruption, the shards are all curve-elongate to irregular in shape with very irregular to concave-convex outlines, and long axes measurements of >100µm. The shards frequently have vesicles which are ovoid to tubular in shape. (**B**) Basaltic shard from Katla displaying an elongate shape and a very irregular outline; long axis >100µm. Vesicles are ovoid in shape. (**C**) Basaltic shard from Iceland displaying a blocky/equant shape; very irregular outline, and a long axis greater than 100µm. Vesicles are spherical to ovoid in shape. Mineral (microlite) inclusions are tabular and irregularly arranged. (**D**) Basaltic shard from Iceland with hydration rim. (**E**) Basaltic shard with surface alteration features . (**F**) Rhyolitic shards from the 'Borrobol' source, shards are blocky with an irregular to concave-convex outline. Shards possess a number of spherical and ovoid vesicles, with inclusions orientating parallel to the long axis of the shard. (**G**) A small rhyolitic shard from Torfajökull exhibiting a highly cuspate structure. (**H**) A flat 'platey' rhyolitic shard from Katla. Images A-E from Matthews (2008); F-H from Timms (this study).

morphological features such as vesicles, fluting or mineral inclusions that are particularly diagnostic (Figure 4.4).

4.6.3 Optical properties

Volcanic glass exhibits several optical properties that can be used to distinguish between shards and mimics. Volcanic glass is isotropic, meaning that under cross-polarised light shards 'extinguish' or darken, as plane polarised light remains unaltered by the glass' amorphous structure (Figure 4.5 A, B). Most minerals that mimic tephra morphologies possess crystalline structures (anisotropic); they thus display birefringence under such light sources, and are seen to glow with bright vivid colours (Nesse 2000; Figure 4.5 A, B). It should be noted, however, that recrystalisation of glass minerals at the edges of weathered shards, and mineral inclusions within the glass body can also result in a faint glow when viewed in cross-polarised light (Figure 4.5 A, C). Thus caution must be used not to disregard objects that may exhibit some birefringence.

Whilst cross-polarised light can assist in distinguishing between volcanic glass and mineral matter, it cannot be utilised to differentiate between tephra shards and biogenic silica (i.e. diatoms, phytoliths and sponge spiricules) due to their similar isotopic characteristics (Figure 4.5 A, B, D). Fortunately in many cases the morphology of these objects is sufficiently different to tephra shards that an experienced operator can quickly discount them as potential candidates. In some circumstances, however, these biogenic objects can become fragmented and weathered to an extent they resemble blocky shards (Figure 4.5 D); in such cases, even an experienced eye can prove inadequate to reliably characterise these objects. Fortunately experiments with differing mounting media have shown that it is possible to differentiate between these troublesome mimics and tephra, based on their respective refractive index (RI). Volcanic glass typically ranges between 42-77% wt SiO_2, whilst in contrast biogenic silica may reach SiO_2 totals of approximately 95-98% wt. Due to these chemical differences biogenic silica has a maximum RI of 1.47 and tephra a minimum RI of 1.485 (Matthews 2008). Using a mounting medium that occurs between these values therefore allows for optical discrimination between shards and mimics via subtle colour differences and the Becke line test (see Enache and Cumming 2006). Several mounting media are available for tephra studies: Naphrax® (RI = 1.7), Canada balsam (RI = 1.55), Euparal™ (RI = 1.483) and Glycerol (RI = 1.475). Whilst Euparal™ and Glycerol have optimum properties to allow for the distinction between tephra shard and biogenic silica, Canada balsam was chosen for this study, as the medium is superior at distinguishing volcanic glass with higher SiO_2 values; a characteristic of the Icelandic

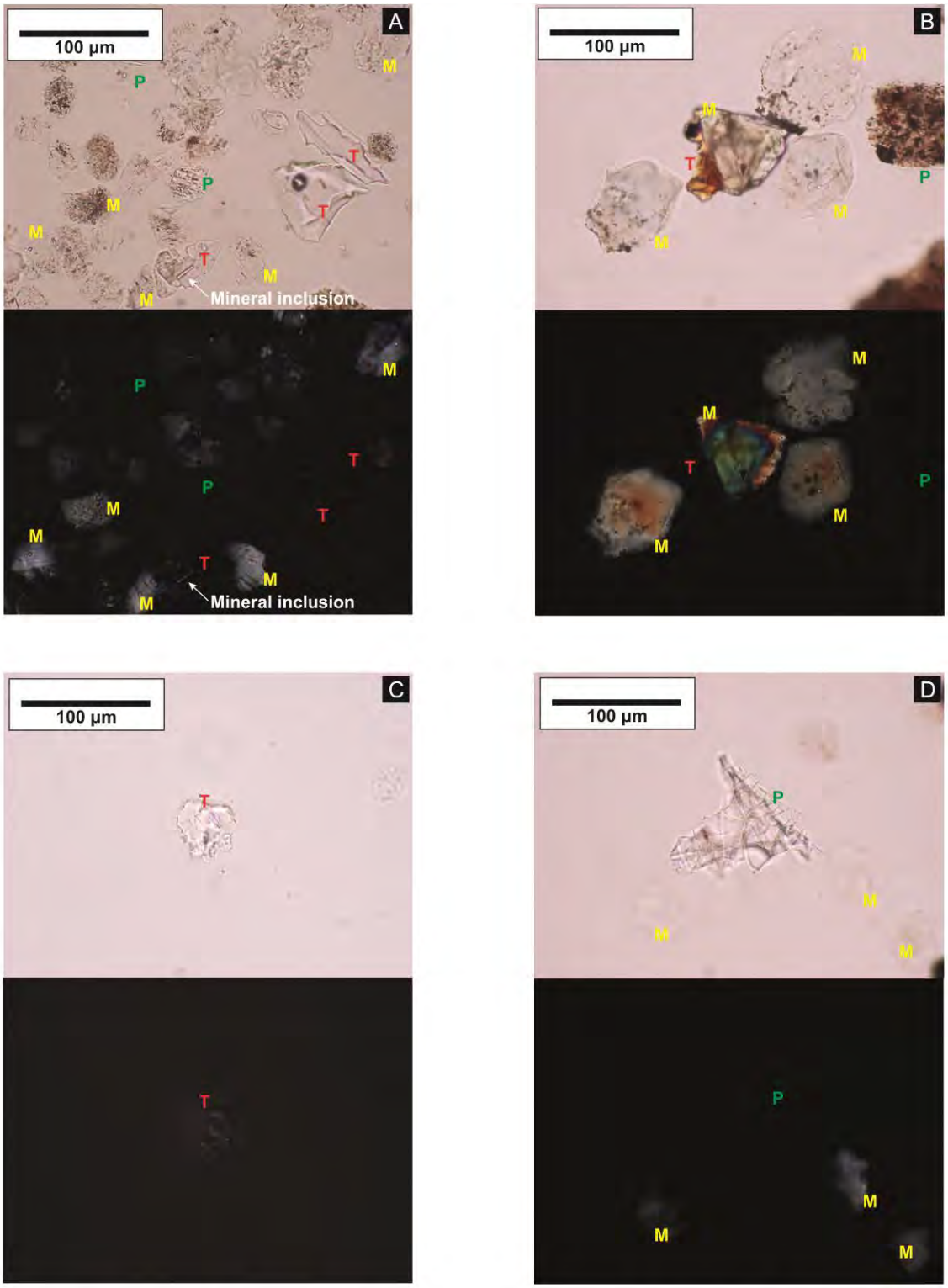

Figure 4.5 Examples of tephra and non-tephra objects in plane polarised and cross-polarised light. Abbreviations: **T** = Tephra, **M** = Mineral grain, **P** = Phytolith. (**A**) Note how the tephra shards and phytoliths 'extinguish' in cross-polarised light whereas the mineral grains 'glow'. Also note the pencil-like mineral inclusion glowing within the lower tephra shard. (**B**) The unusual occurrence of tephra fused with a mineral grain. Also note the birefringence of the minerals. (**C**) A small blocky shard that appears to 'glow' in cross-polarised light, this is likely due to surface alteration and/or the inclusion of minerals within the glass. (**D**) A blocky phytolith that could be mistaken for a shard.

province. In Canada balsam silicic shards often exhibit pinkish hues, whilst basaltic shards possess greeny-brown to black colouring.

Unfortunately optical identification of volcanic glass is not an exact science, the process of categorising shards based on optical and morphological characteristics is subjective (see Hardiman 2012: 78), and on occasion shard-like objects may emerge that are difficult to classify; in these circumstances the approach taken by the operator must remain consistent. In this study, any questionable shard-like objects were discounted and not included in the final tally; the shard totals presented in this study are therefore minimum counts.

4.6.4 Quantification of cryptotephra horizons

Fundamental to cryptotephra studies is the quantification or enumeration of shard concentrations. In the terrestrial setting these are typically recorded as a total number of shards counted within a sample; quantified as a value per volume of wet/ dry sediment (shards cm^3); or quantified as a value per gram/milligram of wet/ dry sediment (shards g^{-1}) (Lowe 2011). Whilst other methods exist, they can be slightly ambiguous e.g. shards per drop (Ranner et al. 2005); shards per 50 inorganic objects (Bennett et al. 1992).

In this study, shards per gram of dry sediment were calculated using the mass of the dried sample derived from the LOI. Shards were rudimentarily classified as either colourless (silicic) or brown (basaltic) before chemical characterisation.

4.6.5 *Lycopodium* counting method for macrotephra horizons

In order to quantify the concentration of macrotephra horizons identified during the course of this study, a technique using *Lycopodium* to 'spike' the sample was employed. The method is common in palynological studies to assess pollen concentrations, but was first applied to tephra sequences by Blackford et al. 1992, and later modified by Bourne (2012) (see Figure 4.2 for preparatory methods). Three vertical transects were made across each slide and the glass shard concentrations were quantified using the following:

$$c = \left(l \times \frac{a}{b}\right) d$$

where c = concentration of glass shards, l = number of *Lycopodium* spores in a tablet, a = glass shard count, b = *Lycopodium* spore count, d = sample dry weight in grams.

4.7 Tephra preparation for geochemical analysis

Within the development of cryptotephra studies, the identification of smaller shards and less concentrated horizons have presented significant challenges for both extraction and reliable chemical characterisation of volcanic glass particles. In the field of quantitative microbeam chemical analysis, it is essential that flat highly-polished surfaces are achieved on individual shards. Typically, this process involves impregnating shards within an epoxy resin before cutting and polishing stages expose shards to the surface. During the course of this research a collaborative effort to devise a new and quicker method to impregnate and section shards was developed by several researchers and technical staff at Royal Holloway. As a result both the existing methodology employed at Royal Holloway and the revised method were used in this study. The details of these are presented in section 4.73 and 4.74 respectively, with the samples produced by each method listed in Appendix A.

4.7.1 Sample preparation

Cryptotephra and macrotephra horizons selected for chemical analyses were prepared following the procedure outline in Figures 4.1 and 4.2 respectively.

4.7.2 Micromanipulation of shards: picking procedure for cryptotephras

Whilst macrotephras can be pipetted directly onto ready flattened stubs, or silicone rubber sheets following extraction, cryptotephra shards need to be manually separated from any remaining substrate before resin impregnation. Samples were pipetted onto well slides mounted under an Olympus CX-41 transmitted light microscope and extracted or 'picked' using a 5 µl gas chromatography syringe, fitted with a 100 µm-diameter needle and mounted on a mechanical manipulation device (Figure 4.6). The picked shards were transferred to a second well slide containing de-ionised water, which acted as a further filtering stage. To prevent this sample drying out, the well slide was periodically topped up with de-ionised water. The concentrated tephra shards were then transferred using the micromanipulator to either a:

- ready flattened silicon stub (existing method)
- piece of silicone rubber sheet, cut to the proportions of a wide diameter glass slide and adhered to the surface (revised method, see below)

Once all shards were transferred to a stub or silicon sheet, the picked sample was covered and allowed to dry. Whilst this process is highly time consuming, the versatility of the micromanipulator allows for the needle to be positioned precisely within the

vicinity of each tephra shard; it is thus highly effective at filtering away any unwanted material from the final sample, and is therefore very efficient at maximising the number of chemical analyses that can be obtained, a factor especially important when analysing small tephra populations (Hall and Hayward 2014).

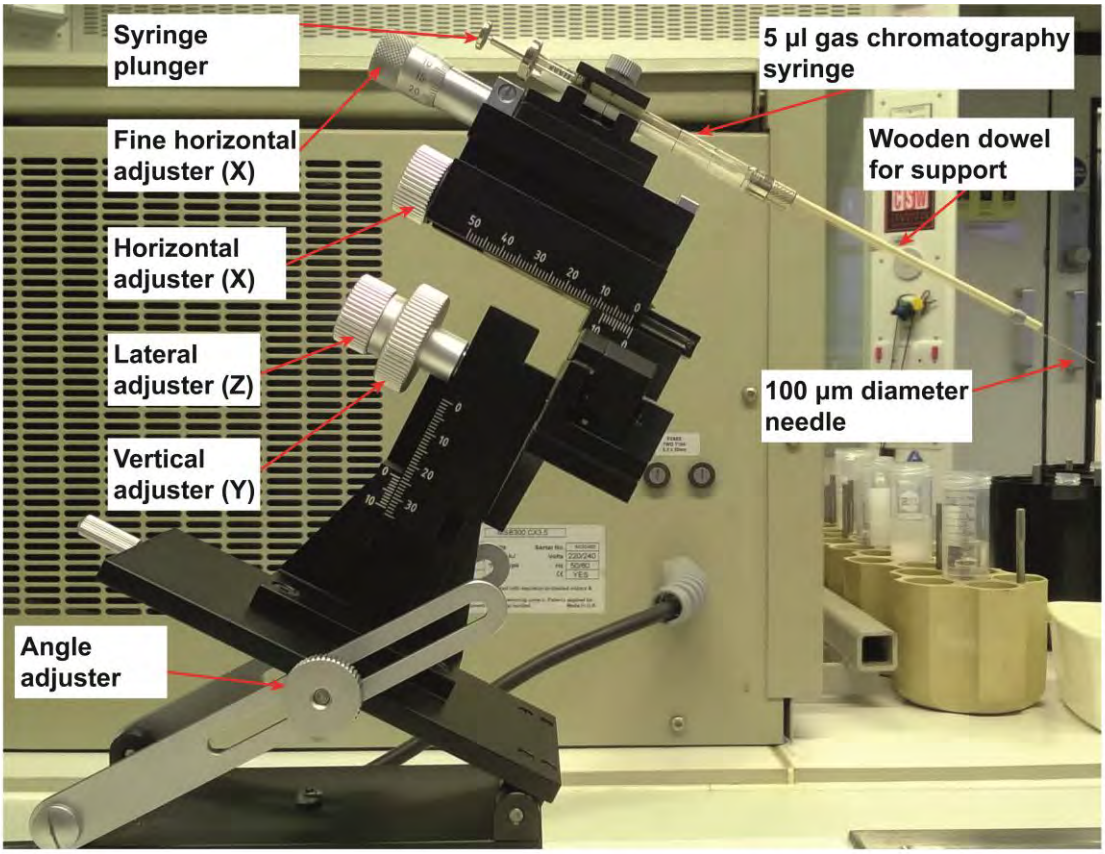

Figure 4.6 Micromanipulator used to extract or 'pick' individual shards for geochemical analyses.

4.7.3 Resin stub preparation (existing procedure)

The existing procedure for resin stub production at Royal Holloway is outlined in Figure 4.7.

4.7.4 Resin stub preparation (revised procedure)

The revised method of stub preparation is outlined in Figure 4.8. The revision was conducted under the supervision of Dr I. Matthews, with contributions from Dr A. MacLeod, Mrs K. Flowers, Mrs D. Weston and Mr R. Timms. The technique combines elements of the existing Royal Holloway procedure, with that of Hall and Hayward (2014). Specifically the technique employs a flat silicone rubber sheet as an alternative to a ready flattened resin stub, in doing so two time demanding phases of the existing methodology can be mitigated:

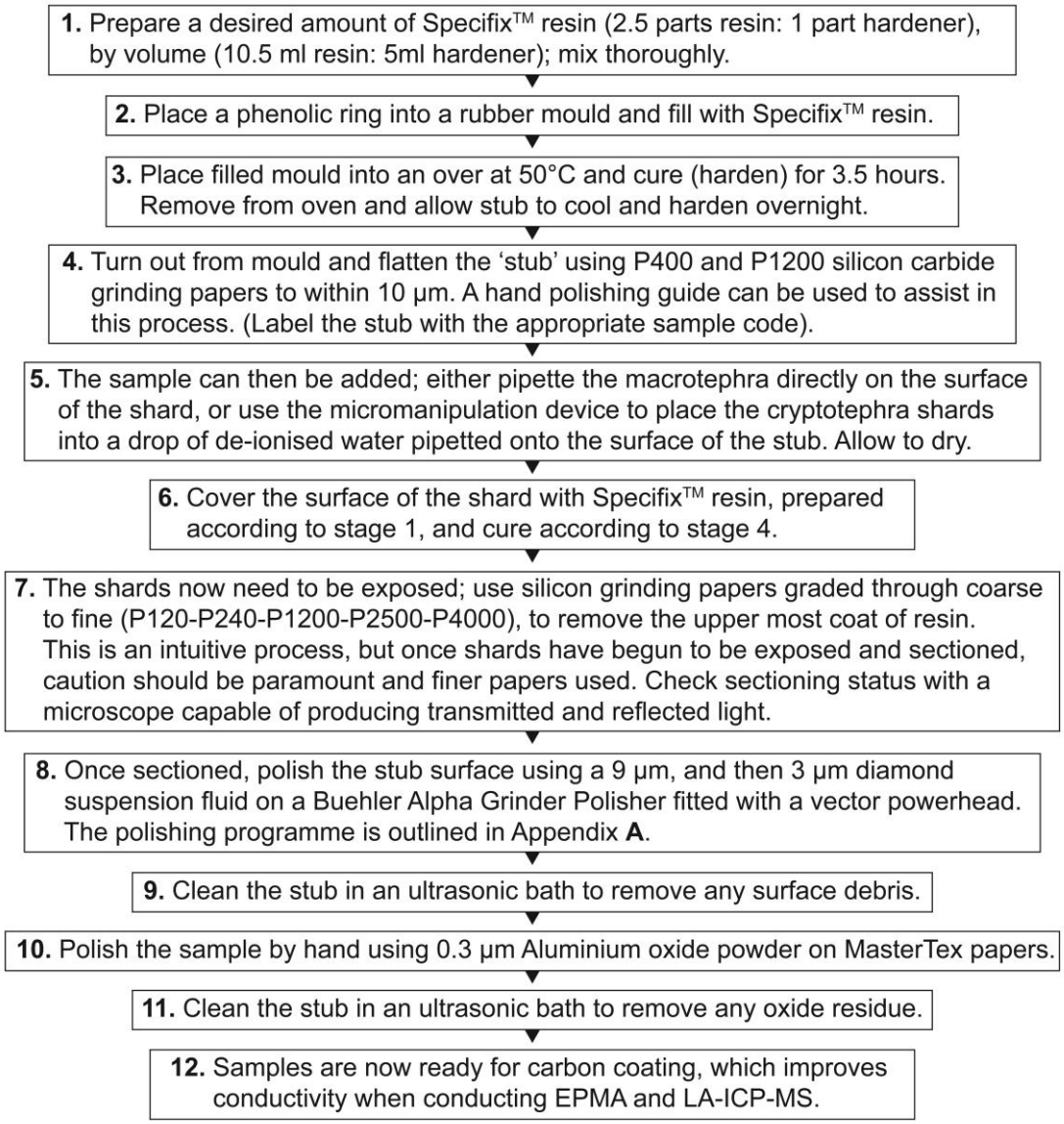

Figure 4.7 Existing procedure for resin stub preparation at Royal Holloway.

1) The moulding, curing, and flattening phases of the resin stub prior to the introduction of tephra shards can be avoided altogether. Instead shards are picked onto a flat pre-prepared sheet of silicone rubber, cut to the proportions of a wide diameter glass slide.
2) Once the shards are impregnated in resin, and following the existing procedure, it is necessary to cut down through the resin cap to expose the shards; this may take several hours depending on the amount of resin to section, the 'flatness' of the mounted surface, and the number of tephra shards that are to be exposed. By using the silicone rubber sheeting in the revised method, shards are within a single plane at or near the surface of the stub. Firstly this is a much quicker method, allowing for more samples to be processed, and secondly by having shards within a single plane allows each sample to be maximised for the number of chemical analyses that can be obtained.

1. Prepare a desired amount of Specifix™ resin (2.5 parts resin: 1 part hardener), by volume (10.5 ml resin: 5ml hardener); mix thoroughly.

2. Place the slide with the mounted silicone square into the curing rack.

3. Place phenolic ring over the dried tephra sample and press down firmly (Image **A**).

4. Fill the ring with the pre-prepared Specifix™ resin, and screw down the curing rack lid (Image **B**).

5. Place rack into an over at 50°C and cure (harden) for 3.5 hours. Remove from oven and allow stub to cool and harden overnight.

6. Label the open side of the stub with the appropriate lab code; invert and remove glass slide and the silicone square; retain the slide for re-use, discard the silicone square

7. Examine stub under a microscope capable of producing transmitted and reflected light; shards should be partially exposed at the surface.

8. Carefully expose and section the remaining shards using P2500 silicon grinding paper. Caution should be paramount.

9. Clean the stub in an ultrasonic bath to remove any surface debris.

10. Polish the sample by hand using 0.3 µm Aluminium oxide powder on MasterTex papers.

11. Clean the stub in an ultrasonic bath to remove any oxide residue.

12. Samples are now ready for carbon coating, which improves conductivity when conducting EPMA and LA-ICP-MS.

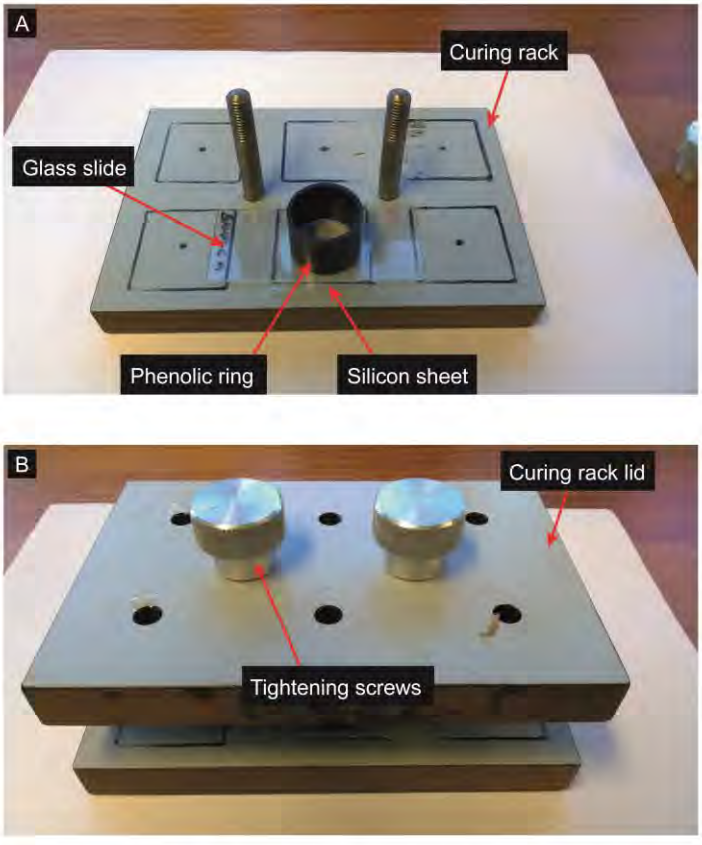

Figure 4.8 New procedure for resin stub preparation at Royal Holloway.

The development of this procedure is ongoing, and several minor problems still beset the technique. Issues associated with air bubble nucleation around shards during resin impregnation have hindered some attempts to section stubs, causing a weakness in the resin, and tendency for the resin to fail within the vicinity of the shards. Sectioned air bubbles may also act as a 'trap' for coarse debris resulting from the sectioning stages, later delivering this material onto a polishing surface. Whilst the ultrasonic treatment between sectioning and polishing can minimise this risk, there is a possibility that this coarser material may remain and subsequently lead to a scratching of the polished stub surface, or in a worst case scenario a 'plucking' of shards from the resin. These problems may be mitigated in future by using a pressure vessel to cure the resin, thereby minimising bubble growth (Hall and Hayward 2014).

4.8 Geochemical techniques

4.8.1 Major and minor elemental analysis (WDS-EPMA)

Within distal tephra studies, the Electron Probe Microanalyser (EPMA) has become the method of choice for determining the major elemental composition of individual glass shards (see section 2.4.3). The technique works by directing a focused beam of electrons onto a sample, ablating the surface, and generating X-rays of particular energies and wavelengths that reflect the elemental composition of the sample (Lowe 2011).

Recent work by Hayward (2012) has developed new analytical protocols for EPMA systems which enable the routine use of narrower diameter beams (5 μm and 3 μm) without Na loss; an issue that has beset cryptotephrochronology for several years (Lowe 2011). This development allows for greater analytical precision on smaller samples and reduces bias in the size of shards that can be analysed, both fundamental and intrinsic factors in this study, and in distal cryptotephrochronology as a discipline.

All chemical analyses were conducted on the Cameca SX100 electron probe microanalyser, located at the Tephra Analysis Unit (TAU), in the School of Geosciences, University of Edinburgh. The instrument is equipped with five WD spectrometers and operates via Cameca's Windows-based PeakSight software. Machine settings followed the 5 μm and 3 μm beam size set-up parameters of Hayward (2012). Eight major elements were analysed Si, Al, Ti, Fe, Mn, Mg, Ca, Na, K, and one minor element P, across all 61 samples of this study, with an additional minor element, Cl, also being analysed on samples TM9A 466, TM9A 467, TM9D 516, TM9D 528, TM9D 545, and TM9D 553. All analyses in this study are expressed as % wt oxide

unless otherwise stated. Primary standards were run prior to tephra analysis and secondary standards, Lipari Obsidian and BCR-2G, were run during and after probing, to ensure precision and to check for machine drift.

4.8.2 Handling geochemical data

Before geochemical data can be thoroughly explored they must undergo a process of 'filtering' to ensure that only robust and reliable analyses of the glass population are presented and interpreted. Whilst it is essential to ensure this geochemical integrity, some practices are not without controversy (see section 2.4.4). In the following section methods employed to 'filter' data produced during the course of this study are outlined. All filtered chemical data produced in this study are presented in Appendix B.

4.8.3 Data quality and removal of outliers

The extraction and refinement process used in this study, i.e. density separation and picking of individual tephra grains, does not guarantee absolute success in preventing sample contamination from crystalline minerogenic materials or biogenic amorphous silicates. Analyses of such non-tephra objects can only be reliably identified after analysis. Under such circumstances analytical totals for each element will likely be outside 'normal' tephra ranges (see section 2.4.4), and thus can be easily excluded based on their 'goodness of fit' with other glass chemical data.

4.8.4 Data quality and low analytical totals

The causes of low analytical totals resulting from EPMA are discussed in section 2.4.4, as are the common methodologies in dealing with such data. This study follows the recommendations of Hunt and Hill (1993) and Pollard et al. (2006), in excluding all analyses (unless otherwise stated) that exhibit totals less than 95 %.

4.8.5 Correlating tephra layers

All geochemical correlations made in this study are based on filtered non-normalised data sets. Correlations have been made graphically, via oxide-oxide bi-plots or 'Harker' diagrams; tri-plots or 'ternary' diagrams have been avoided due to the additional data manipulation that is required for their plotting (Matthews 2008) (see section 2.4.5.1). Graphical correlations have been made using the plotting software Geochemical Data Toolkit (GCDkit) v 3.0 (Janoušek et al. 2006). Reference data has been gathered from published journal articles, PhD theses and the RESET database (Bronk Ramsey et al. 2015a). The latter archives chemical information produced during the course of the RESET project, and also stores information gathered from previous publications and other data collation exercises; in total 22,000 major element analyses from 240 known

eruptions are catalogued within the system (Bronk Ramsey 2015a). A list of reference data sets used in correlation are provided in Appendix B.

4.9 Age modelling

All age models derived from this study are based on tephra layers and the current best-age estimate of those horizons. Age modelling in the context of this study has three primary applications: 1) to provide site specific chronologies; 2) as a means to improve the ages of less well dated horizons; and 3) to facilitate in the comparison of palaeoclimate data with other high resolution records.

Age models were constructed using OxCal v 4.2 (Bronk Ramsey and Lee 2013) coupled with the IntCal13 calibration curve (Reimer et al. 2013). The age depth model for all stratigraphic sequences was determined using the ***P_Sequence*** function in OxCal v. 4.2; the approach uses the relative position of dated horizons in order to produce a constrained age-depth relationship between horizons. The model employs a Poisson depositional construct that allows for variable sedimentation rates between dated horizons, and calculates the most likely age for undated intervals. ***Boundary*** functions typically placed to represent litho-stratigraphic boundaries were excluded from all models in this study, following the recommendations of Bronk Ramsey et al. (2015b); the exclusion of these allows the model greater freedom in determining sedimentation rates. Additional control over the sedimentation rate is governed via the model's ***K value*** (a Poisson constraining parameter) which sets the number of accumulation events per unit depth (Bronk Ramsey 2008). In previous iterations of the programme the *K value* had to be manually set and manually varied to achieve the optimum model output. However, developments in OxCal v. 4.2 allow for the specification of a variable *K value*, thereby removing any user bias in constraining model iterations, a distinct problem in previous versions (Bronk Ramsey 2009; Bronk Ramsey and Lee 2013). Where two dates were found for a single horizon the ***Combine*** function was used to amalgamate the ages based on their probability density functions; the process tests for whether the ages are statistically similar and allow a 'common' age to be derived. The resulting model can be evaluated via the total ***Agreement Index***; if the associated indices (^{A}overall and ^{A}model) do not total 60 % or greater, then the model should be considered for rejection (Bronk Ramsey 2001; 2009). All age-model parameters and output data are presented in Appendix C. Modelled ages are presented as convention dictates, with either 95.4 % confidence limits or as the mean with 2σ range.

4.10 Chapter summary

This chapter has detailed the laboratory methods used in this project. Tephra sampling and extraction procedures have been modified from recognised published methods, and reflect a gradual iterative development of the technique. Key modifications are: 1) contiguous high resolution sampling; 2) sieving at larger and smaller grain size fractions (125-15 μm); 3) refined density separation protocols; 4) quicker geochemical preparation methods; and 5) improved microprobe protocols for the analysis of shards with smaller surface areas (Hayward 2012). In conjunction, these developments and revisions enable sedimentary units to be examined more thoroughly and more robustly for the presence of tephra horizons than has previously been undertaken in minerogenic sediments of this age in the British Isles.

Chapter 5. Quoyloo Meadow Results

5.1 Introduction and chapter structure

Quoyloo Meadow is a calcareous rich basin in the west central region of Orkney Mainland. This location makes it, along with Crudale Meadow (Chapter 6), one of the most northerly marl basins in the British Isles. These sites offer some of the best opportunities in NW Europe to develop high resolution palaeoenvironmental records of LGIT age (e.g. Whittington et al. 2015). The high latitude of the Orcadian archipelago also offers significant opportunities to improve tephrostratigraphic links between Britain and other parts of NW Europe. It is thought that tephras which have previously eluded detection in Britain, but have been found elsewhere in Northern Europe, may well be detected within Orcadian stratigraphies (Chapter 3).

Quoyloo Meadow has previously been the focus of a detailed palynological assessment, and was the second site in the British Isles to yield a tephra of LGIT age (Bunting 1994). More recent work on the island has shown how these small carbonate basins have the potential to provide a detailed insight into the abrupt climatic oscillations that took place during the LGIT (Whittington et al. 2015). However, in both instances these studies and their conclusions were limited by the accuracy of site chronologies; a particular problem typical of carbonate basins due to the potential effect of hardwater contamination of radiocarbon samples. The focus of this chapter along with Chapter 6 is to therefore assess the viability of carbonate basins for capturing, and preserving tephra horizons of LGIT age, with an ultimate aim of developing robust age models capable of centennial-scale precision.

The geological and glaciological history of the Orkney Isles, along with the regional tephrostratigraphy and previous studies conducted at the site, are reported and discussed in the context of Chapter 3. This chapter therefore details the main litho- and tephrostratigraphic findings from this study, and provides a detailed discussion and interpretation of the tephra geochemical data. Elements of this chapter are quoted verbatim from Timms et al. (2016).

5.2 Results

Nine boreholes were cored from the Quoyloo Meadow site using 0.5 m Russian samplers in February 2014 (Figure 5.1). Due to time constraints a full basin survey was not completed; instead, a series 1.0 m Russian rods were used to provisionally sound basin depth, working systematically every 10-15 m along a NNE-SSW transect, which

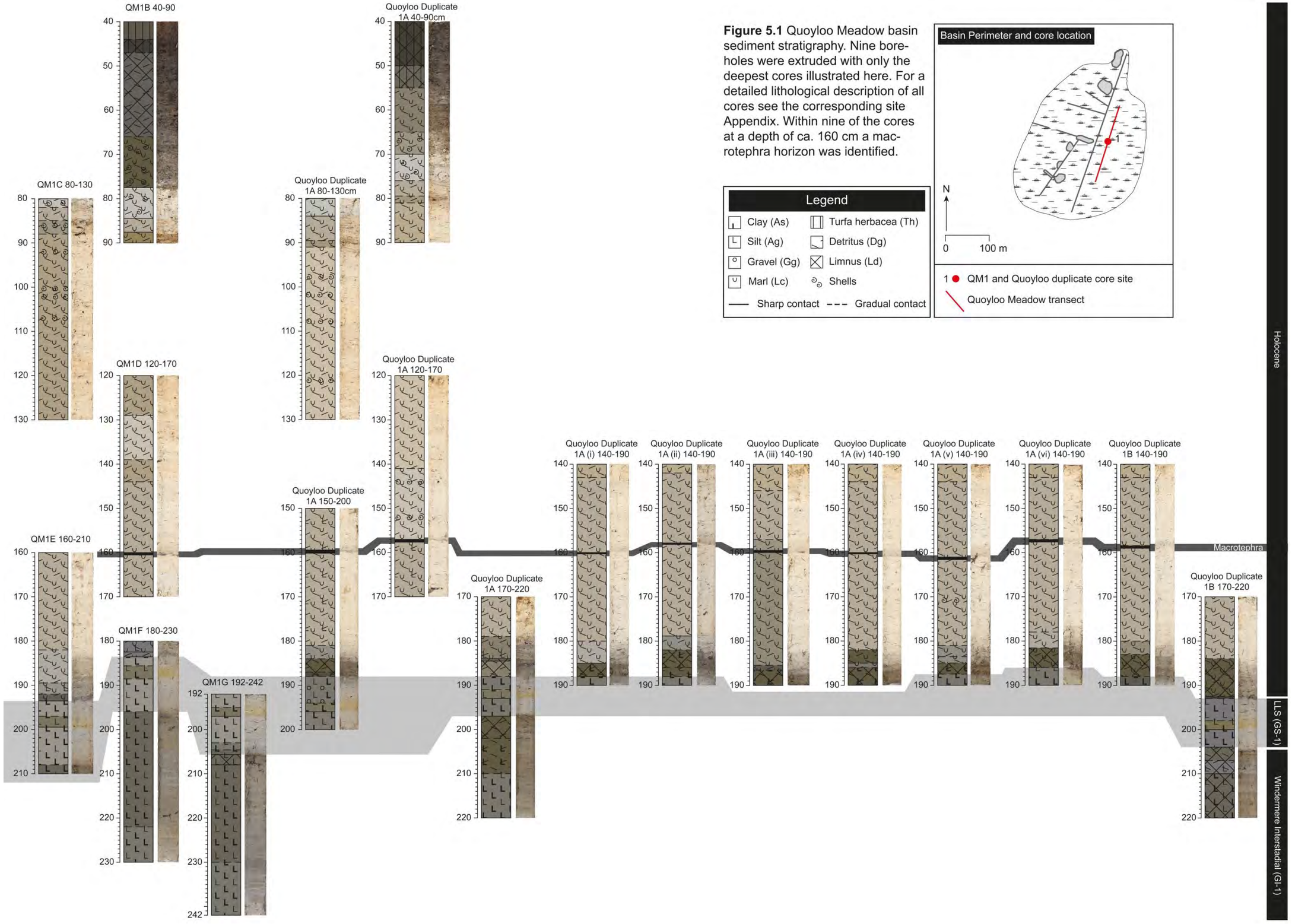

Figure 5.1 Quoyloo Meadow basin sediment stratigraphy. Nine boreholes were extruded with only the deepest cores illustrated here. For a detailed lithological description of all cores see the corresponding site Appendix. Within nine of the cores at a depth of ca. 160 cm a macrotephra horizon was identified.

ran parallel with the central Quoyloo drainage ditch (Figure 5.1). It was decided that the core site should be away from the areas modified by drainage ditches, and the deepest area was identified at (59.066417 -3.309333), which became the focus of QM1, as well as the QM duplicate sequence's (Figure 5.1).

5.2.1 Basin sedimentology

Figure 5.1 illustrates the deepest Crudale Meadow cores, with climatic zones delineated and inferred from lithological changes. Detailed sedimentological descriptions of each of the cores can be found in Appendix D. The QM1 sequence is the longest and most complete record obtained from the site, and was therefore chosen for further analysis in this study. Cores QM1G, QM1F, QM1E, and QM1D (Figure 5.1) were matched and aligned using lithological changes, LOI, $CaCO_3$, and magnetic susceptibility values to form a composite sediment stratigraphy (Figure 5.2).

The two basal units in the Quoyloo Meadow composite stratigraphy are characterised by silty clays, with a minor, but gradually increasing organic content (Figure 5.2). Based on these properties it is not clear when in time sedimentation began at Quoyloo Meadow. The sequence does not exhibit a 'typical' tri-partite sequence (i.e. minerogenic sediments-organic gytja/ lake marls-minerogenic sediments) that is considered diagnostic of other LGIT aged sequences in Scotland (see section 1.6; Lowe and Walker 2015 p.156). Whilst a correlation of these lower units to the stratigraphy and hence bio-stratigraphy of Bunting (1994) can be made, these additional data fail to clarify the situation. The low pollen concentrations and the sparseness of the vegetation record is unlike the pollen succession so distinctly observed at more southerly sites on the Scottish mainland (Bunting 1994; 1996). Whilst Bunting (1994) suggests these are of Windermere Interstadial age, the dominance of minerogenic sediments, and the very low organic content, suggest that the lowermost silts and clays (i.e. unit 1a) may in fact relate to the Dimlington Stadial. Independent chronological or stratigraphic information (tephra) must therefore be used to clarify the onset of sedimentation at Quoyloo Meadow.

The silts and clays of unit 1b likely relate to the Windermere Interstadial, and these are capped by a small organic detrital horizon, which likely reflects the onset of cold conditions and the degradation and inwash of the catchment's limited vegetation cover. This unit is succeeded by further silts and clays deposited during the Loch Lomond Stadial. Mid way through this unit, a distinctive pale brown/ orange horizon is identified, and is common to all cores spanning the Loch Lomond at Quoyloo Meadow (Figure 5.1). This horizon gradually grades out and is replaced by grey clastic sediments.

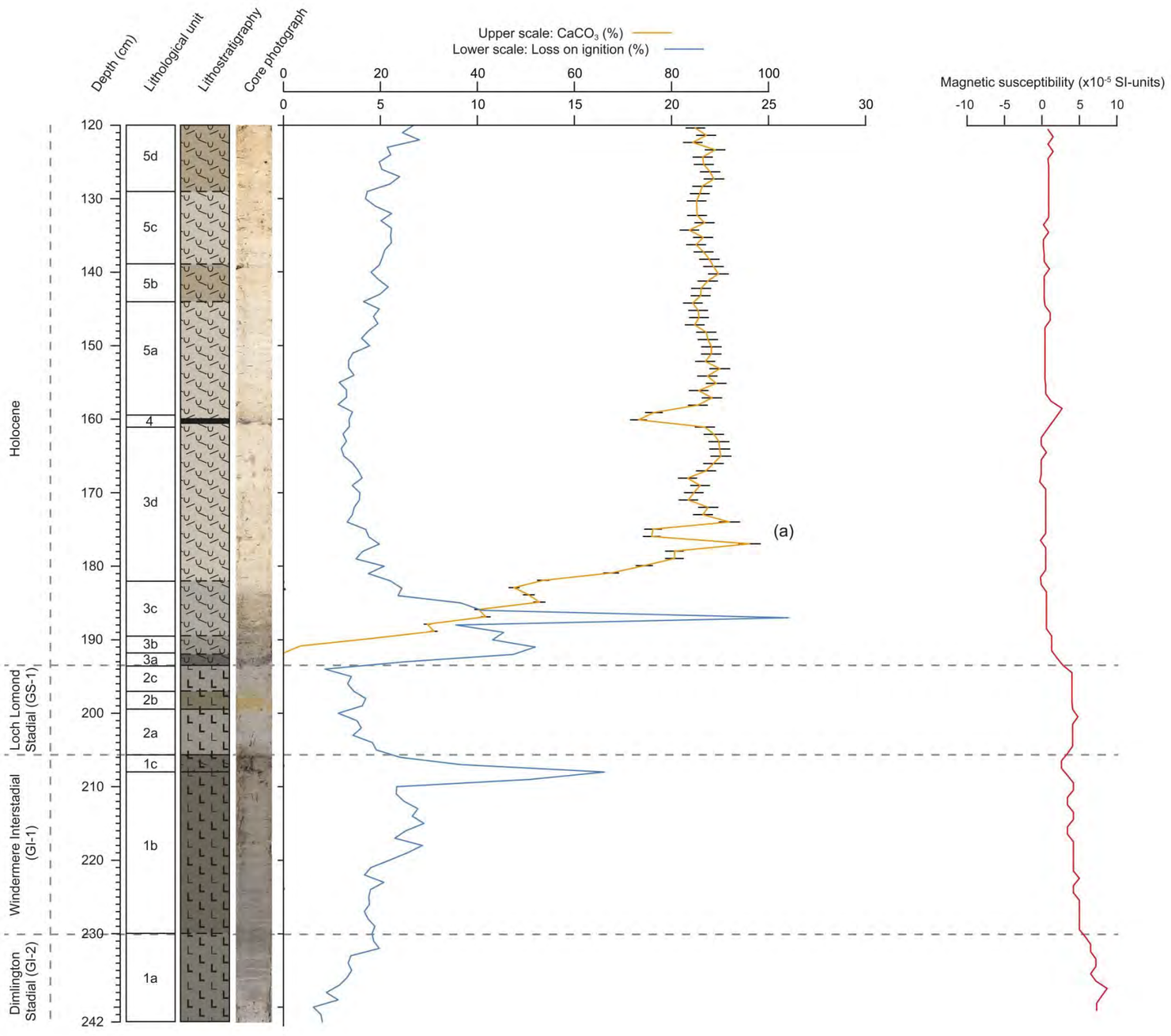

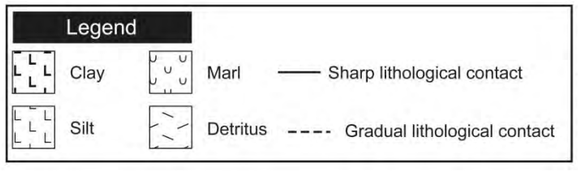

Figure 5.2 Composite sediment stratigraphy for QM1 derived from four overlapping Russian cores. LOI, $CaCO_3$ (with error bars), and Magnetic susceptibility values also shown. There is some uncertainty governing the chronostratigraphic context of unit 1a at Quoyloo Meadow, and whether it relates to the Dimlington Stadial or Windermere Interstadial. See Appendix D for a detailed lithological description.

In turn these are overlain by detrital marl horizons, which signifies the climatic amelioration and environmental/ catchment stabilisation of the early Holocene. Within unit 3d, a short lived, but distinct oscillation in the $CaCO_3$ signal centred on 175-176 cm is noted, and may represent one of the many early Holocene climatic oscillations that are known to characterise this period (e.g. Björck et al. 1996; 1997; Rasmussen et al. 2007). Higher in the stratigraphy at 160 cm, the marl unit is intersected by a black horizontal band of visible ash. This macrotephra likely correlates to the Saksunarvatn Ash, which was identified by Bunting (1994) at a comparable depth of 163 cm. This correlation is discussed further in the ensuing section.

5.2.2 Tephrostratigraphy

QM1D, QM1E, and QM1F were processed for tephra at contiguous 1 cm intervals (see section 4.5), whilst QM1G was sampled only in the lower 11 cm as defined by the overlap with QM1F. Magnetic separation to identify basaltic shards was conducted at select intervals encompassing highly concentrated silicic horizons i.e. 211-215 cm and 196-200 cm. The calcareous deposits of the early Holocene were largely devoid of minerogenic material, thus from a depth of 183 cm upwards only the cleaning phase of the extraction process was necessary (see section 4.5). This enabled the early Holocene sequence to be examined for both silicic and basaltic shards, with the latter often remaining unidentified in limnic deposits due to biases associated with the extraction methodology (see section 4.5). A composite tephrostratigraphy is presented in Figure 5.3 and has been constructed in the same manner as the composite lithostratigraphy. Raw count data can be found in Appendix D.

Due to constraints on time and facilities not all peaks in tephra concentration could be processed for chemical analyses. In total ten horizons were analysed across all of the aforementioned cores. (Figure 5.3). Table 5.1 provides a summary of horizons analysed, their climato-stratigraphic placing, and notes the corresponding composite depth for the tephra.

In the following sections, the shard type which is most abundant within a horizon is termed population A. Shard-types of lesser prominence are given a sequential letter e.g. B, C, D reflecting their lower concentration within the horizon. For consistency, single shard analyses are also referred to as ‘populations’. The justification for this approach is that it is impossible to fully characterise every shard within a horizon, thus whilst a single shard may appear anomalous and hence be considered an ‘outlier’, it

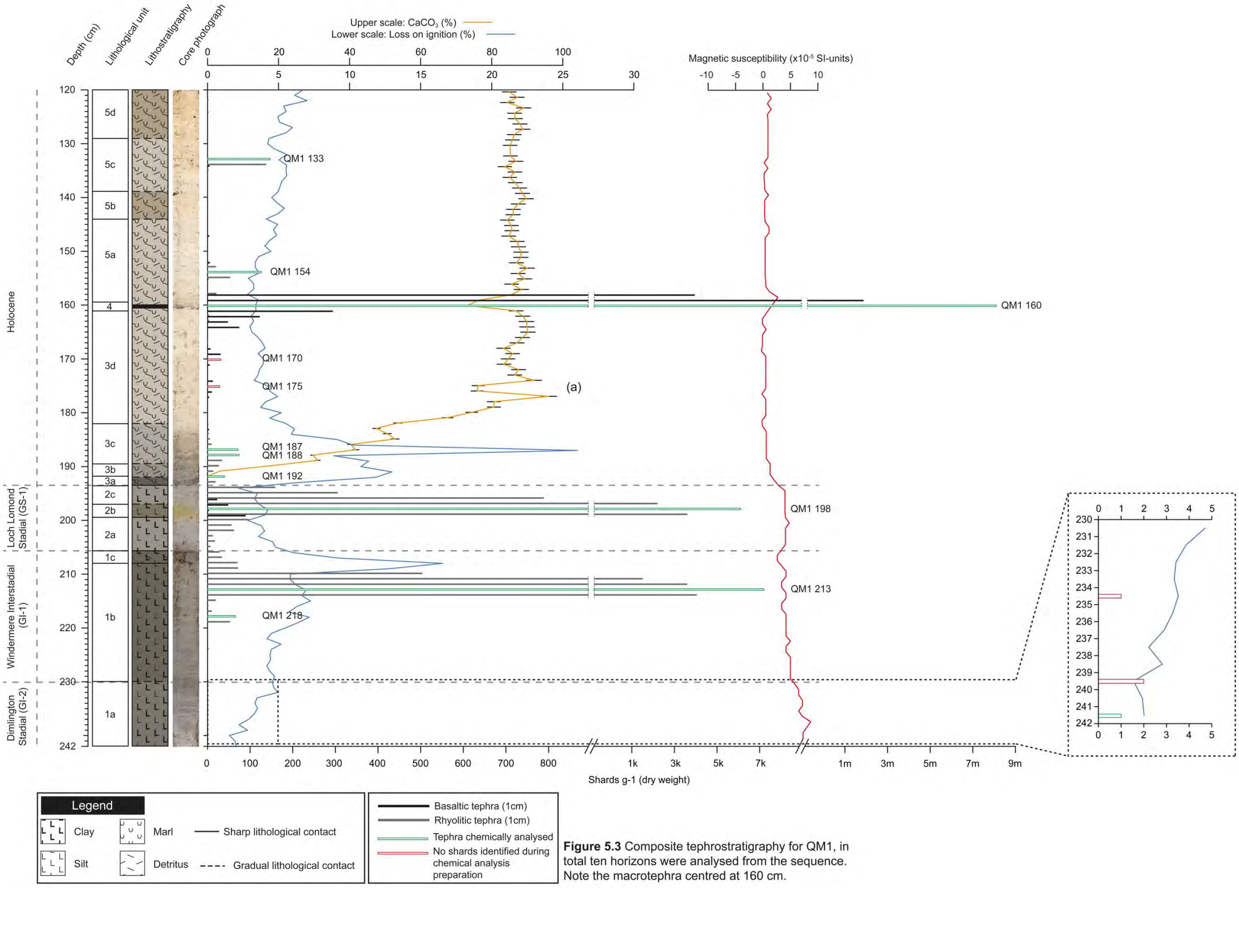

Figure 5.3 Composite tephrostratigraphy for QM1, in total ten horizons were analysed from the sequence. Note the macrotephra centred at 160 cm.

may also represent a sparsely concentrated component, and its dismissal as an outlier based upon a user defined concentration should be considered poor practice. The chemical characteristics of tephra horizons and the populations within, are based on non-normalised filtered data sets. Mean chemical data is presented in Table 5.2. For all geochemical data see Appendix B, and for analytical conditions see section 4.8.1.

Table 5.1 Tephra samples from the Quoyloo Meadow 1 cores and their corresponding composite depth.

Core	Horizon (cm)	Stratigraphic position	Composite coding	Notes
QM1D 120-170	133	early Holocene	QM1 133	analysed
	154		QM1 154	analysed
	160		QM1 160	No shards identified for geochem
QM1E 160-210	168		QM1 169	
	169		QM1 170	analysed
	186		QM1 187	analysed
	187		QM1 188	analysed
QM1F 180-230	191	early Holocene transition	QM1 192	analysed
	187	Loch Lomond Stadial	QM1 198	analysed
	202	Windermere Interstadial	QM1 213	analysed
	207		QM1 218	analysed
QM1G 192-242	234		QM1 235	analysed
	239		QM1 240	sample destroyed in prep
	241		QM1 242	analysed

QM1 242

The lowermost tephra horizons identified in the Quoyloo Meadow sequence lay within the silty-clays of unit 1a (Figure 5.3). Within this unit, three intervals were identified as containing tephra. QM1 242 is the deepest, and attained a concentration of 1 shard g^{-1}, whilst slightly higher in the stratigraphy QM1 240 and QM1 235 attained concentrations of 2 and 1 shard g^{-1} respectively (Figure 5.3). Morphologies of shards across the two horizons are predominantly defined by small blocky shapes, with elongated closed vesicles and circular open vesicles (Figure 5.4 A-D). The single shard identified in QM1 242 is a platey featureless specimen. Whilst all three horizons were prepared for chemical analyses only the shards picked for QM1 242 survived the entire process. Four analyses were obtained from this interval which produced a homogenous series defined by relatively low FeO (ca. 1.45 wt %) and CaO (ca. 0.82 wt %) values (Table 5.2).

Table 5.2 Mean EPMA geochemical data for QM1, values expressed as (%) weight oxide.

Composite code	SiO_2	TiO_2	Al_2O_3	FeO	MnO	MgO	CaO	Na_2O	K_2O	P_2O_5	Total
QM1 133	71.55	0.19	11.80	2.84	0.07	0.05	0.37	5.08	4.42	0.01	96.38
2 std dev (n=11)	1.03	0.01	0.89	0.35	0.01	0.04	0.17	0.37	0.15	0.01	1.39
QM1 154	73.46	0.11	11.80	1.47	0.04	0.07	0.67	4.13	3.84	0.01	95.61
2 std dev (n=11)	0.99	0.02	0.83	0.36	0.01	0.06	0.23	0.29	0.54	0.01	0.99
QM1 160	49.42	3.06	12.99	14.32	0.23	5.46	9.85	2.81	0.47	0.32	98.92
2 std dev (n=31)	0.77	0.34	0.55	1.22	0.02	0.90	0.73	0.35	0.12	0.10	1.38
QM1 187 (pop A)	75.12	0.10	12.09	1.05	0.03	0.02	0.42	3.39	5.30	0.01	97.53
2 std dev (n=4)	2.14	0.01	0.58	0.37	0.01	0.04	0.13	0.70	1.78	0.01	2.49
QM1 187 (pop B)	73.64	0.29	12.06	2.54	0.08	0.22	1.56	4.49	2.51	0.05	97.45
2 std dev (n=2)	2.10	0.01	1.55	0.44	0.02	0.00	0.01	0.42	0.04	0.01	3.65
QM1 187 (pop C)	70.49	0.19	12.36	2.59	0.06	0.08	0.49	5.21	4.38	0.02	95.86
2 std dev (n=2)	1.31	0.00	2.36	0.39	0.02	0.13	0.31	0.52	0.18	0.01	1.41
QM1 187 (pop D)	69.41	0.27	12.71	3.65	0.13	0.20	1.27	5.35	3.39	0.05	96.43
2 std dev (n=2)	2.64	0.00	0.56	0.47	0.03	0.06	0.01	0.53	0.14	0.01	3.99
QM1 188	73.29	0.29	11.66	2.48	0.09	0.24	1.57	4.32	2.48	0.05	96.48
2 std dev (n=8)	1.99	0.01	0.33	0.31	0.01	0.03	0.12	0.39	0.08	0.02	1.92

QM1 192 (pop A)	70.74	0.28	13.16	3.89	0.15	0.20	1.28	5.01	3.51	0.04	98.26
2 std dev (n=6)	2.53	0.01	0.65	0.31	0.02	0.04	0.09	0.57	0.24	0.01	3.51
QM1 192 (pop B)	74.54	0.08	11.99	1.09	0.03	0.04	0.62	4.60	3.69	0.01	96.69
QM1 198	69.67	0.28	12.92	3.76	0.15	0.21	1.31	5.35	3.40	0.03	97.08
2 std dev (n=15)	1.77	0.01	0.44	0.34	0.01	0.04	0.11	0.43	0.16	0.01	2.60
QM1 213	73.10	0.12	12.02	1.44	0.04	0.06	0.72	4.24	3.79	0.01	95.55
2 std dev (n=17)	1.41	0.02	0.48	0.30	0.02	0.04	0.17	0.39	0.17	0.01	1.14
QM1 218	73.43	0.12	12.10	1.47	0.04	0.08	0.75	4.03	3.78	0.01	95.81
2 std dev (n=11)	0.76	0.02	0.24	0.12	0.01	0.04	0.09	0.16	0.19	0.01	0.97
QM1 242	72.66	0.12	12.13	1.45	0.05	0.06	0.82	4.11	3.78	0.02	95.20
2 std dev (n=4)	2.09	0.01	0.47	0.21	0.01	0.01	0.09	0.37	0.30	0.02	2.33

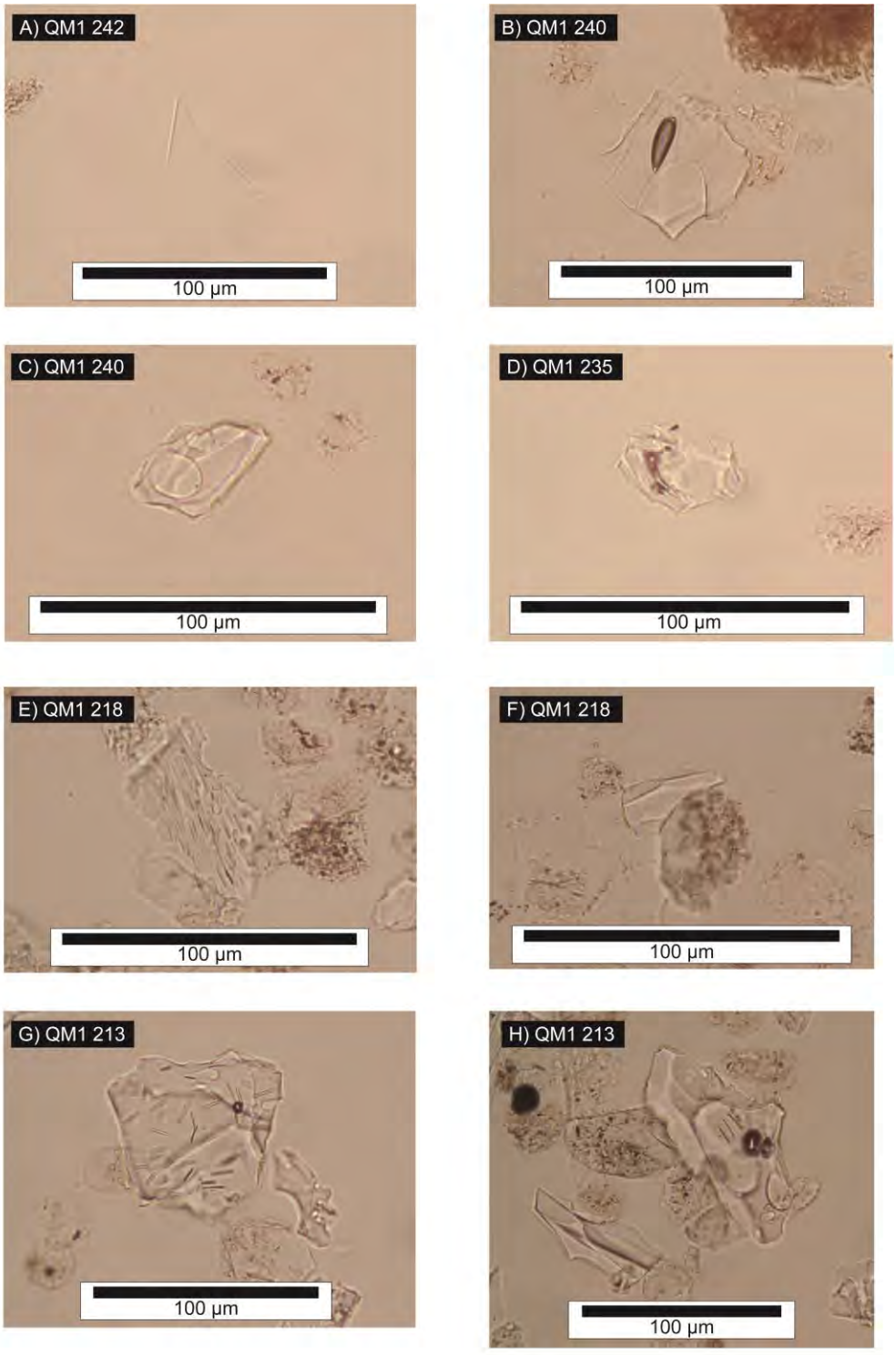

Figure 5.4 Photographs of tephra horizons identified in QM1. (A) A featureless platey shard. (B) A blocky cuspate shard, with an elongate closed vesicle. (C) A small blocky shard exhibiting large open vesicles. (D) A small blocky shard exhibiting small irregularly shaped closed vesicles. (E) A thin damaged shard exhibiting numerous pencil-like mineral inclusions, and elongate open vesicles all aligned in the same direction. (F) A small blocky shard with a single pencil-like mineral inclusion. (G) A large blocky shard possessing numerous pencil-like mineral inclusions aligned in a variety of directions. A single closed vesicle is also present. (H) Two blocky cuspate shards. The larger specimen on the right exhibits some large open vesicles and smaller closed vesicles. Three pencil-like mineral inclusions are also present.

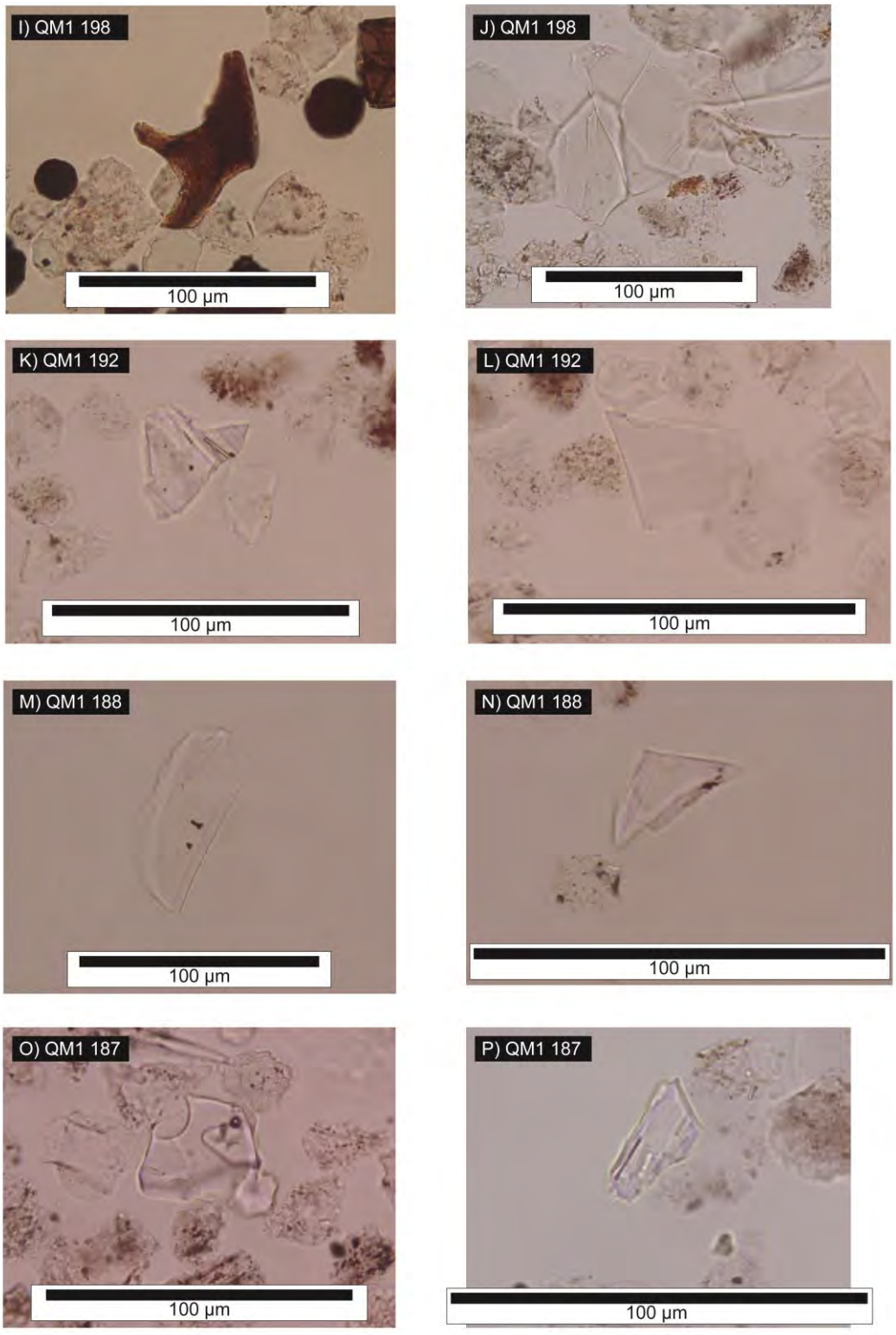

Figure 5.4 continued (I) A highly weathered basaltic shard, exhibiting extensive surface corrosion. (J) Three platey shards and one shard exhibiting some fluting (left hand shard). (K) A small, slightly fluted shard containing a mineral inclusion. (L) A small platey shard showing signs of a cuspate upper edge. (M) An elongated fluted shard which also exhibits an open vesicle on the upper left hand corner. (N) A very small fluted shard. (O) A small blocky shard showing evidence of open and closed vesicles. (P) A very small shard with a single pencil-like mineral inclusion.

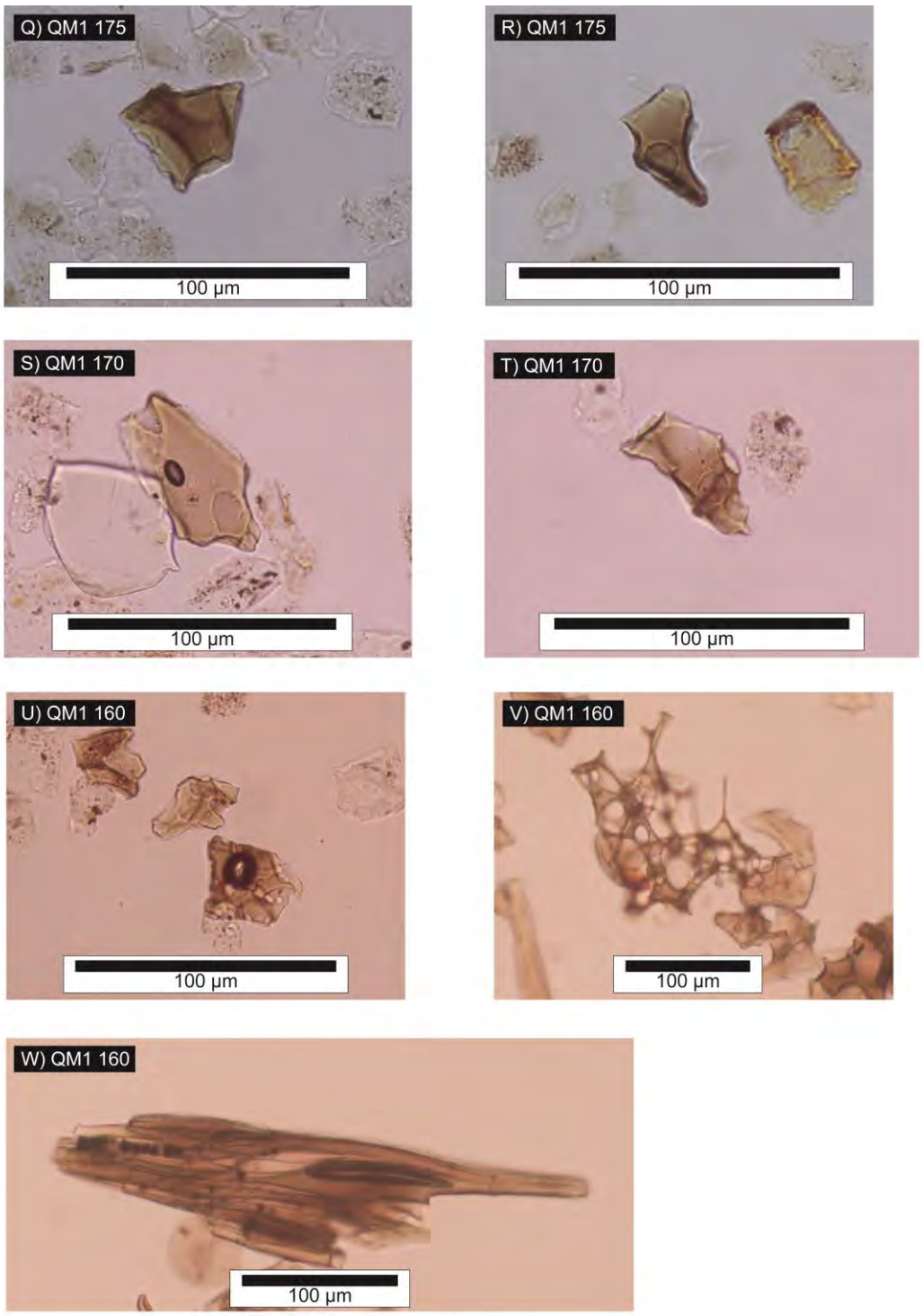

Figure 5.4 continued (Q) A blocky basaltic shard showing signs of damage to the left hand margin. (R) A small basaltic cuspate shard with a single open vesicle. (S) A basaltic shard showing signs of surface pitting and leaching from the left hand margin. (T) A small blocky basaltic shard with a single open vesicle. (U) Three blocky basaltic shards showing signs of surface pitting and glass leaching. A single large closed vesicle is present in the lower specimen. (V) Very unusual 'web-like' morphology, possibly resultant from high levels of degassing and subsequent frothing within the magma body. (W) An exceptionally large shard with an A-axis measurement of 346 µm.

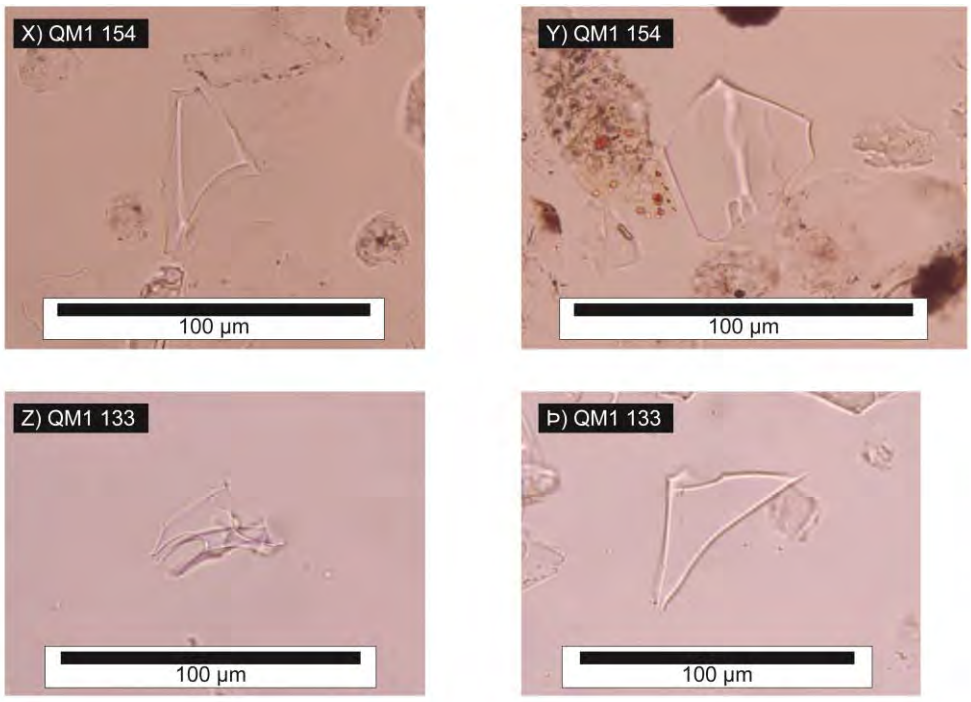

Figure 5.4 continued X) A blocky, platey shard exhibiting some cuspate tendencies. (Y) A 'wing-like' shard with a thicker backbone and thinner flanking sails or 'wings'. (Z) A small cuspate and fluted shard. (Þ) A platey featureless shard.

QM1 218 and 213

The lithological unit 1b is defined by two prominent peaks in shard concentration (Figure 5.3). The lower is centred at 218 cm within silt and clays, and coincides with a minor peak in the LOI; the layer attains a peak concentration of 65 shards g^{-1}. The second peak in shard concentrations at 213 cm occurs just prior to a large influx of organic material, represented in the LOI as a major rise (Figure 5.3), and is defined by a much greater concentration of 7230 shards g^{-1}. Both peaks are typified by large, blocky, colourless shards with an abundance of microlitic inclusions, and some open and closed vesicles (Figure 5.4 E-H). Eleven analyses were obtained for QM1 218 and seventeen for QM1 213; both sets of analyses returned homogenous values, which are defined by relatively low FeO (ca. 1.47 and 1.44 wt %) and CaO (ca. 0.75 and 0.72 wt %) values, respectively (Table 5.2).

QM1 198

Within unit 2 and centred at a depth of 198 cm (unit 2c), i.e. the pale brown/ orange horizon, a tephra was identified (Figure 5.3). The horizon possesses an abundance of colourless vitreous shards that appear plate like, fluted and in some cases exhibited 'wing-like' morphologies (Figure 5.4 I-J). This morphological component of the horizon attained a maximum concentration of 6098 shards g^{-1}. Magnetic separation of the heavy residues also yielded brown-coloured shards which are characterised by a

double peak either side of the 198 cm interval. The highest concentration of 94 shards g^{-1} was attained at 199 cm, whilst a secondary peak of 46 shards g^{-1} was identified at 196 cm. Chemical analyses of the colourless shards (n=15) returned chemistries typified by high FeO (ca. 3.76 wt %), CaO (ca. 1.31 wt %) and Na_2O (ca. 5.35 wt %) values (Table 5.2).

QM1 192

At 192 cm a tephra layer was identified that coincides with an upturn in LOI, and a change in sedimentation from the silt-clay dominant unit 2, to a silty organic-rich calcium carbonate deposit (unit 3a; Figure 5.3). The layer has a concentration of 40 shards g^{-1}, and possesses a variety of shard morphologies ranging from plate-like featureless specimens to blocky microlitic shards (Figure 5.4 K-L). Six chemical analyses produced chemistries, which possessed relatively high FeO (ca. 3.89 wt %), TiO_2 (ca. 0.28 wt %), and CaO (ca. 1.28 wt %) values, while a single shard returned chemistries typified by much lower FeO (1.09 wt %), TiO_2 (0.08 wt %) and CaO (0.61 wt %) totals (Table 5.2).

QM1 188 and 187

Within the detrital marls of unit 3c, two consecutive samples, 188 cm and 187 cm attained comparable shard concentrations of 74 and 71 shards g^{-1} respectively (Figure 5.3). Both intervals were prepared for chemical analyses; the lower peak (188 cm) coincides with a minor reduction in LOI and $CaCO_3$, and is comprised of small, fluted shards, with a fraction containing open and closed vesicles (Figure 5.4 M-N). Eight chemical analyses were obtained, which are defined by comparatively high SiO_2 (ca. 73.29 wt %), low K_2O (ca. 2.48 wt %) and intermediary CaO (ca. 1.57 wt %) values (Table 5.2). QM1 187, conversely coincides with a peak in LOI and exhibits shards of varying size and morphology (Figure 5.4 O-P). The deposit is comprised of small blocky microlitic shards, alongside cuspate, fluted and vesicular shards. Ten chemical analyses were obtained for this horizon, and four distinct populations were identified. Population A (n=4) possess low FeO (ca. 1.05 wt %), TiO_2 (ca. 0.10 wt %), and CaO (ca. 0.42 wt %) values. Population B, (n=2) exhibits low K_2O (ca. 2.51 wt %), and higher CaO (ca. 1.56 wt %), and MgO (ca. 0.22 wt %) values. Population C (n=2) reveals low CaO (ca. 0.49 wt %) and high Na_2O + K_2O values (ca. 5.21 + 4.38 wt %). Population D (n=2) is typified by relatively high FeO (ca. 3.65 wt %) and CaO (ca. 1.27 wt %) (Table 5.2).

QM1 175 and QM1 170

At QM1 175 and QM1 170 two separate peaks of brown shards were identified and quantified to 31 and 29 shards g^{-1} respectively (Figure 5.3). Shards possessed a variety of shapes and sizes (Figure 5.4 Q-T), but also showed signs of chemical corrosion, with leaching and surface pitting present on several specimens (Figure 5.4 S-T). These horizons were subsequently resampled for chemical preparation, but on further investigation no shards were found. This suggests that the shards previously identified were likely a product of contamination from the overlying visible ash layer at QM1 160 and therefore no further analysis was conducted.

QM1 160

The macrotephra identified at 160 cm exhibits exceptionally high concentrations of brown vitreous shards which attained a value of between 8-9 million shards g^{-1}. Optical examination revealed the layer to be dominated by specimens of varied size and morphology (Figure 5.4 U-W). A small percentage of shards were also noted to possess one or more axis >125μm (Figure 5.4 W). Thirty-one chemical analyses were obtained for the horizon which returned a chemical signature defined by comparatively low SiO_2 (ca. 49.42 wt %) and $Na_2O + K_2O$ (ca. 2.81 wt % + 0.47 wt %) values.

QM1 154

Occurring in close stratigraphic proximity to the highly concentrated basaltic horizon of QM1 160, and within unit 5a, is a tephra horizon attaining a peak concentration of 126 shards g^{-1}. The tephra is defined by colourless, blocky, cuspate and 'wing-like' shards (Figure 5.4 X-Y), and ten chemical analyses were obtained. The homogenous analyses are defined by low totals of FeO (ca. 1.47 wt %) and CaO (ca. 0.67 wt %), and comparatively high SiO_2 (ca. 73.46 wt %) values.

QM1 133

The youngest cryptotephra identified in the sequence is identified within unit 5c and is composed of small, faint, platey colourless shards, with some specimens exhibiting open vesicles (Figure 5.4 Z-Þ). A peak concentration of 147 shards g^{-1} was identified, and ten analyses were successfully acquired to classify the horizon. Shard chemistries are typified by high $Na_2O + K_2O$ (ca. 5.08 wt % + 4.41 wt %) values and relatively low CaO (ca. 0.37 wt %) totals.

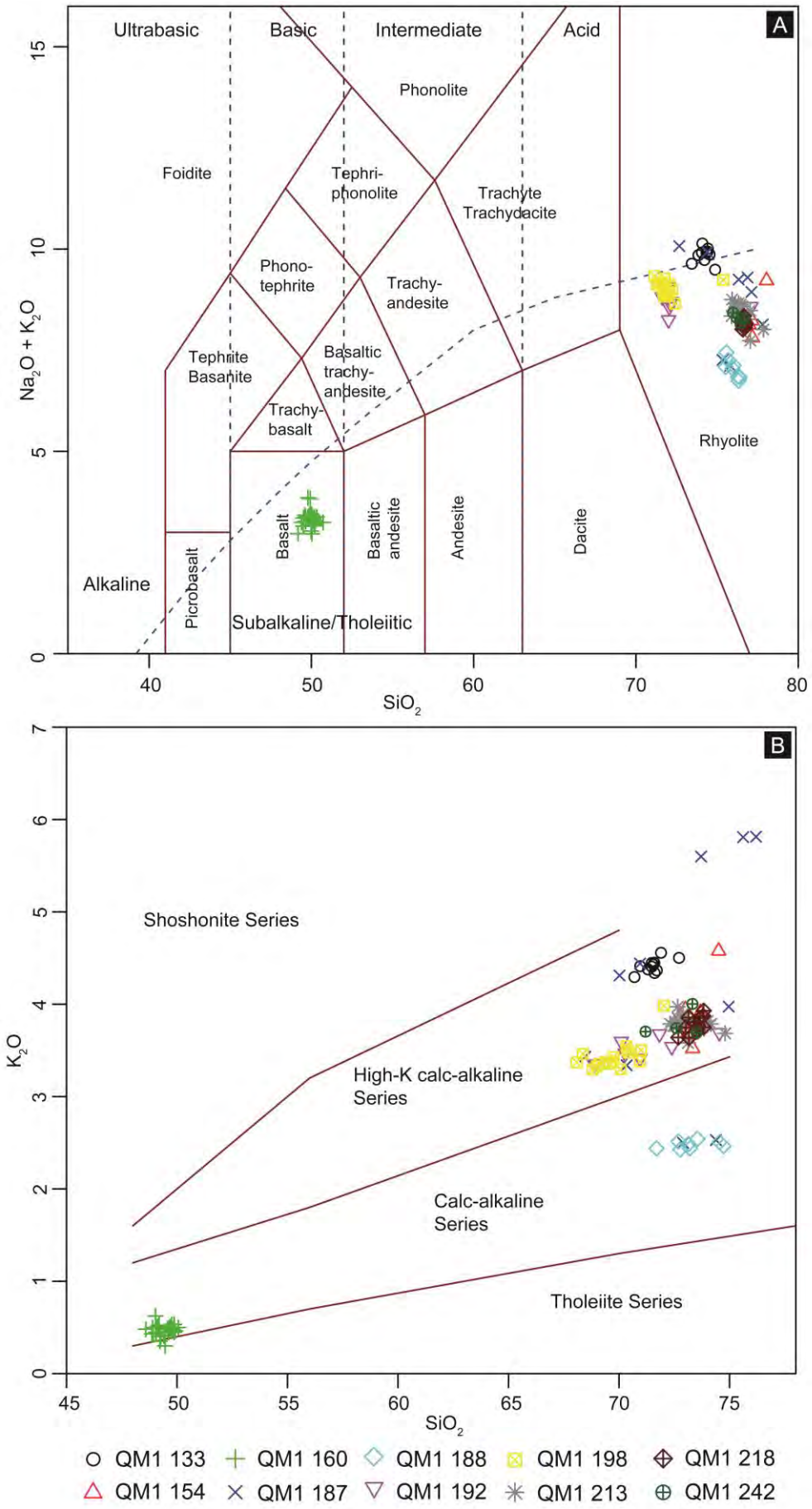

Figure 5.5 Chemical classification of tephra horizons from QM1. (A) Total Alkali vs Silica diagram (Le Bas 1986). (B) K-series plot (Pecorillo and Taylor 1976).

5.3 Interpretation

5.3.1 Tephra correlations

In this section tephra correlations are proposed based on current published data sets. The local and wider significance of these correlations is discussed in Chapter 10 and 11. Primary classification of the tephra layers is made via Total Alkali vs Silica diagrams (Figure 5.5 A), and by potassium value plots (Figure 5.5 B) as defined by Le Bas (1986), and Pecorillo and Taylor (1976) respectively. Data sources for the tephra correlations are summarised in Appendix B.

QM1 242, 218 and 213

The tephras identified across these three intervals can be characterised as sub-alkali rhyolites possessing high potassium values (Figure 5.5). QM1 242, 218 and 213 correlate to an increasing number of tephras in northwest Europe that are described as 'Borrobol-type', after the type-site in northern Scotland where the first of these layers was described (Turney et al. 1997; Pyne-O'Donnell 2007; Pyne-O'Donnell et al. 2008; Lind et al. 2016). These tephras have no known provenance in northern Europe, and suggestions of Snæfellsjökull, Torfajökull, Hekla, and Öræfajökull as source volcanoes have all subsequently been refuted (Lind et al. 2013; Lind et al. 2016). In the British Isles, two tephras are known to occur within the Windermere Interstadial which possess such chemical characteristics; the Borrobol and the Penifiler (Turney et al. 1997; Pyne-O'Donnell 2007; Pyne-O'Donnell et al. 2008). A third tephra layer also bearing this chemical signature has been identified at Lochan An Druim (Ranner et al. 2005). This tephra has a younger age than the accepted range for both the Borrobol and the Penifiler, suggesting that it may represent a separate eruption from the Borrobol source. However, uncertainties on age ranges for all three horizons, and the absence of three clearly defined peaks within any one studied sequence, prevent a more definitive statement, and conclusion being drawn.

The uncharacteristic stratigraphic and biostratigraphic sequence at Quoyloo Meadow means that assigning likely correlatives to the three horizons identified here is particularly challenging. No distinct chemical difference exists between the three horizons which agrees with previous analyses of the Borrobol-type tephras (Lind et al. 2016; Figure 5.6). Due to these chemical and stratigraphic uncertainties, several plausible scenarios are suggested below, to explain the pattern of shards identified within the Quoyloo sequence.

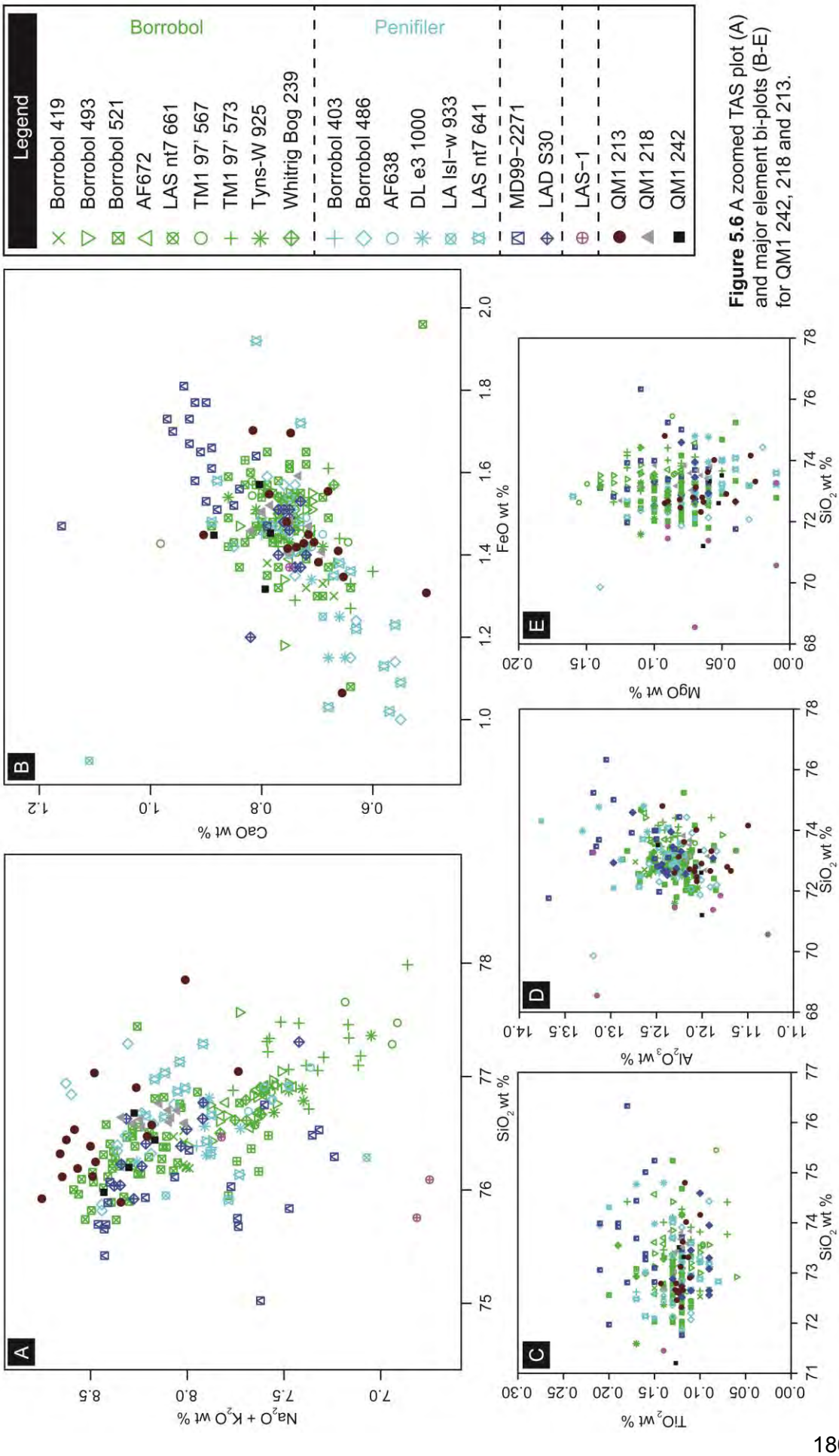

Figure 5.6 A zoomed TAS plot (A) and major element bi-plots (B-E) for QM1 242, 218 and 213.

Scenario 1

Firstly the shards at the base of the sequence, i.e. QM1 242, may represent an older eruption from the Borrobol source. Three sites in particular are known to have yielded Borrobol-type tephras of a Late-Devensian age, which are the marine-core records HM107-05 and MD99-2271/ MD99-2275 situated on the Icelandic shelf (Eiríksson et al. 2000; Gudmundsdóttir et al. 2011; 2012 Figure 5.6). Given correlation to either of these would mean that unit 1a relates to the end of the Dimlington Stadial, whilst the transition into the Windermere Interstadial i.e. GI-1e would be represented by the lower part of unit 1b. Consequently the horizons identified at 213 and 218 cm may therefore be correlated to the Borrobol and Penifiler Tephras respectively. It would also mean that sedimentation rates were particularly high during the late Dimlington Stadial/ early Windermere Interstadial, but reduced markedly after the deposition of the Penifiler Tephra i.e. QM1 213. Subsequent sedimentation at Quoyloo Meadow would seem to be almost non-existent until the onset of the Loch Lomond Stadial, where rates appear to increase. This hypothesis may help to explain the low pollen concentration identified by Bunting (1994) and the predominance of minerogenic sedimentation at the site.

Scenario 2

A second explanation is that the analyses at the base of the sequence (QM1 242) represent material of the Borrobol eruption, and that the long spread of tephra between 220-205, represents the Penifiler Tephra. It has been noted in other locales that the Penifiler Tephra often exhibits a diffuse profile composed of numerous minor peaks (e.g. Matthews et al. 2011; Lind et al. 2016). This potentially means that the sediment between QM1 242 and QM1 218/213 can be attributed to the cold climate GI-1d event. This hypothesis would help to explain the dominance of minerogenic sedimentation at Quoyloo, and would also fit well with the tephrostratigraphy. Current understanding places the Borrobol Tephra slightly before GI-1d, whilst the Penifiler Tephra is often observed coinciding with it, or occurring on the upturn in LOI associated with the subsequent climatic amelioration (e.g. Pyne-O'Donnell et al. 2008; Matthews et al. 2011; Brooks et al. 2012; Lind et al. 2016). A potential caveat on this interpretation is that magnetic separation of the heavy residues coinciding with QM1 218 returned no shards of a basaltic composition, a characteristic of the Penifiler Tephra at Loch Ashik (Pyne-O'Donnell et al. 2008). This hypothesis, like the previous, hints at a possible sedimentary hiatus following QM1 213 and before the onset of Loch Lomond Stadial.

Scenario 3

Thirdly it is plausible that the basal shards i.e. QM1 242 represent the Penifiler, and that sedimentation at Quoyloo only commences after GI-1d. This would mean that that

the sediments at Quoyloo represent the mid-Windermere Interstadial, and that the tephras identified at QM1 218 and 213 represent an eruption, or eruptions, from the Borrobol source at the end of the Interstadial. This is not a pattern which has been previously identified in Scottish sequences, however, a single shard characterised amongst the late Interstadial LAS-1 horizon at Loch an t'Suidhe seemingly offers a potential correlative (Davies 2003; Figure 5.6). However, the majority of the 6 analyses characterising the LAS-1 horizon do not plot within the vicinity of the Borrobol-type chemical field, meaning this horizon cannot therefore be considered a reliable correlative (Figure 5.6). Whilst QM1 218 and 213 may therefore represent new tephras for the LGIT, at present it is difficult to ascertain where chronologically these reside in the lateglacial.

Further work is therefore needed to clarify the stratigraphic context of these tephras. This has already begun, and a provisional Chironomid inferred temperature reconstruction would suggest that temperatures were warm and stable through unit 1b (Steve Brooks pers. comm. 2016). This tentative result eliminates scenario 3 as a plausible contender, as cold climatic conditions would dominate through this interval if the unit was related to GI-1d. At present, it is hard to distinguish between Scenario 1 or 2, however, the first seems more plausible at this time. It is assumed therefore that unit 1a and hence QM1 242 relates to the late Dimlington Stadial. It should be noted, that due to the low concentrations it is not immediately clear whether the shards are representative of the isochron, or whether this lies beneath the extracted unit. This finding is discussed further in section 10.3.3.1 in light of other evidence derived from this study and elsewhere.

QM1 198

The horizon at QM1 198 can be classified as a sub-alkali rhyolite tephra with high potassium values (Figure 5.5). The position of the tephra mid-way through the Loch Lomond Stadial sediments, and its distinctive Katla-type chemistry, would suggest a correlation to the Vedde Ash (Figure 5.7), a tephra widely distributed across Europe and the North Atlantic during this time (e.g. Ruddiman and McIntyre 1981; Mangerud et al. 1984; Wastegård et al. 2000b; Mortensen et al. 2005; Lane et al. 2012b). Whilst there are a number of tephras to possess this chemical affinity (e.g. Lane et al. 2012b), the presence of brown shards thought to be representative of basaltic glass, the clay-dominated stratigraphic unit and its correlation to Bunting's (1994) QM1-Pb, would further support this hypothesis, suggesting the landscape was sparsely vegetated and dominated by a cold climate regime at the time of this tephra's deposition.

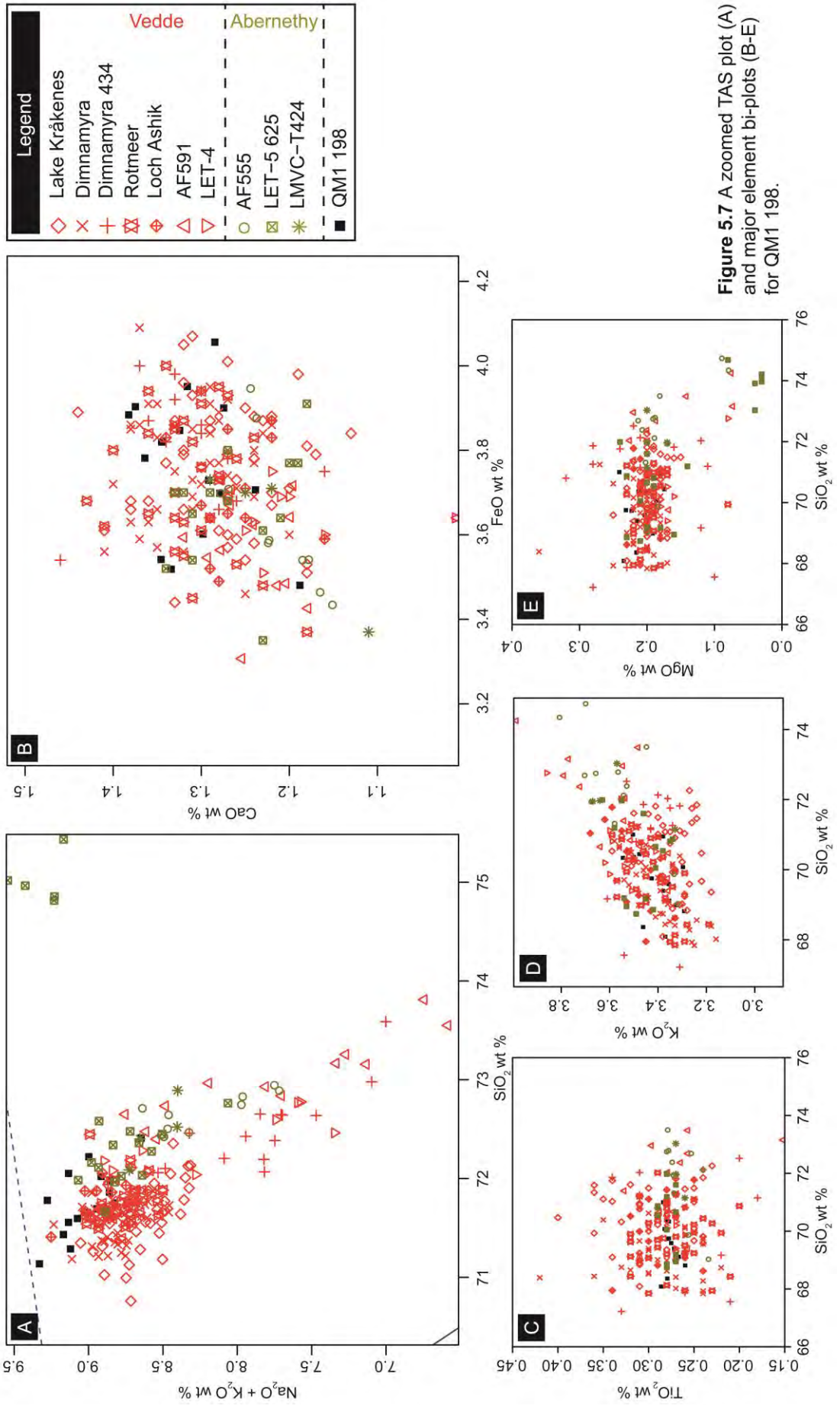

Figure 5.7 A zoomed TAS plot (A) and major element bi-plots (B-E) for QM1 198.

QM1 192

The horizon at QM1 192 returned a bi-modal chemical signature, but all analyses can be classified as sub-alkaline rhyolites with high potassium values (Figure 5.5). Population A as defined by six analyses can be correlated to the Katla volcanic system (Figure 5.8). A second tephra isochron for the Younger Dryas has now been recognised across Scotland, i.e. the Abernethy Tephra (Matthews et al. 2011; MacLeod et al. 2015). It is geochemically indistinguishable from its stratigraphic neighbour, the Vedde Ash, based on major element analysis, being both derived from the same provenance (e.g. Lane et al. 2012b). This fact makes it difficult to discern whether this horizon is the result of primary deposition from the Abernethy Tephra, or, owing to the close proximity of the Vedde Ash, a reworking of the latter. Such an incidence has been shown to be common within Scottish sequences of the period (Pyne-O'Donnell 2011), and the lack of a clear stratigraphic separation between the Vedde Ash and QM1 192 prevents a correlation to the Abernethy Tephra in this case.

The single outlying analyses from QM1 192 (population B) is quite distinct from the accompanying Katla-type shards and shows a chemical affinity to tephras that have previously been correlated to Snæfellsjökull (Davies et al. 2003; Wastegård 2002; Lind and Wastegård 2011; Figure 5.8). In the early Holocene, two tephras are thought to originate from this volcanic centre: the Hässeldalen (11,543-11,232 cal. BP) and Hovsdalur (10,695-10,285 cal. BP), although this has yet to be verified robustly (Lind and Wastegård 2011). The lithostratigraphy and LOI upturn coinciding with QM1 192 would suggest that this interval is indicative of the Younger Dryas/Preboreal transition, the period in which the Hässeldalen was originally described (Davies et al. 2003). Further support for this interpretation is provided by the discovery of the Askja-S/10ka Tephra, which is identified within the stratigraphy 4cm above this horizon, and which possesses a younger age than the Hässeldalen but is considered older than the Hovsdalur. In combination, this evidence would elude to the interpretation that the single shard is more likely representative of the older Hässeldalen Tephra than the Hovsdalur. However, due to the low number of shards identified, and the spread of tephra which characterises this interval (Figure 5.3), it is difficult to ascertain whether or not this interval represents the isochron of the Hässeldalen Tephra. It is possible that the isochron may lie within the surrounding sediments, and quite plausibly masked by reworked Vedde Ash shards.

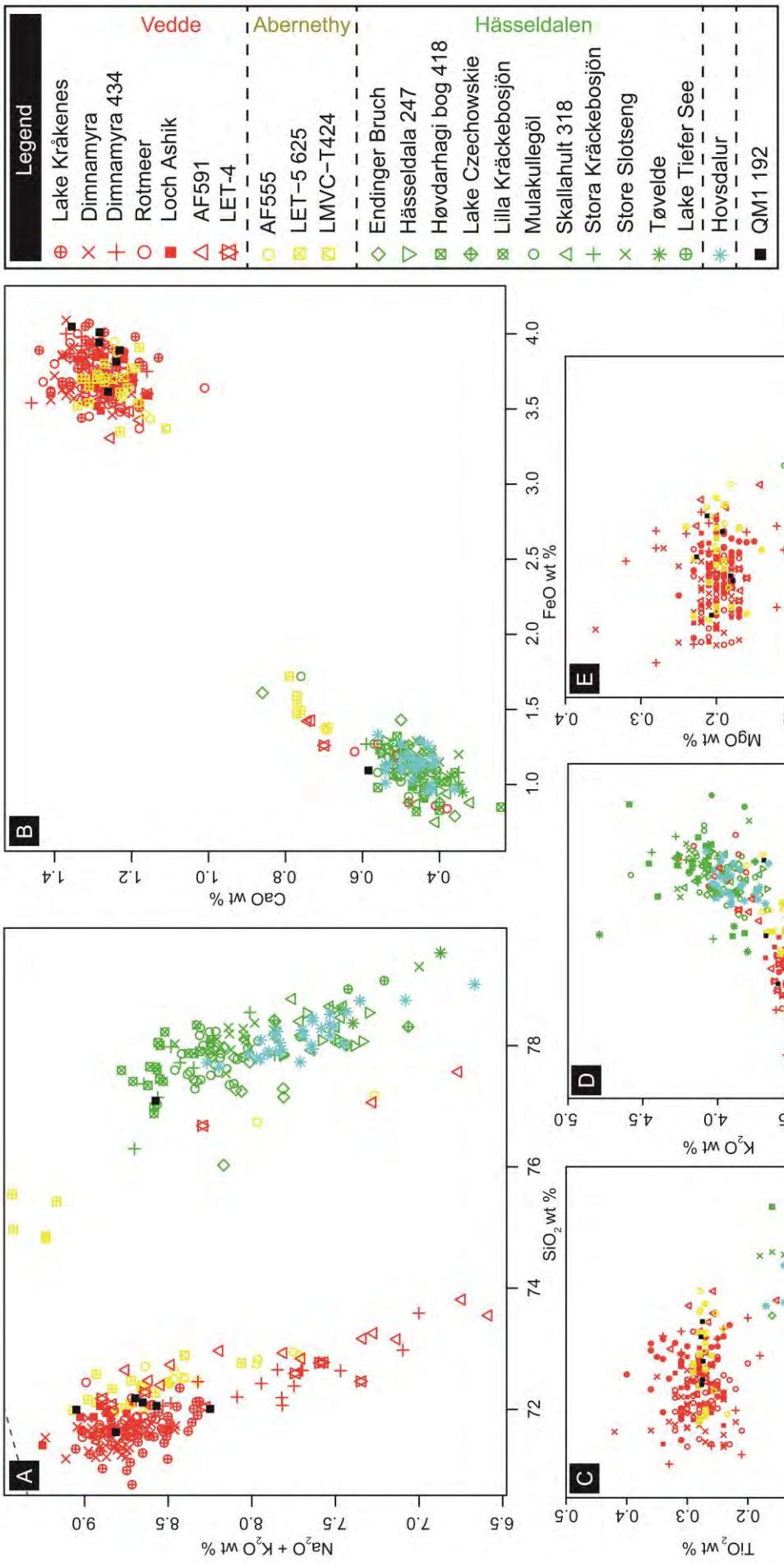

Figure 5.8 A zoomed TAS plot (A) and major element bi-plots (B-E) for QM1 192.

QM1 188 and QM1 187

The chemical characteristics of QM1 188 place it as a sub-alkaline rhyolite with medium potassium values (Figure 5.5). The eight analyses obtained returned a unimodal chemical signature that can be correlated to the Askja volcanic system. For the LGIT only one eruption is known to have occurred from this centre: the Askja-S/10ka (Sigvaldason 2002; Davies et al. 2003). This tephra has a strong representation in mainland Europe, but had remained relatively elusive in sequences from the British Isles until relatively recently (Kelly et al. 2016). Despite this, QM1 188 can be confidently assigned to the Askja-S/10ka eruption (Figure 5.9).

Population A (n=4) of QM1 187 can be classified as a sub-alkaline rhyolite, but potassium values are split between 'high' values and that of the Shoshonite series (Figure 5.5). These abnormally high totals can be ascribed to K-feldspar contamination during analysis of the shards glass. As shown in Figure 5.4 K, shards identified in this interval were very small and contained numerous pencil like mineral inclusions. In plots excluding potassium, the analyses of QM1 187 show a chemical resemblance to tephras previously ascribed to Snæfellsjökull (Davies et al. 2003; Wastegård 2002; Lind and Wastegård 2011; Figure 5.9). Given this tephra's position, i.e. in unit 3c, it is likely that this interval of tephras was deposited early in the Holocene. Hitherto, the only known tephra from this period to possess such chemical characteristics, and to post-date the Askja-S/10ka Tephra (identified 1 cm below; QM1 188), is the Hovsdalur, to which a correlation is therefore proposed.

QM1 187 population B (n=2) can also be classified sub-alkaline rhyolite, but in this instance potassium values are more indicative of an 'intermediate' classification (Figure 5.5). This population is recognised as the Askja-S/10ka (Figure 5.9), which can be explained by a remobilisation of shards from the isochron in the underlying horizon at QM1 188.

QM1 187 population C (n=2) is an alkaline rhyolite with high potassium values (Figure 5.5), and shows an affinity to tephras derived from Torfajökull (Ranner et al. 2005; Pyne-O'Donnell 2007; Lind and Wastegård 2011; Figure 5.9). In the early Holocene there are three tephras that are thought to originate from the Torfajökull province: the Ashik Tephra (10,550-10,250 cal. BP; Pyne-O'Donnell 2007), the Høvdarhagi Tephra (9850-9600 cal. BP; Lind and Wastegård 2011) and the An Druim Tephra (9671-9490 cal. BP; Ranner et al. 2005). The age of the Ashik Tephra is somewhat uncertain, being described in relation to a LOI downturn considered to be the PBO, and older than the Saksunarvatn Ash (Pyne-O'Donnell 2007). Notably, QM1 187 also

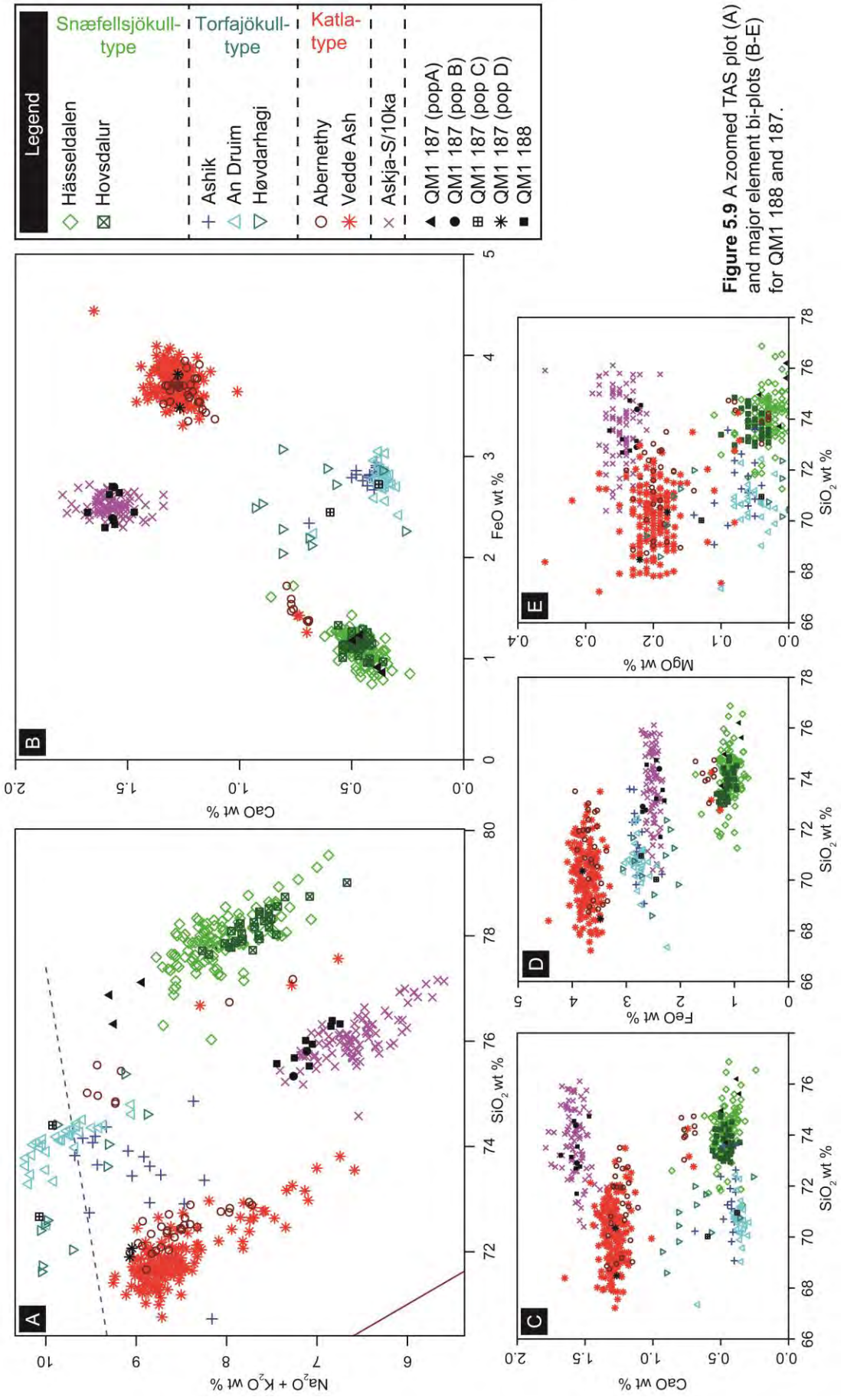

Figure 5.9 A zoomed TAS plot (A) and major element bi-plots (B-E) for QM1 188 and 187.

occurs just after an LOI downturn (Figure 5.3), which may also be representative of the climatic deterioration associated with the PBO. Further evidence to support a connection to the Ashik Tephra is given by the occurrence of the Saksunarvatn Ash stratigraphically above this horizon at QM1 160 (see below). The Saksunarvatn Ash is younger than the Ashik Tephra and older than both the An Druim and Høvdarhagi tephras; therefore, on the premise of superposition, population C can be confidently assigned to the Ashik Tephra.

QM1 187 population D (n=2) is a sub-alkaline rhyolite showing high potassium values (Figure 5.5), and has an overlapping chemical signature with that of the Katla volcanic system (Figure 5.9). Whilst a number of rhyolitic eruptions from Katla are known to have occurred during the LGIT (e.g. Bond et al. 2001; Koren et al. 2008; Lane et al. 2012b; Tomlinson et al. 2012a), the shards identified here cannot be assigned to a primary event. No eruption from Katla is known from this time period (ca. 10.7 cal. BP), which suggests reworking of the Vedde Ash (QM1 198) or the uncorrelated Katla rhyolites (QM1 192), and may have continued to have influence on the tephrostratigraphic profile of the site well into the early Holocene. A low sedimentation rate at this point in the sequence has likely exacerbated this mixing of tephra layers, and, when coupled with the low number of shards identified, means that the placing of the Hovsdalur/Ashik Isochron must be treated with caution.

QM1 160

The macrotephra analysed at this interval provided a unimodal chemical signature that can be classified as a Tholeiitic basalt with low potassium values (Figure 5.5), and more specifically can be correlated to the Grímsvötn system (Figure 5.10). It has recently been demonstrated that this system was particularly active during the early Holocene, where as many as seven eruptions may have characterised this system (Jennings et al. 2002; Jóhannsdóttir et al. 2005; Kristjánsdóttir et al. 2007; Kylander et al. 2011; Jennings et al. 2014; Thordarson 2014; Neave et al. 2015). This has put doubt on whether the Saksunarvatn Ash is an isochronous layer derived from a single eruption, or an amalgam of several closely-spaced events (Thordarson 2014). At present however, all evidence for a multi-modal eruptive series lies to the west of the Grímsvötn caldera (e.g. Jóhannsdóttir et al. 2005; Jennings et al. 2014), with only the Saksunarvatn Ash *sensu stricto* identified in sediment sequences to the east. Whilst all of these tephras are considered to be indistinguishable based on major elemental chemistries, trace element work has noted a distinct chemical offset between tephras identified in the Greenland ice cores and those identified at terrestrial sites in the Faroes and in Germany (Davies et al. 2012; Bramham-Law et al. 2013). Importantly the

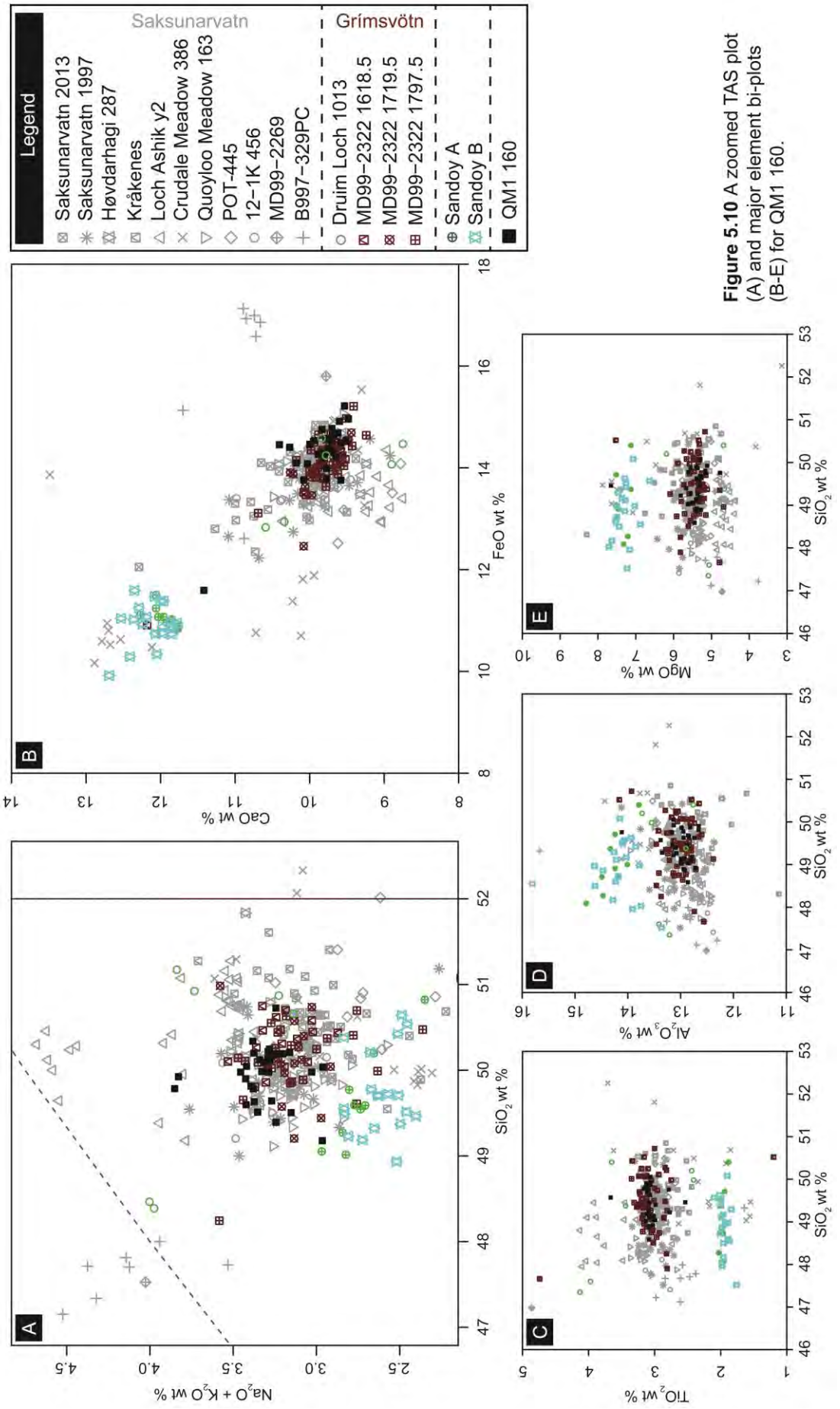

Figure 5.10 A zoomed TAS plot (A) and major element bi-plots (B-E) for QM1 160.

analyses conducted in the Faroes and Germany were indistinguishable from one another, thus suggesting that they were derived from the same event. Whilst further work is needed on the additional layers identified to the west of Grímsvötn, at present it would seem that only one Grímsvötn eruption i.e. the 'Saksunarvatn Ash' proper, was of sufficient magnitude to deposit large quantities of tephra over NW Europe during the Holocene. It is therefore likely that the macrotephra identified in this interval correlates to the well-known Saksunarvatn Ash.

QM1 154

The colourless tephra identified in close proximity to the Saksunarvatn Ash can be classified as a sub-alkaline rhyolite, with high potassium values (Figure 5.5). The tephra exhibits a chemical signature indicative of the Borrobol source (Figure 5.11). In the early Holocene, five tephras bear some chemical resemblance to this group (Lind et al. 2013): the Fosen tephra ca. 10,200 cal. yrs BP (Lind et al. 2013); the Högstorpsmossen ca. 10,200 cal. yrs BP (Björck and Wastegård 1999); a component of L-274 ca. 10,200 cal. yrs BP (Lind and Wastegård 2011); population 3 of the QUB-608 ca. 9500 cal. yrs BP (Pilcher et al. 2005); and the SSn ca. 7300 cal. yrs BP (Boygle 1999). All of these tephras can be described as 'Borrobol-type', and there is a strong possibility that at least the first four of these layers may represent the same event, but poor age controls have prevented a more robust correlation from being made (Lind et al. 2013; Lind et al. 2016). It would seem, however, that QM1 154 most likely correlates to the Fosen Tephra, as this horizon has been defined as occurring immediately after the Saksunarvatn Ash (Lind et al. 2013), as is the case at Quoyloo Meadow.

QM1 133

The uppermost tephra identified in the Quoyloo Meadow sequence can be classified as a sub-alkali/ alkali rhyolite exhibiting high potassium values (Figure 5.5). The unimodal population exhibits a chemical signature akin to tephras which have formerly been correlated to the Torfajökull volcanic system (Figure 5.12). QM1 133 therefore represents the second horizon in the sequence that can be chemically correlated to this system, and, as noted above, three tephras are considered to originate from this province in the early Holocene: the Ashik Tephra 10,550-10,250 cal. BP (Pyne-O'Donnell 2007), the Høvdarhagi Tephra 9850-9600 cal. BP (Lind et al. 2011) and the An Druim Tephra 9671-9490 cal. BP (Ranner et al. 2005). It is likely that the previous occurrence of Torfajökull-type shards in this sequence at QM1 187 can be ascribed to the Ashik Tephra; thus this horizon can be eliminated as a potential candidate. Given

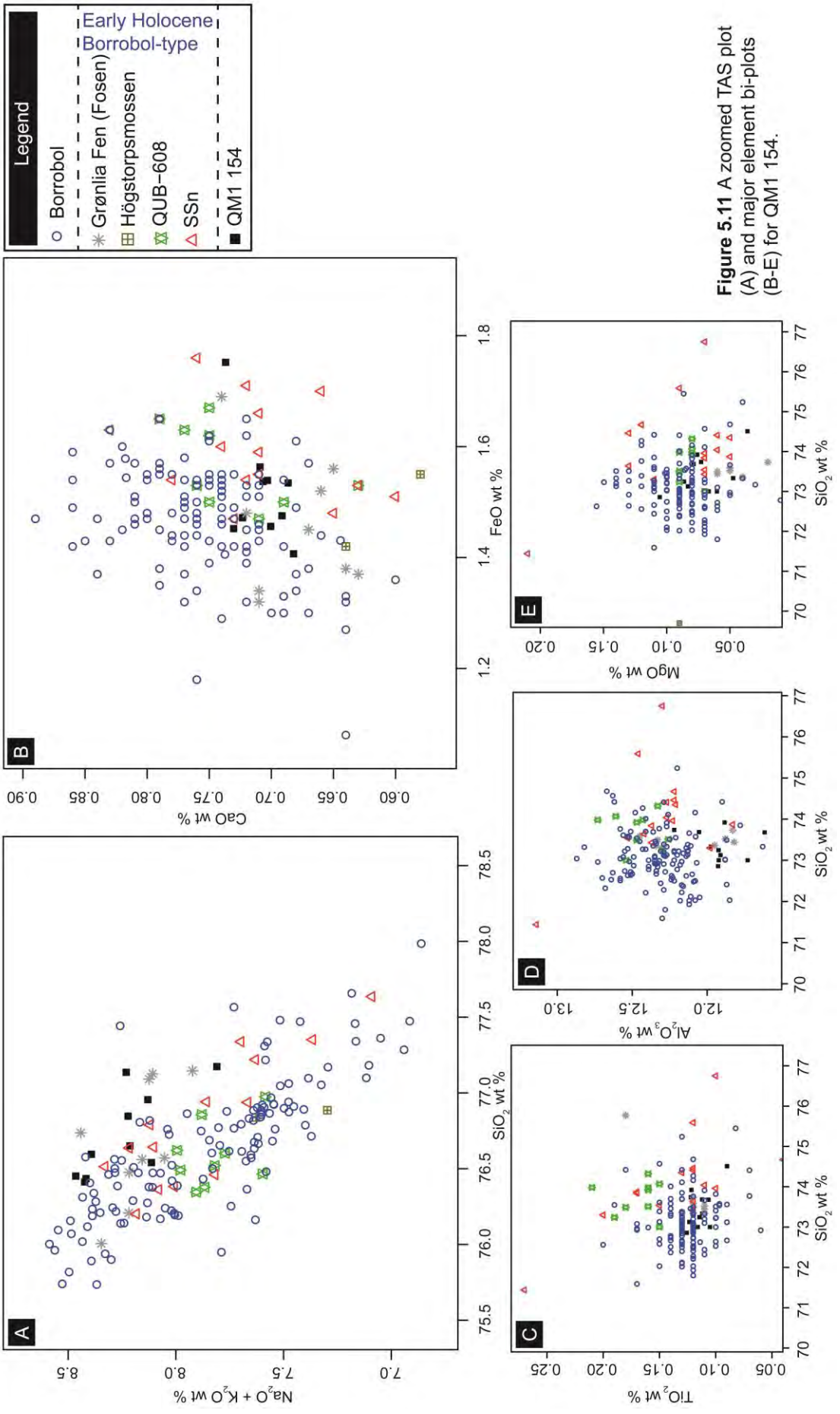

Figure 5.11 A zoomed TAS plot (A) and major element bi-plots (B-E) for QM1 154.

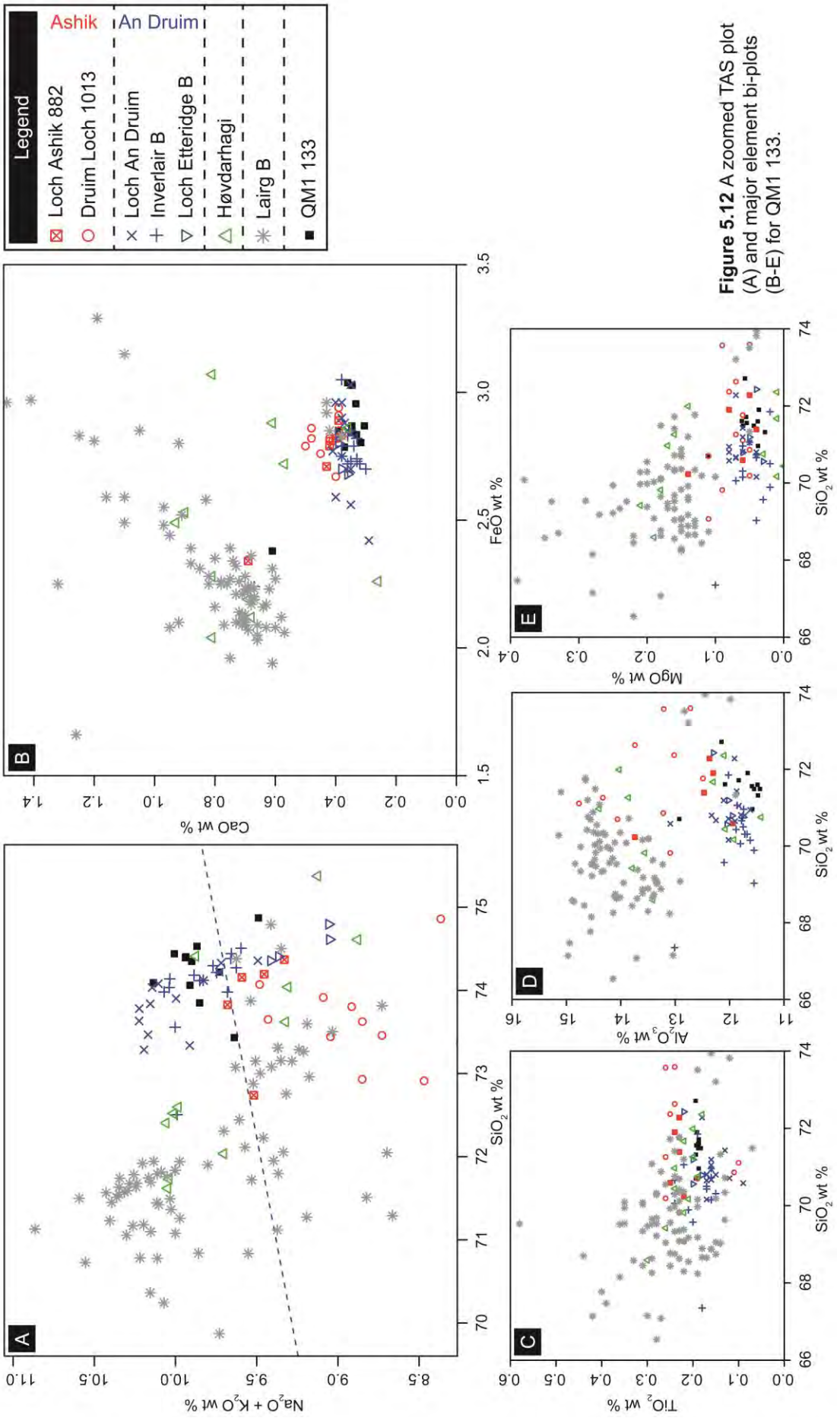

Figure 5.12 A zoomed TAS plot (A) and major element bi-plots (B-E) for QM1 133.

the overlapping ages of the An Druim and the Høvdarhagi, there is some suggestion that these may in fact represent the same eruption (Lind et al. 2011). However, Lind et al. (2011) argue that the Høvdarhagi exhibits a bi-modality that is absent from the An Druim Tephra, and is thus more characteristic of the Ashik Tephra and later Holocene tephras deriving from the Torfajökull system, for example the Lairg B horizon (Dugmore et al. 1995; Pilcher et al. 1996). To emphasise this bi-modal trend, analyses of the mid-Holocene Lairg B Tephra are also shown in Figure 5.12, although this is not considered a potential correlative. The data presented here cluster with the An Druim Tephra; however, one data point consistently plots away from the main body of analyses, and falls broadly within the bi-modal field as illustrated by the spread of Høvdarhagi and Lairg B analyses (Figure 5.12 B). On this basis, the horizon at Quoyloo bears a greater resemblance to the An Druim Tephra, however, the possibility of bi-modality may strengthen the links to the Høvdarhagi Tephra and further consolidate them as a single eruption; this is discussed further in section 10.3.3.4.

5.4 Chapter summary

- This chapter presents litho- and tephrostratigraphic data from Quoyloo Meadow, a basin from Orkney Mainland, Scotland. This data would suggest that the site is indicative of a LGIT age sequence, which agrees with previous investigations of the basin. Contiguous high-resolution (1 cm) sampling throughout the entire sequence yielded a tephrostratigraphic record that exhibits greater complexity than has previously been recognised for the site. Ten horizons were analysed as part of the tephrostratigraphic study, with the main findings summarised in Table 5.3.

- The identification of the Saksunarvatn Ash (QM1 160) as a macrotephra has not previously been reported from the site. This makes the horizon at Quoyloo Meadow the third known incidence of a visible tephra layer in the British Isles, and only the second known occurrence of this particular tephra as visible within the British Isles.

- The Askja-S/10ka Tephra has been firmly identified within the Quoyloo Meadow sequence (QM1 188). This is only the second time this tephra has been confirmed in Scotland after Inverlair by Kelly et al. (2016). The tephra is a particularly valuable early Holocene marker horizon for two reasons: firstly it possesses a very well constrained age estimate (Bronk Ramsey et al. 2015b),

and; secondly it resides in close stratigraphic association with the PBO (e.g. Davies et al. 2003).

- The presence of the Hässeldalen Tephra at Quoyloo Meadow (population B, QM1 192) is recognised in Scotland for the first time. In conjunction with the Askja-S/10ka Tephra, these isochrons offer considerable potential in accurately constraining the PBO in the British Isles for the first time (e.g. Davies et al. 2003).

Table 5.3 Summary of tephra horizons identified in the QM1 composite sequence.

Composite code	Unit	Stratigraphic position	Correlation	Notes
QM1 133	5c	early Holocene	An Druim Tephra	
QM1 154	5a		Fosen Tephra	
QM1 160	4		Saksunarvatn Ash	macrotephra
QM1 187	3c		Hovsdalur? & Ashik Tephra	mixed horizon of Snæfellsjökull-type, Torfajökull-type, Askja-type and Katla-type shards
QM1 188			Askja-S/10ka Tephra	
QM1 192	3a/3b		Hässeldalen Tephra? Abernethy Tephra?	mixed horizon of Katla-type and Snæfellsjökull-type shards
QM1 198	3b	Loch Lomond Stadial	Vedde Ash	
QM1 213	1b	Windermere Interstadial	uncertain	difficulties differentiating between the Borrobol and Penifiler, and the undiagnostic stratigraphy of Quoyloo Meadow prevents a more secure conclusion from being made concerning these horizons
QM1 218				
QM1 242	1a			

- The apparent identification of the Hässeldalen (QM1 192) and Hovsdalur (QM1 187) in the same sequence is a significant find. Both of these tephras thought to derive from Snæfellsjökull, and hence exhibit an indistinguishable chemical signature from one another. There has been some suggestion that they may represent the same eruption (Lind and Wastegård 2011), but this discovery places some doubt on this hypothesis, and highlights that further work is necessary to establish their identity as independent isochrons.

- The Ashik and Hovsdalur Tephras have been identified in the same interval (QM1 187), and closely follow the deposition of the Askja-S/10ka. The exclusively Scottish found Ashik Tephra, can therefore be placed into a refined

regional tephrostratigraphy, and said to be a younger tephra than the Askja-S/10ka Tephra and older than the Saksunarvatn Ash. The development of a site age model for Quoyloo Meadow (Chapter 11) will also provide the first reliably quantified age estimate for this tephra horizon.

- A large amount of ambiguity surrounds the name and age of the early Holocene Borrobol-type eruptions. However, the presence of one of these layers at Quoyloo Meadow (QM1 154) can likely be correlated to the Fosen Tephra. The Fosen occupies a similar stratigraphic position as QM1 154, in that it is found immediately after the Saksunarvatn Ash at Grønlia Fen in Norway (Lind et al. 2013). Thus for the first time in the British Isles this tephra has been reliably identified and placed into a robust tephrostratigraphy.

- There is some debate within the literature as to whether the An Druim and Høvdarhagi represent the same event. Analyses from QM1 133 match more closely with the An Druim Tephra, but there is also some suggestion of a bi-modality in the record. At present it is this lack of bi-modality in the An Druim record which has prevented a consolidation of these two tephras. This is discussed further in section 10.3.3.4 where evidence from Quoyloo Meadow is considered in the wider context of results from all study sites.

- These results have demonstrated that Quoyloo Meadow and the Orkney archipelago are ideally suited to capture and record the multiple Icelandic eruptions that characterised the early Holocene. In combination, the eleven tephra horizons identified in this sequence provide an unparalleled opportunity in the British Isles to develop a robust age model derived purely from tephra horizons. The development of tephra based age models are presented in Chapter 11.

Chapter 6. Crudale Meadow Results

6.1 Introduction and chapter structure

Crudale Meadow is located in the south west of Orkney Mainland (Chapter 3). With Quoyloo Meadow (Chapter 5) it is one of the most northerly basins containing marl sediments in the British Isles, and offers one of the best opportunities in NW Europe to develop a multi proxy record of LGIT age (e.g. Whittington et al. 2015). In addition, it is postulated that the sites northerly position off the coast of Caithness and Sutherland will improve the links between mainland Britain and other parts of NW Europe, where tephras so far absent in the Scottish or British tephra frameworks have been detected.

Crudale Meadow resides within the same catchment as Spretta Meadow (see Chapter 3), and unlike the former, exhibits a sedimentological profile that spans the entirety of the LGIT. The site has previously been the focus of several detailed palynological studies (Moar 1969a; Bunting 1994; Whittington et al. 2015), as well as a more recent stable isotopic assessment (Whittington et al. 2015). However, the wider significance of these studies have been limited by the lack of a robust chronology; a problem which besets many palaeoenvironmental records from carbonate basins due to the effects of geological carbonate contamination of radiocarbon samples. The focus of this chapter along with Chapter 5 is to assess the viability of carbonate basins for capturing, and preserving tephra horizons of LGIT age, with the ultimate aim of developing robust age models capable of centennial to decadal scale precision.

The geological, glaciological, and tephrostratigraphical context of the site is presented in Chapter 3, as is a summary of previous studies on the basin. This chapter therefore focuses on the main litho- and tephrostratigraphic findings of this study, and provides an interpretation of the tephra series based upon the current understanding of LGIT aged tephras in NW Europe.

6.2 Results

Three boreholes were recovered from the Crudale Meadow site using 0.5 m Russian samplers in February 2014 (Figure 6.1). Site coordinates from Whittington et al. (2015) were used in order to replicate previously studied stratigraphies. CRUM 1 (59.016111 -3.328639) is positioned in the same locality as the Bunting and Whittington cores, whereas CRUM 2 (59.016028 -3.32875) and CRUM 3 (59.015833 -3.328556) are cores from deeper parts of the basin. These deeper locations were determined by a systematic basin sounding, using 1.0 m Russian rods to ascertain point depth measurements every 15-20 m from CRUM 1.

Figure 6.1 Crudale Meadow basin sediment stratigraphy. Only the lower-most cores are illustrated here, for a lithological description of all cores see corresponding Appendix. The deeper CRUM 2 and CRUM 3 sequences have been aligned with the CRUM 1 sequence. Note the stratigraphic mismatch between CRUM 1I 520-570 and CRUM 1J 560-610. At a depth of 398 cm a macrotephra horizon was identified within the CRUM 1E 360-410 core.

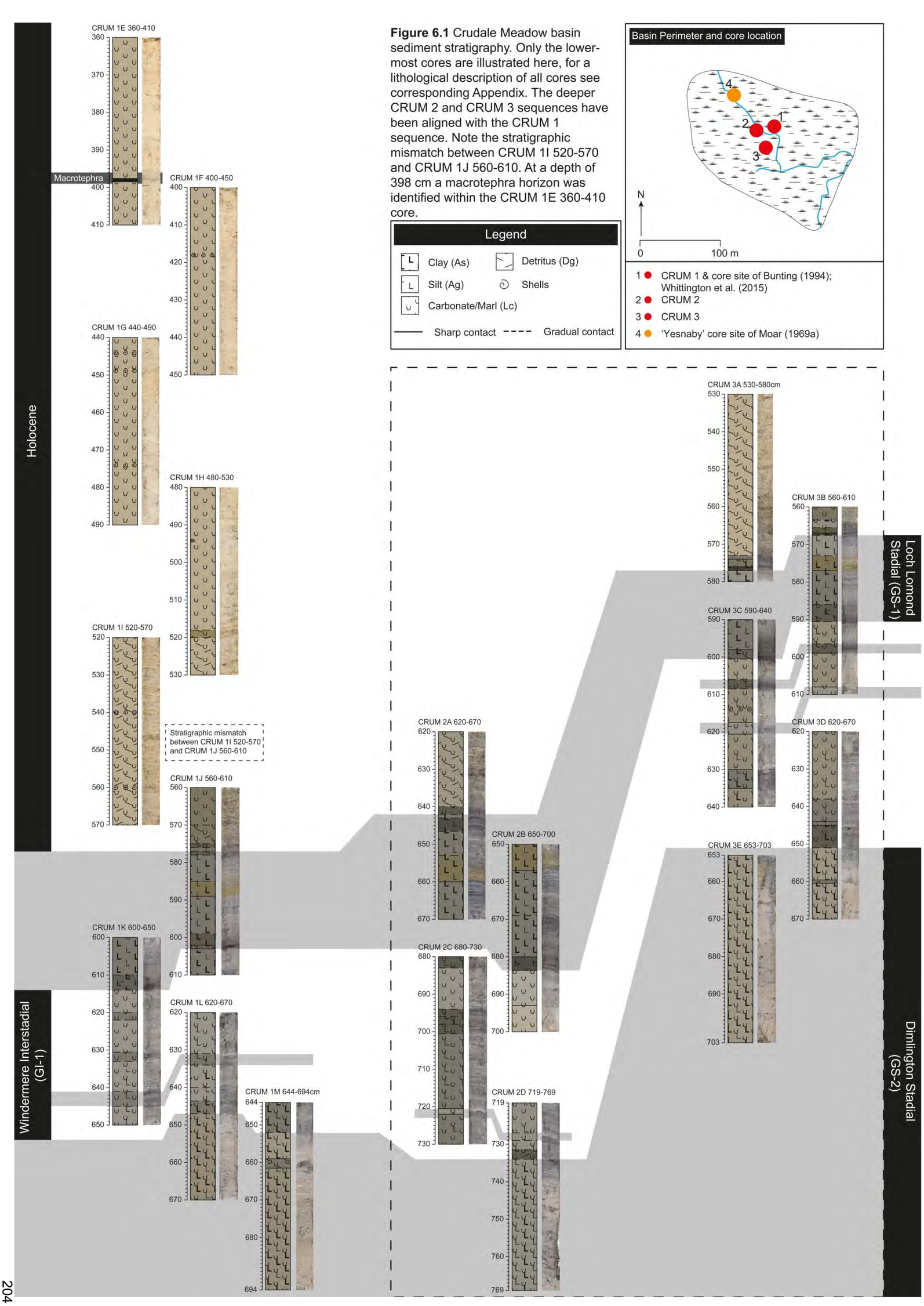

6.2.1 Basin sedimentology

Figure 6.1 illustrates the deepest Crudale Meadow cores, with climatic zones inferred from lithological changes. Detailed sedimentological descriptions of each of the cores can be found in Appendix E. The CRUM 1 sequence was chosen in this study due to the potential correlations that could be drawn with the Whittington et al. (2015) lithostratigraphy.

Cores from the CRUM1 sequence (Figure 6.1) were matched and aligned using lithology, LOI, $CaCO_3$, and magnetic susceptibility changes. This enabled a composite sediment stratigraphy to be constructed. However, problems were encountered when aligning CRUM 1J 560-610 and CRUM 1I 520-570, which are thought to span the Loch Lomond Stadial/ early Holocene transition (Figure 6.1). A clear mismatch can be observed in the stratigraphy, with the upper unit of CRUM 1J 560-610 exhibiting a much darker and more mottled marl substrate than the lower unit of CRUM 1I 520-570. This is further evident in the LOI, $CaCO_3$ and magnetic susceptibility values between the two cores, which cannot be aligned reliably (Figure 6.2). Using the CRUM 3A 530-580 core, which spans the same interval, it is evident that approximately 15 cm is absent from the CRUM1 stratigraphy (Figure 6.2). Using this information, a corrected composite stratigraphy was developed (Figure 6.3). In the correction process, the Holocene portion of the sequence was shifted upwards by 15 cm. This is justified by the stratigraphic alignment of tephra: moving the sequence upwards by 15 cm places the depth of the basaltic macrotephra at 380 cm, at a comparable depth to the Saksunarvatn Ash as reported by Bunting (1994) and Whittington et al. (2015), 386.5 and 384 cm, respectively.

The basin contains sediments spanning the entirety of the LGIT and Holocene. Clastic deposits at the base of the sequence relate to the Dimlington Stadial, and these grade progressively into Windermere Interstadial marls. What is particularly interesting about the Interstadial sequence at Crudale Meadow is that marl sedimentation, indicative of warm stable conditions, appears to be punctuated by two, and potentially three, intervals where minerogenic sedimentation is dominant. These may be correlated to three sedimentological and proxy-inferred climatic ‘events’ as identified by Whittington et al. (2015). The depths of these units within this sequence are centred on (a) 632, (b) 621, and (c) 610 cm (Figure 6.3). The Windermere Interstadial sediments are succeeded by Loch Lomond Stadial age silts and clays, and mid-way through the deposit, a distinctive pale brown/ orange horizon is identified. Notably this is common

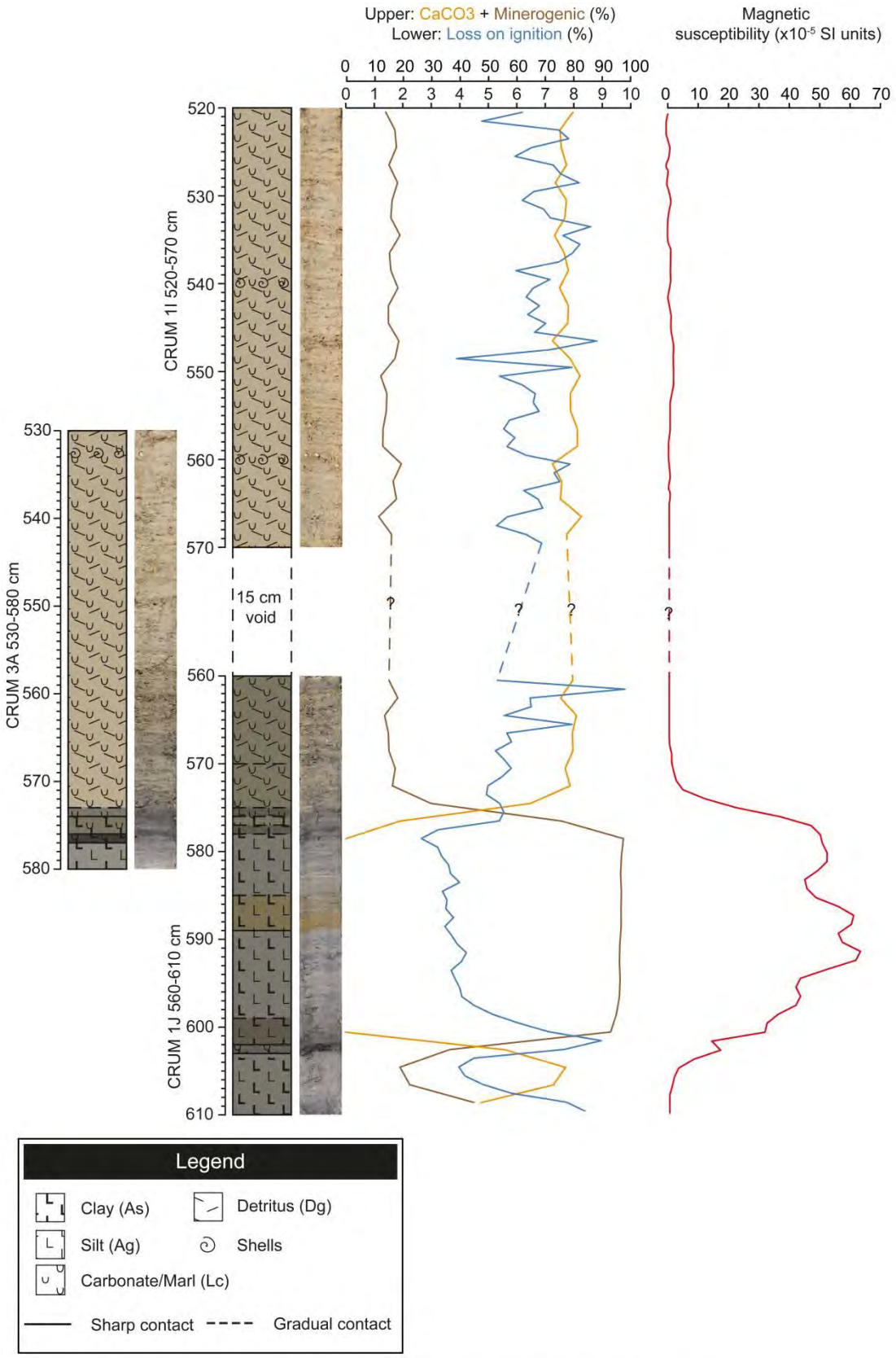

Figure 6.2 Schematic illustrating a 15 cm offset between CRUM 1J 560-610 and CRUM 1I 520-570 as inferred from the CRUM 3A 530-580 core.

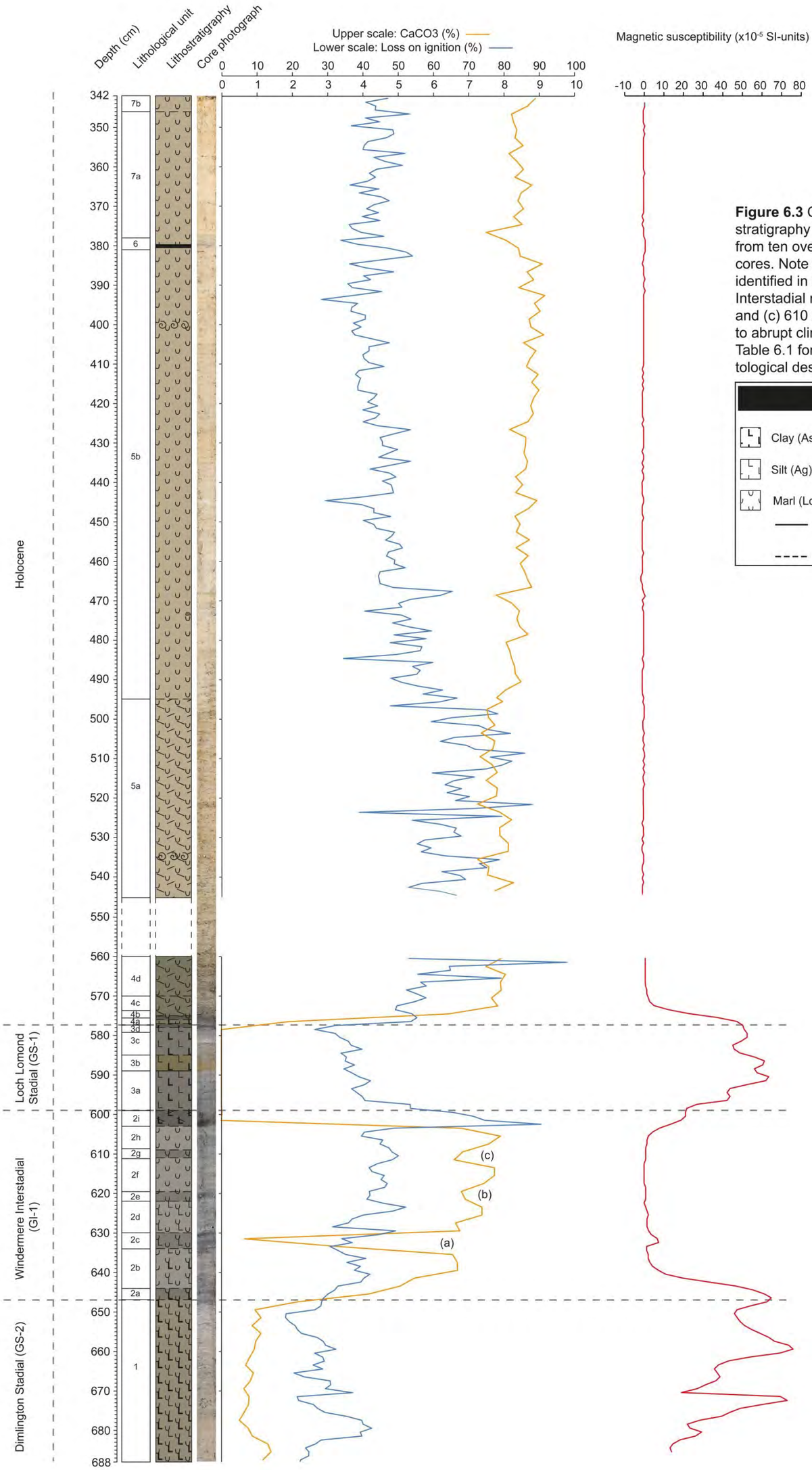

Figure 6.3 Composite sediment stratigraphy for CRUM1 derived from ten overlapping Russian cores. Note the three oscillations identified in the Windermere Interstadial marls (a) 632, (b) 621, and (c) 610 cm, which may relate to abrupt climatic oscillations. See Table 6.1 for a detailed sedimentological description.

across all four cores taken from this unit within the basin (Figure 6.3). Holocene marl overlies the Loch Lomond Stadial deposits, with the lowermost of these marl unis exhibiting abundant moss layers. These units become largely devoid of moss bands at a depth of ca. 495 cm. At 380 cm a black horizontal band composed of visible tephra intersects the marl substrate, and likely correlates to the Saksunarvatn Ash identified by Bunting (1994) and Whittington et al. (2015) at respective depths of 386.5 and 384 cm. This correlation is discussed further in the next section.

6.2.2 Tephrostratigraphy

CRUM 1E 360-410, CRUM 1F 400-450, CRUM 1G 440-490, CRUM 1H 480-530, CRUM 1I 520-570, CRUM 1J 560-610, CRUM 1K 600-650, CRUM 1L 620-670 and CRUM 1M 644-694 were processed for tephra at contiguous 1 cm intervals (see section 4.5). Magnetic separation to identify basaltic shards was conducted at select intervals surrounding the mid Loch Lomond Stadial silicic tephra i.e. 585-588 cm. The calcareous deposits of the early Holocene were largely devoid of minerogenic material, thus from a depth of 545 cm upwards only the cleaning phase of the extraction process was necessary (see section 4.5). This enabled the early Holocene sequence to be examined for both silicic and basaltic shards, with the latter often remaining unidentified in limnic deposits due to biases associated with the extraction methodology (see section 4.5). A composite tephrostratigraphy is presented in Figure 6.4 and has been constructed on the same basis as the construction of the composite sediment stratigraphy. Raw count data can be found in Appendix E.

Due to constraints on time and facilities not all peaks in tephra shard concentration could be chemically analysed. In total sixteen horizons were analysed across all of the aforementioned cores. Overlapping analyses occur at CRUM 1L 630 cm and CRUM 1K 643 cm which relate to a tephra situated within unit 2c (Figure 6.4). CRUM 1K 608 cm and CRUM 1J 597 cm relate to a tephra that spans unit 2i/ 3a. CRUM 1I 522 cm and CRUM 1H 518 cm relate to a silicic tephra at the end of unit 5a. As a result thirteen tephra horizons comprise the composite tephrostratigraphy (Figure 6.4). Table 6.1 provides a summary of horizons analysed, their climato-stratigraphic placing, and notes the corresponding composite coding.

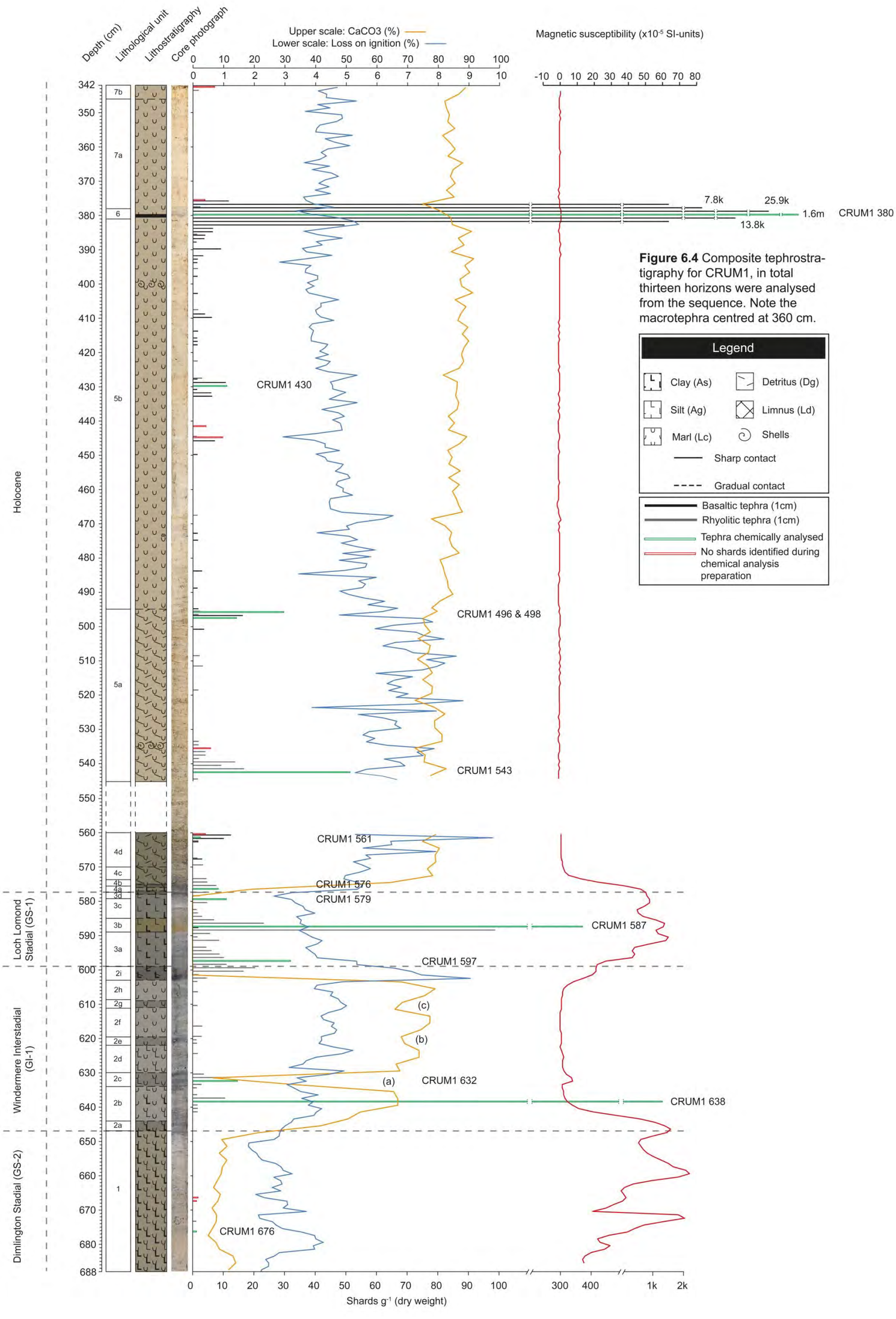

Figure 6.4 Composite tephrostratigraphy for CRUM1, in total thirteen horizons were analysed from the sequence. Note the macrotephra centred at 360 cm.

Table 6.1 Tephra samples from Crudale Meadow 1, and their corresponding composite depth.

Core	Horizon (cm)	Stratigraphic position	Composite coding	Notes
CRUM 1E 360-410	360	early Holocene	CRUM1 343	No shards identified for geochem
	393		CRUM1 376	No silicic shards identified for geochem
	396		CRUM1 380	analysed
CRUM 1G 440-490	451	early Holocene	CRUM1 430	analysed
	463		CRUM1 442	No shards identified for geochem
	466		CRUM1 445	No shards identified for geochem
CRUM 1H 480-530	518	early Holocene	CRUM1 498	analysed
CRUM 1I 520-570	520	early Holocene	CRUM1 496	analysed
	522	early Holocene transition	CRUM1 498	analysed
	560		CRUM1 536	No shards identified for geochem
	567		CRUM1 543	analysed
CRUM 1J 560-610	560	early Holocene transition	CRUM1 560	No shards identified for geochem
	561		CRUM1 561	analysed
	576		CRUM1 576	analysed
	579	Loch Lomond Stadial	CRUM1 579	analysed
	587		CRUM1 587	analysed
	597		CRUM1 597	analysed
CRUM 1K 600-650	608	Loch Lomond Stadial	CRUM1 597	analysed
	643	Windermere Interstadial	CRUM1 632	analysed
CRUM 1L 620-670	630	Windermere Interstadial	CRUM1 632	analysed
	637		CRUM1 638	analysed
	665	Dimlington Stadial	CRUM1 666	No shards identified for geochem
	666		CRUM1 667	Not tephra when analysed
CRUM 1M 644-694	681	Dimlington Stadial	CRUM1 676	analysed

In the following sections, the most numerous chemical analyses of the same type are described as population A, with subsequent horizons assigned sequential lettering e.g. B, C denoting a lesser prominence within the horizon. For consistency, single shard analyses are also referred to as 'populations'. The chemical characteristics of tephra horizons and the populations within are based on non-normalised filtered data sets. Mean chemical data is presented in Table 6.2. For all chemical data see Appendix B, and for analytical conditions see section 4.8.1.

Table 6.2 Mean EPMA geochemical data for CRUM1.

Composite code	SiO_2	TiO_2	Al_2O_3	FeO	MnO	MgO	CaO	Na_2O	K_2O	P_2O_5	Total
CRUM1 380	49.21	3.03	12.82	14.27	0.23	5.45	9.92	2.75	0.45	0.30	98.43
2 std dev (n=29)	1.23	0.24	0.80	1.37	0.02	0.44	0.97	0.50	0.11	0.04	1.90
CRUM1 430	48.33	3.04	12.76	14.30	0.23	5.40	9.76	2.44	0.49	0.53	97.28
2 std dev (n=8)	1.89	0.17	0.86	0.68	0.01	0.25	0.42	1.01	0.08	0.93	3.24
CRUM1 498	75.57	0.30	12.09	2.53	0.09	0.24	1.60	4.29	2.56	0.05	99.31
2 std dev (n=13)	0.93	0.01	0.41	0.22	0.01	0.06	0.12	0.37	0.08	0.01	1.28
CRUM1 496 (pop A)	49.24	3.05	12.80	14.26	0.23	5.31	9.73	2.64	0.47	0.30	98.05
2 std dev (n=27)	0.95	0.12	0.71	0.83	0.02	0.36	0.46	0.50	0.05	0.05	2.24
CRUM1 496	75.22	0.31	12.13	2.70	0.09	0.22	1.67	4.36	2.43	0.04	99.17
CRUM1 498 (pop A)	74.21	0.30	11.92	2.56	0.09	0.23	1.62	4.26	2.55	0.04	97.78
2 std dev (n=29)	1.73	0.01	0.40	0.20	0.02	0.04	0.13	0.23	0.17	0.01	2.07
CRUM1 498 (pop B)	49.49	3.05	12.88	14.10	0.23	5.25	9.63	2.61	0.49	0.36	98.09
2 std dev (n=2)	0.01	0.06	0.44	0.97	0.01	0.11	0.03	0.48	0.01	0.08	1.02
CRUM1 498 (pop C)	68.70	0.26	13.05	3.42	0.13	0.21	1.28	4.93	3.33	0.03	95.35
CRUM1 543 (pop A)	74.14	0.09	11.35	1.08	0.03	0.02	0.40	3.38	4.01	0.01	94.50
2 std dev (n=4)	1.59	0.01	0.24	0.29	0.02	0.03	0.05	2.26	0.24	0.01	1.20

CRUM1 543 (pop B)	73.13	0.16	12.45	1.30	0.04	0.05	0.76	3.72	3.72	0.02	95.34
2 std dev (n=3)	2.48	0.01	0.62	0.20	0.02	0.03	0.10	1.00	0.21	0.00	2.55
CRUM1 561 (pop A)	72.97	0.16	11.77	2.42	0.07	-0.01	0.36	4.57	4.20	0.01	96.53
2 std dev (n=2)	3.95	0.00	1.25	0.02	0.00	0.01	0.01	0.74	0.49	0.01	5.01
CRUM1 561 (pop B)	69.09	0.28	13.14	3.53	0.15	0.20	1.24	5.11	3.32	0.04	96.11
CRUM1 576 (pop A)	73.41	0.12	12.01	1.45	0.04	0.06	0.77	4.12	3.75	0.01	95.76
2 std dev (n=5)	1.14	0.01	0.69	0.10	0.01	0.02	0.05	0.20	0.10	0.01	1.35
CRUM1 576 (pop B)	71.21	0.28	13.44	3.65	0.14	0.19	1.31	5.23	3.53	0.03	99.01
2 std dev (n=4)	1.52	0.01	1.36	0.11	0.02	0.03	0.07	0.42	0.13	0.01	3.35
CRUM1 576 (pop C)	73.72	0.16	11.43	2.66	0.07	0.00	0.41	4.73	3.86	0.00	97.04
CRUM1 579 (pop A)	73.68	0.12	12.07	1.54	0.04	0.07	0.66	4.19	3.60	0.00	95.98
CRUM1 579 (pop B)	71.10	0.27	12.79	3.88	0.14	0.22	1.31	5.08	3.38	0.03	98.21
CRUM1 587 (pop A)	71.11	0.28	13.08	3.71	0.15	0.19	1.29	5.00	3.47	0.02	98.31
2 std dev (n=21)	1.72	0.01	0.53	0.40	0.02	0.06	0.17	0.35	0.19	0.01	1.94
CRUM1 587 (pop B)	73.05	0.13	11.79	1.55	0.04	0.07	0.71	4.00	3.77	0.01	95.11
CRUM1 587 (pop C)	73.43	0.16	11.52	2.45	0.07	-0.02	0.33	4.46	4.07	0.00	96.47

CRUM1 587 (pop D)	73.05	0.29	8.37	6.45	0.29	0.00	0.27	5.51	4.38	0.01	98.62
CRUM1 597	73.29	0.12	12.10	1.47	0.04	0.07	0.76	4.11	3.74	0.01	95.70
2 std dev (n=30)	0.81	0.01	0.40	0.19	0.01	0.03	0.09	0.31	0.19	0.01	1.14
CRUM1 632	73.59	0.12	12.16	1.45	0.04	0.07	0.74	4.12	3.79	0.01	96.08
2 std dev (n=13)	1.24	0.01	0.62	0.17	0.01	0.03	0.09	0.30	0.18	0.00	1.74
CRUM1 638 (pop A)	73.82	0.12	12.16	1.49	0.04	0.07	0.73	4.14	3.74	0.01	96.33
2 std dev (n=41)	1.65	0.01	0.45	0.20	0.01	0.05	0.11	0.25	0.24	0.01	2.27
CRUM1 638 (pop B)	70.07	0.27	13.28	3.44	0.15	0.18	1.24	5.29	3.34	0.04	97.29
CRUM1 676	62.15	1.24	15.00	5.12	0.14	1.42	3.67	5.12	2.47	0.93	97.26
2 std dev (n=2 same shard)	0.56	0.02	0.88	0.38	0.00	0.00	0.39	0.83	0.12	0.15	1.44

CRUM1 676

The lowermost tephra horizons identified in the Crudale Meadow sequence lies within the carbonate rich silts and clays of the Dimlington Stadial i.e. unit 1 (Figure 6.4). Within this unit four intervals were identified as containing tephra. CRUM1 676 and 673 are isolated shards and are quantified as 1 shard g^{-1}, whilst the interval of CRUM1 666-667 exhibits a peak concentration of 2 shards g^{-1}. Shard morphologies from these intervals are varied (Figure 6.5 A, B), with specimens exhibiting fluted and blocky shapes. CRUM1 666-667 did not return any viable chemical data, and CRUM1 673 was not sampled for analysis; however, a single shard from CRUM1 676 was successfully extracted and analysed twice. The analyses revealed a chemical signature defined by intermediate SiO_2 values (ca. 62.15 wt %), high FeO values (ca. 5.12 wt %) and high Al_2O_3 totals (ca. 15.0 wt %) (Table 6.2).

CRUM1 638

Shortly after the onset of marl formation and within unit 2b of the Windermere Interstadial a stratigraphically distinct and highly concentrated tephra occurs. The peak of the tephra is quantified at 1328 shards g^{-1}, with shards exhibiting blocky, cuspate, and vesicular morphologies (Figure 6.5 C, D). Chemical analysis of this horizon returned a predominantly homogenous signature, although a single shard was identified amongst the 42 analyses that did not correlate with the rest of the series. Population A is therefore defined by 41 analyses, and possesses relatively low FeO (ca. 1.64 wt %) and CaO values (ca. 0.73 wt %). In comparison the single shard comprising population B is defined by higher FeO (3.44 wt %) and CaO values (1.24 wt %) (Table 6.2).

CRUM1 632

Within unit 2c, and observed around the oscillation marked (a) in Figure 6.4, a tephra horizon is identified. Shard concentration reaches a peak of 15 shards g^{-1}, and exhibit morphologies identical to those seen in CRUM1 638, i.e. blocky, vesicular along with occasional mineral inclusions (Figure 6.5 E, F). Thirteen chemical analyses returned a homogenous population characterised by low FeO (ca. 1.45 wt %) and CaO values (ca. 0.74 wt %), respectively (Table 6.2).

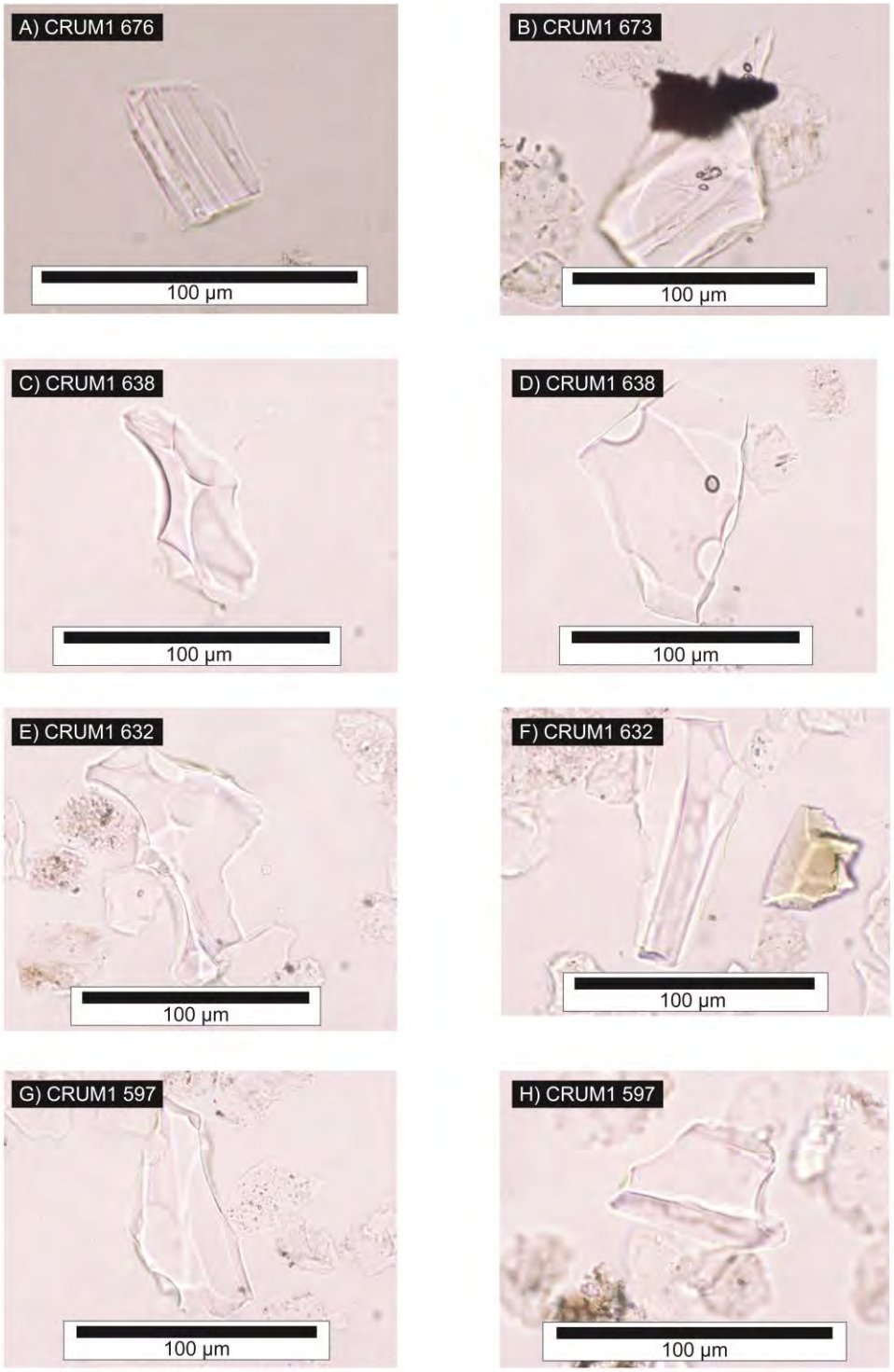

Figure 6.5 Photographs of tephra horizons analysed from CRUM1. (A) A thin and delicate fluted shard. (B) A blocky shard with an irregular morphology and irregular shaped mineral inclusions. (C) A blocky cuspate shard. (D) A large platey shard, with cuspate edges and a ovoid shaped closed vesicle. The shard also exhibits a hydration crack running across the upper surface. (E) A blocky cuspate shard, which exhibits a number of fine pencil-like mineral inclusions on the lower limb. (F) A blocky shard with a weathered left and right flank. (G) A blocky shard with cuspate edges. (H) A blocky shard with cuspate edges.

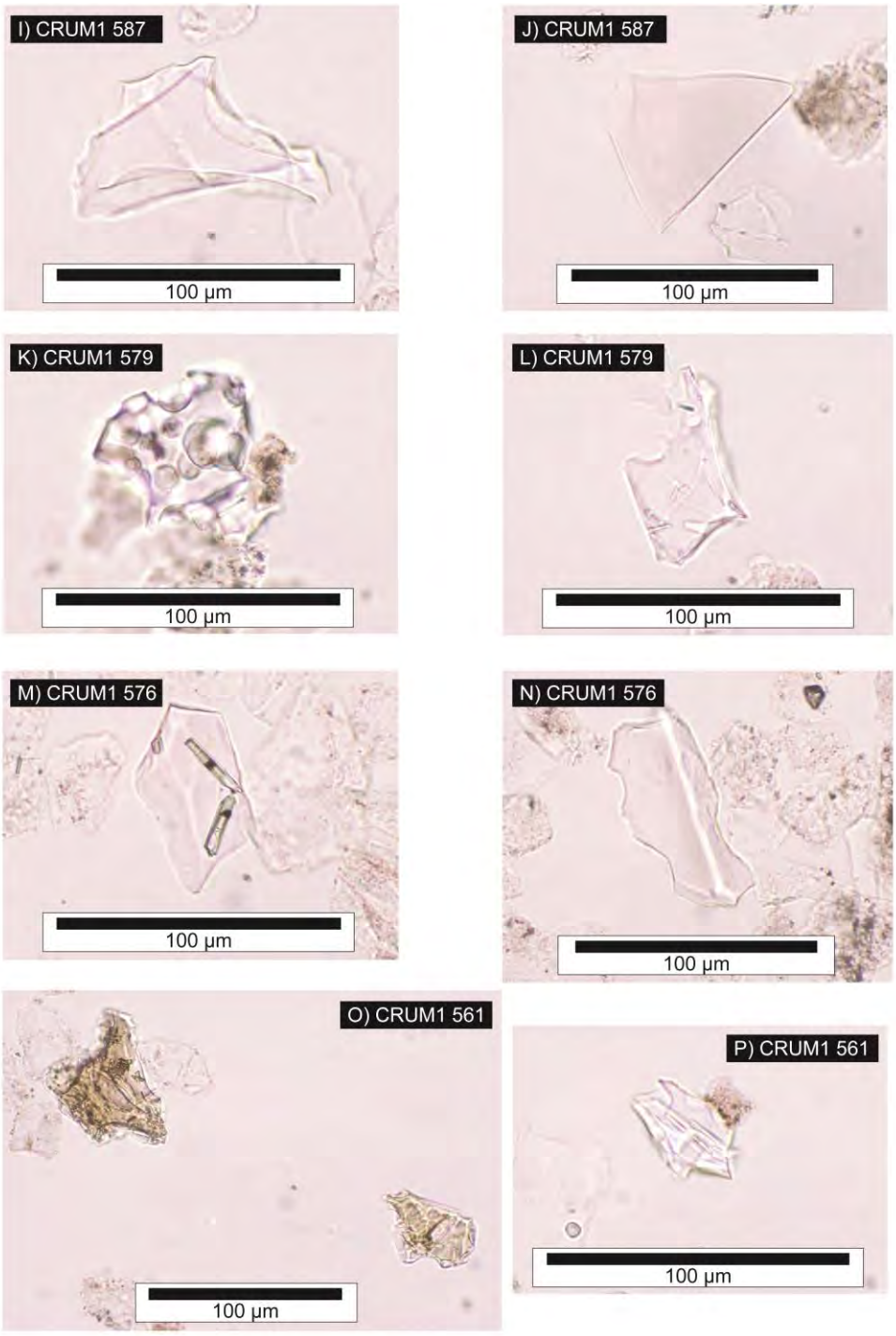

Figure 6.5 continued (I) A blocky shard with cuspate edges. (J) A featureless platey shard. (K) A very blocky and highly vesicular shard with some pencil-like mineral inclusions. (L) A thin battered shard, with irregularly placed pencil-like mineral inclusions and evidence of open vesicles. (M) A small shard with large pencil-like mineral inclusions. (N) A shard exhibiting a thicker central 'spine' with two thinner 'wings' either side ('Butterfly shaped'). (O) Two highly weather basaltic shards. Both exhibit varying degrees of surface pitting a leaching. (P) A small shard with very fine mineral inclusions aligned with the long axis.

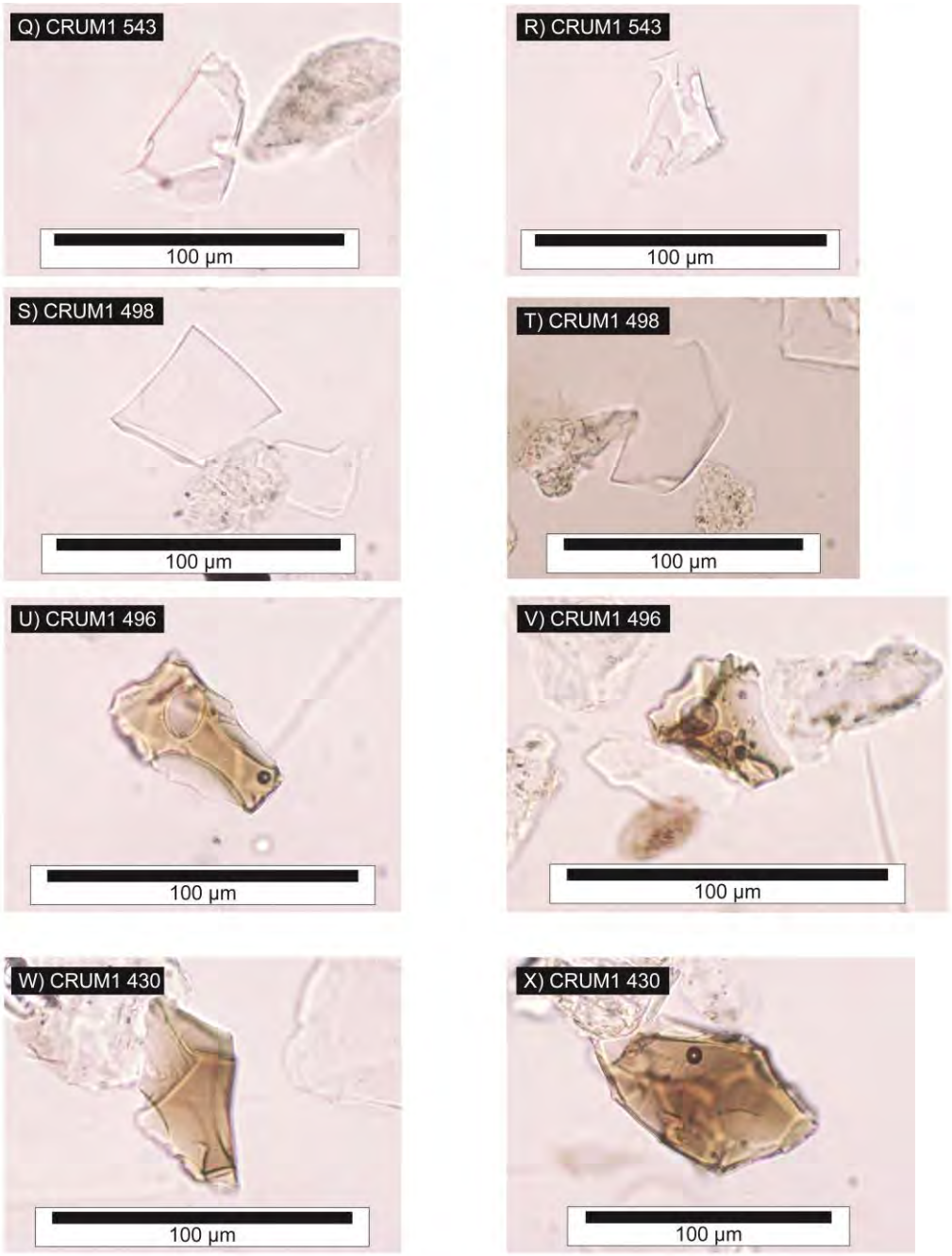

Figure 6.5 continued (Q) A small shard with cuspate edges and evidence of open vesicles. (R) A small shard with several open vesicles forming cuspate edges. The shard also exhibits a small mineral inclusion. (S) A featureless platey shard. (T) A featureless platey shard. (U) A blocky basaltic shard exhibiting both open and closed vesicles, as well as a degree of colour leaching on the outer flanks. (V) A small vesicular basaltic shard showing signs of surface pitting. (W) A blocky basaltic shard showing signs of surface leaching on the lower left hand margin. (X) A blocky basaltic shard with a single closed vesicle, evidence of surface pitting, and a degree of surface leaching on the upper margin.

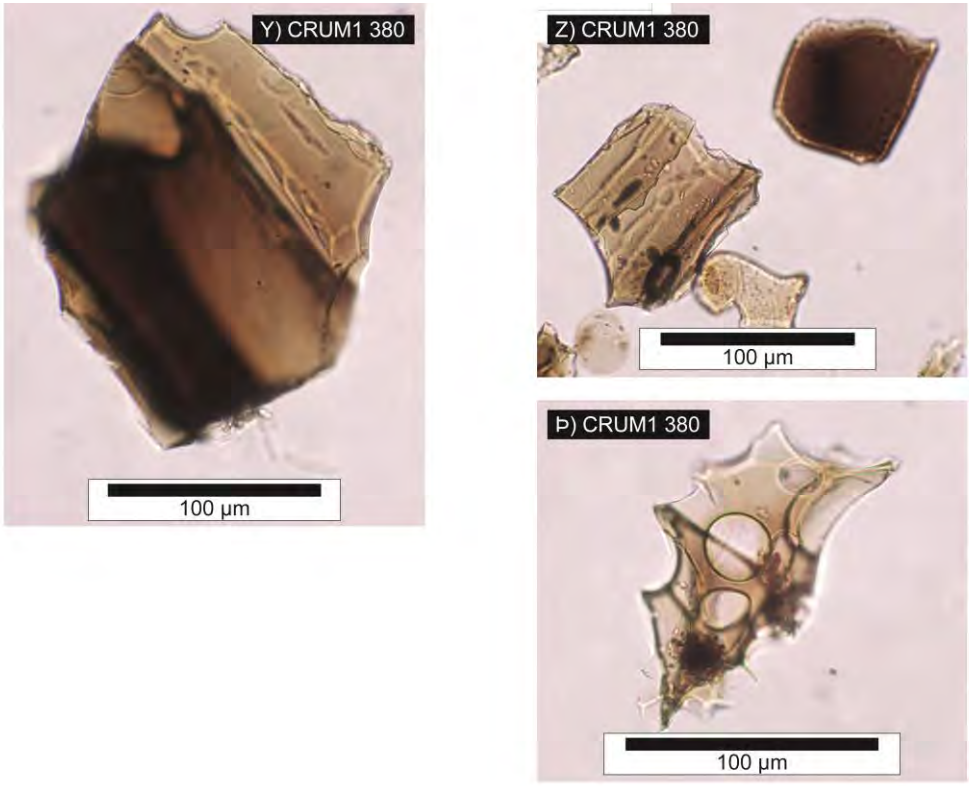

Figure 6.5 continued (Y) A very large basaltic shard with an A-axis of ca. 140 µm. (Z) Two basaltic shards of differing morphologies. The shard to the left exhibits a partially fluted, cuspate shape, with elongated closed vesicles The shard on the right exhibits a darker hue, and has a largely featureless surface aside from some surface pitting. (Þ) A highly vesicular basaltic shard exhibiting some surface corrosion on the lower and right hand margins.

CRUM1 597

At the end of the Windermere Interstadial (unit 2i) and within the transition to the Loch Lomond Stadial (unit 3a), a tephra is present which is spread over 11 cm and is defined by three peaks. The most concentrated of these is located at a depth of 597 cm and reaches a value of 32 shards g^{-1}. Shards exhibit similar morphologies to the previous two horizons described from the Crudale Meadow sequence, being blocky, cuspate with the occasional mineral inclusion (Figure 6.5 G, H). Chemical characterisation of the horizon (n=30) produced a homogenous series defined by low FeO (ca. 1.47 wt %) and CaO values (ca. 0.76 wt %), respectively (Table 6.2).

CRUM1 587

Mid-way through the Loch Lomond Stadial and in association with the pale brown/ orange unit of 3b, a tephra exhibiting relatively high concentrations of colourless shards was identified. The tephra peak has a concentration of 372 shards g^{-1}, and magnetic separation yielded a low concentration of brown shards (2 shards g^{-1}). Colourless shards are defined as possessing platey, cuspate and fluted morphologies (Figure 6.5 I, J). Chemical characterisation of this component returned a predominantly

homogenous main population, but three additional populations were identified, which all possess slightly differing chemistries. Population A (n=21) exhibits relatively high values of Al_2O_3 (ca. 13.01 wt %), FeO (ca. 3.65 wt %) CaO (ca. 1.25 wt %), respectively. Population B (n=1) exhibits lower values of Al_2O_3 (11.79 wt %), FeO (3.65 wt %) and CaO (1.25 wt %). Population C (n=1) possesses lower values of Al_2O_3 (11.59 wt %), FeO (2.44 wt %) and CaO (0.33 wt %). Population D (n=1) possesses lower values of Al_2O_3 (8.37 wt %), higher values of FeO (6.45 %) and much lower CaO totals (0.27 wt %) (Table 6.2).

CRUM1 579 and 576

An interval of tephra spread over 8 cm is observed between the end of the Loch Lomond Stadial and the onset of the early Holocene. The two largest peaks were chosen for chemical analyses: CRUM1 579, which, situated within the Loch Lomond Stadial, attained a concentration of 11 shards g^{-1}, and CRUM1 576, which resides within the early Holocene and totalled 8 shards g^{-1}. Morphologically, both horizons exhibited shards with variable characteristics, including blocky, vesicular, inclusion-rich and cuspate shapes (Figure 6.5 K-N). Two analyses were obtained from CRUM1 579 which had two distinct populations. Population A is defined by low FeO (1.54 wt %) and CaO (0.66 wt %) whereas population B exhibits higher totals of both FeO (3.88 wt %) and CaO (1.31 wt %). Analyses for CRUM 576 returned a tri-modal population: population A (n=5) is defined by low FeO (ca. 1.45 wt %) and low CaO (0.77 wt %). Population B (n=4) in comparison returned values of higher FeO (ca. 3.65 wt %) and CaO (ca. 1.31 wt %). Population C is defined by a single analyses with intermediary values of FeO (2.66 wt %) and the lowest totals of CaO (0.41 wt %) identified within the horizon (Table 6.2).

CRUM1 561

At the top of unit 4d and within the detrital marls of the early Holocene, a tephra horizon distributed over 3 cm, and defined by both colourless and brown shards, was identified (Figure 6.5 O, P). Notably the brown shards were identified within the 2.5 g/cm^{-3} floated fraction, which suggests the density of the brown shards had been altered diagenetically. The peak interval for both shard types is at 560 cm, where colourless and brown shards reach a concentration of 4 and 13 shards g^{-1} respectively. This interval was sampled twice for chemical analyses, however, in both cases no shards were identified. The adjacent interval (561 cm) where colourless and brown shards were quantified at 3 and 10 shards g^{-1}, respectively, and were therefore sampled for chemical analyses. The 561 cm sample yielded several colourless shards; however, no brown shards were identified. Three successful analyses of the colourless shards were

obtained, which returned a bi-modal population. Population A (n=2) defined by relatively low Al_2O_3 (ca. 11.77 %), FeO (ca. 2.42 wt %) and CaO (ca. 0.36 wt %), whereas the single shard defining population B is characterised by higher Al_2O_3 (13.14 wt %), FeO (3.53 wt %) and CaO (1.24 wt %) values (Table 6.2).

CRUM1 543

Following the absent section of core, and within the early Holocene sediments of unit 5a, a 10 cm zone of tephra was identified. Here three peaks at 543, 540 and 536 cm with concentrations of 51, 14, and 6 shards g^{-1}, respectively, were identified. A morphological analysis of the shards revealed populations defined by small cuspate and vesicular shards (Figure 6.5 Q, R). The samples 543 and 536 were chosen for chemical preparation; however, upon resampling the latter interval did not yield any identifiable shards. A number of specimens were successfully extracted from CRUM1 543 cm; however, during the analysis it became evident that applying the 95 % cut off for analytical totals as recommended by Hunt and Hill (1993) and Pollard et al. (2006), would mean that most of the analyses were rejected. These consistently low totals likely reflect a relatively high water content, and as a result a lower cut off of 94 % (two decimal places) was applied. Seven successful analyses were obtained, with the chemical results showing a similar but distinctly bi-modal population. Population A (n=4) is defined by relatively lower Al_2O_3 (ca. 11.35 wt %), FeO (ca. 1.08 wt %) and CaO (ca. 0.40 wt %) values, whereas population B (n=3) exhibits higher Al_2O_3 (ca. 12.45 wt %), FeO (ca. 1.30 wt %) and CaO (ca. 0.76 wt %) totals (Table 6.2).

CRUM1 498 and 496

Occurring at the top of unit 5a and just prior to the cessation of moss bands within the early Holocene marls at Crudale Meadow, an interval of tephra exhibiting both colourless and brown shards is identified. The interval of tephra spans over 4 cm, with the peak in colourless shards (14 shards g^{-1}) occurring at 498 cm, and the peak in brown shards (30 shards g^{-1}) residing at 496 cm (Figure 6.4). An analysis of shard shape revealed rhyolitic specimens defined predominantly by platey morphologies, whilst basaltic shards are notably blockier, feature some open and closed vesicles, and also exhibit some chemical alteration (Figure 6.5 S-V). Chemical characterisation of the 498 cm sample, as defined by 45 analyses, which returned a tri-modal chemical distribution. Population A (n=42) exhibits high SiO_2 values (ca. 74.63 wt %), relatively low FeO (ca. 2.55 wt %) and intermediary CaO (ca. 1.61 wt %) totals. Population B (n=2) has much lower SiO_2 values (ca. 49.49 wt %) and much higher FeO (ca. 14.10 wt %) and CaO (ca. 9.63 wt %) totals. The third population, as defined by a single

analyses has a chemical signature defined by intermediary SiO_2 (68.7 wt %), and FeO (3.42 wt %) totals, and the lowest CaO value in the horizon (1.28 wt %).

CRUM 496 is defined by 28 analyses, and these are predominantly of a single chemical type. However, one analysis was obtained that does not fit into this group. Population A therefore is characterised by low SiO_2 values (ca. 49.24 wt %), and high FeO (ca. 14.26 wt %) and CaO (ca. 9.73 wt %) totals, whereas the analyses defining the single shard of population B exhibits much higher SiO_2 values (75.22 wt %), and much lower FeO (2.7 wt %) and CaO (1.67 wt %) totals.

CRUM1 430

Between 428-433 cm a 6 cm zone of brown shards is identified, with morphologies defined by blocky shapes and closed vesicles (Figure 6.5 W, X). Two consecutive samples, 429 and 430 reach a peak concentration of 11 shards g^{-1}, with the lowermost horizon being selected for chemical characterisation. Eight analyses were obtained which revealed a homogenous population defined by low SiO_2 values (ca. 48.33 wt %), and high FeO (ca. 14.30 wt %) and CaO (ca. 9.76 wt %) totals (Table 6.2).

CRUM1 380

At 380 cm a macrotephra was identified, with shards associated with such distributed between 376-388 cm. (Figure 6.4). The peak of the horizon is quantified at 1.6 million shards g^{-1}, and optical analysis revealed the dominance of brown vitreous shards exhibiting a mixed size and morphology (Figure 6.5 Y-Þ). Chemical analysis of the peak (n=29), yielded a chemically homogenous population defined by low SiO_2 values (ca. 49.21 wt %), and high FeO (ca. 14.27 wt %) and CaO (ca. 9.92 wt %) totals (Table 6.2).

6.3 Interpretation

6.3.1 Tephra correlations

In this section tephra correlations are proposed based on current published data sets. The local and wider significance of these correlations are discussed in Chapter 10 and 11. Primary classification of the tephra layers is made via Total Alkali vs Silica diagrams (Figure 6.6 A), and by potassium value plots (Figure 6.6 B) as defined by Le, Bas (1986), and Pecorillo and Taylor (1976) respectively. Data sources for the tephra correlations are summarised in Appendix B

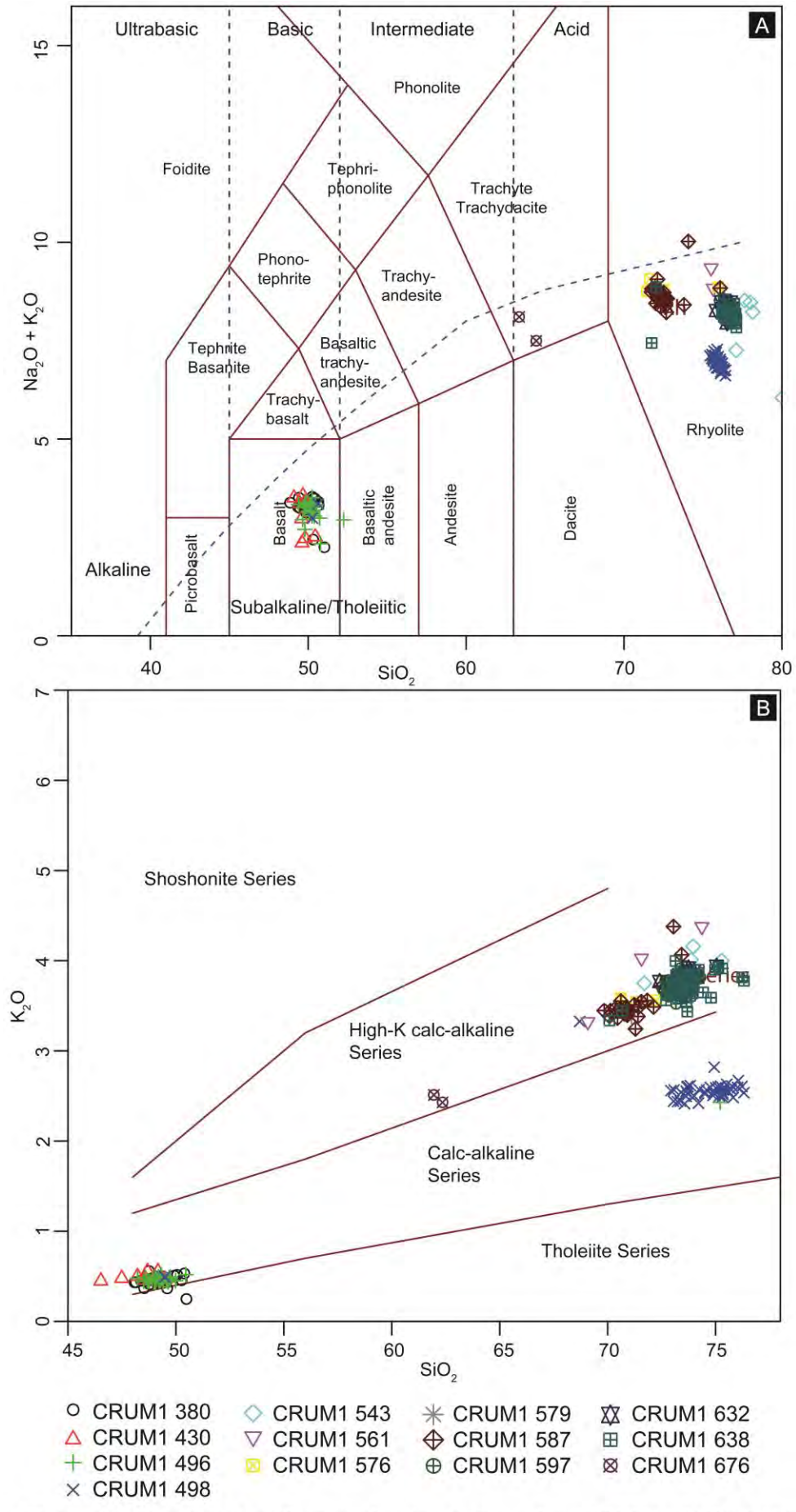

Figure 6.6 Chemical classification of tephra horizons from CRUM1. (A) Total Alkali vs Silica diagram (Le Bas 1986). (B) K-series plot (Pecorillo and Taylor 1976).

CRUM1 676

The single shard from CRUM1 676 was analysed twice and returned a chemical signature that can be classified as a Trachydacite, with a high potassium value (Figure 6.6). The tephra resides within Dimlington Stadial aged sediments; of the very few horizons which have been characterised from this interval in NW Europe, only one horizon bears some chemical similarity, the Hekla-derived NGRIP 1619.58 m Tephra (Mortensen et al. 2005). However, whilst some elements (e.g. SiO_2) reach comparable 'intermediate' values, significant differences exist in other key elements (e.g. FeO and CaO), which attain much higher values of ca. 8.4 and ca. 5.12 %, respectively in NGRIP 1619.58 m, compared to the mean values of ca. 5.12 and 3.67 % for FeO and CaO in CRUM1 676.

When plotted against a series of broader Icelandic geochemical envelopes, further comparisons can be drawn with Hekla, with correlations particularly strong where TiO_2 forms one axis of a bi-plot (Figure 6.7 B). It is conceivable therefore that the existing chemical envelope for NGRIP 1619.58 m does not reflect the whole eruptive suite of this Hekla derived layer, with the analysis at CRUM1 676 perhaps representing a previously unanalysed phase of this eruption. However, enough dissimilarity exists with other major elements to raise doubt on this hypothesis, and this is further confounded by apparent correlations that can be drawn with the Katla volcanic system (Figure 6.7). One chemical series derived from Katla that correlates most closely with CRUM1 676 is the mid-late Holocene dacite tephras i.e. SILK layers (e.g. Larsen et al. 2001; Óladóttir et al. 2005), and the early Holocene Skopun Tephra (Lind and Wastegård 2011). Current understanding of SILK layers limits them to a 6000 year interval, and it is uncertain whether an earlier period of SILK genesis characterised the Katla system (Larsen et al. 2001; Óladóttir et al. 2005).

An alternative explanation may lie with the Sólheimar Ignimbrite, a hypothesised proximal correlative of the Katla derived Vedde Ash, and one which exhibits a broader intermediate chemical range to that of its supposed distal counterpart (Lane et al. 2012b; Tomlinson et al. 2012a). What is particularly characteristic of the Katla system through the LGIT is its ability to repeatedly produce tephras of an indistinguishable 'Vedde-like' chemical signature (Lane et al. 2012b). During the latter phases of GS-2, two eruptions are known to exhibit a Katla rhyolite signal; the Dimna Ash (Koren et al. 2008) and the 10-1P 192 (Thornally et al. 2011). It is possible therefore that CRUM1 676 may represent an intermediate chemical correlative of either of the two aforementioned rhyolitic tephras. The absence of any proximal correlative like the Sólheimar Ignimbrite can be explained by the occurrence of a thick ice cap covering

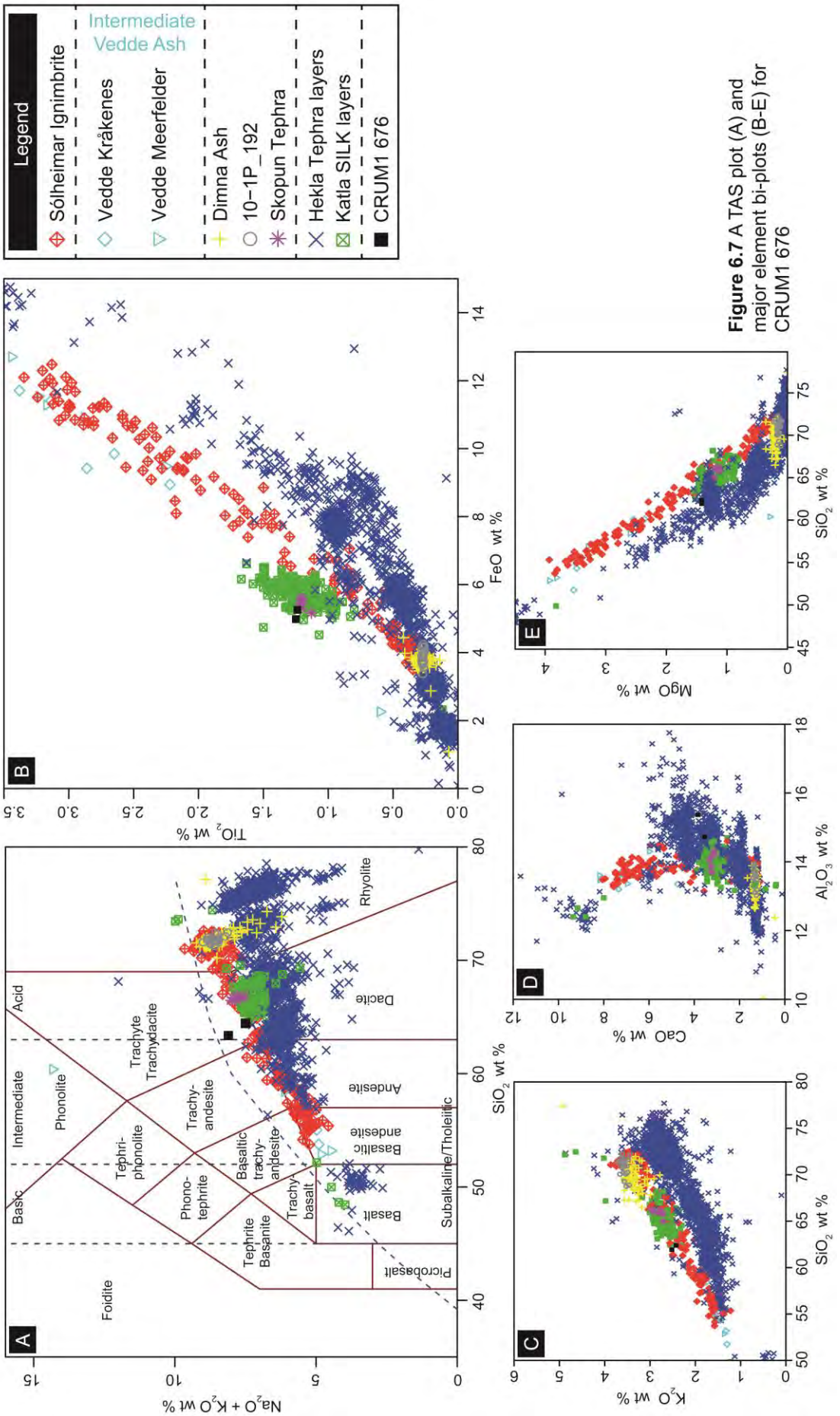

Figure 6.7 A TAS plot (A) and major element bi-plots (B-E) for CRUM1 676

Katla during the latter phases of GS-2 (e.g. Hubbard et al. 2006; Norðdahl et al. 2008). Any eruption from the system would have had to have broken through this barrier, before ejecting tephra into the atmosphere. The point at which this occurred cannot be determined, but feasibly this may have happened as the magmatic series was evolving from a more basic to a more silicic chemistry. Thus the chemical composition of the Dimna and 10-1P 192 horizons, as currently characterised, may not represent the full compositional range of magma associated with the eruption.

Due to the limited number of analyses obtained for CRUM1 676 and the lack of robust correlatives only tentative and hypothetical correlations can be made at this stage. Further analysis is required from the CRUM1 676 horizon to see whether a greater overlap can be made between either the Hekla or Katla systems. However, for the time being, a correlation to the Katla system is accepted, and owing to the uncertainties revolving around ice rafting and the origin of the 10-1P 192 tephra, the preferred correlative is that of the Dimna Ash.

CRUM1 638

Forty-two analyses were obtained from CRUM1 638 which can be characterised as a sub-alkali rhyolite possessing high potassium values (Figure 6.6). Forty-one of these data points can be correlated to the Borrobol-type tephras, with the data clustering around the more recent analyses of the Borrobol and Penifiler obtained by Lind et al. (2016) (Figure 6.8). This occurrence likely reflects the refined analytical conditions which have arisen in recent years for the characterisation of major and minor elemental geochemistry (e.g. Hayward et al. 2012). Whilst the Borrobol and Penifiler express an indistinguishable chemical signature (e.g. Pyne-O'Donnell et al. 2008; Lind et al. 2016), the stratigraphic position of the horizon, i.e. within the early Windermere Interstadial, would suggest a correlation to the Borrobol Tephra, a position from which the Borrobol has been previously described (e.g. Turney et al. 1997; Turney 1998a; Pyne-O'Donnell et al 2008; Matthews et al. 2011; Lind et al. 2016).

The single shard characterising population B can be correlated to the Katla volcanic system. Several Katla rhyolites exhibiting a 'Vedde-like' chemistry have been described from sites across NW Europe throughout the LGIT (Lane et al 2012b), although none have been described from a similar stratigraphic position to the Borrobol Tephra. The Katla shard may have therefore been remobilised from horizons with lower shard concentrations in unit 1 (Figure 6.4). The occurrence of this shard therefore adds some weight to the argument that CRUM1 676 may relate to a previously unrecognised

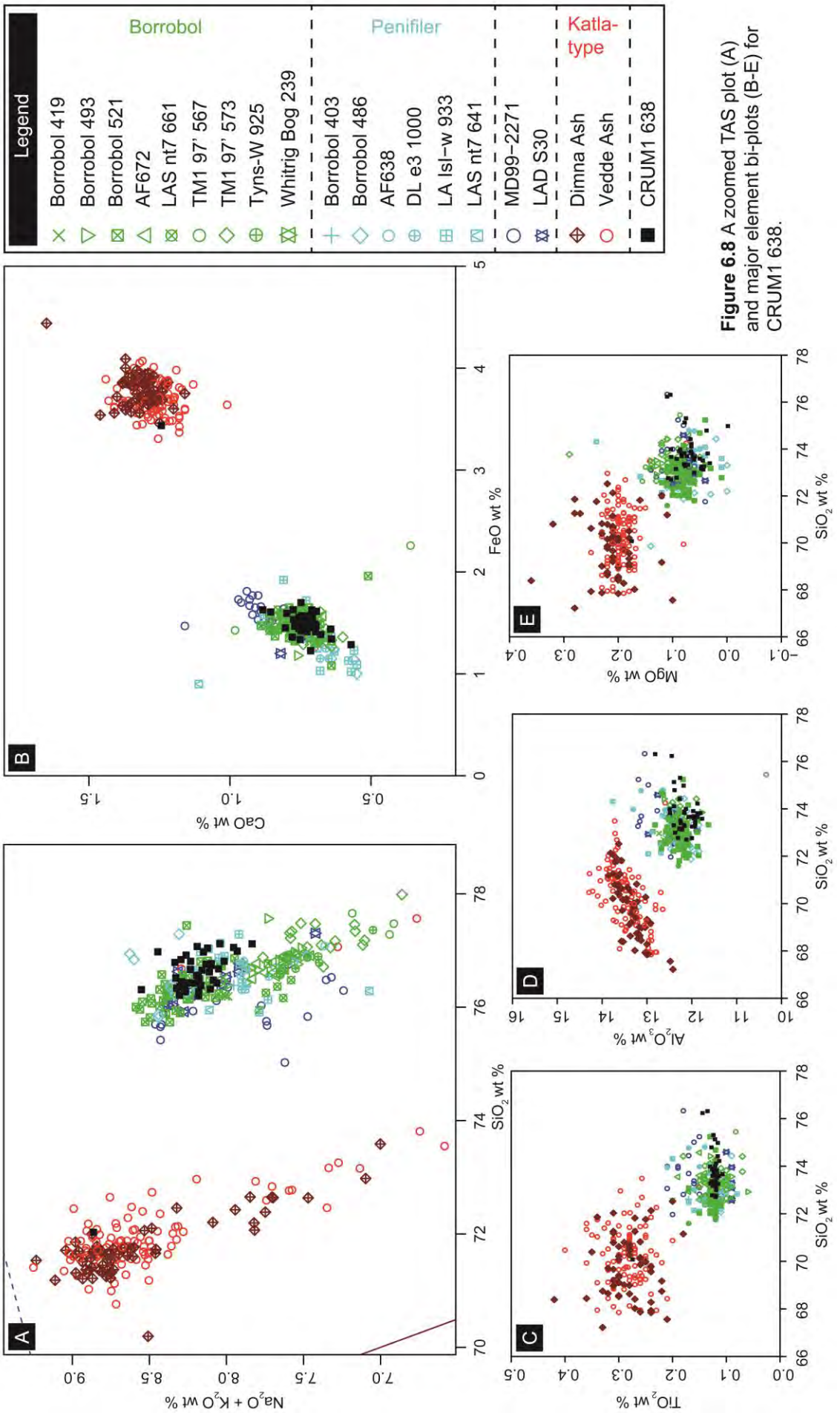

Figure 6.8 A zoomed TAS plot (A) and major element bi-plots (B-E) for CRUM1 638.

intermediate fraction of the Dimna Ash (see above), as downward mobilisation seems unlikely.

CRUM1 632

Within unit 2c, and in association with the downturn in $CaCO_3$, a chemically homogenous tephra is identified. This tephra can be classified in Figure 6.6 as a sub-alkali rhyolite possessing high potassium values. As with the previous horizon, the tephra possesses a chemical signature indicative of the Borrobol-type tephras, and clusters most closely with the recent analyses of Lind et al. (2016) (Figure 6.9). The oscillation observed within the $CaCO_3$ signal has been correlated on lithostratigraphic grounds to a similar occurrence within the Whittington et al. (2015) stratigraphy, where palaeoclimatic data suggests the unit is representative of GI-1d. Given the occurrence of the Borrobol stratigraphically below this horizon, and the incidence of the Penifiler Tephra in close association with GI-1d as inferred from Chironomidae analyses at Abernethy Forest and Loch Ashik (Matthews et al. 2011; Brooks et al. 2012), it is most likely that CRUM1 632 relates to the Penifiler Tephra.

CRUM1 597

The data points from CRUM1 597 are chemically homogenous, and can be classified as sub-alkali rhyolites with high potassium values (Figure 6.6). The chemical signature of the horizon is typical of tephras which have previously been ascribed to one of the Windermere Interstadial Borrobol-type tephras, i.e. the Borrobol and the Penifiler. The stratigraphic position of these tephras occur much earlier in the Windermere Interstadial with the Borrobol often related to the amelioration with in climate following the Dimlington Stadial, and the Penifiler occurring in association GI-1d (e.g. Pyne-O'Donnell et al. 2008; Matthews et al. 2011; Brooks et al. 2012; Lind et al. 2016). However, the occurrence of this Borrobol-type horizon at the transition from Interstadial to the Loch Lomond Stadial is not a pattern which has been previously reported for NW European records. A single shard characterised amongst the late Windermere Interstadial LAS-1 horizon at Loch an t'Suidhe may offer a potential correlative (Davies 2003; Figure 6.10). However, the majority of the six data points characterising this horizon do not attain the 95 % cut-off recommended for analytical totals (Hunt and Hill 1993; Pollard et al. 2006), and do not plot within the vicinity of the Borrobol-type chemical field (Figure 6.10). Whilst this horizon is thought to represent a new tephra layer for the LGIT, the possibility of reworking from either the Borrobol or Penifiler Tephra's already identified in the sequence cannot be excluded. This theme is discussed further in section 10.3.3.2.

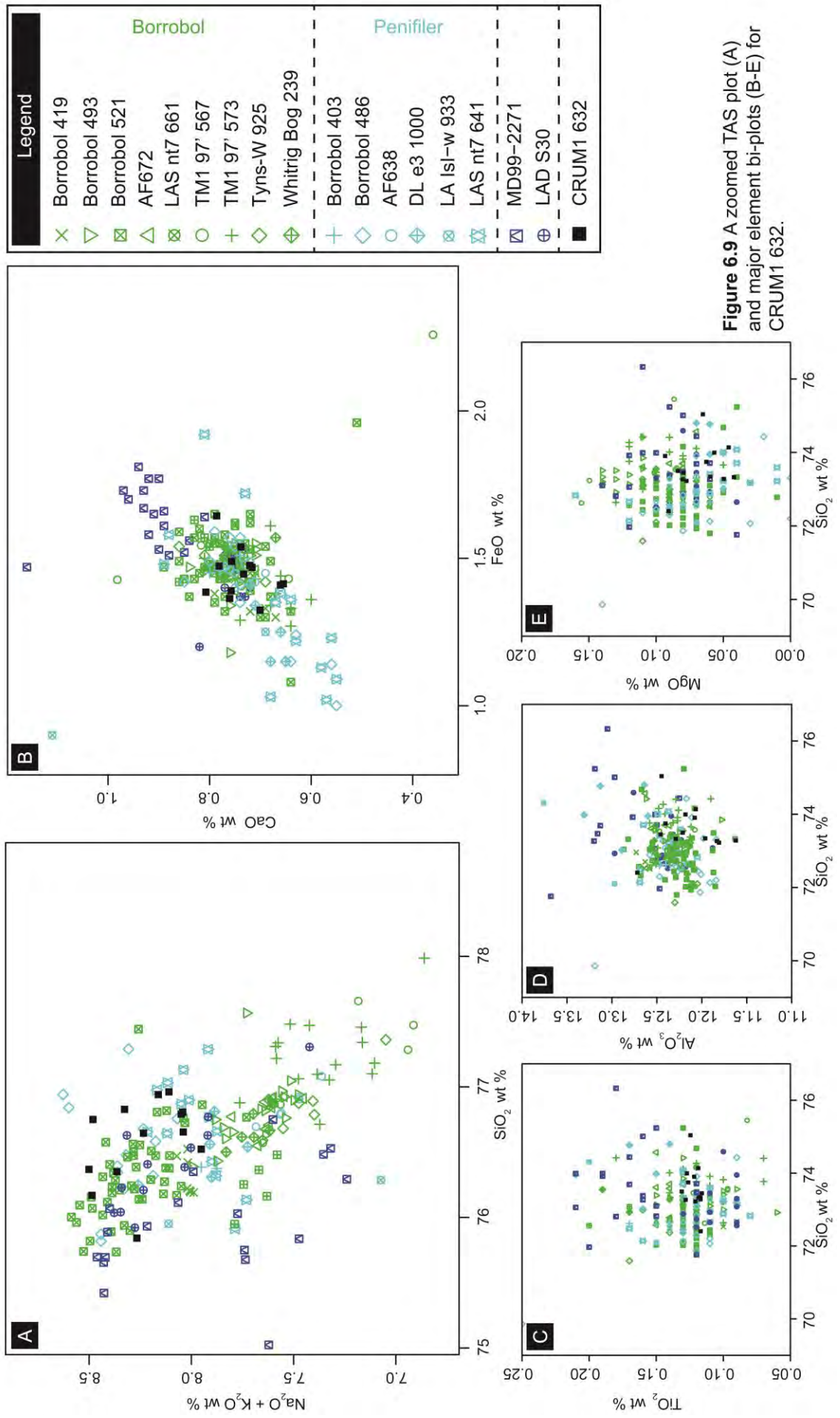

Figure 6.9 A zoomed TAS plot (A) and major element bi-plots (B-E) for CRUM1 632.

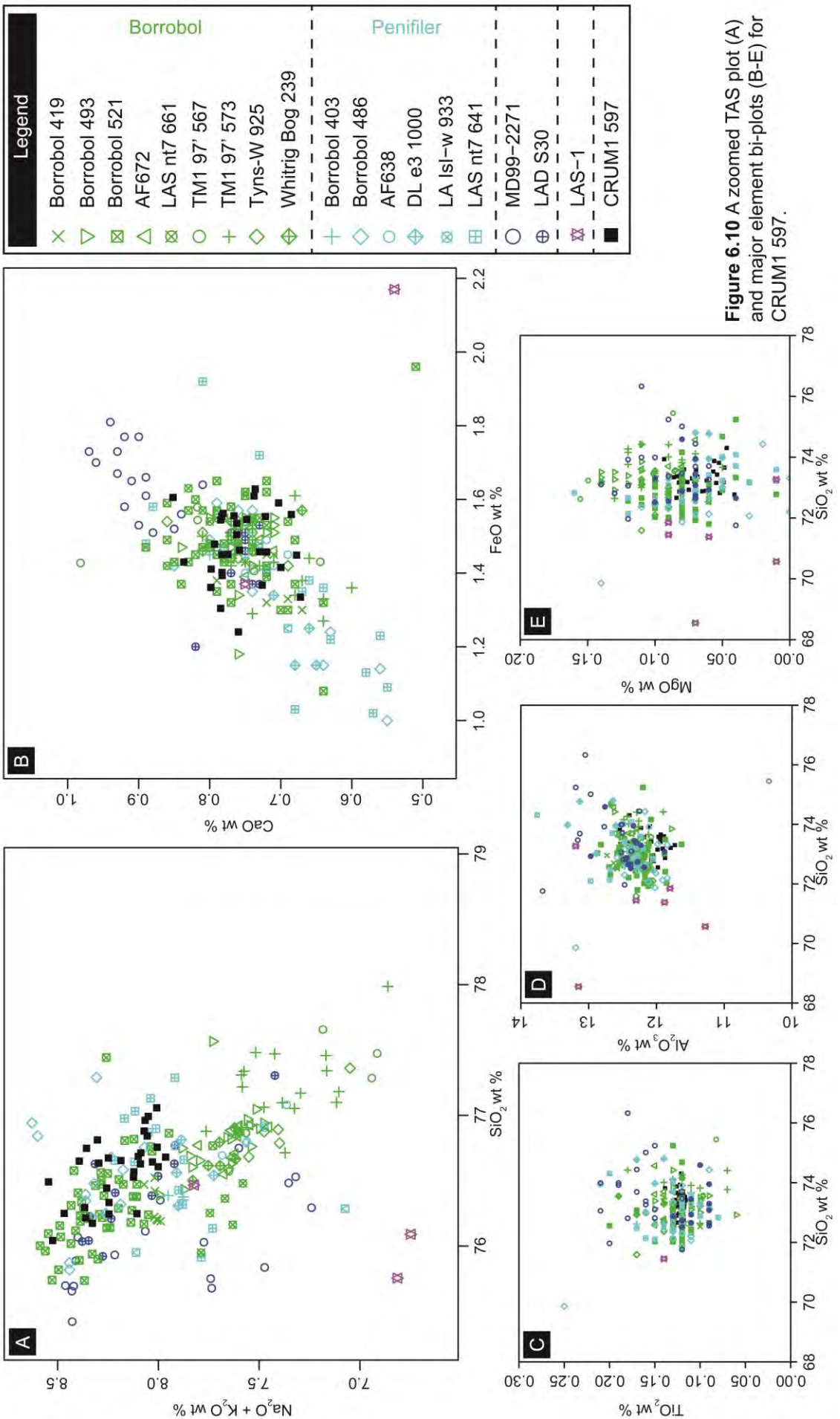

Figure 6.10 A zoomed TAS plot (A) and major element bi-plots (B-E) for CRUM1 597.

CRUM1 587

The tephra identified mid-way through the Loch Lomond Stadial sediments can be classified as a sub-alkali rhyolite tephra with high potassium values (Figure 6.6). The predominant chemical signature of the horizon is characteristic of the Katla volcanic system, Iceland (Figure 6.11). Whilst it is now recognised that several incidences of Katla rhyolites characterised the LGIT, the stratigraphic position of this horizon i.e. within a minerogenic unit indicative of a cold climate regime, would suggest a correlation to the Vedde Ash. Population B, as defined by a single analyses, correlates with the Borrobol-type tephras, and has probably been remobilised from the underlying CRUM1 597 horizon, or the overlying CRUM1 576 horizon (see below).

Two other populations, each defined by a single analysis, were also identified within the CRUM1 587 interval. Population C exhibits an unusual geochemical signature for an LGIT aged sequence, with the analyses correlating most closely with the Torfajökull and Tindfjallajökull systems. For ease of interpretation this population is absent from Figure 6.11, however, its occurrence is discussed in the context of CRUM1 561 (see below), where the predominant population also exhibits a chemical signature of this type.

Population D closely resembles the Vedde Ash in many aspects, but appears to have elevated FeO, Na_2O and MnO values, this suggests the analysis has been altered by the partial measurement of a mineral inclusion; as a result the shard is considered an outlier and removed from the interpretation.

CRUM1 579 and 576

The horizons at 579 and 576 yielded a mixed chemical signature, but all analyses can be classified as representing sub-alkali rhyolites with high potassium values (Figure 6.6). CRUM1 579 is characterised by two analyses which returned a split chemical distribution, population A and B therefore have the same significance in this instance. Population A correlates with the Borrobol-type tephras, whereas population B shares an affinity with Katla-type tephras (Figure 6.12). CRUM1 576 also shares this geochemical assemblage, with population A (n=5) correlating to the Borrobol-type tephras, and population B (n=4) being characteristic of the Katla system (Figure 6.12).

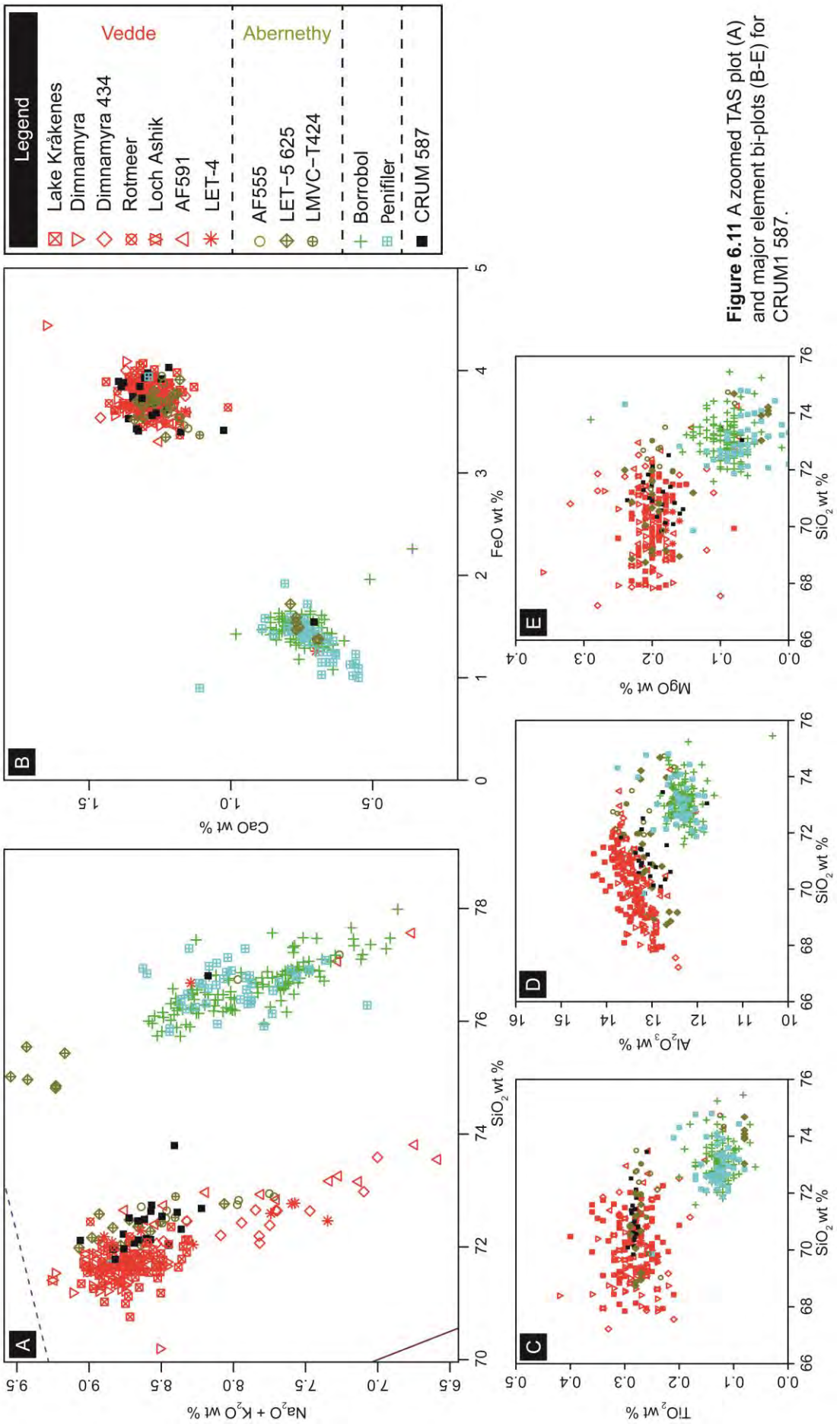

Figure 6.11 A zoomed TAS plot (A) and major element bi-plots (B-E) for CRUM1 587.

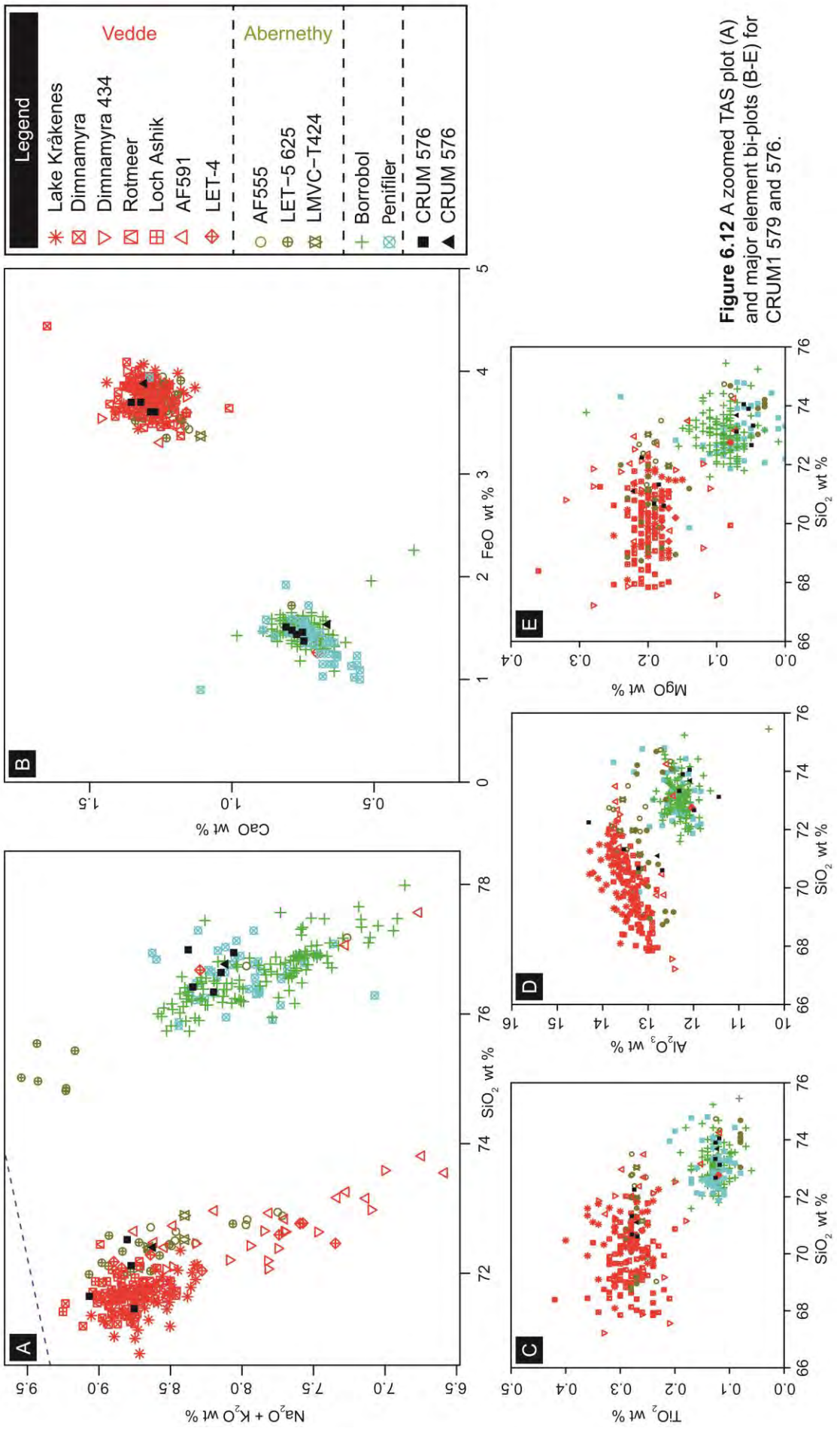

Figure 6.12 A zoomed TAS plot (A) and major element bi-plots (B-E) for CRUM1 579 and 576.

In regards to the Katla derived chemistries from both intervals, the Loch Lomond Stadial is now thought to contain at least two tephras which originated from this province: the older and more prominent Vedde Ash, deposited approximately mid-way through the Stadial, and the Abernethy Tephra which occurs at the transition from Stadial into the Holocene (e.g. Matthews et al. 2011; Lane et al. 2012b; MacLeod et al. 2015). It is likely that the horizon represented by CRUM1 587 is that of the Vedde Ash, thus by the laws of superposition a more likely correlative for CRUM1 579 and 576 is that of the Abernethy Tephra. However, in both instances at Crudale Meadow an occurrence of Borrobol-type shards is noted, and in CRUM1 576, these shards are more prominent within the chemical assemblage. Notably, however, a small number of Borrobol-type shards appear in the chemical analyses of the Abernethy Tephra at Abernethy Forest and Loch Etteridge, i.e. the AF555 and LET-5 (Matthews et al. 2011; MacLeod et al. 2015). This potentially suggests that a synchronous eruption from the Borrobol source may have accompanied an eruption from Katla during the transition from the Loch Lomond Stadial to the Holocene. Alternatively the mixed population of shards in both CRUM1 579 and 576 may have arisen as a result of reworking and remobilisation, either from within the basin or from elsewhere in the catchment. It has been hypothesised that during the early Holocene a lowering of lake levels may have taken place (Digerfeldt 1988; Pyne-O'Donnell 2011). Lowering of lake levels at Crudale Meadow would have exposed tephra-laden sediments to erosive processes. It is difficult to ascertain therefore, whether the shards present in CRUM1 579 and 576 are genuine isochronous events, a product of erosion, or a combination of both scenarios. These themes are discussed further in section 10.3.3.3, but due to these uncertainties no robust tephra correlations can be made at present.

A third population was also identified in CRUM1 576 (population C), which is not shown in Figure 6.12. The single data point returned a chemical profile that matches closely with the Torfajökull and Tindfjallajökull systems, and as above, this correlation is discussed further in the context of CRUM1 561 which also bears a chemical signature of this type.

CRUM1 561

The horizon analysed in this interval returned a mixed chemical assemblage, with both components being classified as sub-alkali rhyolites with high potassium values (Figure 6.6). Population B is defined by a single analysis and can be correlated to the Katla volcanic system. As previously discussed, a number of Katla-derived tephras are recognised in LGIT aged sequences around NW Europe (e.g. Lane et al. 2012b). However, in this instance, due to the low number of shards identified, the occurrence

likely relates to a reworking of the Vedde Ash, or uncorrelated Katla rhyolites identified in the preceding horizon.

Population A (n=2) from this interval, along with population C (n=1) from CRUM1 587 and population C (n=1) from CRUM1 576 (see above) exhibit a chemical signature that bears some similarity to tephras that have been previously ascribed to the Torfajökull volcanic system. Three eruptions from this province are thought to have deposited tephra in NW European sequences during the LGIT: these are the rhyolitic component of the Ashik Tephra, the An Druim Tephra and the Høvdarhagi Tephra (Pyne-O'Donnell 2007; Ranner et al 2005; Lind and Wastegård 2011). However, the aforementioned populations possess slightly higher SiO_2 values than is typical for Torfajökull, and do not consistently plot within the chemical envelope derived from the LGIT age Torfajökull eruptions (Figure 6.13). Pollard et al. (2003) demonstrate that tephra derived from Torfajökull is amongst the least chemically stable of ashes found in the North Atlantic periphery, therefore, in order to provide a broader and more feasible chemical envelope for correlation, three additional Holocene aged Torfajökull eruptions were used for correlative purposes i.e. the Lairg B Tephra, the Hoy Tephra, and the Gullbergby Tephra. These tephras were chosen for their higher SiO_2 values but are not considered potential correlatives. Even with this broader chemical envelope, sufficient differences exist to suggest that Torfajökull cannot be considered a reliable correlative (Figure 6.13).

It would seem that a more reliable correlation can be made with a tephra that has its origins in the Tindfjallajökull system (Tomlinson et al. 2010). The Tindfjallajökull data shown in Figure 6.13 are derived from the 54,500 ± 2000 year-old Thórsmörk Ignimbrite, which is considered to be one of the largest Icelandic eruptions in the last 2 Ma (Lacasse and Garbe-Schönberg 2001). Since this caldera forming event, it is believed that Tindfjallajökull has remained relatively inactive, although the volcanic history and stratigraphy of the volcano are poorly studied and largely unknown (Lacasse et al. 1998; Guðmundsson 2015). The most recent activity in the volcano is understood to have culminated in a series of small basaltic lava flows (<1 km^2) at the onset of the Holocene, however, a central rhyolitic dome has also formed since the Thórsmörk Ignimbrite eruption, although the timing of this event is unknown (Guðmundsson 2015). It is possible therefore that a silicic eruption from the Tindfjallajökull edifice transpired during this period of early Holocene activity, perhaps extruding the rhyolitic dome, and perhaps being of sufficient magnitude to eject silicic tephras into the upper atmosphere. Whether the limited number of analyses identified here represents a new ash layer for the early Holocene is difficult to ascertain.

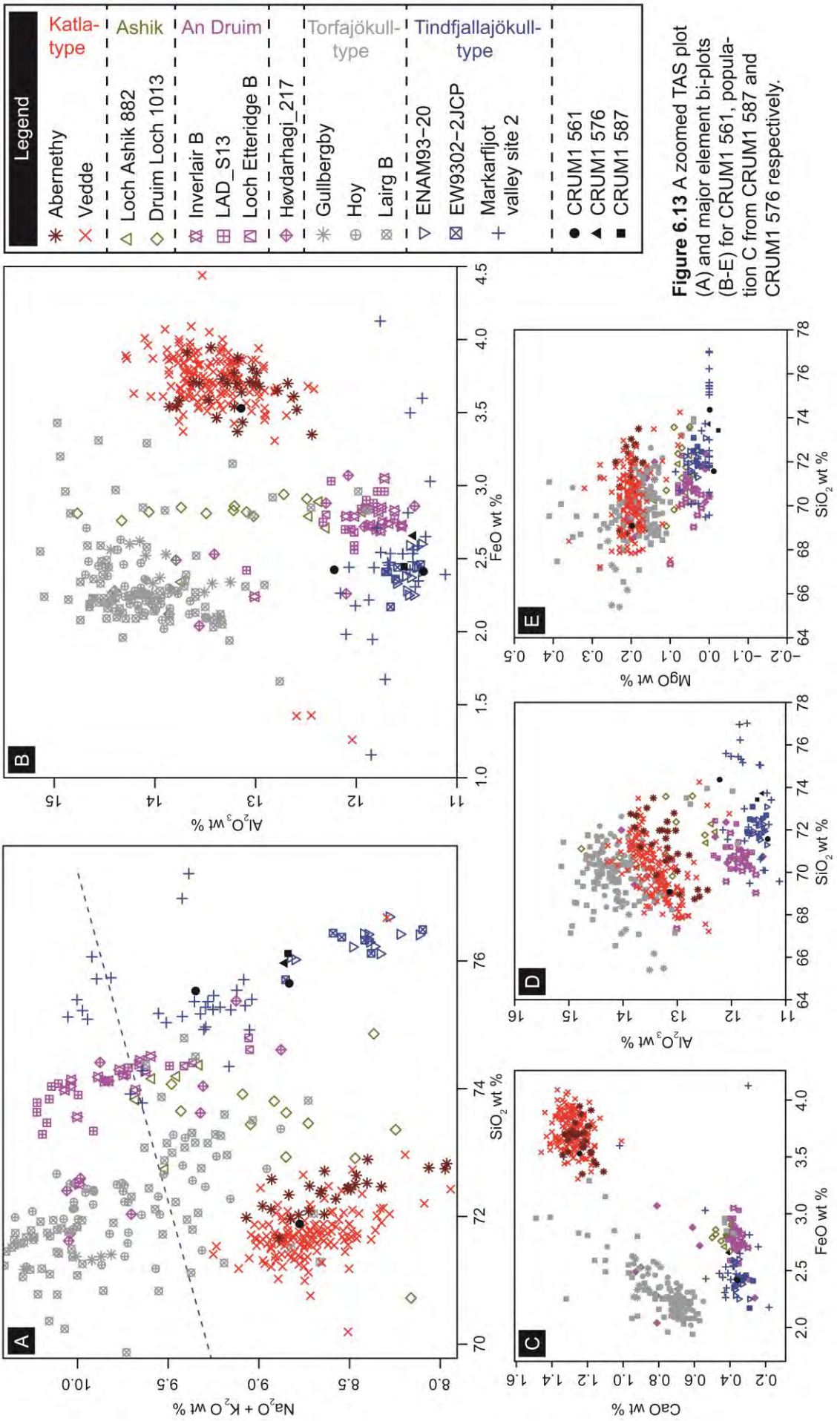

Figure 6.13 A zoomed TAS plot (A) and major element bi-plots (B-E) for CRUM1 561, population C from CRUM1 587 and CRUM1 576 respectively.

The shards are distributed over three intervals spanning 26 cm, and it has been noted by Jennings et al. (2014) that weathering of Katla-type shards may produce a chemical profile that closely resembles material derived from Tindfjallajökull. Given the occurrence of these shard types alongside shards of a Katla provenance, this explanation may hold some weight; however, analytical totals for the Tindfjallajökull analyses do not appear erroneously low, which suggests that chemical weathering has not had a major effect on their chemical composition. Nevertheless, in order to test this proposal, further chemical analyses are required. Given the diffuse pattern of shards identified thus far, and the very few shards identified in the intervals between CRUM1 576 and CRUM1 561 (Figure 6.4), it seems possible that a greater concentration of Tindfjallajökull-type shards may reside above CRUM1 561, i.e. the interval in which the greatest concentrations were observed. Unfortunately the CRUM1 561 interval occurs just prior to the hiatus in the stratigraphy (Figure 6.4); however, it may be possible to trace this horizon to the CRUM 3A 530-580 core. At present it is therefore not possible to reliably state the provenance of CRUM1 587 population C, CRUM1 576 population C, and CRUM1 561 population A, only that there is the potential for a new early Holocene tephra to be identified in the future.

CRUM1 543

The analyses at CRUM1 543 produced a chemical series defined by two populations, population A (n=4) and population B (n=3), although both can be classified as sub-alkali rhyolites with high potassium values (Figure 6.6). Population A shares a chemical affinity with tephras that have previously been correlated with Snæfellsjökull, and population B can be correlated with the Borrobol-type tephras (Figure 6.14). In the LGIT there are two tephras which are thought to derive from Snæfellsjökull, the Hässeldalen Tephra (11,543-11,232 cal. yrs BP; Davies et al. 2003) and the Hovsdalur Tephra (10,695-10,285 cal. yrs BP; Wastegård 2002). Stratigraphically both of these horizons are found in early-Holocene sequences. Thus, without the assistance of an independent chronology, these tephras can only be distinguished based upon their relative tephrostratigraphic position and respective ages. At several sites across NW Europe the Hässeldalen Tephra is described as occurring before the Askja-S/10ka Tephra (e.g. Davies et al. 2003; Wohlfarth et al. 2006; Lane et al. 2012a; Lilja et al. 2013; Ott et al. 2016), which has a current best age estimate of 10,956-10,716 cal. yrs BP (Bronk Ramsey et al. 2015b). The Hovsdalur, by comparison, has to date only been identified at the base of a single site in the Faroe Islands, where it was described as being below the Saksunarvatn Ash (Wastegård 2002).

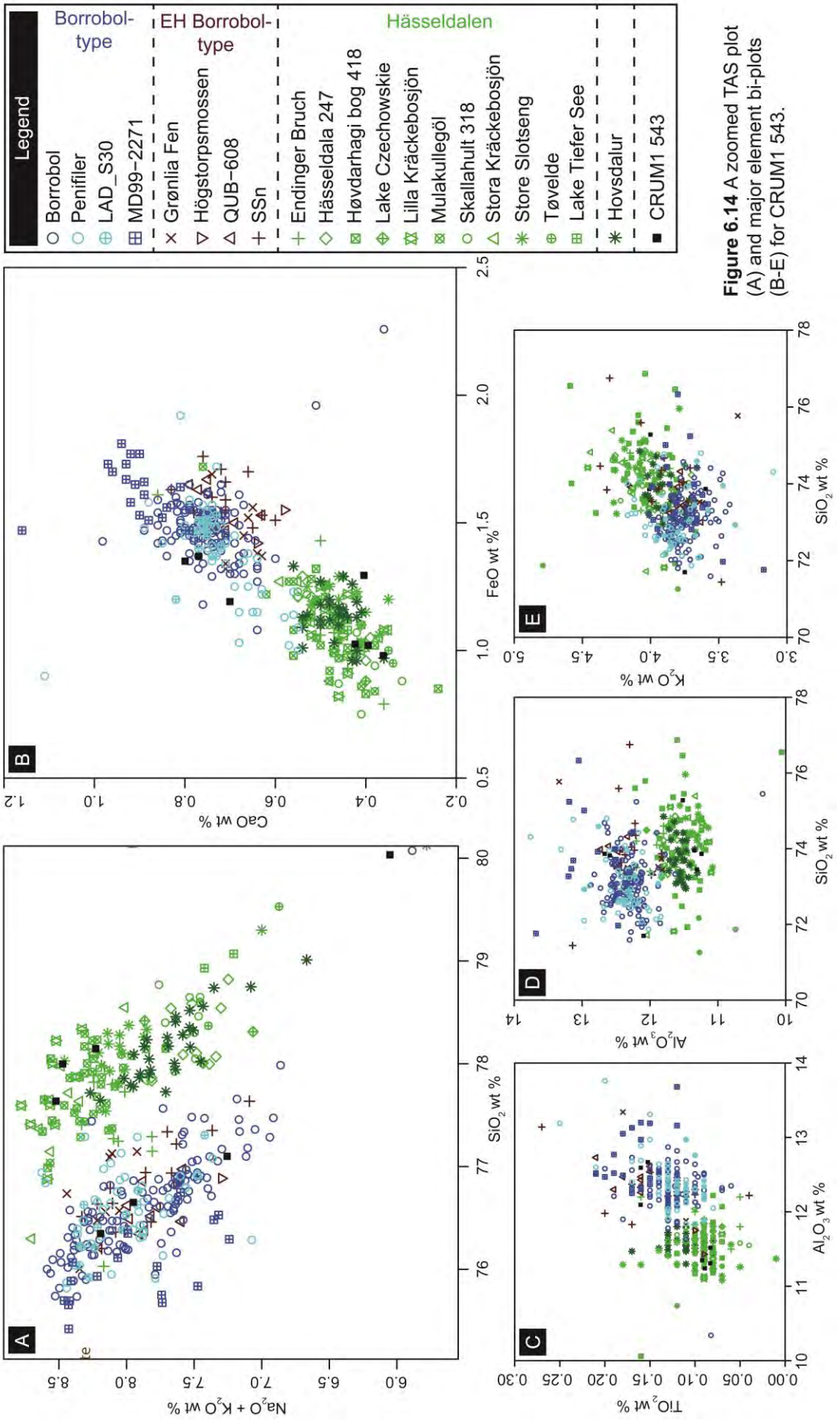

Figure 6.14 A zoomed TAS plot (A) and major element bi-plots (B-E) for CRUM1 543.

In the Crudale Meadow sequence, both the Askja-S/10ka and the Saksunarvatn Ash are identified above the CRUM1 543 interval, at a depth of 498 and 360 cm, respectively (see below). Therefore a correlation to the Hovsdalur Tephra is not feasible, and it is most likely population A in CRUM1 543 is the Hässeldalen Tephra.

In regards to population B, in the early Holocene, several horizons have been described that exhibit a Borrobol-type chemical signature (e.g. Lind et al 2016). They are: the Fosen Tephra ca. 10,200 cal. yrs BP (Lind et al. 2013); the Högstorpsmossen ca. 10,200 cal. yrs BP (Björck and Wastegård 1999); a component of L-274 ca. 10,200 cal. yrs BP (Lind and Wastegård 2011); population 3 of the QUB-608 ca. 9500 cal. yrs BP (Pilcher et al. 2005); and the SSn ca. 7500 cal. yrs BP (Boygle 1999). There is some suggestion that the first four of these tephras may be indicative of the same eruption, but limited age controls have prevented a more reliable conclusion from being drawn (Lind et al. 2013; Lind et al. 2016). Nevertheless, the current best age estimate of all of these, would place them after the Askja-S/10ka Tephra, which as fore-mentioned is stratigraphically above this interval at a depth of 498 cm. Thus it seems unlikely that the Borrobol-type shards identified in CRUM1 543 correlate to any of the previously described early Holocene tephra horizons. The Borrobol-type shards may therefore constitute a reworking of existing Borrobol-type material within the basin or catchment, or may represent a previously unidentified eruption. Reworking seems unlikely, however, as if this were the case, a mix of Katla-type and Tindfjallajökull-type shards might also be expected within the CRUM1 543 analyses.

What is interesting to note with other occurrences of the Hässeldalen Tephra, and most specifically analyses derived from Mulakullegöl, Sweden (Lilja et al. 2013) and Endinger Bruch, Germany (Lane et al. 2012a), is that a number of analyses classified as Hässeldalen Tephra clearly exhibit a more Borrobol-like chemical signature. This is exemplified most clearly in the FeO vs CaO plot (Figure 6.14 B). This pattern suggests that a contemporaneous eruption of the Borrobol-source may have accompanied an eruption from the Hässeldalen source, i.e. Snæfellsjökull, and thus conceivably that the Borrobol-source may lay in proximity to the Snæfellsjökull volcano. At present therefore, population B of CRUM1 543 cannot be confidently assigned to any known eruption of LGIT age.

CRUM1 498 and 496

The stratigraphically-discrete horizon at 498-496 was analysed and returned a chemical population dominated by two types. Population A (n=42) of CRUM1 498 and population B (n=1) of CRUM1 496 can be classified as sub-alkaline rhyolites with

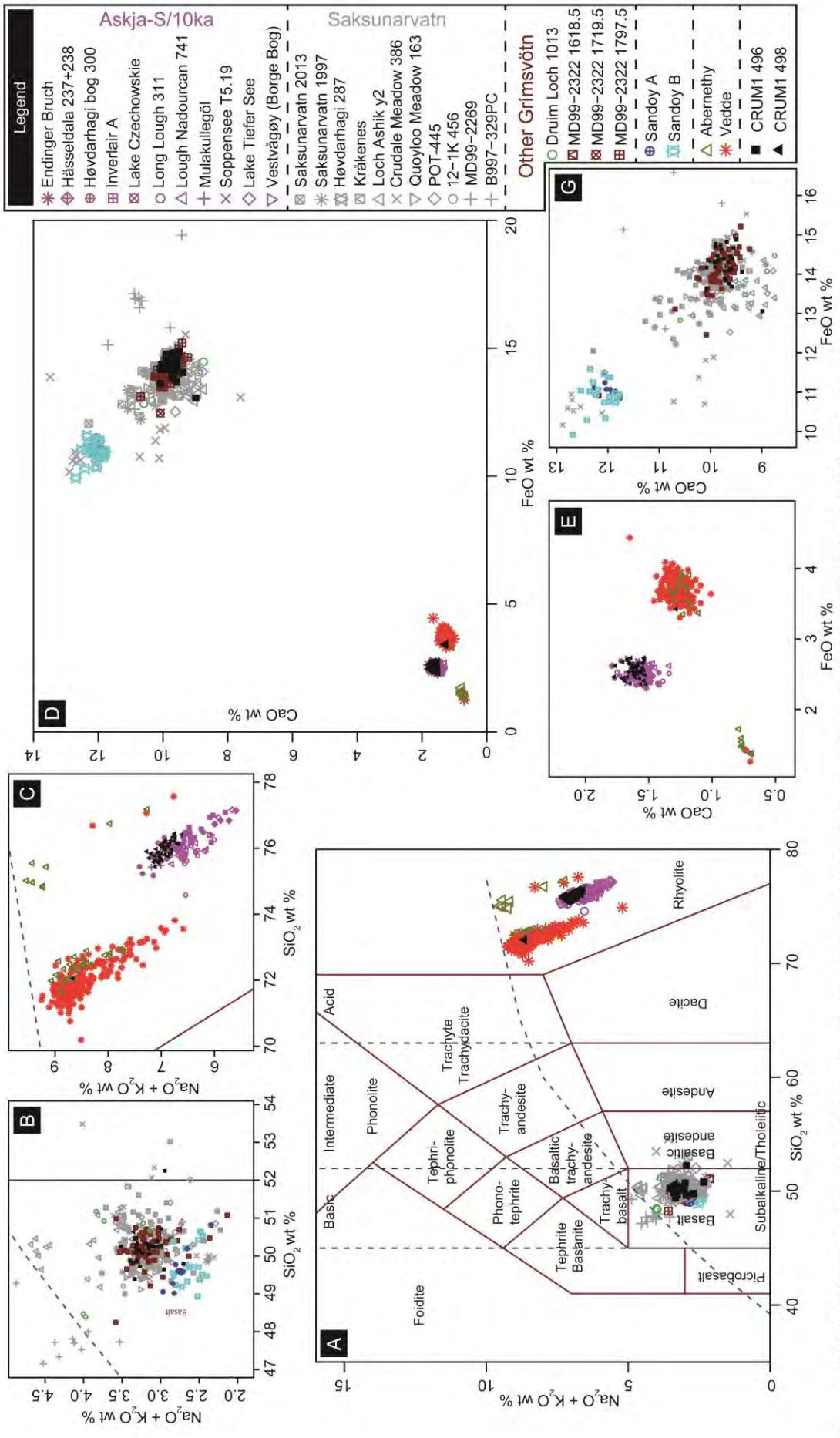

Figure 6.15 A TAS plot with zoomed insets (A- C), and major element bi-plots with zoomed insets (D-L) for CRUM1 498 and 496.

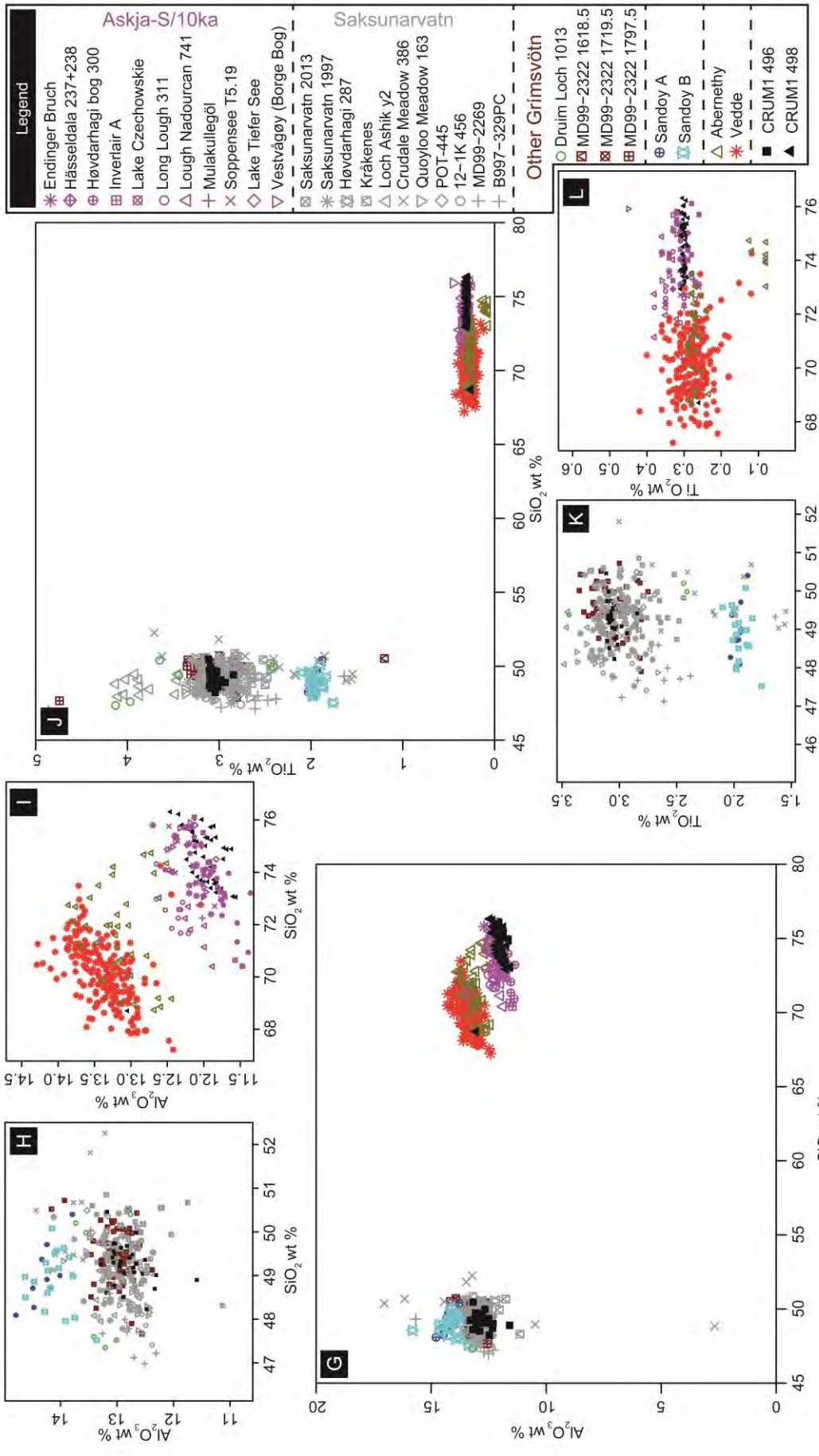

Figure 6.15 continued A TAS plot with zoomed insets (A- C), and major element bi-plots with zoomed insets (D-L) for CRUM1 498 and 496.

medium potassium values (Figure 6.6). Population B (n=2) of CRUM1 498 and population A (n=27) of CRUM1 496 can conversely be classified as a Tholeiitic basalt with low potassium values (Figure 6.6). A third population was identified in the CRUM1 498 interval, and is defined by a single analyses which can be classified as a sub-alkaline rhyolite with high potassium values.

The chemical signature of CRUM1 498 population A and CRUM1 496 population B is unique for LGIT age sequences, with only a single eruption known which exhibits such chemical characteristics; the Askja-S/10ka, derived from a Plinian eruption of the Askja caldera, Iceland (Sigvaldason 2002; Davies et al. 2003). Thus a confident correlation can be made to this eruption (Figure 6.15).

The two basaltic shards from CRUM1 498 and the dominant population from CRUM1 496 are indicative of the Grímsvötn volcanic system, Iceland (Figure 6.15). Recent work to the west of Grímsvötn in Iceland, and around the continental margin of Iceland have revealed that as many as seven eruptions from Grímsvötn may have occurred over a five hundred year interval during the early Holocene ca. 10.4-9.9 ka, (Jennings et al. 2002; Jóhannsdóttir et al. 2005; Kristjánsdóttir et al. 2007; Kylander et al. 2011; Jennings et al. 2014; Thordarson 2014; Neave et al. 2015). These results, in conjunction with Thornally et al. (2011), suggest that Grímsvötn was amongst the most active volcanic centres during the late Pleistocene and early Holocene. The close association of this horizon with the Askja-S/10ka Tephra would suggest an age of ca. 10,800 cal. yrs BP for the CRUM1 496 interval that at present does not correlate with any previously-described occurrence of a Grímsvötn tephra layer. Notably at Loch Ashik, Scotland, Pyne-O'Donnell (2007) describes a coeval basaltic tephra layer with that of the silicic Torfajökull-derived Ashik Tephra horizon. This basaltic component possess a mixed chemical signature, which in part can be correlated to the Grímsvötn system. However neither the silicic or basaltic components of the 'Ashik Tephra' possesses a robust age estimate, being estimated instead to ca. 10,400 cal. yrs BP (Pyne-O'Donnell 2007). Interestingly, in parts of the Loch Ashik basin, the Askja-S/10ka Tephra was identified in the same stratigraphic position as the Ashik Tephra, but the latter was unexpectedly absent in such incidences (Sean Pyne-O'Donnell pers. comm. 2016). Furthermore significant is the fact that the 'Ashik Tephra' identified alongside the Grímsvötn tephra layer at Loch Ashik, was never chemically confirmed as the Ashik Tephra. This perhaps suggests that there is a more complicated relationship between the Ashik Tephra, the Askja-S/10ka Tephra and the aforementioned Grímsvötn horizon than has previously been recognised, this is discussed further in section 10.3.3.4.

With regard to the single data point characterising population C in CRUM1 498 a correlation can be made to the Katla-volcanic system. No record eruption of Katla is known from this approximate time period, ca. 10,800 cal. yrs BP, but notably, shards of a Katla affinity were identified alongside the Askja-S/10ka tephra at Borge bog in Vestvågøy, Noway by Pilcher et al. (2005). In summary CRUM1 498 can be correlated to the Askja-S/10ka tephra, whereas the interval at CRUM1 496 seems to represent a previously unrecognised Grímsvötn tephra horizon.

CRUM1 430

The homogenous analyses identified at this interval can be classified as a Tholeiitic basalt with low potassium values (Figure 6.6). The horizon has a chemical signature which can be correlated to the Grímsvötn system (Figure 6.16), which as noted above was particularly active during the early Holocene ca. 10.4-9.9 (Jennings et al. 2002; Jóhannsdóttir et al. 2005; Kylander et al. 2011; Jennings et al. 2014; Thordarson 2014; Neave et al. 2015). A recent study by Neave et al. (2015) has demonstrated that at least five of the Grímsvötn eruptions that typified this period possess identical major element characteristics, with the other two as yet unanalysed (Jennings et al. 2002; Jennings et al. 2014). Whilst the tephra identified at CRUM1 430 may therefore correlate to one of the seven known Holocene eruptions from Grímsvötn, it is particularly difficult to assign a robust correlation in this instance without further chemical distinction between these horizons, or other chronological information,.

CRUM1 380

Analyses of the macrotephra associated with this interval produced an homogenous chemical series that can be classified as a Tholeiitic basalt with low potassium values (Figure 6.6). The interval, like the basaltic tephra horizons characterised at CRUM1 496 and CRUM1 430, can be correlated to the Grímsvötn system (Figure 6.17). Recent studies have revealed that a 500-year interval of increased activity characterised the Grímsvötn system during the early Holocene, and that the 'Saksunarvatn Ash', as originally described from the Faroe Islands (e.g. Waagstein and Jóhansen 1968; Jóhansen 1975; Mangerud et al. 1986), may not be the product of a single ash fall event (Jennings et al. 2002; Jóhannsdóttir et al. 2005; Kristjánsdóttir et al. 2007; Kylander et al. 2011; Jennings et al. 2014; Thordarson 2014; Neave et al. 2015). Work by Thordarson (2014) in particular has illustrated that the volume of material ascribed to the Saksunarvatn Ash, if produced by a single event, would have been >450 km^3, approximately 40 times larger than the most explosive Holocene aged silicic eruptions

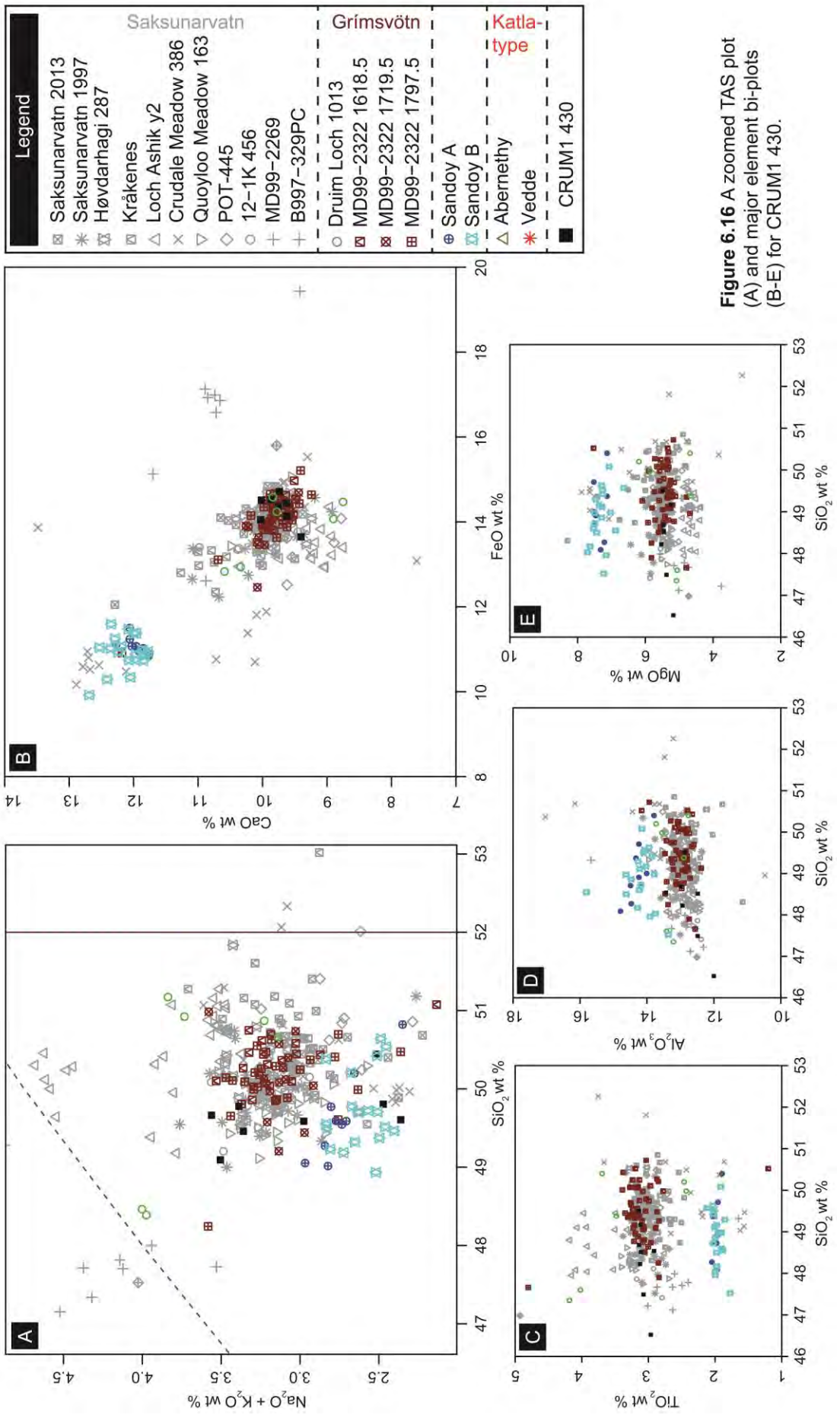

Figure 6.16 A zoomed TAS plot (A) and major element bi-plots (B-E) for CRUM1 430.

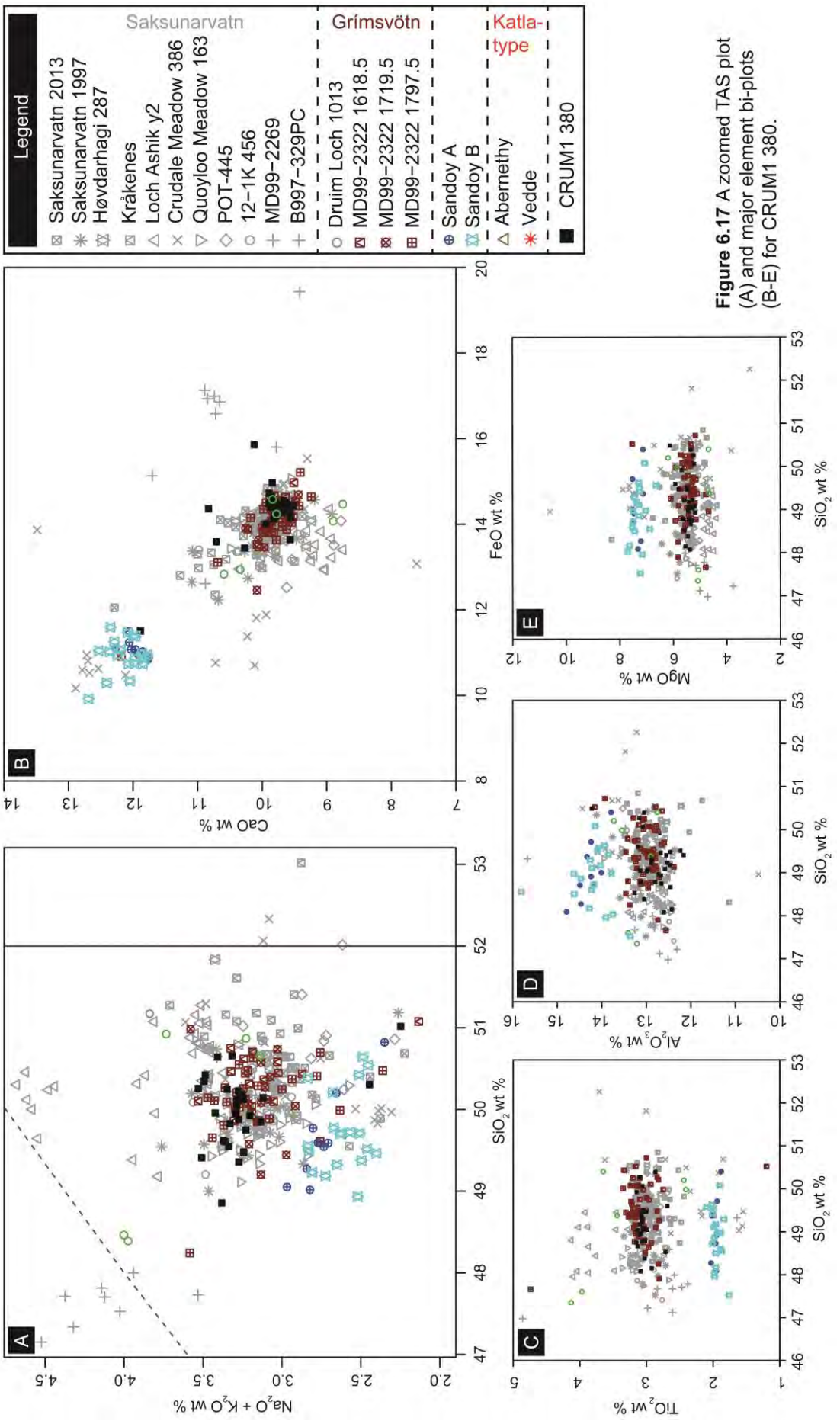

Figure 6.17 A zoomed TAS plot (A) and major element bi-plots (B-E) for CRUM1 380.

from Iceland, and bordering on a 'super-eruption' classification. Evidence from lake Hvítárvatn in Iceland, and from marine sites on the Greenland Shelf, have revealed that as many as seven ash layers may have been produced from Grímsvötn during this period of activity (Jóhannsdóttir et al. 2005; Jennings et al. 2014). However, it is not clear exactly how many of these Grímsvötn eruptions dispersed tephra in an eastwards direction towards mainland Europe. At present all evidence for a multi-eruption model lies to the west of the Grímsvötn volcanic centre (Jóhannsdóttir et al. 2005; Jennings et al. 2014), with only the Saksunarvatn Ash *sensu stricto* identified in terrestrial sediment sequences to the east. Trace element analyses conducted by Davies et al. (2012) and Bramham-Law et al. (2013) would further supported this multi-eruption model; these studies demonstrated that a chemical distinction could be made between 'Saksunarvatn' shards identified in Greenland and those identified in several European sequences. Significantly, these studies also illustrated that a chemical homogeneity exists between the trace element analysis of 'Saksunarvatn' deposits identified in European sequences. Thus, at present, it would seem that only one Grímsvötn eruption i.e. the 'Saksunarvatn Ash', was of sufficient magnitude to deposit large quantities of tephra over NW Europe during the Holocene. Whilst the other Grímsvötn layers identified in the CRUM1 stratigraphy may provide evidence for the multi-eruption model proposed from proximal sites in Iceland, the clear prominence of the horizon identified at 380 cm most likely correlates to the Saksunarvatn Ash identified in the Faroe Islands and in other sites across NW Europe.

6.4 Chapter summary

- This chapter presents litho- and tephrostratigraphic data from Crudale Meadow, a basin from Orkney Mainland, Scotland. Litho- and tephrostratigraphic data would suggest that the site is indicative of a typical LGIT age sequence in Scotland, which agrees with previous investigations of the basin. Contiguous, high-resolution (1 cm) sampling has yielded a tephrostratigraphic record that exhibits a much greater level of complexity than has previously been recognised at the site. Fourteen horizons were analysed as part of the tephrostratigraphic study, with the main findings summarised in Table 6.3.

- The occurrence of a silicic tephra at the base of Crudale Meadow (CRUM1 676) is a significant find. Very few terrestrial sites in NW Europe have yielded a Dimlington Stadial-aged tephra. The horizon identified here has been tentatively correlated to the Dimna Ash, a tephra only previously identified in Norway, and in the Summer Isles, Scotland (Koren et al. 2008; Weston 2012). However,

some ambiguity surrounds this correlation, and further chemical analyses are required to test this hypothesis.

- The occurrence of a Borrobol-type tephra at the Windermere Interstadial/ Loch Lomond Stadial transition is an important discovery. At present it is not certain whether this horizon is a product of primary airfall, or secondary re-deposition. It will thus be essential to trace this tephra to other sites before a more definite conclusion can be made.

Table 6.3 Summary of tephra horizons identified in the CRUM1 composite sequence

Composite code	Unit	Stratigraphic position	Correlation	Notes
CRUM1 380	6	early Holocene	Saksunarvatn Ash	macrotephra
CRUM1 430	5b	early Holocene	unknown Grímsvötn eruption	
CRUM1 496	5a	early Holocene	unknown Grímsvötn eruption	small quantities of Askja-type and Katla-type shards present
CRUM1 498	5a	early Holocene transition	Askja-S/10 ka Tephra	small quantities of Grímsvötn-type shards present
CRUM1 543	5a	early Holocene transition	Hässeldalen Tephra & unknown Borrobol-type	mixed horizon
CRUM1 561	4d	early Holocene transition	unknown Tindfjallajökull	mixed horizon of Tindfjallajökull-type and Katla-type shards
CRUM1 576	4a	early Holocene transition	Abernethy Tephra?	mixed horizon of Borrobol-type and Katla-type shards
CRUM1 579	3c	Loch Lomond Stadial	Abernethy Tephra?	mixed horizon of Borrobol-type and Katla-type shards
CRUM1 587	3b	Loch Lomond Stadial	Vedde Ash	small quantities of Borrobol-type shards also present
CRUM1 597	2i/3a	Loch Lomond Stadial	unknown Borrobol-type eruption	
CRUM1 632	2c	Windermere Interstadial	Penifiler Tephra	
CRUM1 638	2b	Windermere Interstadial	Borrobol Tephra	
CRUM1 676	1	Dimlington Stadial	uncertain, potentially Dimna Ash or 10-1P 192 Tephra	more analyses required

- The Hässeldalen (CRUM1 543) and Askja-S/10ka (CRUM1 498) Tephra's have been reliably identified within the Crudale Meadow sequence. These early Holocene tephras are key marker horizons in constraining the PBO at other sites in NW Europe (e.g. Davies et al. 2003). After Quoyloo Meadow (Chapter 5.0; Timms et al. 2016), this is only the second time these two tephras have been identified in the British Isles. Their identification therefore offers new

tephrostratigraphic links, and an exciting opportunity to accurately constrain the PBO in the British Isles.

- A Grímsvötn basaltic tephra has been identified in close association with the Askja-S/10ka Tephra (Table 6.3). The tephra is thought to reside just outside the period of increased Grímsvötn activity, as identified in Iceland and on the Greenland Shelf. It is thus believed that this tephra represents a previously unrecognised horizon, and hence is termed the CRUM1 496 Tephra.

- A tephra with a chemical signature akin to the Tindfjallajökull system has been tentatively identified in the Crudale Meadow sequence (Table 6.3). This is potentially a very significant find, which may necessitate a re-evaluation of the Tindfjallajökull system as a viable producer of distal tephra during the LGIT.

- The Saksunarvatn Ash at Crudale Meadow has previously been reported by Bunting (1994) and Whittington et al (2015), but not a being visible within the stratigraphy. This is an important discovery, and along with Quoyloo Meadow brings the total number of known visible Saksunarvatn Ash layers in the UK to four.

Chapter 7. Spretta Meadow Results

7.1 Introduction and chapter structure

Spretta Meadow is a previously unreported site, and the only non-carbonate record that was examined as part of the tephrostratigraphic study on Orkney. Given the uncertainties governing tephra preservation in carbonate sequences (e.g. Pollard et al. 2003), it was hoped that Spretta Meadow would act as a 'control' for the Northern Sector; exhibiting tephras which may otherwise be chemically altered or dissolved entirely within the Quoyloo Meadow and Crudale Meadow stratigraphies (Chapter 5 and 6). With this site, and the additional Orcadian basins, it is anticipated that the Northern Sector will offer one of the best opportunities to identify tephras which have previously alluded detection in more southerly locations. In this regard these sites should help to further the tephrostratigraphic framework of Scotland, and hence provide valuable tephrostratigraphic links to Scandinavia, and Europe (Chapter 3). This chapter presents the main litho- and tephrostratigraphic results from the Spretta Meadow basin, and also provides a discussion on the likely geochemical correlations of the tephra series. For the local and regional site context see Chapter 3.

7.2 Results

Three boreholes were cored from the Spretta Meadow site using 0.5 m Russian samplers in February 2014 (Figure 7.1). Due to constraints on time and access arrangements with Scottish Natural Heritage, a full basin survey was not completed. Instead, a series of 1.0 m Russian rods were used to provisionally sound basin depth, working systematically every 20 m along a broad arcing transect from west to east. The two deepest areas identified became the focus of SPME 1 (59.012283 -3.332733) and SPME 3 (59.012056 -3.33295), whilst SPME 2 (59.012217 -3.331983) was taken to illustrate that the basin shallowed from west to east, and toward the outlet of the Burn of Sowadee. SPME 1 is the only complete sequence retrieved from the basin, as sediments pertaining to the LGIT were the preliminary focus of this project. Consequently only the basal core was extracted from SPME 2 and 3 (Figure 7.1).

7.2.1 Basin sedimentology

Figure 7.1 illustrates the deepest SPME cores, with climatic zones delineated and inferred from lithological changes. Detailed sedimentological descriptions of each of the cores can be found in Appendix F. SPME1 R, Q and P were matched and aligned using lithological, LOI and magnetic susceptibility changes to form a composite sediment stratigraphy (Figure 7.2). A detailed description of the composite core sedimentology is presented in Appendix F.

Figure 7.1 Spretta Meadow basin sediment stratigraphy. Only the lowermost cores are illustrated here, for a lithological description of all cores see corresponding Appendix. SPME2 A has been aligned with the rest of the sequence, but note its depth offset with that exhibited by SPME1 R, and SPME3 A. This is evidence to suggest the basin shallows toward the east (see inset), whilst still possessing sediments relating to the Loch Lomond Stadial at base.

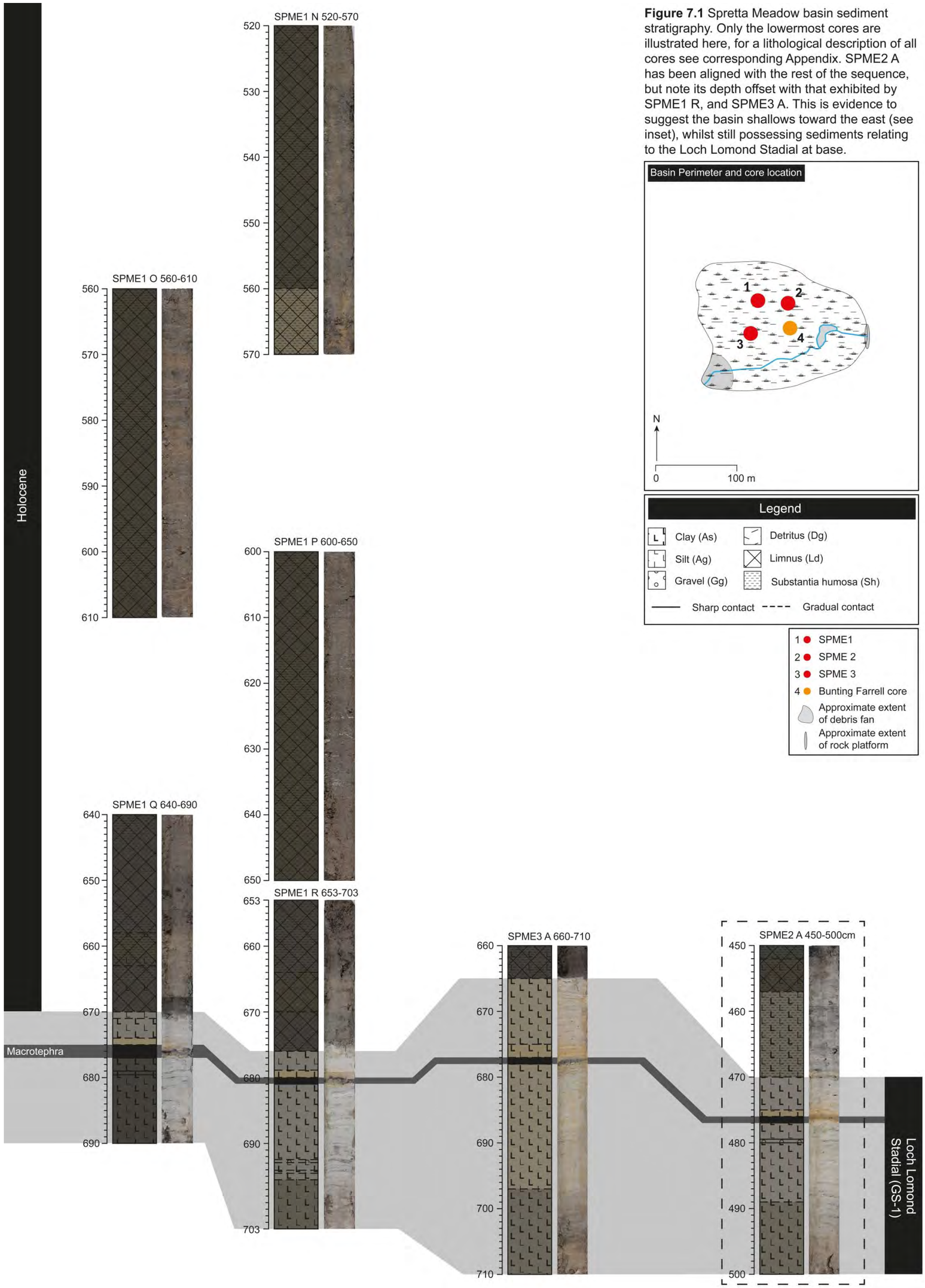

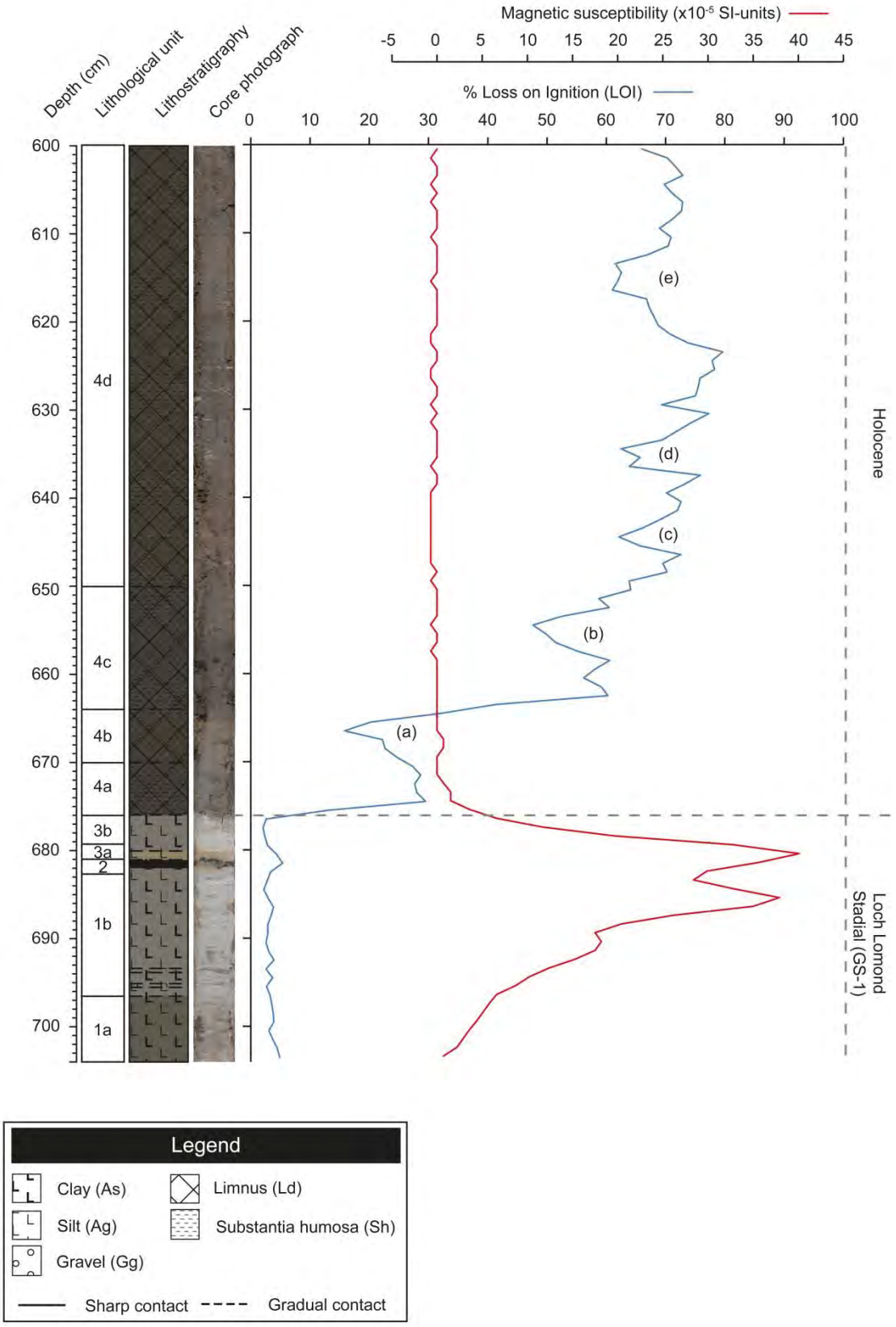

Figure 7.2 Composite stratigraphy for the Spretta Meadow basin derived from cores SPME1 R, Q and P. Note the peak in magnetic susceptibility in association with the macrotephra centred on 681 cm. Also note the five oscillations (a-e) as depicted by downturns in the LOI signal. These oscillations are centred on (a) 666, (b) 654, (c) 644, (d) 634, and (e) 616 cm.

The absence of an archetypal 'tri-partite' sequence (Lowe and Walker 2015 p.g. 156) suggests the lowermost units are representative of Loch Lomond Stadial silts and clays. This Stadial deposit is punctuated by a macrotephra horizon, which holds significance due to the fact such a discovery has only previously been made at one other site in the UK; Loch Ashik, on the Isle of Skye (Davies et al. 2001). The ash layer is found across all three basal cores, although it appears less pronounced in SPME2 A (Figure 7.1). Associated with the tephra in all three basal cores is a pale brown/ orange horizon, which occurs concurrently with the tephra, but also appears to progressively grade into the overlying gray coloured silts and clays which typify the remaining cold climate deposits. These Loch Lomond Stadial sediments are in turn overlain by organic lake muds of the early Holocene, which show a progressive increase in the organic content. However, at least five downturns as inferred from the LOI appear to intersect this trend (Figure 7.2). These oscillations are centred on (a) 666, (b) 654, (c) 644, (d) 634, (e) 616 cm. At an approximate depth of 408 cm (not shown in Figures 7.1 and 7.2) the lake muds transition into peats, demonstrating the basins continued hydroseral succession and gradual terrestrialisation of the basin.

7.2.2 Tephrostratigraphy

SPME1 R and P were processed for tephra at contiguous 1 cm intervals throughout the entire core (see section 4.5), whereas SPME1 Q was sampled only in the upper 19 cm as defined by the overlaps in the sequence. A composite tephrostratigraphy is presented in Figure (7.3) and has been constructed in the same manner as the composite lithostratigraphy. Raw count data can be found in Appendix F.

Silicic tephra shards were identified in almost every sample through the stratigraphic sequence (Figure 7.3). Magnetic separation to identify basaltic shards was conducted at select intervals surrounding the most voluminous silicic tephras i.e. 676-686 cm and 647-652 cm. 92 shards were recovered from the lower interval, but no shards were identified in the upper samples. From 600-647 i.e. within the early Holocene organic unit 4d, a single drop of the 'heavy fraction' left residual from the density separation process was mounted and assessed for the presence of basaltic shards. No basaltic shards were identified.

Due to constraints on time and facilities not all peaks in shard concentration could be processed for chemical analyses. In total ten horizons were analysed across SPME1 R, P and Q, with the analysis of a stratigraphically comparable tephra between P and Q cores at a depth of SPME1 Q 642 cm, SPME1 P 649 cm and SPME1 P 645 cm. These depths relate to a highly concentrated and diffuse silicic tephra, positioned between

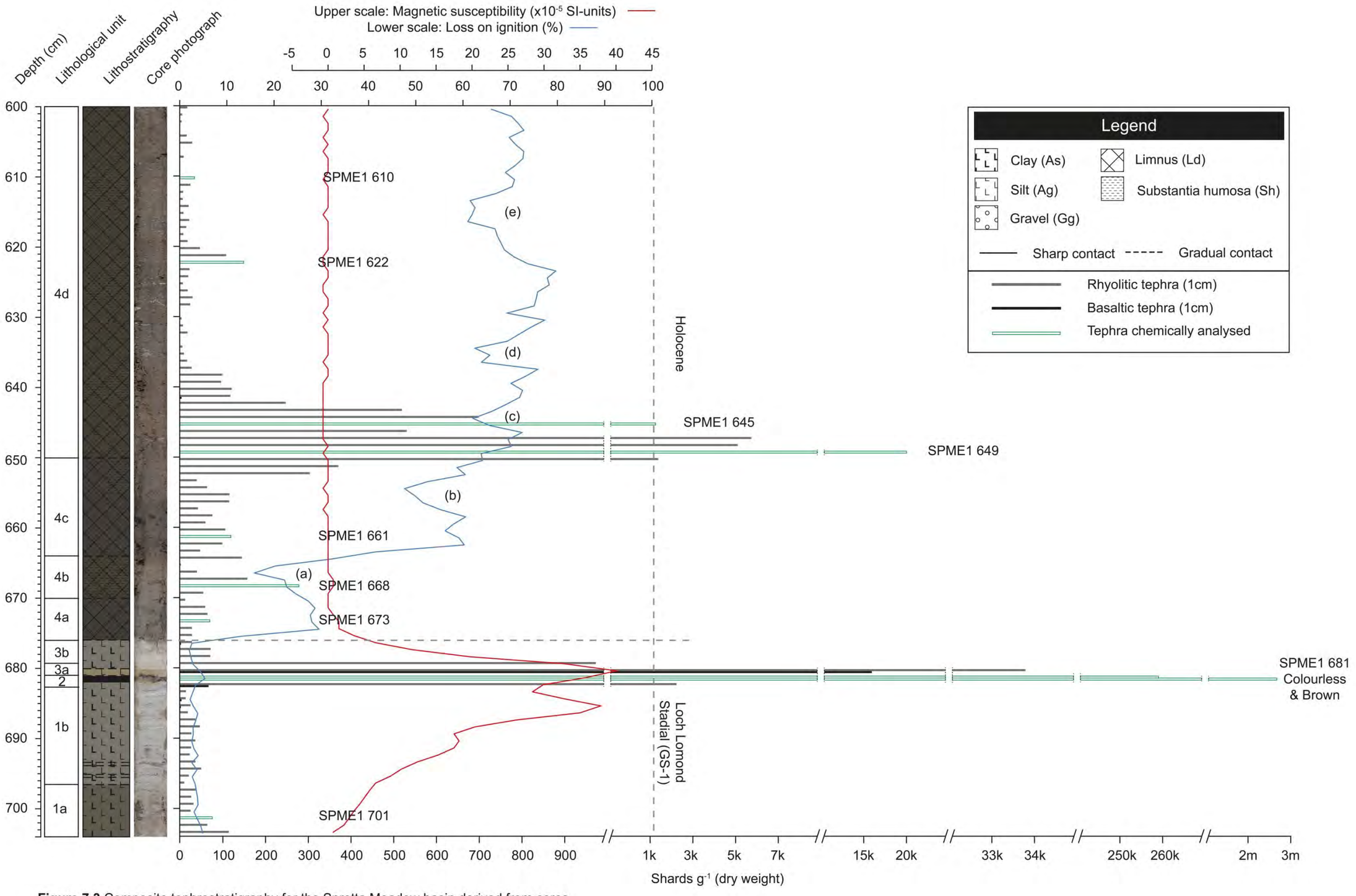

Figure 7.3 Composite tephrostratigraphy for the Spretta Meadow basin derived from cores SPME1 R, Q and P. Note the almost continuous distribution of tephra through the core. Basaltic shards were only identified in the 681 cm interval and in the surrounding 8 cm.

oscillations (b) and (c) in Figure 7.3. Table 7.1 provides a summary of horizons analysed, their climo-stratigraphic placing, and notes the corresponding composite coding.

Table 7.1 tephra samples from the Spretta Meadow 1 cores, and their corresponding composite depth.

Core	Horizon	Stratigraphic position	Composite coding
SPME1 P 600-650	610	early Holocene	SPME1 610
	622	early Holocene	SPME1 622
	645	early Holocene	SPME1 645
	649	early Holocene	SPME1 649
640-690	642	early Holocene	SPME1 649
SMPE1 R 653-703	661	early Holocene	SPME1 661
	667	LLS/Holocene transition	SPME1 668
	672	LLS/Holocene transition	SPME1 673
	680	Loch Lomond Stadial	SPME1 681
	700	Loch Lomond Stadial	SPME1 701

In the following sections, population A is defined as the most numerous within the horizon, with subsequent horizons given letters denoting their lower prominence within the series, i.e. population B, C etc. The chemical characteristics of tephra horizons and the populations within, are based on non-normalised filtered data sets. Mean chemical data is presented in Table (7.3). For all chemical data see Appendix B, and for analytical conditions see section 4.8.1.

SPME1 701

Within the Loch Lomond Stadial sediments, between the base of the SPME1 sequence, and the macrotephra horizon at 681 cm (unit 1a/1b), an interval of tephra spanning approximately 20 cm can be identified. The spread of shards does not possess a discernible peak, although two intervals toward the base 701, and 703 cm exhibit slightly higher totals of 76 and 114 shards g^{-1} respectively. A morphological analysis of the shards present within the 20 cm section showed that blocky cuspate specimens with open vesicles and mineral inclusions predominated (Figure 7.4 A, B). The interval at 701 cm was chosen for chemical analyses. Nine analyses were obtained which returned a homogenous population defined by low FeO (ca. 1.47 wt %) and CaO (ca. 0.72 wt %) values (Table 7.2).

Table 7.2 Mean geochemical data for SPME1, values expressed as (%) weight oxide.

Composite code	SiO_2	TiO_2	Al_2O_3	FeO	MnO	MgO	CaO	Na_2O	K_2O	P_2O_5	Total
SPME1 610 (pop A)	71.54	0.19	11.56	2.82	0.07	0.07	0.34	5.10	4.42	0.01	96.13
2 std dev (n=2)	0.58	0.02	0.78	0.02	0.01	0.05	0.04	0.09	0.11	0.01	1.67
SPME1 610 (pop B)	73.54	0.11	11.84	1.47	0.05	0.07	0.59	4.11	3.71	0.01	95.51
SPME1 622 (pop A)	70.16	0.26	12.54	3.66	0.15	0.13	1.21	5.01	3.57	0.03	96.71
2 std dev (n=5)	2.74	0.07	0.70	0.21	0.01	0.05	0.23	0.53	0.14	0.01	2.87
SPME1 622 (pop B)	74.69	0.10	11.73	1.23	0.03	0.03	0.52	3.90	3.97	0.00	96.20
2 std dev (n=2)	0.03	0.01	0.01	0.04	0.02	0.03	0.04	0.39	0.03	0.01	0.45
SPME1 622 (pop C)	71.21	0.19	11.51	2.93	0.07	0.05	0.36	5.23	4.33	0.01	95.89
2 std dev (n=2)	0.79	0.01	0.04	0.14	0.00	0.00	0.06	0.32	0.16	0.02	0.57
SPME1 645	71.75	0.19	11.88	2.76	0.07	0.05	0.41	5.08	4.30	0.01	96.50
2 std dev (n=18)	1.92	0.03	1.00	0.42	0.01	0.07	0.20	0.53	0.26	0.01	1.77
SPME1 649	71.32	0.19	11.98	2.77	0.07	0.06	0.40	5.12	4.34	0.01	96.27
2 std dev (n=28)	2.14	0.01	1.27	0.47	0.01	0.05	0.19	0.40	0.20	0.01	1.74
SPME1 661 (pop A)	71.82	0.27	13.22	3.73	0.15	0.22	1.35	5.21	3.44	0.04	99.46
2 std dev (n=4)	2.57	0.02	1.06	0.21	0.03	0.07	0.16	0.31	0.20	0.01	4.15

SPME1 661 (pop B)	72.32	0.42	13.05	2.75	0.15	0.26	0.93	5.14	3.66	0.04	98.73
2 std dev (n=3)	1.52	0.01	0.84	0.31	0.01	0.07	0.07	0.27	0.18	0.01	2.63
SPME1 661 (pop C)	73.69	0.11	12.38	1.46	0.05	0.07	0.68	4.15	3.64	0.01	96.24
2 std dev (n=2)	0.74	0.00	0.20	0.02	0.02	0.07	0.09	0.13	0.24	0.01	1.02
SPME1 668 (pop A)	70.99	0.28	12.96	3.71	0.15	0.20	1.27	5.18	3.37	0.04	98.15
2 std dev (n=18)	1.63	0.03	0.47	0.43	0.02	0.03	0.11	0.23	0.16	0.01	2.27
SPME1 668 (pop B)	73.52	0.12	12.11	1.56	0.05	0.09	0.71	4.04	3.73	0.01	95.93
2 std dev (n=2)	1.07	0.00	0.16	0.17	0.00	0.05	0.01	0.09	0.13	0.02	1.02
SPME1 673 (pop A)	73.63	0.12	11.92	1.52	0.05	0.06	0.71	4.15	3.70	0.01	95.87
2 std dev (n=10)	1.67	0.02	0.58	0.23	0.01	0.06	0.19	0.22	0.17	0.01	1.37
SPME1 673 (pop B)	71.03	0.28	13.08	3.75	0.15	0.20	1.32	5.15	3.36	0.04	98.35
2 std dev (n=8)	2.19	0.01	0.57	0.23	0.01	0.04	0.09	0.39	0.17	0.01	2.98
SPME1 681 (pop A)	47.22	4.52	12.77	14.58	0.22	4.98	9.82	3.10	0.75	0.47	98.41
2 std dev (n=25)	2.27	0.43	1.03	2.22	0.02	0.79	0.99	0.45	0.19	0.06	2.53
SPME1 681 (pop B)	69.33	0.28	12.89	3.68	0.14	0.21	1.28	5.20	3.42	0.04	96.47
2 std dev (n=16)	1.60	0.02	0.51	0.24	0.01	0.04	0.10	0.32	0.12	0.01	2.16

SPME1 701	73.17	0.12	11.92	1.47	0.04	0.07	0.72	4.13	3.69	0.01	95.35
2 std dev (n=9)	0.92	0.01	0.50	0.28	0.03	0.08	0.20	0.23	0.13	0.01	0.97

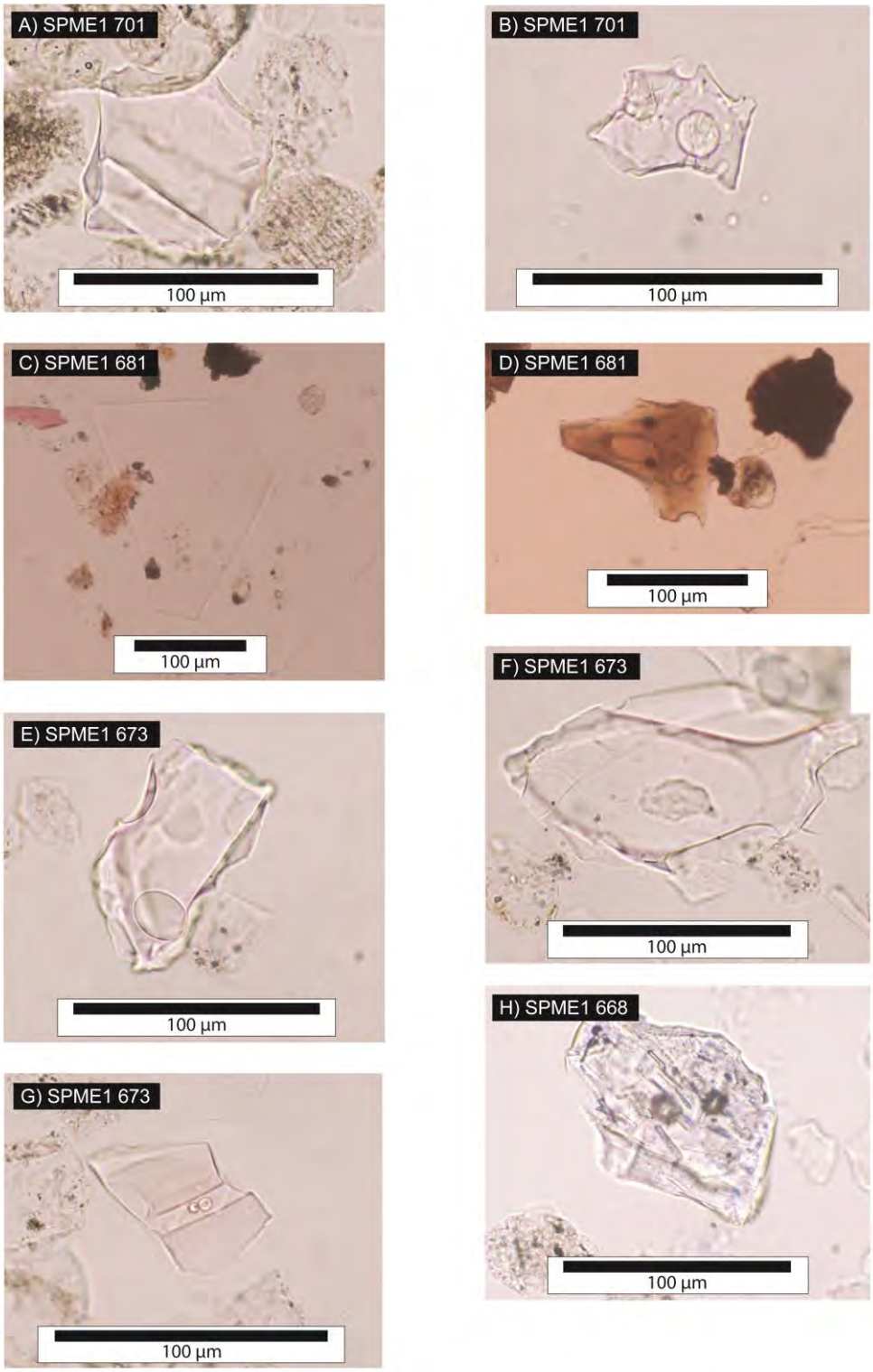

Figure 7.4 Photographs of horizons analysed from SPME1. (A) A blocky cuspate shard with a single pencil-like mineral inclusion toward the right edge. (B) A small blocky shard exhibiting one large open vesicle and evidence of surface pitting from chemical attack. (C) An abnormally large platey shard with an A-axis of 190 µm. (D) A blocky basaltic shard with both open and closed vesicles. Also note the opaque back object in the upper right hand corner, this material is believed to be micro-pumice. (E) A blocky shard exhibiting one large open vesicle and several damaged and corroded edges. (F) A large blocky shard showing some signs of hydration fractures on the left hand side. (G) A fluted and platey shard. (H) An inclusion rich blocky shard which also exhibits a number of closed vesicles.

Figure 7.4 continued (I) A blocky irregular sharped shard exhibiting a number of open and closed vesicles, as well as several pencil-like mineral inclusions. (J) A delicate looking cuspate shard with a notably thin upper edge. (K) A delicate looking cuspate shard. (L) A shard exhibiting a 'winged-shaped' morphology i.e. a central thick spine flanked by two more lightly constructed 'wings'. (M) Four small shards two of which feature small closed vesicles, one circular and the other elongate. (N) A feint delicate shard with a proportionally large closed and ovoid vesicle. (O) An delicate elongated shard, exhibiting some fluting as well as ovoid shaped open and closed vesicles. (P) A blocky shard in possession of two small circular closed vesicles.

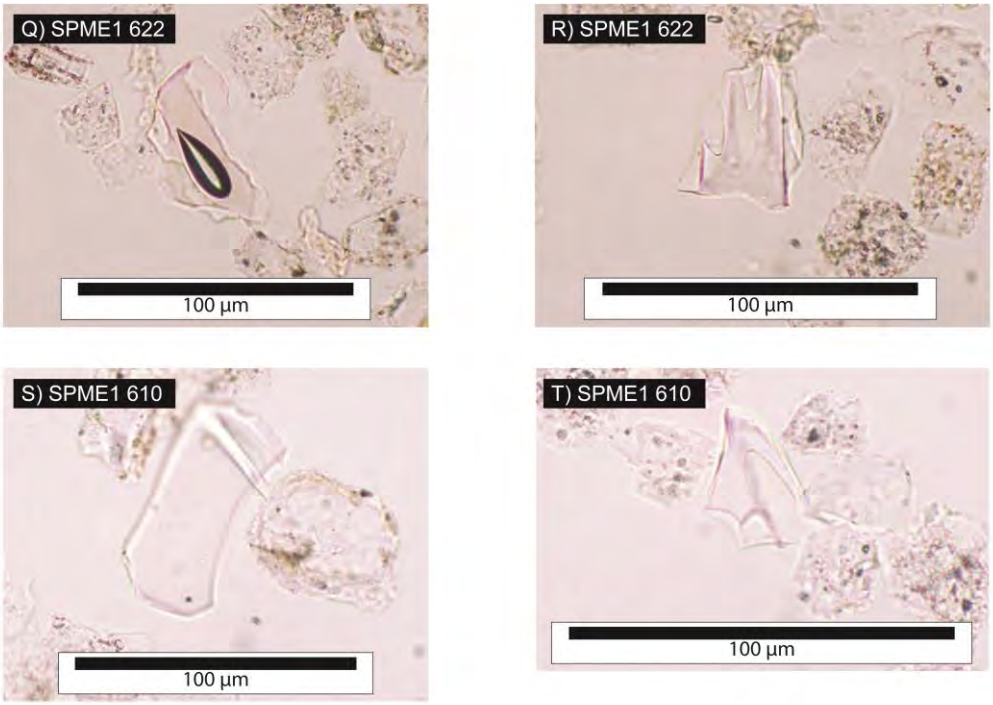

Figure 7.4 continued (Q) A small blocky shard exhibiting a large tear-drop shaped closed vesicle and a slightly tatty right flank. (R) A small shard with an open vesicle. (S) A broadly platey shard exhibiting a thicker upper edge. (T) A small cuspate shard with one proportionally large vesicle.

SPME1 681

The macrotephra horizon identified at 681 cm exhibited both brown (population A) and colourless (population B) shards; the respective totals of each were quantified using the lycopodium spiking method (see section 4.6.5). The colourless fraction attained a peak concentration of ca. 259,000 shards g^{-1}, whilst the brown population exhibited much higher concentrations of ca 2.7 million shards g^{-1}. Colourless shards tended to possess platey, fluted and 'winged' shaped morphologies (Figure 7.4 C), whereas the brown population was distinctly blockier, and also exhibited open and closed vesicles (Figure 7.4 D). Some abnormally large shards were identified in the colourless fraction, with a number of specimens exhibiting an A-axis value >125 µm (Figure 7.4 C). Chemical analyses of the brown population returned SiO_2 totals of ca. 47.22 wt %, FeO values of ca. 14.58 wt % and K_2O totals of ca. 0.75 wt %. The colourless fraction in comparison returned chemistries defined by much higher SiO_2 totals of ca. 69.33 wt %, lower FeO values of ca. 3.68 wt % and higher K_2O totals of ca. 5.20 wt % (Table 7.2).

SPME1 673

Shortly after the onset of organic sedimentation and within unit 4a, three consecutive intervals are noted to exhibit slightly higher shard concentrations than the preceding and succeeding samples (Figure 7.3). The first interval at 673 cm possesses the

highest concentration of 70 shards g^{-1}. The horizon exhibits shards with a varied morphology, where smaller platey and fluted shards are interspersed with large blocky specimens (Figure 7.4 E, F, G). Eighteen data points were obtained for the interval and returned a bi-modal distribution. Population A (n=10) is defined by shards exhibiting relatively low FeO (ca. 1.52 wt %) and CaO (ca. 0.71 wt %) values when compared to population B (n=8), which possesses FeO values in the order of (ca. 3.75 wt %) and CaO totals of (ca. 1.32 wt %) (Table 7.2).

SPME1 668

Within unit 4b and on the downturn into the oscillation marked (a) in Figure 7.3, a clear peak in tephra concentrations can be observed against the seemingly continuous 'background' of tephra which typifies this early Holocene interval. The horizon attains a value of 278 shards g^{-1}, and is characterised by a mixed morphological population. Shards exhibit large blocky microlitic forms, as well as smaller platey and cuspate morphologies (Figure 7.4 H, I, J). Twenty chemical analyses were obtained for the horizon which returned a bi-modal distribution. Population A (n=18) the most dominant of the two series exhibits shards defined by relatively high FeO (ca. 3.71 wt %) and CaO (ca. 1.27 wt %) when compared to population B (n=2) which possesses FeO totals of (ca. 1.55 wt %) and CaO values of (0.71 wt %) (Table 7.2).

SPME1 661

The sequence between 664 and 653 i.e. unit 4c is defined by a continuous spread of tephra. Concentrations fluctuate broadly between horizons exhibiting totals of ~40-60 shards g^{-1} and intervals totalling ~100-120 shards g^{-1}. A decision was made to sample the interval at 661 cm which attains a concentration of 119 shards g^{-1} and is the second highest 'peak' within this spread of tephra (Figure 7.3). Morphologically the horizon appears to be dominated with delicate looking cuspate shards with some exhibiting wing-like shapes (Figure 7.4 K, L). Nine chemical analyses were obtained for the horizon, which returned a tri-modal population (Table 7.2). Population A (n=4) exhibited the highest FeO (ca. 3.73 wt %), CaO (ca. 1.35 wt %) and Na_2O (ca. 5.21 wt %) values of the three. Population B (n=3) in comparison had marginally lower totals in these elements; FeO (ca. 2.75 wt %), CaO (ca. 0.93 wt %) and Na_2O (ca. 5.14 wt %), whilst population C (n=2) had the lowest comparable totals; FeO (ca. 1.46 wt %), CaO (ca. 0.68 wt %), and K_2O (ca. 4.15 wt %) (Table 7.2).

SPME1 649 and 645

Straddling the transition into unit 4d and spreading over approximately 18 cm is a highly concentrated and diffuse tri-peaked tephra interval. The three major peaks are

situated between the oscillations marked (b) and (c) in Figure 7.3, and occur specifically at 649 (20,180 shards g^{-1}), 647 (5733 shards g^{-1}) and 645 cm (1318 shards g^{-1}). The entire tephra series is defined by small cuspate and blocky shards, which often exhibit closed vesicles (Figure 7.4 M-P). The first and third most significant peaks i.e. SPME1 649 and SPME1 645 cm were chosen for chemical analyses and both returned homogenous populations with matching chemical signatures. Twenty-eight analyses were obtained for SPME1 649 and eighteen for SPME1 645; SiO_2 values reach ca. 71.32 wt % and ca. 71.75 wt % respectively, FeO totals ca. 2.77 wt % and ca 2.76 wt % respectively, and CaO attains a value of ca. 0.40 wt % and 0.41 wt % respectively (Table 7.2).

SPME1 622

Within unit 4d, and occurring on a decline in LOI marked as oscillation (e) in Figure 7.3, a peak in tephra is noted. Concentrations reach 149 shards g^{-1}, and morphologies exhibit cuspate and vesicle rich forms (Figure 7.4 Q, R). Nine chemical analyses were obtained for the interval, which revealed a tri-modal population. Population A (n=5) can be characterised by relatively high FeO (ca. 3.66 wt %), Al_2O_3 (ca. 12.54 et %) and CaO (ca. 1.21 wt %) totals. Population B (n=2) in comparison has much lower FeO (ca. 1.23 wt %), lower Al_2O_3 (ca. 11.73 wt %) and also lower CaO (ca. 0.52 wt %). Population C (n=2) has intermediary FeO (ca. 2.93 wt %) values, the lowest Al_2O_3 (ca. 11.51 wt %) totals, and intermediary CaO (ca 0.36 wt %) values (Table 7.2).

SPME1 610

The uppermost horizon examined in the SPME1 sequence occurs on the LOI upturn of the oscillation marked (e) in Figure 7.3. The horizon reached a concentration of 34 shards g^{-1}, and morphologies are defined by platey cuspate specimens (Figure 7.4 S, T). Three chemical analyses were obtained for the horizon which returned a bi-modal population. Population A (n=2) returned chemistries defined by relatively higher FeO (ca. 2.82 wt % and Na2O (ca. 5.10 wt %) values. Whereas the single shard defining population B exhibited comparably lower FeO (1.47 wt %) and Na2O (4.11 wt %) totals (Table 7.2).

7.3 Interpretation

7.3.1 Tephra correlations

In this section tephra correlations are proposed based on current published data sets. The local and wider significance of these correlations are discussed in Chapter 10 and 11. Primary classification of the tephra layers is made via Total Alkali vs Silica

diagrams (Figure 7.5 A), and by potassium value plots (Figure 7.5 B) as defined by Le Bas (1986), and Pecorillo and Taylor (1976) respectively. Data sources for the tephra correlations are summarised in Appendix B.

SPME1 701

Within this interval a homogenous population classified as a sub-alkali rhyolite with a high potassium value was identified (Figure 7.5). The analyses can be correlated to the suite of tephras known as Borrobol-type tephras (Figure 7.6), for which there are several known incidences in the LGIT (Davies et al. 2004; Pyne-O'Donnell 2007; Pyne-O'Donnell et al. 2008; Lind et al. 2013; Lind et al. 2016). Such tephras are chemically inseparable based on current major and trace element analyses (Lind et al. 2016); thus additional stratigraphic evidence must be considered when dealing with such horizons. In this instance a long spread of shards exhibiting the same morphological properties as those analysed in SPME 701 can be found from the base of the deposit to the macrotephra horizon identified at 681 cm. The lithological properties of this interval are defined by silts and clays, which are often indicative of the Loch Lomond Stadial (Lowe and Walker 2015). At present no tephra horizon has been analysed from a Loch Lomond Stadial, or Younger Dryas deposit which has returned exclusively Borrobol-type chemistries. Such chemistries have, however, been identified alongside the Katla derived Vedde Ash and Abernethy Tephra at Abernethy Forest and Loch Etteridge, Scotland (Matthews et al. 2011; MacLeod et al. 2015).

The source of these shards may therefore lie with either the Borrobol and Penifiler Tephras. However, both deposits occur within the Windermere Interstadial, and deposits of this age are not known from the Spretta Meadow basin. It is plausible, that there are tephra bearing deposits of Interstadial age, higher in the Spretta catchment. These may have undergone progressive denudation during the Stadial, thus remobilising Borrobol/ Penifiler shards into the lower Spretta catchment. However, it is also plausible that an eruption from the Borrobol source occurred concurrently with the onset of deposition in the Spretta basin. This would agree with the finding of a Borrobol-type tephra within the late Interstadial/ early Loch Lomond Stadial at Crudale Meadow i.e. the CRUM1 597 horizon (Chapter 6.0). Given a lack of information to support the former hypothesis of upper catchment denudation, this latter suggestion of a distinct and separate eruption is favoured here. The implications of this finding are discussed further in Chapter 10.

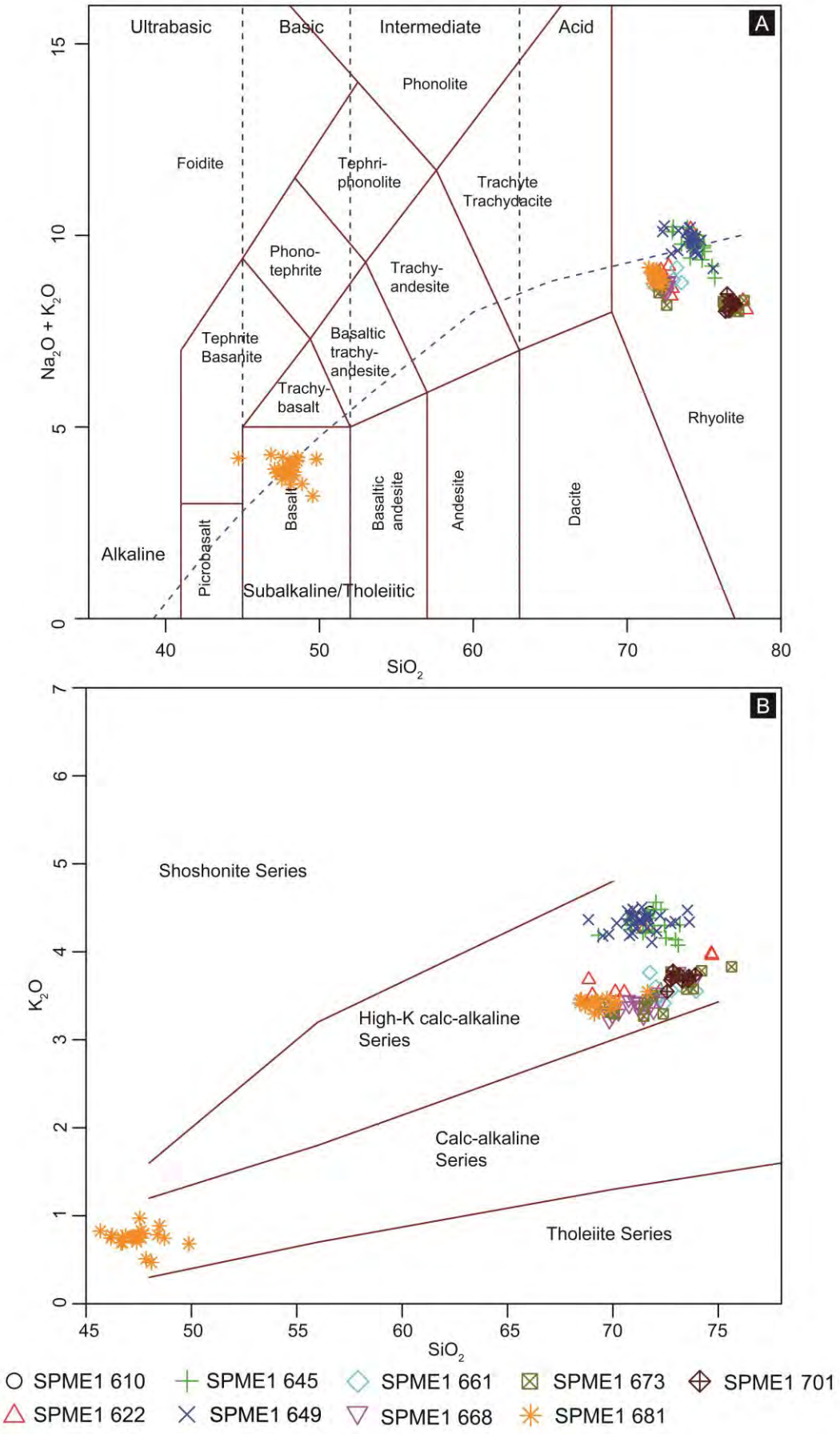

Figure 7.5 Chemical classification of tephra horizons from SPME1. (A) Total Alkali vs Silica diagram (Le Bas 1986). (B) K-series plot (Pecorillo and Taylor 1976).

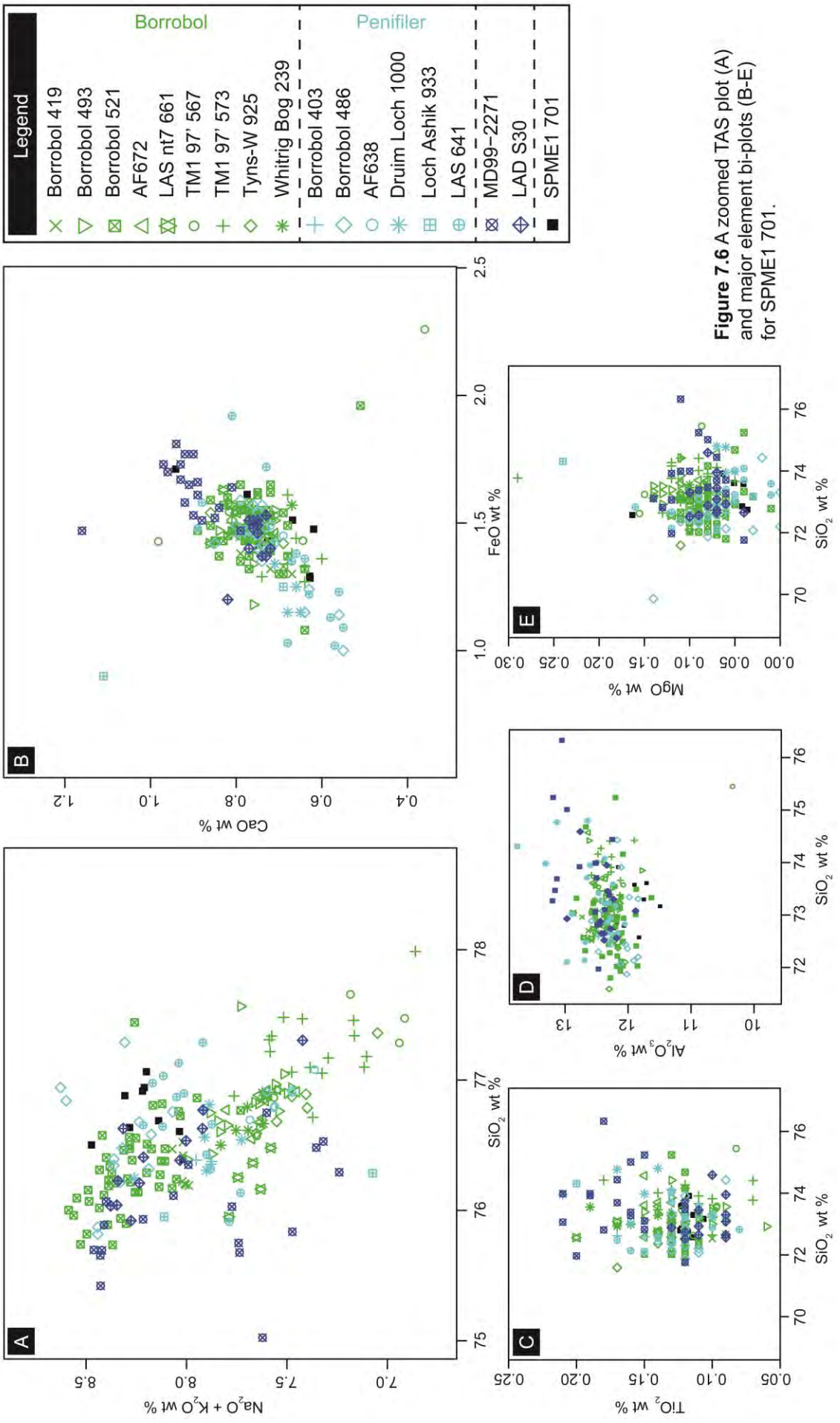

Figure 7.6 A zoomed TAS plot (A) and major element bi-plots (B-E) for SPME1 701.

SPME1 681

The morphological bi-modalism of the colourless and brown shards identified in this interval is reflected in the chemistry of the shards. The colourless population can be classified as a sub-alkali rhyolite with a high potassium value, whereas the brown shards are defined as a basalt with high potassium values (Figure 7.5). Both populations return chemistries which are indicative of the Katla-volcanic system, Iceland (Figure 7.7). Whilst a number of Katla derived horizons are recognised across NW Europe during the LGIT (e.g. Lane et al. 2012b), only one such incidence is known to have produced both silicic and basaltic shards contemporaneously: the Vedde Ash (Mangerud et al. 1984; Lane et al. 2012b; Tomlinson et al. 2012a). This chemical correlation is furthermore supported by the lithostratigraphic position of the tephra, i.e. mid way through sediments relating to the Loch Lomond Stadial/ Younger Dryas. These two lines of evidence distinguish the Vedde Ash from its stratigraphic and chemically identical neighbour, the Abernethy Tephra. Thus a correlation to the Vedde Ash is proposed.

SPME1 673

The analysis of this interval straddling the Loch Lomond Stadial/ Holocene transition returned a chemically bi-modal tephra, which can be broadly classified as a sub-alkali rhyolite with a high potassium value (Figure 7.5). Population A (n=10) can be correlated to a suit of tephras known as the Borrobol-type tephras, and Population B (n=8) can be correlated to tephras which have previously been assigned to the Katla volcanic system (Figure 7.8). The Loch Lomond Stadial is now thought to contain at least two tephras derived from the Katla system: the Vedde Ash, deposited approximately mid-way through the cold phase, and the Abernethy Tephra which occurs at the transition from Stadial into the Holocene (Matthews et al. 2011; Lane et al. 2012b; MacLeod et al. 2015). The former is undoubtedly represented in the SPME1 record by the macrotephra centred on 681 cm (see above), thus the stratigraphic position of the Abernethy Tephra would present a more favourable correlation in this instance. However, the primary population of SPME1 673 is not of Katla-type shards, but Borrobol-type, and this limits the likely correlation to the Abernethy Tephra. What is interesting, however, is that the presence of Borrobol-type shards has been noted in association with other occurrences of the Abernethy Tephra at several sites in Scotland, including the type-site i.e. Abernethy Forest (Matthews et al. 2011; MacLeod et al. 2015). It may be that in this instance, the Borrobol-type population is more dominant in the Abernethy Tephra horizon than the Katla derived population.

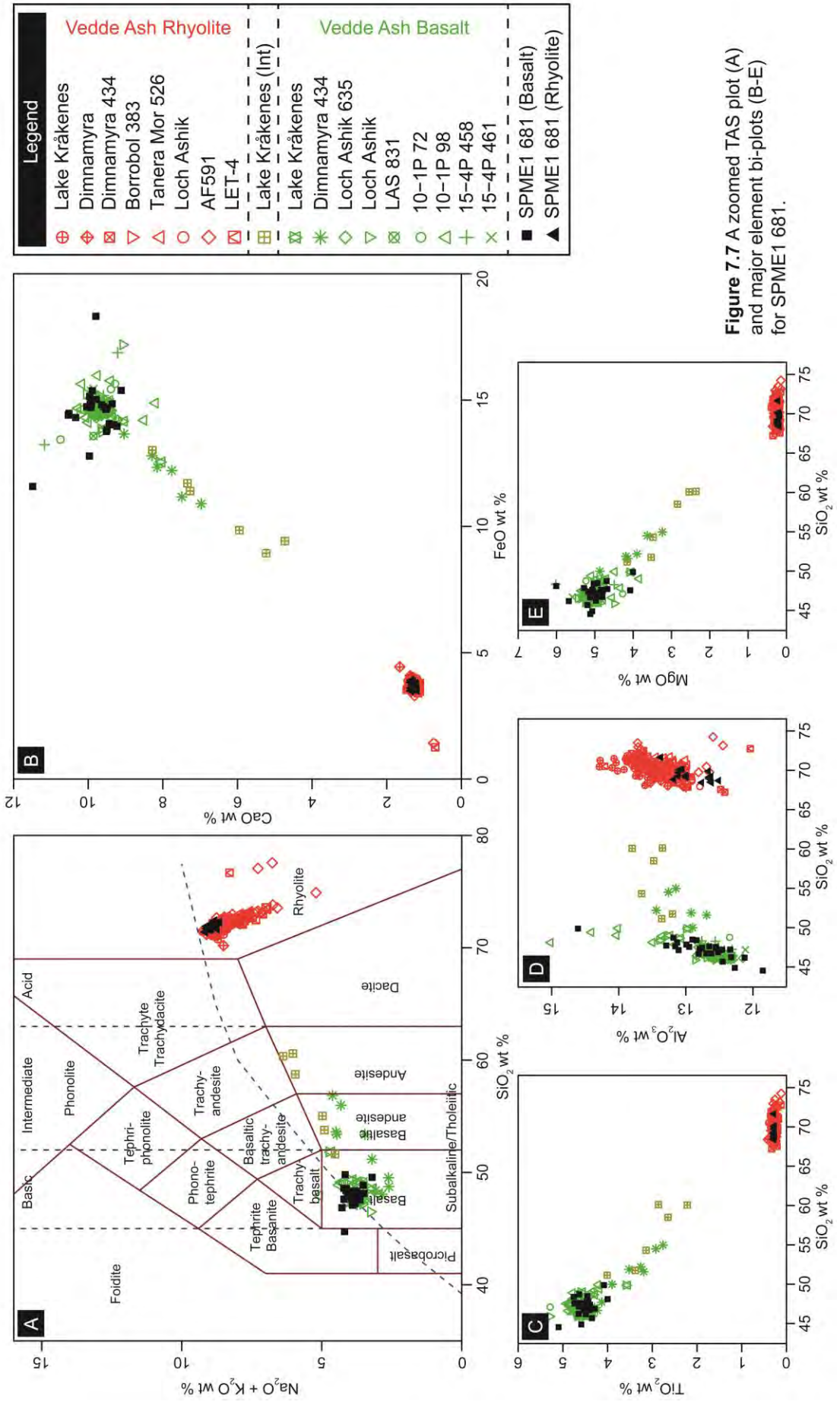

Figure 7.7 A zoomed TAS plot (A) and major element bi-plots (B-E) for SPME1 681.

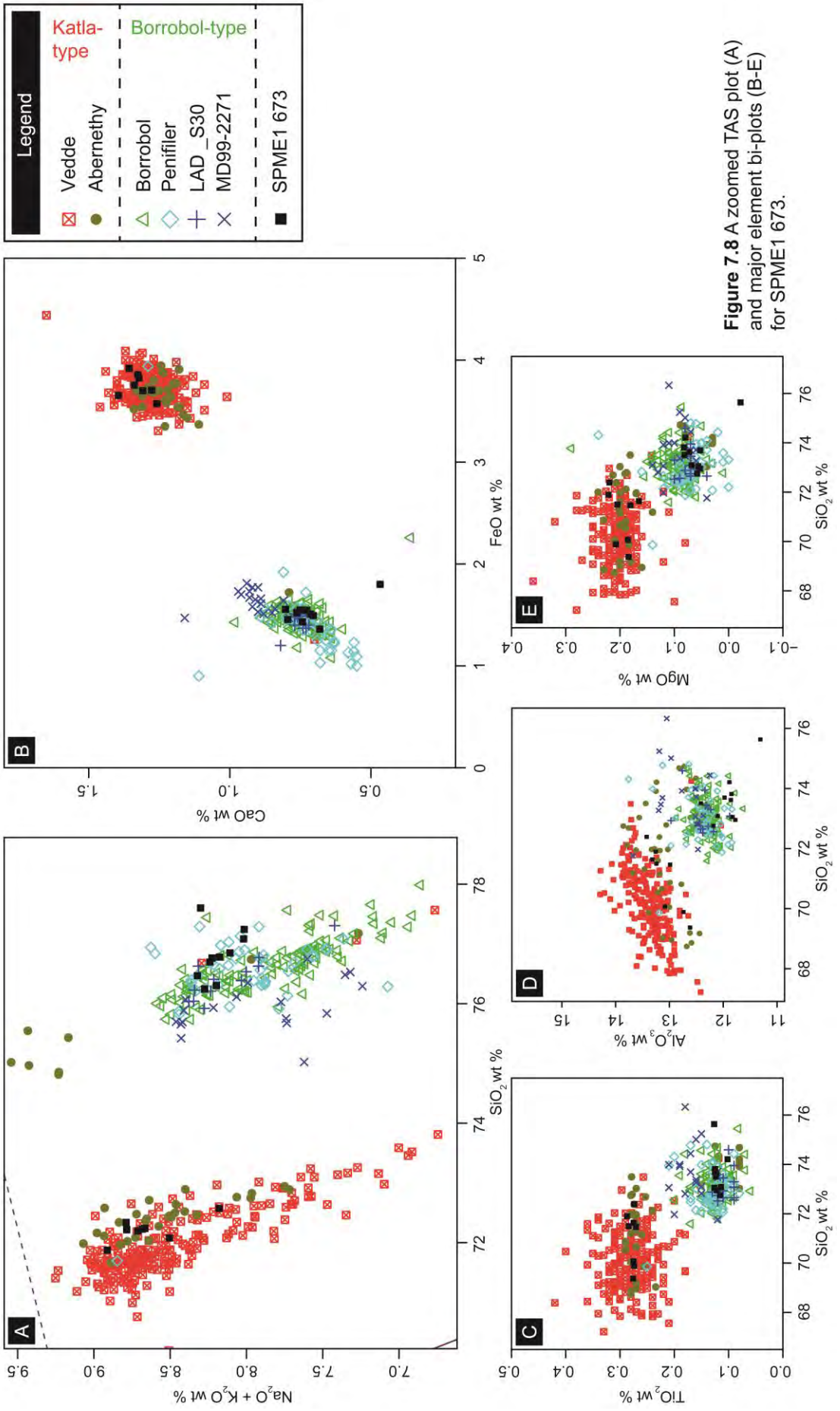

Figure 7.8 A zoomed TAS plot (A) and major element bi-plots (B-E) for SPME1 673.

A caveat on this interpretation is the presence of an exceptionally high concentration of Katla-type shards centred on 681 cm i.e. the Vedde Ash, and the prevalence of Borrobol-type shards throughout the earlier phases of the Loch Lomond Stadial. It is certainly plausible that the mechanism by which Borrobol-type shards were being spread through the early part of the stadial record, continued to have an influence on the basin through the later Stadial and into the Holocene. These taphonomic uncertainties and the uncharacteristic chemical dominance of Borrobol-type shards in SPME1 673 makes a robust correlation for this horizon to the Abernethy Tephra uncertain.

SPME1 668

The peak in shards at 668 cm just prior to the LOI downturn marked (a) in Figure 7.3 yielded a bi-modal chemical composition, with both populations being classified as a sub-alkali rhyolites with high potassium values (Figure 7.5). Population A (n= 18) in this instance can be correlated to the Katla volcanic system, whereas population B (n=2) shows affinity to Borrobol-type tephras (Figure 7.9). As discussed above, it is believed that there are at least two Katla derived eruptions through the Loch Lomond Stadial. The position of this horizon within organic gytjas correlates well with the stratigraphic position of the Abernethy Tephra reported elsewhere in Scotland and NW Europe (MacLeod et al. 205). But as before, the presence of such a highly concentrated Vedde Ash horizon 13 cm below this interval places a considerable limit on the robustness of any such correlation, especially as there is a continuous profile of tephra between the respective horizons. Whilst an argument could be made that the peak at 668 cm stands in contrast to what could be classified as ‘background’ tephra at the site, the presence of the LOI downturn signifies that organic sedimentation was decreasing, and likely that clastic sedimentation was increasing in this interval. It is possible therefore, that the apparent ‘peak’ in the tephra signal may be a product of increased minerogenic recycling within the catchment. As such, no firm correlations to the Abernethy Tephra can be made.

SPME1 661

The horizon at 661 cm has returned a tri-modal population. All three populations can be classified as sub-alkali rhyolites exhibiting high potassium values (Figure 7.5). Population A (n=4) can be correlated to the Katla volcanic system, and population C (n=2) correlates with the Borrobol-type group of tephras (Figure 7.10). As discussed in the previous two intervals, the continued occurrence of shard types exhibiting these same two chemical signatures limits the establishment of a reliable and robust isochron. The presence of Katla-type shards may have come from the Vedde Ash

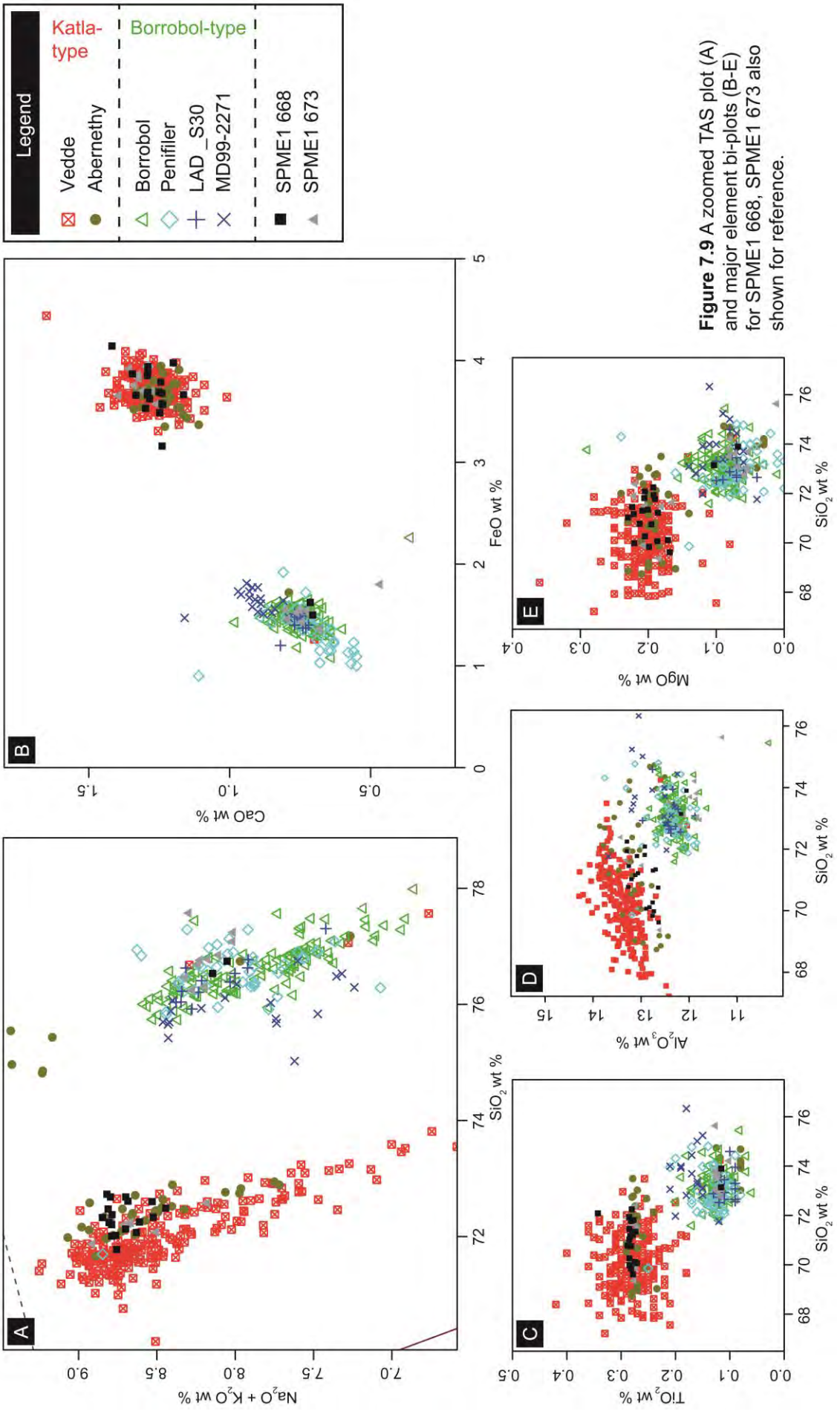

Figure 7.9 A zoomed TAS plot (A) and major element bi-plots (B-E) for SPME1 668, SPME1 673 also shown for reference.

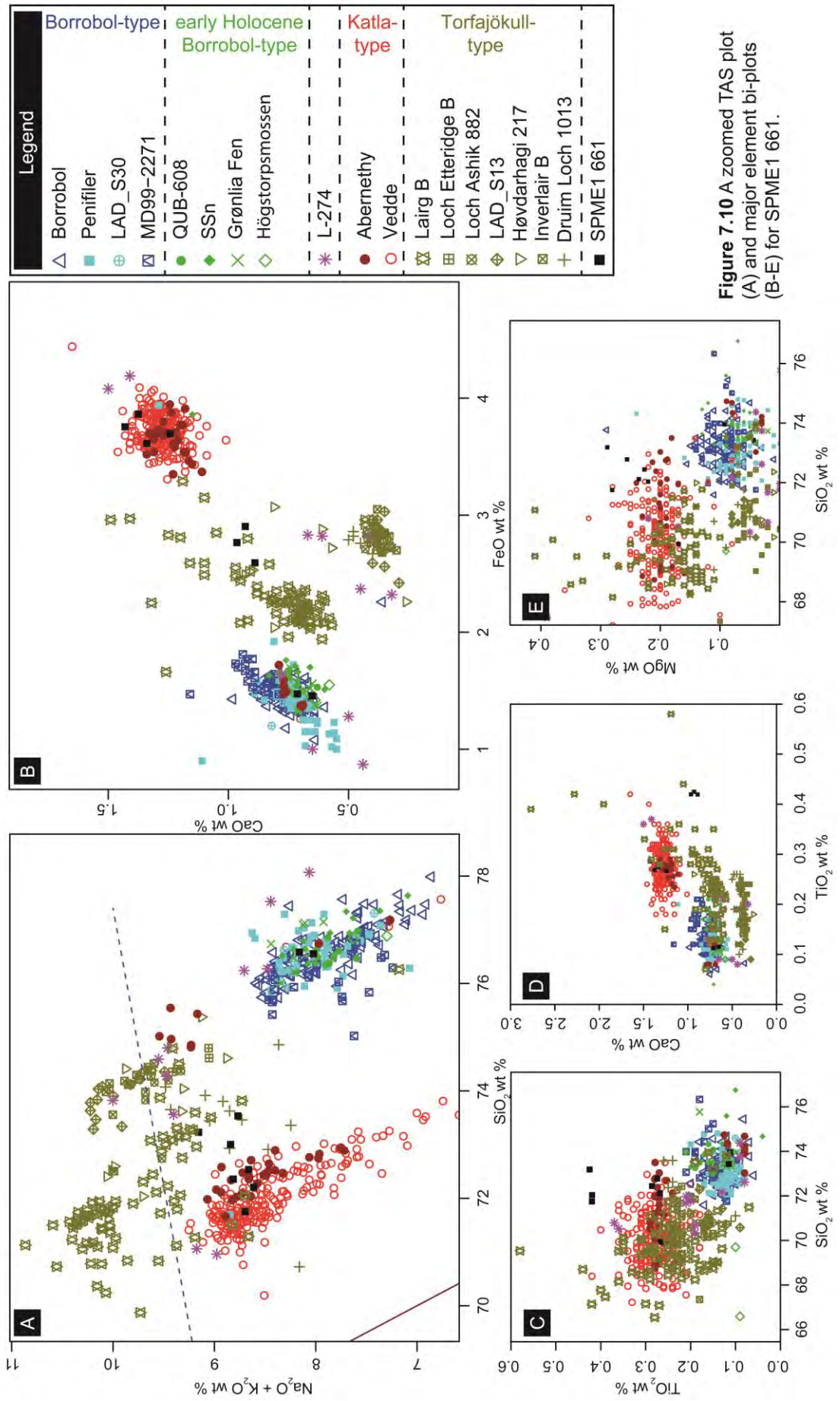

Figure 7.10 A zoomed TAS plot (A) and major element bi-plots (B-E) for SPME1 661.

horizon, or potentially the Abernethy Tephra horizon if indeed SPME1 668 is representative of this isochron. The Borrobol-type shards may have reworked from deeper within the Stadial stratigraphy, or potentially from one of the several early Holocene Borrobol-type eruptions which typify this period (e.g. Lind et al. 2013; 2016). Such candidates are the Fosen tephra (ca. 10,200 cal BP; Lind et al. 2013); the Högstorpsmossen (10,556-9931 cal BP; Björck and Wastegård 1999); population 3 of the QUB-608 (ca. 9500 cal BP; Pilcher et al. 2005); and the SSn (9400-9500 cal BP; Boygle 1999). It has been hypothesised by Lind et al. (2013) and later by Lind et al. (2016) that the four layers may represent the same event, but insufficient age control has prevented a more reliable conclusion from being drawn.

Population B (n=3) shows some affinity to the Torfajökull volcanic system, Iceland, although not in all elements (Figure 7.10). TiO_2 values in particular do not correlate well with tephras which have previously been ascribed to the system (Figure 7.10 C). The mid-Holocene Lairg B Tephra is also plotted in Figure 7.10 to supplement the limited range of analyses that stem from the three LGIT aged Torfajökull eruptions (see below); although it is not considered a potential candidate. Even with this additional data, population B cannot be confidently ascribed to Torfajökull. Pollard et al. (2003) illustrated that tephra derived from Torfajökull is amongst the least chemically stable of ashes typically found in the North Atlantic periphery. It is possible therefore that this component of SPME1 661 has been down-worked and chemically altered from the highly concentrated horizon at SPME 649, but without further evidence must be considered an outlier.

SPME1 649 and 645

The homogenous chemistry of these two peaks can be classified as a sub-alkali/ alkali rhyolite exhibiting high potassium values (Figure 7.5). The single population exhibits a chemical composition akin to tephras which have previously been ascribed to the Torfajökull volcanic system (Figure 7.11). Three eruptions from this centre are thought to have deposited tephra in NW Europe during the LGIT; these are the rhyolitic component of the Ashik Tephra, the An Druim Tephra and the Høvdarhagi Tephra (Pyne-O'Donnell 2007; Ranner et al. 2005; Lind and Wastegård 2011). The Ashik Tephra dates to 10,250-10,550 cal BP and is described as occurring just after an LOI oscillation, which most likely represents the PBO at Loch Ashik, Druim Loch and Loch an t'Suidhe (Pyne-O'Donnell 2005; Pyne-O'Donnell 2007). The An Druim Tephra and the Høvdarhagi Tephra occur later in the Holocene and possess a similar age of 9671-9490 cal BP and 9850-9600 cal BP respectively. Whilst this difference in age can be used to separate the Ashik with that of the An Druim Tephra and the Høvdarhagi

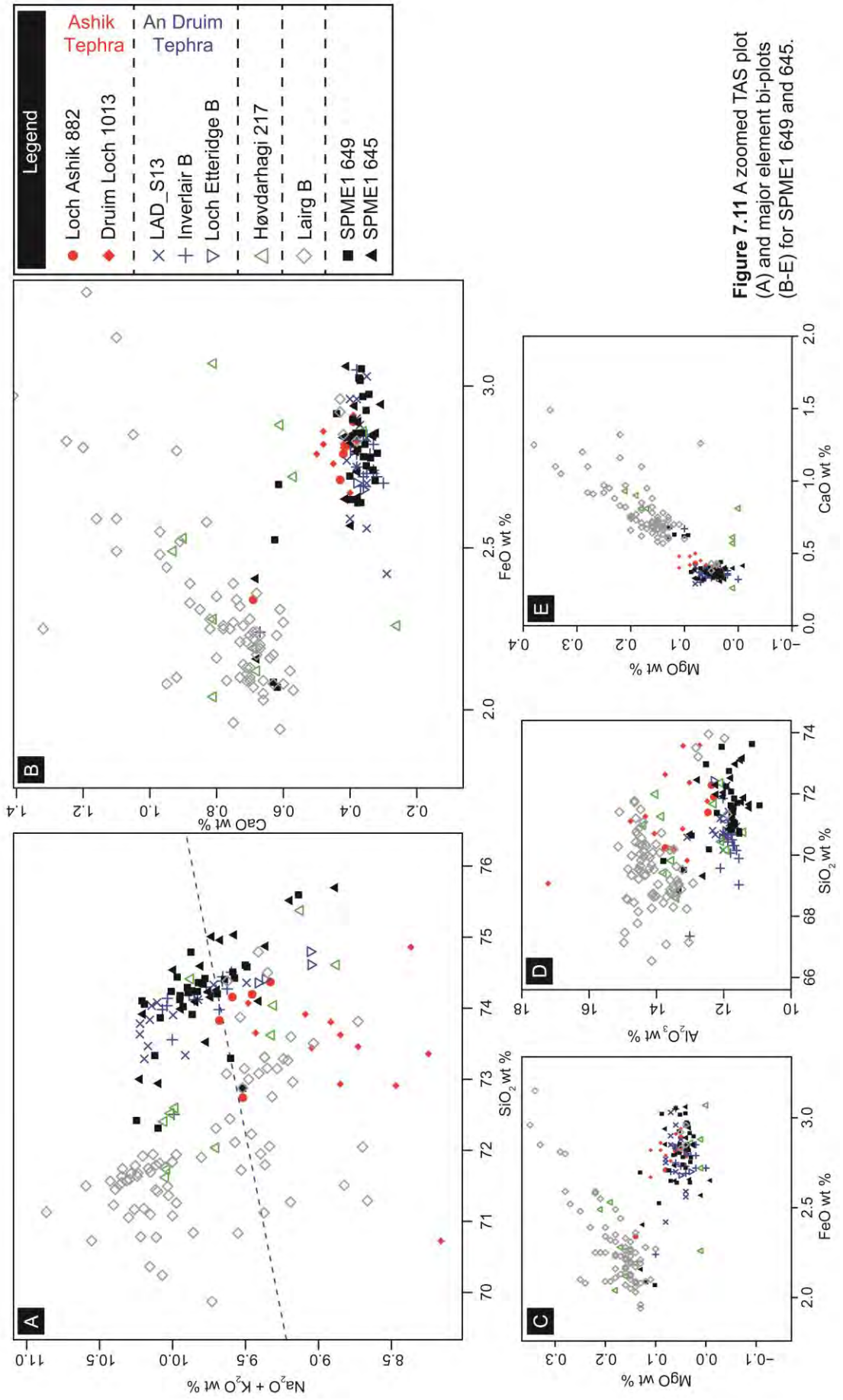

Figure 7.11 A zoomed TAS plot (A) and major element bi-plots (B-E) for SPME1 649 and 645.

from Iceland, and bordering on a 'super-eruption' classification. Evidence from lake Hvítárvatn in Iceland, and from marine sites on the Greenland Shelf, have revealed that Tephra, the Ashik Tephra also possesses a basaltic component which is absent from the latter two tephras (Pyne-O'Donnell 2007). Furthermore it has been established by Kelly et al. (2016) that a distinction can also be drawn between these tephra based upon the biostratigraphic position of the *Corylus* rise in Scottish sequences. At several sites it has been shown that the *Corylus* rise occurs after the deposition of the Ashik, but before the occurrence of the An Druim/ Høvdarhagi horizons (Kelly et al. 2016).

However, in this instance such biostratigraphic indicators are absent, thus the superposition of tephras identified above this horizon must be used to guide interpretation; these are described below, and a final interpretation of this part of the Spretta Meadow sequence is given at the end of the section.

SPME1 622

The horizon at 622 cm returned a tri-modal chemical population. Population A and B can be classified as sub-alkali rhyolites which exhibit high potassium values, whilst population C is classified as an alkali rhyolite, also with a high potassium value (Figure 7.5). Population A (n=5) can be correlated with tephras which have previously been ascribed to the Katla volcanic system, and in the early Holocene this would favour a correlation to the Suðuroy Tephra (8310-7868 cal BP; Wastegård 2002; Figure 7.12). Population B (n=2) shares a chemical signature with tephras which have previously been correlated to Snæfellsjökull, which in the LGIT are specifically the Hässeldalen Tephra (11,543-11,232 cal BP; Davies et al. 2003) and the Hovsdalur Tephra (10,695-10,285 cal BP; Wastegård 2002; Figure 7.12). Population C (n=2) correlates to the Torfajökull suite of tephras, which in the LGIT to reiterate are the Ashik Tephra (10,250-10,550 cal BP; Pyne-O'Donnell 2007), the An Druim Tephra (9671-9490 cal BP; Ranner et al. 2005) and the Høvdarhagi Tephra (9850-9600 cal BP Lind and Wastegård 2011; Figure 7.12).

The presence of these three differing chemical populations in SPME1 622 makes correlating the analyses to specific eruptions very difficult. The potential candidates as listed above all exhibit markedly different ages with no apparent overlap. This leads to the conclusion that the horizon, at least in part, is a product of reworking. The horizon sits on the downturn into the LOI oscillation marked (e) in Figure 7.3, which may signify an increased clastic contribution into the basin, and hence also signify a potential increase in sediment reworking from basin margins and from tephra bearing sediments

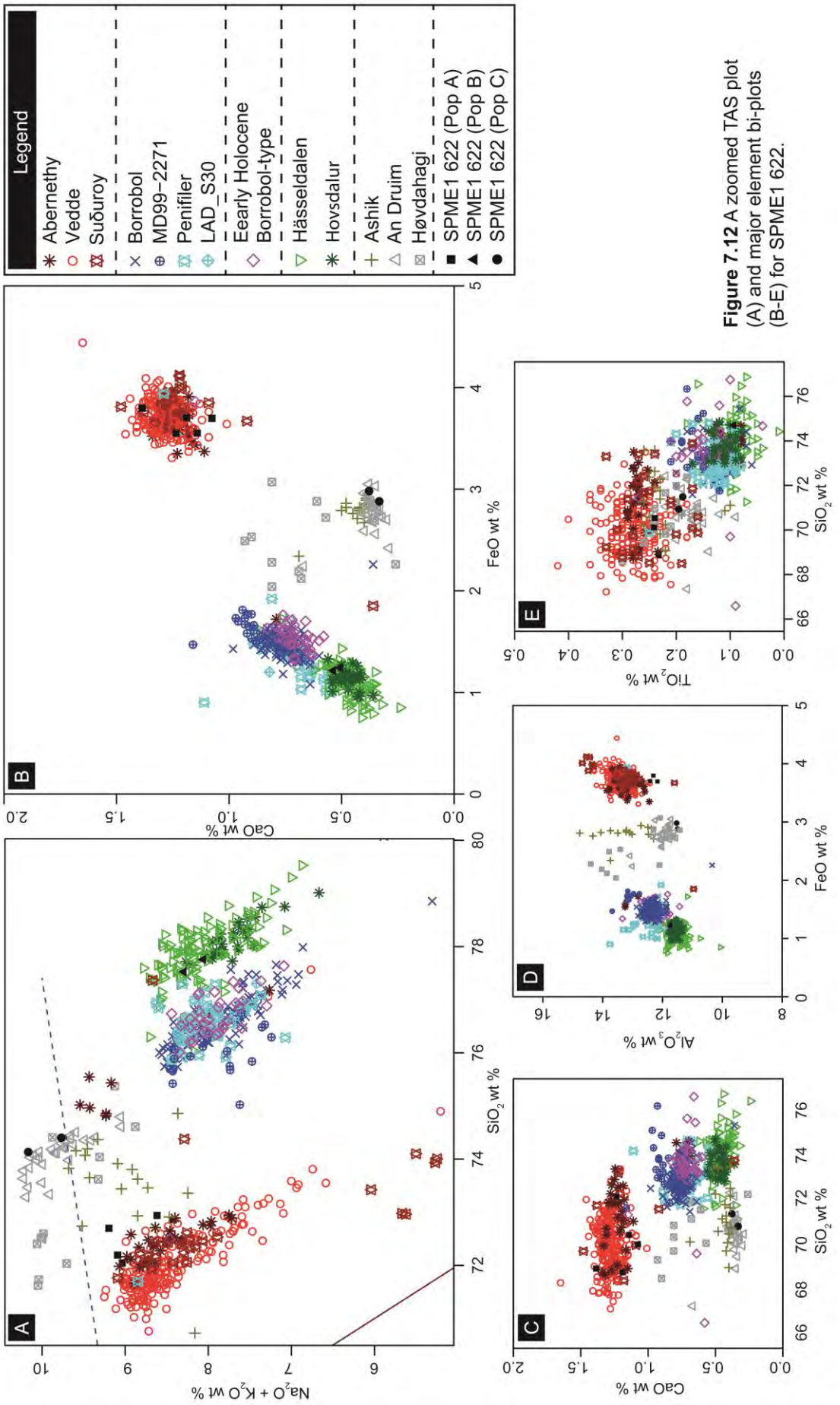

Figure 7.12 A zoomed TAS plot (A) and major element bi-plots (B-E) for SPME1 622.

higher in the catchment. It is important to note that whilst the appearance of Snæfellsjökull-type shards has not previously been described from the sequence, these shards may have been remobilised from one of the several unanalysed peaks or not detected in an analysed horizon due to the predominance of other shard types. This prospect of sediment recycling and remobilisation is supported by an almost contiguous profile of tephra extending from the base of the sequence to this horizon at 622 cm (Figure 7.3). Nevertheless, based on the available evidence it is suggested that the Snæfellsjökull-type tephra may represent a genuine isochron, exactly which is discussed at the end of the section.

SPME1 610

The uppermost horizon in the Spretta Meadow tephrostratigraphy returned a bi-modal population with population A (n=2) being classified as an alkali rhyolite with high potassium values, and population B (n=1) being classified as a sub-alkali rhyolite with high potassium values. The former possesses a chemical signature that is indicative of a Torfajökull derived tephra, whilst the latter single analyses can be correlated to Borrobol-type tephras (Figure 7.13). A conflation of tephras, for example the SSn (9450 ± 50 cal BP), QUB 608 (ca. 9500 cal BP) or Fosen (ca. 10,200) with the An Druim (9671-9490 cal BP) or Høvdarhagi (9850-9600 cal BP) may explain the chemical signature of this horizon. These tephra possess similar and in some instances overlapping ages, but as discussed above sediment recycling cannot be excluded, which is a factor that offers an equally plausible answer given the rest of the mixed tephra deposits at Spretta Meadow.e

SPME1 649/ 645, 622 and 610 interpretation

It is evident that the depositional regime characterising the Spretta Meadow basin during the early Holocene interval, has led to the development of a complicated and diffuse tephrostratigraphic record. Interpreting this sequence is particularly challenging, however, following the premise of superposition one clear and viable scenario emerges. Recent work at neighbouring Quoyloo Meadow, by Timms et al. (2016; Chapter 5.0) has identified the Snæfellsjökull derived Hovsdalur in the same 1 cm sample as the Torfajökull derived Ashik Tephra. This finding clearly illustrates a close stratigraphic relationship between these two tephras, and importantly no Snæfellsjökull derived horizon has been identified in close proximity to the An Druim or Høvdarhagi Tephras (Ranner et al. 2005; Lind and Wastegård 2011; Kelly et al. 2016; Timms et al. 2016; Chapter 5.0).

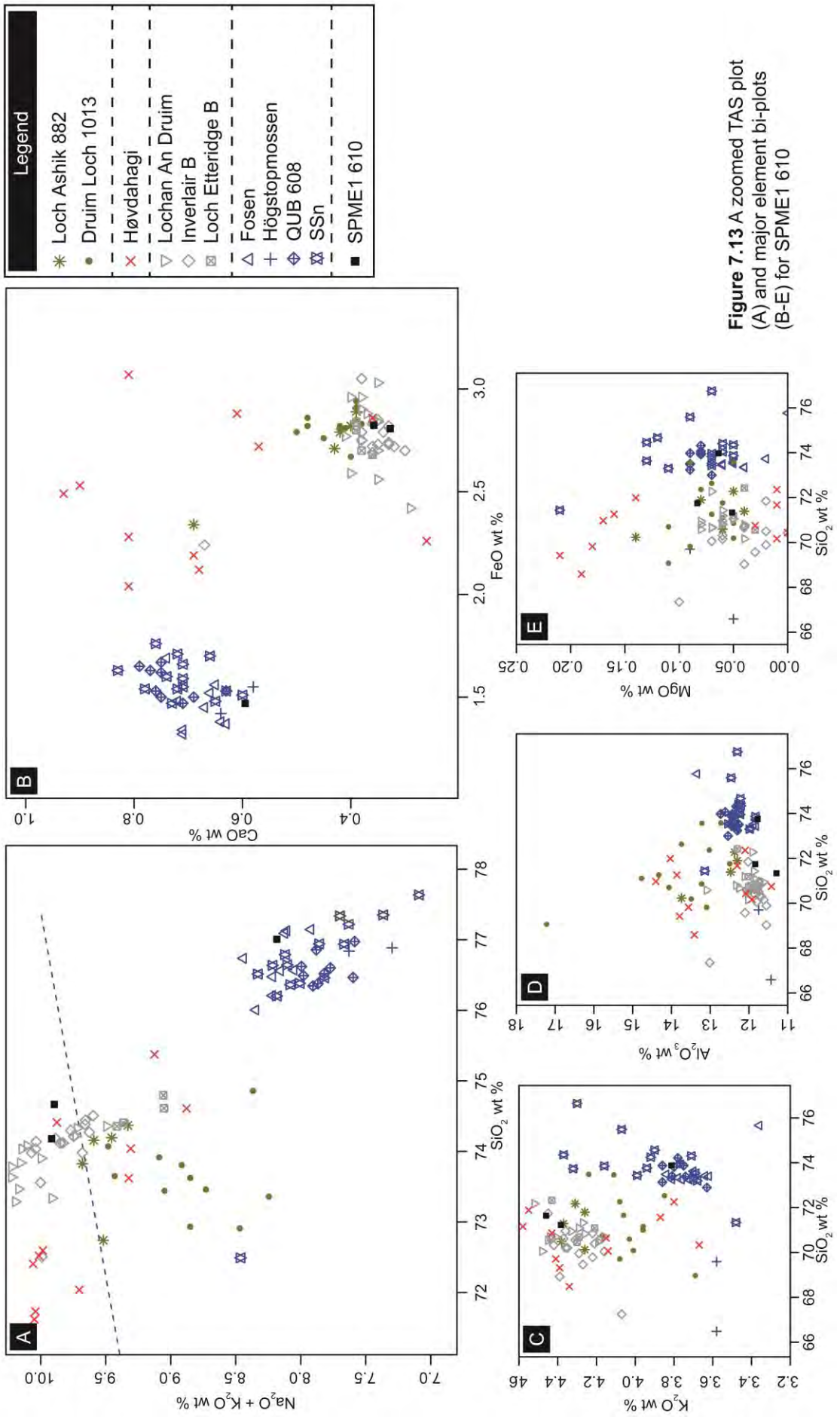

Figure 7.13 A zoomed TAS plot (A) and major element bi-plots (B-E) for SPME1 610

The interpretation of the Spretta Meadow sequence based on these findings therefore, is that the horizon characterised by SPME1 649/645 relates to the Ashik Tephra, whilst the horizon at SPME1 622 correlates to the Hovsdalur Tephra. The higher sedimentation rate in this instance allowing for a stratigraphic distinction between these two isochrons. If these correlations are correct, then the most likely correlation for the Borrobol-type shard identified in SPME1 610 is either the Fosen Tephra (ca. 10,200 cal BP; Lind et al. 2013), the Högstorpsmossen (ca. 10,200 cal BP; Björck and Wastegård, 1999), a component of L-274 (ca. 10,200 cal BP; Lind and Wastegård, 2011), population 3 of the QUB-608 (ca. 9500 cal BP; Pilcher et al. 2005) or the SSn (ca. 7300 cal BP; Boygle, 1999). Given that the age estimate of these tephras with the exception of the SSn are similar, and that all with the exception of the Fosen are poorly characterised, it is quite possible that they represent the same eruption (Lind et al. 2013). At present the Fosen tephra is the only horizon of those which has been traced to several sequences, and it is furthermore the only tephra which exhibits a viable and robust age estimate (Lind et al. 2013). Based on these factors, a correlation to the Fosen Tephra is therefore proposed for the SPME1 610 interval.

This interpretation, however, does not account for the Katla and Torfajökull-type tephras identified throughout the stratigraphic sequence at Spretta Meadow. It is likely, however, that due to the highly concentrated amounts of tephra characterising these intervals, an abundance of these shard types remained mobile within the catchment well after their primary deposition. Such an occurrence has probably been further exacerbated by the unconsolidated, highly organic gytja which has presumably allowed the free movement of shards through the stratigraphic column. With this in mind correlations, and isochron placement must be treated with caution, however, it certainly seems a viable explanation to account for the diffuse spread of shards and the masking of subsequent tephras with shards of these chemical types.

7.4 Chapter summary

- This chapter presents litho- and tephrostratigraphic data from Spretta Meadow, a basin from Orkney Mainland, Scotland. Litho- and tephrostratigraphic data would suggest that the site possess sediments spanning from the Loch Lomond Stadial to the present. Although the onset of stadial conditions i.e. the transition from the Windermere Interstadial is not identified. Contiguous high-resolution (1 cm) sampling through this interval has yielded an almost continuous distribution

of tephra. From this, ten horizons were selected for analysis, with the main findings summarised in Table 7.3.

Table 7.3 Summary of tephra horizons identified in the SPME1 composite sequence

Composite code	Unit	Stratigraphic Position	Correlation	Notes
SPME1 610	4d	early Holocene	Fosen Tephra	Mixed horizon of Torfajökull-type and Borrobol-type. Reworked material?
SPME1 622	4d	early Holocene	Hovsdalur Tephra	Mixed horizon, of Katla-type, Snæfellsjökull-type, and Torfajökull-type. Reworked material?
SPME1 645	4d	early Holocene	Ashik Tephra	
SPME1 649				
SPME1 661	4c	early Holocene	Uncertain	Mixed horizon, of Katla-type, Borrobol-type and potentially Torfajökull-type. Reworked material?
SPME 668	4b	early Holocene	Abernethy Tephra?	Further work necessary
SPME 673	4a	early Holocene	Uncertain	Mixed horizon of Abernethy Tephra or reworked Vedde and Borrobol-type material?
SPME 681	2/3a	Loch Lomond Stadial	Vedde Ash	
SPME 701	1a	Loch Lomond Stadial	Uncertain	Late Interstadial/ Loch Lomond Stadial Borrobol-type tephra or reworked Borrobol or Penifiler shards?

- The identification of a macrotephra relating to the Vedde Ash is only the second time this horizon has been detected as a visible layer in the British Isles. It is also only the third site in the British Isles to have yielded the basaltic population of the Vedde Ash, and the fifth site to host a visible macrotephra of LGIT age.

- The occurrence of an exclusively Borrobol-type tephra in Loch Lomond Stadial deposits adds further complexity to the LGIT aged tephrostratigraphic record in Scotland. Whether this tephra represents a genuine isochronous event is difficult to ascertain. However, at present it is suggested that a correlation to the CRUM1 597 Tephra can be made (Chapter 6.0). The occurrence of this tephra may help to explain the identification of Borrobol-type shards amongst analyses of the Vedde Ash and Abernethy Tephra at other sites in Scotland, thus suggesting that this tephra may have a greater extent than is currently recognised.

- Further evidence has been presented for the Hovsdalur and Fosen Tephra's within the Orkney Isles. In conjunction with the findings at Quoyloo Meadow, these results enable new tephrostratigraphic links to be made with early Holocene sequences in the Faroe Islands, Norway, and Denmark (Wastegård 2002; Lind et al 2011; Larsen 2013).

- Detailed chemical analyses through the early Holocene has yielded a tephrostratigraphic record dominated by the repeated occurrence of Katla-type, Borrobol-type and Torfajökull-type tephras. The repeating chemical signature of three shard types, suggests that taphonomic process may be more prevalent than previously supposed. These themes are discussed further in Chapter 10.

Chapter 8. Tanera Mòr Results

8.1 Introduction and chapter structure

Tanera Mòr 1 is a small isolation basin located on the island of Tanera Mòr in the Summer Isles archipelago. This island group is of regional significance due its position between the northerly most tephrostratigraphic study sites of Loch An Druim and Borrobol, and the more southerly Druim Loch and Loch Ashik basins on the Isle of Skye. The geological and glaciological history of this NW sector is summarised in Chapter 3.0, along with further details of the regional tephrostratigraphy, and a review of previous studies conducted on the basin. This chapter outlines the main lithostratigraphic and tephrostratigraphic findings of this study, and also provides an interpretation and geochemical correlation of the tephra series.

8.2 Results

Ten borehole locations were identified on a north-south transect across TM1 (Figure 8.1). At nine of these sites, cores were extracted using 1.0 m Russian samplers, and at a single location, samples were drilled using a stitz closed coring chamber (location 10; Figure 8.1). The deepest records were attained in the centre of the basin and are represented by TM1 BH5 and TM1 BH4 (Figure 8.1). However, sediments pertaining to the Windermere Interstadial are not particularly well resolved in these sequences, and a better representation of the full LGIT record is provided by cores from borehole 9. It was decided therefore that TM1 BH9A and TM1 BH9D would provide the primary material for tephra analysis in this study, whilst TM10B would be used to conduct a provisional plant macrofossil analysis of the site.

8.2.1 Basin sedimentology

Figure 8.1 illustrates the TM1 cores from the central deepest part of the basin, with climatic zones inferred from lithological changes. Detailed sedimentological descriptions along with the magnetic susceptibility measurements of each of the cores can be found in Appendix G. TM1 BH9A and TM1 BH9D were matched and aligned based on lithological, LOI and magnetic susceptibility changes to form a composite sediment stratigraphy (Figure 8.2). A detailed description of this core and proposed correlations to the sequence of Roberts (1997) is presented in Appendix G.

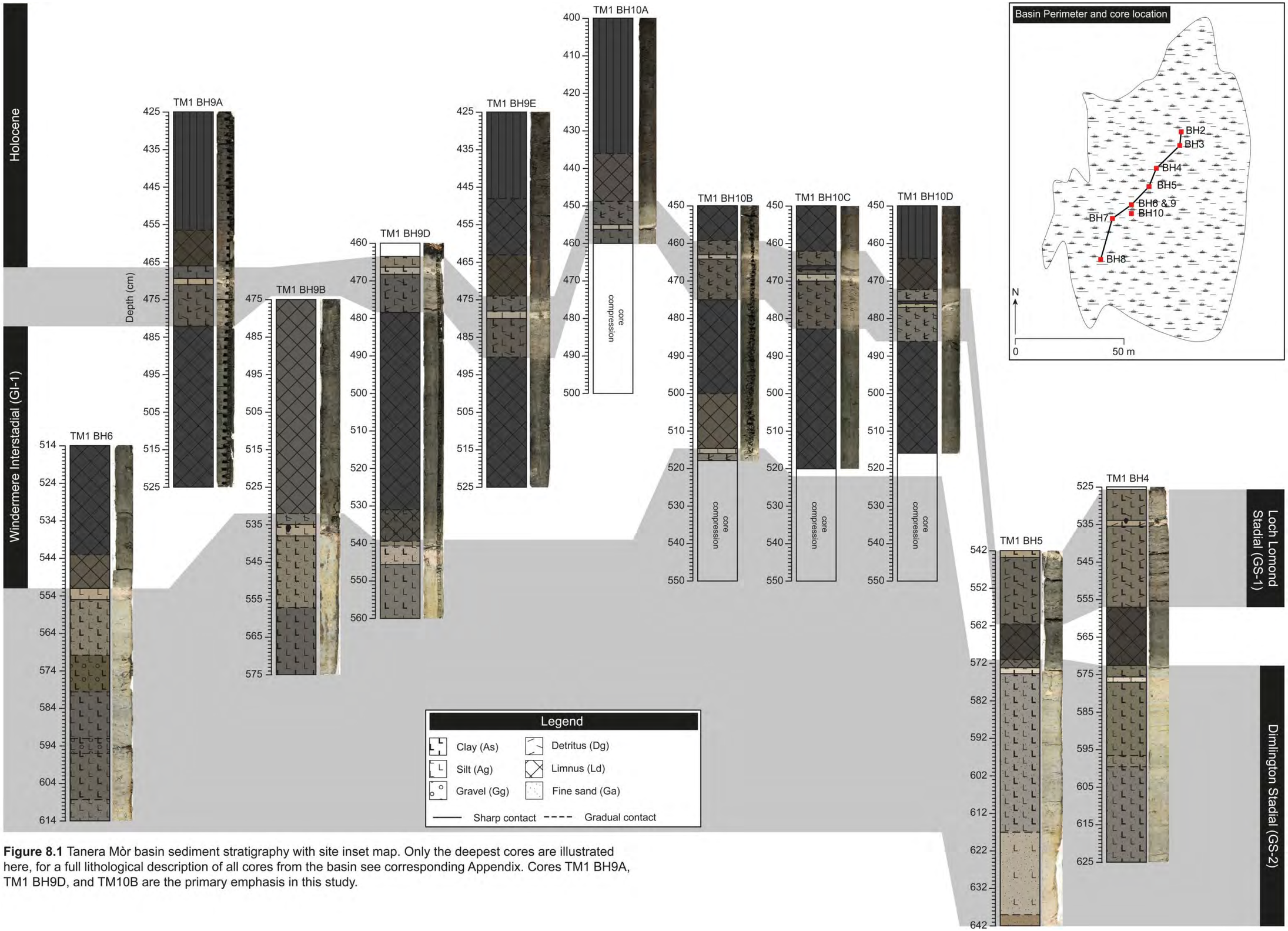

Figure 8.1 Tanera Mòr basin sediment stratigraphy with site inset map. Only the deepest cores are illustrated here, for a full lithological description of all cores from the basin see corresponding Appendix. Cores TM1 BH9A, TM1 BH9D, and TM10B are the primary emphasis in this study.

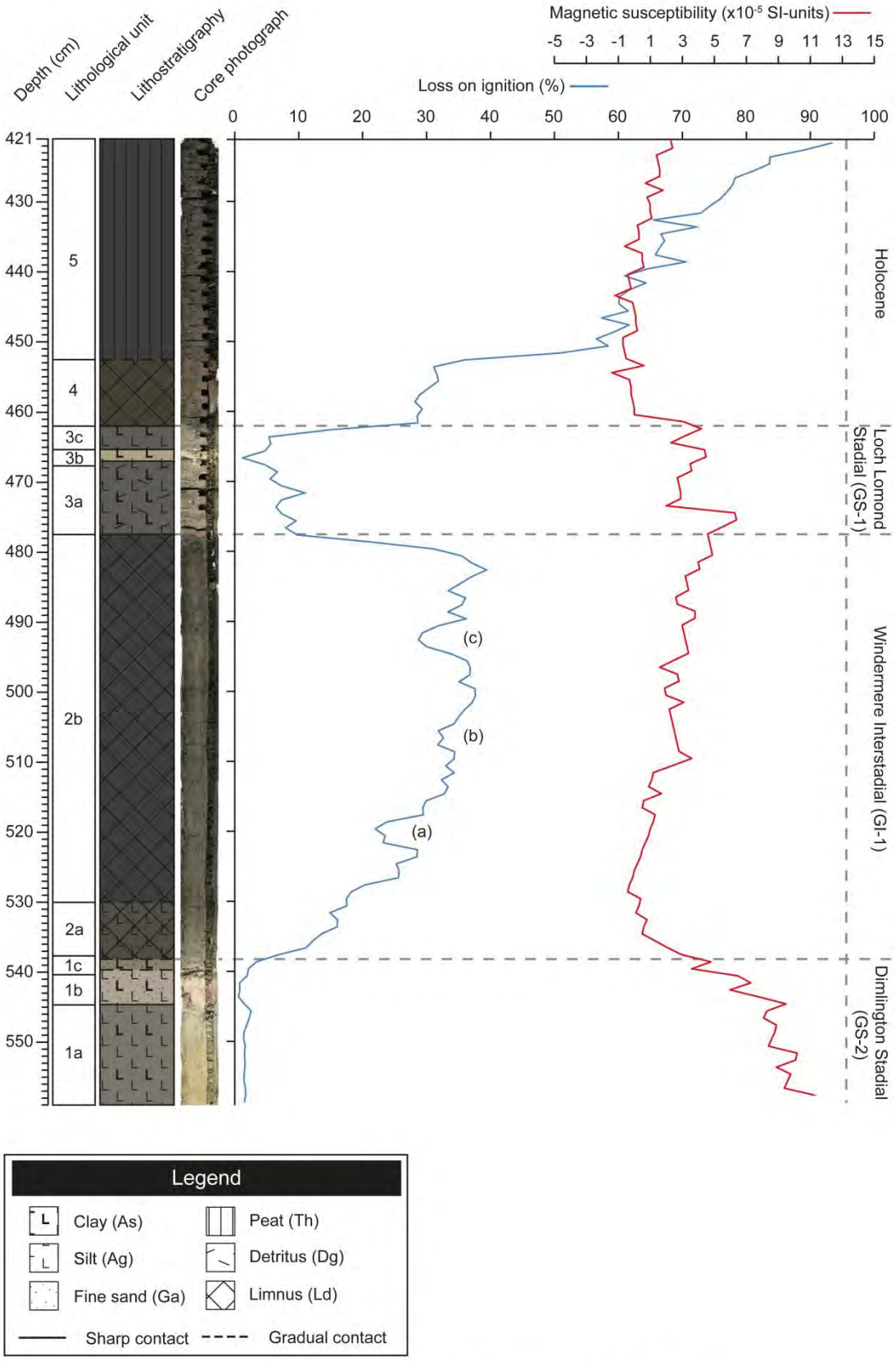

Figure 8.2 Composite stratigraphy derived from TM1 BH9A and TM1 BH9D.

The basin is indicative of a traditional Scottish LGIT sequence (Lowe and Walker 2015). At the base of the sequence, Dimlington Stadial aged clastic sediments grade into organic gyttja of the Windermere Interstadial. Within this unit, organic content progressively rises, but is punctuated by three distinct oscillations as inferred from the LOI signal; these are centred on (a) 519, (b) 506, and (c) 492 cm. The Windermere Interstadial organics are capped by Loch Lomond Stadial silts and clays, which contain detrital moss bands. This unit is subsequently overlain by organic gyttja of the early Holocene, which is superceded by a detrital peat deposit as the basin progressively becomes terrestrialised.

8.2.2 Tephrostratigraphy

TM1 BH9A and TM1 BH9D were processed for tephra at contiguous 1 cm intervals, (see section 4.5). Raw count data can be found in Appendix G. A composite tephrostratigraphy is presented in Figure 8.3. Sixteen horizons were chemically analysed across TM1 BH9A and TM1 BH9D, with an overlapping analysis between the two cores occurring at TM1 BH9A 520 cm and TM1 BH9D 516 cm. These depths relates to a horizon situated within sediments of the Windermere Interstadial, which occurs just after the suspected oscillation (a) in Figure 8.2. Table 8.1 provides a summary of horizons analysed, their climato-stratigraphic placing, and critically provides the corresponding depth for the tephra horizon in the composite lithostratigraphy. The composite depth for the tephra horizon is used in the following description.

In the following sections, population A is defined as the most numerous within the horizon, with subsequent horizons given letters denoting their lower prominence within the series i.e. population B, C etc. The chemical characteristics of tephra horizons and the populations within are based on non-normalised filtered data sets. Mean chemical data is presented in Table 8.2. For all chemical data see Appendix B, and for analytical conditions see section 4.8.1.

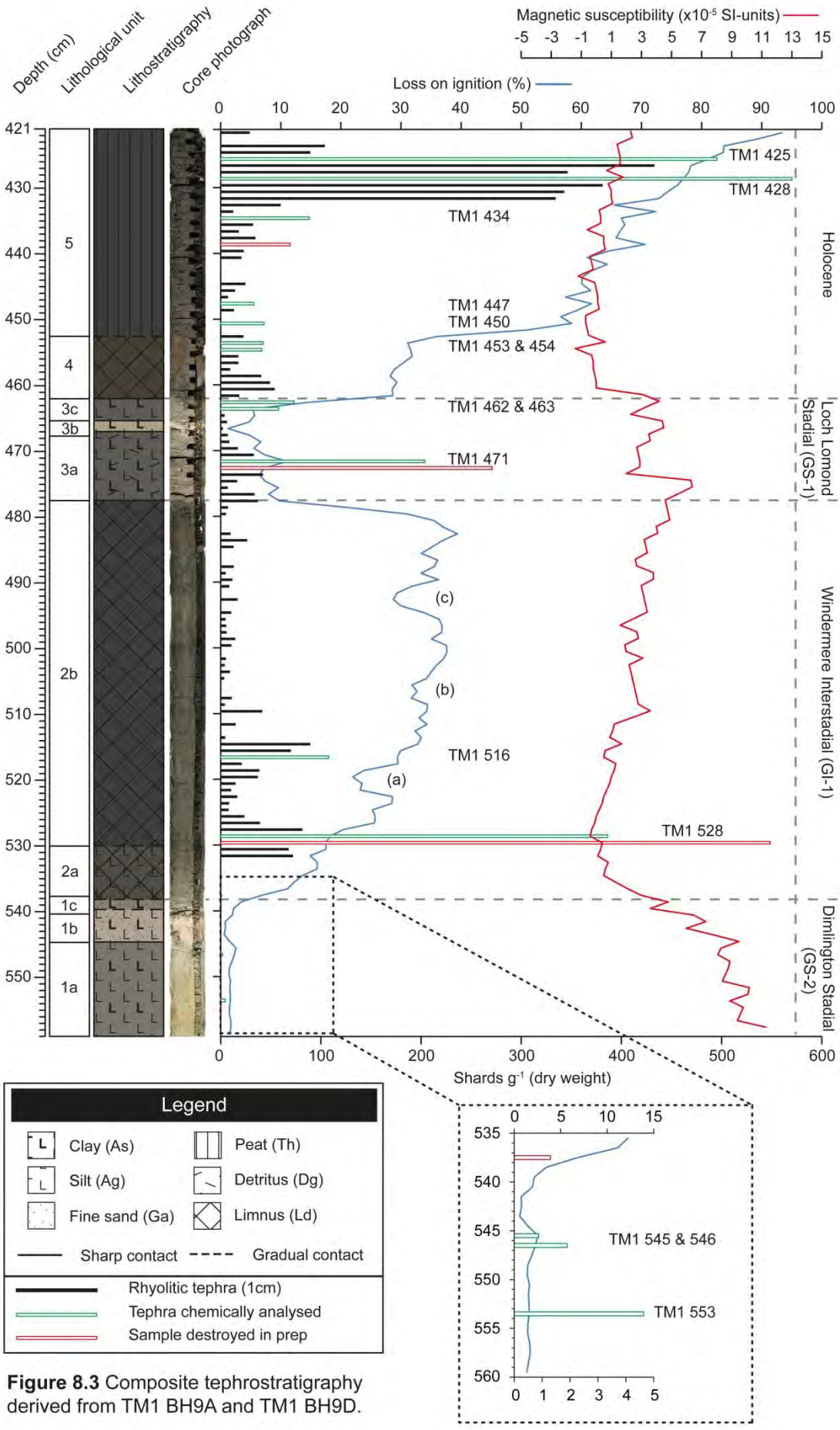

Figure 8.3 Composite tephrostratigraphy derived from TM1 BH9A and TM1 BH9D.

Table 8.1 Tephra samples from the two Tanera Mòr 1 cores, and their corresponding composite depth.

Core	Horizon (cm)	Stratigraphic position	Composite coding	Notes
TM1 BH9A	429	early Holocene	TM1 425	analysed
	432	early Holocene	TM1 428	analysed
	438	early Holocene	TM1 434	analysed
	442		-	sample destroyed in prep
	451	early Holocene	TM1 447	analysed
	454	early Holocene	TM1 450	analysed
	457	early Holocene	TM1 453	analysed
	458	early Holocene	TM1 454	analysed
	466	Loch Lomond Stadial	TM1 462	analysed
	467	Loch Lomond Stadial	TM1 463	analysed
	475	Loch Lomond Stadial	TM1 471	analysed
	476		-	sample destroyed in prep
	496		-	sample destroyed in prep
	499		-	sample destroyed in prep
	520	mid Windermere Interstadial	not part of composite, horizon considered the same as TM1 BH9D 516	analysed
TM1 BH9D	516	mid Windermere Interstadial	TM1 516	analysed
	528	early Windermere Interstadial	TM1 528	analysed
	529		-	sample destroyed in prep
	537		-	sample destroyed in prep
	545		-	sample destroyed in prep
	546	Dimlington Stadial	TM1 546	analysed
	553	Dimlington Stadial	TM1 553	analysed

Table 8.2 Mean geochemical data for TM1, values expressed as (%) weight oxide. Note: In relation to interval TM1 516 only the populations with the most secure correlations have been averaged, the remaining data is presented in its raw format.

Composite code	SiO_2	TiO_2	Al_2O_3	FeO	MnO	MgO	CaO	Na_2O	K_2O	Cl	P_2O_5	Total
TM1 425	71.45	0.19	11.71	2.81	0.04	0.07	0.38	5.05	4.39		0.01	96.10
2 std dev (n=17)	1.24	0.01	0.86	0.42	0.04	0.01	0.15	0.20	0.17		0.01	1.10
TM1 428	70.96	0.19	11.92	2.76	0.06	0.07	0.43	5.11	4.42		0.01	95.92
2 std dev (n=23)	1.68	0.01	1.28	0.48	0.08	0.01	0.21	0.25	0.17		0.01	1.36
TM1 434 (pop A)	71.43	0.19	12.09	2.72	0.06	0.07	0.41	5.04	4.50		0.01	96.53
2 std dev (n=4)	1.41	0.01	0.69	0.45	0.03	0.01	0.06	0.21	0.05		0.01	0.86
TM1 434 (pop B)	72.83	0.12	12.10	1.53	0.05	0.04	0.73	4.33	3.78		0.01	95.53
2 std dev (n=2)	1.18	0.05	0.88	0.21	0.02	0.01	0.24	0.10	0.09		0.01	0.22
TM1 434 (pop C)	75.00	0.05	11.98	0.94	0.04	0.05	0.52	3.54	5.22		0.00	97.33
TM1 434 (pop D)	72.07	0.12	12.39	3.89	0.85	0.07	2.47	4.48	3.04		0.01	99.39
TM1 447 (pop A)	69.82	0.27	12.87	3.71	0.20	0.14	1.28	5.19	3.55		0.03	97.05
2 std dev (n=4)	1.11	0.02	0.33	0.30	0.05	0.02	0.12	0.19	0.25		0.01	1.47
TM1 447 (pop B)	74.09	0.30	11.82	2.44	0.24	0.09	1.59	4.33	2.56		0.04	97.49
2 std dev (n=2)	1.76	0.00	0.76	0.22	0.03	0.02	0.06	0.12	0.34		0.00	3.10
TM1 450 (pop A)	74.60	0.30	11.96	2.55	0.25	0.09	1.65	4.31	2.59		0.03	98.33

2 std dev (n=9)	2.07	0.01	0.58	0.26	0.04	0.01	0.15	0.21	0.08		0.01	3.04
TM1 450 (pop B)	69.91	0.27	13.07	3.64	0.17	0.15	1.31	5.36	3.62		0.03	97.52
2 std dev (n=2)	3.01	0.02	0.78	0.46	0.04	0.01	0.06	0.23	0.14		0.02	4.65
TM1 453 (pop A)	73.57	0.30	11.72	2.53	0.24	0.09	1.62	4.24	2.47		0.03	96.81
2 std dev (n=11)	1.62	0.01	0.33	0.29	0.05	0.01	0.16	0.30	0.16		0.01	1.95
TM1 453 (pop B)	69.36	0.27	12.95	3.70	0.19	0.15	1.34	5.24	3.44		0.03	96.67
2 std dev (n=4)	2.17	0.01	0.73	0.25	0.06	0.02	0.19	0.14	0.30		0.01	3.28
TM1 454 (pop A)	72.96	0.30	11.55	2.54	0.23	0.09	1.60	4.34	2.51		0.03	96.15
2 std dev (n=22)	1.39	0.01	0.39	0.24	0.04	0.02	0.18	0.21	0.13		0.01	1.84
TM1 454 (pop B)	69.63	0.28	12.63	3.57	0.18	0.15	1.23	5.17	3.45		0.03	96.32
2 std dev (n=3)	0.87	0.03	0.41	0.27	0.09	0.01	0.13	0.54	0.21		0.01	2.32
TM1 462 (pop A)	70.09	0.27	13.03	3.68	0.14	0.20	1.28	5.25	3.56	0.17	0.04	97.71
2 std dev (n=18)	1.85	0.02	0.49	0.31	0.02	0.06	0.14	0.27	0.17	0.01	0.01	1.86
TM1 462 (pop B)	72.88	0.12	12.06	1.50	0.03	0.09	0.79	4.19	3.79	0.12	0.01	95.59
TM1 463 (pop A)	71.68	0.28	13.28	3.76	0.15	0.20	1.28	5.11	3.56	0.17	0.04	99.51
2 std dev (n=13)	1.52	0.01	0.42	0.15	0.01	0.05	0.12	0.34	0.22	0.01	0.01	1.83
TM1 463 (pop B)	73.55	0.13	12.24	1.36	0.04	0.07	0.76	4.06	3.77	0.12	0.01	96.11
2 std dev (n=3)	1.33	0.01	0.55	0.05	0.03	0.05	0.06	0.08	0.06	0.00	0.01	1.67

TM1 471	70.60	0.27	13.00	3.65	0.19	0.15	1.23	5.01	3.58		0.03	97.70
2 std dev (n=13)	2.87	0.02	0.81	0.35	0.05	0.02	0.21	0.37	0.20		0.01	4.03
TM1 516 (pop A)	73.81	0.11	12.07	1.29	0.04	0.05	0.66	4.13	3.88	0.13	0.01	96.13
2 std dev (n=24)	1.55	0.02	0.50	0.34	0.03	0.05	0.15	0.20	0.24	0.02	0.01	1.80
TM1 516 (pop B)	71.84	0.27	13.21	3.70	0.16	0.15	1.30	5.10	3.62	0.17	0.03	99.51
2 std dev (n=3)	0.87	0.04	0.43	0.11	0.06	0.06	0.01	0.43	0.10	0.01	0.01	1.11
TM1 516 (pop C1)	65.7707	0.0353	18.9784	2.7535	0.0797	0.2492	1.1712	6.4007	4.973	0.0252	-0.0021	100.4346
TM1 516 (pop C1)	67.0214	0.0008	18.5995	2.0572	0.0994	0.2286	1.8603	7.4642	2.8639	0.0917	0.0032	100.29
TM1 516 (pop C1)	65.694	-0.0019	18.7034	2.4444	0.1005	0.2789	2.0828	7.5155	2.8289	0.1056	-0.0008	99.7513
TM1 516 (pop C2)	67.9472	-0.0076	18.7061	0.2075	0.0114	-0.0004	0.9039	7.0749	4.7999	0.0202	0.0034	99.6666
TM1 516 (pop C2)	66.4342	-0.0558	19.0409	-0.0036	-0.001	0.0087	0.7483	6.8481	5.6696	0.0043	0.0016	98.6951
TM1 516 (pop D)	75.9882	0.0637	13.5129	0.9378	0.3005	0.0039	1.7928	5.3172	1.3023		0.0128	99.2321
TM1 516 (pop D)	75.8988	0.1686	13.799	1.0302	0.4143	0.0021	1.8596	5.3627	1.1689		0.0118	99.716
TM1 516 (pop E)	75.9661	0.3049	11.7479	2.1898	0.1996	0.0864	1.5787	4.1999	2.6064		0.0294	98.9091
TM1 516 (pop E)	74.0152	0.5525	12.1603	3.6969	0.9326	0.0462	1.6557	4.6485	2.4778		0.0667	100.2524
TM1 516 (pop F)	70.7792	0.2541	14.4927	2.9807	0.5149	0.1101	1.9419	4.9799	3.2097		0.0224	99.2856
TM1 516 (pop F)	70.407	0.1344	15.6742	2.1776	0.0551	0.1591	1.6468	5.8768	3.6278	0.0595	0.0057	99.8241
TM1 516 (pop G)	74.197	0.0215	11.4748	0.4607	0.0104	0.0322	0.6479	3.1554	4.9847	0.0092	0.0047	94.9988

TM1 516 (pop G)	75.5839	0.0134	12.4212	0.2237	0.0088	0.0156	0.0487	4.3411	4.937	0.0079	0.0005	97.6019
TM1 516 (pop H)	68.9557	0.0602	14.6063	1.2338	0.0651	0.0132	0.9625	4.72	4.4949		0.0439	95.1557
TM1 516 (pop I)	68.3326	-0.0075	15.3149	0.542	0.0594	0.0139	0.6499	5.7993	5.1144		0.0008	95.8197
TM1 516 (pop J)	72.0557	0.2034	13.9338	1.0223	0.1717	0.0289	0.1832	5.0048	3.2119		0.0059	95.8215
TM1 528	73.14	0.12	12.18	1.53	0.04	0.07	0.74	4.15	3.85	0.12	0.01	95.95
2 std dev (n=19)	1.37	0.01	0.47	0.24	0.01	0.03	0.10	0.19	0.15	0.01	0.01	1.59
TM1 545 (pop A)	72.77	0.14	12.68	1.66	0.03	0.10	0.83	3.99	3.75	0.12	0.02	96.09
2 std dev (n=2)	0.44	0.01	0.69	0.02	0.01	0.04	0.06	0.74	0.17	0.02	0.01	0.50
TM1 546 (pop B)	73.87	0.13	12.20	1.51	0.07	0.05	0.89	4.00	3.71		0.02	96.46
TM1 553 (pop A)	72.15	0.14	12.46	1.57	0.04	0.13	0.84	3.99	3.76	0.14	0.01	95.22
2 std dev (n=2)	0.03	0.00	1.12	0.07	0.01	0.05	0.16	0.54	0.06	0.02	0.01	0.79
TM1 553 (pop B)	68.21	0.26	12.99	3.67	0.14	0.15	1.23	5.29	3.46	0.18	0.03	95.61
2 std dev (n=2)	1.16	0.00	0.35	0.41	0.01	0.00	0.13	0.17	0.34	0.00	0.01	1.23

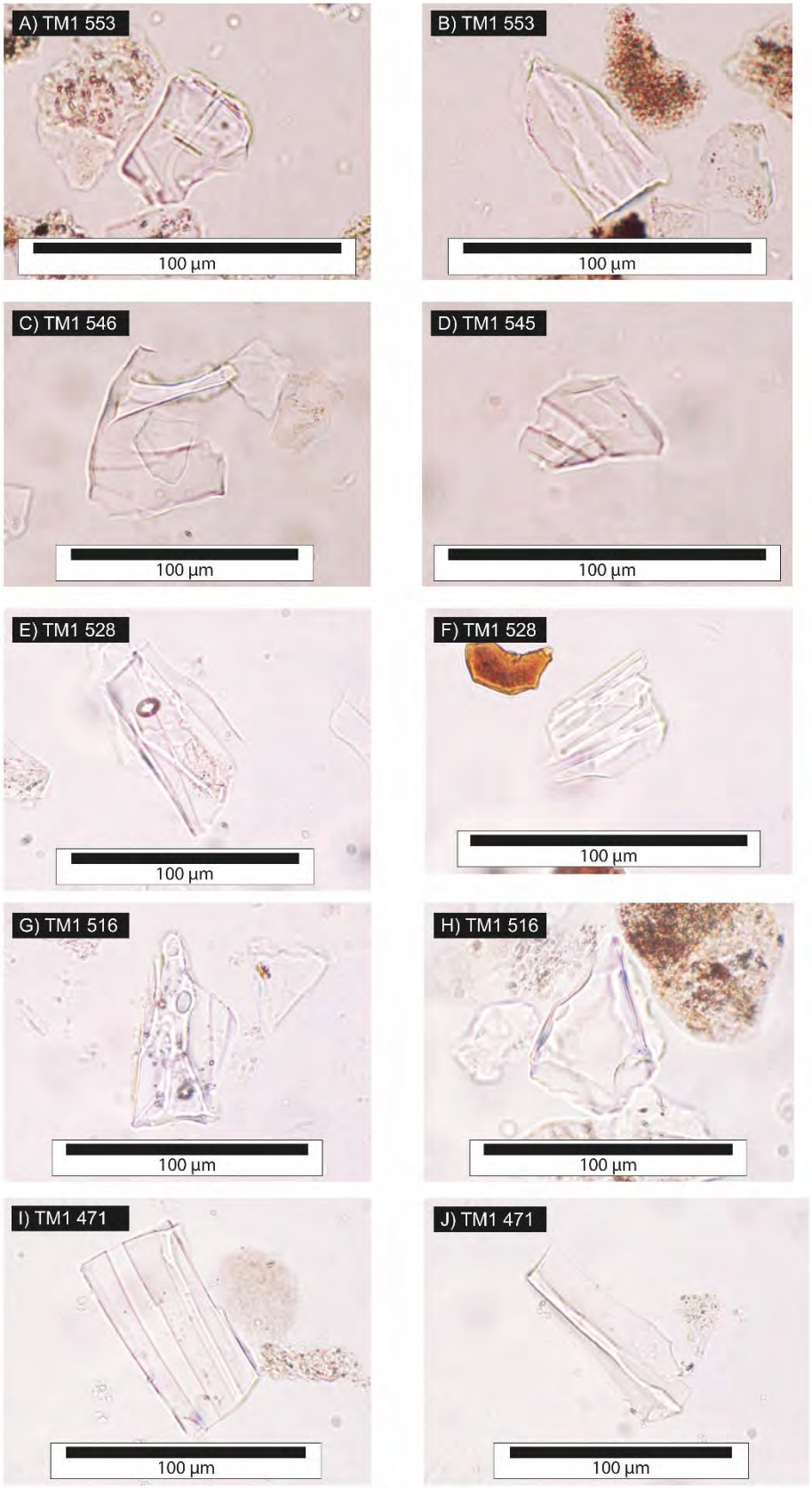

Figure 8.4 Photographs of horizons analysed from Tanera Mor 1. (A) A blocky shard with several pencil like mineral inclusions, evidence of surface pitting also present. (B) A elongate shard exhibiting signs of surface pitting and slight chemical alteration. (C) A large cuspate shard with a slightly degraded upper 'limb'. (D) A small blocky shard with some fluting. (E) An elongate shard exhibiting extensive surface alteration, and characterised by a closed vesicle and large flutes. (F) A shard possessing extensive fluting. (G) An elongate blocky shard with open and closed vesicles, fluting and extensive surface alteration features (surface pitting). (H) A blocky cuspate shard, with a degraded right flank. (I) A large rectangular fluted shard. (J) A large elongate shard with slightly cuspate features.

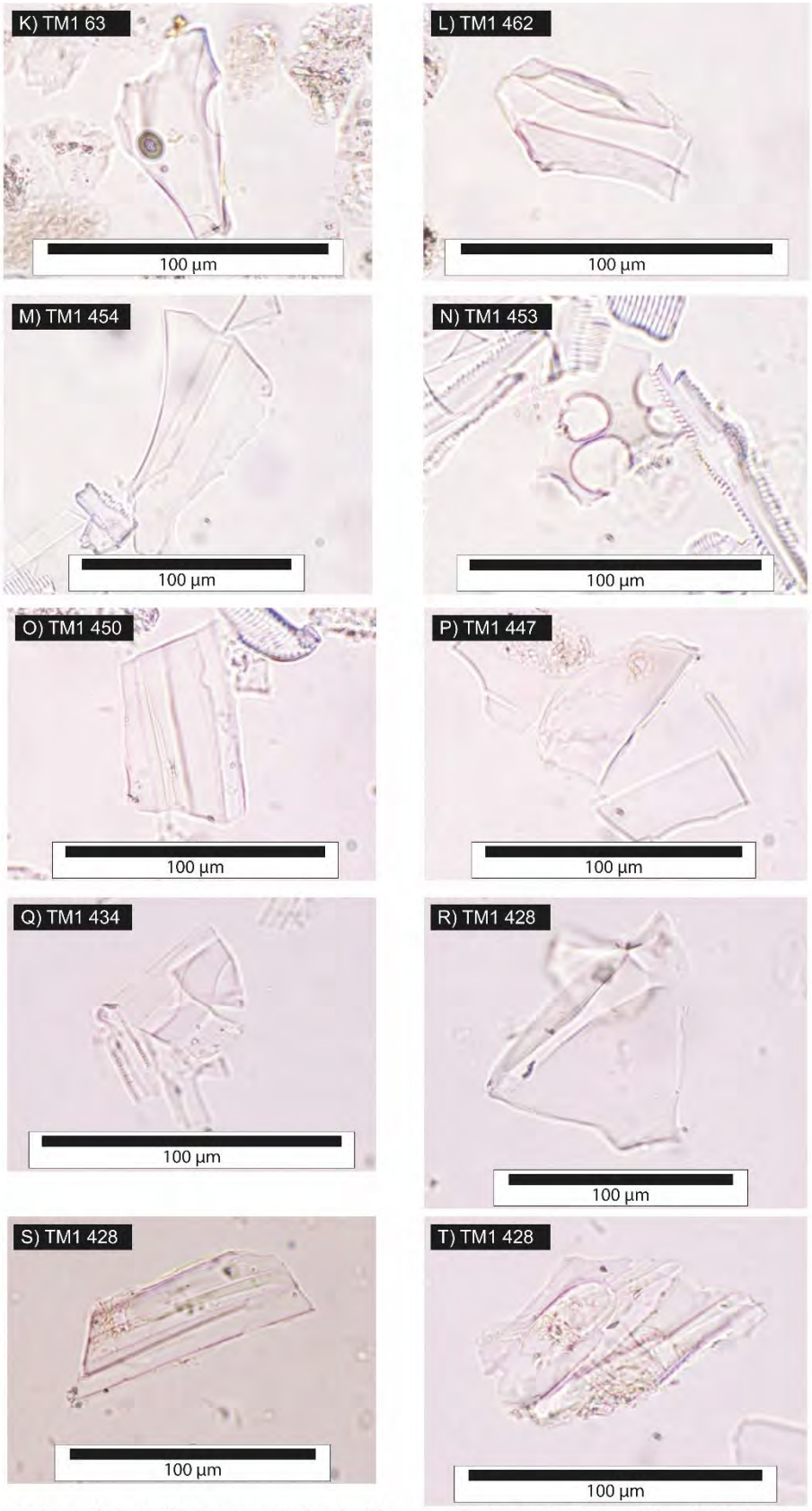

Figure 8.4 continued (K) A cuspate shard with a singular large closed vesicle. (L) A blocky shard with fluting and a slightly degraded upper edge. (M) A large elongated fluted shard, with cuspate features and a degraded right flank. (N) A small cuspate shard with numerous large open vesicles. Siliceous diatom fragments also present. (O) A rectangular fluted shard, with evidence of some surface pitting. (P) A blocky platey shard with a degraded upper side. Siliceous mimic material also present. (Q) A small feint and fluted shard. (R) A large blocky shard with a cuspate upper edge and signs of surface alteration. (S) A large rectangular fluted shard with some chemical alteration. (T) A large shard with large open vesicles, flutes and small irregular mineral inclusions. Extensive surface alteration is present along the lower edge.

TM1 553

The basal tephra of Tanera Mòr 1 is found within the silty-clay substrate of unit 1a, which relates to sediments to the late Dimlington Stadial. The horizon has a concentration of 5 shards g^{-1} restricted to a single cm within the stratigraphy. Shards exhibit a blocky and degraded morphology, with evidence of surface pitting (Figure 8.4 A, B). Four chemical analyses were obtained from three shards, one analysis using a 5 µm beam setup, and three using a 3µm beam setup (Hayward 2012). Two distinct populations were identified; population A, n=2 defined by low FeO (ca. 1.57 wt %) and CaO (0.84 wt %) values and population B , n=2 (1 shard) defined by relatively higher FeO (ca. 3.67 wt %) and CaO (ca.1.23 wt %) values (Table 8.2).

TM1 545 and TM1 546

A second horizon is also situated in unit 1a and was successfully analysed. The tephra is situated over two consecutive centimetres and concentrations of TM1 545 and TM1 546 reach 1 and 2 shards g^{-1} respectively. Shard morphology is defined by blocky cuspate forms, with some fluting also present (Figure 8.4 C,D). A single analyses from TM1 546 returned chemistries defined by low FeO (1.51 wt %) and CaO (0.88 wt %) values. Three analyses from two shards were obtained for TM1 545 which revealed two distinct populations; population A defined by low FeO (ca. 1.66 wt %) and CaO (ca. 0.83 wt %), and population B where the single shard was defined by relatively high FeO (3.74 wt %) and CaO (1.22 wt %) values (Table 8.2).

TM1 528

Between 531-513 cm, a continuous spread of shards spanning across two lithological units (2a and 2b), which represent Windermere Interstadial deposits, is observed. The 18 cm distribution is characterised by one discernible peak of 548 shards g^{-1} at a depth of 529 cm, and several minor peaks centred on 518, 516, and 514 cm (Figure 8.3). Shard morphologies through the entire suit are typified by blocky, cuspate forms with some instances of microlitic inclusions, as well as open and closed vesicles (Figure 8.4 E-H). Sample TM1 529 was lost during the sectioning stage, however, the consecutive sample TM1 528 was successfully analysed. A homogenous population n=18 was characterised with low FeO (ca. 1.53 %) and CaO (ca. 0.74 wt %) values (Table 8.2).

TM1 516

The analyses comprising the horizon TM1 516 are amalgamated from analyses of TM1 BH9D 516 and TM1 BH9A 520, which based on core lithology, LOI magnetic susceptibility values and shard distribution pattern are thought to represent the same event. Forty-three analyses were obtained for this interval which yielded several

differing chemical signatures. For ease of interpretation and discussion, only the populations with the most secure correlations have been averaged, the remaining data for TM1 516 is presented in Table 8.2.

The most numerate population identified (n=24) possess low FeO and CaO values (ca. 1.29 wt %) and (0.66 wt %). A second smaller, but chemically distinct group is also present; population B (n=3), which exhibits higher FeO and CaO values (ca. 3.70 wt % and 1.30 wt %). Population C1 is defined by at least three analyses, and are characterised by Intermediate SiO_2 totals (ca. 65-67 wt %), high Al_2O_3 values (ca. 18.7 wt %) and high Na_2O values (ca. 6.4-7.5 wt %). A further two analyses (C2) appear to exhibit similar trends in these elements SiO_2, Al_2O_3 and Na_2O + K_2O, however, FeO, MgO and CaO values appear to be much less than that exhibited by those characterising population C1 (Table 8.2). The remaining eleven analyses are presented in Table 8.2, which have been grouped in accordance to the similarity of their chemical signature.

TM1 471

Within organic-rich silty-clays of the Loch Lomond Stadial (unit 3a) a notable tephra peak was identified against a consistent background of shards which spans 27 cm and intersects three major units (Figure 8.3). The peak coincides with an organic band centred on 471 cm, which is thought to be a product of basin inwash. Shards are exclusively colourless and exhibit platy, fluted and cuspate morphologies (Figure 8.4 I, J). Concentrations reach a maximum of 271 shards g^{-1} at a depth of 472 cm, however, this sample was destroyed during chemical preparations. The consecutive sample, TM1 471 (204 shards g^{-1}) was successfully processed and returned homogenous analyses (n=12) defined by relatively high FeO (ca. 3.65 wt %) and Na_2O (ca. 5.01 wt %) values.

TM1 462 and TM1 463

At the top of unit 3c bordering the transition into unit 4 (early Holocene), two consecutive intervals, TM1 462 and TM1 463, were analysed. Both horizons are defined broadly by two types of shard morphology, one exhibiting platy, fluted and cuspate morphologies and a second appearing blockier, with occasional mineral inclusions as well as closed vesicles (Figure 8.4 K, L). The horizons reach concentrations of 73 and 58 shards g^{-1} in 462 and 463 respectively, and comprise the second and third largest peaks in the 27 cm long spread of tephra that defines this portion of the stratigraphy (Figure 8.3). Both horizons possess a bi-modal distribution. Population A (n=16) of TM1 462 is characterised by high FeO (ca. 3.68 wt %) and

Na_2O (ca. 5.25 wt %) values, whereas population B (n=1) has much lower FeO (1.50 wt %) and Na_2O (4.18 wt %) totals. TM1 463 exhibits a similar chemical division; population A (n=12) has relatively high FeO (ca. 3.76 wt %) and Na_2O (ca. 5.11 wt %) totals, with population B (n=3) being characterised by lower FeO (ca. 1.36 wt %) and Na_2O (ca. 4.06 wt %) values.

TM1 453 and TM1 454

Toward the end of the 27 cm long continuous tephra spread, and within early Holocene lacustrine muds (unit 4), two lesser consecutive peaks were analysed. Morphologies of the shards are mixed, with some exhibiting colourless cuspate and fluted forms, whilst others possess a more vesicular profile (Figure 8.4 M, N). Both intervals possess comparable totals of 43 shards g^{-1} for TM1 453 and 41 shards g^{-1} for TM1 454, with both also possessing bi-modal chemical distributions. Population A of TM1 453 (n=10) is characterised by relatively high SiO_2 values (ca. 73.57 wt %) and comparatively low Na_2O totals (ca. 4.24 wt %), whereas in population B (n=4) the comparative figures of SiO_2 (ca. 69.36 wt %) are lower, and Na_2O totals (ca. 5.24 wt %) are higher. TM1 454 exhibits a similar chemical division; Population A (n=21) exhibits higher SiO_2 values (ca. 72.96 wt %) and lower Na_2O totals (ca. 4.34 wt %) in comparison to population B which possesses SiO_2 totals of (ca. 69.63 wt %) and Na_2O totals (ca. 5.17 wt %).

TM1 450

Following the transition into unit 5 (early Holocene peats) the continuous tephra signal that characterised units 3 and 4 ceases. However, 1 cm above this termination a single isolated peak of shards is identified which attains a concentration of 43 shards g^{-1}. The morphology of shards defining the interval are predominantly platy and fluted (Figure 8.4 O), although smaller vesicular specimens also occur. The horizon exhibits a bi-modal distribution; Population A (n=8) is defined by relatively high SiO_2 values (ca. 74.60 wt %) and lower FeO totals (ca. 2.55 wt %) in comparison to that attained by population B (n=2), which possesses SiO_2 values of (ca. 69.91 wt %) and FeO totals of (ca. 3.64 wt %).

TM1 447

The second of five intervals to be chemically characterised from unit 5 occurs as a peak within a distribution of shards extending over 5 cm. The horizon is characterised by predominantly featureless platy shards (Figure 8.4 P), with concentrations reaching a value of 33 shards g^{-1}. The horizon is bi-modal in distribution, with population A (n=4) possessing relatively lower SIO_2 values (ca 69.82 wt %) and higher FeO values (ca.

3.71 wt %) than population B (n=2), which in contrast is defined by SiO_2 totals of (ca. 74.09 wt %) and FeO values in the order of (ca. 2.44 wt %).

TM1 434

Between 440-423 lies a continuous spread of tephra, and within this five peaks can be observed. A stub containing shards from the first peak at 438 cm was destroyed during preparations, however, a neighbouring peak 4 cm above, and reaching a concentration of 88 shards g^{-1}, was successfully analysed. TM1 434 is characterised by small feint shards with some exhibiting a fluted morphology (Figure 8.4 Q). The horizon is chemically variable, being composed of three to four populations, with the uncertainty deriving from similar chemical characteristics. Population A (n=4) possesses high Na_2O and K_2O values (ca. 5.04 wt % and 4.50 wt %). Population B (n=2) exhibits comparatively lower alkali values (ca. 4.33 wt % and 3.78 wt %) respectively, and also has relatively low FeO and CaO values (ca. 1.53 wt % and 0.73 wt %). Population C (n=1) is chemically similar to population B, but has lower FeO and CaO values (0.94 wt % and 0.51 wt %) and notably high K2O totals (5.22 wt %). Population D (n=1) exhibits high FeO and CaO values (3.8 wt % and 2.4 wt %).

TM1 428 and TM1 425

The two most prominent peaks within the diffuse 17 cm horizon characterising the 440-423 interval, are TM1 428 and TM1 425, which attain concentrations of 570 and 495 shards g^{-1} respectively. Both peaks are characterised by tephras that possess large fluted and vesicular morphologies (Figure 8.4 R-T). Chemically, both intervals have returned homogenous populations which are specifically defined by high Na_2O values (ca. 5.11 % and ca. 5.05 %) and low CaO totals (ca. 0.38 wt % and ca. 0.43 wt %) in TM1 428 and TM1 425 respectively. The total number of a analyses for each peak is 22 for TM1 428 and 16 for TM1 425.

8.3 Interpretation

8.3.1 Tephra correlations

In this section tephra correlations are proposed based upon current published data sets, with the local and wider significance of these correlations discussed in Chapters 10 and 11. Primary classification of the tephra layers is made via Total Alkali vs Silica diagrams (Figure 8.5 A), and by potassium value plots (Figure 8.5 B) as defined by Le, Bas (1986), and Pecorillo and Taylor (1976) respectively. Data sources for the tephra correlations are summarised in Appendix B

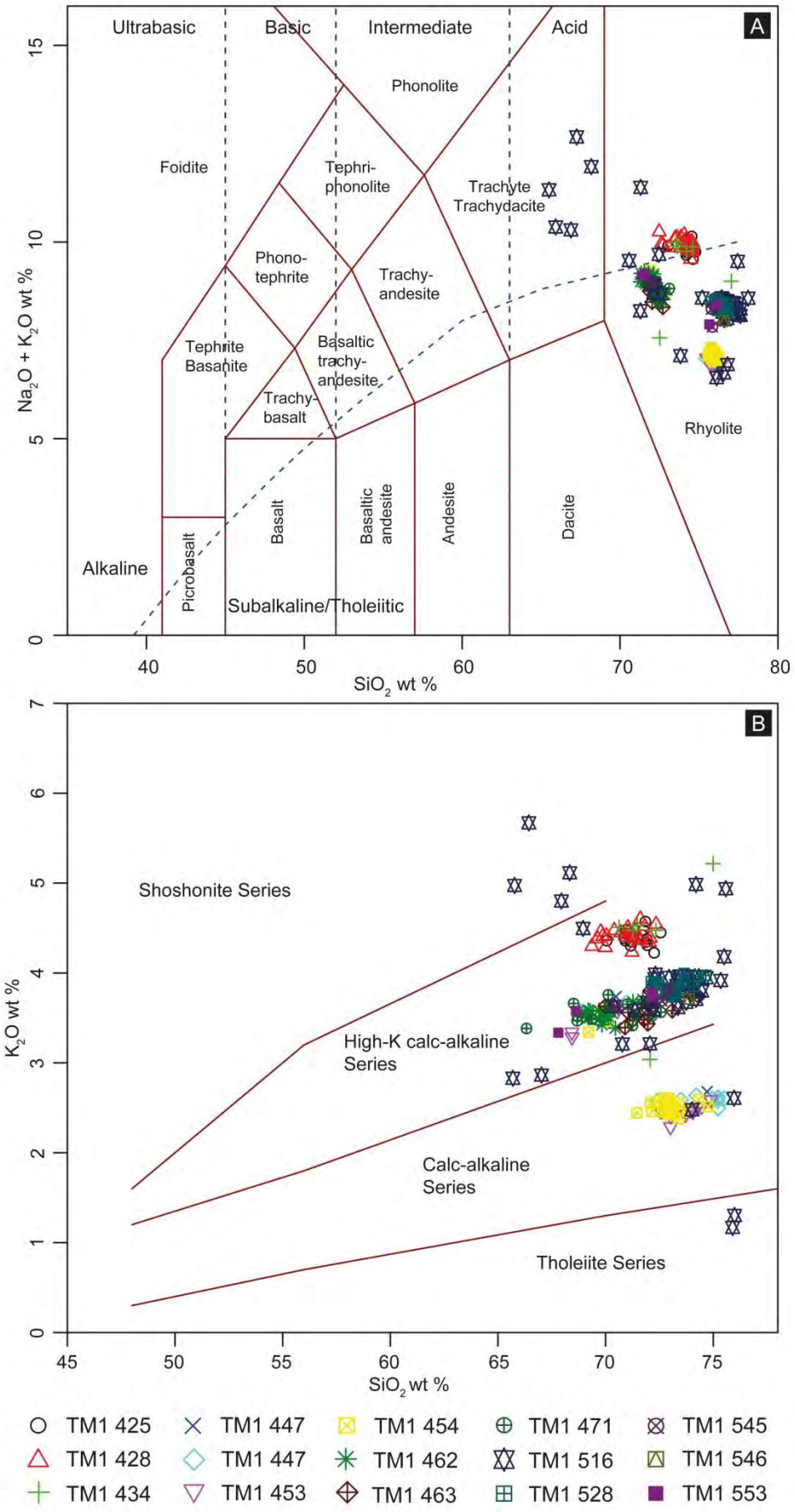

Figure 8.5 Chemical classification of tephra horizons from TM1. (A) Total Alkali vs Silica diagram (Le Bas 1986). (B) K-series plot (Pecorillo and Taylor 1976).

TM1 9 553

This interval within unit 1a yielded two populations derived from the analysis of three shards. Both populations can be classified as sub-alkali rhyolites with high potassium values (Figure 8.5). Population A (n=2) can be chemically correlated to a suit of tephras known as Borrobol-type (Figure 8.6), whereas population B (n=2, 1 shard) correlates to tephras which have previously been ascribed to the Katla volcanic system, Iceland (Lane et al. 2012b; Tomlinson et al. 2012a; Figure 8.6). Tephras classified as Borrobol-type, are chemically inseparable based on the available major, minor and trace elemental analyses (Lind et al. 2016). This is also evident for rhyolitic Katla-type tephras of the LGIT (Lane et al. 2012b; Tomlinson et al. 2012a). Additional chronological and stratigraphic information must therefore be considered when dealing with tephra deposits which possess these chemical signatures. The litho- and biostratigraphies from TM 1 place this tephra layer within Dimlington Stadial aged deposits. This is in agreement with the deglaciation model of Hughes et al. (2016), which suggests that Tanera Mòr became ice-free sometime between 15-16 kyrs, i.e. prior to Windermere Interstadial warming at ca. 14.7 kyrs (Brooks et al. 2012). The absence of a radiometric age from the lower organic sediments on Tanera Mòr prevents a minimum age from being calculated, and so several potential correlatives are suggested.

Three sites that are known in the North Atlantic region to have yielded Borrobol-type tephras of a Late Dimlington age, are the marine cores HM107-05, MD99-2271/MD99-2275, situated on the Icelandic shelf (Eiríksson et al. 2000; Gudmundsdóttir et al. 2011; 2012). The Borrobol-type tephras from these cores have been assigned ages of 16,650-16,490 cal. yrs BP and 15,400-14,850 cal. yrs BP respectively, making them both potential correlatives to TM1 553. However, in neither of the records were Katla-type shards reported alongside the Borrobol-type chemistries. Explaining the Katla-type shard within TM1 553 may lie with one of the two Dimlington Stadial tephras known to have originated from the Katla system through this interval. These are the Dimna Ash (15,400-14,850 cal. yrs BP), and the 10-1P 192 Tephra (ca. 14.7 kyrs), identified at Dimnamyra, Norway and within the North Atlantic marine core 10-1P respectively (Koren et al. 2008; Thornally et al. 2011). It should be noted that the age for the Dimna Ash is a minimum age, and the tephra is plausibly older (Koren et al. 2008). It is also possible that the 10-1P is older than stated, as it is possible this horizon is a product of ice rafting (Thornally et al. 2011).

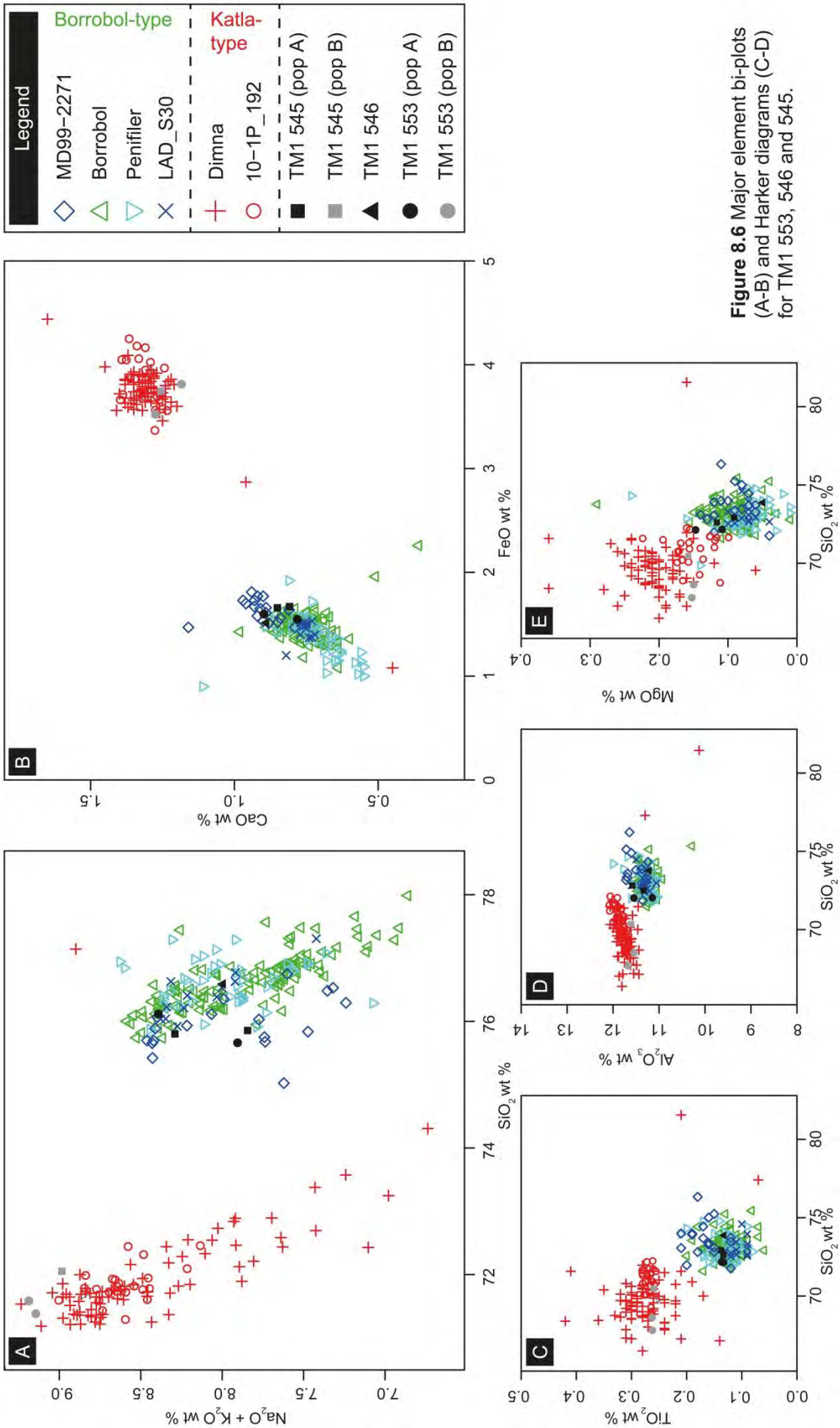

Figure 8.6 Major element bi-plots (A-B) and Harker diagrams (C-D) for TM1 553, 546 and 545.

Based on a number of uncertainties concerning the ages and superposition of the tephras, along with potential uncertainties concerning marine reservoir offsets, it is difficult to ascertain which, if any, of the aforementioned layers TM1 553 may correlate with. It is plausible that the horizon is an amalgam of eruptions either occurring concurrently, or deposited on the Late Devensian Ice Sheet, being subsequently washed into the basin as ice receded from the landscape. This problem of tephra taphonomy in newly deglaciated landscapes is discussed in the wider context of all Dimlington Stadial tephras identified in this thesis in section 10.3.3.1. It is also within this section that final correlatives shall be proposed.

TM1 545 and TM1 546

Two consecutive samples situated within unit 1a i.e. the Dimlington Stadial sediments, were analysed, and can be classified as sub-alkali rhyolites with high potassium values (Figure 8.6). TM1 546 (n=1) can be correlated to a Borrobol-type eruption, as can TM1 545 population A (n=2, shard); whereas population B (n=1) of TM1 545 is indicative of the Katla volcanic system. As with TM1 553, discerning the exact eruption or mechanism of deposition i.e. primary airfall or secondary inwash is particularly difficult in the context of the Dimlington Stadial sediments of the TM1 basin. In this regard only tentative correlations are made to the aforementioned eruptions. Taphonomic issues and stratigraphic discrimination concerning the Summer Isles region are discussed further in section 10.3.3.1.

TM1 528

A homogenous population classified as a sub-alkali rhyolite, and possessing high potassium values was extracted from this depth within unit 2b (Figure 8.7). The eighteen analyses plot entirely within the field of the Borrobol-type tephras and group most consistently with the recent analyses of the Borrobol and Penifiler Tephras by Lind et al. (2016) (Figure 8.7). This clustering of new data likely reflects improved analytical conditions for cryptotephras, which have been developed in recent years, and therefore postdate much of the existing comparative data (e.g. Hayward 2012). Stratigraphically, the tephra occurs on the rising limb of LOI values at the onset of the Windermere Interstadial, and marks the first major occurrence of a tephra within the TM1 sequence. This position within early Windermere deposits would suggest a probable correlation with the Borrobol Tephra, as it is from within such deposits that the Borrobol has been previously described in Scotland (e.g. Turney et al. 1997; Turney 1998a; Pyne-O'Donnell et al. 2008; Matthews et al. 2011; Lind et al. 2016). This correlation reproduces the analyses of Roberts (1997), who identified the Borrobol Tephra in association with an LOI upturn in TM2 97' (see section 3.5.1).

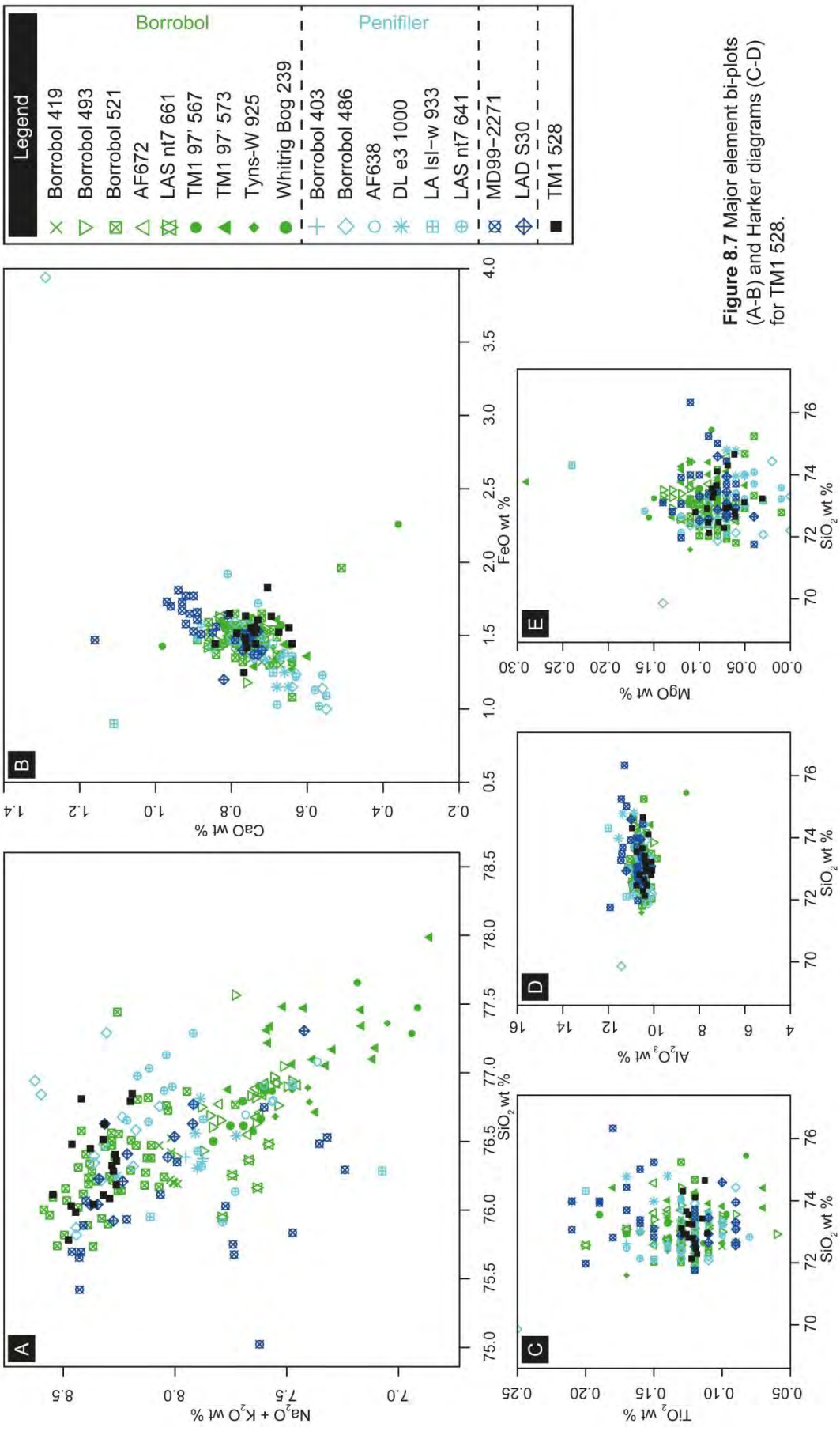

Figure 8.7 Major element bi-plots (A-B) and Harker diagrams (C-D) for TM1 528.

TM1 516

The shards identified in this interval exhibit highly varied chemical signatures, spread from sub-alkali rhyolites through to alkaline rhyolites and into the trachyte trachydacite field (Figure 8.5 A). Potassium values are also as equally spread, with values ranging from low to high.

The predominate group of shards identified within this interval can be classified as sub alkaline rhyolites with high potassium values. These analyses (n=24) correlate to the Borrobol-source (Figure 8.8). In the Windermere Interstadial, two tephras are known in Scottish sequences which exhibit such a chemical signature; the Borrobol Tephra and the Penifiler Tephra. There has been much debate concerning the origin, age and stratigraphic position of these tephras (e.g. Davies et al. 2004; Pyne-O'Donnell et al. 2008; Lind et al. 2016). But it is now widely recognised that the Borrobol Tephra can be placed within the Bølling interval/ GI-1e of the North Atlantic event stratigraphy, whilst the younger Penifiler Tephra occurs in close association with the Older Dryas/ GI-1d cold climate oscillation (Pyne-O'Donnell et al. 2008; Matthews et al. 2011). The interval at 516 cm occurs just after an oscillation in the LOI signal which is centred at 519 cm (Figure 8.3). It is plausible therefore that this downturn in organic production may represent GI-1d in the Tanera Mòr sequence, and hence the interval at 516 may relate to the Penifiler Tephra. It is important to note that in the original work conducted at Tanera Mòr, Roberts (1997) identified three groups of shards at the base of the sequence (Figure 3.16 G). Two of these peaks (BTM1 and 2) were analysed, and returned chemistries of a Borrobol-type affinity. At that time, only the Borrobol Tephra was known to exhibit this chemical signature in sequences dating to the Windermere Interstadial, and so a correlation of both peaks to the Borrobol was proposed. More recent work by Lind et al. (2016) has hypothesised that the secondary peak (i.e. BTM2), which occurs in close association with the LOI downturn, likely relates to the Penifiler Tephra. Whilst this is the preferred interpretation of the 516 cm horizon, the varied chemical signature indicates that other tephras might also be present.

One of these secondary series (population B, n=3) is classified as sub alkaline rhyolite with high potassium values, and can be correlated more specifically to the Katla volcanic system (Figure 8.8). Several Katla rhyolites with a 'Vedde-like' chemical signature have now been recognised in the LGIT period (e.g. Lane et al. 2012b); including the R1 tephra, which is dated to ca. 13.6 kyrs (Thornally et al.. 2011). No age errors are presented by Thornally et al. (2011) but it is conceivable that they would overlap substantially with that of the Penifiler Tephra which has an accepted age range of 14.09–13.65 cal. BP, although there is some uncertainty in this value (Matthews et

al. 2011; Bronk-Ramsey et al. 2015; Lind et al. 2016). It is also plausible that the Katla rhyolites may have been reworked from previous deposits i.e. the hypothesised Dimna Ash/ 10-1P horizons identified at TM1 553, 546, and 545. The climate conditions associated with the GI-1d would have been extremely harsh, and periglacial processes would have likely contributed to a reworking and remobilisation of sediments. These themes are discussed further in section 10.3.3.1.

The sixteen other analyses characterising TM1 516 are much more difficult to correlate robustly. Five of the analyses possess a very unusual chemical signature for NW European tephra records of an LGIT age as they plot with the trachyte trachydacite field, and exhibit high potassium values (Figure 8.5). Only one province local to Scotland is capable of producing tephras of this chemical composition; the Chaîne des Puys in the Massif Central, France. Notably, the Les Roches Tephra derived from this system has an age of 13,875 ± 175 cal. yrs BP (Vernet et al. 2000) which would therefore also place it within the age estimate of the Penifiler Tephra. However, caution must be exhibited with this correlation, due to the lack of published glass data from the Les Roches Tephra, the Chaîne des Puys, and the Massif Central in general. The correlation in this instance has been made using younger data relating to the Vasset-Killian Tephra, which is believed to have originated from the Chaîne des Puys, but at a much later date of 9525 ± 495 cal. yrs BP (Juvigne et al. 1996). The potential identification of French tephra in northern Scotland is unexpected; tephras derived from the Massif Central region have only been mapped in the most local and proximal settings (Figure 3.8), although there has been little emphasis to trace these to the distal environment. Whilst the finding here therefore holds much significance for the tephrostratigraphy of NW Europe, it is essential to establish whether these results can be replicated, and whether the interval at 516 cm represents the highest concentration of this chemical type.

The remaining eleven analyses of TM1 516 cannot be ascribed to any of the major volcanic systems in Iceland, nor do they correlate to either of the large Cascade eruptions characterising this interval in North America (Figure 8.8; Pyne-O'Donnell et al. 2016). Whilst similarities and tentative correlations can be made concerning some major element characteristics, inconsistencies across several fields prevent reliable correlation. This is most clearly exemplified in Figure 8.8 B. As such, eleven of these analyses remain uncorrelated at present.

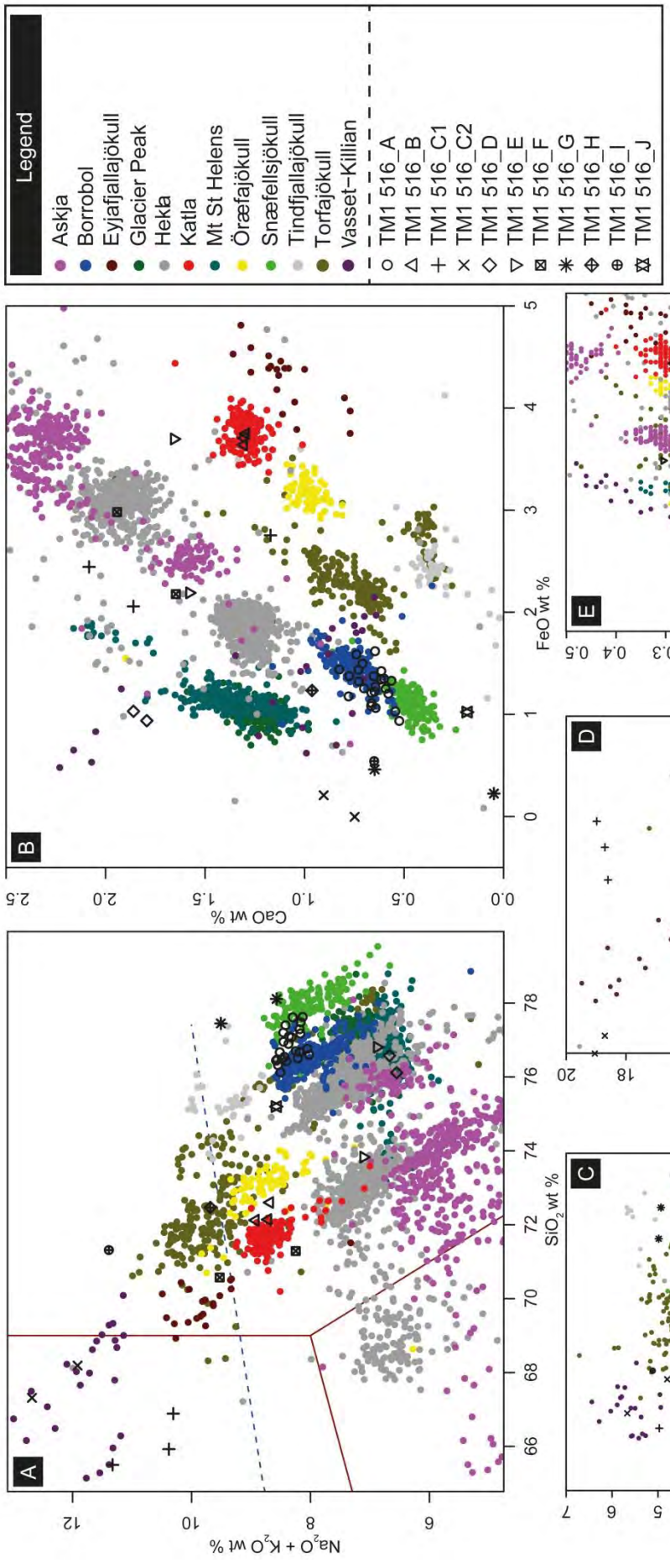

Figure 8.8 Major element bi-plots (A-E) for TM1 516.

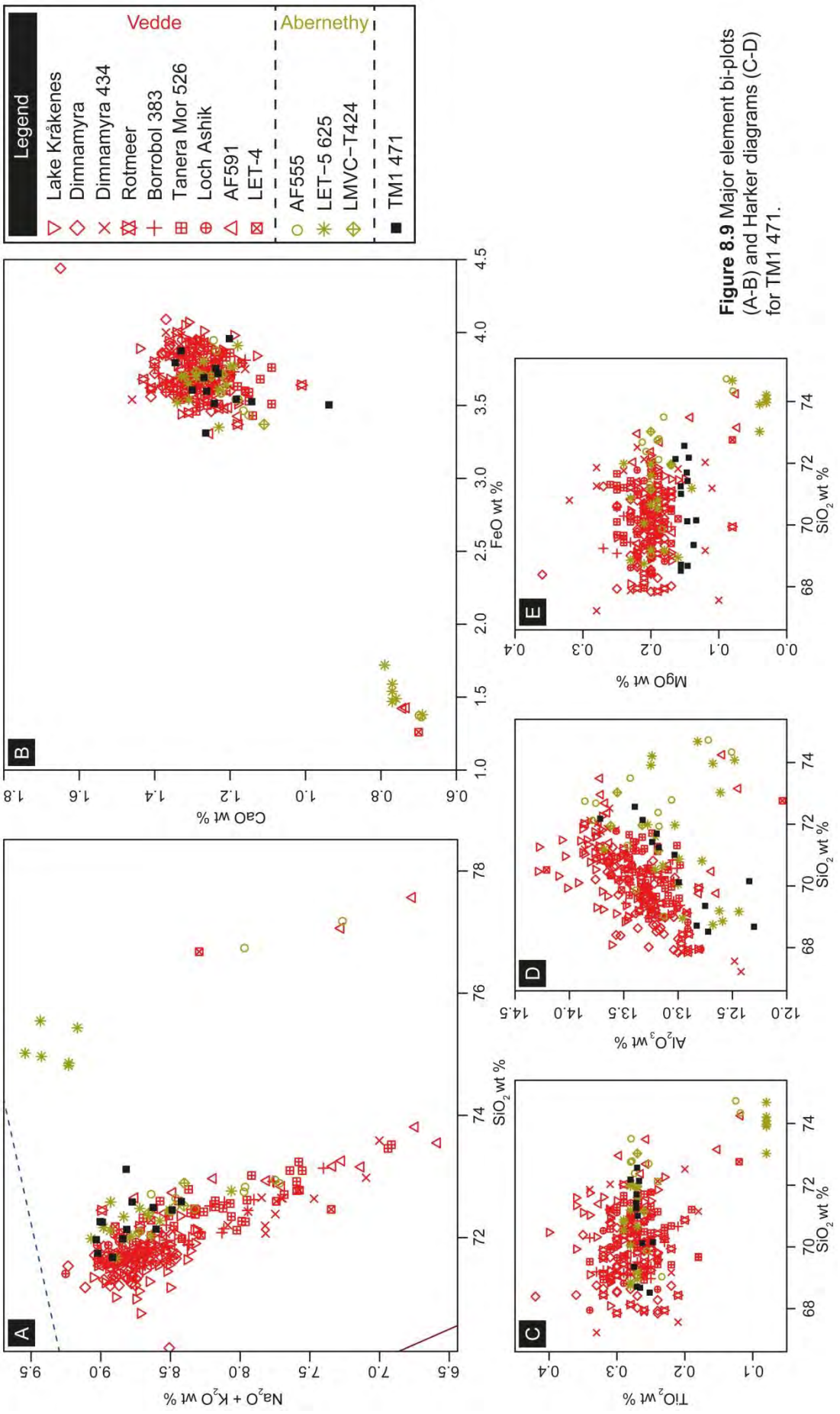

Figure 8.9 Major element bi-plots (A-B) and Harker diagrams (C-D) for TM1 471.

TM1 471

This interval within unit 3a yielded a single population as defined by twelve analyses. The tephra can be classified as a sub-alkali rhyolite possessing high potassium values (Figure 8.5). The data is chemically correlated to tephras that have previously been assigned to the Katla volcanic system, Iceland (Figure 8.9). The tephra's prominence mid-way through Loch Lomond Stadial silts and clays would suggest a strong correlation to the Vedde Ash (e.g. Lacasse et al. 1995; Lane et al. 2012b). However, a second tephra isochron derived from the Katla system, and dating from the Loch Lomond Stadial/Holocene transition has been recognised in a number of deposits in Scotland and Scandinavia; the Abernethy Tephra (Matthews et al. 2011; MacLeod et al. 2015). The data from TM1 9 471 plots well within the field for the Vedde Ash, but appears to overlap consistently with that of the Abernethy Tephra in a number of plots (Figure 8.9 A, C). The stratigraphic position of the Abernethy Tephra, however, is more closely associated with that of the transition into the Holocene (MacLeod et al. 2015), and so is an unlikely correlative here. The chemical similarity between TM1 9 471 and the Abernethy Tephra is likely due to recent advances in electron-microprobe analyses, which have been developed to minimise Na loss during analyses (Hayward 2012). Much of the Vedde Ash data pre-dates these developments and so an analytical offset can be observed in some of the elemental bi-plots. This correlation is in agreement with the results produced by Roberts (1997), who identified the Vedde Ash (VTM2) in association with Loch Lomond Stadial deposits in TM2 97' (see section 3.5.1).

TM1 462 and TM1 463

Two consecutive samples bordering the transition from the Loch Lomond Stadial into the early Holocene (unit 3c) were analysed, and can be classified as sub-alkali rhyolites with high potassium values (Figure 8.5). Both horizons returned bi-modal populations; TM1 462 (pop A = 17, pop B = 1), TM1 463 (pop A =13, pop B = 3). Population A in both horizons can be correlated to tephras previously assigned to the Katla volcanic system, whereas population B correlates to the Borrobol-type tephras (Figure 8.10). As fore-mentioned, the Loch Lomond Stadial is currently thought to contain at least two Katla derived tephras, the Vedde Ash and the Abernethy Tephra (Matthews et al. 2011; Lane et al. 2012b; MacLeod et al. 2015). The Abernethy Tephra is described as occupying a stratigraphic position close to the Loch Lomond Stadial/Holocene transition (MacLeod et al. 2015). However, problems have been encountered in validating the presence of the Abernethy Tephra in several sequences due to the Abernethy's indistinguishable chemical signature from that of its stratigraphic neighbour, the Vedde Ash. This problem has been exacerbated by the tendency of the Vedde to exhibit a diffuse depositional profile, which may obscure and mask shards

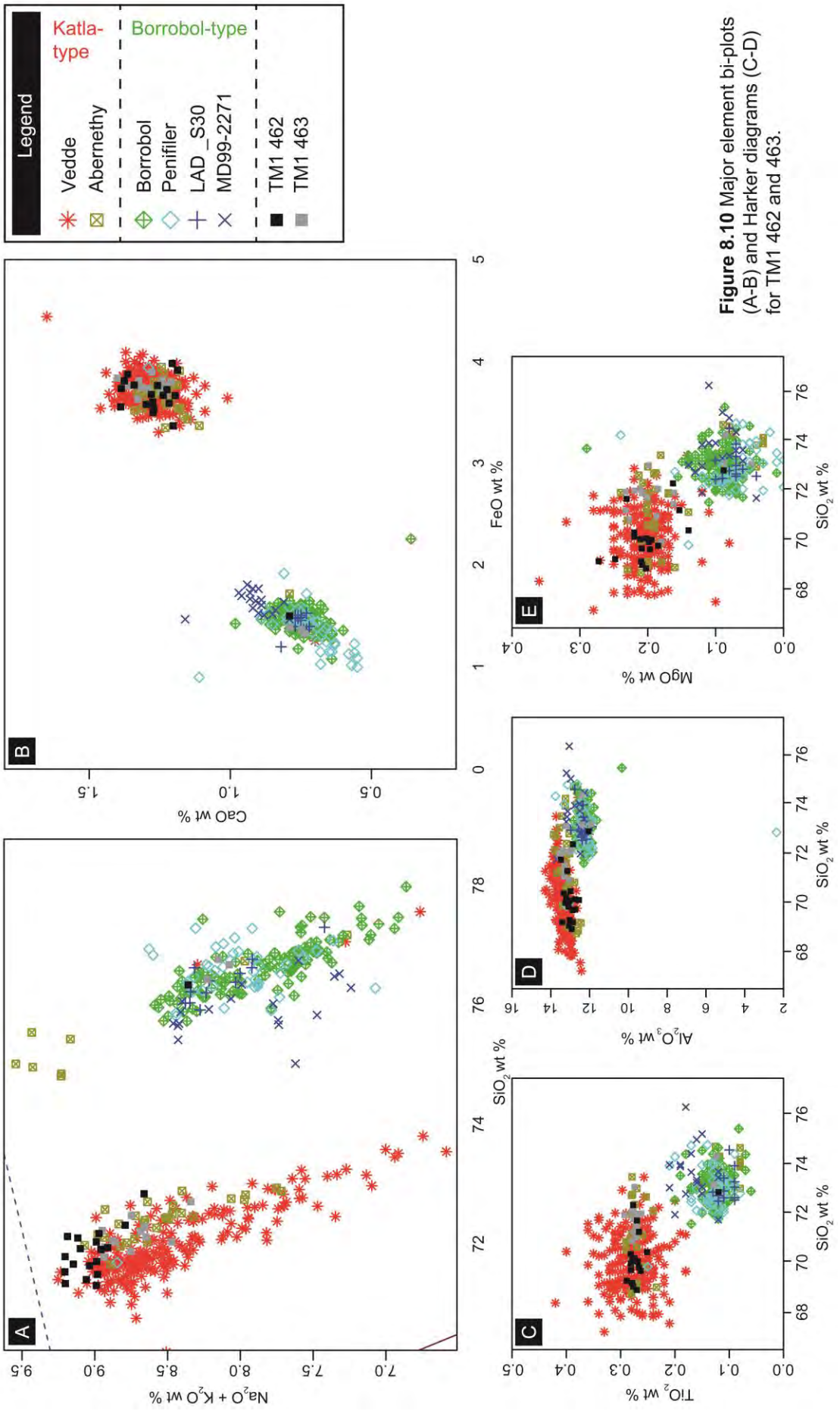

Figure 8.10 Major element bi-plots (A-B) and Harker diagrams (C-D) for TM1 462 and 463.

from subsequent eruptions (MacLeod et al. 2015). This has led to the suggestion that the 'Abernethy Tephra' may be a product of reworked material, and hence not a genuine isochronous marker horizon (MacLeod et al. 2015). Whilst a tail of shards from the Vedde Ash can be observed in TM1 (Figure 8.3), the peaks at TM1 462 and TM 1 463 contrast this diminishing trend.

One line of evidence that suggests a possible correlation to the Abernethy Tephra is the occurrence of a slight chemical offset in SiO_2 values between the samples of TM1 462 and 463, with the latter exhibiting slightly higher values (Figure 8.10 A). This structuring in the data series would seem unlikely if the horizons were a product of indiscriminate reworking of the Vedde Ash. Both horizons were analysed successively on the same day, and no appreciable change in analytical conditions was noted. However, if the raw SiO_2 data for TM1 462 (71.69 wt %) and TM1 463 (70.09 wt %) is normalised, then there is no statistical difference between the samples, i.e. the SiO2 values for TM1 462 and TM1 463 become 71.94 and 71.73 wt % respectively.

What is interesting to note, and what has so far eluded comment in the literature, is the presence of Borrobol-type tephras in association with the Abernethy Tephra. The occurrence of these shard types is noted in TM1, but also occur in the type site of Abernethy Forest and Loch Etteridge i.e. AF555 and LET-5, although the latter shows erroneously high K_2O values (Matthews et al. 2011; MacLeod et al. 2015). This suggests that a contemporaneous eruption from the Borrobol source may have taken place during the latter stages of the Loch Lomond Stadial. Alternatively these shards may be remnant from previous eruptions of the Borrobol source, and have been reworked into the basin during the onset of warming and the transition into the Holocene. If this is the case, the robustness of the Abernethy Tephra isochron is brought into question, as is any possibility of a correlation here. These findings, along with the potential implications of such are discussed further in section 10.3.3.3.

TM1 453 and TM1 454

Within early Holocene lacustrine muds, and just prior to an upturn in LOI and transition into Holocene detrital peats, two consecutive peaks were analysed and both returned bi-modal populations; TM1 453 (pop A = 10, pop B = 4), TM1 9 454 (pop A 21, pop B = 3). In both instances population A is defined as a sub-alkali rhyolite with medium potassium values (Figure 8.5), and can be correlated to tephras which have previously been ascribed to the Askja volcanic system, Iceland (Figure 8.11). In contrast, population B which is also a sub-alkaline rhyolite, exhibits a higher potassium content

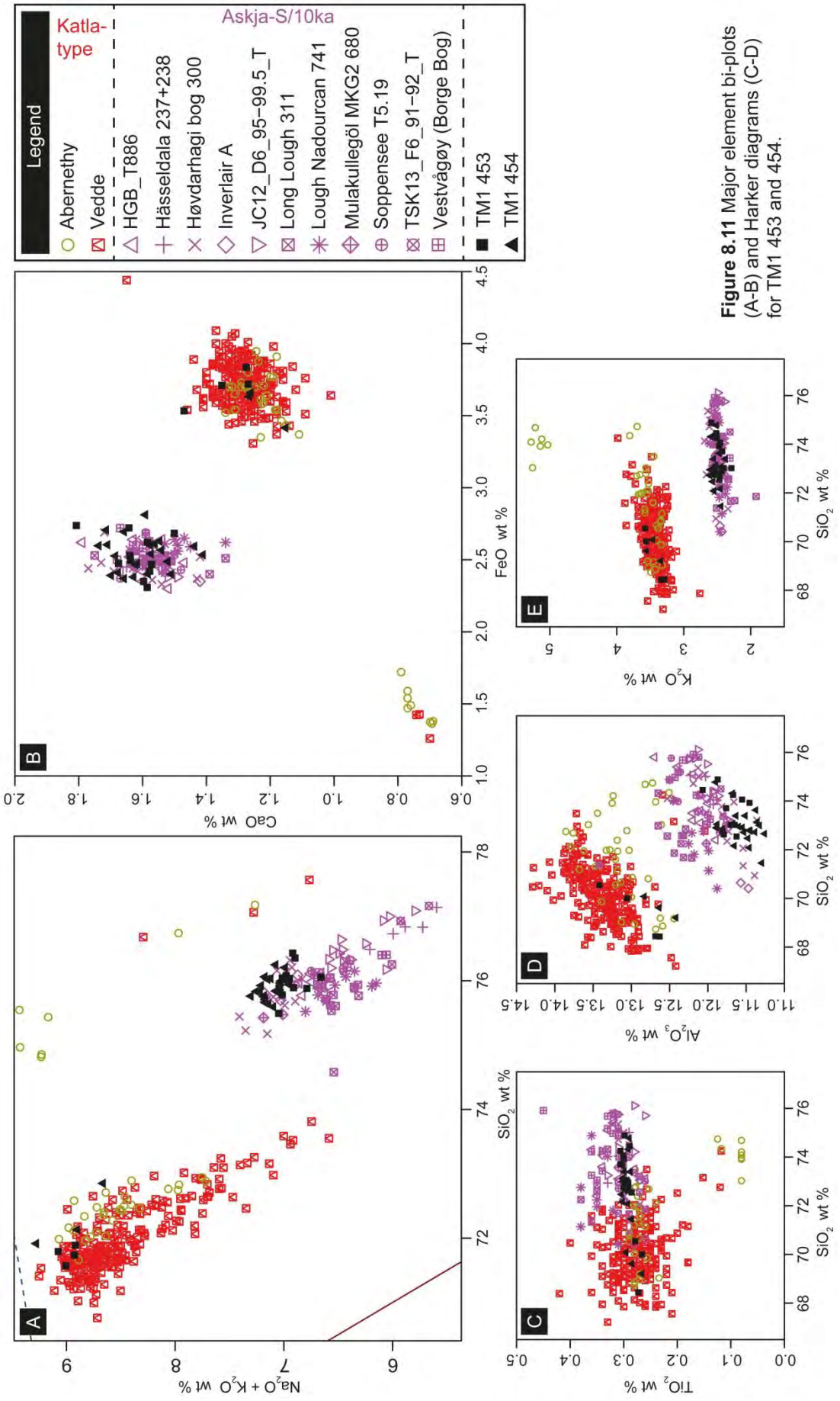

Figure 8.11 Major element bi-plots (A-B) and Harker diagrams (C-D) for TM1 453 and 454.

(Figure 8.5), and shows affinity to tephras correlated to the Katla volcanic system (Figure 8.11). The chemical data from population A suggests a link to the Askja-S/10ka Tephra, derived from a Plinian eruption of the Askja caldera (Sigvaldason 2002; Davies et al. 2003). The presence of Katla rhyolites within the early Holocene sediments is difficult to ascribe to a primary eruption. A number of Katla horizons are known throughout the LGIT (e.g. Bond et al. 2001; Koren et al. 2008; Matthews et al. 2011; Lane et al. 2012b; Tomlinson et al. 2012a), however, only one is known from this period, the Abernethy Tephra (Matthews et al. 2011; MacLeod et al. 2015). This isochron may be a possible correlative, although it is believed that this eruption is represented by TM1 462 and TM1 463, which makes greater sense due to the stratigraphic placing and chemical characteristics of these layers (see above). It is possible therefore that the Katla rhyolites identified in these intervals are reworked shards from the Vedde Ash or Abernethy Tephra isochrons. A similar finding of Katla shards alongside the Askja-S/10ka was identified at Borge bog in Vestvågøy, Norway (Pilcher et al. 2005). Conclusions from this study suggest such an occurrence was the result of either a low sedimentation rate between the Younger Dryas and early Holocene, or more likely as a product of sediment disturbance and reworking. No firm correlation can be given here and the possibility of another eruptive event cannot be entirely excluded (see section 10.3.3.3).

TM1 447 and TM1 450

Both of these intervals within the lower portion of unit 5 i.e. early Holocene detrital peats, yielded bi-modal populations of the same chemistries, however, the dominant population i.e. population A varied between the two intervals. Population A (n=4) in TM1 447 and population B (n=2) in TM1 450 can be classified as a sub-alkaline rhyolite, with a high potassium content (Figure 8.5), and which has a chemical signature indicative of tephras previously ascribed to the Katla volcanic system (Figure 8.12). Population B (n=2) in TM1 447 and Population A (n=8) in TM1 450 can also be classified as a sub-alkaline rhyolite, but exhibit a lower potassium content (Figure 8.5). The chemical signature of these populations may be correlated to tephras previously identified as originating from the Askja volcanic system (Figure 8.12). It is likely that the Askja-type shards can be correlated to the Askja-S/10ka eruption, however, the occurrence of shards exhibiting the same chemical signature in TM1 453 and TM1 454 somewhat complicates the placing of the isochron. The Katla-type shards also add additional complexity to the tephrostratigraphic record, suggesting either that the Katla system was particularly active during the early Holocene, or that reworking within the TM1 basin was extensive and prolonged enough so that shards originating from the Vedde Ash horizon and Abernethy Tephra horizon continued to have influence on the

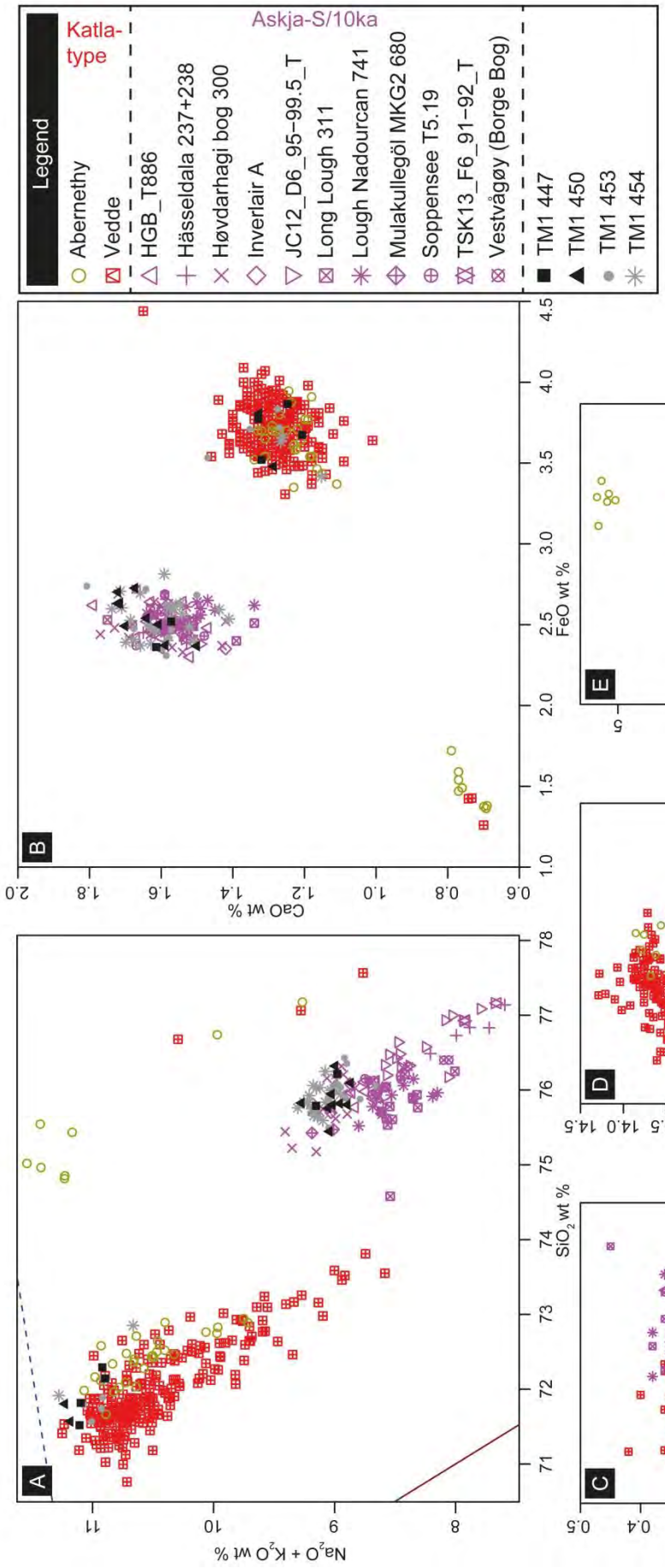

Figure 8.12 Major element bi-plots (A-B) and Harker diagrams (C-D) for TM1 447 and 450. TM1 453 and 454 also shown for comparison.

tephrostratigraphy of the site well into the early Holocene. As before, no firm correlation can be given to the Katla-type shards.

TM1 9 434

This interval consists of approximately four populations, with a slight uncertainty in this number deriving from the chemical similarity between populations B and C when compared with reference data. Population A is alkali rhyolite, possessing high potassium values (Figure 8.5). Population B is a sub-alkali rhyolite, possessing high potassium values (Figure 8.5). Population C is sub-alkaline rhyolite with high potassium values bordering on the Shosonite series (Figure 8.5). Population D sub-alkaline rhyolite with potassium values bordering on the calc-alkaline/ high-K calc-alkaline transition (Figure 8.5). To ease interpretation, populations A and D are plotted in Figure 8.13 whereas population B, C and D are shown in Figure 8.14. Population D has been marked as an outlier in both figures, with the rationale explained below.

Population A (n=4) shows affinity to the Torfajökull volcanic system, Iceland (Figure 8.13), and during the course of the LGIT three eruptions are thought to have derived from this centre; the rhyolitic component of the Ashik Tephra, the An Druim Tephra and the Høvdarhagi Tephra (Pyne-O'Donnell 2007; Ranner et al. 2005; Lind and Wastegård 2011). It is also important to note that shards exhibiting Torfajökull-like chemistries were also identified in combination with Katla-type and Borrobol-type shards as a discrete horizon termed the L-274 in Høvdarhagi, Faroe Islands (Lind and Wastegård 2011). Incidentally this sits stratigraphically below the Høvdarhagi Tephra, but above the Saksunarvatn Ash in the same sequence (Lind and Wastegård 2011).

Torfajökull eruptions typically exhibit a bi-modal distribution (Dugmore and Newton 1995; Pilcher et al. 1996), which is particularly evident with the Høvdarhagi Tephra, but less so with the Ashik and An Druim tephras, and absent entirely from the analyses of the L-274. To emphasise this feature and to provide a plausible geochemical envelope for correlation, the mid-Holocene Lairg B Tephra is also plotted in Figure 8.13, although it is not considered a potential candidate. Of the early Holocene Torfajökull eruptions, population A plots most consistently with tephras previously ascribed to the An Druim Tephra, however, due to the small size of the population some ambiguity with this interpretation exists. Additional stratigraphic control can be sought from the recent work of Kelly et al. (2016), who has established that these tephras can be reliably separated based upon the associated palynological signal, and vegetation succession in Scotland. TM1 434 occurs after the *Corylus* (hazel) rise in TM1, which first occurs at a

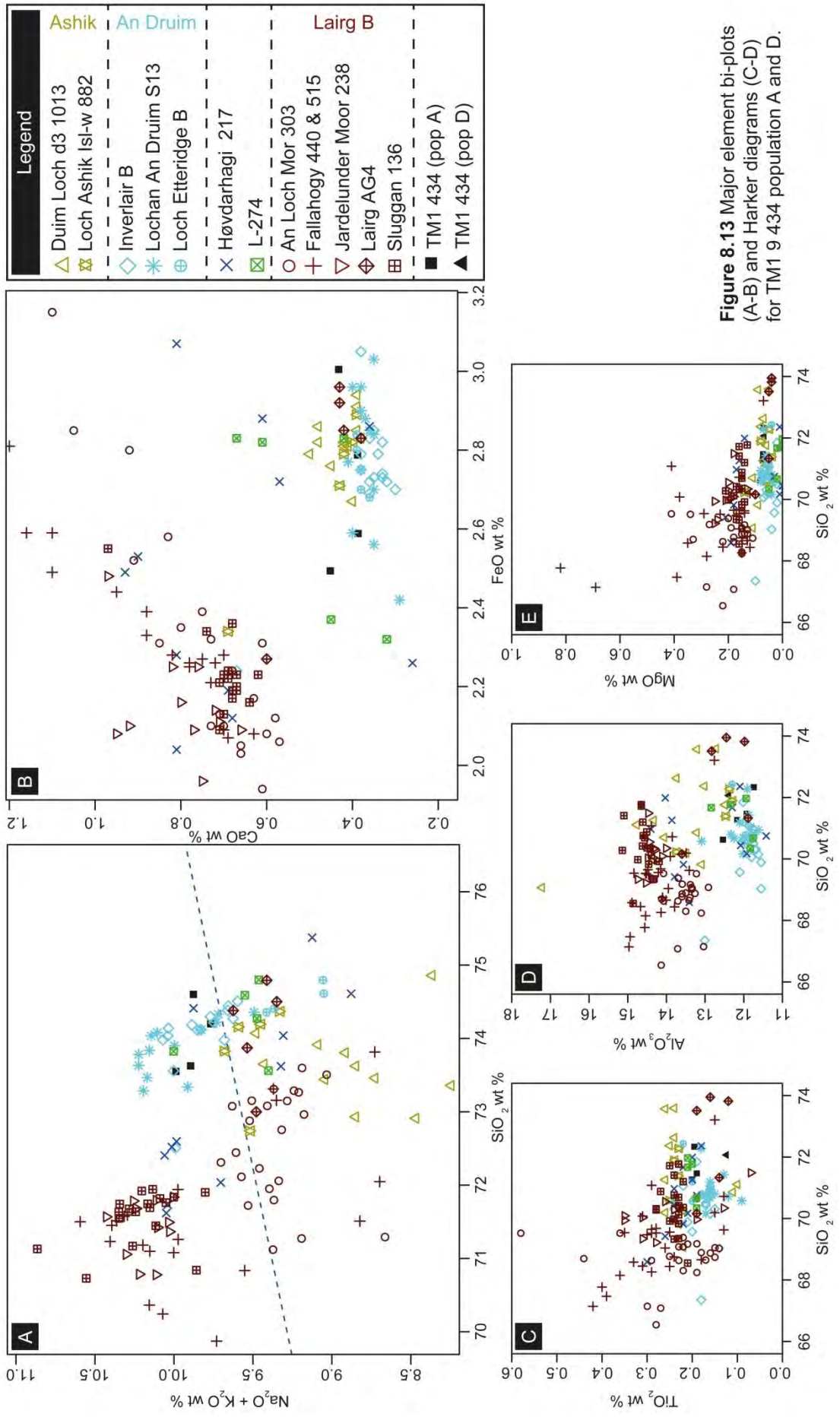

Figure 8.13 Major element bi-plots (A-B) and Harker diagrams (C-D) for TM1 9 434 population A and D.

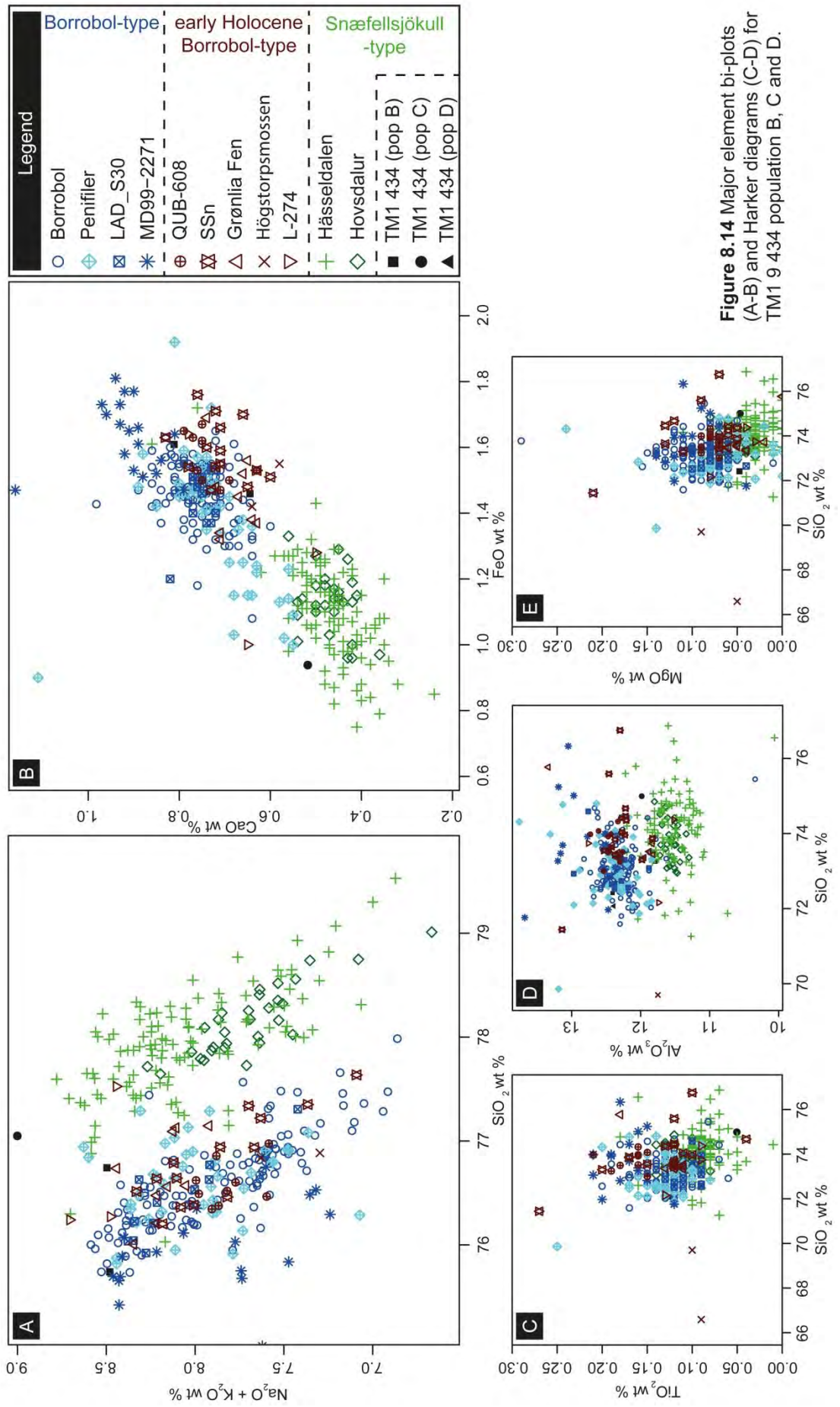

Figure 8.14 Major element bi-plots (A-B) and Harker diagrams (C-D) for TM1 9 434 population B, C and D.

pers. comm 2016). Crucially, in Scottish sequences this has been shown to occur after the Ashik Tephra, but before the An Druim Tephra (Kelly et al. 2016). This rise has also been shown to pre-date, or be broadly coincidental with that of the Saksunarvatn Ash (Bunting 1994; Brooks et al. 2012; Whittington et al. 2015; Kelly et al. 2016). Thus by association, if the L-274 and Høvdarhagi Tephras were deposited in Scottish sequences they would also fall after the *Corylus* rise. On the premise of this chemical evidence, and from the palynological data, a correlation to the Ashik Tephra can be ruled out, but a correlation to the L-274, An Druim or Høvdarhagi Tephras cannot be reliably established at this stage.

Population B (n=2) plots within the field of the Borrobol-type tephras (Figure 8.14), and within the early Holocene there are a number of horizons which exhibit such affinities (Lind et al. 2016). These are, the Fosen tephra (Lind et al. 2013); the Högstorpsmossen (Björck and Wastegård 1999); a component of L-274 (Lind and Wastegård 2011); population 3 of the QUB-608 (Pilcher et al. 2005); and the SSn (Boygle 1999). There is a strong possibility that the first four of these layers may represent the same event, but poor age controls have prevented a more robust conclusion from being made (Lind et al. 2013; Lind et al. 2016). None of these tephras have yet been identified reliably in Scotland, although there is some suggestion that the SSn has been identified at Loch Laggan (MacLeod 2008). In NW European sequences the Fosen and L-274 are the best stratigraphically constrained of the aforementioned horizons, occurring just after the deposition of the Saksunarvatn Ash. To reiterate, whilst the Saksunarvatn Ash has not been identified in TM1, where it has been identified in Scotland, it is found after the *Corylus* rise (e.g. Bunting 1994; Brooks et al. 2012; Whittington et al. 2015). Thus based on the position of the *Corylus* rise in this sequence, it is likely that Population B is a correlative of one of these early Holocene Borrobol-type tephras, however at this stage it is not possible to any more specific.

Population C (n=1), whilst similar to population B, exhibits a signature that is more indicative of tephras previously ascribed to the Snæfellsjökull volcanic system, Iceland i.e. the Hässeldalen (e.g. Davies et al. 2003) and the Hovsdalur (Wastegård 2002) (Figure 8.14). As both tephras are found within early Holocene sediments, there is insufficient stratigraphic evidence at Tanera Mòr to favour one over the other. What is interesting to note, however, is that there is an overlap between the chemical series of the Borrobol-type and the Hässeldalen Tephras. This is exemplified in the FeO vs CaO plot (Figure 8.14 B), with analyses previously being correlated to the Hässeldalen in Mulakullegöl (Lilja et al. 2013) and Endinger Bruch (Lane et al. 2012a) plotting within

the Borrobol field. It is also interesting to note that a single analysis of the L-274 plots within the Snæfellsjökull-type tephra field.

Population D (n=1) does not correlate to any known tephra of the LGIT, or any tephra held within the RESET database. Some chemical similarity can be observed with the Glen Garry Tephra (not shown), the source of which is the Askja volcanic system, Iceland. However, the alkali values for population D are consistently higher than what has previously been attained for an Askja derived tephra, and several other of the major elements e.g. TiO_2, MgO and MnO do not correlate sufficiently. Given the occurrence of the Askja-S/10ka through multiple intervals of the TM1 sequence stratigraphically below TM1 434, it is plausible that this single shard is representative of a reworked and chemically altered specimen.

Overall TM1 9 434 is a heterogeneous ash zone most similar to the L-274 i.e. exhibiting Torfajökull-type, Borrobol-type and Snæfellsjökull-type chemistries (Figure 8.13, 8.14). However, the origin of this horizon is uncertain and it is debatable of whether the layer is representative of primary deposition or a product of reworking (Lind and Wastegård 2011). This is also the case at TM1, and given the available evidence it is not possible to discern whether reworking, a conflation of closely spaced eruptions, or genuine primary airfall from several sources, is responsible for the tephras identified in this interval. Nevertheless the identification of Snæfellsjökull-type shards is an important finding due to the comparative sparsity of these shard types identified in the British Isles prior to undertaking of this study.

TM1 428 and TM1 425

Both of these horizons are composed of a homogenous chemical population that is classified as an alkali rhyolite with high potassium values (Figure 8.5). The chemistries returned are indicative of tephras which have previously been correlated to the Torfajökull volcanic system (Figure 8.15). The stratigraphic position of these horizons i.e. above the *Corylus* rise means, that a correlation to either the An Druim or Høvdarhagi Tephra is most likely. There is some suggestion that these two horizons may be different components of the same eruption, but such correlations have remained equivocal based on the lack of bi-modalism exhibited by the An Druim chemical data (Lind and Wastegård 2011; Kelly et al. 2016). The analyses here occur as a bi-modal distribution, however this is only prominent within the FeO vs CaO plot (Figure 8.15 B) and not in the SiO2 vs MgO plot (Figure 8.15 E) which is particularly key in the distinction of the Høvdarhagi. On this evidence a correlation to the An Druim

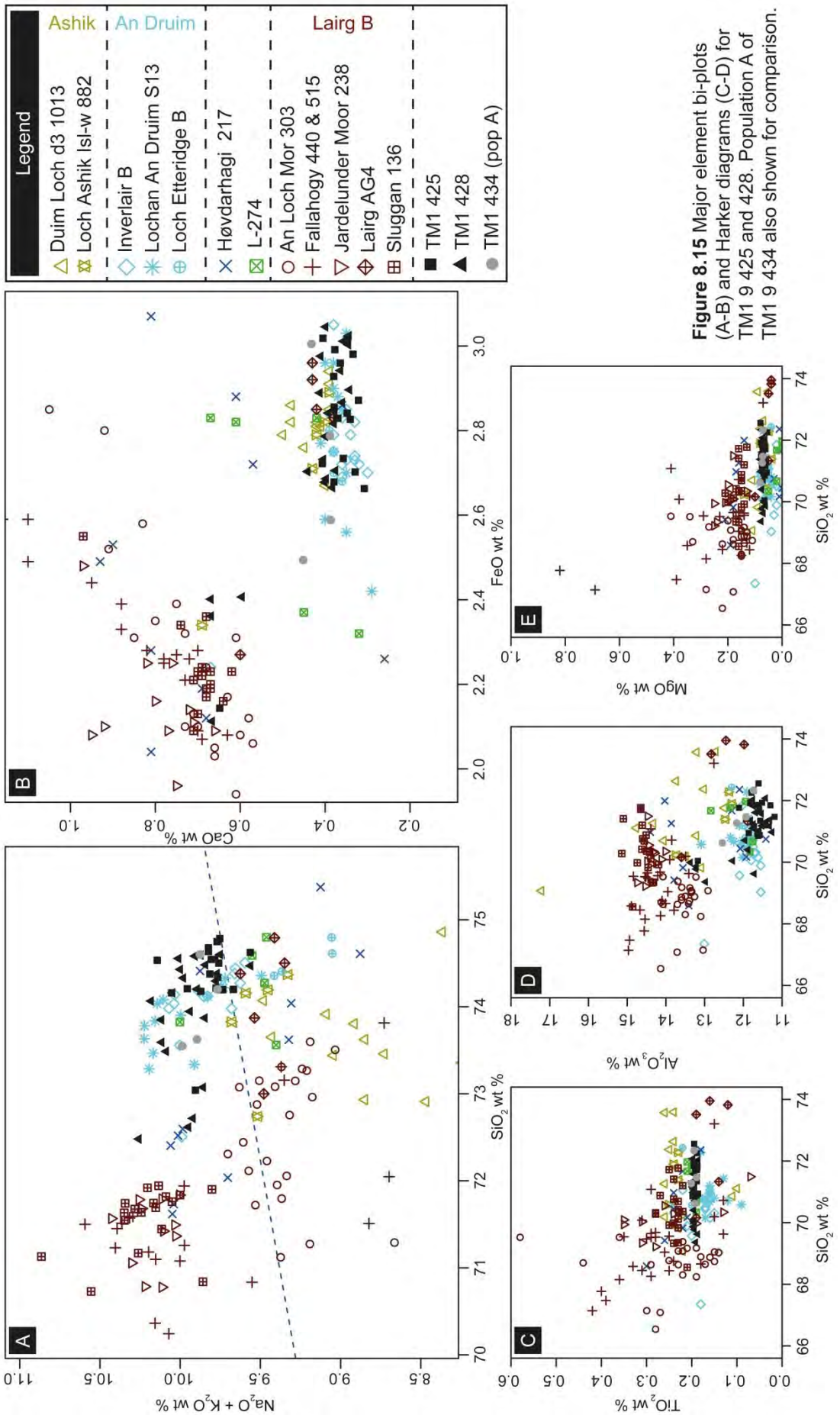

Figure 8.15 Major element bi-plots (A-B) and Harker diagrams (C-D) for TM1 9 425 and 428. Population A of TM1 9 434 also shown for comparison.

is proposed, whilst the question of whether the An Druim and Høvdarhagi represent the same eruption requires further investigation.

8.4 Chapter summary

- This chapter presents litho- and tephrostratigraphic data from Tanera Mòr 1, a basin from the island of Tanera Mòr situated within the Summer Isles archipelago, Scotland. Contiguous high-resolution (1 cm) sampling throughout the entire sequence yielded a tephrostratigraphic record that exhibits greater complexity than is typically recognised in Scottish sequences of comparable age. Sixteen horizons were chemically analysed, with the main findings summarised in Table 8.3.

- The chemical composition of basal tephras identified within the Dimlington Stadial sediments agrees only in part with the findings of Weston (2012). Several intervals (TM1 553, 546, 545; Table 8.3) exhibited mixed populations of Katla-type and Borrobol-type chemistries. The identification of a Dimlington aged Borrobol Tephra, or 'pre-Borrobol' further supports the evidence from Quoyloo Meadow of a Borrobol-type tephra from this interval (Chapter 5.0). The site and depth code of this tephra's first occurrence i.e. TM1 553 is proposed as the informal name of this horizon until further evidence determines otherwise.

- A high level of chemical variability in association with the TM1 516 'Penifiler' horizon suggests the early-mid Windermere Interstadial was a particularly active period for volcanic centres with the capability to deposit tephras in NW Europe. At present most of the populations within the TM1 516 interval cannot be reliably correlated to a known volcanic centres. However, there is tentative evidence for a tephra deriving from the Massif Central, France. Accumulatively this variance in chemistry, and hence possibility of multiple eruptions, may help to explain why this interval often exhibits a diffuse spread of shards. Further high-resolution sampling and accompanying chemical analyses will be required to further investigate this possibility of multiple eruptions, both at Tanera Mòr and elsewhere.

- Further evidence has been provided for the presence of the Askja-S/10ka tephra in Scotland (Table 8.3); hence facilitating improved tephrostratigraphic links to Ireland and the rest of Europe.

- Additional evidence has been provided to suggest that the An Druim and Høvdarhagi Tephra's may be representative of the same eruption (Table 8.3). At present some ambiguity remains in this statement, however, this topic is reinvestigated in light of all chemical data obtained in this thesis in section 10.3.3.3.

Table 8.3 Summary of tephra horizons identified in the TM1 composite sequence

Composite code	Unit	Stratigraphic position	Correlation	Notes
TM1 425	5	early Holocene	An Druim Tephra	
TM1 428	5	early Holocene	An Druim Tephra	
TM1 434	5	early Holocene	Uncertain	Mixed horizon with similarities to the L-274 i.e. Torfajökull-type, Borrobol-type and Snæfellsjökull-type (Lind and Wastegård 2011)
TM1 447	5	early Holocene	Askja-S/10ka Tephra & unknown Katla rhyolite	Mixed horizon
TM1 450	5	early Holocene	Askja-S/10ka Tephra & unknown Katla rhyolite	Mixed horizon
TM1 453	4	early Holocene	Askja-S/10ka Tephra & unknown Katla rhyolite	Mixed horizon
TM1 454	4	early Holocene	Askja-S/10ka Tephra & unknown Katla rhyolite	Mixed horizon
TM1 462	3c	Loch Lomond Stadial/ Holocene	Abernethy Tephra?	
TM1 463	3c	Loch Lomond Stadial/ Holocene	Abernethy Tephra?	
TM1 471	3a	Loch Lomond Stadial	Vedde Ash	
TM1 516	2b	Windermere Interstadial	Penifiler Tephra	Mixed horizon with Katla-type and potentially also shards from the Massif Central, France. Further work needed.
TM1 528	2b	Windermere Interstadial	Borrobol Tephra	
TM1 545	1a	Dimlington Stadial	Uncertain	Mixed horizon with several potential candidates (HM107-05 and MD99-2271- Borrobol type) (Dimna Ash and 10-1P 192 - Katla-type)
TM1 546	1a	Dimlington Stadial	Uncertain	
TM1 553	1a	Dimlington Stadial	Uncertain	

Chapter 9. Little Lochans Results

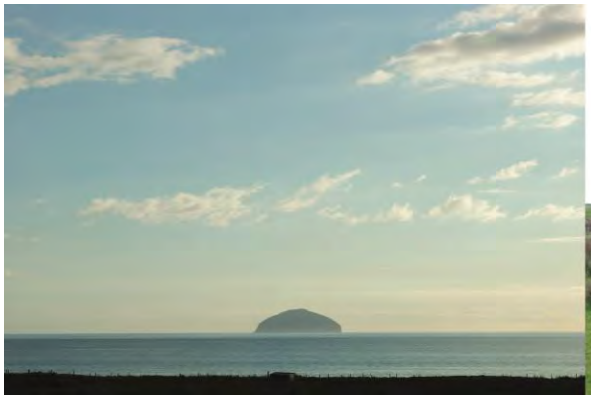

9.1 Introduction and chapter structure

This final results chapter presents the findings from Little Lochans, the only site in this study from the South Western sector of Scotland (Chapter 3). This southerly location is important for understanding the tephrostratigraphic disparity observed between Ireland and the rest of the British Isles. As previously noted the Irish tephra framework appears to exhibit a suite of tephras, which are either less well represented in Scotland, or absent entirely. This difference is most notable in the Windermere Interstadial and early Holocene. In the context of the Windermere Interstadial, the Borrobol and Penifiler Tephras, so common to Scottish sequences, are seemingly absent from Irish tephrostratigraphies. Instead this interval in Ireland features the Roddans Port A and B Tephras, which, at present, have not been identified outside the region (Turney et al. 2006). Considering the early Holocene, the Askja-S/10ka Tephra is seemingly much more ubiquitous in Ireland than it is in Scotland, where currently only one verified occurrence has been documented (Kelly et al. 2016). It is hoped therefore that the Little Lochans site will provide a tephrostratigraphic 'bridge' between these two regions, and enable a more robust tephrostratigraphic framework to be constructed across the British Isles.

The geological, glaciological and tephrostratigraphical context of this site is presented in Chapter 3, along with a summary of lithological and palynological results from Moar (1969b). This chapter therefore presents the main litho- and tephrostratigraphic findings of this project.

9.2 Results

Access to the site was restricted due to flooding, consequently only one complete sequence was extracted from the south-westerly margin of the lochans (Figure 3.27). Five 0.5 m Russian cores were extruded with 0.10-0.0.20 m overlaps between cores. A composite stratigraphy with corrected depth measurements has been produced by aligning lithological changes, LOI, TOC, $CaCO_3$ and magnetic susceptibility values (Figure 9.1). Detailed sedimentological descriptions for each of the five cores, along with raw data detailing the LOI, TOC, $CaCO_3$ and magnetic susceptibility measurements can be found in Appendix H.

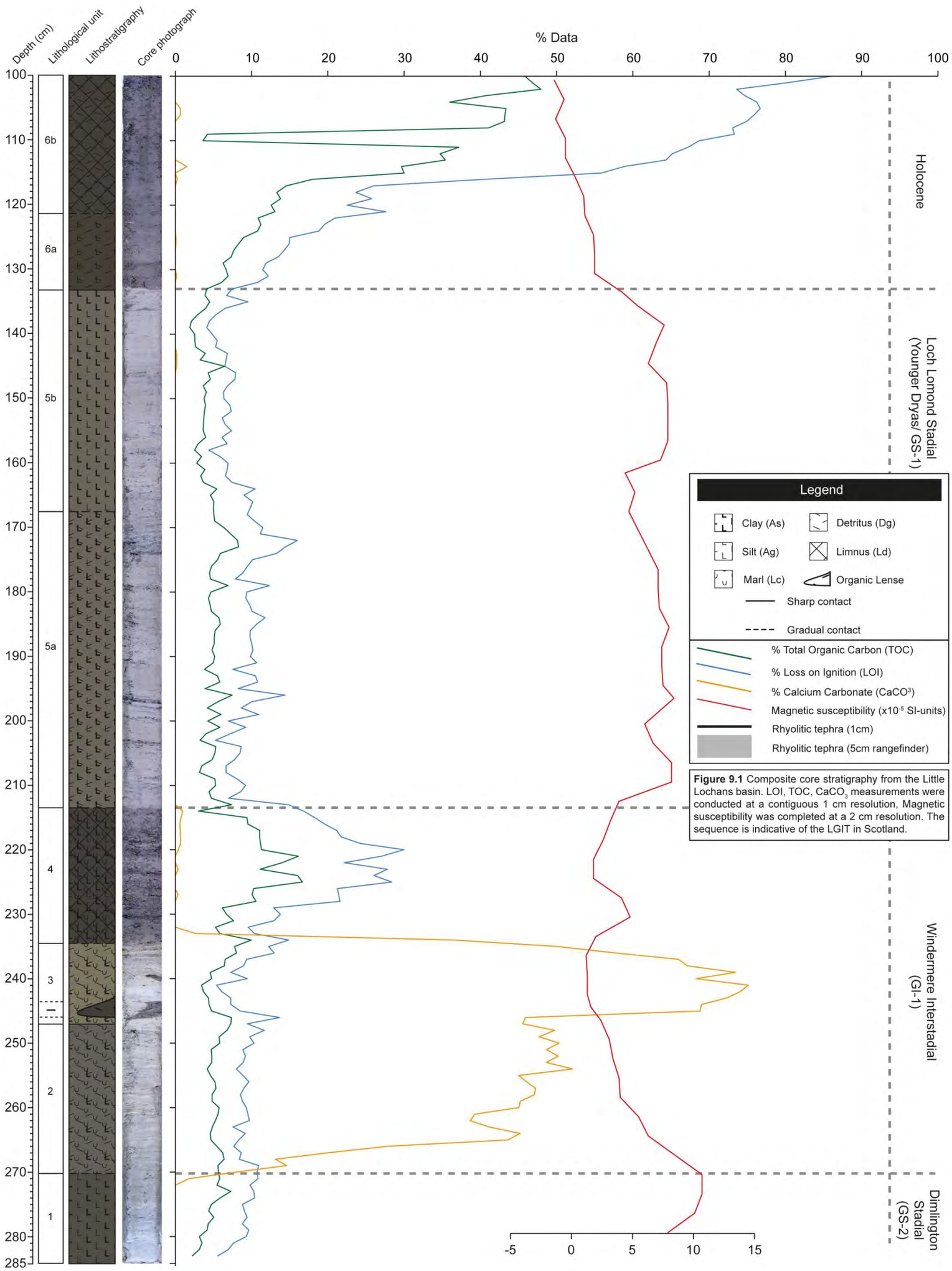

Figure 9.1 Composite core stratigraphy from the Little Lochans basin. LOI, TOC, $CaCO_3$ measurements were conducted at a contiguous 1 cm resolution, Magnetic susceptibility was completed at a 2 cm resolution. The sequence is indicative of the LGIT in Scotland.

9.2.1 Basin sedimentology

A detailed description of the sedimentological units is given in Appendix H, the sequence is divided into six stratigraphic units, with units 5 and 6 comprising two sub-units (Figure 9.1).

The basin contains sediments that relate to the LGIT and early Holocene (Figure 9.1). At the base of the sequence silty clays with trace organic matter would suggest either a late Dimlington Stadial or early Windermere Interstadial age. At ca. 270 cm this minerogenic sediment grades into a calcareous limnic deposit (marl), signifying a climatic amelioration and a relative stability in the landscape typical of the Windermere Interstadial. At ca. 244 cm a discontinuous organic band intersects the sequence, this band was identified in the overlap of two cores, suggesting a genuine 'event' and not a coring artefact. At ca. 235 cm the marl unit is succeeded by an organic rich gyttja. This succession can either be interpreted as the onset of climatic deterioration and the inwashing of organic material into the basin, or as part of a gradual process of terrestrialisation. At ca. 213 cm this organic unit is replaced by a silty clay. This silty clay unit initially contains banded moss layers, but at ca. 168 cm upwards these become less frequent. This transition from organic to minerogenic sedimentation is interpreted as the transition from the Windermere Interstadial to the Loch Lomond Stadial. At 133 cm the silty clay Loch Lomond Stadial unit ceases, and is replaced by silty organic rich lake muds signalling the re-colonisation of the landscape and the onset of Holocene warming.

In comparison with the stratigraphy from Moar (1969b; Table 3.4; Figure 3.27), the lithology of the two studied sequences is similar despite a clear offset in the absolute depth and unit thicknesses. The cause of these differences may relate to deflation, and increased decomposition of the peat surface due to landscape drainage and consolidation since the late 1960's (Boelter 1972; Coulson et al. 1990). The variations in lake sediments probably relate to a variable basal topography, and preferential sediment focussing during differing climatic regimes (Figure 9.2). Sediments pertaining to the Windermere Interstadial are represented by a longer sequence in Moar (1969b) 70 cm vs 57 cm in this study, whereas sediments of the Loch Lomond Stadial are notably shorter 30 cm vs 77 cm. Palmer et al. (2015) illustrate that sedimentation in lacustrine sequences is variable through time, with clastic inputs derived from overland or streamflow processes being preferentially focused around basin margins (Figure 9.2). The cooler climate of the Loch Lomond Stadial and the short lived climatic oscillations that characterised the Windermere Interstadial are considered to have had a profound effect on landscape stability (Lowe and Walker 2015), thus the inwash

potential of freshly exposed land surfaces would have been high through this period. At Little Lochans this in-washing of sediments is represented by the organic lense identified in the Windermere Interstadial marls, and the banded moss layers that can be observed within the lower half of the Loch Lomond Stadial sediments i.e. units 3 and 5a respectively. These layers may have been deposited during storm events, or periods of high overland flow. Interestingly the moss banding in the Loch Lomond Stadial deposits reduces in the upper half of the sediments i.e. unit 5b, suggesting that in-washing becomes less dominant within the local area, vegetation becomes much reduced within the local catchment, and/ or that the landscape begins to stabilise. No comment is made on the presence of moss banding within the sequence from Moar (1969b), and no organic content is depicted within the lithostratigraphy. This adds further weight to the suggestion that Moar (1969b) extracted a sequence that was less susceptible to periods of high inwash and overland flow, and hence a more central core compared to the one retrieved in this study.

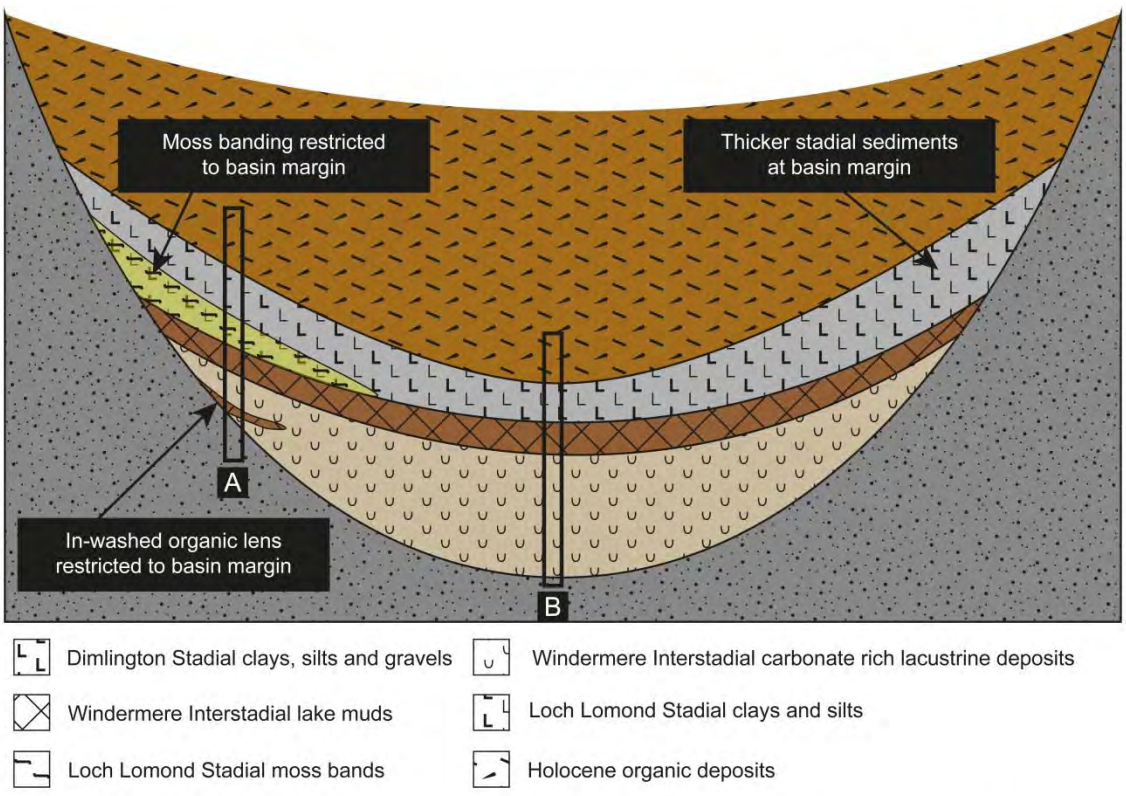

Figure 9.2 Theoretical basin stratigraphy of Little Lochans, the more peripheral core extracted in this study is represented by core A with the more central core of Moar (1969b) being represented by core B. The longer Interstadial unit of Moar (1969b) and shorter stadial unit is likely the result of preferential sediment focussing during different climatic regimes. Not to scale.

9.2.2 Tephrostratigraphy

Due to the unknown tephra content of the basin, and the lack of neighbouring sites for comparison, it was decided to implement the low resolution scan and resample

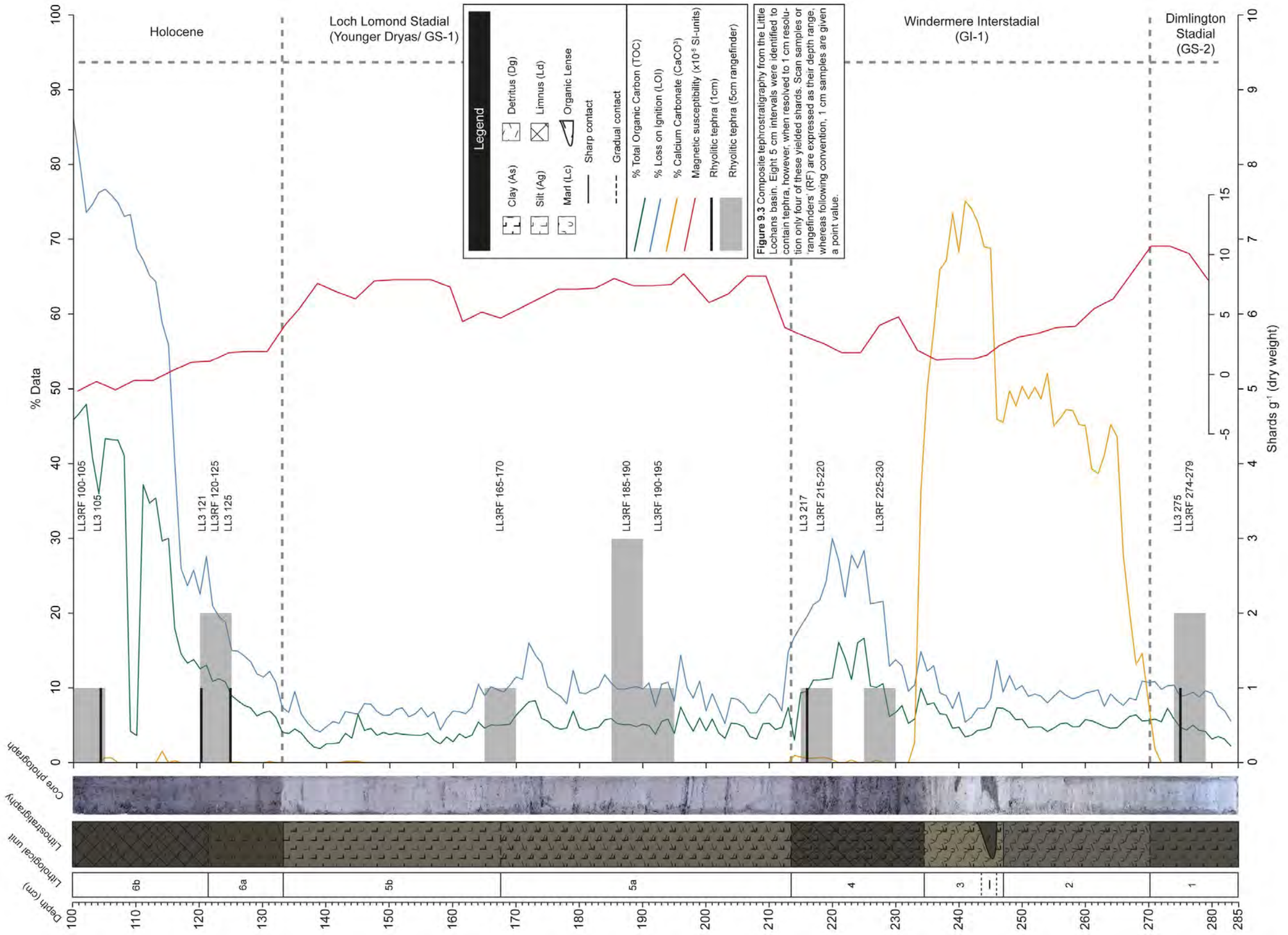

Figure 9.3 Composite tephrostratigraphy from the Little Lochans basin. Eight 5 cm intervals were identified to contain tephra, however, when resolved to 1 cm resolution only four of these yielded shards. Scan samples or 'rangefinders' (RF) are expressed as their depth range, whereas following convention, 1 cm samples are given a point value.

strategy as a first order of determining tephra content. Low resolution 5 cm scans of the sequence identified eight intervals in which tephra was present (Figure 9.3). These horizons possessed very low concentrations of no more than 3 shards g^{-1} dry weight. Subsequent refinement to a 1 cm resolution failed to yield higher concentrations, and in four of the intervals no tephra was identified when reprocessed at these higher resolutions (LL3RF 165-170; LL3RF 185-190; LLRF 190-195; and LLRF 215-220). Figure 9.4 illustrates shard morphologies taken from both low and high resolution samples. Due to these very low concentrations it was decided that the horizons would not be pursued for chemical characterisation. Tentative correlations based on morphology and stratigraphic position are therefore outlined below.

LL3RF 274-279 and LL3 275

Within the basal sediments of unit 1 two shards were identified, and each with a differing morphology. The shard depicted in Figure 9.4 (A) is perhaps more diagnostic than the fainter shard exhibited in Figure 9.4 (B), being that it possess a large mineral inclusion, which is an indicative feature of the Borrobol and Penifiler tephras (Pyne-O'Donnell et al. 2008). The presence of the horizon below the onset of marl sedimentation at the start of the Windermere Interstadial may therefore support a correlation to the Borrobol Tephra over the Penifiler, as the latter is often associated with a short lived climatic oscillation early in the interstadial (Pyne-O'Donnell et al. 2008; Matthews et al. 2011). However, in the context of the site and the relatively proximity of Northern Ireland, a correlation to one or both of the Roddans Port Tephras cannot be excluded.

LL3RF 225-230

In unit 4 two peaks are identified, the lower is comprised of a solitary shard depicted in Figure 9.4 (C). The shard is the largest identified within the sequence and exhibits a fluted morphology; a characteristic that is uncommon for either the Borrobol or Penifiler tephras. A number of other tephras have been identified in the period encompassing the Lateglacial Interstadial around NW Europe and the Atlantic margin (Table 2.3), but few details exist on their morphological properties. At present no correlation may be suggested without further data.

LLRF 215-220 and LL3 217

The second of the peaks within unit 4 contains a cuspate and vesicular shard (Figure 9.4 D), and one which is morphologically characteristic of the Borrobol-type tephras (Pyne-O'Donnell et al. 2008). As with the preceding horizon, It's position late in the Windermere Interstadial limits correlations to either the Borrobol or Penifiler but may

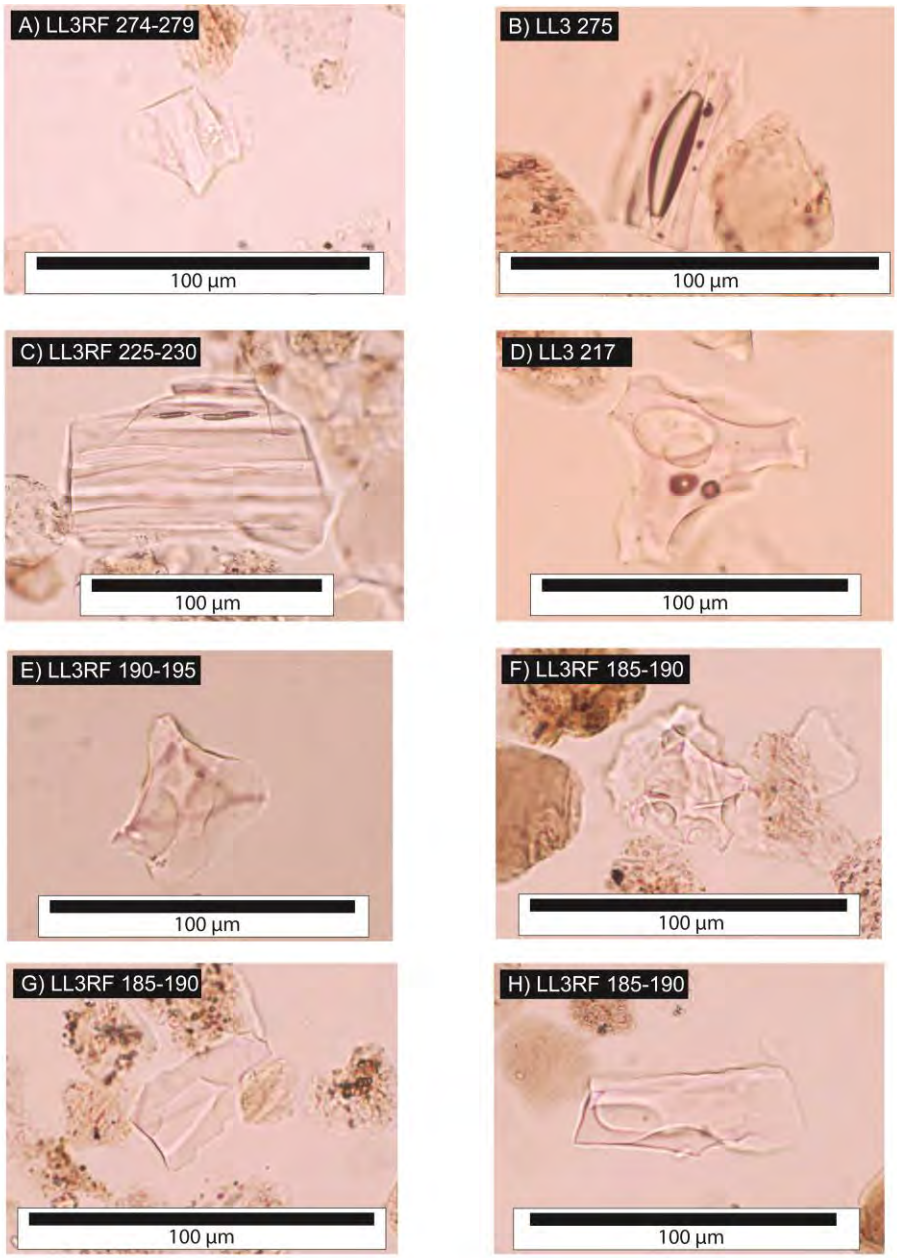

Figure 9.4 Photographs of shards identified within the Little Lochans sequence. (A) Small faint shard showing some surface alteration within flutes. (B) Small elongate shard with one large closed vesicle and a number of smaller closed vesicles. Some surface pitting also present. (C) Large elongate shard with fluting, as well as open and closed vesicles. (D) Highly cuspate shard with open and closed vesicles. (E) Blocky cuspate shard showing signs of surface pitting and a rounding of edges. (F) Blocky irregular cuspate shard, with microlitic inclusions. (G) Cuspate shard. H) Cuspate shard with rounded edges (right hand side).

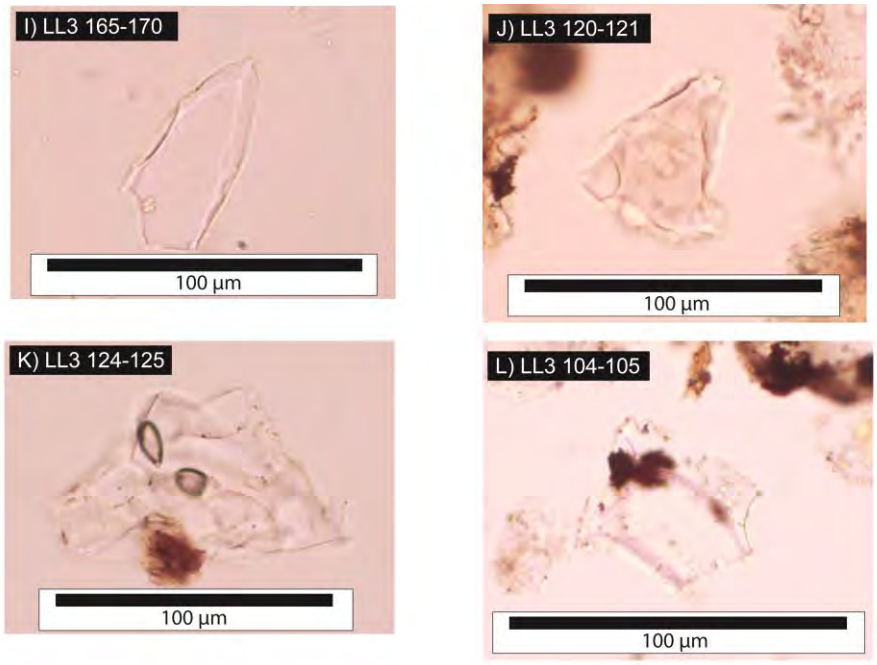

Figure 9.4 continued (I) Long cuspate shard with some signs of surface alteration (bottom left). (J) A Blocky vesicular shard. (K) A large blocky irregular shard with closed vesicles. (L) A faint shard exhibiting signs of surface pitting and chemical alteration.

signify a second occurrence of the LAS-1; a tephra previously only identified at Loch an t'Suidhe at the end of the Interstadial (Davies 2003). Notably the tephra is one that is described as containing circular vesicles (Davies 2003). Another candidate may be the CRUM1 597 Tephra identified at Crudale Meadow and Spretta Meadow which also possesses cuspate morphologies (Chapter 6.0 and 7.0). Chemical characterisation will be needed to establish whether these are viable candidates for correlation.

LLRF 185-190 and LLRF 190-195

Two consecutive scan samples within unit 5a returned tephras, with the uppermost horizon exhibiting the highest concentration of shards identified within the sequence (ca. 3 shards $g^{-}1$). The shards are predominantly cuspate (Figure 9.4 E-H), with one depicted in Figure 9.4 (F) also exhibiting small 'pencil-like' mineral inclusions. All shards show signs of weathering with rounded edges and pitted surfaces common. The ubiquitous cuspate morphology is characteristic of the Vedde Ash, and their position mid-way through sediments relating to the Loch Lomond Stadial also supports this correlation.

LLRF 165-170

Straddling the division between the sub-unit 5a/b is a second peak within Loch Lomond Stadial sediments. The tephra is depicted in Figure 9.4 (I) and is a featureless cuspate

shard which may indicate a Katla origin (e.g. Mangerud et al. 1984). The horizon henceforth may correlate to the Abernethy Tephra, second tephra isochron derived from Katla during the Loch Lomond Stadial that is now well recognised in Scotland and parts of NW Europe (Matthews et al 2011; MacLeod et al. 2015).

LL3RF 120-125, LL3 121 and LL3 125

Within unit 6a of the early Holocene, a blocky cuspate tephra with irregular mineral inclusions was identified (Figure 9.4 J and K). A number of tephras have been identified in sediments of this period around NW Europe, thus making even tentative correlations problematic. However, the morphology of the shards may suggest a correlation to the Hässeldalen Tephra, which has been described as highly vesicular (Lind and Wastegård 2011; Wulf et al. 2016).

LLRF 100-105 and LL3 105

The uppermost tephra identified in the sequence is depicted in Figure 9.4 (L). The tephra is faint and shows signs of chemical alteration. As with the preceding horizon a number of potential correlatives exist, but more robust correlations cannot be made currently. However, the oscillation in the TOC values may be indicative of a short lived, climatic event, in which case the tephra identified here may correlate to the Ashik Tephra, which is described as occurring shortly after the PBO in the early Holocene (Pyne-O'Donnell 2007).

9.3 Discussion

The lack of tephra shards and the inconsistent presence of tephra identified at Little Lochans could be related to either basin and catchment characteristics, or geographical restrictions relating to ash plume dynamics.

9.3.1 Basin and catchment factors

A detailed account of the likely factors influencing tephra accumulation and preservation is provided in section 2.3.3. In relation to the Little Lochans sequence it is the spatially variability of tephra deposits within lacustrine basins which is key (e.g. Mangerud et al 1984; Boygle 1999; Davies et al. 2001; Pyne-O'Donnell 2011; Bertrand et al. 2014). Little Lochans possesses no inlet channels, and is surrounded by relatively subdued topography, in a catchment barely larger than the basin itself. This situation is similar to the Druim Loch basin studied in Pyne-O'Donnell's (2011) tephrostratigraphic experiment (Figure 9.5). Pyne-O'Donnell (2011) notes that with the absence of inlet channels and fluvial focussing, the predominant factor governing tephra input is direct

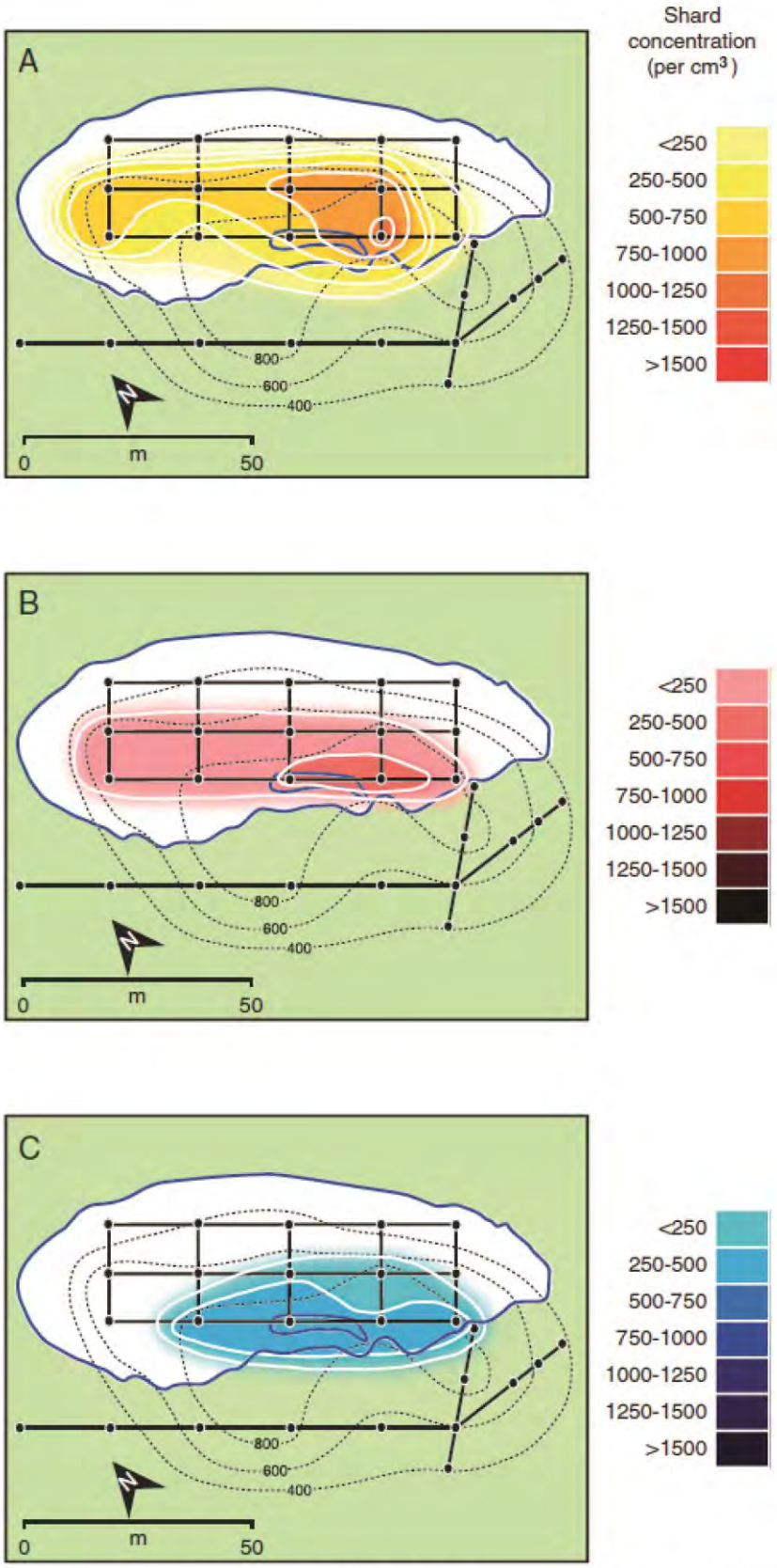

Figure 9.5 Distribution and concentration of tephras in association with the (A) Ashik Tephra; (B) Vedde Ash; (C) Penifiler Tephra at Druim Loch, Isle of Skye. Toward the periphery of the basin tephra concentrations are markedly reduced, if present at all. The absence of inflows into Druim Loch, and the small surface area to catchment ratio is similar to the Little Lochans basin (from Pyne-O'Donnell 2011).

airfall, and the factors controlling the distribution and concentration is basin depth. Figure 9.5 illustrates that towards the periphery of Druim Loch concentrations of tephra are greatly reduced, if present at all. If related to Little Lochans, it seems plausible to suggest that the small catchment size and more peripheral core being retrieved in this instance, has greatly reduced the chance of developing a quantifiable tephrostratigraphy at the site. In addition to this a high proportion of the tephra identified exhibited some kind of post depositional alteration i.e. chemical dissolution or mechanical weathering (Figure 9.5). The presence of calcium carbonate in the basin may have resulted in unfavourable preservation conditions during the mid-Interstadial, potentially leading to the dissolution of some shard types (e.g. Pollard et al. 2003). However, the calcium carbonate content is negligible in other climato-stratigraphic zones. It is therefore unlikely that the presence of a marginally alkaline environment has had any significant control on the preservation of more silicic shards within the basin. The occurrence of rounded and physically degraded shards may indicate a reworking of sediments during certain periods, this is especially notable in the shards identified within the stadial units 5a/5b. However, it seems unlikely that mechanical weathering would be so severe as to degrade shards to the extent that they were no longer recognisable.

9.3.2 Geographical restrictions in tephra plume pathways

Many of the sites which encompass the regional tephrostratigraphy have not yielded high tephra concentrations through the LGIT (Figure 3.24). In particular, the closest sites to Little Lochans in mainland Britain i.e. Rubha Port an t-Seilich to the north (max conc. ca. 15 shards g^{-1}; Mithen et al. 2015), and St Bees and Hallsenna Moor to the south east (max conc. ca. 25-30 shards g^{-1}; Lane 2004). This is made particularly more evident by the total absence of tephra identified by Wastegård et al. (2000a) Lang et al. (2010) and Matthews (pers. comm) along the Irish Sea coast and within the Lake District. To the west of Little Lochans, Roddans Port and Long Lough also fail to produce high concentrations of tephra through the Interstadial; although the Vedde Ash is moderately well represented at Roddans Port (max conc. 189 shards cm^3), and the Askja-S/10ka Tephra is quantified to ca. 325 shards cm^3 at Long Lough. Notably further to the east, Whitrig Bog and Howburn Farm display much higher tephra concentrations than the other sites within the region, with the Vedde Ash reaching a value close to, and in excess of, 800 shards g^{-1}, respectively. This suggests that the western coastline of southern Scotland, and northern England resides within a low tephra concentration zone (Figure 9.6), which may reflect a lack of tephra delivery to this area. Lacasse (2001) suggests that prevailing westerly winds are most likely to distribute tephras originating in Iceland eastwards towards Scandinavia and northern Scotland. Whilst

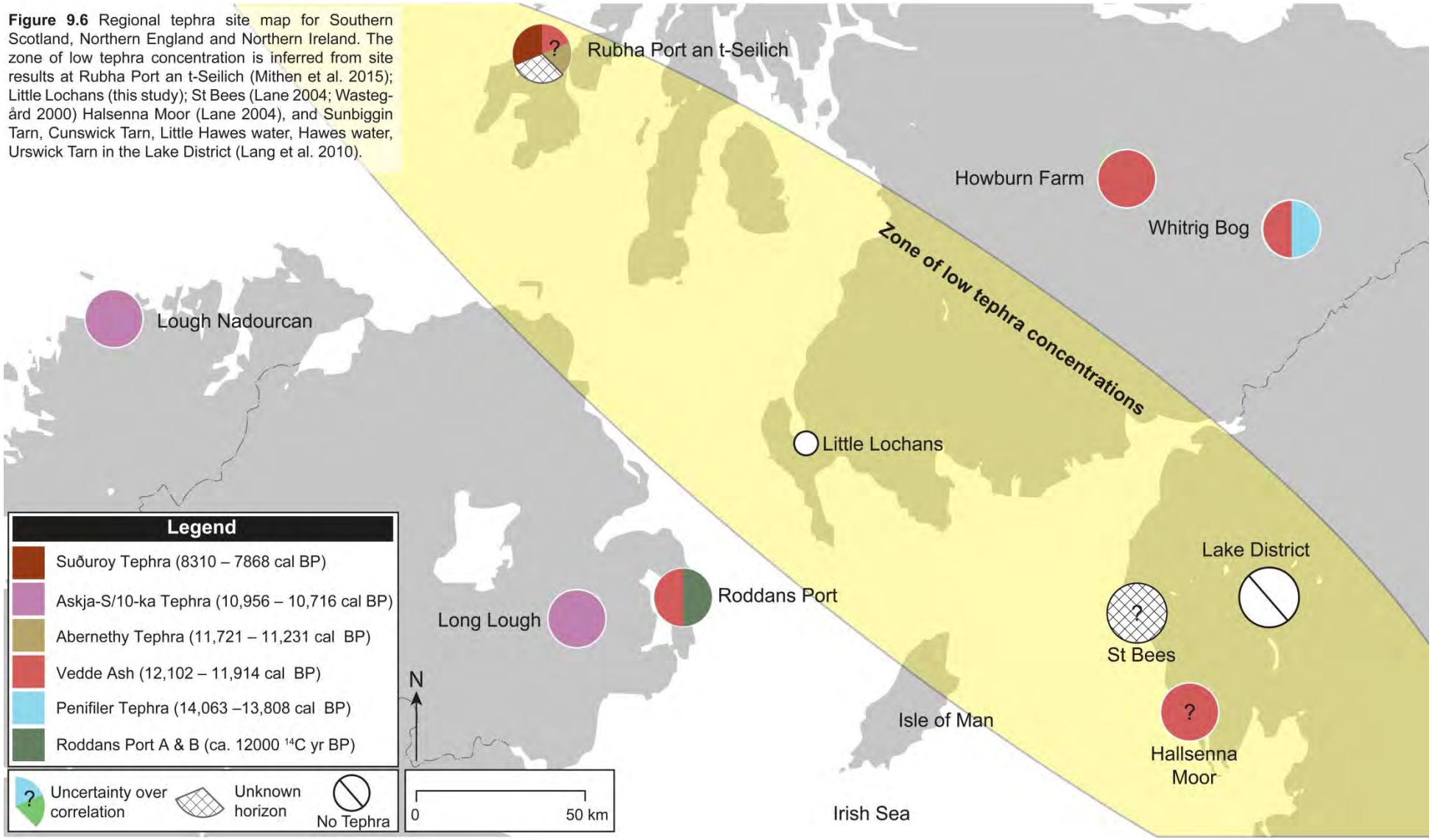

Figure 9.6 Regional tephra site map for Southern Scotland, Northern England and Northern Ireland. The zone of low tephra concentration is inferred from site results at Rubha Port an t-Seilich (Mithen et al. 2015); Little Lochans (this study); St Bees (Lane 2004; Wastegård 2000) Halsenna Moor (Lane 2004), and Sunbiggin Tarn, Cunswick Tarn, Little Hawes water, Hawes water, Urswick Tarn in the Lake District (Lang et al. 2010).

Swindles et al. (2011) have noted that an abundance of mid-late Holocene tephra sites in Ireland is likely due to anticyclonic airflows dispersing tephras southwards. Fluctuations in zonal air masses and hence ash cloud dynamics, may therefore help to explain the disparity observed within the tephrostratigraphies of Ireland and mainland Britain i.e. the absence of the Borrobol, Penifiler and Ashik Tephras in Ireland and the absence of the Roddans Port Tephras in mainland Britain (Chapter 3.0). It is also possible that these factors have contributed to differences in shard concentrations between sites. Southwest Scotland, western England and Wales may lie just outside these dominant zonal airflows and therefore may experience less frequent and less concentrated ash clouds than neighbouring areas (Figure 9.6). In order to test this hypothesis, and to rule out other factors related to taphonomy or preservation, a denser network of sites is necessary.

9.4 Chapter summary

Little Lochans is the most south-westerly tephra bearing site dating from the LGIT in Scotland. However, low concentrations and the absence of tephra in some horizons when resolved to higher resolutions has prevented further analyses. As a consequence only limited conclusions, and tentative suggestions as to why the site does not exhibit higher concentrations can be made. It is likely that a location such as Little Lochans, is highly dependent upon tephra delivery directly from airfall. The Stranraer Isthmus still holds promise in developing a local tephrostratigraphy, even if the specific locale of Little Lochans is limited. A more extensive search is necessary therefore to find a basin than exhibits a larger catchment area, and with that a better chance of extracting shards for geochemical analyses; an essential prerequisite in establishing new links between Ireland and mainland Britain. At present therefore these tephrostratigraphic sectors of the British Isles remain disparate, nevertheless these findings add important information to the understanding of LGIT tephra distributions in the British Isles.

Chapter 10. A Revised Tephrostratigraphy for Scotland

10.1 Introduction and chapter structure

Tephrochronology provides a unique means of linking, dating and correlating geological, palaeoenvironmental, and archaeological sequences with a greater chronological control than is typically available for late Pleistocene and early Holocene sedimentary records (Lowe 2011; Lowe et al. 2015). It is essential therefore that reliable tephrostratigraphies are developed, which ensure confident correlations and minimise uncertainties. If this is not achieved, inaccurate stratigraphic alignments can lead to the development of imprecise age estimates for both tephra horizons and for stratigraphic sequences, inherently leading to erroneous conclusions concerning palaeoenvironmental or palaeoclimatic processes and events.

This chapter outlines and reviews the recent developments in the tephrostratigraphy of Scotland during the LGIT (ca. 16-8 cal. yrs BP), and considers the importance and palaeoenvironmental significance of this research in a broader European context. Emphasis is placed on the results which have arisen from this study, but discussion also includes a host of published and unpublished works, conducted prior to, and during the course of this project.

The chapter is divided into four main sections. Firstly the role of tephrostratigraphic refinement in tephra studies is considered, and how different sampling strategies can impact the number of tephras identified. Secondly, these refinement issues are considered in the context of existing research and the overall effect this has had on the spatial disparity of tephras in Scotland and NW Europe. Thirdly a tephrostratigraphic framework for Scotland is presented, before finally, a section addressing fundamental questions that continue to hamper tephrostratigraphic developments in NW Europe, as well as tephrostratigraphy as a discipline. Sections of this chapter are quoted verbatim from Timms et al. (2016).

10.2 Tephrostratigraphic refinement

This study marks the first attempt to apply a contiguous (1 cm) resolution sampling strategy to multiple sites within the Scottish Lateglacial and early Holocene. Methods for extracting, quantifying and chemically analysing cryptotephras have undergone a progressive evolution in the decades since their first application, with studies reforming procedures which have been shown to have detrimental or undesired affects (e.g. Froggatt 1992; Hunt and Hill 1993; Blockley et al. 2005). By comparison, sampling resolution and the methods by which horizons are prioritised for chemical analyses

have not been through this same iterative development. As a consequence, these steps have remained *ad hoc*, subjective, and untested in terms of the impact they have on resolving tephrostratigraphies. At present, the best methods for detecting and quantifying tephras held within minerogenic and organic substrates are destructive laboratory techniques (Gehrels et al. 2008; Davies 2015; see section 2.4.2). Unfortunately these procedures are time consuming, labour intensive, and thereby significant limiters on the volume of material that can be realistically examined in typical tephrostratigraphic studies.

An approach that has found favour amongst the cryptotephra community to minimise these issues is the 'scan and resample' or 'rangefinder' technique (e.g. Pilcher and Hall 1992; Langdon and Barber 2004; Lane et al. 2014; Davies 2015). This approach, where 5-10 cm scan or 'rangefinder' samples serve as a preliminary investigative tool, are used to establish the approximate depth of peak shard concentration, before a refinement of the peak is conducted at a higher (typically 1 cm) resolutions, and chemical analyses of the peak is conducted. This approach, advocated for its efficiency in covering stratigraphic sections with reduced effort, inherently focuses the operator to primarily consider the largest peaks as a priority over the occurrence of more minor, or less well expressed tephras. As a consequence of this, less prominent peaks are frequently explained as reworked isochrons, or deemed unviable for chemical characterisation because of comparatively low concentrations (e.g. Bourne et al. 2015; Matthews et al. 2015; Mithen et al. 2015; Mackay et al. 2016).

Studies at Loch Laggan (MacLeod 2008) and Abernethy Forest (Matthews et al. 2011) have demonstrated that targeted and contiguous high resolution sampling, i.e. at 1 cm or higher, can provide a more coherent and complex narrative to the history of volcanic events deposited during the Scottish Lateglacial and early Holocene than has been appreciated hitherto. By taking this 'targeted' approach and applying it to complete stratigraphic sequences, the results from Tanera Mòr, Spretta Meadow, Crudale Meadow and Quoyloo Meadow clearly demonstrate the tephrostratigraphic complexity that can beset such sites, and further illustrates that the tephrostratigraphy of Scotland and of NW Europe is yet to be fully resolved. The results from these sites also specifically highlight the limitations and inadequacies of current sampling and refinement protocols, whilst also illustrating the level of complexity that can be reliably deciphered, given sufficient time and resources. Outlined below are examples from each of the four aforementioned sites, where contiguous high resolution sampling and chemical characterisation took place, and how these results may have differed if the study had been conducted at lower, more 'standardised' sampling resolutions.

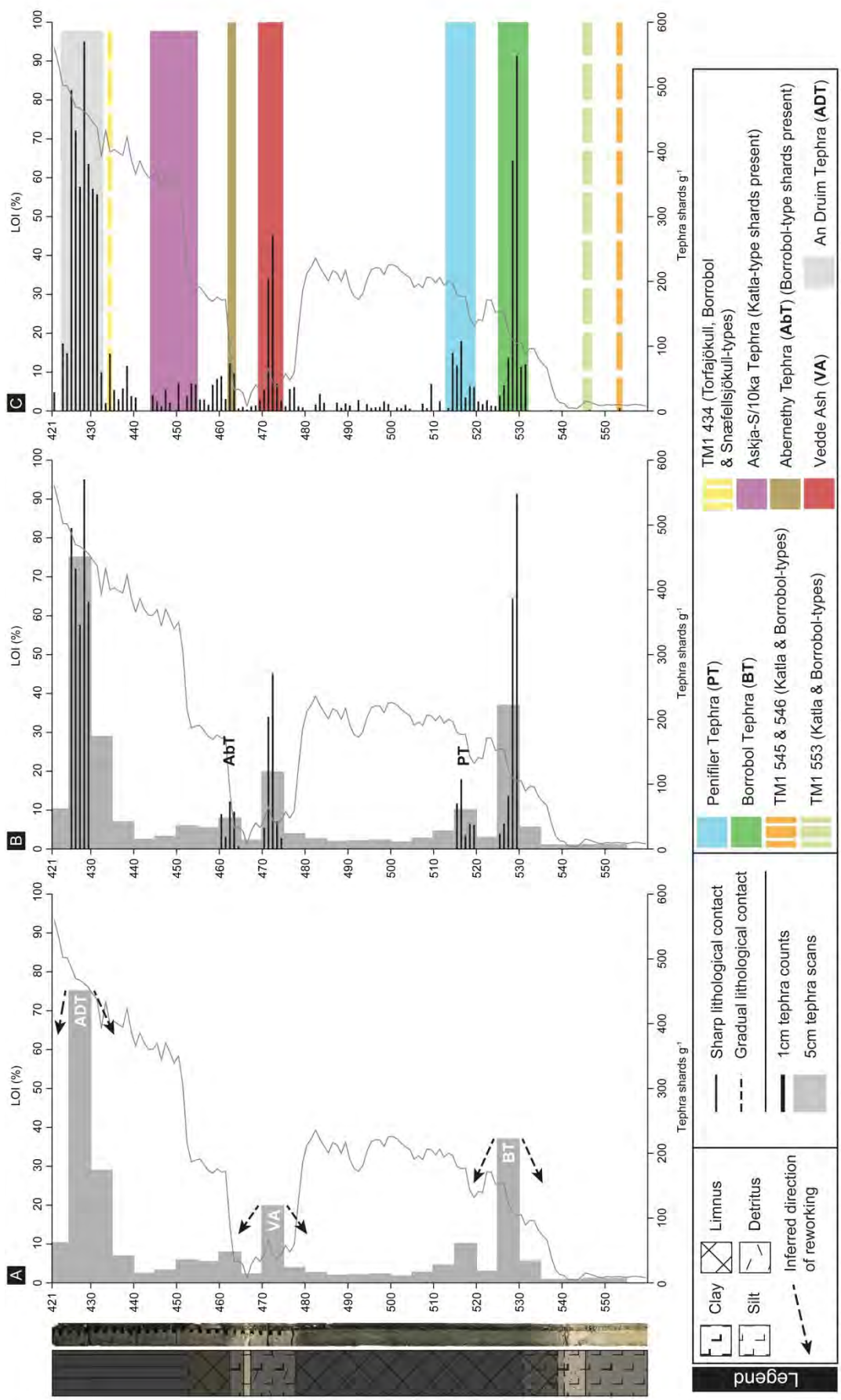

Figure 10.1 The Tanera Mor sequence at various phases of tephrostratigraphic refinement. (A) Sequence resolved to a typical 5 cm scan sample resolution. (B) Peaks in concentration identified in the 5 cm scans refined to a 1 cm resolution. (C) Complete refinement of the stratigraphic profile at a 1 cm resolution.

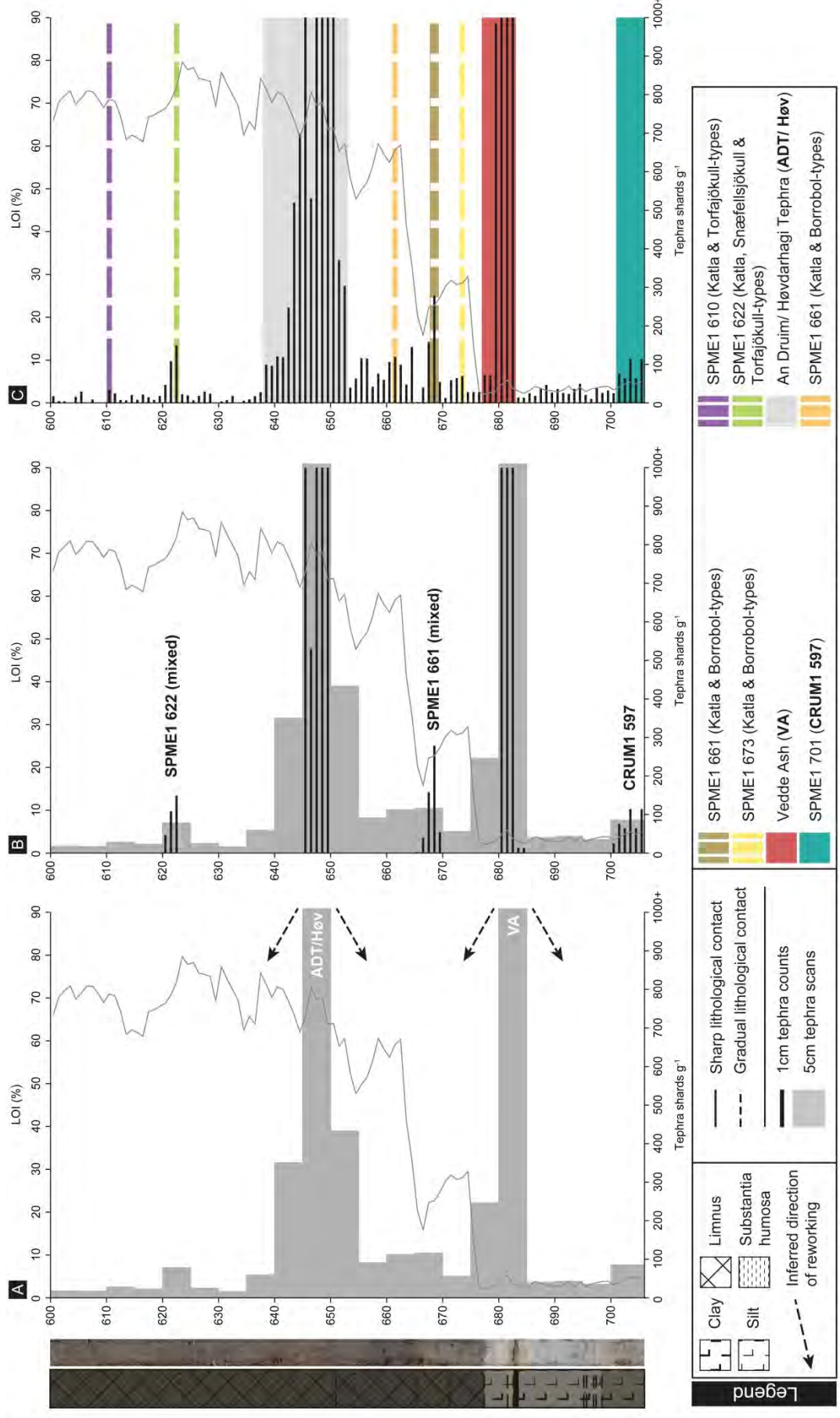

Figure 10.2 The Spretta Meadow sequence at various phases of tephrostratigraphic refinement. (A) Sequence resolved to a typical 5 cm scan sample resolution. (B) Peaks in concentration identified in the 5 cm scans refined to a 1 cm resolution. (C) Complete refinement of the stratigraphic profile at a 1 cm resolution.

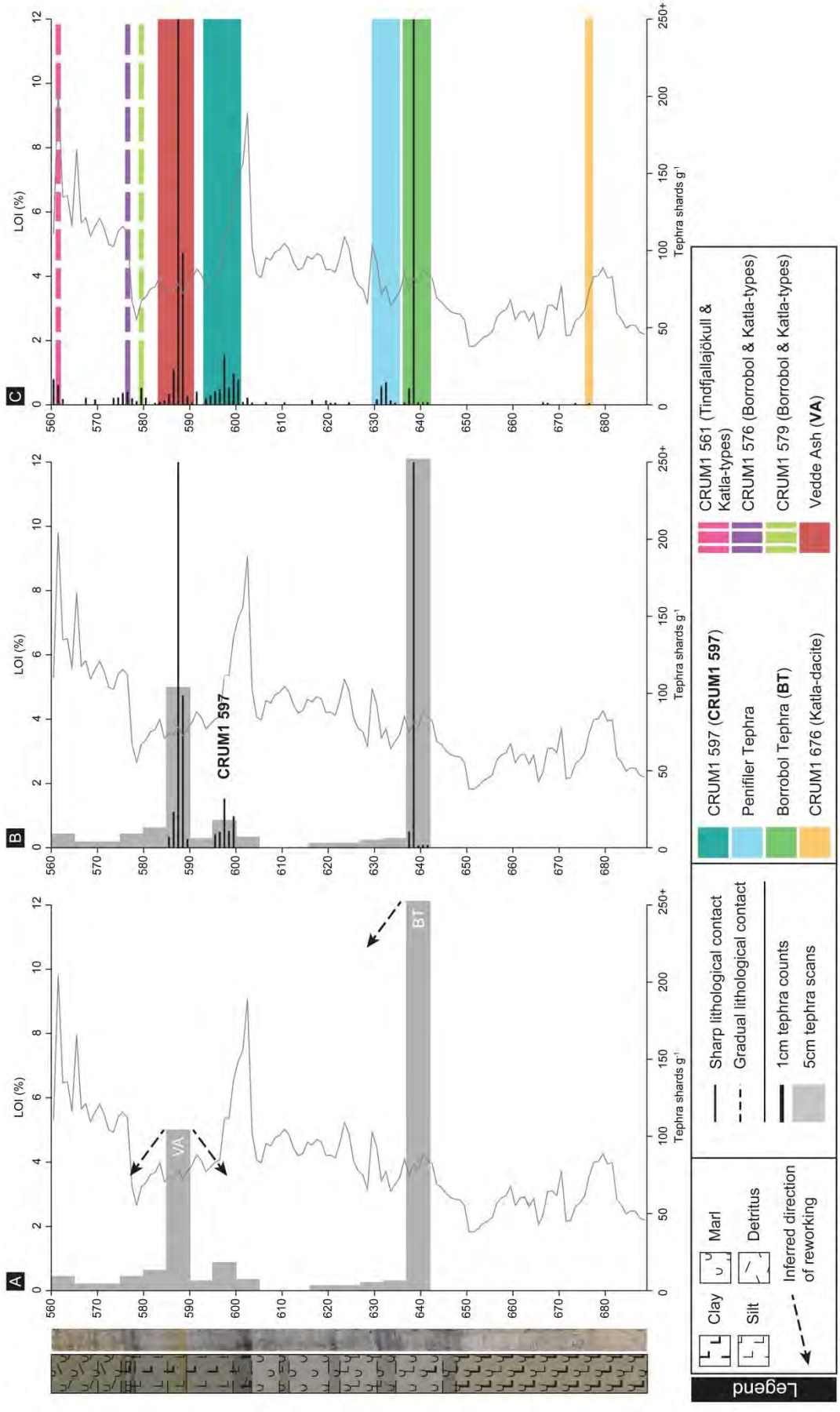

Figure 10.3.1 The Crudale Meadow lateglacial sequence at various phases of tephrostratigraphic refinement. (A) Sequence resolved to a typical 5 cm scan sample resolution. (B) Peaks in concentration identified in the 5 cm scans refined to a 1 cm resolution. (C) Complete refinement of the stratigraphic profile at a 1 cm resolution.

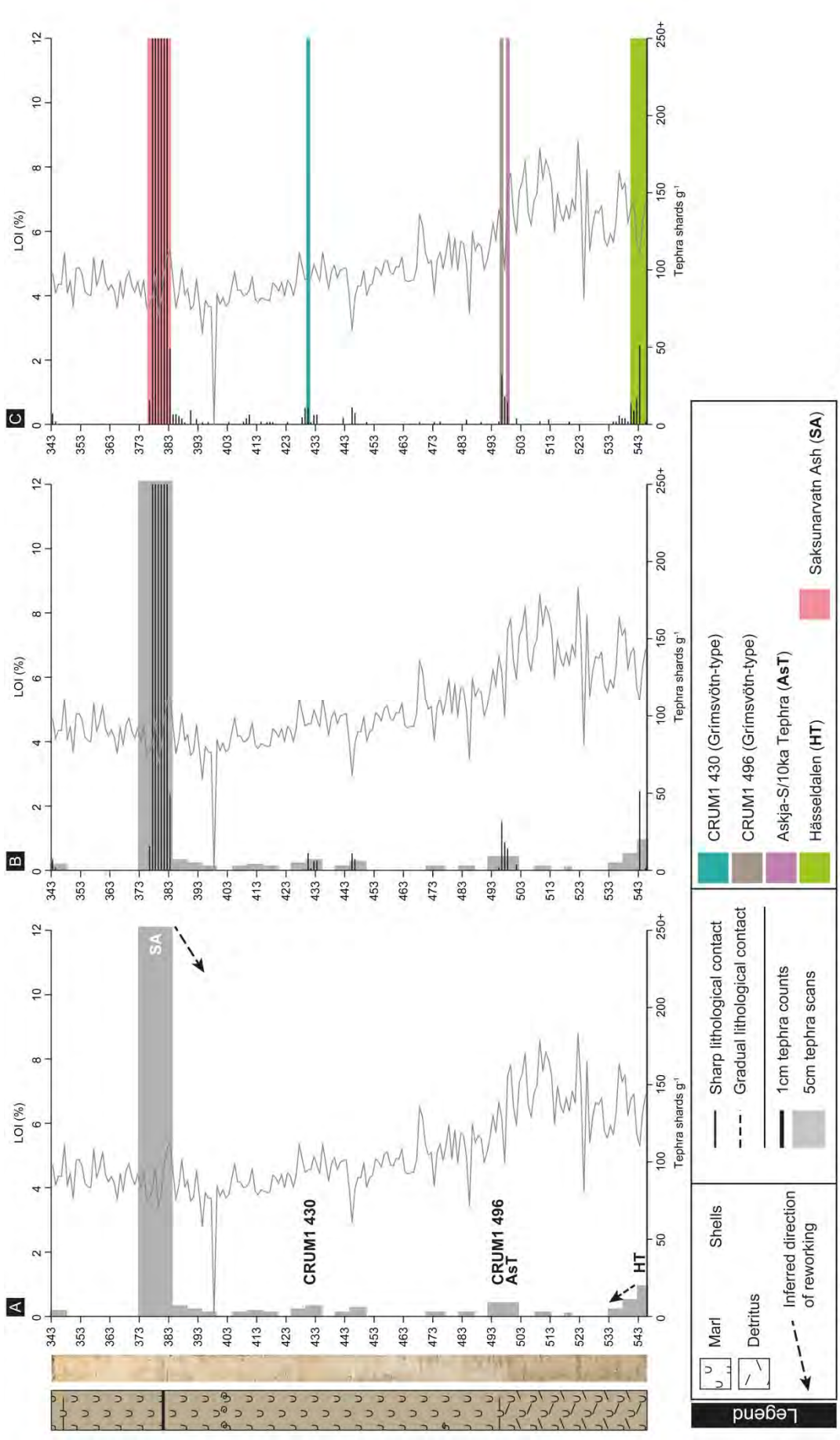

Figure 10.3.2 The Crudale Meadow Holocene sequence at various phases of tephrostratigraphic refinement. (A) Sequence resolved to a typical 5 cm scan sample resolution. (B) Peaks in concentration identified in the 5 cm scans refined to a 1 cm resolution. (C) Complete refinement of the stratigraphic profile at a 1 cm resolution.

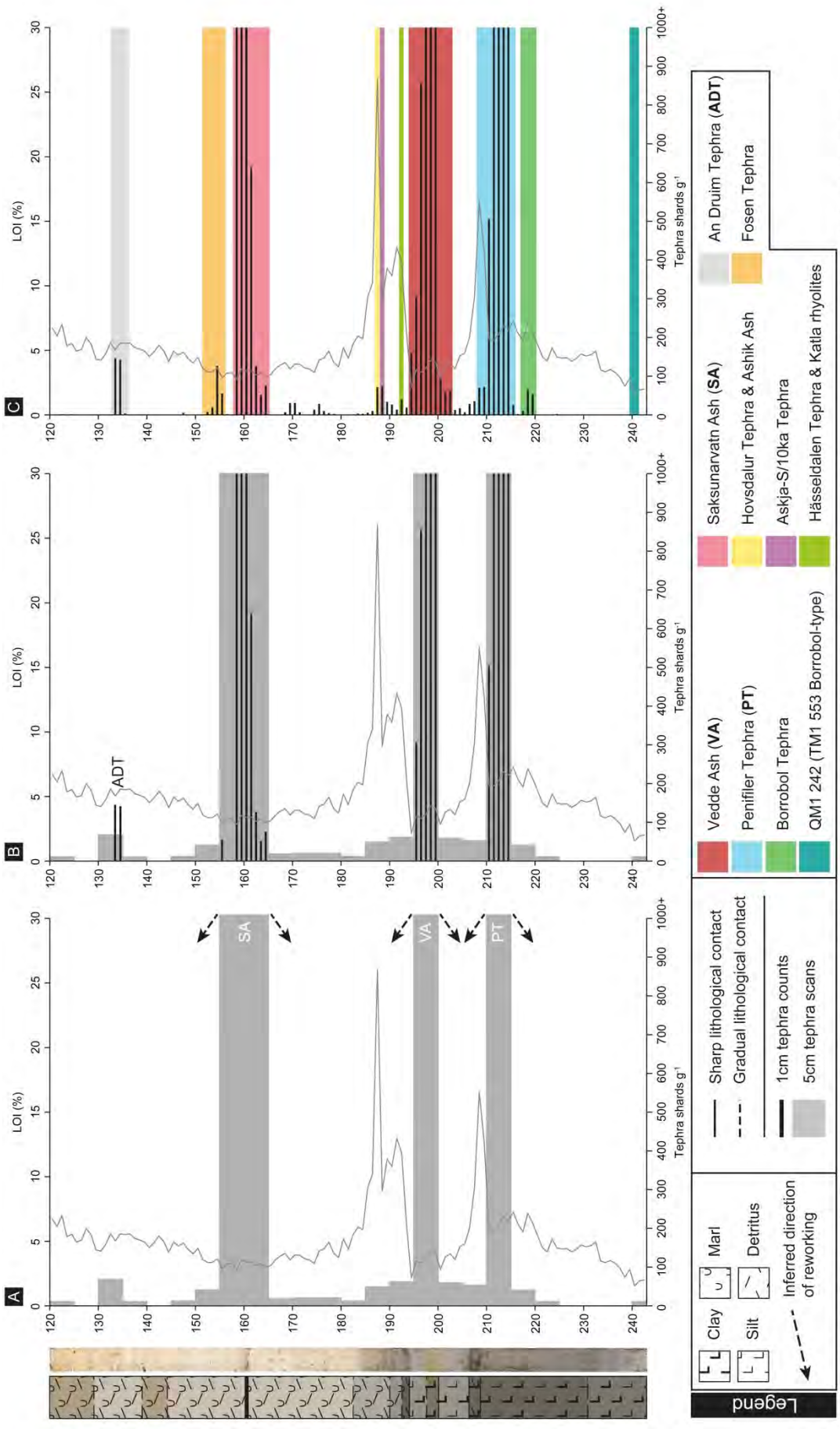

Figure 10.4 The Quoyloo Meadow sequence at various phases of tephrostratigraphic refinement. (A) Sequence resolved to a typical 5 cm scan sample resolution. (B) Peaks in concentration identified in the 5 cm scans refined to a 1 cm resolution. (C) Complete refinement of the stratigraphic profile at a 1 cm resolution.

10.2.1 High resolution sampling vs low resolution scanning

Figures 10.1, 10.2, 10.3.1, 10.3.2 and 10.4 illustrate the Tanera Mòr, Spretta Meadow, Crudale Meadow, and Quoyloo Meadow tephrostratigraphies at varying stages of refinement. Due to the length of the Crudale Meadow sequence, and the issues associated with the alignment of the Lateglacial and early Holocene portions of the core (see section 6.2.1), these have been divided and are shown in 10.3.1 and 10.3.2 respectively; the rest of the sequences are shown in their full extent. Table 10.1 shows the number of discreet tephra horizons and the number of mixed chemical assemblages that would have been identified within the four sequences following three different sampling strategies. These stages are: (A) a 5 cm resolution scanning strategy; (B) a 5 cm scan and 1 cm resolution resample strategy, and; (C) a contiguous 1 cm sampling of the whole sequence.

Stage (A) in Figure 10.1-10.4 is illustrative of the sequences had they been resolved using a 5 cm resolution scanning method only. It is evident that pursuit of this approach would have produced tephrostratigraphic profiles, that are dominated by few, large scale or highly concentrated tephra horizons (Table 10.1). At Tanera Mòr these horizons are the Borrobol Tephra, the Vedde Ash and the An Druim Tephra; at Spretta Meadow these are the Vedde Ash and the Ashik Tephra horizon; at Crudale Meadow the sequence is dominated by the Borrobol Tephra, the Vedde Ash, and the Saksunarvatn Ash; and at Quoyloo Meadow, the Penifiler Tephra, the Vedde Ash, and the Saksunarvatn Ash predominate. It is clear that the most ubiquitous and common tephras found in these sequences, i.e. the Borrobol Tephra, the Vedde Ash, and the Saksunarvatn Ash, are also amongst the most frequently found within Scottish and NW European tephrostratigraphies (see section 2.8 and 3.2).

Following standard protocols, and refining the peaks of this scan phase to a 1 cm resolution, would have resulted in the tephrostratigraphic profiles as illustrated as stage (B) in Figures 10.1-10.4. In these instances, minor horizons that occur inbetween or in close proximity to the larger peaks, have also been refined to 1 cm, although this is not always conducted as a standard procedure (see section 10.2.2). As highlighted above, these more minor peaks are often interpreted or disregarded as a reworking, and/or an amalgamation of tephra derived from the neighbouring major horizons; this is indicated by the dashed arrows spreading away from the larger peaks in Figure 10.1-10.4 stage (A). Nevertheless, the additional tephras that would have been revealed in this instance by a targeted high resolution re-sampling are: at Tanera Mòr, the Penifiler and Abernethy Tephras; at Spretta Meadow, a basal Borrobol-type horizon (SPME1 701); at Crudale Meadow, the late Interstadial Borrobol-type horizon (CRUM1 597), the

Table 10.1 Tephrostratigraphic summary of the four main sites examined in this thesis. The three different refinement methods show how many tephras could be reliably identified at each stage. In this instance a *discreet tephra* is defined as a clear peak with more than 50 % of the main analyses correlating to a known tephra horizon or volcanic source. A *mixed assemblage* in this instance is defined by the most numerate population comprising 50 % or less of the total number of chemical analyses, or sufficient doubt exists as to the isochronous nature of the deposit. As can be observed a greater number of both discreet and mixed horizons can be identified with finer levels of stratigraphic refinement.

	5 cm scan phase		5 cm scan phase + 1 cm targeted sampling		1 cm contiguous sampling	
Site	Discreet tephras	Mixed assemblage	Discreet tephras	Mixed assemblage	Discreet tephras	Mixed assemblage
Tanera Mor	3	0	5	0	6	3
Spretta Meadow	2	1	3	2	3	4
Crudale Meadow	3	0	8	0	10	3
Quoyloo Meadow	4	0	4	0	11	2
Average	3	0.25	5.25	0.25	7.5	3

Hässeldalen Tephra, the Askja-S/10ka Tephra, and two uncorrelated Grímsvötn eruptions (CRUM1 496, CRUM1 430); and at Quoyloo Meadow the An Druim Tephra would have been identified (Figure 10.4; Table 10.1). In total therefore, following standardised scan and resample strategies, the Tanera Mòr sequence would be characterised by five tephras, Spretta Meadow by three tephras, Crudale Meadow by eight tephras, and Quoyloo Meadow by four tephras (Table 10.1).

It is evident, however, that this level of tephrostratigraphic refinement underestimates the total number of tephras that have been identified within these stratigraphies (Figure 10.1-10.4 stage C). By applying contiguous, high resolution sampling at the four sites, and by systematically analysing major and minor peaks, on average, two additional discrete tephra layers were identified per site (Table 10.1).

At Tanera Mòr and Crudale Meadow, high resolution sampling through the Dimlington Stadial-aged sediments at the base of the sequence has successfully identified discreet and amalgamated populations of shards. The concentration of these horizons are exceptionally low, and on occasion <1 shard g^{-1} dry weight. With coarser sampling, it is doubtful that these horizons would have been detected. Scan sampling is also likely to have had a detrimental impact on the results obtained from Windermere-aged deposits at Quoyloo Meadow and Crudale Meadow. Contiguous sampling though these intervals has revealed the presence of three horizons exhibiting Borrobol-type chemistries. At lower resolutions only two horizons would have been revealed in the Crudale Meadow sequence (Figure 10.3.1), whilst only a single horizon would have been identified at Quoyloo Meadow (Figure 10.4). Due to the indistinguishable major element signature that is common for all Borrobol-type tephras, underestimating the total number of these horizons would likely have led to miscorrelations within the site (see section 10.2.2), and ultimately to the development of erroneous age-depth models.

Whilst sampling resolution plays a key role in identifying additional tephra isochrones, positive results have also been obtained from the contiguous chemical characterisation of diffuse tephra profiles at several sites. At Quoyloo Meadow, consecutive sampling has identified three tephras in a 2 cm interval. Analysis of QM1 187 and QM1 188 identified a conflated occurrence of the Hovsdalur and Ashik in the former, and the Askja-S/10ka Tephra as a distinct isochron in the latter. Therefore, by preparing several intervals of a tephra horizon for chemical analyses, additional discriminatory data may be obtained. Contiguous chemical profiling has also revealed that reworking and conflation of tephra horizons is much more common than previously suggested

(Figure 10.1-10.4). The occurrence of such is likely to be related to a host of taphonomic processes, and confirms that in reality, tephrostratigraphies are 'messy' entities, prone to taphonomic processes as much as any other environmental proxy (e.g. Pyne-O'Donnell 2005; 2011; Zalwana-Geer et al. 2016).

The realisation and acceptance of 'messy horizons' is an important development in tephrostratigraphic studies. Detailed measurements of conflated or mixed horizons can provide information about the mobility and residence time of tephras on the landscape, and how long shards may remain available for catchment and basin recycling. Diffuse tephra profiles may also inform researchers about the likelihood of displacement and mobility of other proxy indicators. It is evident in all sites presented here, that Katla-type shards are deposited within the early Holocene sediments well after the deposition of the Vedde Ash or Abernethy Tephra (Figure 10.1-10.4). This is also evident for Borrobol-type tephras, which like the Katla-type horizons appear to have a presence within early Holocene stratigraphies, despite the passing of several millennia since their initial deposition. This may have significant implications for the successful identification and discrimination of any tephra that stratigraphically follows a horizon of the same chemical signature e.g. the Borrobol/Penifiler/Fosen tephras, Vedde Ash/Abernethy Tephra, the Ashik/ An Druim/ Høvdarhagi tephras. If shards are preserved in the landscape or can be easily re-mobilised by basin or catchment-wide processes, such an occurrence may provide a false 'eruption' signal (see section 10.3.3). Whilst potentially problematic for the reliable distinction of these tephras, this process does allow greater insight into catchment and basin dynamism, and should in theory also allow a more objective assessment to be made concerning potential taphonomic processes and the reliability of any accompanying environmental and palaeoclimatic data.

Widespread heterogeneous shard populations masking discreet horizons, further supports the argument that peak shard sampling, in many instances, does not characterise the entire tephra population. In cryptotephra studies, where variable shard concentrations have been shown to occur across closely spaced sites and within the same basin (e.g. Boygle 1999; Pyne-O'Donnell 2011; Watson et al. 2015), there is now a genuine uncertainty that peak shard characterisation as defined by scan sampling is truly representative of the entire suite of tephras preserved within a stratigraphic sequence. The current scan and resample method is likely to be too crude to discriminate multiple events that deposit low shard concentrations and/or that might cause overlap/mixing of the ashes within a palaeoenvironmental record. Examples of this might include: 1) high frequency eruptions; 2) low magnitude volcanic events; 3)

short duration events; 4) events where ash clouds only partially cover a region; or 5) where sedimentation rates are low and hence encourage the conflation of horizons. With the discovery of trans-Atlantic tephras in Northern Europe (Jensen et al. 2014), the methodological predisposition to focus on larger events may be masking the subtleties of both relatively low-concentration ultra-distal tephras, and smaller-scale, 'local' volcanic events. The method is one that promotes coverage over detail, and incomplete refinement of the stratigraphic record is often the result. It is a technique, therefore, which has likely contributed to an artificial disparity and a perceived irregularity in the tephra record between the British Isles and NW Europe.

Following these themes, it may be necessary for future studies to devise and implement more refined sampling strategies, and/or more appropriate site specific strategies. It has become evident during this study that a 1 cm sampling resolution is insufficient in some circumstances to fully resolve tephrostratigraphies, and to confidently assign the position of isochrons when a conflation of tephras occurs e.g. the Katla-type and Snæfellsjökull-type shards in QM1 192. Higher sampling intervals of 0.5 cm and 0.1 cm have previously been applied to LGIT aged tephrostratigraphies (e.g. MacLeod 2008; Matthews et al. 2011; Pyne-O'Donnell 2011). Applying these techniques to sequences exhibiting low sedimentation rates such as Quoyloo Meadow, may help to decipher the superposition and hence chronostratigraphic placing of tephras that fall within 1 cm samples. However, whilst these studies have shown that the quantification of tephra is possible at very high resolutions, this has not been matched consistently by the resolution of chemical analyses. It is this factor which needs to be addressed if the conflation of closely-spaced tephras is to be fully resolved. However, with existing laboratory techniques it may not be feasible to sample contiguously and chemically analyse tephras at such high resolutions, especially when studies are limited by factors including the finite availability of sediment, time, as well as financial considerations. To counter this problem of conflation, it may be appropriate for future studies to instead focus on longer sequences with naturally higher sedimentation rates. In doing so this should enable a clear stratigraphic distinction between horizons, thereby avoiding this issue. However, accessing longer sequences may not always be feasible with standardised coring equipment, and may instead require specialist extraction equipment. At present, therefore, it would seem that refinement of crypto-tephrostratigraphic records has reached a limit as defined by methodological, technological and site specific constraints.

10.2.2 Implications for existing tephra records in Scotland

Considering the above discussion, it is necessary to evaluate the existing tephra sites in Scotland, and their potential for further tephrostratigraphic refinement. Twenty-four tephra records spanning the LGIT have been published from this region, with a further fifteen unpublished locales characterised in Undergraduate, Masters, and PhD projects from studies conducted at Royal Holloway and, in one instance, the University of Exeter. Table 10.2 lists these sites, and provides information of the chronostratigraphic extent of the site, the level of refinement that has been applied, the tephras that have been found, and how these have been correlated i.e. by geochemical or stratigraphic means. It should be noted that this table incorporates those studies which have been conducted during the course of this project, and so differs from that presented in Chapter 3 (Table 3.1).

The sites containing the greatest number of discrete and correlatable tephras are: Quoyloo Meadow (n=11; this study), Crudale Meadow (n=10; this study), Loch Ashik (n=7; Davies et al. 2001; Pyne O'Donnell 2007; Brooks et al. 2012); Tanera Mòr 1 (n=6; this study) and Loch an t'Suidhe (n=6; Roberts 1999; Davies 2003; Pyne O'Donnell 2007). These five sites have either been sampled contiguously and analysed at high resolution i.e. Quoyloo Meadow, Crudale Meadow and Tanera Mòr, or as is the case of Loch Ashik and Loch an t'Suidhe have been subject to repeated examination by a number of authors, including the seminal tephro-taphonomy work of Pyne-O'Donnell (2005; 2011; Table 10.2). These sites stand out as having an unusually high number of tephra isochrones, which is partly due to the sediments from these basins being examined to their fullest temporal extent i.e. sediments relating to the Windermere Interstadial, the Loch Lomond Stadial, and the early Holocene. In contrast, many of the other sites listed in Table 10.2 have been subject to more selective tephrostratigraphic refinement i.e. only one or two chronostratigraphic zones have been scrutinised. Given the number of tephras that are routinely found in sequences across NW Europe, and the findings of this study, it is highly probable that the number of tephras identified in many Scottish sequences only represents a small proportion of the horizons present.

Table 10.2 Complication of published and unpublished LGIT aged tephra sites in Scotland. The number of tephras is based on the number of discreet and reliable isochrons. In the sites presented in this study there are several mixed assemblages of shards, and at present these are not considered distinct or reliable enough to be included here. The green background in the four chronostratigraphic columns signifies that sediments relating to the respective zones exist, whilst the crosses illustrate whether a tephrostratigraphic study has been undertaken in the interval.

EH = early Holocene, LLS = Loch Lomond Stadial, WI = Windermere Interstadial, DS = Dimlington Stadial, (v) = visible/macrotephra, (b) = basaltic fraction present, ? = uncertainty with the correlation.

Site	Chronozone				Tephra(s)	Number of tephras	Chemistry	Super-position	Level of refinement	Reference
	EH	LLS	WI	DS						
Dallican Water	x				Saksunarvatn	1	x		1 cm contiguous	Bennett et al. 1992
Loch of Benston	x				Saksunarvatn (v)	1	x		direct sampling of macrotephra	Bondevik et al. 2005
The Loons		x	x		Loons 350 (no geochem), Vedde, Loons 427 (Borrobol-type)	3	x		5 cm scan and resample	Callicott 2015 unpublished MSc
Quoyloo Meadow 94'	x				Saksunarvatn	1	x		1 cm contiguous	Bunting 1994
Quoyloo Meadow	x	x	x		An Drium, Fosen, Saksunarvatn(v), Hovsdalur, Ashik, Askja-S/10ka, Hässeldalen, Vedde(b), Penifiler, Borrobol, QM1 242 (Borrobol-type)	11	x		1 cm contiguous	Timms et al. 2016; this study
Crudale Meadow 94'	x				Saksunarvatn	1	x		1 cm contiguous	Bunting 1994; Whittington et al. 2016
Crudale Meadow		x	x	x	Saksunarvatn(v), CRUM1 430 (Grímsvötn), CRUM1 496 (Grímsvötn), Askja-S/10ka, Hässeldalen, Vedde(b), CRUM 597 (Borrobol-type), Penifiler, Borrobol, CRUM1 679	10	x		1 cm contiguous	this study

					(Katla dacite)					
Spretta Meadow	x	x			Fosen; Hovsdalur; Ashik; Vedde(v,b), SPME1 701 (Borrobol-type)	5	x		1 cm contiguous	this study
Lochan An Druim	x	x	x		An Druim, S20 (no geochem), Vedde, S30 (Borrbol-type)	4	x		5 cm scan and resample	Ranner et al. 2005
Borrobol 97'		x	x		Saksunarvatn (no geochem) Vedde, Borrobol	3	x	x	5 cm scan and resample	Turney et al. 1997; Turney 1998a
Borrobol 07'		x	x		Penifiler, Borrobol	2	x		5 cm scan and resample	Pyne O'Donnell 2007; Pyne O'Donnell et al. 2008
Borrobol 16'		x	x		Vedde (no geochem), Penifiler, Borrobol	3	x	x	5 cm scan and resample	Lind et al. 2016
Tanera Mòr 1	x	x	x	x	An Druim, Askja-S/10ka, Abernethy, Vedde, Penifiler, Borrobol, TM1 9 545 (Katla-Borrobol mix), TM1 9 546 (Katla-Borrobol mix), TM1 9 553 (Katla-Borrobol mix)	6	x		1 cm contiguous	this study
Tanera Mòr 2 97'		x	x		Vedde, Borrobol	2	x		selected 1 cm resolution	Roberts 1997; Wastegård et al. 2000a
Tanera Mòr 2		x	x	x	Vedde, Penifiler (no geochem), Borrobol (no geochem), Dimna	4	x	x	5 cm scan and resample	Weston 2012
Eilean Fada Mòr			?	?	Three intervals of tephra with 'Borrobol type' morphologies	3?			5 cm scan and resample	Callicott 2013 unpublished BSc
Priest Island		x	x	x	Vedde (no geochem), Penifiler, Borrobol, PRI 700 (Borrobol-type), PRI 756 (no geochem), PRI 811 (no geochem)	6?	x	x	5 cm scan and resample	Valentine 2015
Druim Loch	x	x	x		Ashik (b), Vedde, Penifiler	3	x		5 cm scan and resample	Dadswell 2002; Pyne O'Donnell 2005; Pyne

										O'Donnell 2007; Pyne O'Donnell et al. 2008
Loch Ashik	x	x	x		Breakish, Saksunarvatn, LAS-a4 339, Askja-S/10ka (unpublished), Ashik (b), Vedde(v,b), Penifiler, Borrobol	7	x		5 cm scan and resample	Davies et al. 2001; Davies 2003; Matthews 2002; Pyne O'Donnell 2004; Pyne O'Donnell 2007; Pyne O'Donnell et al. 2008; Pyne O'Donnell 2011; Brooks et al. 2012
Kennethmont		x			Vedde	1	x		selected 1 cm resolution	Roberts 1997; Turney 1998a; Wastegård et al. 2000
Abernethy Forest	x	x	x		Abernethy, Vedde, Penifiler, Borrobol	4	x		0.5 cm contiguous	Matthews et al. 2011
Loch Laggan East	x				Suðuroy, SSn, An Druim/Ashik, Vedde? (no geochem)	3	x		1 and 0.5 cm contiguous	MacLeod 2008; MacLeod et al. 2015
Glen Turret Fan	x				Abernethy?	1	x		5 cm scan and resample	MacLeod et al. 2015
Glen Turret Bank	x				Askja-S/10ka, Abernethy/Vedde?	2	x		5 cm scan and resample	Carter-Champion 2015
Mishnish		x			Vedde	1	x		5 cm scan and resample	Davies 2003; Mackie et al. 2002
Loch Torr a'Beithe		x	x		Vedde, Penifiler (no geochem), Borrobol (no geochem)	3	x	x	5 cm scan and resample	Weston (unpublished PhD data)
Loch a'Beithe		x	x		Vedde (no geochem), Penifiler (no geochem), Borrobol (no geocehm)	3	x	x	5 cm scan and resample	Weston (unpublished PhD data)
Inverlair	x				An Druim, Askja-S/10Ka	2	x		5 cm scan and resample	Kelly et al. 2016
Loch Etteridge	x	x	x		Ashik/An Druim?, Abernethy, Vedde, Penifiler, Borrobol	5	x		5 cm scan and resample/1 cm contiguous	Albert 2007; Hardiman 2007; Lowe et al. 2008b; MacLeod et al. 2015; Kelly et al. 2016
Kingshouse 2	x				Askja-S/10ka, Abernethy/Vedde?	2	x		5 cm scan and resample	Stocker 2014; Mayfield 2015
Larig Mor 1	x				No tephra identified	0			5 cm scan and	Harding 2013

									resample	
Larig Mor 2	x				Abernethy/Hässeldalen? (no geochem), AnDruim? (no geochem)	2		x	5 cm scan and resample	Harding 2013
Drumochter	x				No tephra identified	0		x	5 cm scan and resample	Harding 2013
Feagour Channel	x				An Druim? (no geochem)	1		x	5 cm scan and resample	Harding 2013
Loch an t'Suidhe	x	x	x		Saksunarvatn? (no geochem), Ashik (no geochem), Vedde(b), LAS-1, Penifiler, Borrobol	6	x	x	5 cm scan and resample	Roberts 1999; Davies 2003; Pyne O'Donnell 2005; Pyne O'Donnell 2007; Pyne O'Donnell et al. 2008; Pyne O'Donnell 2011
Pulpit Hill		x	x		Ashik? (no geochem), Vedde, Penifiler (no geochem), Borrobol? (no geochem)	4?	x	x	5 cm scan and resample	Lincoln 2011
Straloch		x	x		Vedde	1	x		5 cm scan and resample	Maclachlan 2014
Tirinie		x	x		Vedde, Penifiler	2	x		5 cm scan and resample	Candy et al. 2016 in press
Tynaspirit West		x	x		Vedde, Penifiler, Borrobol	3	x		selected 1 cm resolution/ 5 cm scan and resample	Roberts 1997; Turney et al. 1997; Pyne O'Donnell 2007; Pyne O'Donnell et al. 2008
Lake of Menteith		?			Vedde?	1		x	unknown	Grosvenor 2009
Muir Park Reservior		x	x		Vedde, Penifiler, Borrobol	3	x		selected 1 cm resolution/ 5 cm scan and resample	Roberts 1997; Cooper 1999; Lowe and Roberts 2003; Brooks et al. 2016
Rubha Port an t-Seilich	x	x			Suðuroy, Borrobol-type/Hasseldalen?, AF555/Vedde?	3	x		5 cm scan and resample	Mithen et al. 2015
Whitrig Bog		x	x		Vedde, Penifiler (no geochem), Borrobol	3	x	x	selected 1 cm resolution/ 5 cm scan and resample	Turney et al. 1997; Pyne O'Donnell et al. 2008

Little Lochans	x	x	x	x	Very low concentrations (no geochem)	7?			5 cm scan and resample	this study
Howburn Farm		x			Vedde	1	x		5 cm scan and resample	Housley et al. 2014; Tipping in press

In order to test this hypothesis, scan sample data were collated from several of these sites, and compared against the intervals which had been chosen for high resolution refinement. Unfortunately in most instances this data was fragmentary, unavailable, or scanning had only been conducted at selective intervals. Complete stratigraphic data was however, available from the work of Pyne-O'Donnell (2005). Figure 10.5, 10.6 and 10.7 therefore depicts the various cores taken from Loch Ashik, Loch an t'Suidhe, and Druim Loch basins, as examined as part of Pyne-O'Donnell's (2005) PhD thesis.

In Figure 10.5-10.7, 1 cm counts are plotted against 5 cm scan samples, with the original tephra correlations of Pyne-O'Donnell shown in blue. Despite the detailed work conducted at these sites, and the level of taphonomic information obtained, it is evident there are numerous peaks within the scan samples that have not been refined (Figure 10.5-10.7). These unrefined 'peaks' have been identified with red arrows, and where appropriate, potential correlatives have been proposed. At Loch Ashik and Loch an t'Suidhe, there appears to be distinct evidence for a peak in tephra towards the end of the Windermere Interstadial that occurs between the Penifiler Tephra and the Vedde Ash (Figure 10.5; 10.6). At Loch an t'Suidhe this tephra has been named the LAS-1 (Davies 2003), but poor chemical analyses have prevented a robust correlation, or a more definitive conclusion being drawn about its origin. As noted in Chapter 5 and 6, some similarity can be drawn with the Borrobol-type tephras, meaning a correlation may be possible with the late Windermere Interstadial Borrobol-type tephras identified at Crudale Meadow (CRUM1 597), and Spretta Meadow (SPME 701), as well as an uncharacterised tephra at Loch Etteridge (LET-3) which exhibits morphological characteristics akin to the Borrobol-type tephras. The late Windermere Interstadial horizon was not pursued by Pyne-O'Donnell, who sought instead to understand the distribution and expression of the Penifiler Tephra, the Vedde Ash and the Ashik Tephra. However, this lack of refinement has meant that a potentially important marker horizon has gone largely unrecognised in Scottish sequences, despite its identification some thirteen years ago by Davies (2003). It also means that some of Pyne-O'Donnell's (2005; 2011) taphonomic conclusions may not be valid, as a miscorrelation of the Penifiler Tephra may have taken place with the late Interstadial Borrobol-type tephra at Loch an t'Suidhe, and Loch Ashik respectively. Problems with the stratigraphic distinction of these Borrobol tephra types is discussed further in section 10.3.3.2.

Similar tephrostratigraphic issues typify the early Holocene sediments across the three sites. Due to the nature of Pyne-O'Donnell's taphonomic project, it was necessary to investigate and correlate a large number of tephra horizons. However, temporal and

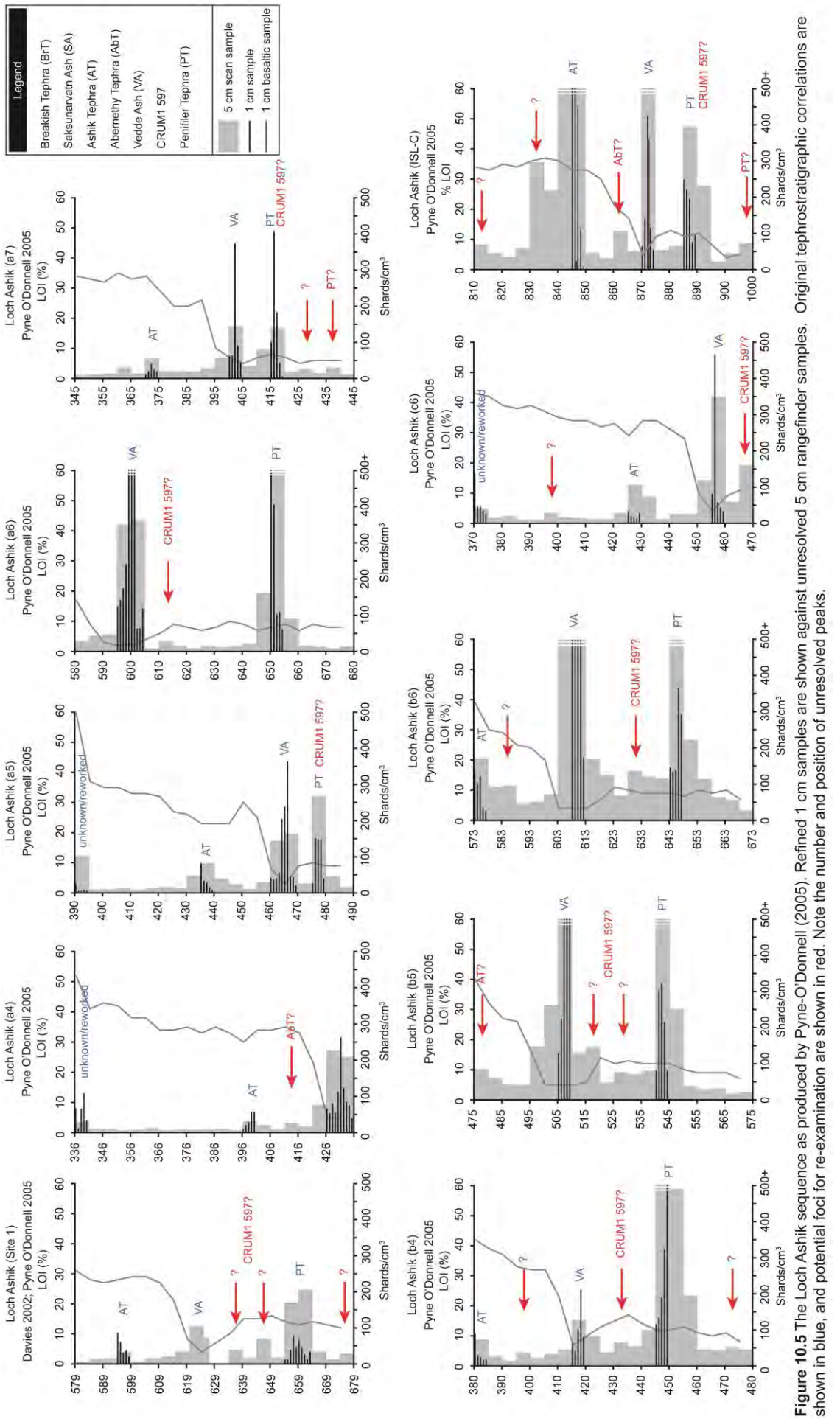

Figure 10.5 The Loch Ashik sequence as produced by Pyne-O'Donnell (2005). Refined 1 cm samples are shown against unresolved 5 cm rangefinder samples. Original tephrostratigraphic correlations are shown in blue, and potential foci for re-examination are shown in red. Note the number and position of unresolved peaks.

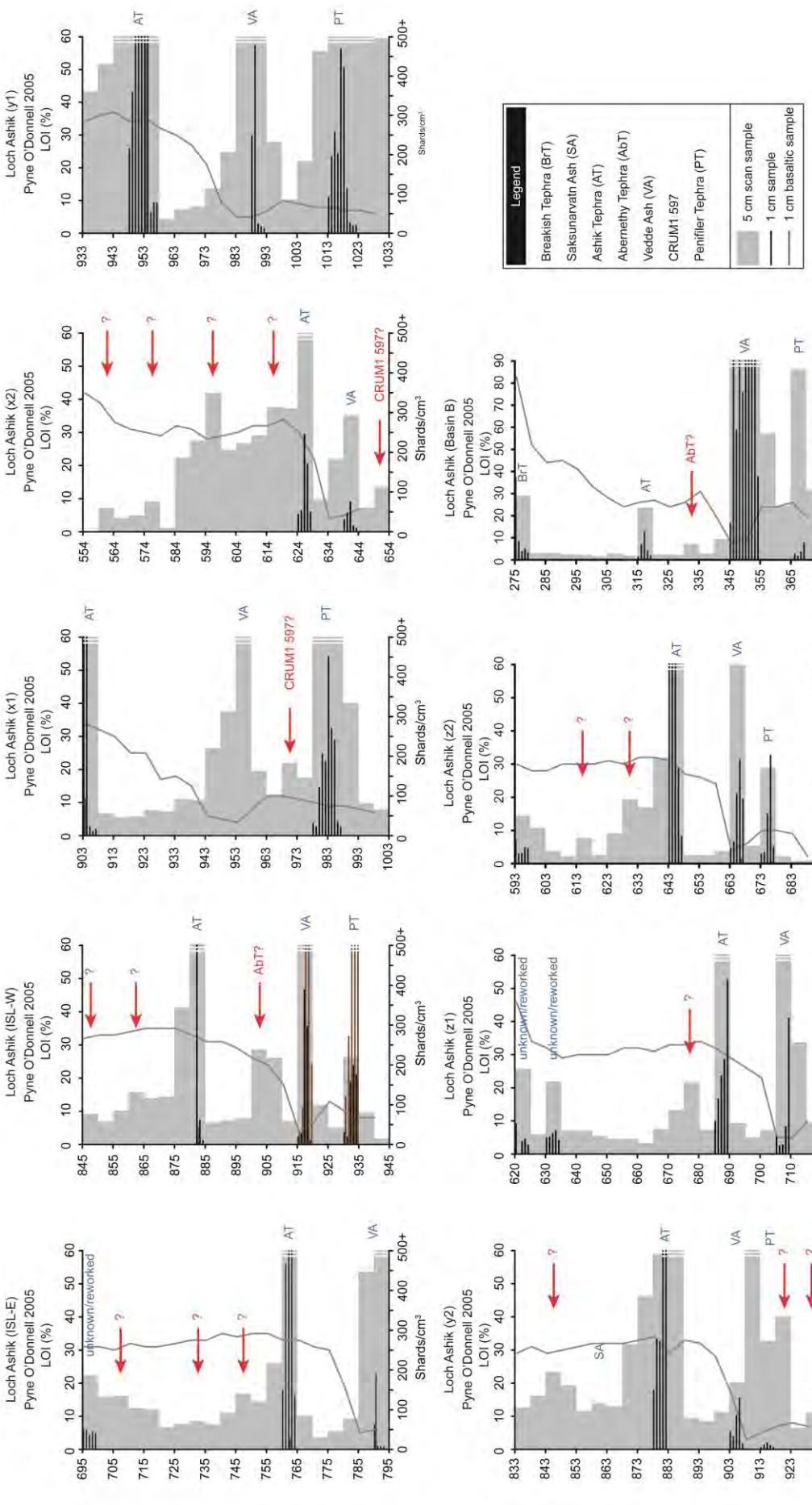

Figure 10.5 continued The Loch Ashik sequence as produced by Pyne-O'Donnell (2005). Refined 1 cm samples are shown against unresolved 5 cm rangefinder samples. Original tephrostratigraphic correlations are shown in blue, and potential foci for re-examination are shown in red. Note the number and position of unresolved peaks.

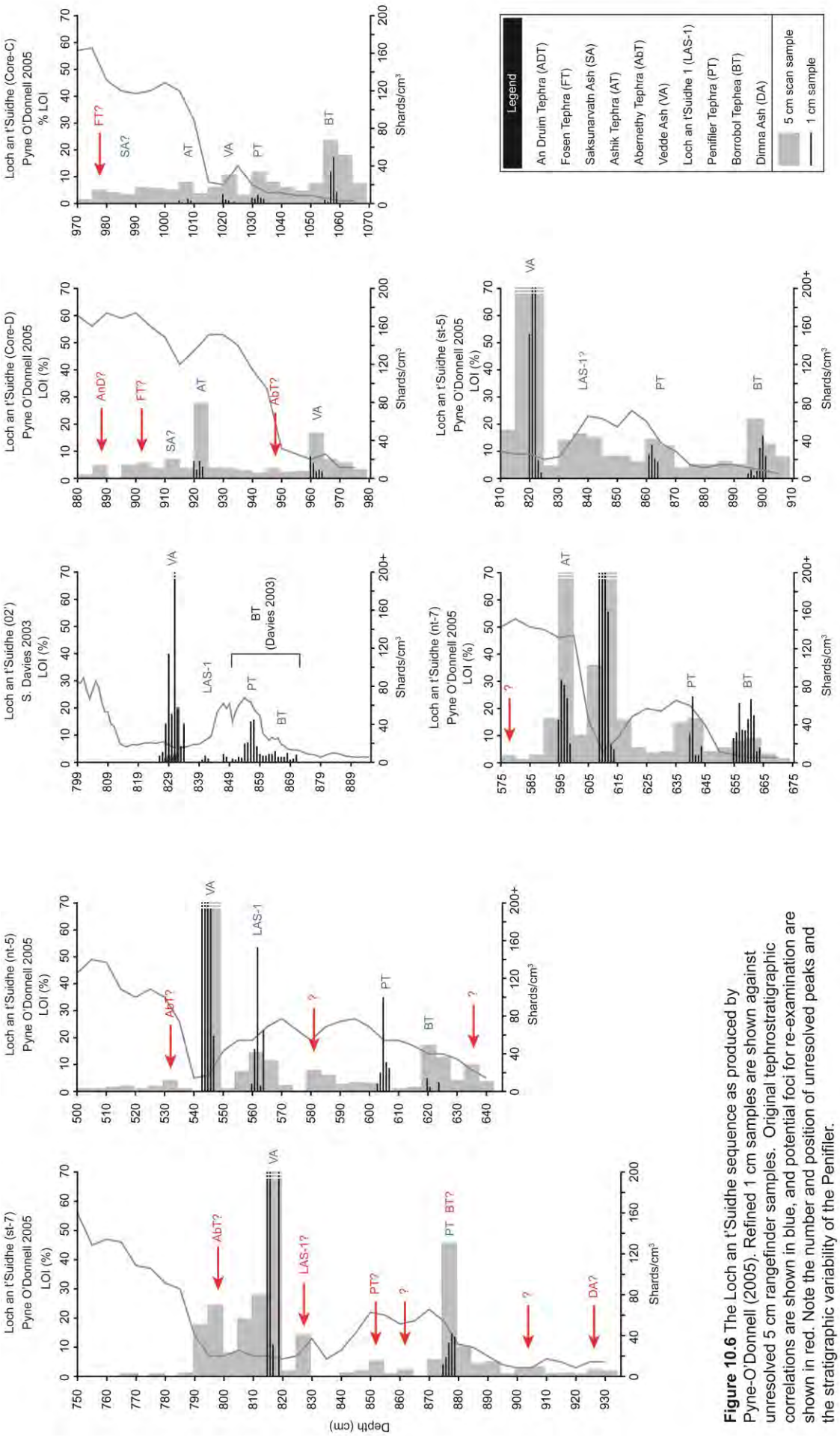

Figure 10.6 The Loch an t'Suidhe sequence as produced by Pyne-O'Donnell (2005). Refined 1 cm samples are shown against unresolved 5 cm rangefinder samples. Original tephrostratigraphic correlations are shown in blue, and potential foci for re-examination are shown in red. Note the number and position of unresolved peaks and the stratigraphic variability of the Penifiler.

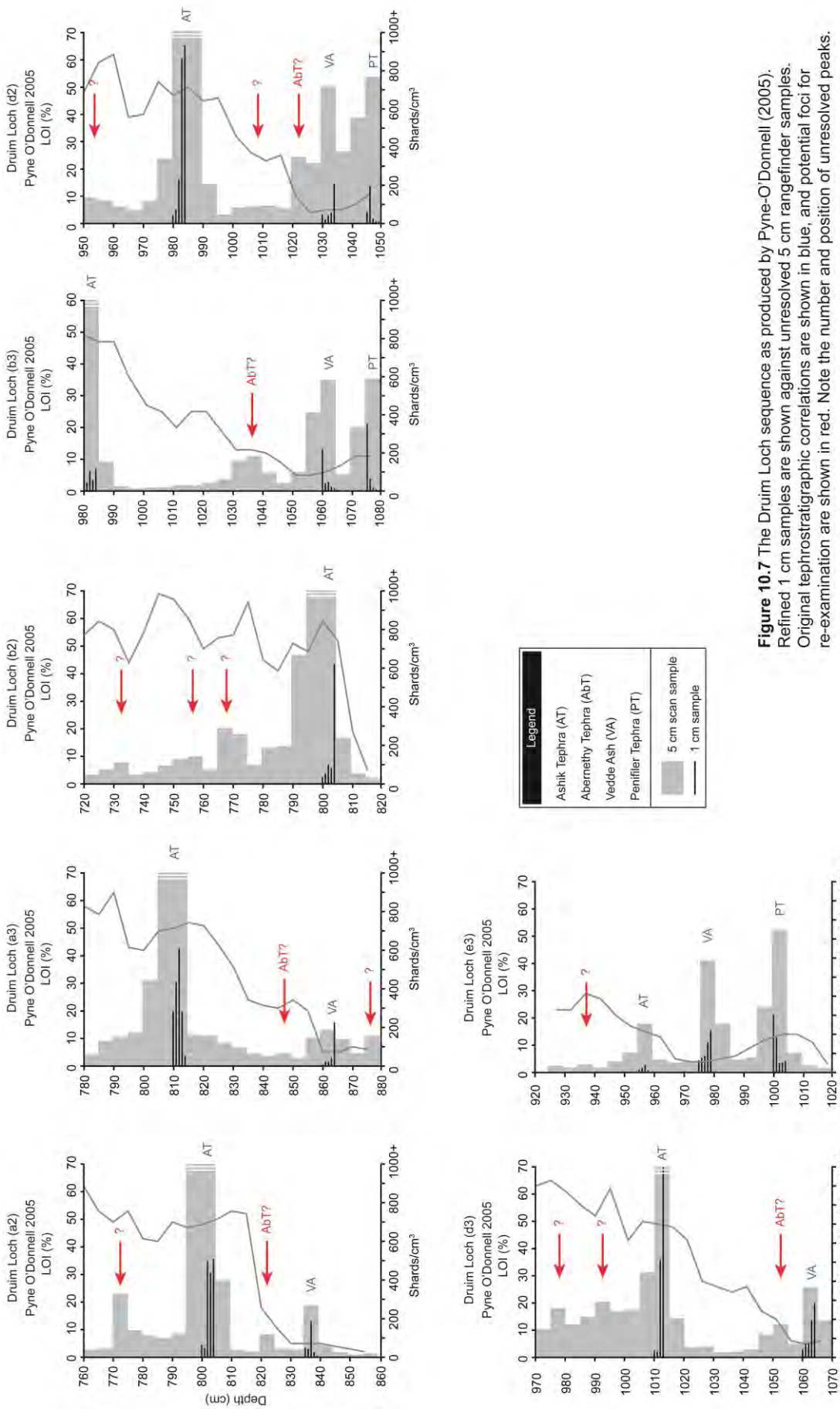

Figure 10.7 The Druim Loch sequence as produced by Pyne-O'Donnell (2005). Refined 1 cm samples are shown against unresolved 5 cm rangefinder samples. Original tephrostratigraphic correlations are shown in blue, and potential foci for re-examination are shown in red. Note the number and position of unresolved peaks.

financial constraints limited the applicability of chemical methods, thus stratigraphic superposition was favoured in most instances. Whilst seemingly robust at the time of completion, given the issues associated with the conflation of tephras and the propensity of mixed horizons identified in this study, some of the correlations and conclusions drawn by Pyne-O'Donnell (2005) may be erroneous. This is further evident given that the 5 cm sampling in all three sites, clearly depicts a consistent level of tephra throughout the Windermere and early Holocene. These findings closely agree with the scan results simulated in this study (Figure 10.1-10.4), and hence suggest that in order to fully resolve these tephrostratigraphies, it is necessary that a contiguous high resolution sampling be applied, which is subsequently accompanied by an complementary level of chemical characterisation.

Based on these findings it is likely that additional, unidentified tephras exist within the Lateglacial and early Holocene sediments at Loch Ashik, Loch an t'Suidhe, and Druim Loch. Given that these sites have already undergone a more thorough and extensive tephrostratigraphic investigation than most sites listed in Table 10.2, it is also highly probable that an extensive reassessment and reanalysis of these and other sites will be necessary.

10.2.3 Recommended refinement protocols

The results, as discussed above, illustrate the necessity to implement stringent and robust protocols when resolving the distribution of tephras within a stratigraphic sequence, and when selecting samples for chemical characterisation. At present too much emphasis is placed on the shape of a shard concentration profile, derived from scan phases, and the vertical distribution of shards within a sequence, especially when: 1) establishing the position of tephra isochrones; 2) prioritising horizons for high resolution refinement; and 3) selecting samples for chemical characterisation. A predisposition to resolve 'peaks' derived from these scan phases in a region where a high frequency of tephra horizons are known to occur may lead to: 1) an under-representation of horizons being identified; 2) a generalisation of the local and regional tephrostratigraphies; and 3) an exaggeration of local and regional tephra disparities.

It is acknowledged that a contiguous high-resolution sampling strategy has only been successfully conducted in northerly locales, and that a more comprehensive survey of sites is needed to test the validity of these findings and their implications in different geographic locations. It is also acknowledged that the proposed methodology is time-consuming, labour intensive and potentially costly if chemical analyses are also required. The following recommendations are therefore made.

- When sampling in well studied regions, or through time periods that are known to exhibit a high frequency of events (e.g. the early Holocene), a sampling resolution of 1 cm or higher should be employed to maximise the number of tephras that can be identified and resolved. A caveat on this recommendation relates to annually-laminated or varve sequences, where sampling resolutions must be dictated by feasible site-specific strategies.

- In new areas, the scan and resample strategy is retained to maximise efficiency, but the identification of all tephra within the scan phase must either be resolved to a higher resolution or in the very least **reported clearly and consistently**. This shall enable subsequent studies to objectively assess the potential for further tephrostratigraphic refinement.

- All processes should be clearly reported in the literature i.e. level of refinement and corresponding depths of analysis. If high-resolution work is not employed then the limitations to the tephrostratigraphy and subsequent correlations should be acknowledged.

- If a thorough and detailed chemical characterisation of horizons is not within the scope of research, then notes documenting any changes to predominant shard morphologies should accompany supplementary information files or appendices, thereby enabling an objective assessment of the potential for further tephrostratigraphic refinement.

- Contiguous or high resolution chemical profiling may help to decipher conflated or closely spaced tephra horizons preserved within diffuse tephra profiles. This additional level of tephrostratigraphic discrimination is essential if robust networks are to be developed. However, due to costs and time this approach may only be warranted where significant refinements in correlation and/or age constraint may be made.

10.3 A tephrostratigraphic framework for Scotland

The importance and potential of tephra frameworks or ‘lattices’ has been repeatedly championed by several groups in recent years (e.g. Lowe et al 2008a; Davies et al. 2012; Blockley et al. 2014; Lowe et al. 2015). The development of these frameworks has revealed that a dense network of interlaced tephra horizons can have a profound

impact on the way climatic and environmental questions are put forth and tested. Studies utilising this approach have demonstrated their importance by emphasising: 1) the dynamic spatial variability of climatic transitions (Lane et al. 2013); 2) the phasing of environmental response to abrupt climate change (Lane et al. 2012a); and 3) the complex interplay between climate and human dispersal (Lowe et al. 2012; Barton et al. 2015). These findings may not have become apparent using more traditional radiometric, or incremental dating techniques alone. However, as discussed in section 2.8 and 3.2, the number and quality of tephra-linkages that can be made across regions of Europe currently limits the effectiveness of this approach. It is essential therefore that efforts are focused on resolving local tephrostratigraphic frameworks, and optimising the number of horizons that can be used to link records at various spatial scales.

Figure 10.8 (A1 fold-out at back of thesis) details the current 'state of play' in regards to the Scottish tephrostratigraphic framework, and illustrates the wealth of research that has been conducted over the past three decades. Highlighted specifically in Figure 10.8 with asterisks are the five sites derived from this thesis. The key tephrostratigraphic contribution of this work is discussed below, and placed into the wider European context.

10.3.1 Newly identified tephras

During the course of this study, three new LGIT aged tephras were identified, these are:

The '***TM1 55 / pre-Borrobol***' Tephra (TM1 553, 545-546; QM1 241).

This tephra exhibits a Borrobol-type chemical signature and lies within Dimlington Stadial aged sediments. The identification of this tephra provides a second isochron in addition to the Dimna Ash in this interval, and is hence crucial for constraining the timing of deglaciation in Scotland. At present these findings at Tanera Mòr 1 and Quoyloo Meadow, represent the only geochemically confirmed occurrences of this tephra in a terrestrial setting, although correlations may be drawn with offshore sequences around Iceland (Eiríksson et al. 2000; Gudmundsdóttir et al. 2011; 2012). This possibility is discussed further in section 10.3.3 and 11.2 respectively.

The '***CRUM1 597***' Tephra (CRUM1 597; SPME1 701).

This tephra is located at the transition between the Windermere Interstadial and Loch Lomond Stadial. The horizon, which was identified at Crudale Meadow and Spretta Meadow, exhibits a Borrobol-type chemical signature, but crucially is stratigraphically

distinct to the Borrobol and Penifiler Tephras which share the same chemical profile. A similarly positioned tephra has been recognised at Loch an t'Suidhe (LAS-1) and Loch Etteridge (LET-3) (Davies 2003; Lowe et al. 2008b), however, chemical data is needed from these to further support this potential correlation. This tephra therefore offers much promise in becoming an important stratigraphic marker for climatic deterioration into the Loch Lomond Stadial.

The '***CRUM1 496***' Tephra (CRUM1 496).
This Grímsvötn derived basalt lies within early Holocene sediments and is associated with the Askja-S/10ka Tephra. A basaltic component of this horizon has not previously been described; however, it is known that the Askja-S/10ka Tephra has a close stratigraphic relationship with the Ashik Tephra (Timms et al 2016; Sean Pyne-O'Donnell pers. comm. 2016); a tephra which does exhibit a Grímsvötn derived basaltic component (Pyne-O'Donnell 2007). This discovery adds an additional level of complexity to the Holocene tephrostratigraphies in Scotland, and also to the Askja-S/10ka-Ashik Tephra relationship. This topic is considered further in section 10.3.3.

These three discoveries lie at important positions in the context of NW European tephrostratigraphies; either toward the end of climatic periods i.e. the Dimlington Stadial and Windermere Interstadial, or within the early Holocene radiocarbon plateau. This makes them particularly valuable chronostratigraphic markers. It will be necessary to trace these horizons to additional sequences, before more 'traditional' names can be allocated to these horizons.

10.3.2 Existing tephras

In addition to the three new tephras, four horizons previously unrecognised in Scotland, but prevalent elsewhere in Europe, were identified. These are:

The '***Hässeldalen Tephra***' (CRUM1 543; QM1 192).
This Snæfellsjökull derived horizon is an important marker for constraining the PBO in Europe. The tephra has been identified at thirteen sites on the European mainland (e.g. Davies et al. 2003; Housley et al. 2013; Figure 10.9), but has previously eluded detection in the British Isles. The identification of this horizon on Orkney provides a new early Holocene isochron for the Scottish tephrostratigraphic framework, and provides another means to tie Scottish sequences to their European counterparts.

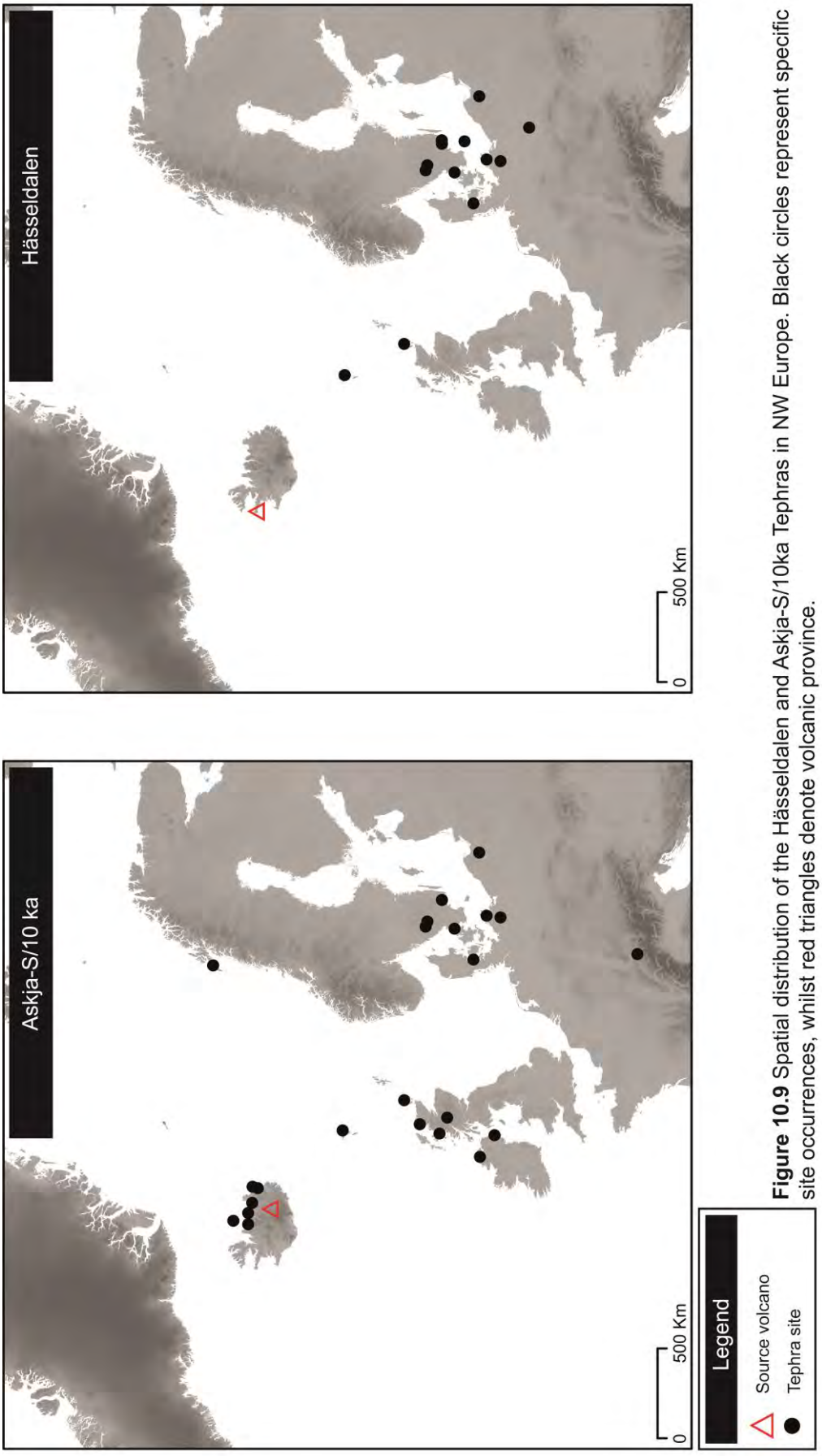

Figure 10.9 Spatial distribution of the Hässeldalen and Askja-S/10ka Tephras in NW Europe. Black circles represent specific site occurrences, whilst red triangles denote volcanic province.

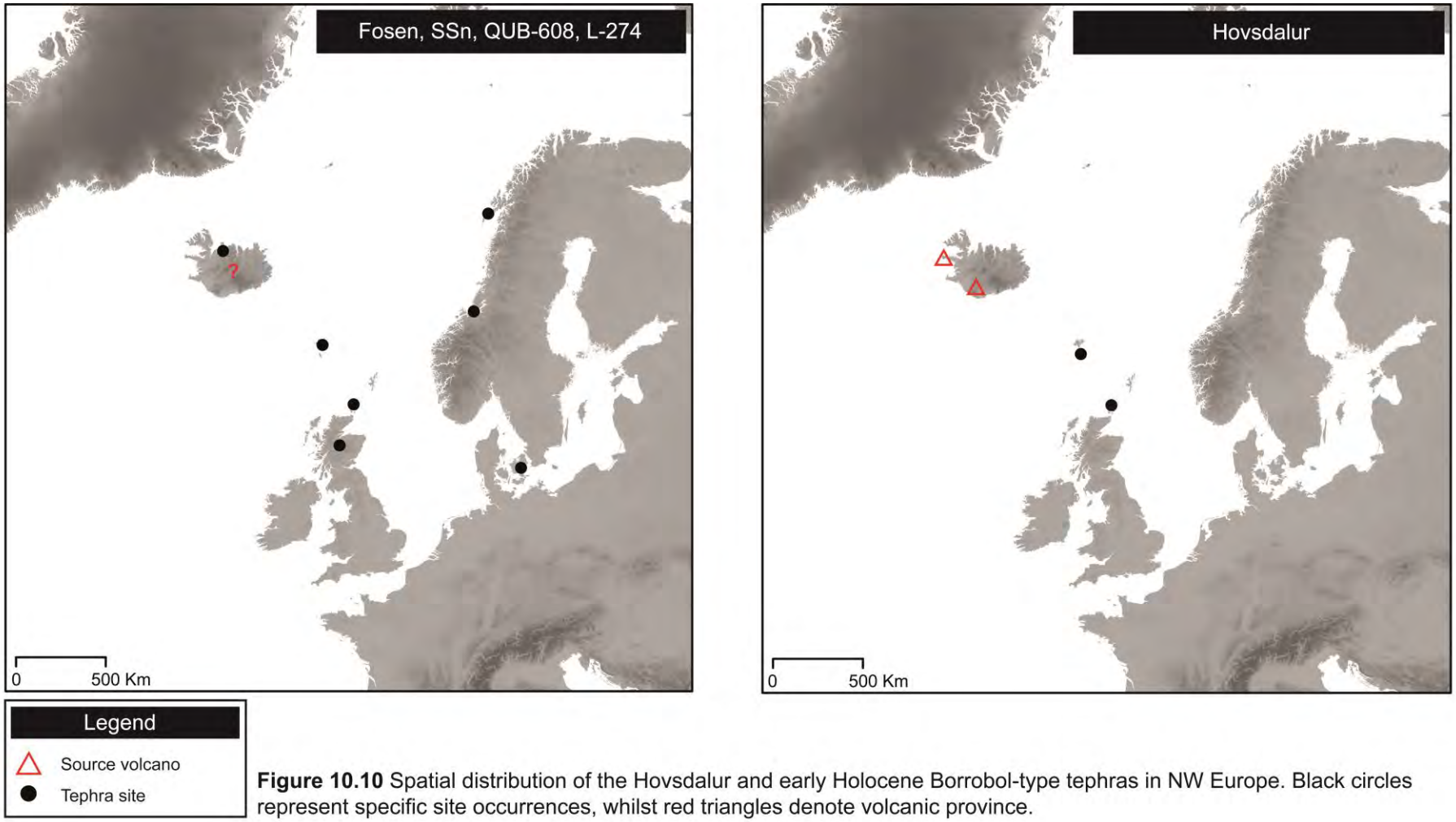

Figure 10.10 Spatial distribution of the Hovsdalur and early Holocene Borrobol-type tephras in NW Europe. Black circles represent specific site occurrences, whilst red triangles denote volcanic province.

The '***Askja-S/10ka Tephra***' (TM1 454-453, 450, 447; QM1 188; CRUM1 496).
Until relatively recently the Askja-S/10ka Tephra has also eluded detection in Scotland, despite its finding within the tephrostratigraphy of Northern Ireland by Turney et al. (2006), and its occurrence in ten sites across mainland Europe (e.g. Davies et al. 2003; Pilcher et al. 2005; Figure 10.9). Like the Hässeldalen Tephra, the Askja-S/10ka Tephra offers much potential in constraining the PBO climatic event (Wohlfarth et al 2006). Thus the tephra's occurrence at Inverlair in central Scotland (Kelly et al. 2016), and within the more northerly sites of this thesis, means there is an exciting possibility of being able to trace the tephra to other sites e.g. Loch Ashik (Sean Pyne-O'Donnell pers. comm). If the Hässeldalen can also be traced to these sites, then there is much potential for this duo to assist in accurately constraining early Holocene perturbations, a task yet to be robustly undertaken in Scotland.

The '***Hovsdalur Tephra***' (QM1 187; SPME1 622)
The identification of the Snæfellsjökull derived Hovsdalur Tephra at Quoyloo Meadow and Spretta Meadow represents the first occurrence of this tephra within the British Isles, and only the second incidence of this tephra in Europe (Figure 10.10). What is further significant is the identification of this tephra in the same sequence as the Hässeldalen Tephra at Quoyloo Meadow. This finding illustrates that these tephras are independent and stratigraphically distinct events, refuting the suggestion of Lind and Wastegård (2011) that these may be representative of the same eruption.

The '***Fosen Tephra***' (QM1 155; SPME1 610)
The early Holocene Borrobol-type tephra has been identified at Quoyloo Meadow and Spretta Meadow, which represents the first incidences of this tephra in the British Isles. There are a number of early Holocene Borrobol-type events described from various sites around the North Atlantic periphery (Figure 10.10), but poor age constraints on these had hiterto prevented a more secure correlation from being made (Lind et al. 2013). Further work is necessary to establish whether these events can be considered analogous, which would provide another useful marker in the early Holocene tephrostratigraphy of NW Europe.

The discovery of the previously unrecognised horizons in Scotland, has increased tephra 'connectivity' across NW Europe by 1.25 % (from 18.75-20 %) (Figure 10.11). This illustrates the impact local refinements can have on the overall number of tephra linkages within regions, and demonstrates how tephra connectivity can be improved by following the recommendations as suggested in section 10.2.3. Despite these positive developments, there are a number of issues which continue to hamper further

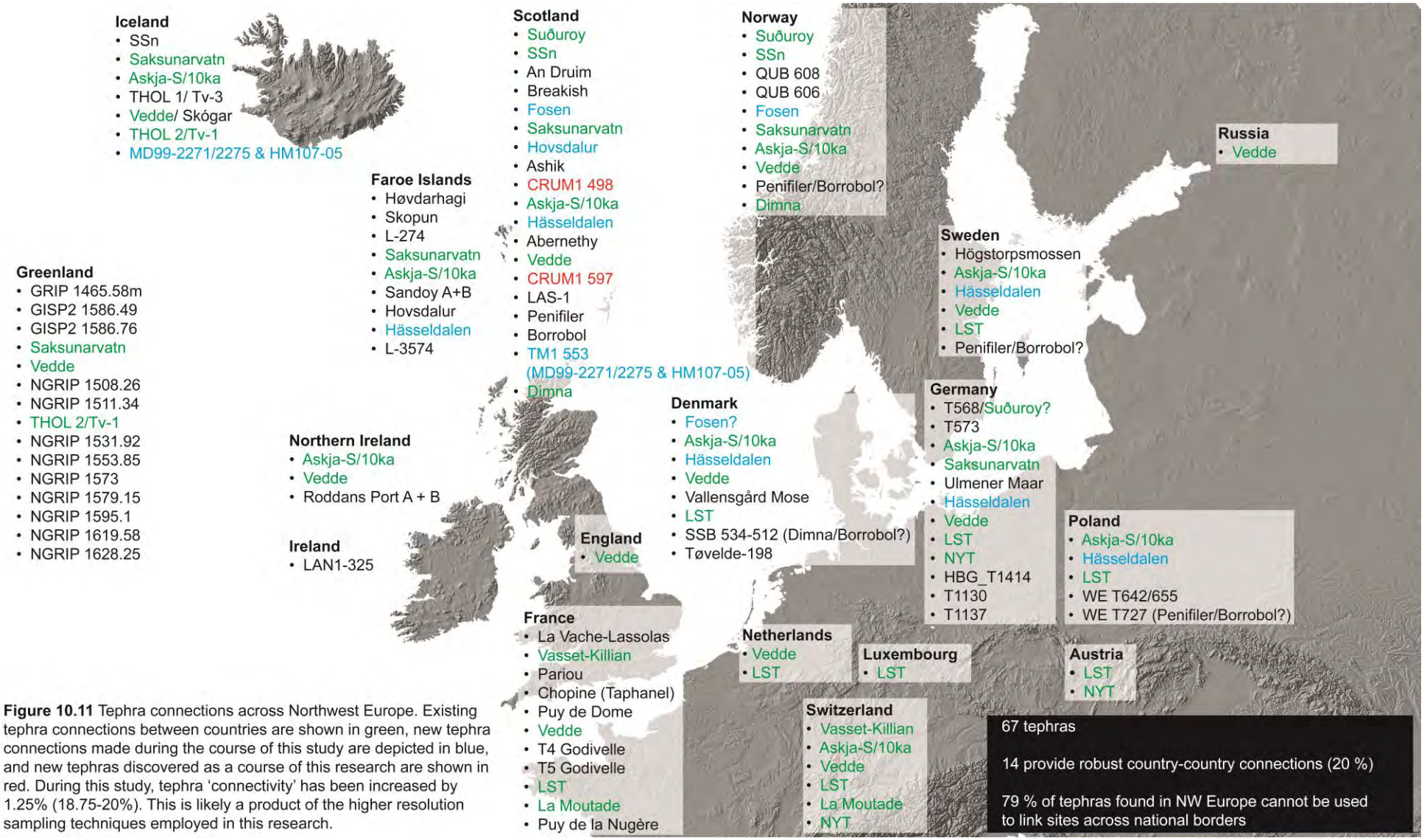

Figure 10.11 Tephra connections across Northwest Europe. Existing tephra connections between countries are shown in green, new tephra connections made during the course of this study are depicted in blue, and new tephras discovered as a course of this research are shown in red. During this study, tephra 'connectivity' has been increased by 1.25% (18.75-20%). This is likely a product of the higher resolution sampling techniques employed in this research.

progression. These unresolved elements of the tephrostratigraphy of Scotland and NW Europe require further focus and are discussed in detail in the ensuing section.

10.3.3 Unresolved tephrostratigraphic issues

Figure 10.12 illustrates a composite or 'optimal' tephrostratigraphy derived from the horizons currently known to exist across Scotland (Figure 10.8). In the right hand margin of the diagram are some of the current issues specifically associated with these tephra isochrons, and these can be divided into two broad themes, 1) stratigraphic/ chronological control and 2) geochemical control. These tephro-specific issues are discussed below, however, such themes and challenges are equally applicable to any tephrostratigraphic network regardless of locality, thus the solutions proposed here may find traction elsewhere.

10.3.3.1 Dimlington Stadial tephras

- Katla rhyolite (Dimna Ash)
- Katla SILK (Dimna Ash?)
- TM1 553 (pre-Borrobol Tephra)

The occurrence of Dimlington-aged tephras has now been recognised at several locations in the Summer Isles, and at two sites in the Orkney Islands (Figure 10.13; 10.8). The first reported occurrence of basal Katla-type shards was at Tanera Mòr 2 by Weston (2012). This tephra was recognised as a discrete and low-concentration horizon, approximately 36 cm below the Borrobol Tephra (Figure 10.13). During the course of this study an analysis of the sediments at the base of Tanera Mòr 1 revealed three separate intervals, two of which were successfully analysed, with the chemical signature of these defined by a mixed assemblage of Katla-type and Borrobol-type shards. Within the Quoyloo Meadow sequence a basal Borrobol-type tephra was also identified (QM1 241), which likely correlates to the basal horizon(s) identified at Tanera Mòr 1 (Figure 10.13). At Crudale Meadow a differing Dimlington aged tephra was identified; the single shard analysis was of a more intermediate composition than the tephras identified in the Summer Isles or Quoyloo Meadow. The limited data derived from this horizon means that correlations are tentative, but a case is made to suggest that the layer is a product of Katla SILK volcanism, and a correlative of the Dimna Ash (see section 6.3). Assuming this is correct, there is now evidence of at least two separate eruptions characterising the late Dimlington in Scotland, a Katla-type deposit and a Borrobol-type deposit (Figure 10.13).

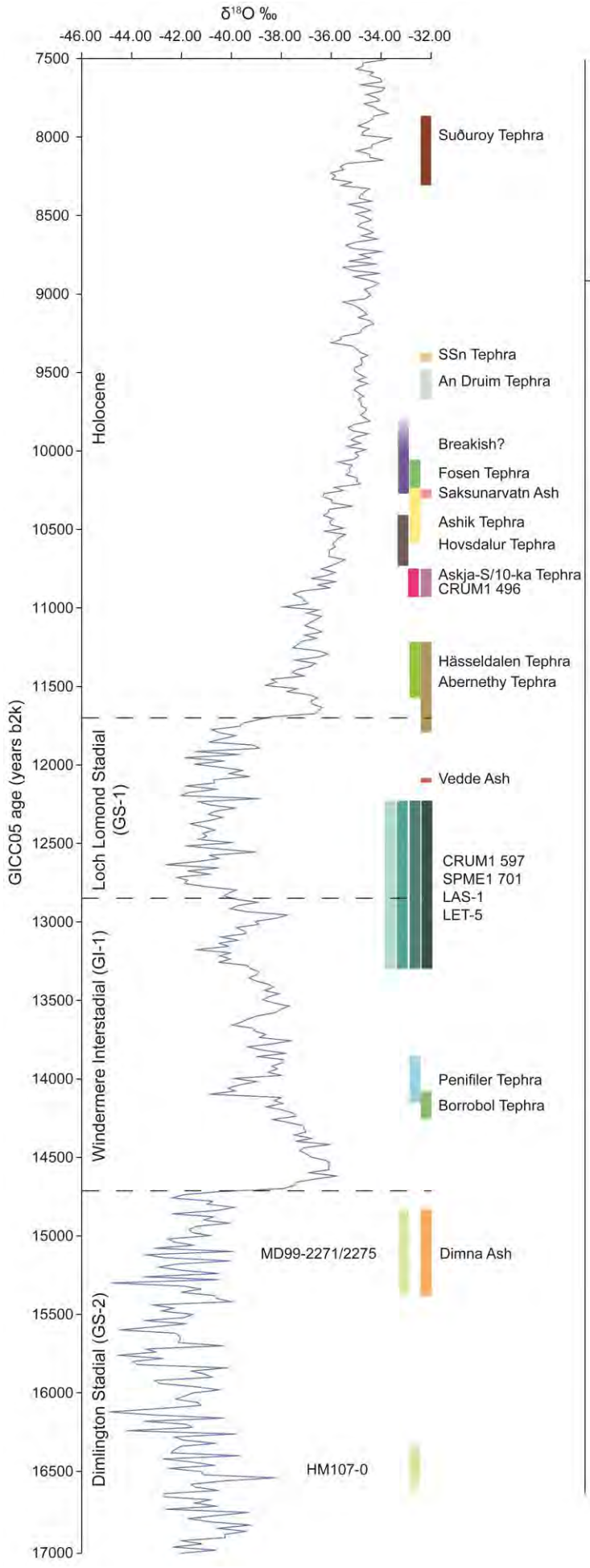

Figure 10.12 Summary diagram of tephras identified in the Scottish tephrostratigraphic framework and their approximate age estimates. Current issues associated with the stratigraphic positioning of these tephra are illustrated in the right hand margin. Note that most of these tephras with the exception of the Saksunarvatn Ash and Vedde Ash are not identified in the Greenland ice core records.

Tephrostratigraphic Issues

There is some suggestion that the An Druim and Høvdarhagi tephras may represent the same eruption

Uncertainty concerns the number and superposition of early Holocene Borrobol-type horizons like the Fosen and SSn

Uncertainty concerns the age of the Ashik Tephra

The occurrence of a Borrobol-type tephra in association with the Abernethy Tephra has raised doubts about the formers isochronous potential

The occurrence of a late Interstadial Borrobol-type tephras at Crudale Meadow (CRUM1 597), is suggested to correlate with the Borrobol-type horizon identified at the base of Spretta Meadow (SPME1 701), but may well also correlated with the Loch an t'Suidhe (LAS-1) and Loch Etteridge (LET-5) tephras

There is mounting evidence to suggest the 'Penifiler Tephra' is composed of more than one chemical population

At Tanera Mòr 1 the presence of Borrobol-type shards intermixed with the Katla-type horizons may suggest a non-air-fall delivery mechanism

It is not clear whether the Borrobol-type shards identified at the base of Tanera Mòr 1, (TM1 553, 545-546) Quoyloo Meadow (QM1 241) and Priest Island (PRI 700) correlate to the Borrobol-type tephras identified in the base of MD99-2271/2275 or HM107-05 if at all

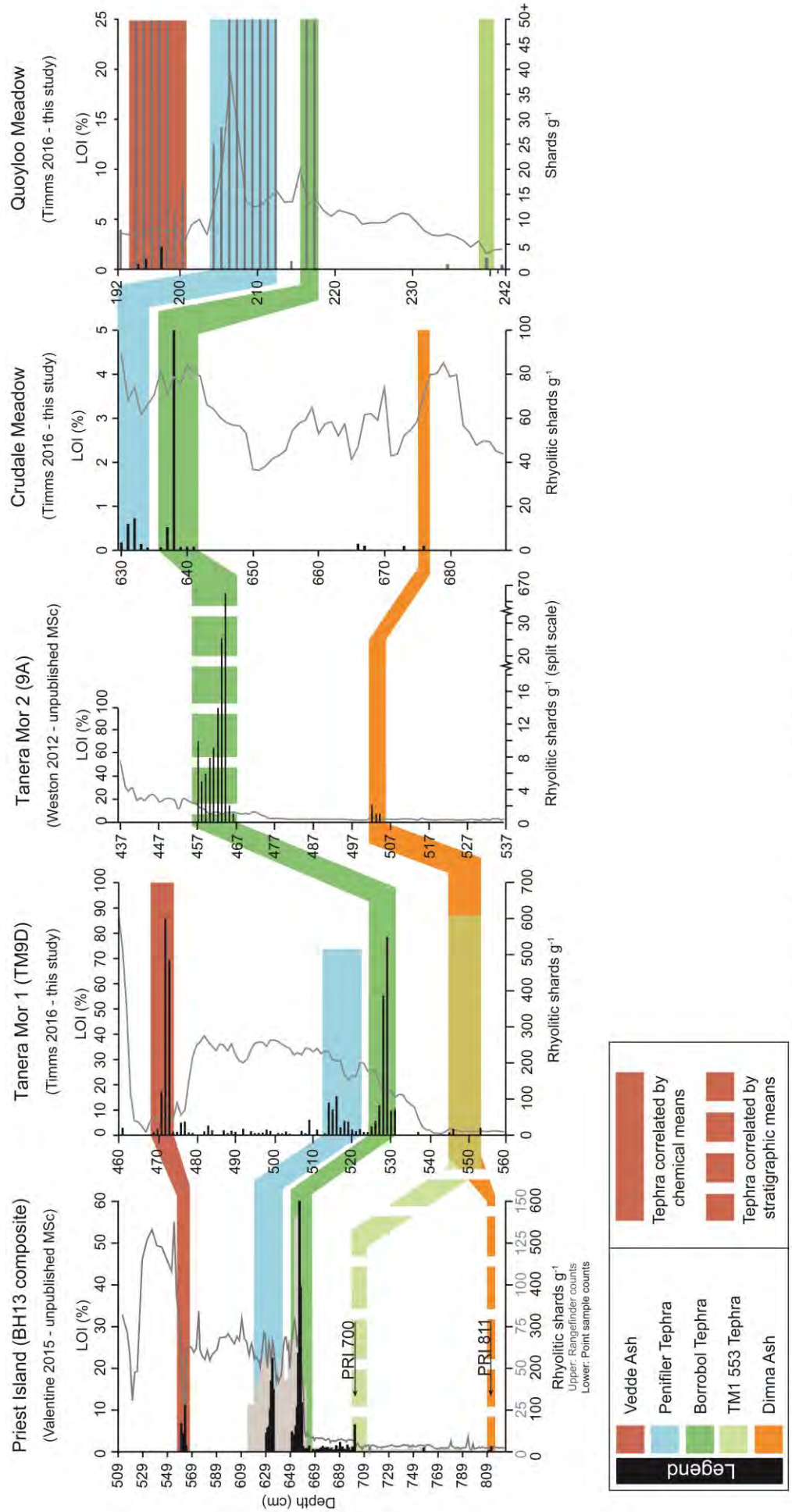

Figure 10.13 Site possessing Dimlington Stadial aged tephras in Scotland and their tephrostratigraphic correlation.

However, the exact taphonomy of these tephra horizons is debatable. Whilst the discreet nature of the horizon at Tanera Mòr 2 would favour airfall as a delivery mechanism, the low concentration and diffuse nature of the horizon(s) at Tanera Mòr 1, Crudale Meadow and Quoyloo Meadow raises some doubt on this hypothesis. It is quite possible that these shards represent much older eruptions, which deposited ash onto the Dimlington ice sheet, and only accumulated within these basins after the gradual retreat of ice, and the subsequent exposure of these basins to proglacial inwash (e.g. Koren et al 2008). It is evident therefore that there are at least two plausible scenarios to account for tephras within these basal sediments: 1) primary airfall from a single or multiple eruptions or 2) a mobilisation of antecedent horizons preserved within the Dimlington ice sheet.

This quandary could be resolved by the chemical characterisation of tephras located within a basin on Priest Island. Work conducted by Valentine (2015) on this site, identified a long and contiguous spread of tephra throughout the basal Dimlington-aged sediments (Figure 10.13). Whilst chemical data is still to be obtained, a morphological assessment revealed that the shards at the very base (PRI 811), and spanning approximately 68 cm, appear to be dominated by platey cuspate specimens (Valentine 2015) morphologies typically associated with Katla-derived eruptions (e.g. Mangerud et al. 1984). This suite progressively grades out and is replaced by shards exhibiting blockier, more vesicle-rich morphologies, which are characteristics common to Borrobol-type tephras (e.g. Pyne-O' Donnell 2007). The isochron of this event is placed at PRI 700, and reflects the highest concentration of this shard prior to the Borrobol *sensu stricto* type at PRI 655 (Valentine 2015). If these physical properties are indeed diagnostic of the chemical suites, the site on Priest Island can be used to illustrate a temporal offset between the Dimlington-aged Katla and Borrobol events. This stratigraphical distinction between the two populations at Priest Island may therefore support the airfall deposition scenario, as such structuring seems unlikely to have arisen from indiscriminate taphonomic processes, or from progressive dead ice melt-out.

At present, evidence from the Summer Isles would suggest that Priest Island and Tanera Mòr 1 and 2 were competent to receive these tephras via means of airfall, although further work at the latter will be needed to establish whether a Dimlington-aged Borrobol event can be identified. The lack of stratigraphic distinction at Tanera Mòr 1 most likely reflects one or a combination of three factors: 1) near simultaneous deposition of the tephras; 2) low sedimentation rates within the basin, or 3) post-depositional alteration of tephra shard profiles. In the context of Quoyloo Meadow and

Crudale Meadow the evidence for airfall or reworking of these basal shards is equivocal. At present therefore it is assumed that these horizons represent airfall events, however, it will be necessary to establish whether the other minor shard occurrences within the basal sediments correlate to the Dimna Ash and TM1 553 Tephra respectively (Figure 10.13).

In order to gain a greater understanding of these Dimlington Stadial tephras and their stratigraphic/ chronological relationship, it will be necessary to trace them to other sites. Whilst it is tempting to hypothesise where such basins may exist and which sites may provide superior and more complete records than so far identified, notable caveats exist on such assumptions. Amongst the most significant of these is that sediments began accumulating in exposed basins immediately after deglaciation, hence allowing for the immediate 'capture' and preservation of any Dimlington aged ash fall event. However, in many cases the basins being studied are ice wastage features e.g. kettle holes, and whilst an area may have become ice free, it is the point in which a basin becomes competent to host sediments i.e. the point in which the ice has melted to form a depression which is fundamental in this process. In periglacial environments dead ice may persist on the landscape for hundreds of years (Ballantyne and Harris 1994), thus sediment accumulation in these features will also be lagged. It is unlikely that sufficient melting would have occurred during the Dimlington Stadial to effectively 'activate' these basins in most instances. Thus preferential focus should be given to basins that reside within geological depressions such as fault scarps, structural basins, or coastal isolation basins as the competency of these to accumulate sediments is not dependent upon ice wastage. It is likely that the basins on the Summer Isles relate to coastal isolation basins, as the islands exhibit very little superficial deposits.

At present, Priest Island therefore offers the most potential in developing a greater understanding of these tephras, as the site exhibits the only known occurrence of the TM1 553 Tephra and Dimna Ash in clear stratigraphic succession. It is likely that the reason for Priest Island's longer more complete Dimlington Stadial tephrostratigraphy, relates to: 1) the geological origin of its basin and 2) the position of the island in the context of the regional ice mass. As shown in Figure 3.19 Priest Island is located further out into the Minch that hosted a palaeo-ice stream, and hence is hypothesised to have been deglaciated earlier than the other islands within the archipelago (Hughes et al. 2015). This potential earlier emergence, and the basin's early competency has allowed for the development of a longer sedimentary unit than any other neighbouring site. This locale can therefore be considered unique in the context of the Scottish

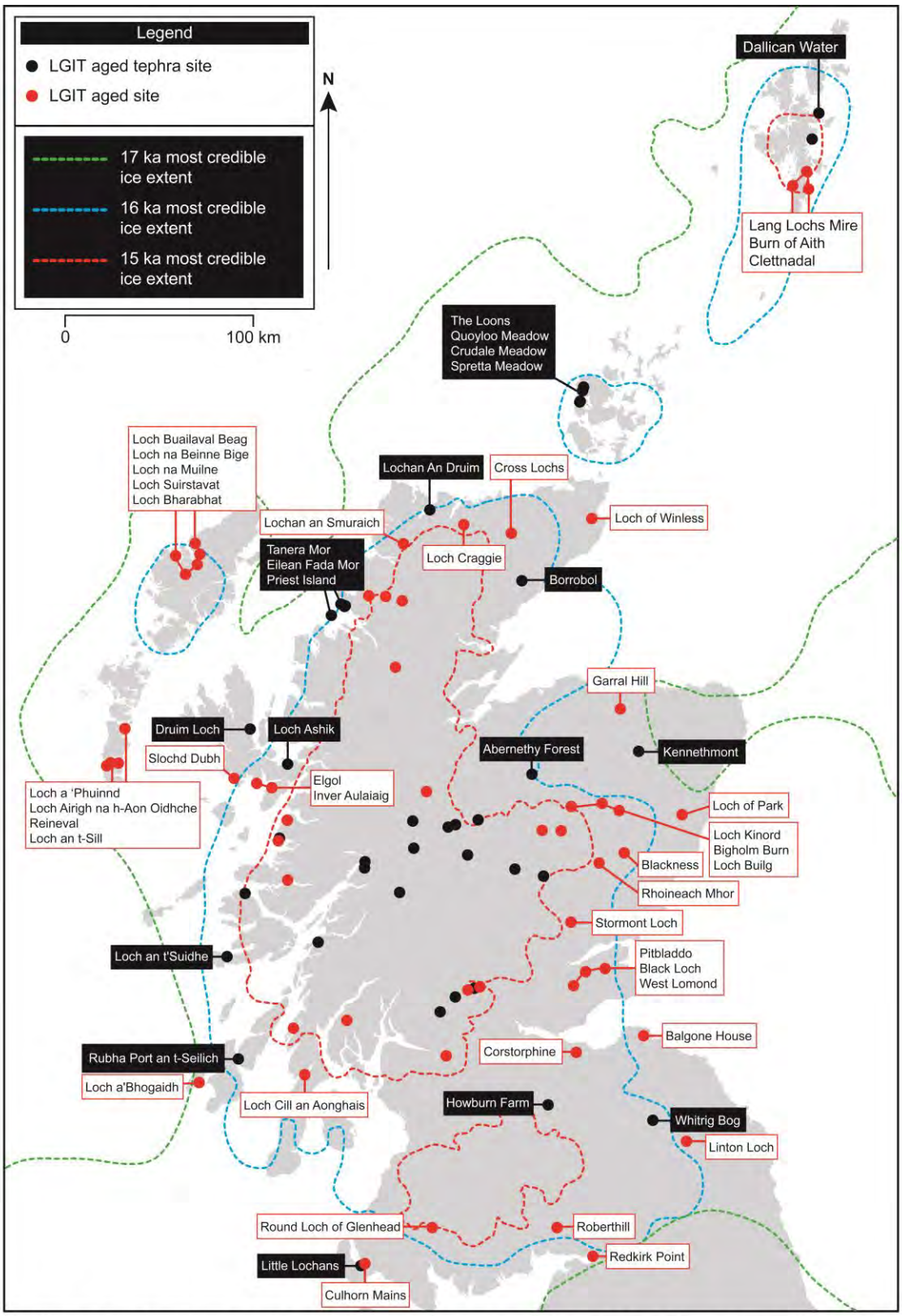

Figure 10.14 Dimlington-aged 'basal' tephras have been recognised at Priest Island, Tanera Mòr 1 & 2, Crudale meadow and Quoyloo Meadow. These sites lie just within or just outside the 16 ka ice limit as proposed by Hughes et al. (2016). There are thus numerous other sites in Scotland which may offer longer, superior tephra records covering the late Dimlington Stadial.

tephrostratigraphic framework (Figure 10.8). However, the conditions arising to its development are probably not. Figure 10.14 compares the position of known LGIT aged sites in Scotland with the 'most credible' model of Devensian ice retreat as proposed by Hughes et al (2015). It is evident that Priest Island lies on the fringes of the 16 ka ice limit, but there are numerous other sites and regions which lie well outside this isoline. These areas, in theory, may contain longer and more complete records of Dimlington tephras than any site so far examined in Scotland, and it will be necessary to investigate these more fully in future.

10.3.3.2 Windermere Interstadial tephras

- Borrobol Tephra
- Penifiler Tephra
- CRUM1 597 (late Windermere Interstadial Tephra)

The number, climatostratigraphic position, age, source and chemical composition of Borrobol-type tephras has been the focus of intense research for more than 15 years (Turney et al. 1997; Davies et al. 2004; Pyne-O'Donnell 2007; Pyne-O'Donnell et al. 2008; Lind et al. 2013; 2016). The current understanding proposes that there are two chemically indistinct Borrobol-type events, that reside within the Windermere Interstadial, the Borrobol Tephra and the Penifiler Tephra. Based on lithostratigraphy and accompanying LOI % measurements, the Borrobol Tephra is recognised as occurring at the onset of Windermere Interstadial warming, broadly equivalent to GI-1e (Björck et al. 1998; Lowe et al. 1999). Whilst the Penifiler Tephra occurs later, and is often found in association with a more minerogenic unit, or downturn in LOI associated with GI-1d (Older Dryas) (Pyne-O'Donnell 2007; Matthews et al. 2011).

Positioned at key climatic transitions, the Borrobol and Penifiler Tephras are hence important stratigraphic markers for LGIT aged sequences, and their presence is recognised at three of the sites examined in this thesis: Tanera Mòr 1, Quoyloo Meadow and Crudale Meadow (Figure 10.8). However, the discovery of a Dimlington Stadial aged Borrobol-type tephra i.e. the TM1 553 horizon at Tanera Mòr 1 and Quoyloo Meadow, as well as a late Interstadial Borrobol-type tephra i.e. the CRUM1 597 at Crudale Meadow and Spretta Meadow, has added further complication to sequences of this age. At present, Scotland is the only region in Europe where multiple Borrobol-type events have been identified through the Lateglacial (Lind et al. 2016). Elsewhere on the continent, the finding of only one Borrobol-type horizon within Interstadial sediments has meant that correlations remain more tentative (e.g. Davies et al 2003; 2004; Pyne-O'Donnell et al. 2008; Koren et al. 2008; Larsen 2013; Lilja et

al. 2013; Lind et al. 2016). Figure 10.15 illustrates the stratigraphic position of the Lateglacial Borrobol-type tephras, and the terminology applied to these horizons.

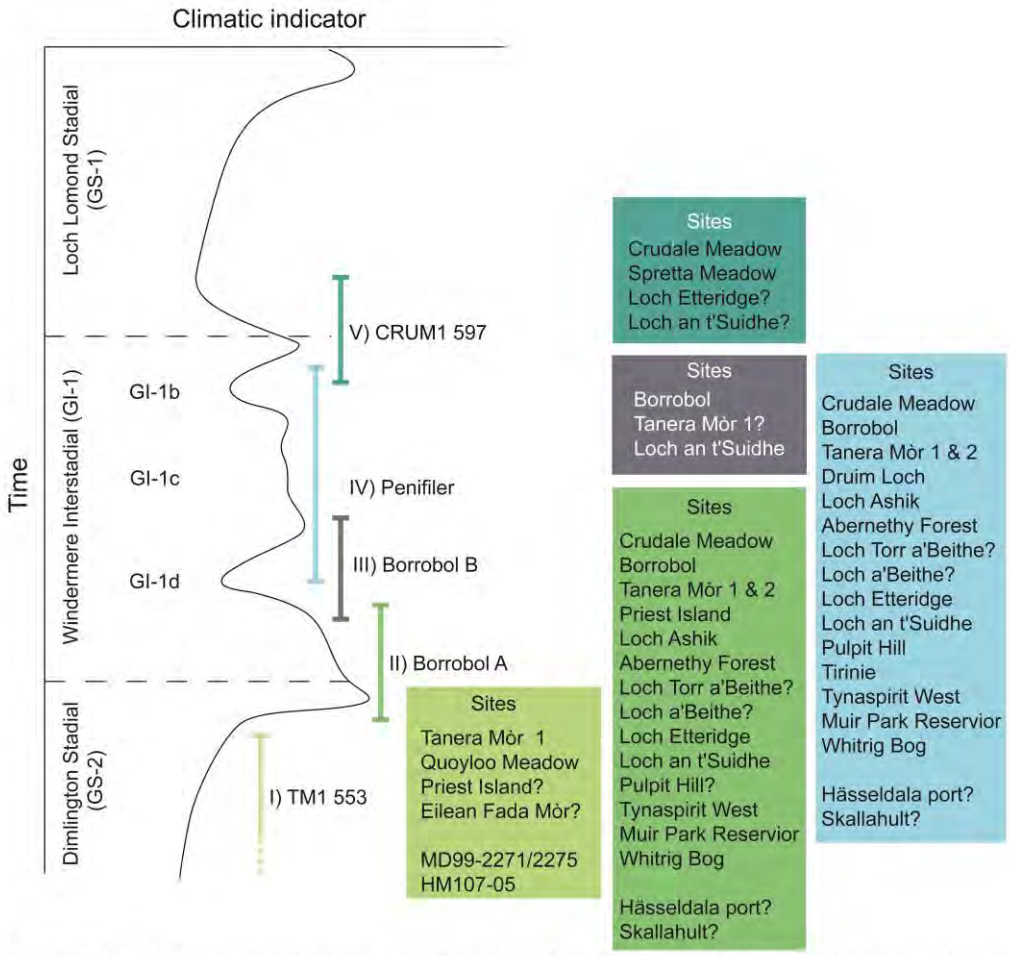

Figure 10.15 Approximate stratigraphic positions of Borrobol-type tephras characterising LGIT sequences in NW Europe. As many as five events may characterise this interval. There is emerging evidence for a 'pre-Borrobol' Borrobol-type Tephra i.e. the TM1 553 Tephra, which is hard to explain by down-working of the original Borrobol Isochron. The original Borrobol horizon is stratigraphically reliable, however isochron placement is a subject for debate. There is tentative evidence for a Borrobol B tephra, although it would seem in most instances this term has become interchangeable with the 'Penifiler'. The original 'Penifiler' was described from a post GI-1d position. However, in most instances where this was shown to be a distinct isochron there appears to be a conflation with the Borrobol once rangefinder samples are considered. There is also now evidence for a late Interstadial Borrobol-type tephra i.e. the CRUM1 597 Tephra, which is seemingly apparent at several sites in Scotland. However, there is a possibility that this also represents reworking of antecedent Borrobol-type horizons, triggered by the climatic decay of the Loch Lomond Stadial.

It is evident that there is much stratigraphic variability associated with the position of these tephras, and an equal inconsistency in the terms used to refer to them. These nuances not only occur between sites, but are also apparent amongst studies conducted in the same basin. One prime example of this is at the Borrobol type-site (Figure 10.16). The original work conducted by Turney et al. (1997) and Turney (1998) identified two distinct and separate horizons within the Windermere Interstadial, both of

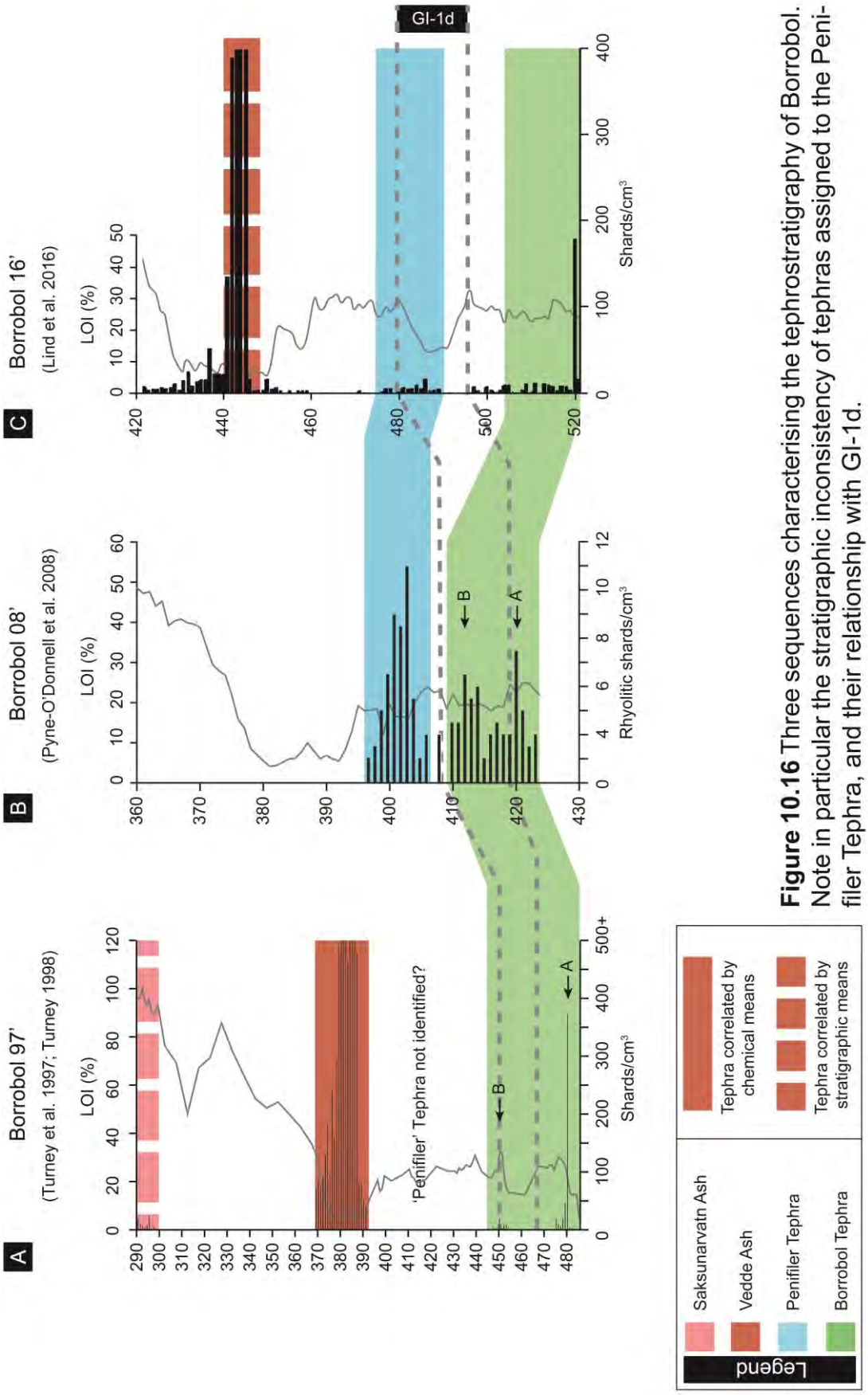

Figure 10.16 Three sequences characterising the tephrostratigraphy of Borrobol. Note in particular the stratigraphic inconsistency of tephras assigned to the Penifiler Tephra, and their relationship with GI-1d.

which exhibited Borrobol-type chemistries (Figure 10.16 A). The lower horizon was termed the Borrobol Tephra, whilst the upper remained undesignated, but was thought to perhaps represent reworking (Turney 1998a). A reinvestigation of the site by Pyne-O'Donnell et al. (2008) produced a new record (Figure 10.16 B), and, from this, a reinterpretation of the Turney sequence was made. In accordance to a pattern observed within the new tephrostratigraphy and other sites in Scotland, Pyne-O'Donnell et al. (2008) assigned both discreet peaks within the original Turney sequence to the Borrobol Tephra (Borrobol A and B), whilst a third peak identified in the new sequence was correlated to the Penifiler Tephra (Figure 10.16 B). Subsequent work by Lind et al. (2016) has produced a third Borrobol tephrostratigraphy, which presents a different interpretation (Figure 10.16 C). Here the tephra peak follows the LOI downturn and is correlated to the Penifiler, rather than the Borrobol B Tephra, whilst the third 'Penifiler' peak of Pyne-O'Donnell et al. (2008) is not recognised (Figure 10.16). It is particularly interesting that the Borrobol Tephra (Borrobol A of Pyne-O'Donnell et al. 2008) appears to be stratigraphically consistent, occurring during the LOI rise or at its peak, whilst the horizon ascribed to the 'Penifiler Tephra' is seemingly much more variable, and totally absent from the original work by Turney et al. (1997) and Turney (1998a).

It could be argued that LOI and other methods for establishing ratios of biogenic and minerogenic sediment are not necessarily reliable chronostratigraphic indicators due to their susceptibility to local catchment processes (e.g. Dearing and Foster 1986). However, the stratigraphic inconsistency of these tephra layers is also apparent when more regional indicators are considered. Figure 10.17 depicts the tephrostratigraphy of Loch Ashik, Muir Park Reservoir and Abernethy Forest in relation to each sites respective Chironomid-inferred temperature reconstruction (Brooks et al. 2012; 2016). It is apparent that the position of the 'Penifiler Tephra' in each record has a markedly different relationship with the GI-1d event. Whilst abrupt climatic transitions associated with the Loch Lomond Stadial/ GS-1 have been shown to be time transgressive (Lane et al. 2013), it is hard to understand how a widely recognised climatic event such as the Older Dryas/ GI-1d would have such a clear spatial irregularity across a relatively small region. It seems more likely therefore, that there is inconsistency in what has been ascribed to the 'Penifiler' in each of these sequences. Considering the evidence presented above it would seem that this inconsistency has also affected other sites within the Scottish tephrostratigraphic framework. This problem may have arisen in part from the incomplete tephrostratigraphic refinement of records, but in this instance the disparity probably also relates to a more complicated taphonomic and/or eruptive scenario than has previously been considered. Discussed below are two different

scenarios which may help to explain the occurrence of events observed in these sequences.

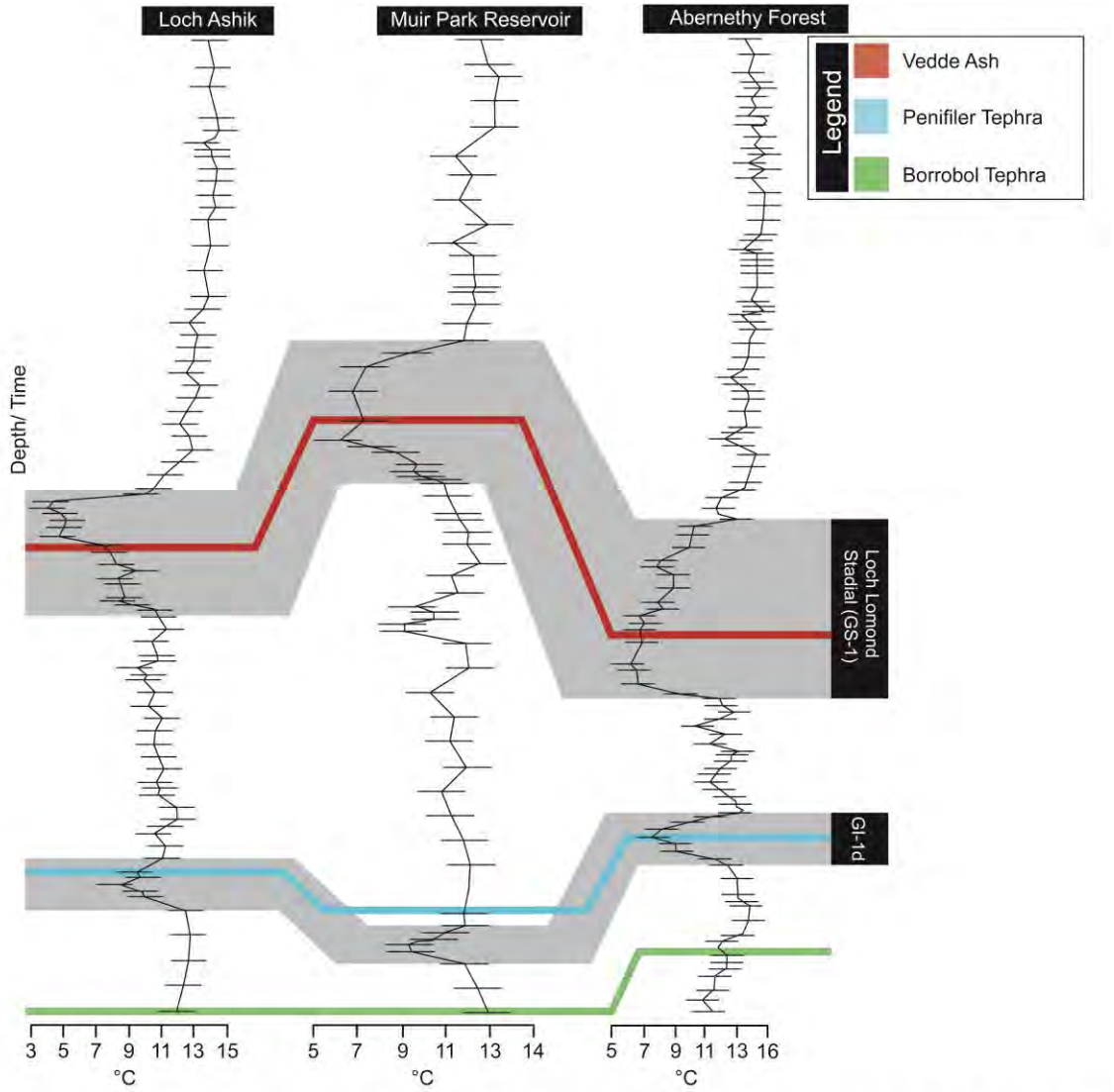

Figure 10.17 The three existing Chironomid inferred temperature reconstructions for Scotland. Note the variable stratigraphic relationship of the Penifiler isochron with the GI-1d cold climate oscillation. This finding would suggest that the 'Penifiler' has not been reliably characterised at all sites.

Scenario 1: reworking

The stratigraphic inconsistency of the Penifiler and its mergence with the Borrobol Tephra in some circumstances might favour a reworking hypothesis to account for its origin (e.g. Larsen 2013). With respect to the Vedde Ash, Mangerud et al. (1984) commented on how the cold climatic regime of the Younger Dryas in Norway, and the sparse vegetation coverage, served to prolong the period in which the Vedde Ash was reworked and re-mobilised from the surrounding catchment into basins. With the deposition of the Borrobol Tephra soon after the Dimlington Stadial (ca. 500 yrs), it is quite probable that the slopes surrounding many basins in Scotland were also sparsely

vegetated (Walker 1984; Ballantyne and Harris 1994; Ballantyne 2002; Lowe and Walker 2015). This would have facilitated the gradual reworking of tephra from primitive, loosely bound catchment soils, and hence contributed to the diffuse profile of shards observed at many sites. It is also likely that a progressive melting of snow and ice, left remnant in sheltered areas, would have also contributed to this signal at several localities, and especially those at higher altitudes. These processes would have continued until the catchment was depleted of shards, or the area became stabilised enough to diminish mineral inwash. The ensuing cold climatic oscillation of GI-1d would have caused an abrupt degradation of the landscape, a reduction in vegetation cover, and the resurgence of periglacial conditions across Scotland (Brooks et al. 2012; 2016; Lowe and Walker 2015). Chironomid-inferred temperature reconstructions through this period suggest that mean summer air temperatures reduced by ca. 2-3°C in Scotland, but it is likely that a greater reduction in temperature typified winter months (Bradwell et al. 2008; Brooks et al. 2012; 2016). This would have had the most detrimental impact on landscape stability; likely causing an increased shard recycling from: 1) cryoturbated soils; 2) a reworking of lacustrine sediments positioned higher in some catchments, and; 3) within basin reworking/ slope failures/ marginal slumping potentially caused by lake level fluctuations (e.g. Larsen 2013). The acceptance of this scenario has inherent implications for the Penifiler and CRUM1 597 Tephras as independent isochronous markers, as both exhibit a close stratigraphic association with the cold climatic events of the period.

Scenario 2: multi-eruption

Whilst scenario 1 is a plausible explanation to account for: 1) the diffuse nature of the Borrobol; 2) the conflated signal between the Borrobol and the Penifiler; 3) the occurrence of the 'Penifiler' tephra in association with GI-1d; and 4) the association of the CRUM1 597 tephra with the transition into the Loch Lomond Stadial. This scenario of shard recycling and remobilisation is less convincing at sites where: 1) the Penifiler Tephra appears stratigraphically distinct e.g. Abernethy Forest and Muir Park Reservoir; 2) the peak in shards occurs after the climatic deterioration associated with GI-1d i.e. after catchment re-stabilisation e.g. Pulpit Hill, Loch Ashik and Tanera Mòr 1 or 3) catchment size is restricted, and sediments relating to the earliest phases of the Windermere are not preserved e.g. Druim Loch and Tirinie (Figure 10.8). A reworking hypothesis in these instances becomes much more difficult to justify and explain. An alternative proposal, and one initially put forth by Davies et al. (2004) to account for the diffuse nature of the Borrobol Tephra, is that several closely spaced eruptions from the Borrobol source typified the early-mid Interstadial. Whilst the exact source of the Borrobol-type tephras has yet to be identified, there is a growing body of evidence to

suggest they derive from the Icelandic province (e.g. Pyne-O'Donnell 2007; Lind et al. 2016). With diminishing ice caps and retreating ice margins characterising the early Interstadial in Iceland (e.g. Hubbard et al. 2006; Norðdahl et al. 2008; Van Vliet-Lanoë et al. 2007), the accompanying isostatic recovery would have greatly increased the potential for explosive volcanism (e.g. Slater et al. 1998; Sigvaldason 2002; Larsen and Eiríksson 2008; Carrivick et al. 2009; Sigmundsson et al. 2010). It is quite possible therefore that pressure within the Borrobol system was released as a series of explosive eruptions during the latter phases of the Dimlington and throughout the Windermere Interstadial (e.g. Turney et al. 1997; Eiríksson et al. 2000; Pyne-O'Donnell et al. 2008; Gudmundsdóttir et al. 2011; 2012).

This multi-eruption theory gathers impetus from recent developments at Lille Slotseng in Denmark (Larsen 2013), Star Carr in Yorkshire (RHUL unpublished) and from Tanera Mòr 1 in this study. At Lille Slotseng, Larsen (2013) established the occurrence of an Interstadial aged Borrobol-type tephra, intermixed with shards exhibiting Askja-type characteristics. The horizon spreads from the upper part of the Bølling (GI-1e), through the Older Dryas, and into the Allerød (GI-1c-a). The lack of a defined or reliable peak in concentration lead Larsen (2013) to term the interval the Bølling-Allerød Ash Zone, and interestingly this same chemical suite has recently been detected at Star Carr in Yorkshire (Figure 10.18). The early Windermere Interstadial, encompassing GI-1d is of high stratigraphic resolution at Star Carr, and tephrostratigraphic investigations have identified two distinct and separate occurrences of tephra in association with the aforementioned climatic downturn. Figure 10.18 illustrates the position of the two tephras; the upper has a Borrobol-type signature, whilst the lower shares a chemical affinity to the Askja-type tephra identified in the Lille Slotseng basin (Ian Matthews pers. comm. 2016). This is a significant discovery for two reasons: 1) the identification of a new tephra isochron in Windermere Interstadial aged sediments offers the potential for a more robust isochron, and; 2) the low concentrations typifying each horizon, and the absence of shards bearing the same chemical signature lower in the stratigraphy at Star Carr provides seemingly robust evidence for the placing of a Borrobol-type isochron within the confines of GI-1d. Results from Tanera Mòr 1, however, would suggest that this interval in much more complex than these sites would allude to. Analyses of the 'Penifiler' horizon at this site has established the presence of a mixed chemical assemblage, with as many as ten different geochemical populations typifying the interval (see section 8.3). At present no analyses of an Askja-type signature have been identified within this suit. However, this discovery adds weight to the idea that the diffuse tephra profile observed in many sequences should perhaps be regarded as an 'Ash Zone' i.e. a period of time which

encapsulates the deposition of several closely spaced eruptions, and perhaps not all derived from the Borrobol source.

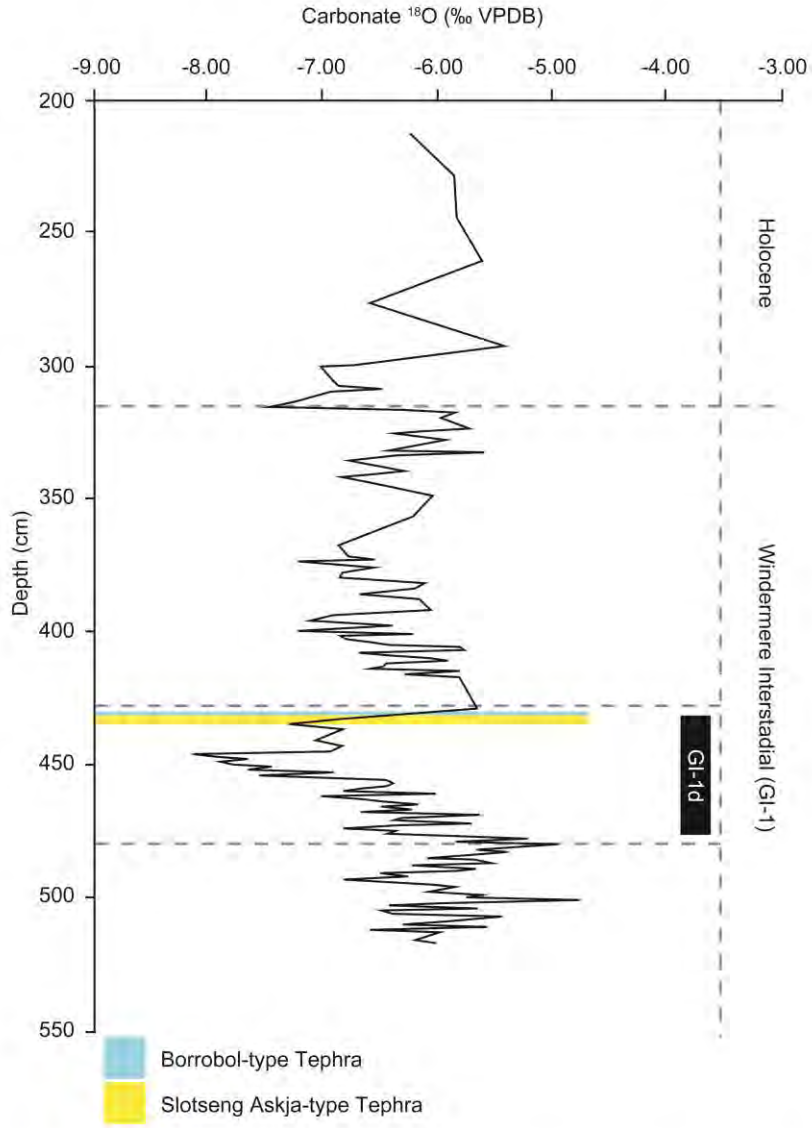

Figure 10.18 The Windermere Interstadial sequence from Star Carr, Yorkshire. The Borrobol-type tephra is found between 430-432 cm, whilst the Slotseng tephra is found slightly lower in 432-435 cm. At the end of the interstadial (ca. 315 cm) a hiatus in the record occurs, with the Holocene sediments directly on top.

Whilst these reworking and multi-eruption scenarios can be considered in isolation, there is the distinct likelihood that both may have been fundamental in the development of site tephrostratigraphies. Distinguishing between these differing mechanisms is inherently problematic, as it is likely their influence and prominence varies between sites. Establishing exactly how many Borrobol-type eruptions, and/ or other eruptions may have typified the Windermere Interstadial is also difficult to decipher. Reliance on more 'traditional' means of tephrostratigraphic distinction such as LOI signals, is less

likely to be a useful discriminator in future, as it has been shown that these Borrobol-type events are more ubiquitous and common than previously thought. Such lithostratigraphic trends are also less applicable to sequences outside of Scotland where the archetypal 'tripartite' sequence may not exist. Outlined below are some recommendations on resolving these tephrostratigraphic and geochemical issues.

- The Dimlington Stadial aged TM1 553 resides within basal sediments prior to Interstadial warming and has been found in close association with the Katla-type Dimna Ash. Identification of this accompanying Katla-type horizon and/or a quantitative reconstruction of temperature may help to distinguish this isochron from the Borrobol *sensu stricto*, and other tephras of the period.

- From a stratigraphic perspective the Borrobol *sensu stricto*, is arguably the most well-defined LGIT aged Borrobol-type tephra. The horizon is defined by a uni-modal chemical signature, and is positioned shortly after early Interstadial warming. Crucially this tephra occurs before the climatic deterioration associated with GI-1d (Brooks et al. 2016), thus at present, quantitative temperature reconstructions are the most reliable means by which this tephra can be constrained and distinguished.

- Of the several Borrobol-type horizons identified in the Lateglacial, the Penifiler Tephra is the horizon which exhibits the greatest level of uncertainty. Stratigraphic inconsistencies, and the emergence of mixed chemical assemblages in association with this layer, suggests that this interval may be better considered an 'Ash zone'. This inherently means that the definition of the Penifiler *sensu stricto* must be reviewed, as must the age of the tephra (Matthews et al. 2011; Bronk Ramsey et al. 2015b). High resolution sampling, and successive chemical characterisation will be necessary to decipher the number and relative placing of eruptions through this interval. Work at Star Carr has shown that a Borrobol-type tephra resides on the upturn of the $\delta^{18}O$ signal associated with GI-1d, and crucially above the Askja-type 'Slotseng Tephra' (Figure 10.18). Tephrostratigraphic superposition, will be a crucial future consideration in delineating the Penifiler isochron, as will quantitative climatic indicators.

- The CRUM1 597 appears to straddle the transition into the Loch Lomond, however, its precise relationship with the downturn has yet to be fully quantified. Developing a more meaningful quantitative estimate of the climate at the

position of the isochron will be necessary to test this horizons validity as a genuine isochron.

What can be determined from these recommendations is that comprehensive and well characterised tephrostratigraphies are essential if accurate correlations are to be made. It is also necessary to consider these horizons in the context of the wider regional climatic signal, which should provide more robust and transferable tie points, than basin specific organic/minerogenic ratios.

10.3.3.3 Loch Lomond Stadial/ early Holocene transitional tephras

- Vedde Ash
- Abernethy Tephra

The Vedde Ash

The discovery of the Vedde Ash in all three Orcadian sites extends the known range of this tephra within the British Isles to its most northerly locale, and further confirms the dominance and importance of this horizon within the European tephra framework. The finding of the Vedde Ash in these sites is made more significant due to the occurrence of the basaltic component, and the visible occurrence of the tephra at Spretta Meadow. Only one other site in the British Isles contains the Vedde Ash as a macrotephra, which is Loch Ashik on the Isle of Skye (Davies et al. 2001; Pyne-O'Donnell 2011). This site is also one of only two sites in the British Isles to host the basaltic fraction of the tephra, which is understood to be more spatially restricted than the rhyolitic fraction (Lane et al. 2012b). Whilst studies have calculated that rhyolitic shards are more likely to reach the British Isles than basaltic ones (Stevenson et al. 2015), the disparity in representation also probably relates to biases associated with the density floatation technique (e.g. Turney 1998b; Blockley et al. 2005). This reason is often cited as being one of the primary inhibitors in establishing the 'true' distribution of basaltic tephras during the LGIT (e.g. Davies et al 2001; Mackie et al 2002). The higher respective densities of basaltic tephra in relation to their more silicic counterparts means that these shards may be left remnant within 'heavy residues' following silicic extraction at 2.5-2.55 g cm^{-3}. Chemical alteration of basaltic shards is also cited as a considerable limiter on their successful identification (e.g. Pollard et al. 2003; Wolff-Boenisch et al. 2004; Parruzot et al. 2015); hydration of the glass, and the development of gel and clay layers can ultimately lead to density changes of the hosting glass, or the complete dissolution of the shard (e.g. Crovisier et al. 2003; Pollard et al. 2003; Rebiscoul et al. 2004; Wolff-Boenisch et al. 2004; Parruzot et al. 2015). Such degraded and altered basaltic shards

are intermittently identified within floated fractions (e.g. Figure 6.5 O). During the course of examining the visible Vedde Ash horizon at Spretta Meadow, it was noted that a considerable quantity of basaltic shards were mobilised and floated off by the 2.0 g cm^{-3} cleaning float. Upon examination, no appreciable morphological difference was observed, although presumably the density of these particular specimens had been modified in the post depositional environment. This phenomenon may require further investigation in future studies; the prospect of basaltic shards being missed due to unexamined 'cleaning floats' is perturbing, but nonetheless easily resolvable by exploring cleaning floats, or subjecting these floats to magnetic separation (e.g. Mackie et al. 2002). By doing so, additional tephra linkages may be achieved across Scotland and NW Europe.

The Abernethy Tephra

The Vedde Ash is now not the only tephra understood to occupy Loch Lomond Stadial sediments. Recent work from Matthews et al. (2011) and MacLeod et al. (2015) has put forth a persuasive case concerning the identification and characterisation of a second tephra isochron; the Abernethy Tephra. This horizon, like its stratigraphic neighbour, is derived from the Katla volcanic system and hence shares a chemical composition indistinguishable from the former, and several other LGIT aged tephras e.g. the Dimna Ash (Koren et al. 2008); the R1 (Thornally et al. 2011); the IA2 (Bond et al. 2001); and the Suðuroy Tephra (Wastegård 2002). This issue of repeating chemical signatures is a particular problem for LGIT sequences, but can be resolved with an understanding of the host sedimentological unit, and the position of the isochron in relation to other tephras i.e. its superposition. As noted, however, the Abernethy Tephra has the unfortunate occurrence of residing in close proximity to the Vedde Ash, leading to some doubt about its validity as a genuine isochron. Post depositional reworking and remobilisation of the Vedde Ash from catchments has been cited as mechanisms to explain the 'double-peak' in shard concentration often observed within Loch Lomond Stadial sediments (e.g. Mangerud et al. 1984; Pyne-O'Donnell 2011). MacLeod et al. (2015) provide a comprehensive review of the sites in NW Europe that exhibit potential evidence of the Abernethy Tephra, and classify these sites into four categories in order to clarify this issue (Table 10.3).

During the course of this study, one horizon was identified which, according to the parameters of MacLeod et al. (2015), exhibited evidence supporting the case for the Abernethy Tephra; this horizon is TM1 462-463 (Tanera Mòr 1), which would fall within MacLeod et al.'s (2015) category C (Table 10.3). At all of the Orcadian sites, there is insufficient evidence to argue a case for the unequivocal presence of the Abernethy

Tephra, despite the identification of Katla-type tephras in sediments relating to the Loch Lomond Stadial/ Holocene transition (Figure 10.2-10.4). In these instances the total number of shards were either indiscriminate from background values, or horizons displayed a mixed assemblage, whereby no single population possessed a concentration of more than 50 %. This chemical heterogeneity highlights an important issue, and one which has seemingly been overlooked by MacLeod et al. (2015). Outlined below are two potential scenarios to explain the occurrence of the Abernethy Tephra.

Table 10.3 Summary of terrestrial sites in NW Europe identified as containing evidence to support the occurrence of a second Loch Lomond Stadial (GS-1) tephra isochron the Abernethy Tephra. Modified from MacLeod et al. (2015).

Site #	Site	Location	Reference
A. Sites containing a single visible layer of tephra			
1	Gjølvatn	Norway	Mangerud et al. 1984
2	Kloppamyra	Norway	Mangerud et al. 1984
3	Kråkenes	Norway	Mangerud et al. 1984
4	Kvaltjern	Norway	Mangerud et al. 1984
5	Lerstadvatn	Norway	Mangerud et al. 1984
6	Saudedalsmyra	Norway	Mangerud et al. 1984
7	Torvløмyra	Norway	Mangerud et al. 1984
8	Loch Ashik	Scotland	Davies et al. 2001
B. Sites containing a single non-visible layer of tephra			
8	Loch Ashik	Scotland	Pyne-O'Donnell 2007
9	Store Slotseng	Denmark	Larsen and Noe-Nygaard 2013
10	Endinger Bruch	Germany	Lane et al. 2012a
11	Meerfelder Maar	Germany	Lane et al. 2013
12	Rotmeer	Germany	Blockley et al. 2007
13	Lago di Laverone	Italy	Lane et al. 2012c
14	Lago Piccolo di Avigliana	Italy	Lane et al. 2012c
15	Roddans Port	Northern Ireland	Turney et al. 2006
16	Kostverloren Veen	Netherlands	Davies et al. 2005
17	Andøya	Norway	Bondevik and Mangerud 2002
18	Borge Bog	Norway	Bondevik and Mangerud 2002
19	Irgenstjørn	Norway	Bondevik and Mangerud 2002

20	Nedre Ærasvatn	Norway	Bondevik and Mangerud 2002
21	Stølsmyra	Norway	Bondevik and Mangerud 2002
22	Medvedeskoye	Russia	Wastegård et al. 2000
23	Pastorskoye	Russia	Wastegård et al. 2000
24	Druim Loch	Scotland	Pyne-O'Donnell 2007
25	Loch an t'Suidhe	Scotland	Pyne-O'Donnell 2007
26	Tanera Mòr	Scotland	Roberts 1997
27	Tynaspirit West	Scotland	Turney et al. 1997
28	Whitrig Bog	Scotland	Turney et al. 1997
29	Lake Bled	Slovenia	Lane et al. 2011a
30	Fågelmossen	Sweden	Björck and Wastegård 1999
31	Götesjön	Sweden	Schoning 2001
32	Högstorpsmossen	Sweden	Björck and Wastegård 1999
33	Kullatorpssjön	Sweden	Wastegård et al. 2000
34	Rotsee	Switzerland	Lane et al. 2012c
35	Soppensee	Switzerland	Blockley et al. 2007
C. Sites containing a double non-visible peak in tephra (no gap between peaks)			
36	Borrobol	Scotland	Lowe and Turney 1997
37	Tanera Mòr	Scotland	This study
38	Madtjärn	Sweden	Wastegård et al. 1998
D. Sites containing a double non-visible peak in tephra (gap between peaks)			
39	Abernethy Forest	Scotland	Matthews et al. 2011
40	Loch Etteridge	Scotland	Lowe et al. 2008b
41	Loch Laggan-Glen Turret Fan	Scotland	MacLeod et al. 2015
42	Lochan an Druim	Scotland	Ranner et al. 2005
43	Muir Park Reservoir	Scotland	Lowe and Roberts 2003

Scenario 1: reworking

To date, the evidence for the Abernethy Tephra as shown in Table 10.3 has, in most incidences, been derived from the pattern of shards identified within a stratigraphy i.e. the occurrence of a second tephra 'peak' following the Vedde Ash. Chemical characterisation has only been conducted in a few cases, and in all but one of these incidences, the results have displayed a bi-modal chemical signature, which has not

been commented upon in the literature (e.g. Matthews et al. 2011; Lane et al. 2012b; MacLeod et al. 2015).

Table 10.4 lists the sites in which the Abernethy has been characterised chemically, the number of analyses obtained, and the proportion of those correlating to the Katla system. It is evident that out of the four sites, three possess mixed chemical assemblages, with the secondary population in all cases correlating to the Borrobol-type tephras. At present, no eruption from the Borrobol source has been reliably described from the Loch Lomond Stadial, which may therefore suggest a reworking of antecedent Borrobol-type deposits. Such Borrobol-type shards have also been identified within Vedde Ash analyses at Abernethy Forest (Matthews et al. 2011), Loch Etteridge (MacLeod et al. 2015), and Crudale Meadow (this study), as well as within early Holocene sediments at all sites chemically analysed as part of this study (Figure 10.1-10.4). This cumulative evidence adds weight to the idea that the Loch Lomond Stadial and early Holocene was a particularly dynamic period for basin and catchment processes, and a time which probably saw a remobilisation of tephra-laden lake sediments by subaerial processes.

Table 10.4 Summery of sites in which the Abernethy Tephra has been recognised and chemically analysed. Note the occurrence of Borrobol-type shards in four of the five sites.

Site	# of analyses obtained	Katla-type (%)	Borrobol-type (%)
Abernethy Forest	12	83	17
Loch Etteridge	20	70	30
Loch Laggan-Glen Turret Fan	4	100	N/A
Tanera Mòr	35	89	11

Whilst indiscriminate reworking of lake deposits can account for the consistent background of shards observed at some sites i.e. category C in Table 10.3, the same mechanism does not so easily explain how a distinct and separate ‘peak’ (Category D) may have arisen (MacLeod et al. 2015). This occurrence may be used to support a case for a distinct and separate eruption at the end of the Stadial, however, this pattern may have also formed by the crossing of a regional temperature threshold, and the melting of tephra-laden snow beds. There is an increasing body of evidence to suggest that the latter half of the Loch Lomond Stadial experienced dramatic changes in ocean-atmospheric circulations, leading to the development of warmer conditions over NW Europe (e.g. Isarin et al. 1998; Bakke et al. 2009; Lane et al. 2013). It is plausible that tephra deposited during the Vedde Ash eruption, may have been held within perennial snow beds, and only liberated from these repositories once summer air temperatures

were of sufficient magnitude to counter the effect of winter precipitation and accumulation (e.g. Davies et al. 2007). The warmer conditions thought to have characterised the latter phases of the stadial would have likely had a detrimental effect on the size and extent of snow beds in Scotland (Isarin et al. 1998; Bakke et al. 2009). With the onset of Holocene warming, this would have triggered the final demise of these repositories, flushing the remaining Vedde shards into basins and causing a secondary 'Abernethy' tephra peak.

MacLeod et al. (2015) rightfully acknowledge that the incidence of tephra peaks ascribed to the Abernethy Tephra may in some incidences represent reworking, but the evidence presented here illustrates that further caution is necessary regarding some site interpretations. These considerations must therefore be paramount when interpreting a tephrostratigraphy based on superposition and limited chemical data.

Scenario 2: multi-eruption

Following the above discussion, it is essential to chemically characterise surrounding sediments and to understand the distribution of tephra throughout the Loch Lomond Stadial and early Holocene. It is the development of protocols, such as contiguous chemical characterisation, that are essential if problematic issues such as repeating chemical signatures and the conflation of tephra horizons are to be fully resolved. It is particularly interesting to note that the Tanera Mòr sequence from Roberts (1997) i.e. the same basin as examined as part of this study, is cited as containing only one, non-visible layer in association with Loch Lomond Stadial sediments (Table 10.4). This is further evidence of the select nature of past tephrostratigraphic studies, and how a reinvestigation of sites in Scotland is necessary if full tephrostratigraphic suits are to be realised. Until this or other means by which the Abernethy Tephra can be distinguished from the Vedde Ash, the uncertainty of the tephra negates its usefulness as an isochron in most instances.

10.3.3.4 Early Holocene tephras

- Ashik
- Askja-S/10ka
- An Druim and the Høvdarhagi

The early Holocene tephrostratigraphy of Scotland is a particularly complicated and understudied subdivision of the overall tephra framework. However, the data presented

here suggests that it is amongst the most promising for future development, and crucial for the temporal constraint of early Holocene climatic perturbations.

Torfajökull-type tephras: the Ashik, An Druim/Høvdarhagi

As highlighted in Chapters 5-8, the early Holocene was a particularly active period for the Torfajökull system, with at least two, and possibly four eruptions emanating from this system. These are: the rhyolitic component of the Ashik Tephra (10,250-10,550 cal. yrs BP); the An Druim Tephra (9671-9490 cal. yrs BP); the Høvdarhagi Tephra (9850-9600 cal. yrs BP); and potentially also a component of the L-274 (10,325-10,125 cal. yrs BP) (Pyne-O'Donnell 2007; Ranner et al. 2005; Lind and Wastegård 2011). These tephras all exhibit a similar chemical signature to one another, and their residence within the early Holocene makes drawing a reliable distinction between them particularly problematic. Intermediary tephra horizons such as the Saksunarvatn Ash or Fosen Tephra occur at higher stratigraphic positions than the Ashik Tephra, and lower than both the An Druim and Høvdarhagi Tephras, thus tephrostratigraphic superposition can assist in this process of distinction. In this study, and following this premise, the Ashik Tephra has been recognised at Spretta Meadow and Quoyloo Meadow, whilst the An Druim/ Høvdarhagi has been recognised at Tanera Mòr 1 and Quoyloo Meadow.

However, such tephras may not always be detectable due to dispersal, taphonomic, preservation or resolution issues. An alternative approach which has emerged is the employment of regional biostratigraphic markers. Kelly et al. (2016) have demonstrated that the Ashik Tephra can be separated from the An Druim and Høvdarhagi Tephra's based on the position of the *Corylus* (hazel) rise in Scottish sequences. The succession from open ground taxa indicative of Loch Lomond Stadial conditions, to the birch and hazel dominated woodland of the Holocene is well documented, and is believed to have been completed broadly within the first millennium of the Holocene (e.g. Walker 1984; Birks 1989; Kelly et al. 2016). This means that the *Corylus* rise occurs after the deposition of the Ashik Tephra, but before the occurrence of the An Druim/ Høvdarhagi horizons (Kelly et al. 2016). Whilst seemingly robust, this time-transgressive method is not applicable in more southerly latitudes where the *Corylus* rise is documented to occur much sooner in the Holocene, or the distribution is affected by the presence of refugia and/ or other ecological restrictions (e.g. Tallantire 2002). At present therefore, radiometric dating methods are arguably amongst the most effective means to distinguish between these three horizons. Having said that, the overlapping age ranges of the An Druim and Høvdarhagi means that these latter tephras are much

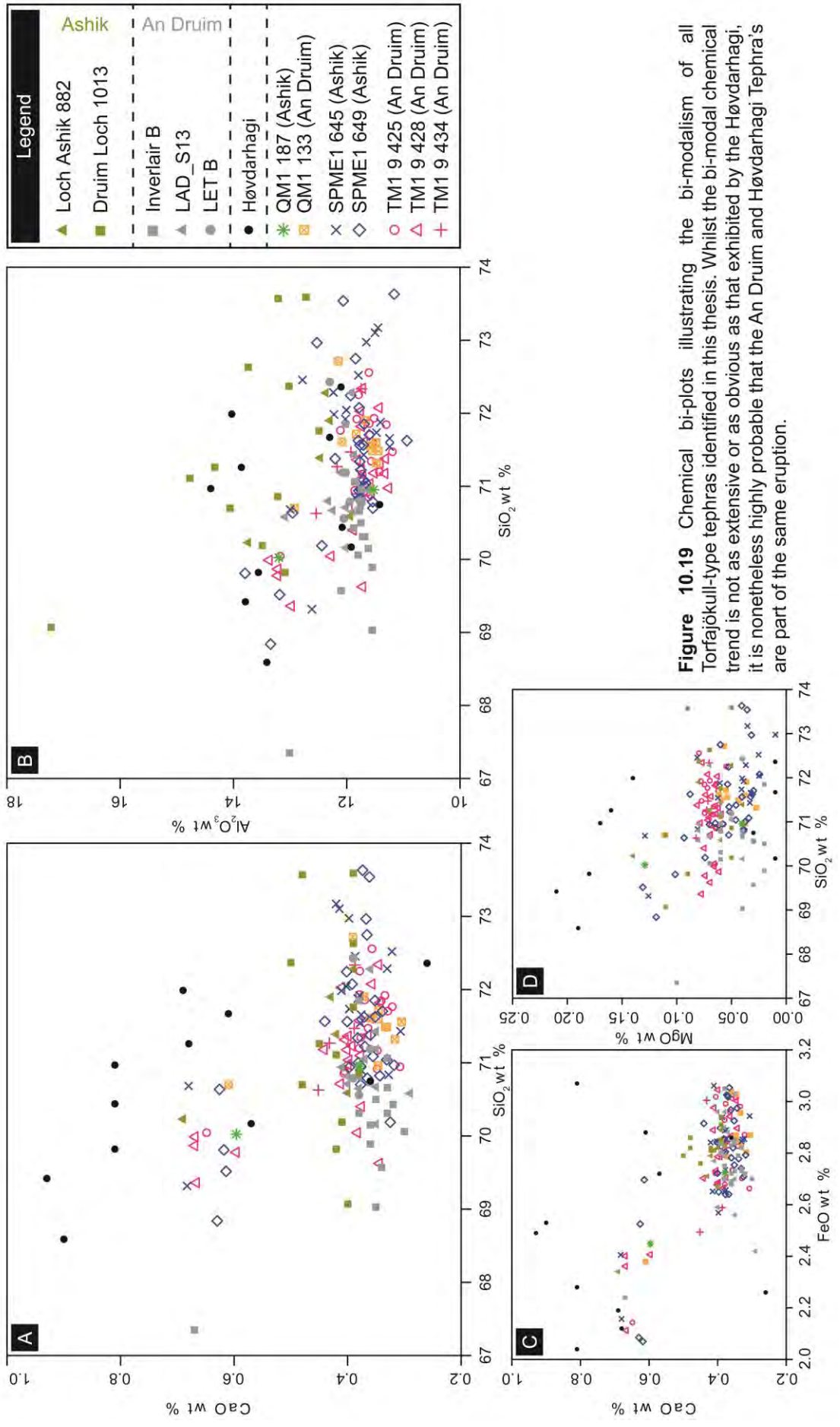

Figure 10.19 Chemical bi-plots illustrating the bi-modalism of all Torfajökull-type tephras identified in this thesis. Whilst the bi-modal chemical trend is not as extensive or as obvious as that exhibited by the Høvdarhagi, it is nonetheless highly probable that the An Druim and Høvdarhagi Tephra's are part of the same eruption.

more difficult to distinguish (see section 11.2). This similarity in age has led Lind and Wastegård (2011), Kelly et al. (2016), and Timms et al. (2016) to suggest that these tephras may be part of the same eruption. However, Lind and Wastegård (2011) also argue that the Høvdarhagi exhibits a bimodality that is absent from the An Druim tephra, and is thus more characteristic of the Ashik Tephra and later Holocene tephras deriving from the Torfajökull system, e.g. the Lairg B horizon (Dugmore and Newton 1995; Pilcher et al. 1996).

Figure 10.19 illustrates the Torfajökull derived tephra horizons analysed as part of this study plotted against the reference data sets for each respective eruption. As can be observed, all of the horizons examined in this study exhibit a degree of bimodality, and that the larger the data set the more convincing the bi-modal trend is (Figure 10.19 A & C). The Høvdarhagi analyses from the Faroe Islands clearly exhibits the most prominent and well developed bi-modalism of these horizons, however, the evidence presented here might lead to the interpretation that the An Druim and the Høvdarhagi tephras represent slightly different phases of the same eruption. The lesser bimodality in records from Scotland (this study; Ranner et al. 2005; Kelly et al. 2016) can possibly be explained by an evolution in the eruptive series and/or a coincidental shift in the direction of North Atlantic weather systems. The delivery of shards possessing a narrower chemical range to Scotland is a plausible hypothesis considering the variable dispersal characteristics of more recent Icelandic eruptions (Davies et al. 2010; Stevenson et al. 2012, 2013).

As a means to test this hypothesis, additional analyses of the An Druim Tephra from the type-site at Lochan An Druim will be required to establish whether the bi-modalism seemingly absent from these analyses, is either a product of a low number of data points or a genuine feature of the An Druim Tephra. Based on the larger data sets acquired in this thesis, an amalgamation of the An Druim and Høvdarhagi would be favoured, although a caveat on this is the seemingly different age estimates of these tephras, this issue is addressed in section 11.2.

The Ashik/Askja-S/10ka relationship

One of the key questions to arise from this study is the relationship between the bimodal chemistry of the Ashik Tephra and the rhyolitic Askja-S/10ka Tephra. These two horizons have a limited spatial extent in Scotland (Figure 10.8) with the most detailed information on the former reported by Pyne-O' Donnell (2005; 2007; 2011). The primary focus of that study was to examine taphonomy of tephra in Scottish basins that necessitated the investigation of multiple core sequences, but this approach

restricted the number of horizons that were characterised chemically. Thus single cores were analysed chemically and additional correlations between cores made on the basis of shard morphology and stratigraphic position. Consequently the Ashik Tephra isochron (and others such as the Penifiler and Breakish) reported in Pyne-O' Donnell (2007) were not necessarily the cores from which chemical analyses were taken. Whilst this was acknowledged by the author at the time, subsequent unpublished analyses of the 'Ashik Tephra' from Loch Ashik basin indicate that this tephra was misidentified in some instances and is instead the Askja-S/10ka Tephra. This finding is perhaps even more significant when it is noted that the 'Ashik Tephra' has never been chemically characterised at Loch an t'Suidhe, only inferred on stratigraphic grounds.

These unpublished developments clearly complicate the taphonomic results of the Pyne-O'Donnell (2005; 2011) study, but they also further stress the necessity for thorough chemical characterisation in tephrostratigraphic projects. It is further evident therefore that the Ashik Tephra and the Askja-S/10ka Tephra clearly have a close stratigraphic relationship, which has been recently replicated by the identification of each aforementioned tephra in consecutive 1 cm samples at Quoyloo Meadow (QM1 187, QM1 188 respectively) (Timms et al. 2016; Chapter 5.0). In this case, high resolution sampling has allowed for a clear stratigraphic distinction to be made, and hence the Ashik Tephra is now known to be younger than the Askja-S/10 Tephra (Timms et al. 2016) (see section 11.4.2).

Whilst the stratigraphic relationship between the rhyolitic fraction of the Ashik Tephra and the Askja-S/10ka Tephra has seemingly been resolved, a new complication has arisen following the discovery of an additional Grímsvötn basalt alongside the Askja-S/10ka tephra at Crudale Meadow (CRUM1 496/498). It is a Grímsvötn basalt and a Torfajökull rhyolite which comprise the bi-modal 'Ashik Tephra' at Loch Ashik, Druim Loch, and Loch an t'Suidhe. However, given the miscorrelations of the 'Ashik Tephra' at Loch Ashik, and the chemically uncorrelated 'Ashik Tephra' at Loch an t'Suidhe, there is some doubt as to whether the Grímsvötn component of the Ashik is genuinely coeval with the Torfajökull rhyolitic fraction. The Grímsvötn basalt may instead have a closer stratigraphic relationship with that of the Askja-S/10ka tephra.

At present, the identification of a Grímsvötn basalt has not been identified in association with the Askja-S/10ka Tephra at any other site in NW Europe, and so this has been declared as a new horizon in this study i.e. CRUM1 496 (see section 10.3.1). However, given the discussion above concerning limitations of the density flotation method, and the infrequent use of magnetic separation techniques, this is not

necessarily conclusive evidence. Further high resolution analyses will be required to establish the stratigraphic relationship between the rhyolitic Ashik, the basaltic Ashik, and the rhyolitic Askja-S/10ka Tephra's. It is suggest that this is conducted at Loch Ashik, as previous studies have already established the presence of all three chemical components.

10.4 Chapter summary

- The results here have shown that tephras which have previously escaped detection in the British Isles, or which are poorly represented, can be identified if high resolution protocols are followed. This has enabled distinctly 'British' or 'Scottish' tephras to be integrated into the tephrostratigraphic framework, and the superposition of tephras in NW Europe to be refined.

- As a result of this study tephra 'connectivity' across Europe has been increased by 1.25 %.

- This chapter has demonstrated the necessity for contiguous high resolution sampling. It has been shown that low resolution scan methods are inadequate to fully resolve records, and had such methods been implemented in this study, the total number of tephra horizons identified per site would have been on average two less.

- An evaluation of existing tephrostratigraphic records in Scotland has shown that it is highly likely that the number of tephra horizons preserved within these sequences is underestimated.

- The exact number of tephra isochrons dispersed across Scotland is therefore a matter for further research; incomplete archives, inconsistent chemical characterisation, and a propensity to focus on specific chronozones instead of entire LGIT sequences has contributed to the spatial disparity and irregular pattern of tephra distributions observed across Scotland and NW Europe.

- Whilst the collective evidence presented here has been used to develop a regional tephrostratigraphical framework (Figure 10.8), following the evidence and discussion above, this scheme and any such like it should be regarded as provisional, ongoing, and open to refinement.

- By producing higher resolution tephrostratigraphies in the future, an improvement to the overall number of tephra-linkages can be made, thus enabling a more competent tephra framework, lattice or web to be constructed across NW Europe. This is an essential requisite for the development of more robust tephrochronologies (Chapter 11.0) and the further testing of climatic leads and lags (Chapter 12.0).

Chapter 11. Site Age Models and Tephrochronological Refinement

11.1 Introduction and chapter structure

The successful integration of dated tephra horizons into site chronologies has refined age depth models in many palaeoenvironmental and archaeological settings (e.g. Lowe et al. 2000; Larsen et al. 2002; Reide et al. 2012). More recently studies have emerged in which site chronologies are exclusively constructed from tephra ages (e.g. Brooks et al. 2012; Timms et al. 2016). It is essential therefore that robust dates are developed for tephra isochrons, and that uncertainties associated with the age transfer process is minimised. Erroneous age transfer can have a detrimental effect on any environmental, climatic or archaeological inference derived from the host sediment, and can also negatively impact the modelled age that is subsequently generated for any undated tephra horizon.

This chapter aims to develop independent age models for all sequences in this study where viable tephra correlations have been made, and to assign either refined or new age estimates for the ashes reported in Chapters 5-8. The chapter is divided into two main sections, with the first dedicated to a synopsis of the main tephrochronological problems facing Scotland and NW Europe during the LGIT. In several instances, revisions of published ages are made by: 1) developing new chronological models for sites; 2) re-running existing models with updated and revised OxCal parameters (Bronk Ramsey 2008; Bronk Ramsey and Lee 2013); and/ or 3) re-running existing models using up-to-date radiocarbon calibration curves (Reimer et al. 2013). In the second section of the chapter, provisional site age models are constructed using the current 'best' tephra age estimates. Using the protocols of Bronk Ramsey et al. (2015b), these site results are subsequently fed into a composite age model, with the purpose of further refining, and minimising uncertainty on tephra ages. The model outputs at this stage will provide a basis from which palaeoenvironmental questions can be asked in the ensuing chapter.

11.2 Current tephrochronological issues in Scotland and NW Europe

This section shall exclusively consider the tephras present within the Scottish tephrostratigraphic framework (see Chapter 10.0). However, it is worth noting that many of these issues will be apparent in other regional tephrostratigraphies across Europe. The input and output of all age models reported in this thesis are shown in Appendix C, and for age model conditions see section 4.10.

The Dimlington aged TM1 553 Tephra

The identification of the Dimlington (GS-2) aged TM1 553 tephra at several sites in Scotland is an intriguing development in the history of the unknown Borrobol volcanic province (Lind et al. 2016). This tephra resides well below the lithostratigraphic onset of the Windermere Interstadial, and hence before the occurrence of organic sedimentation. The potential for direct radiometric dating this horizon is therefore negligible. However, the occurrence of this tephra at Priest Island (Valentine 2015), and its position between the Borrobol Tephra and Dimna Ash, offers the best opportunity for the development of an interpolated age in Scotland. Figure 11.1 illustrates the age model for the Priest Island sequence developed in this study using the composite tephrostratigraphy of Valentine (2015).

The position of the Dimna Ash (PRI 811) and the TM1 553 isochron (PRI 700) in the Priest Island sequence, are denoted by the first occurrence of characteristic shard types. Between PRI 811 and PRI 700, shard morphologies are dominated by platey, fluted and 'butterfly' like specimens, which are considered characteristic of Katla-type eruptions (e.g. Mangerud et al. 1984; see section 10.3.3.1). At PRI 700, the dominant shard morphology shifts to a style more indicative of Borrobol-type tephras i.e. blocky, and vesicular (e.g. Turney et al. 1997; Pyne-O'Donnell 2007). This morphological inference is further supported by two chemical analyses denoting a Borrobol-type correlation for PRI 700 (Valentine 2015).

Tephrostratigraphic information from Valentine (2015), and the best age estimates for the Borrobol Tephra and the Dimna Ash (Bronk Ramsey et al. 2015b; Koren et al. 2008) were used to develop a *P_Sequence* age model in OxCal v 2.4. The output of this would suggest that the TM1 553 (PRI 700) has an age of ***14,951-14,035 cal. BP*** (Figure 11.1). This broad range reflects the lack of chronological constraint within the Dimlington interval, and hence the age of the horizon can be seen to overlap with the age of the Borrobol and Penifiler Tephra's. The age of this horizon is largely controlled by the age of the Dimna Ash, which itself is a minimum value derived from a basal radiocarbon date at Dimnamyra, Norway (Koren et al. 2008). The likelihood therefore is that both the TM1 553 Tephra and Dimna Ash layers are markedly older than these age estimates suggest, and hence like the Dimna Ash, the TM1 553 age reported here, should only be considered as a minimum. An older age for the TM1 553 may feasibly allow it to be correlated to tephras identified in offshore sequences around Iceland e.g. Eiríksson et al. (2000); Gudmundsdóttir et al. (2011; 2012). The ages of these horizons from marine cores HM107-05 and MD99-2271/2275 are purportedly 16,650-16,490 cal. yrs BP and 15,400-14,850 cal. yrs BP respectively. However, these ranges are also

likely to be inaccurate due to the variable marine reservoir offsets identified around the North Atlantic during this period (Lowe and Walker 2015).

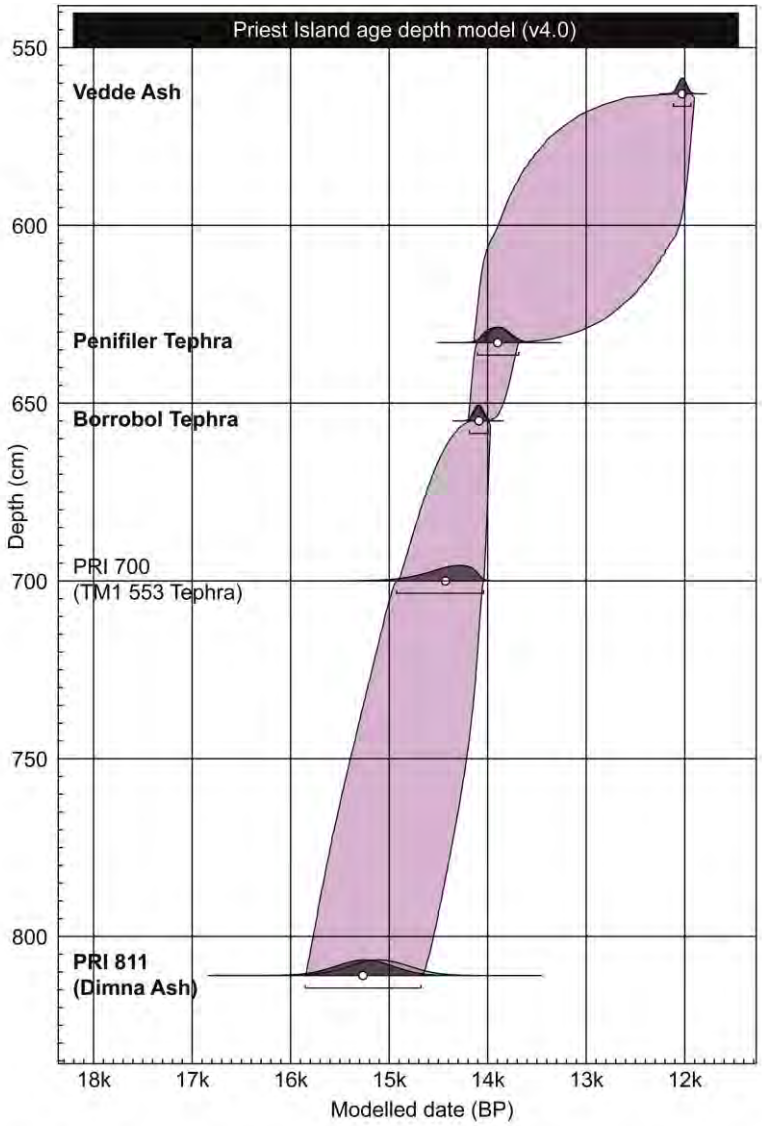

Figure 11.1 Interpolated age model derived for Priest Island, derived from the tephrostratigraphy of Valentine (2015). Modelled in OxCal v4.2 using the recommendations of Bronk Ramsey (2008), outlier analysis (Bronk Ramsey 2009), and variable rigidity (Bronk Ramsey and Lee 2013). Tephras contributing to the age model are highlighted in bold.

The age of the Borrobol type tephra in HM107-05 was generated by applying a modern averaged marine reservoir correction of 400 years to a radiocarbon date of 13,390 ± 120 ^{14}C yrs BP (Eiríksson et al. 2000). Marine sequences are notoriously difficult to date using radiocarbon techniques as appropriate correction factors may not always be reflected by current conditions (Lowe and Walker 2015). Palaeoceanographic changes, and variations in the strength and direction of ocean circulations can have a considerable effect on reservoir ages (e.g. Björck et al. 2003; Eiríksson et al. 2004). In the context of core HM107-05, a correction factor of 400 years

has been shown to be applicable at the level of the Saksunarvatn Ash (ca. 10,200 cal. BP), however, the value is likely to be inappropriate during earlier intervals (Eiríksson et al. 2000; Haflidason et al. 2000; Eiríksson et al. 2004). During the Lateglacial, cold Arctic water masses prevailed in the region, and a reservoir correction of 750–800 years has been suggested as a more viable alternative during the deposition of the Vedde Ash (ca. 12,100) (Eiríksson et al. 2004). During GS-2, it is therefore likely that a correction factor of 400 years is also insufficient to account for the radiocarbon offset. Eríksson et al. (2000) comment that in order for the tephra identified in HM107-05 to correlate with the Borrobol Tephra, a marine reservoir correction factor of 1500 years would be needed. Whilst a correlation to the Borrobol Tephra is unlikely due to the characteristically GS-2 aged biozone in which the HM107-05 Borrobol-type tephra resides, it does nonetheless illustrate that the 16,650-16,490 cal. yrs BP age is likely to be too old due to the 400 year correction factor.

The ages of the Borrobol-type tephras located in marine core MD99-2271 and MD99-2275 were derived from the Borrobol age reported by Pyne-O'Donnell et al. (2008). Subsequently this age has been revised by Matthews et al. (2011), and Bronk-Ramsey et al. (2015), hence the 15,400-14,850 cal. yrs BP estimate is no longer appropriate. Whether this tephra therefore actually relates to the Borrobol Tephra *sensu stricto*, or a late GS-2 age 'pre-Borrobol' horizon is open to debate. The only stratigraphic description of these horizons is that they lie just above glacial sediments (Gudmundsdóttir et al. 2011). Given that the timing and pattern of deglaciation in Iceland is yet to be fully understood (e.g. Norðdahl et al. 2008; Geirsdóttir et al. 2009), and that there is a lack of independent dates from the lower margins of MD99-2271 and MD99-2275, it is possible that a correlation to either the Borrobol or the TM1 553 could be argued for.

At present therefore, the TM1 553 Tephra in Scotland has no viable correlative elsewhere in Europe. There is some suggestion that Borrobol-type Tephras older than the Borrobol *sensu stricto* have been identified in the Greenland ice-core records (Eliza Cook pers. comm. 2013). However, at present this data remains unpublished and any correlations untestable. Future links for the TM1 553 tephra will no doubt emerge in due course, and at other sites with greater stratigraphic control. However, until that time, the provisional ***14,951-14,035 cal. yrs BP*** age of the pre-Borrobol horizon or subsequent revisions as determined by Bayesian age modelling in this thesis, should be considered the best chronological estimate of this tephra in terrestrial sequences in Europe.

The Penifiler Tephra

As discussed in section 10.4.2 there is considerable stratigraphic uncertainty associated with the Borrobol-type tephras of the Windermere Interstadial. Inconsistent stratigraphic correlation may have been exacerbated by several, spatially variable Borrobol-type tephras, previously unrecognised as individual isochrones through this interval. Of particular concern is the Penifiler Tephra which in some instances exhibits a relationship associated with a cold oscillation broadly equivalent to GI-1d, whilst in other instances the isochron has been correlated to a tephra that seemingly post-dates this event (see section 10.4.2).

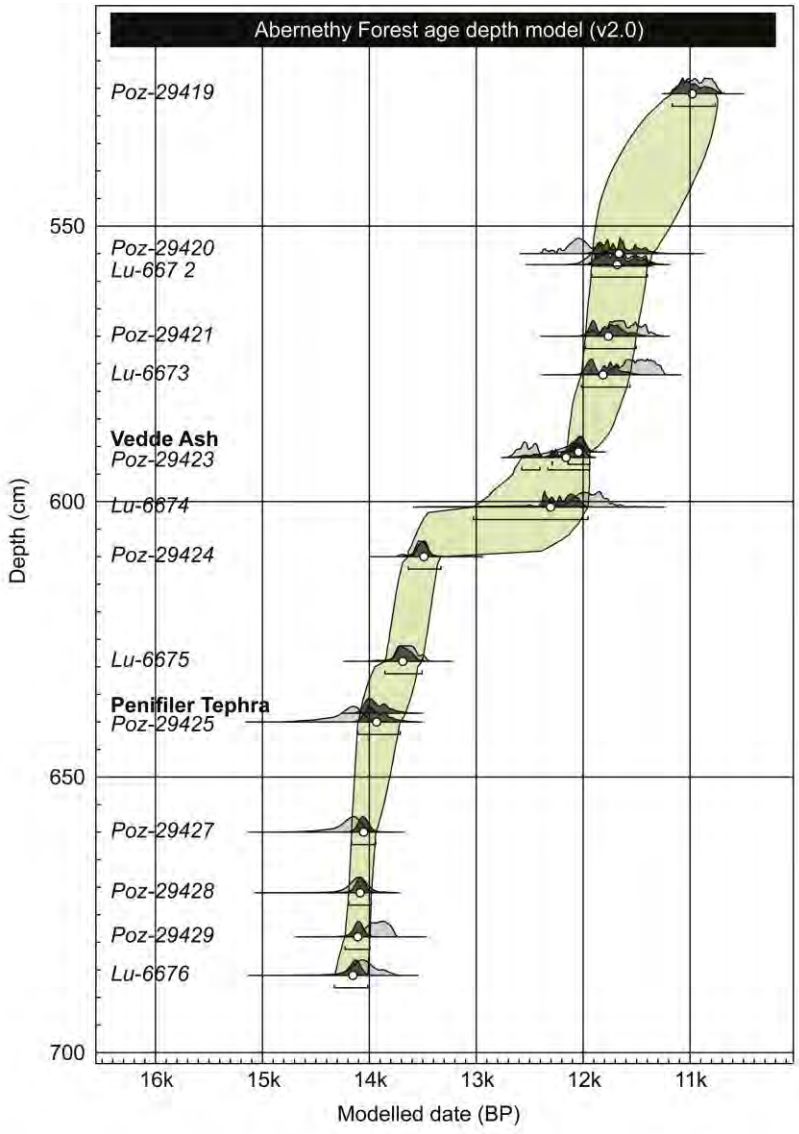

Figure 11.2 Interpolated age model for Abernethy Forest, modified from Matthews et al. (2011). Modelled in OxCal v4.2 using the recommendations of Bronk Ramsey (2008), outlier analysis (Bronk Ramsey 2009), and variable rigidity (Bronk Ramsey and Lee 2013). Tephras highlighted in bold, radiocarbon dates are italicised.

At present the best age of this horizon is derived from an amalgamation of the Penifiler isochron at Abernethy Forest, and a Borrobol-type tephra identified within the Hässeldala port sequence (Bronk Ramsey et al. 2015b). However, as has been commented on by Lind et al. (2016), the Penifiler layer at Abernethy Forest extends over 20 cm, that inherently raises doubt over the accuracy of the isochron placement. There is also some confusion surrounding the Borrobol-type tephra within the Hässeldala port sequence, which has been ascribed to both the Borrobol Tephra (Davies et al. 2003; Lind et al. 2016), and the Penifiler Tephra (Pyne-O'Donnell et al. 2008; Bronk Ramsey et al. (2015b). The stratigraphic placing i.e. within sediments pertaining to the end of the 'Older Dryas' (ca. GI-1d), and an age estimate generated by Davies et al. (2003) and Wohlfarth et al. (2006) would favour the latter. However, this thesis suggests there is sufficient doubt as to the validity of the unified Scottish and Swedish 'Penifiler' Tephra, that the age estimate from Hässeldala port has been excluded in this work as a matter of caution.

In an effort to minimise the uncertainty associated with the 'Penifiler' horizon, and to improve the constraints on the 'Penifiler' *per se*, the Abernethy Forest age model has been re-run with the recommendations and updated OxCal parameters of Bronk Ramsey (2008; 2009); Bronk Ramsey and Lee (2013), and utilising the IntCal13 calibration curve (Reimer et al. 2013). The result of this model is illustrated in Figure 11.2, and the age of the Penifiler from Abernethy Forest is now estimated to be ***14,082-13,655 cal. BP***.

The Askja-S/10ka

The unique geochemical signature of the Askja-S/10ka during the LGIT and the highly constrained age estimate of this horizon makes it a fundamental pinning point in early Holocene tephrostratigraphies (Wohlfarth et al. 2006; Lane et al. 2011b; Bronk Ramsey et al. 2015b). The horizon has a close relationship with the Hässeldalen Tephra, with both horizons flanking the upper and lower margins of the PBO respectively (Davies et al. 2003; Wohlfarth et al. 2006; Ott et al. 2016). Current best age estimates of these tephras, derived from Bayesian based age models (95.4 % confidence intervals), date the Hässeldalen Tephra to 11,596-11,164 cal. yrs BP (Wohlfarth et al. 2006), and the Askja-S/10ka Tephra to 10,956-10,716 cal. yrs BP (Bronk Ramsey et al. 2015b). This suggests there is a minimum age difference between these tephras of 208 years. However, recent work by Ott et al. (2016), where the Askja-S/10ka and Hässeldalen Tephra's were traced to a varved sequence in Poland, has suggested that this age difference is incorrect, and that previous age estimates of the Askja-S/10ka are too young. The varved record at Lake Czechowskie, suggests that the difference between

the two tephras must be 152 +11/-8 varve years, approximately 50 years less than what is theoretically possible if the age models of Wohlfarth et al (2006) and Bronk Ramsey et al. (2015b) are correct. Using the Hässeldalen Tephra age of 11,380 ± 216 cal. yrs BP as an anchor, and adding the differential varve counts from Lake Czechowskie, Ott et al. (2016) present an age for the Askja-S/10ka Tephra of 11,454–11,002 cal. BP; one which is significantly older than existing models would suggest (Figure 11.3).

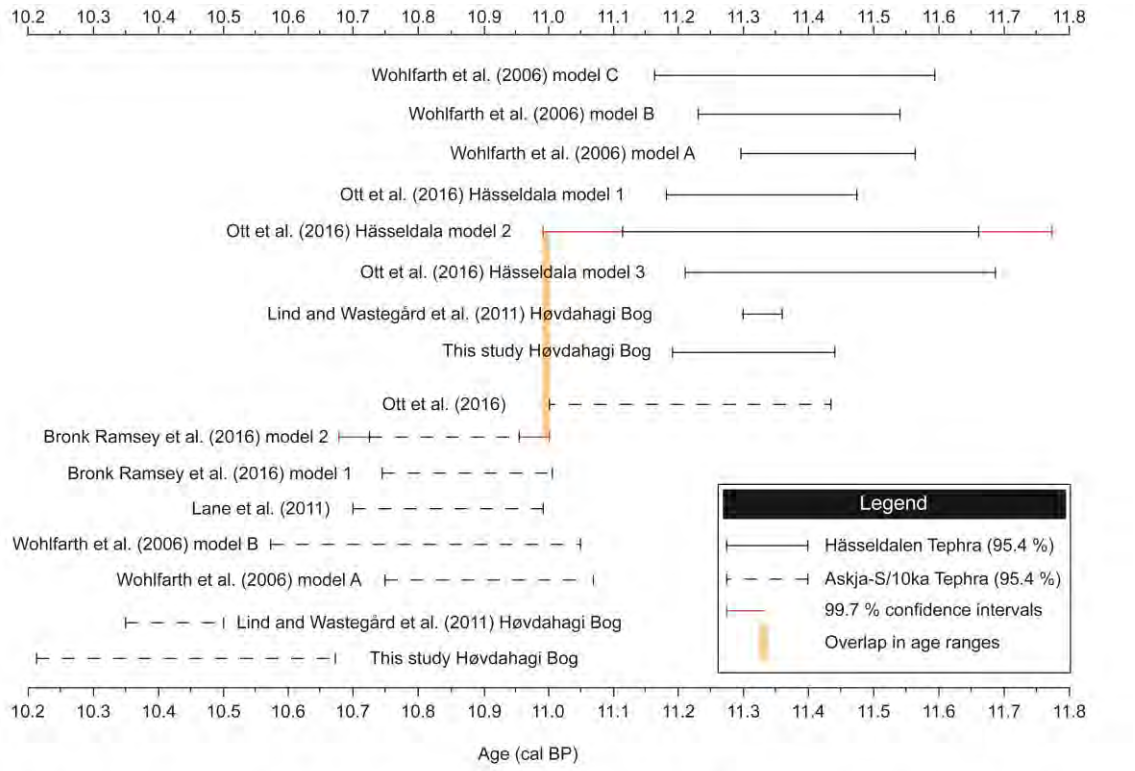

Figure 11.3 Compilation of the published ages ranges for the Hässeldalen and Askja-S/10ka Tephra's (95.4 % confidence interval). The red line indicates the 99.7 % confidence interval for the two most robust age estimates of the tephras, which can be observed to overlap. The Askja-S/10ka Tephra from Ott et al. (2016) is notably older than the ranges suggested at other sites, this in part is likely derived from the 'anchor point' used to tie the varve chronology into absolute time (see text for details). Also shown are the remodelled age estimates from Høvdahagi Bog (see An Druim Høvdahagi age discussion).

However the 'floating' nature of the Lake Czechowskie varve chronology negates a revision of tephra ages in this manner. Simply accepting the Hässeldalen Tephra age as proposed by Wohlfarth et al. (2006) as an anchor, but discrediting the equally viable age of the Askja-S/10ka (Bronk-Ramsey et al. 2015) because it does not fall within the 152+11/-8 varve year period is not statistically valid. If the 99.7% confidence intervals are plotted for the most robust age estimates of the Hässeldalen and the Askja-S/10ka Tephras (Figure 11.3), then an overlap in the ages between these two horizons can be observed. This illustrates that further work is necessary to anchor the Czechowskie varve chronology at a point independent from the two isochrons that are being

scrutinised. At present therefore, whilst the results from Lake Czechowskie offer an excellent opportunity to refine the ages of the tephras, it is not immediately apparent whether it is the absolute age of the Hässeldalen Tephra, the Askja-S/10ka Tephra, or both which need revision. Until further more conclusive evidence is provided, the best age estimates for these two tephras should, in respect to the Hässeldalen Tephra, be considered the 'model 2' age of Ott et al. (2016) (***11,657-11,117 cal. BP***), derived from the recalibration of the Wohlfarth et al (2006) 'model B'. Whilst the most robust estimate for the Askja-S/10ka tephra, should be considered the 'model 2' age from Bronk Ramsey et al (2015b) (***10,956-10,716 cal. BP***), which combines the well constrained ages from Hässeldala port (Wohlfarth et al. 2006) and Soppensee (Lane et al. 2011b).

The Ashik and Hovsdalur Tephras

The Ashik and Hovsdalur Tephras are two early Holocene isochrons which, at present possess poor temporal constraints. The former exhibits no quantifiable age estimate, and instead is defined only by stratigraphic association with an LOI downturn, thought to reflect the PBO (Pyne-O'Donnell 2007; Brooks et al. 2012). To date therefore, the inclusion of this horizon within a chronological framework has necessitated a 'best guess' at the age range based on this climato-stratigraphic inference e.g. the 11,200-10,700 cal. BP estimate of Brooks et al. (2012). For the Hovsdalur, temporal constraint is also limited, being previously only identified in the Faroe Islands (Wastegård 2002). Here a tentative age of 10,695-10,285 cal. BP was assigned, based on the premise of a simple linear age model, extrapolating well below a basal radiocarbon date (Wastegård 2002).

The limited identification of these tephras around the North Atlantic periphery has severely hindered their chronological refinement, and hence their value as isochronous markers. The lack of a robust and reliable age estimate for the Ashik Tephra in particular, negates its use in the individual site chronologies of this thesis. Tephras positioned within the early Holocene make invaluable marker horizons, and are of considerable benefit for site chronologies considering the radiocarbon 'plateaux' of the early Holocene (e.g. Kitagawa and van der Plicht 1998). It is necessary therefore that the ages of these horizons are refined where possible, and that a greater effort be placed on resolving early Holocene tephrostratigraphies in Northern Europe.

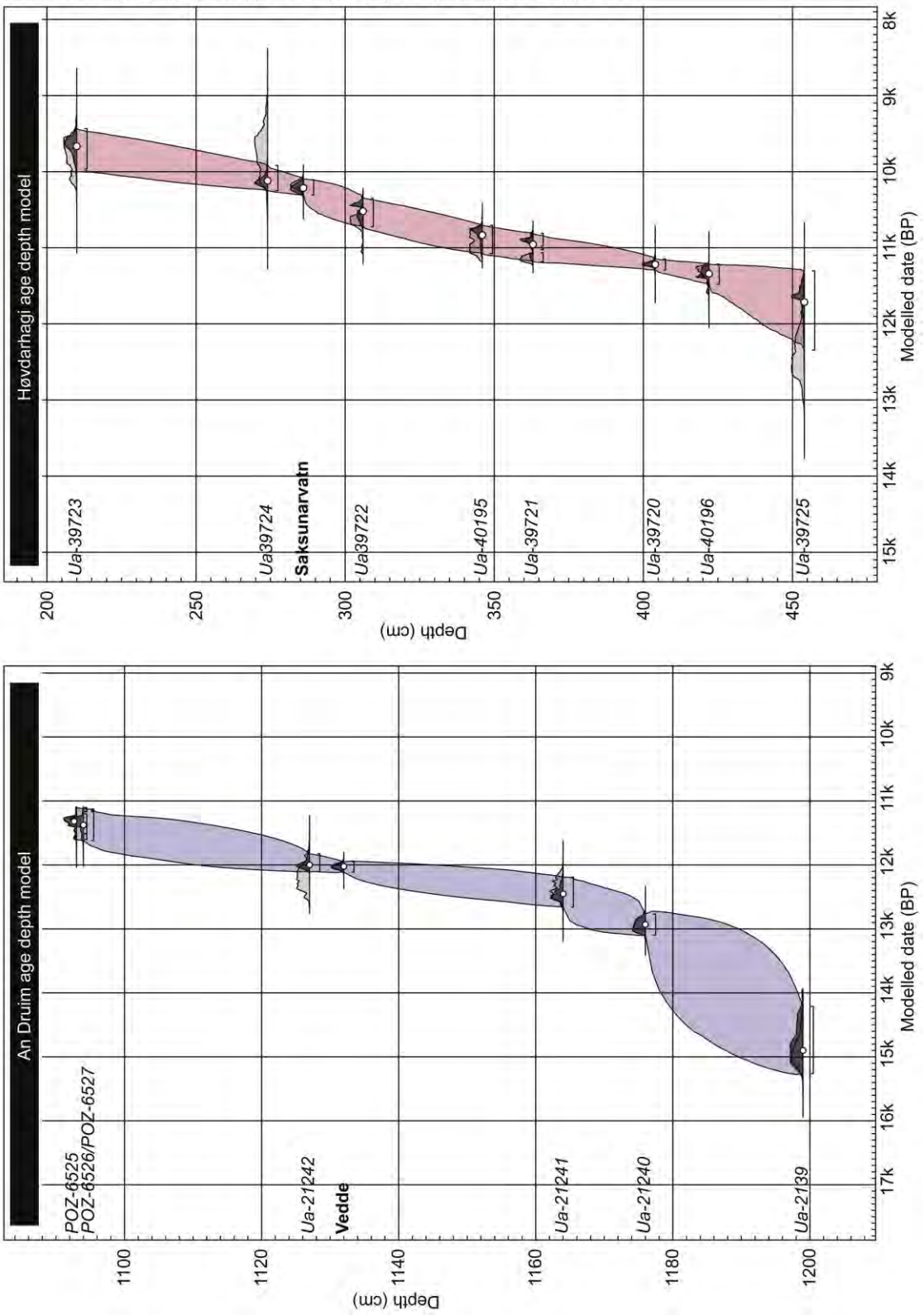

Figure 11.4 Remodelled Lochan An Druim and Høvdarhagi site age models using the OxCal recommendations of Bronk Ramsey (2008), outlier analysis (Bronk Ramsey 2009) and variable rigidity (Bronk Ramsey and Lee 2013). It is likely that the much broader range of the Høvdarhagi illustrates the over constraint of the original age model by (Lind and Wastegård 2011). Tephras contributing to the age model are highlighted in bold, radiocarbon dates are italicised. The depth of the An Druim Tephra at Lochan An Druim is 1094 cm, and the depth of the Høvdarhagi Tephra at Høvdarhagi is 217 cm.

The An Druim/ Høvdarhagi

As discussed in section 10.4.4 the An Druim and the Høvdarhagi Tephra's may represent slightly different phases of the same eruption. The chemical bi-modality of the Høvdarhagi and the absence of such a convincing trend from analyses of the An Druim have been used to argue a distinction between the two tephras (Lind and Wastegård 2011). However, it is evident from the analyses obtained in this thesis and from the work of Kelly et al. (2016) that the absence of a bi-modal trend within the original An Druim analyses (Ranner et al. 2005) may have been an artefact of the small sample size.

Whilst this still needs to be chemically confirmed by reinvestigating the An Druim type-site, impetus for their mergence can be obtained from a reinvestigation of the respective age estimates. Currently the An Druim is reported as 9671-9490 cal. yrs BP, whereas the Høvdarhagi exhibits a seemingly older range of 9850-9600 cal. yrs BP. At present therefore, there is a 71 year overlap in the two age ranges based on these 95.4% confidence intervals. Remodelling of these type-site chronologies using the recommendations, and updated OxCal parameters of Bronk Ramsey (2008; 2009); Bronk Ramsey and Lee (2013), and utilising the IntCal13 calibration curve (Reimer et al. 2013) has produced an age of ***9884-9536 cal. BP*** for the An Druim Tephra, and an age for the Høvdarhagi Tephra of ***10,016-9490 cal. BP*** (Figure 11.4). At Lochan An Druim two bulk radiocarbon dates were used in the original analyses. These were omitted from this remodelling exercise for two reasons: firstly there is a history of erroneous bulk sediment radiocarbon dates where ages are altered through the inclusion of carbon from geological sources (Birks 1984), and, secondly, the absence of accompanying $\delta^{13}C$ values (Ranner 2005; Ranner et al. 2005), which provide an objective assessment of contamination (e.g. Walker et al. 2001).

In the context of the Høvdarhagi, it would seem that the broader age range in this instance is likely a consequence of the original age model being over-constrained, a phenomenon already illustrated in Figure 11.3 in the context of the Hässeldalen and Askja-S/10ka Tephra from Høvdarhagi Bog. The over constraining of age depth models is a particular problem in earlier versions of OxCal, where the *K value*, a parameter setting the number of accumulation events per depth, was manually controlled (Bronk Ramsey 2008). A high *K value* would hence constrain the data very rigidly, leading to a false level of precision, and thus in the context of tephra age estimates, narrow age ranges. This revaluation of the Høvdarhagi Tephra age, and its encapsulation of the An Druim date, adds further weight to the argument that the Høvdarhagi and An Druim Tephras are representative of the same eruption.

11.3 Provisional age depth models

As demonstrated, there are numerous factors and caveats that require careful consideration and revision prior to the development of tephra based age models. It is probable that in many instances such issues will be beyond immediate and feasible resolve, thus models will inevitably reflect the limitations of the current 'state of play'. It is necessary that studies remain transparent with the data they use to compile chronological models, and be fully aware of the limitations of such outputs. Table 11.1 lists the tephras and their respective ages used within the provisional site age models described in the ensuing sections. These are predominately the 'best' age estimates from current published work, but also include the revised ages suggested in the previous section.

Table 11.1 Compilation of the best age determinations for the tephras identified during the course of this study. Several of the published sites were remodelled in OxCal v4.2 using the recommendations of Bronk Ramsey (2008),outlier analysis (Bronk Ramsey 2009), and variable rigidity (Bronk Ramsey and Lee 2013). The remodelling of the Penifiler, the An Druim, the Høvdarhagi, and the reasons behind that are discussed in section 11.2. The remodelling of the Fosen age from Grønlia fen was also conducted; this was due to the absence of error reporting in Lind et al. (2013).

Tephra	Mean age	Error (1σ)	Error (2σ)	Age range (95.4 %)	Reference
An Druim	9648	79	158	9884-9536	this study; Ranner et al. (2005)
Høvdarhagi	9719	128	256	10,016-9490	this study; Lind et al. (2011)
Fosen	10,177	68	136	10,251-10,019	this study; Lind et al. (2013)
Saksunarvatn	10,176	49	98	10,257-10,056	Bronk Ramsey et al. (2015b)
Hovsdalur	10,475	175	350	10,695-10,285	Wåstegård (2002)
Askja-S/10ka	10,830	57	114	10,956-10,716	Bronk Ramsey et al. (2015b)
Ashik Tephra	No quantified age				Pyne-O'Donnell (2007); Brooks et al. (2012)
Hässeldalen Tephra	11,387	135	270	11,657-11,117	Ott et al. (2016)
Abernethy Tephra	11,462	122	244	11,721-11,231	Bronk Ramsey et al. (2015b)
Vedde Ash	12,023	43	86	12,102-11,914	Bronk Ramsey et al. (2015b)
Penifiler Tephra	13,885	115	230	14,082-13,655	this study; Matthews et al. 2011
Borrobol Tephra	14,098	47	94	14,190-14,003	Bronk Ramsey et al. (2015b)
pre-Borrobol Tephra (PRI 700)	14,426	253	506	14,951-14,035	this study; Valentine (2015)
Dimna Ash	15,100	300	600	15,400-14,850	Koren et al. (2008)

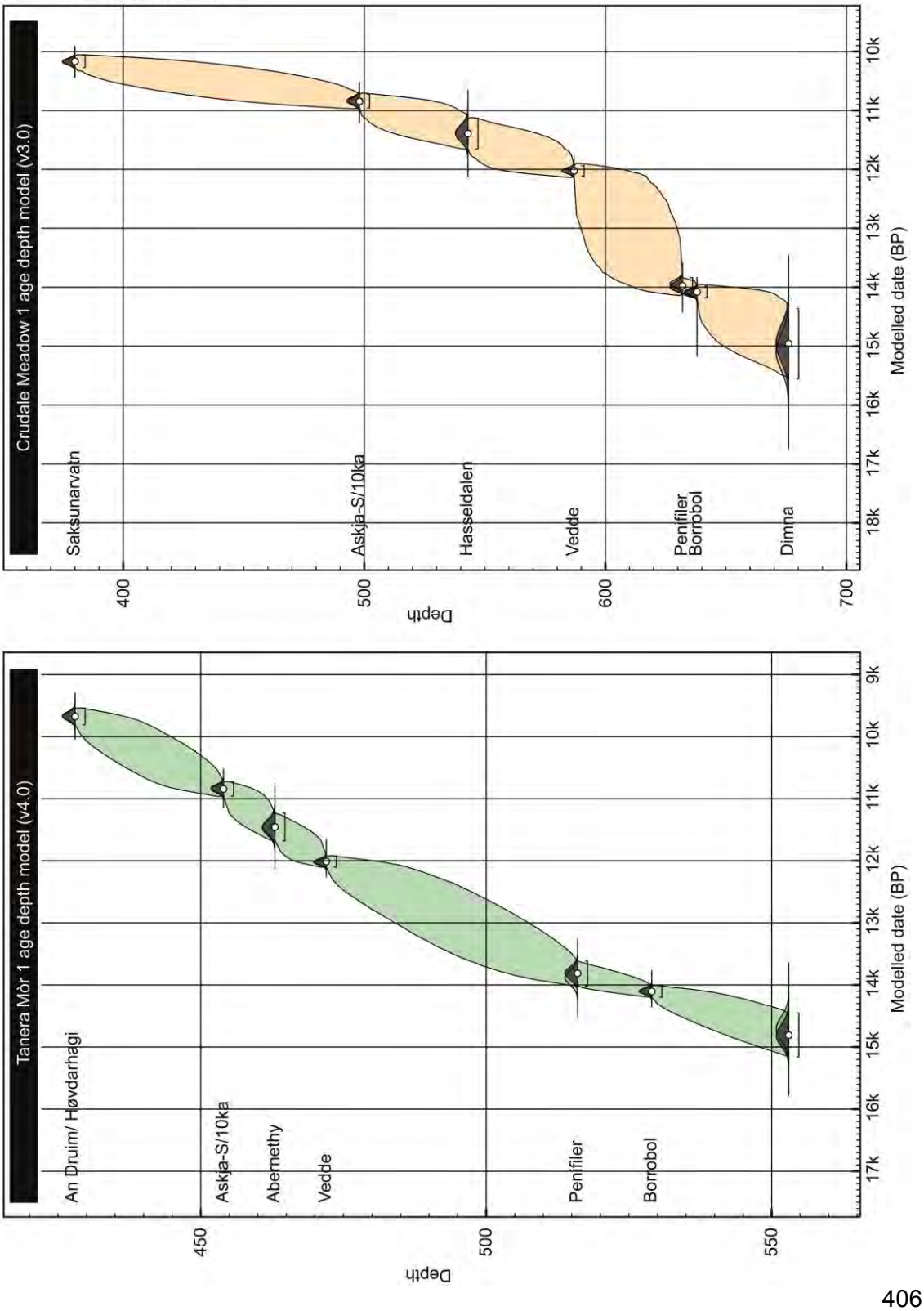

Figure 11.5 Tanera Mòr 1 and Crudale Meadow provisional age depth model. Modelled in OxCal v4.2 using the recommendations of Bronk Ramsey (2008), outlier analysis (Bronk Ramsey 2009) and variable rigidity (Bronk Ramsey and Lee 2013).

11.3.1 Tanera Mòr provisional age model

Eight tephra isochrons form the basis of the provisional Tanera Mòr age model (Figure 11.5) which is based on the following assumptions:

1) The basal Borrobol-type shards and the Dimna Ash exhibit a diffuse and conflated signature at the base of the sequence. In this instance, the first occurrence of these shards is believed to represent the 'isochron' of the two tephras (TM1 553), although it is unlikely that these eruptions were coeval due to their stratigraphic distinction at Priest Island (Valentine 2015; see section 10.4.1).

2) The diffuse nature of the Askja-S/10ka tephra, and the similar concentrations across the four intervals analysed in the Tanera Mòr 1 sequence makes isochron placement problematic. In this case, the first stratigraphic appearance of shards exhibiting a Askja-S/10ka signature has been chosen to mark the isochron (TM1 454).

3) Given the previous discussions on the nature of the An Druim and Høvdarhagi Tephras, both ages were used by applying the *Combine* function in OxCal. This tool considers the entire age range of these two estimates to provide the most probable, and statistically robust age estimate for the TM1 428 horizon.

11.3.2 Crudale Meadow provisional age model

Seven tephra isochrons form the basis of the provisional Crudale Meadow age model (Figure 11.5) which is based on the following assumption:

1) The dacitic tephra toward the base of the sequence (CRUM1 676) is suggested to be a previously unrecognised intermediate phase of the Dimna Ash (see section 6.3.1).

11.3.3 Spretta Meadow provisional age model

Five tephra isochrons form the basis of the provisional Spretta Meadow age model (Figure 11.6) and is based on the following assumptions:

1) The Borrobol-type tephra analysed at the base of the sequence (SPME1 701) is assumed to be a correlative of the Borrobol-type tephra identified at the Windermere Interstadial/ Loch Lomond Stadial transition in Crudale Meadow (CRUM1 597). The age of this horizon is estimated to be ***13648-11936 cal. BP***, and hence has been used to date the lowest interval in the SPME sequence (SPME1 703). It should be noted, however, that this interval may not represent the isochron of the event, which may reside in the irretrievable sediments at the very base of the Spretta sequence.

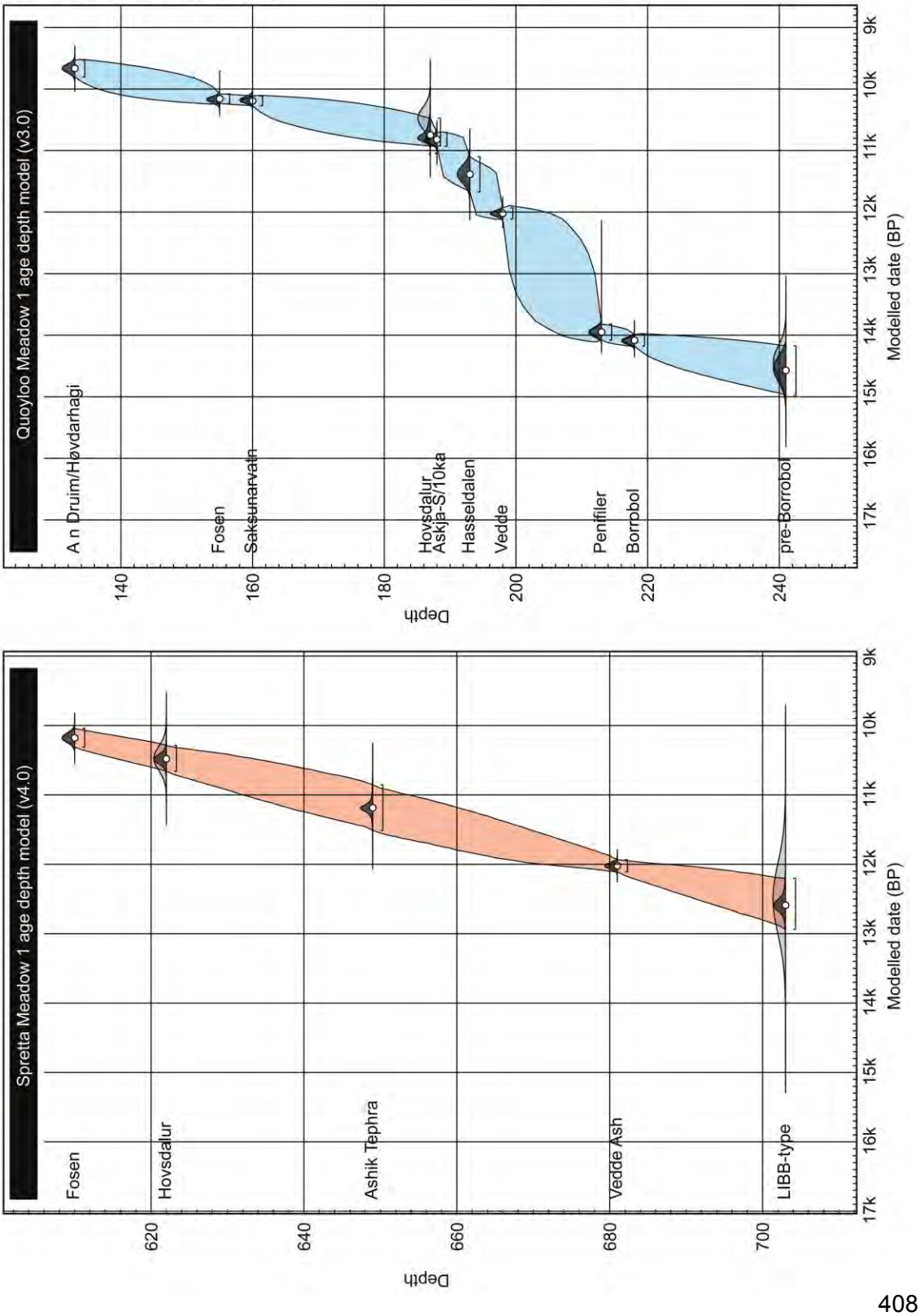

Figure 11.6 Spretta Meadow and Quoyloo Meadow provisional age depth model. Modelled in OxCal v4.2 using the recommendations of Bronk Ramsey (2008),outlier analysis (Bronk Ramsey 2009) and variable rigidity (Bronk Ramsey and Lee 2013).

2) An arbitrary 1σ error range of 300 years is given to the Ashik Tephra due to an uncertain stratigraphic position, and being described only as older than the Saksunarvatn Ash and potentially younger than the PBO (Pyne-O'Donnell, 2007). This magnitude of uncertainty permits the model to find a plausible route through the layer while not constraining the age in a meaningful way.

3) The Hovsdalur and Fosen correlations at SPME1 (622) and (610) respectively, are based on low shard concentrations. There is perhaps some doubt as to the robustness of correlations based on low concentrations especially when these are in the presence of mixed chemical assemblages. However, given the stratigraphic positioning of these tephras, and the absence of similar chemical types within close proximity of the horizons, such correlations seem plausible and have been accepted in this instance.

11.3.4 Quoyloo Meadow provisional age model

Eleven tephra isochrons form the basis of the provisional Quoyloo Meadow age model (Figure 11.6), which is based on the following assumptions:

1) The Borrobol-type tephra analysed at the base of the sequence (QM1 241) has been correlated to the pre-Borrobol tephra, and hence utilises the age derived from the Priest Island record (PRI 700). As iterated elsewhere, this age should be considered a minimum with the likelihood of this isochron being older than the stipulated estimate.

2) The Hässeldalen Tephra has been incorporated into the age model despite only one shard in QM1 192 characterising this horizon. It is considered unlikely that the occurrence of the solitary Snæfellsjökull-type shard at this depth is down-worked from the more abundant and chemically-identical Hovsdalur Tephra horizon (QM1 187), as no shards bearing this chemical affinity were identified in the intervening horizon (QM1 188).

3) As previously stated, the Ashik Tephra has an uncertain age range, being described only as older than the Saksunarvatn Ash and likely younger than the PBO (Pyne-O'Donnell, 2007). As is the case at Spretta Meadow, an arbitrary 1σ error range of 300 years is used to constrain this tephra.

4) The occurrence of both the Ashik and the Hovsdalur Tephra's in QM1 187 has been addressed by using the *Combine* function in OxCal. This parameter enables the entire age range of these tephras to be considered, and hence provides the most statistically viable age for the amalgamated horizon. It should be noted, however, that it is unlikely

that these eruptions were coeval, instead the low sedimentation rate at Quoyloo Meadow has prevented a distinct stratigraphic separation of the horizons (see section 10.2.1).

5) As is the case at Tanera Mòr 1 both the An Druim and Høvdarhagi Tephra ages were merged using the *Combine* function in OxCal. This provides the most statistically viable age for this Torfajökull derived horizon.

11.3.5 Provisional model output

Table 11.2 provides a summary of the tephra ages produced by each site simulation. Whilst there are inherent similarities in the ages of some of the tephras, for example the Vedde Ash and Saksunarvatn Ash i.e. those exhibiting the smallest inputted error ranges, there is significant disparity in those that are typified by much broader age estimates. Tephras such as the Ashik and Hovsdalur, inevitably exhibit a much greater difference between the respective site simulations. This is primarily due to the way in which the model has dealt with the respective stratigraphical and chronological information available from each site. The simulated age of the Ashik Tephra for example at Spretta Meadow and Quoyloo Meadow, differs by approximately 439 years if the mean value is taken as a correlative. This same trend can be observed for the Hovsdalur, in which a difference of 267 years can be seen between the two mean values. At present therefore it is not possible to accurately determine a best age estimate for these early Holocene tephras from these sites in isolation.

It is evident therefore, that single site chronologies may not be adequate to fully extract the chronological potential of tephra isochrons. Furthermore, where poorly dated tephras comprise a significant proportion of a sites chronological framework, large uncertainties may arise. The development of individual age models when developing site chronologies may need revision and studies should instead consider individual site determinations only as the first stage in a multi-part modelling process. This second step, where the individual site chronology is considered within the context of the region but uses additional stratigraphic and chronological information from previous studies, may assist in the overall age refinement of the site (e.g. Bronk Ramsey et al. 2015b). This is considered in the following section.

Table 11.2 Summary of the tephra ages derived from the provisional site age depth models.

	Tanera Mor 1				Crudale Meadow				Spretta Meadow				Quoyloo Meadow			
Tephra	**Mean**	**1σ**	**2σ**	**95.4 % Range**	**Mean**	**1σ**	**2σ**	**95.4 % Range**	**Mean**	**1σ**	**2σ**	**95.4 % Range**	**Mean**	**1σ**	**2σ**	**95.4 % Range**
An Druim/ Høvdarhagi	9676	67	134	9809-9541									9665	67	134	9803-9532
Fosen									10177	67	134	10,312-10,044	10158	39	78	10,238-10,081
Saksunarvatn					10168	51		10,270-10,070					10193	39	78	10,273-10,116
Hovsdalur									10480	87	174	10,660-10,287	10747	113	226	10,927-10,476
CRUM1 496					10825	76	152									
Ashik									11186	139	278	11,513-10,855	10747	113	226	10,927-10,476
Askja-S/10ka	10844	58	116	10,958-10,727	10845	59	118	10,960-10,727					10821	60	120	10,934-10,704
Hässeldalen					11393	131	262	11,654-11,130					11385	143	286	
Abernethy	11455	112	224	11,680-11,231												
Vedde	12012	48	96	12,104-11924	12025	44	88	12,112-11,937	12022	44	88	12,108-11,935	12021	45	90	12,110-11,932
CRUM1 597					12494	512	1024	13,648-11,936	12590	156	312	12,938-12,203				
Penifiler	13812	100	200	14,018-13,615	13976	69	138	14,101-13,837					13949	73	146	14,079-13,819
Borrobol	14196	46	92	14,196-14,012	14079	53	106	14,179-13,982					14083	47	94	14,177-13,988
pre-Borrobol	14808	175	350	15,158-14,450									14571	204	408	
Dimna	14808	178	356	15,158-14,450	14958	296	592	15,553-14,365								14,975-14,173

11.4 Composite age model

11.4.1 Composite model development

A reduction in errors from site-specific age models can be achieved by linking records together using common tephras as tie points. The resulting composite model is able to boast refined age estimates, and further improve model output confidence. Figure 11.7 provides a schematic representation of how the tephras from the four sites in this study, were linked together using the composite model approach of Bronk Ramsey et al. (2015b).

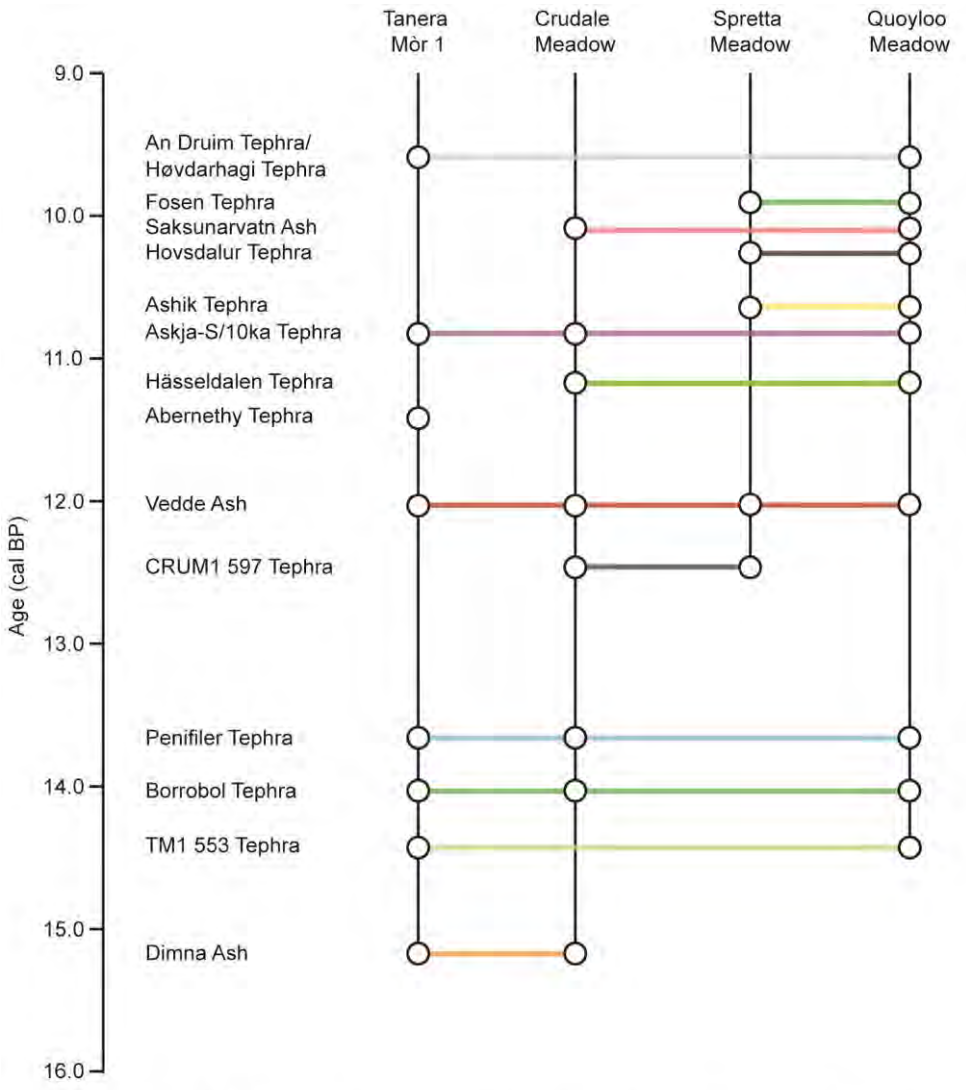

Figure 11.7 Schematic representation of the tephras and sites utilised to create the composite age model.

Eleven main models were produced following the code and approach outlined in Bronk Ramsey et al. (2015b). Experimentation with syntax, and the various parameters and settings available in OxCal (v.4.2), eventually culminated in composite model version

11.2b (Figure 11.8; see Appendix C for the finalised code). Unlike the previous site specific age models, O*utlier analysis* and *Combine* functions were removed from this finalised model. Whilst these two parameters provide invaluable means of assigning prior probabilities of error, and provide the model with the ability to merge equally likely age estimates; as complexity increased i.e. as stratigraphies were added, it was evident that this was having a detrimental impact on the overall stability of the model. To minimise this complexity, yet retain all of the stratigraphical and chronological information, the *Combine* of similarly aged or conflated tephras was undertaken in isolation prior to the running of the model, with the results of these being subsequently inputted into the sequence as individual age determinations.

The *Outlier analysis* was used in previous individual models from which this composite was built. In none of those cases did the function highlight a problem, thus it is logical that it should not be needed at this stage. Nevertheless, in order to compensate for its removal, a greater scrutiny was placed on the overall *Agreement Index*; a numerical value calculated by OxCal as a process of model development (Bronk Ramsey 1995). As convention dictates, if the associated indices (^{A}overall and ^{A}model) do not total 60% or greater, then the model is not statistically robust, and should be considered for rejection (Bronk Ramsey 2001; 2009). For model v.11.2b, the ^{A}overall and ^{A}model indices totalled 74.8 % and 69.3 % respectively, confirming the robustness and stability of the model's output.

11.4.2 Composite model output

Table 11.3 provides a summary of all of tephra ages determined as part of this modelling exercise. In all instances, tephra age uncertainties were reduced when compared to input ages (Table 11.1), and those generated as part of the individual site determinations (Table 11.2). Table 11.3 should therefore be considered to represent the best age estimates of these tephras in NW Europe, although some of these may require further work based on previous discussions (see section 11.2). The model was most successful in further constraining those horizons considered to be poorly dated e.g. the early Holocene Tephras such as the Ashik and Hovsdalur.

The exclusion of an input age for the Ashik Tephra has enabled the composite model to produce a most likely age range based on the superposition of the horizon at Spretta Meadow and Quoyloo Meadow. In doing so this has reduced the uncertainty of this horizon, and eliminated the site-specific variability evident from the individual site determinations (see section 11.3.5). This tephra now exhibits an improved age estimate of ***10,994-10,731 cal. BP***, and as a consequence, a greater distinction

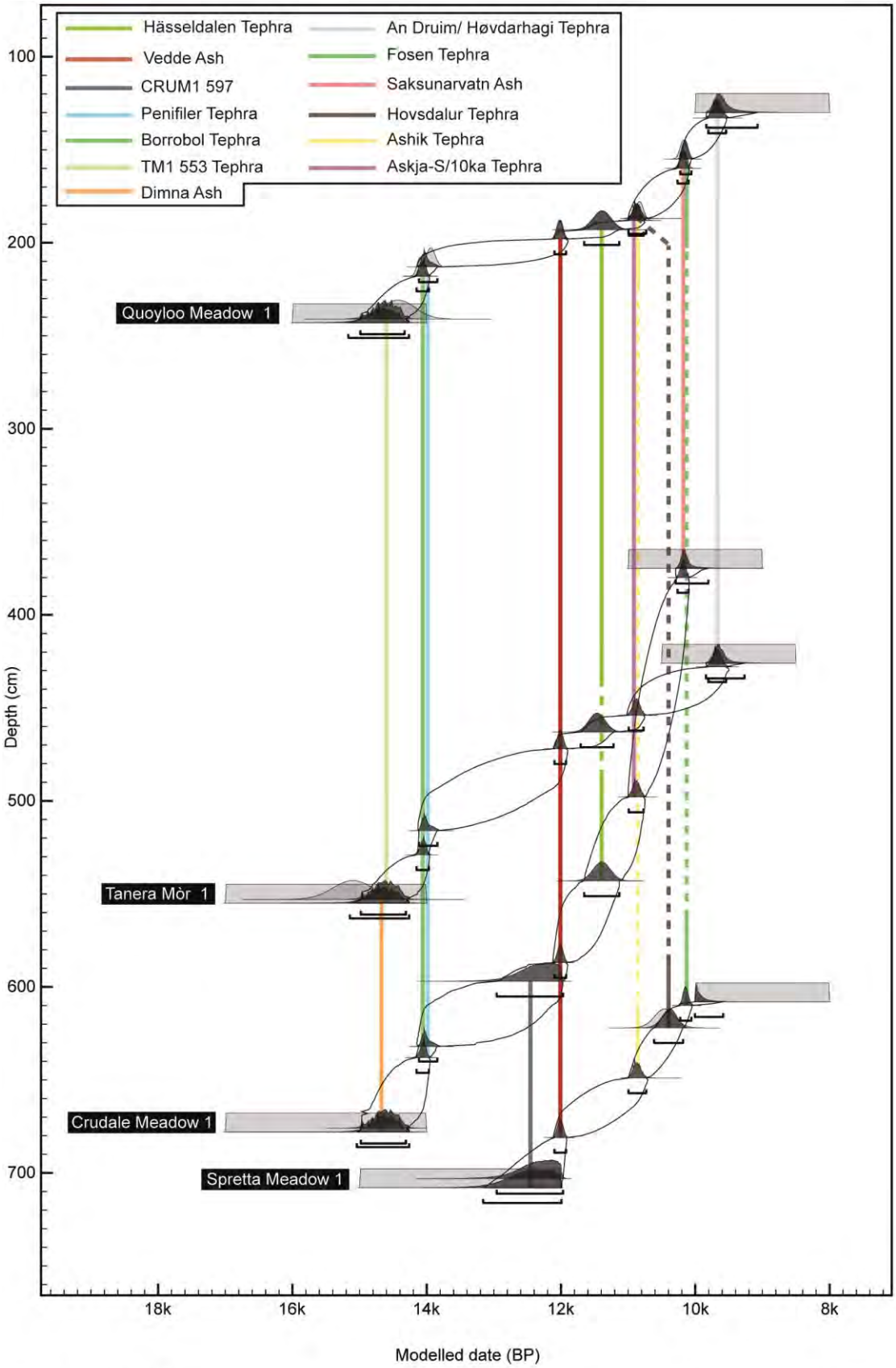

Figure 11.8 Composite age model (version 11.2b). The composite was generated by combining tephrostratigraphic and tephrochronological data from the four main tephra bearing sites examined in this thesis. By using the tephras as common tie points between the stratigraphies, more information could be incorporated into the model, hence improving its robustness and precision. See corresponding Appendix for the finalised code. The model was created using OxCal version 4.2.

between the Ashik Tephra and the Hovsdalur Tephra is now possible. The latter tephra is estimated to reside between ***10,613-10,183 cal. BP***, which is in agreement with the original age estimate of Wastegård et al. (2002), and significantly younger than what is suggested by the Quoyloo Meadow sequence alone (Table 11.2; Timms et al. 2016).

Table 11.3 Summary of the tephra ages derived from the composite age depth model. These tephra ages can be considered the 'best' determinations for these horizons in NW Europe. However, given the above discussion such ages should be considered open to continual refinement.

Tephra	Mean	Error 1σ	Error 2σ	Age range (95.4%)
An Druim/ Høvdarhagi	9676	66	132	9807-9540
Fosen	10,142	41	82	10,223-10,057
Saksunarvatn	10,182	40	80	10,264-10,100
Hovsdalur	10,394	108	216	10,613-10,183
CRUM1 496	10,860	71	142	10,999-10,719
Ashik	10,864	66	132	10,994-10,731
Askja-S/10ka	10,879	55	110	10,992-10,770
Hässeldalen	11,393	130	260	11,656-11,131
Abernethy	11,462	122	244	11,706-11,218
Vedde	12,011	43	86	12,097-11,925
CRUM1 597	12,388	286	572	12,957-11,970
Penifiler	14,000	70	140	14,116-13,843
Borrobol	14,057	46	92	14,151-13,966
TM1 553	14,621	174	348	14,989-14,328
Dimna	14,621	173	346	14,989-14,309

It is evident that a low sedimentation rate e.g. like that found at Quoyloo Meadow and the co-occurrence of tephras in the same stratigraphic level (see section 5.3.1) can have a significant influence on tephra age estimates. This is particularly the case where a well-dated tephra, in this instance the Askja-S/10ka, lies in close stratigraphic proximity to less well-resolved horizons i.e. the Ashik and Hovsdalur Tephras. Such an occurrence has forced these poorly-dated horizons into the upper (older) range of their prospective age estimates. Thereby exacerbating the temporal discrepancy of the early Holocene tephras identified in the Orkney sites. The inclusion of the stratigraphically expanded Spretta record therefore illustrates the necessity to consider multiple sites when constructing age depth models derived in part from poorly dated tephras.

However, compiling multiple lines of evidence may not always provide the best output. The results obtained in association with the Dimlington aged TM1 553 Tephra, and Dimna Ash horizons, illustrate that a level of caution, and a critical evaluation of outputs

is necessary. The TM1 553 Tephra and Dimna Ash horizons were each identified at two sites during the course of this study, once as a unimodal and distinct isochron (TM1 553 Tephra at Quoyloo Meadow; Dimna Ash at Crudale Meadow), and a second where the two horizons were conflated and diffuse (Tanera Mòr 1). Due to this latter occurrence, the composite model determined that it was most likely that both the TM1 553 and Dimna Tephras were coeval i.e. that they exhibit broadly the same age range (Table 11.2). However, work at Priest Island (Valentine 2015), has shown that these horizons are stratigraphically distinct (see section 10.4.1). Hence in this instance, the data derived from the modelled sites is insufficient to drive a distinction in age between these respective tephras. Further work will be necessary in the context of these late Dimlington age tephras, to refine age estimates more akin to their stratigraphic position.

Whilst multi-site modelling can clearly provide further constraint on tephra age estimates, and help refine the relative superposition of horizons, the technique does have inherent limitations. It is necessary therefore that the output of such modelling exercises be considered in the context of wider stratigraphic evidence before the acceptance of ages are made, or before final conclusions are generated.

11.4.3 Chronological refinement and palaeoenvironmental questions

It is evident that a refinement of age, and an improvement to the chronological confidence of tephra horizons can arise from composite age modelling. However, errors of the magnitude depicted in Table 11.3 are at present still too great to reliably address many palaeoenvironmental questions concerning the spatial and temporal manifestation of abrupt climatic transitions. In Greenland, such events have been shown to operate at sub-decadal resolutions (Steffensen et al. 2008), whilst phasing in the climate system may at times operate at decadal to centennial scales (e.g. Lane et al. 2013). Thus if tephras are to be of maximum use in constraining these climatic oscillations, or used in the testing of leads and lags within the climate system, further refinement must be sought. At present, however, this may lie beyond what is feasible with the technique, and the true value of tephra layers may lie with their stratigraphic positioning relative to climatic events e.g. the Vedde Ash demarking a shift in Younger Dryas conditions (Bakke et al. 2009; Lane et al. 2013). If chronological improvements are to be made it is essential to trace tephras to sites where continuous, independent, high-precision and accurate chronologies exist, e.g. ice core records, or annually laminated lake sequences. In these contexts more precise tephra age estimates may be identified while synchronously providing direct links between incrementally-dated records which may be at annual resolution. This concept has been at the forefront of

several multi-institutional research projects such as RESET and INTIMATE, who have aimed to correlate and align numerous spatially disparate tephrochronological records, with several 'key' sites and tephras acting as major pinning points or anchors in the resulting tephra lattices (e.g. Lowe et al. 2008a; Blockley et al. 2014; Lowe et al. 2015; see section 2.7).

However, such research initiatives have understandably focused on large and widespread tephras which address the research questions of those projects e.g. the Vedde Ash and Campanian Ignimbrite. It will be necessary in future to develop a more holistic approach, that will enable all tephras to benefit from a collective chronological and stratigraphic refinement. Certain tephras will always occur in more 'useful' positions, be more widespread, or exhibit more distinctive chemical signatures. As a result tephrochronological hierarchies based around these, and other criteria are inevitable. However, this type of approach cannot be based on partial data, and it is only when a widespread and robust tephrochronological framework exists that this should even be contemplated. To facilitate a greater inclusion of tephras into such projects, it is necessary therefore to further develop stratigraphical and chemical controls on 'troublesome' horizons which caused their omission in some recent projects (e.g. Bronk Ramsey et al. 2015b). By reducing these uncertainties, and by building a greater knowledge of stochastic, non-quantifiable error e.g. taphonomic processes, then greater confidence in these tephras as distinct isochrons can be developed, hence easing their inclusion into such composite frameworks. Whether the inclusion of all known LGIT aged tephras, and all known tephra-bearing sites, is currently computationally possible, is another question open for debate, but a perpetual and continually updating framework of improved tephra age estimates is certainly a plausible long term goal.

11.5 'Best' age estimates and chronostratigraphic developments

Work conducted as part of this thesis has led to the following developments in the tephrochronology of NW Europe (Figure 11.9):

The age of the late Dimlington Stadial tephras have been updated, with the current best age estimates for the TM1 553 Tephra and Dimna Ash at ***14,989-14,328 and 14,981-14,309 cal. BP*** respectively. Whilst these ages possess a similar range, work at Priest Island has established that the Dimna Ash lies stratigraphically lower than the TM1 553 Tephra.

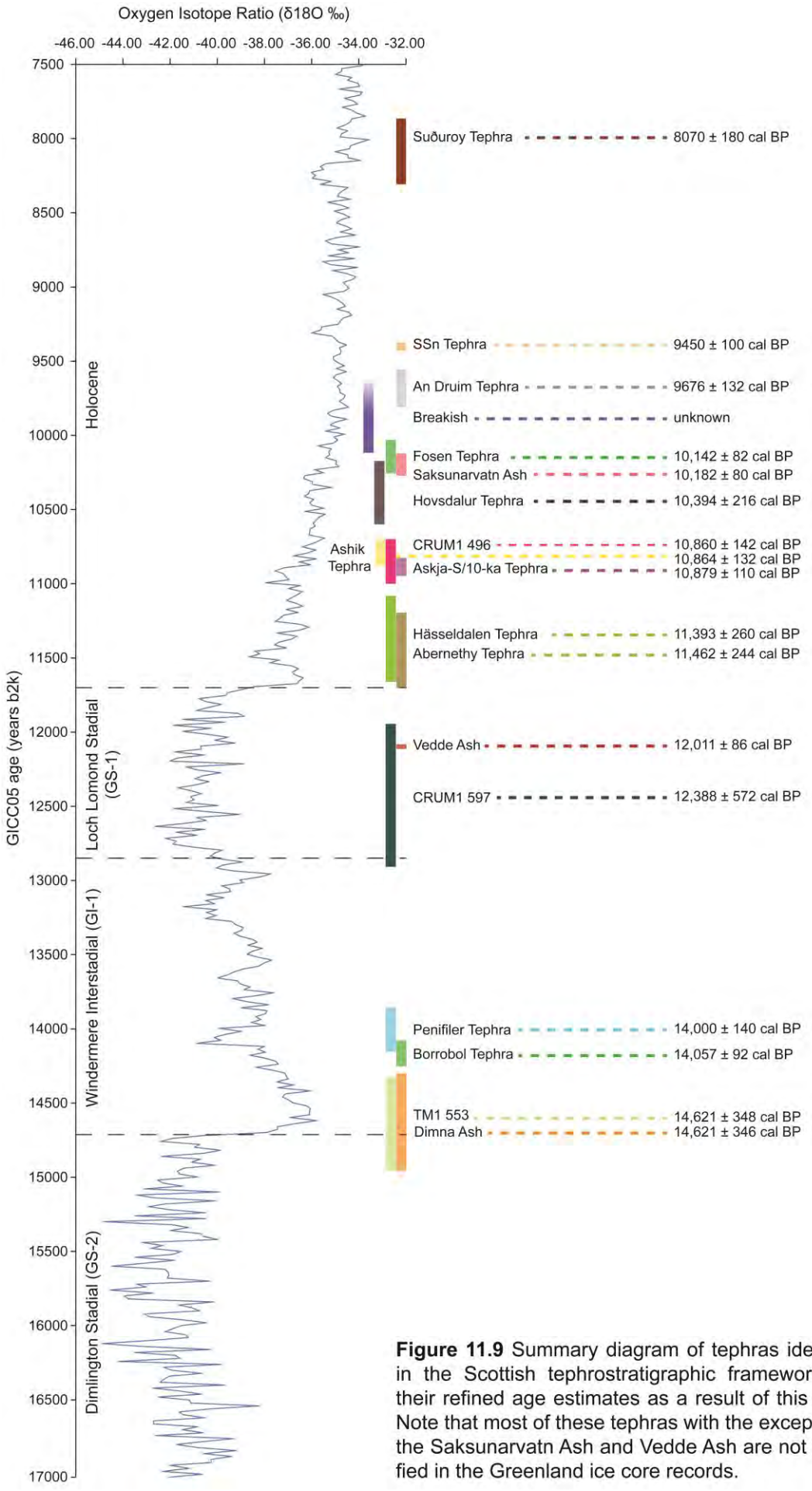

Figure 11.9 Summary diagram of tephras identified in the Scottish tephrostratigraphic framework and their refined age estimates as a result of this study. Note that most of these tephras with the exception of the Saksunarvatn Ash and Vedde Ash are not identified in the Greenland ice core records.

The CRUM1 597 Tephra has a modelled age range of ***12,957-11,970 cal. BP***, as determined by its presence at Crudale Meadow and Spretta Meadow. Currently this is a very broad age estimate, but its postulated occurrence across other sites in Scotland suggests there is potential to refine this. At present, the lithostratigraphic positioning of the layer at the end of the Windermere Interstadial would suggest an age at the older end of this range is more plausible.

The conflated age of the Ashik and Hovsdalur presented by Timms et al. (2016) has been refined through composite modelling of the Quoyloo Meadow and Spretta Meadow sequences. The age ranges of these tephras now lie at ***10,994-10,731 cal. BP*** and ***10,613-10,183 cal. BP*** respectively.

The basaltic tephra identified alongside the Askja-S/10ka Tephra at Crudale Meadow (CRUM1 496) exhibits an age range of ***10,999-10,719 cal. BP***, and adds another relatively well dated isochron into the early Holocene tephrochronological framework.

Age modelling results for the Ashik Tephra and Askja-S/10ka Tephra have further confirmed that these tephras exhibit a close chrono-stratigraphic relationship. For sites in Scotland, the Askja-S/10ka Tephra, has until relatively recently remained rather elusive, thus the improved age estimate of the Ashik Tephra may offer a viable alternative for constraining early Holocene climatic perturbations such as the PBO where the Askja-S/10ka has yet to be identified.

In light of geochemical and geochronological results presented in this thesis, it is formally proposed that the An Druim and Høvdarhagi Tephras are merged, and that the collective term for these horizons be the ‘An Druim Tephra’, due to the emergence of this term before that of the Høvdarhagi (Ranner et al. 2005; Lind and Wastegård 2011). The best age range of this tephra should now be considered ***9807-9540 cal. BP***.

Figure 11.9 presents the current ‘best’ age estimates for tephras identified within the Scottish tephrostratigraphic framework. A number of these e.g. the Suðuroy, the SSn and the Breakish have not been updated, due to the absence of these in the tephrostratigraphic sequences examined in this study. However, considering the above discussion, this diagram and the ages within should be considered provisional, and open to further refinement.

11.6 Chapter Summary

- It has been shown that tephra horizons have the potential to develop robust age-depth models without other chronological data, and that the resulting models have a precision that rivals more traditionally dated radiocarbon age models.

- There is still considerable uncertainty concerning the age of some tephras in NW Europe, with several discordant ages typifying some horizons e.g. the Hässeldalen and Askja-S/10ka Tephras. Refining the age of these isochrons will be essential, for both palaeoenvironmental and tephrochronological studies, especially where these horizons form key pinning points.

- Reduction in tephra age uncertainties are essential if chronological questions focused on the timing or phasing of climatic transitions are to be reliably answered. Composite modelling, and the inclusion of multiple age determinations for a horizon can help build chronological confidence into age models, and eliminate site specific bias's.

- Individual age depth models may benefit from composite age modelling, and should perhaps be conducted as standard when refining site chronologies.

- Future studies tasked with developing tephrochronological frameworks should strive for the inclusion of multiple tephras, and not necessarily just those that are thought to be most applicable in answering project questions. This avoids the situation where a few, well-dated horizons dominate tephrochronological or tephrostratigraphic projects e.g. the Vedde Ash.

- Troublesome tephras are an inevitable component of regional and continental frameworks and should not be dismissed. Improvements in their identification and 'refinement' are essential to in developing a 'total-tephra' strategy i.e. where every layer is fully optimised and integral in age modelling exercises.

Chapter 12. Tephro-stratigraphical and -chronological applications

12.1 Introduction and chapter structure

This final discussion chapter addresses the application of high resolution tephro -stratigraphies and -chronologies. The aim here is not to produce an extensive suite of palaeoclimatic indicators, but to illustrate how well-defined and robustly dated tephras may break the practices of 'tuning' and 'wiggle-matching' (e.g. Lowe et al. 2008a; Blaauw 2012). The process of aligning records has fuelled the "coherent myth", "reinforcement syndrome", and "suck-in effect", terms used to describe the self-confirming practice, that accepts environmental and climatic transitions of the Quaternary were regionally or globally synchronous (Baillie 1991; Wunsch 2006; Blaauw et al. 2006; 2007; Blaauw 2012). Such an approach has been repeatedly demonstrated to be misleading, unscientific, and detrimental to Quaternary investigations (e.g. Wunsch 2010; Blaauw 2012; Lane et al. 2013), yet the practice remains common within the discipline (e.g. Marshall et al. 2002; Lang et al. 2010), particularly in sediment sequences where radiometric dating is frequently problematic e.g. marine records or carbonate-rich lake sequences. A fundamental critique of 'alignment' has been provided by the INTIMATE initiative, which has set out a series of recommendations and principles by which climate and environmental questions can be objectively posed (Lowe et al. 2008a). These are:

1) Palaeoenvironmental interpretations should be based on independent and (preferably) quantified proxy data.
2) Site records should be defined using a local stratigraphic terminology.
3) The timing and duration of palaeoenvironmental events should be based on independently generated chronologies.
4) Palaeoenvironmental reconstructions, and chronologies that emerge, should then be compared with an independent regional stratotype, and the degree of compatibility with the stratotype sequence assessed, taking account of any dating uncertainties.

Following these themes, this chapter outlines two main ways in which the stratigraphical and chronological properties of tephra can be maximised to address palaeoenvironmental questions. These approaches are:

1) *Tephra time-slices (stratigraphical approach)*
By extracting quantified palaeoclimatic data from the same interval as a tephra isochron, high-resolution temporal time slices can be generated across large geographic regions. These offer precise 'snapshots' of climatic data and henceforth

may be more useful than the chronological averaging approach that is frequently employed in these types of studies e.g. Brooks and Langdon (2014).

2) *Tephra age-depth models (chronological approach)*
The development of tephra based age models allows: i) studies to highlight the temporal offsets in proxy response time; ii) a reliable and independent comparison of the site to the regional strato-type e.g. Greenland, and; iii) a flexible age model that can be periodically updated following improvements to tephra age estimates.

This chapter reviews these approaches in the context of the sites examined in this thesis.

12.2 Tephra time-slices (stratigraphical approach)

12.2.1 Isopleth maps

One of the most striking and efficient ways to illustrate late Quaternary climate change is through the use of isopleth maps. Successful applications include vegetation changes (e.g. Birks 1989), sea-level change (e.g. Shennan and Horton 2002), and temperature variability (e.g. Coope et al. 1998), which have all illustrated the diachronous tendencies of climatic transitions and landscape response during the LGIT. Thus, whilst each of these topics can find relevance in this study, it is the latter category of isothermal variance which shall be considered here. Studies such as Coope et al. (1998), Isarin and Bohncke (1999), and Brooks and Langdon (2014) have used Coleoptera, palaeobotanical indicators, and Chironomids to generate isothermal time-slices across Europe for the LGIT. These outputs have revealed strong temperature gradients, and have crucially illustrated that there was significant variability in these gradients between cooler and warmer periods (Figure 12.1).

Coope et al. (1998) remarked that changes in climate should be seen as a dynamic response to local geographical factors, which are overlain on broader patterns of amelioration. However, it is this very dynamism and short-term variability that is removed by the methods of reconstruction favoured by these studies. The approach undertaken by all has been to amalgamate and average data sets into multi-centennial and millennial scale time slices. This partly reflects the dating uncertainties characterising many sites through the LGIT (e.g. Blockley et al. 2007). However, given the nature of abrupt climate change through this interval (e.g. Brauer et al. 2008; Steffensen et al. 2008), there is a likelihood that local, short-lived, and potentially

important thermal anomalies may be 'smoothed', or lost entirely by their inclusion within large temporal envelopes.

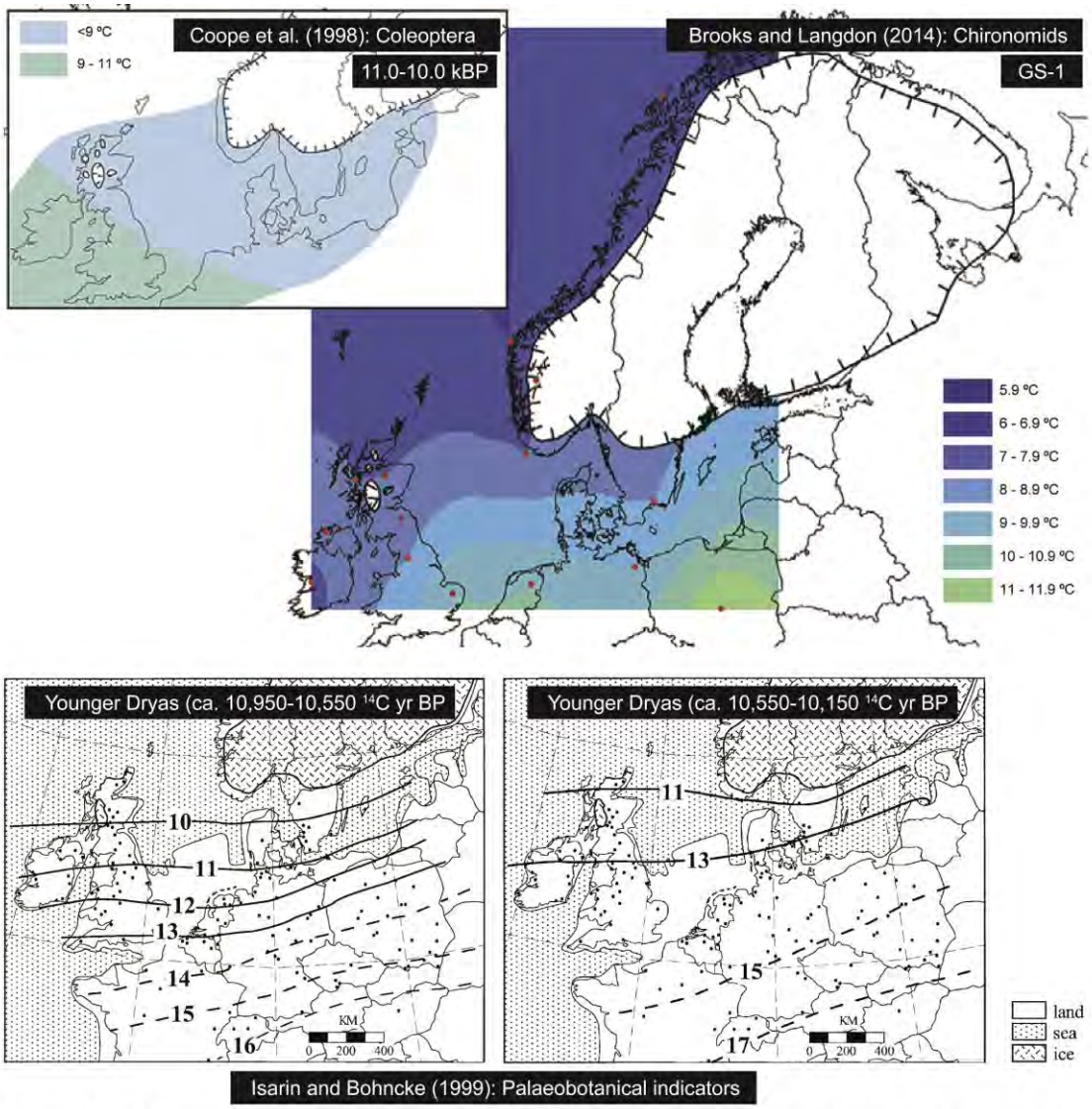

Figure 12.1 Previous isotherm maps illustrating summer temperature variability across NW Europe during the Younger Dryas. Compiled from Coope et al. (1998); Isarin and Bohncke (1999); Brooks and Langdon (2014).Temperatures from Isarin and Bohncke in °C.

This 'loss' of spatial and temporal information by averaging data is a particular concern for the Loch Lomond Stadial. Figure 12.1 illustrates the previously generated isothermal maps for this interval, which suggests that there is a north to south temperature gradient, and potential evidence from palaeo botanical indicators of a warmer second-half. The notion of a two or multi-part Stadial is an idea which has existed in the literature for many years (e.g. Atkinson et al. 1987; Berglund et al. 1994 Isarin and Bohncke 1999). It has been reinvigorated by the studies of Bakke et al. (2009) and Lane et al. (2013), who have demonstrated that the Younger Dryas (Loch Lomond Stadial/ GS-1) was a highly dynamic, and spatially diachronous, period of

climate change. Given that an ultimate goal in understanding abrupt change is to untangle the climatic drivers and responses which may vary both spatially and temporally, it is not particularly useful to therefore consider this period as a single or even as a two stage episode (Figure 12.1).

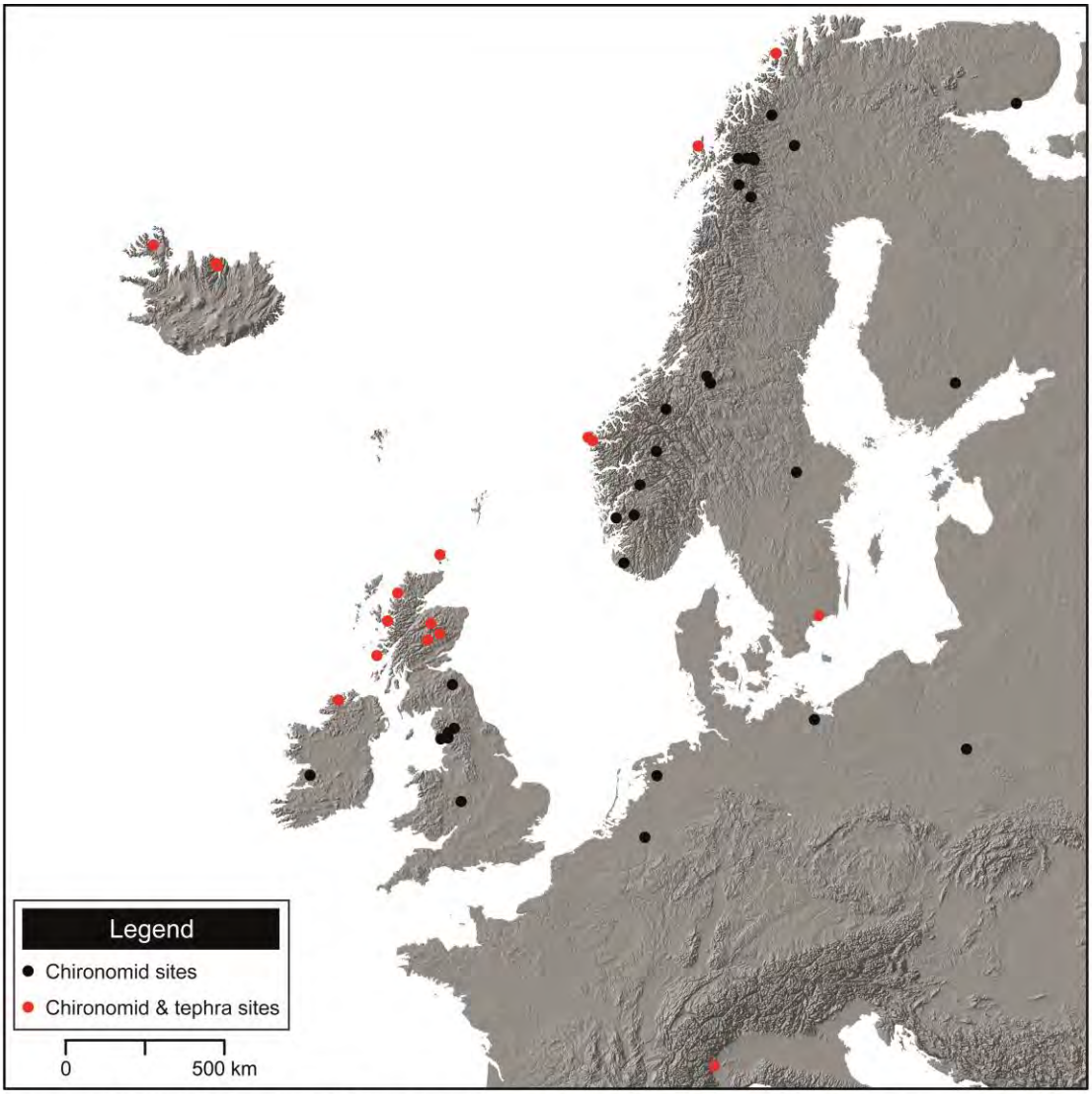

Figure 12.2 LGIT sites in NW Europe where C-IT reconstructions have been developed (black circles), and sites where C-IT exist alongside known tephra horizons (red circles).

12.2.2 Tephra-based isothermal maps

One way in which isothermal reconstructions can be refined is to utilise the isochronous potential of tephra horizons. By extracting a quantifiable climate indicator e.g. Chironomid-inferred summer temperature from the same interval as a tephra isochron, chronological uncertainties associated with amalgamating data sets can be avoided. Whilst sedimentation rate at the chosen site will be an important factor, it is not uncommon for LGIT-age tephra isochrons to be constrained to only a few centimetres and thus have decadal to centennial-scale uncertainties (see Chapter 11). Therefore, an isothermal map produced in association with a well-constrained tephra,

represents a significant development for the time slice approach, and an outcome that is arguably more representative and informative of the time period in question than a multi-centennial average.

Table 12.1 Chironomid samples in association with the Vedde Ash. A number of these sites are unpublished and subject to further refinement, provisional data for Tirinie can be found in Appendix I, whereas data for Quoyloo Meadow and Tanera Mòr 1 can be found in the relevant site appendices.

Site	lat	long	Altitude	Temp (°C)	Sea level temp (°C)	Reference
Quoyloo Meadow	59.06642	-3.30933	31	5.56	5.746	Brooks unpublished
Tanera Mòr 1	58.00616	-5.39348	18	8.2	8.308	Kwong (2016)
Abernethy Forest	57.23697	-3.70713	340	7.8	9.8	Brooks et al. 2012
Loch Ashik	57.24243	-5.82775	40	5.8	6.1	Brooks et al. 2012
Tirinie	56.78752	-3.81517	320	8.2	10.1	Turner (2016)
Muir Park Reservoir	56.09951	-4.42954	206	7.2	8.4	Brooks et al. (2016)
Whitrig Bog	55.60556	-2.6	125	8.9	9.7	Brooks and Birks (2000)
Kråkenes	62.03333	5	40	6.4	6.7	Brooks and Birks (2001)
Myklevatnet	61.92028	5.221389	580	8.5	12.3	Nesje et al. (2014)
Lago Piccolo di Avigliana	45.05446	7.392411	350	16	18.1	Finsinger et al. (2008)

Figure 12.2 depicts the number of LGIT aged Chironomid sites in NW Europe, allied to the number of sites where accompanying tephras have been identified. Chironomids offer many benefits over beetles as a temperature indicators, not least their abundance in freshwater lake sediments, and ability to be sampled at contiguously high resolutions (e.g. Battarbee 2000; Brooks 2006; Heiri and Lotter 2001). These attributes amongst others, makes them ideal proxies to combine with tephra horizons. At present, however, the coeval occurrence of Chironomid and tephra data is limited (Figure 12.2). Nonetheless, there is sufficient evidence to demonstrate the potential of the technique with a case study of the Vedde Ash. Table 12.1 lists the sites where Chironomid temperature reconstructions exist in association with this isochron. Figure 12.3 illustrates the isotherm map for the Vedde Ash; this figure is produced using the data presented in Table 12.1 and follows the protocols of Brooks and Langdon (2014). The isotherms are generated by weighted spatial interpolation (kriging), with the point temperature data in this instance being corrected to sea level using a 0.65°C/100 m environmental lapse rate.

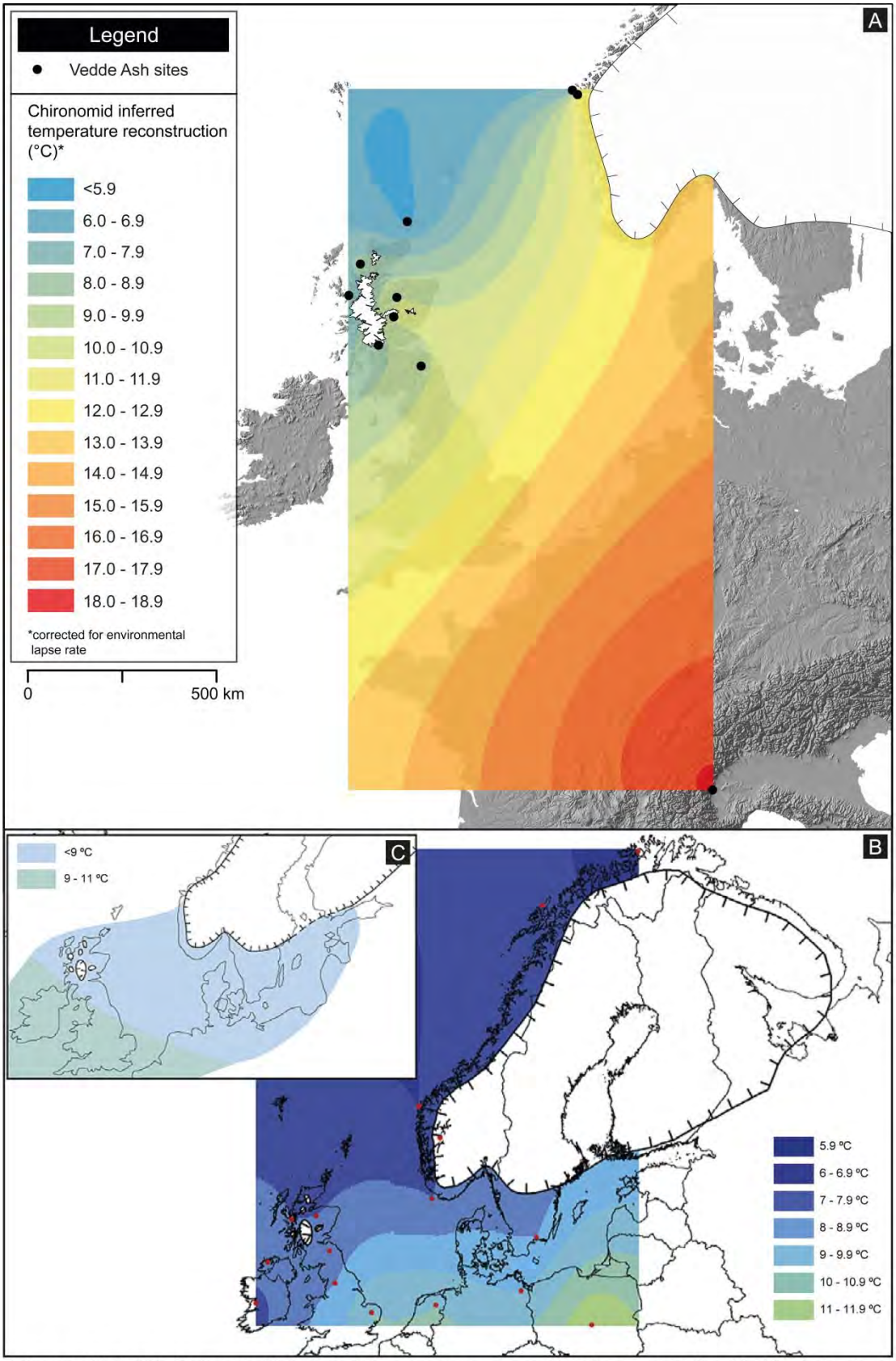

Figure 12.3 (A) Chironomid inferred temperature reconstruction using the Vedde Ash as a temporal marker. Compared with: (B) Brooks and Langdon (2014) and; (C) Coope et al. (1998) where a chronological averaging approach of the Younger Dryas has been used.

It is interesting to note that whilst a general N-S temperature gradient can be observed, there is also a significant NW-SE trend; a pattern which can be tentatively identified in the Chironomid reconstruction of Brooks and Langdon (2014), but one which is absent from the other temperature reconstructions. It also suggests that: 1) the temperature variability across Scotland is much greater than previously recognised; 2) thermal gradients in association with ice masses are stronger than previously shown, and; 3) despite the predominance of the FIS in western Norway, the mean July air temperature at sites such as Myklevatnet are seemingly warmer than much of northern Britain (Figure 12.3; Table 12.1). At present too many areas of the reconstruction rely on single sites or highlight discrepancies between sites, and further work will be needed to see whether these overall trends and local variability can be detected elsewhere, however, the results here offer an exciting possibility to gain a refined insight into the thermal regime of this dynamic interval.

At present therefore, the tephra time-slice approach can only be employed on the most widespread tephras, and at sites where the most detailed palaeoclimatic reconstructions exist. Tephras such as the Vedde Ash, Askja-S/10ka and Saksunarvatn Ash consequently offer the best opportunities in NW Europe to address continental scale questions of climate variability. An advantage of the approach, however, is that it is not immediately necessary to conduct full palaeoclimatic reconstructions, but only sample in association with tephra isochrons. In that respect, a wealth of palaeoclimatic information with very precise age constraints can be generated quickly. The application of this technique will be particularly useful where tephras are positioned at: 1) key climatic transitions e.g. Loch Lomond Stadial/ Holocene (Abernethy Tephra/ Hässeldalen); 2) either side of a climatic event e.g. GI-1d (Borrobol and Penifiler), and 3) intervals where a number of closely spaced tephras occur e.g. the early Holocene. Such data will be useful in: 1) illustrating the spatially diachronous changes known to characterise these intervals; 2) demonstrating how chronological averaging is an oversimplification and misleading practice, and 3) providing a means to objectively test climate models with a greater level of precision than is currently available (e.g. Heiri et al. 2014).

12.3 Tephras as a chronological tool (chronological approach)

The precise age estimates that are associated with many tephra horizons make them ideal chronological markers for age modelling. As a consequence, tephras are becoming an increasingly important method for the development of site age-depth models, particularly when combined in more traditional radiocarbon models (e.g.

Blaauw 2010), and when forming chronologies in their own right (e.g. Brooks et al. 2012; Timms et al. 2016; this study). The level of chronological refinement in association with some horizons has allowed site models to produce age estimates with decadal scale error e.g. between the Fosen Tephra and Saksunarvatn Ash at Quoyloo Meadow, where 2σ error estimates equate to 82 years (Chapter 11.0). Thus, the age models produced for this thesis, are in places, of comparable precision to the regional stratotype i.e. GICC05 (Vinther et al. 2006; Rasmussen et al. 2006; 2007; 2014a). This has particular significance for two reasons: firstly, age estimates for lacustrine records, and especially those of the Holocene frequently exhibit centennial scale errors at best (e.g. Blockley et al. 2007); and secondly, site where dating with radiocarbon techniques is difficult, but offer potential to extract high-resolution proxy-data e.g. carbonate basins such as Quoyloo Meadow, can now be more reliably dated with the identification of cryptotephra horizons.

12.3.1 Quoyloo Meadow: Site proxy data

As the aim of this chapter is to act as a proof of concept, and to highlight what can be achieved using tephras in a palaeoenvironmental context, the ensuing sections are discussed in specific regard to Quoyloo Meadow. The site was chosen to act as the case study due to: 1) the number of tephra horizons identified; 2) the precision of the ensuing age depth model, and; 3) the wealth of palaeoclimatic data that could be developed. In regards to the latter, a high resolution $\delta^{18}O$ and $\delta^{13}C$ stable isotope record for the early Holocene marl sediments, alongside a high-resolution $CaCO_3$ and LOI curve has been produced in this study and supplemented by a variable resolution Chironomid-inferred temperature reconstruction (C-IT) for the whole of the LGIT (Brooks unpublished), and; a high resolution palynological assessment for the whole LGIT (Abrook unpublished) (see Chapter 4.0 for sampling resolution details).

It is beyond the scope of this chapter to discuss in detail each of the proxy data sets, such intricacies will be reported elsewhere. Instead, outlined below and in table 12.2 are brief synopses of the data, and the main interpretation thereafter. Raw data for all proxies, as well as summary diagrams against depth, can be found in Appendix D. Figure 12.4 illustrates the proxy data vs the Quoyloo Meadow stratigraphy. For details of the LOI and $CaCO_3$ signal see section 5.2.1.

Table 12.2 Summary of the proxy data associated with the four early Holocene climatic oscillations identified at Quoyloo Meadow.

	Event	Chronology (cal. yrs BP)	Event	Chronology (cal. yrs BP)	Event	Chronology (cal. yrs BP)
	1		2		3	
Onset	193.5 cm	11,469 (± 362)	188 cm	10,879 (± 111)	172 cm	10,484 (± 340)
Termination	190.5 cm	11,138 (± 435)	185 cm	10,809 (± 217)	167 cm	10,358 (± 301)
Mean duration	3 cm	331 years	3 cm	70 years	5 cm	126 years
LOI trend	Increasing		Increasing		Slight increase	
LOI peak/trough	191 cm (12.9 %)	11,187 (± 221)	187 (26 %)	10,863 (± 132)	N/A	
$CaCO_3$ trend	Increasing		Increasing (saw tooth pattern)		Decreasing	
$CaCO_3$ peak/trough	No discernible peak		Peak at termination (185 cm)	10,809 (± 217)	trough: 168 cm (83.2 %)	10,384 (± 313)
PC trend	Increasing instability		Minor oscillations		Oscillating	
PC peak/trough	192 cm (0.77)	11,290 (± 199)	No discernible peak		peak: 170 cm (0.35)	10,434 (± 330)
C-IT trend	Increasing		Increasing		Increasing	
C-IT range (°C)	8.2-11.5		no change		no change	
C-IT average (°C)	10.2		12.1		13.3	
$\delta^{18}O$ trend	Depleting		Depleting		Depleting	
$\delta^{18}O$ event onset value	193.5 cm (-4.11 ‰)		188 cm (-3.92 ‰)		172 cm (-3.18 ‰)	
$\delta^{18}O$ peak/trough	trough: 191.5 cm (-4.18 ‰)	11,238 (± 420)	trough: 186.5 (-4.03 ‰)	10,847 (± 161)	trough: 170.5 cm (-3.51 ‰)	10,446 (± 333)
$\delta^{18}O$ difference	0.7 ‰		0.11 ‰		0.33 ‰	
$\delta^{13}C$ trend	Depleting		Depleting		Enriching	
$\delta^{13}C$ event onset value	193 cm (3.09 ‰)		188 cm (2.59 ‰)		172 cm (1.87 ‰)	
$\delta^{13}C$ peak/trough	end: 190.5 cm (2.81 ‰)		end: 185 cm (2.00 ‰)		peak: 170.5 cm (2.03 ‰)	10,446 (± 333)
$\delta^{13}C$ difference	0.28 ‰		0.59 ‰		0.16 ‰	

Table 12.2 continued.

	Event	Chronology (cal. yrs BP)	Event	Chronology (cal. yrs BP)	Event	Chronology (cal. yrs BP)
	4a		4b		4c	
Onset	165 cm	10,308 (± 269)	158.5 cm	10,168 (± 82)	154 cm	10,118 (± 134)
Termination	159.5 cm	10,177 (± 80)	155 cm	10,142 (± 82)	150 cm	10,034 (± 221)
Mean duration	5.5 cm	131 years	3.5 cm	26 years	4 cm	84 years
LOI trend	Slight increase		Slight increase		Slight increase	
LOI peak/trough	N/A		N/A		N/A	
$CaCO_3$ trend	Decreasing		Decreasing		Stable	
$CaCO_3$ peak/trough	value affected by Saksunarvatn Ash horizon		value affected by Saksunarvatn Ash horizon		N/A	
PC trend	Large peak noted at event onset, increasing stability through 'event'		Stable		Increasing	
PC peak/trough	peak: 165 cm (0.68)	10,308 (± 269)	N/A		peak: 151.5 cm (0.35)	10,066 (± 196)
C-IT trend	Decreasing		Stable		Stable	
C-IT range (°C)	13.3-12.1		no change		no change	
C-IT average (°C)	12.7		12.1		12.1	
$\delta^{18}O$ trend	Depleting		Depleting		Depleting	
$\delta^{18}O$ event onset value	165 cm (-3.03 ‰)		159 cm* (-2.93 ‰)	10,172 (± 81)	154.5 cm* (-3.03 ‰)	
$\delta^{18}O$ peak/trough	trough: 163.5 cm (-3.26 ‰)	10,271 (± 236)	trough: 156.5 cm (-3.44 ‰)	10,154 (± 83)	trough: 153.5 cm (-3.38 ‰)	10,108 (± 149)
$\delta^{18}O$ difference	0.23 ‰		0.51 ‰		0.35 ‰	
$\delta^{13}C$ trend	Depleting		Enriching		Depleting	
$\delta^{13}C$ event onset value	165 cm (1.50 ‰)		159 cm* (1.10 ‰)	10,172 (± 81)	154 cm (1.46 ‰)	
$\delta^{13}C$ peak/trough	end: 159.5 cm (1.13 ‰)		peak: 156 cm (1.58 ‰)	10,151 (± 83)	end: 150 cm (1.19 ‰)	
$\delta^{13}C$ difference	0.37 ‰		0.48 ‰		0.27 ‰	
			* value taken from peak between event 4a/4b		* value taken from peak between event 4b/4c	

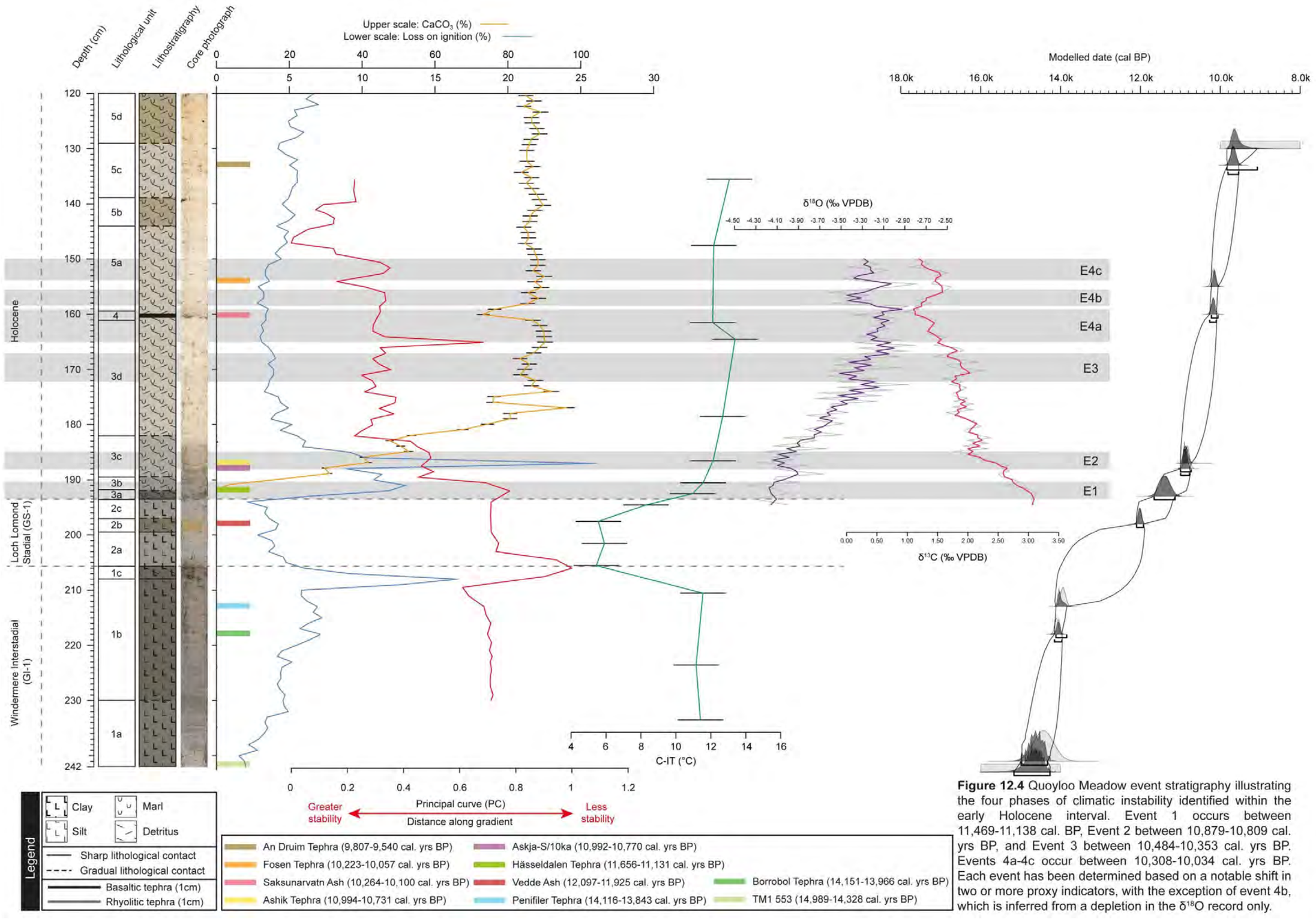

Figure 12.4 Quoyloo Meadow event stratigraphy illustrating the four phases of climatic instability identified within the early Holocene interval. Event 1 occurs between 11,469-11,138 cal. BP, Event 2 between 10,879-10,809 cal. yrs BP, and Event 3 between 10,484-10,353 cal. yrs BP. Events 4a-4c occur between 10,308-10,034 cal. yrs BP. Each event has been determined based on a notable shift in two or more proxy indicators, with the exception of event 4b, which is inferred from a depletion in the $\delta^{18}O$ record only.

$\delta^{18}O$ and $\delta^{13}C$ stable isotopes

There is a notable degree of variability or 'noise' in the $\delta^{18}O$ and $\delta^{13}C$ records, thus in order to highlight the general trends a three-point moving average has been applied to both data sets. Comparisons will be based these 'smoothed' averages, with the acknowledgement that this may limit some interpretations. No significant evidence of co-variance exists between the data sets, with an R^2 value of 0.54. From the basal analyses at 195 cm, there is a general isotopic enrichment of the $\delta^{18}O$, rising from -4.16 ‰ to -3.28 ‰ at 150 cm, which is mirrored by a gradual depletion in the $\delta^{13}C$ from 3.07 ‰ to 1.19 ‰ (Figure 12.4). Intersecting these general trends are several oscillations, the most notable of which are highlighted in Figure 12.4.

In British lake sequences the $\delta^{18}O$ of the carbonate is frequently assumed to be the more significant with regard to reconstructing past climate change (Leng and Marshall 2004; Candy et al. 2015). This is because the $\delta^{18}O$ of lake carbonate primarily reflects the $\delta^{18}O$ of the lake water (fractionated in association with lake water temperature) which records the $\delta^{18}O$ of rainfall (Candy et al. 2016). As the $\delta^{18}O$ of rainfall is strongly controlled by air temperature, it is often assumed that variations in the $\delta^{18}O$ of lake carbonates reflect variability in prevailing temperatures (Candy et al. 2016). The $\delta^{13}C$ of lake carbonates more commonly reflects local factors such as biological processes within the lake and rates of carbon dioxide equilibration (Leng and Marshall 2004). Discussion will focus on the $\delta^{18}O$ record, which is interpreted as depicting a general period of climatic amelioration (as indicated by increasing $\delta^{18}O$ values), but one which is punctuated by at least three oscillations (identified on the basis of short-lived decreases in $\delta^{18}O$ values). These oscillations vary in magnitude, but are all relatively subdued (<1 ‰) when compared to other $\delta^{18}O$ records of the period (e.g. Whittington et al 1996; 2015). Nonetheless, it is likely that decreases of this scale could still reflect temperature oscillations in the order of 2-3°C (Andrews 2006; Candy et al. 2011). When considered together, the oscillatory pattern of the $\delta^{18}O$ and $\delta^{13}C$ suggests that the early Holocene at Quoyloo Meadow was an interval typified by a long-term trend of climatic amelioration, but one which was punctuated by multiple cold events.

Chironomid inferred temperature reconstruction (C-IT)

The low resolution C-IT for Quoyloo Meadow exhibits consistently warm values throughout the Windermere Interstadial of ca. 11.3 °C. This declines sharply into the Loch Lomond Stadial where temperatures attain an early low of 5.4 °C centred on 205 cm. Progressive warming into the Holocene is consistent, and continues until a depth of 164 cm where a reduction from 13.3-12.1 °C is noted. This lower temperature

persists, but is seen too warm toward the end of the record, and reaches a value of 13.0 °C at 135 cm.

The trend exhibited in the C-IT reconstruction mirrors the pattern exhibited in many records developed for this period i.e. a warm, cold, warm succession, and hence agrees with the previous climo-stratigraphic interpretation of the site (see section 3.4.4 and Chapter 5.0). However, due to the resolution of the record it is not currently possible to ascertain exactly where key climatic shift may reside, not is it possible establish whether any other shorter term variance may exist within the record.

Pollen analyses

For brevity and simplicity, the pollen data has been synthesised and condensed into a single principal curve (PC). Principal curves fit smooth one-dimension connections through the middle of data-sets generated by a PCA, they thus provide a non-linear summary of data variance, and hence provide a quantitative means to illustrate vegetation change (Simpson and Birks 2012).

In the context of Quoyloo Meadow the PC explains 88.4 % of the total variability in the pollen data and can be interpreted as a model of landscape stability; high values in the accompanying PCA are driven by species such as *Artemisia* and *Pediastrum* i.e. taxa which thrive in cooler more unstable climes. Whilst low values are controlled by higher order taxa such as *Corylus* and *Salix* i.e. species which dominate in warmer, more stable environments. It is evident that during the Windermere Interstadial and Loch Lomond Stadial that the greatest shifts exhibited by the PC, coincide with major lithological changes previously inferred to represent climatic transitions (Figure 12.4). This illustrates periods of landscape instability accompanied these climatic transitions. During the early Holocene there is a general trend of increased stability; however, this is punctuated by several phases of revertence and/or stagnation within the vegetation record (Figure 12.4).

12.3.2 Quoyloo Meadow: An event stratigraphy

Due to the highest resolution proxy information and high-precision chronological data this section will concentrate on abrupt events during the early Holocene interval. The proxy information produced for Quoyloo Meadow has been used to delineate four abrupt ‘events’, or periods of apparent climatic revertence, with the last of these divided into three sub units labelled a-c (Figure 12.4). Each of these events has been characterised based on a notable shift in two or more proxy indicators, with the exception of event 4b, which has been distinguished solely by a depletion in the $\delta^{18}O$

record (Figure 12.4). Table 12.2 summarises the main attributes of each of these events.

Event 1 occurs between 11,469-11,138 cal. BP, Event 2 between 10,879-10,809 cal. yrs BP, and Event 3 between 10,484-10,353 cal. yrs BP. Events 4a-4c occur between 10,308-10,034 cal. yrs BP, and have been grouped together as these oscillations seem to characterise a period of increased variability, only separable by a brief enrichment in $\delta^{18}O$, and an apparent stabilisation of the landscape as inferred from the PC trend. It is important to note that other periods of instability can be tentatively identified within this interval. For example there appears to be a minor revertence event around 175 cm, as well as around 143 cm. However, at present evidence remains less conclusive and further work will be necessary to determine whether these are of any significance.

12.3.3 Climatic events in the early Holocene at Quoyloo Meadow and their correlation to North Atlantic records

The proxy record and the 'events' highlighted in Figure 12.4 and Table 12.2 clearly illustrate that, at Quoyloo Meadow, the early Holocene was a particularly dynamic and complex interval. The predominant signal is interpreted as one that is driven primarily by climatic variability, however, it is worth reiterating that not all proxies between the events respond in the same manner (Table 12.2). This suggests that other factors play a key role over the resulting signal. Such factors likely to relate to: 1) the magnitude of the event and the severity of this on Orkney (e.g. LeGrande et al. 2006); 2) the duration of the event (e.g. Hughen et al. 2004); 3) the response or lag time of the proxy (e.g. Williams et al. 2002; Willis et al. 2010), and 4) the sampling resolution of the proxy vs the sedimentation rate of the basin. Despite these potential caveats, the precision of the accompanying age model permits an excellent opportunity to make an independent chronological comparison to the Greenland stratotype; a key achievement of this thesis.

In Greenland during the early Holocene, the $\delta^{18}O$ trend is one typified by gradual isotopic enrichment (Rasmussen et al. 2006; 2007; Figure 12.5). Punctuating this trend are three major isotopic excursions, the 11.4 kyrs event (PBO), the 9.3 kyrs event and the 8.2 kyrs event (Rasmussen et al. 2007). These events are ubiquitous across DYE-3, GRIP and NGRIP, and hence represent regionally, if not globally significant climatic oscillations (Rasmussen et al. 2007).

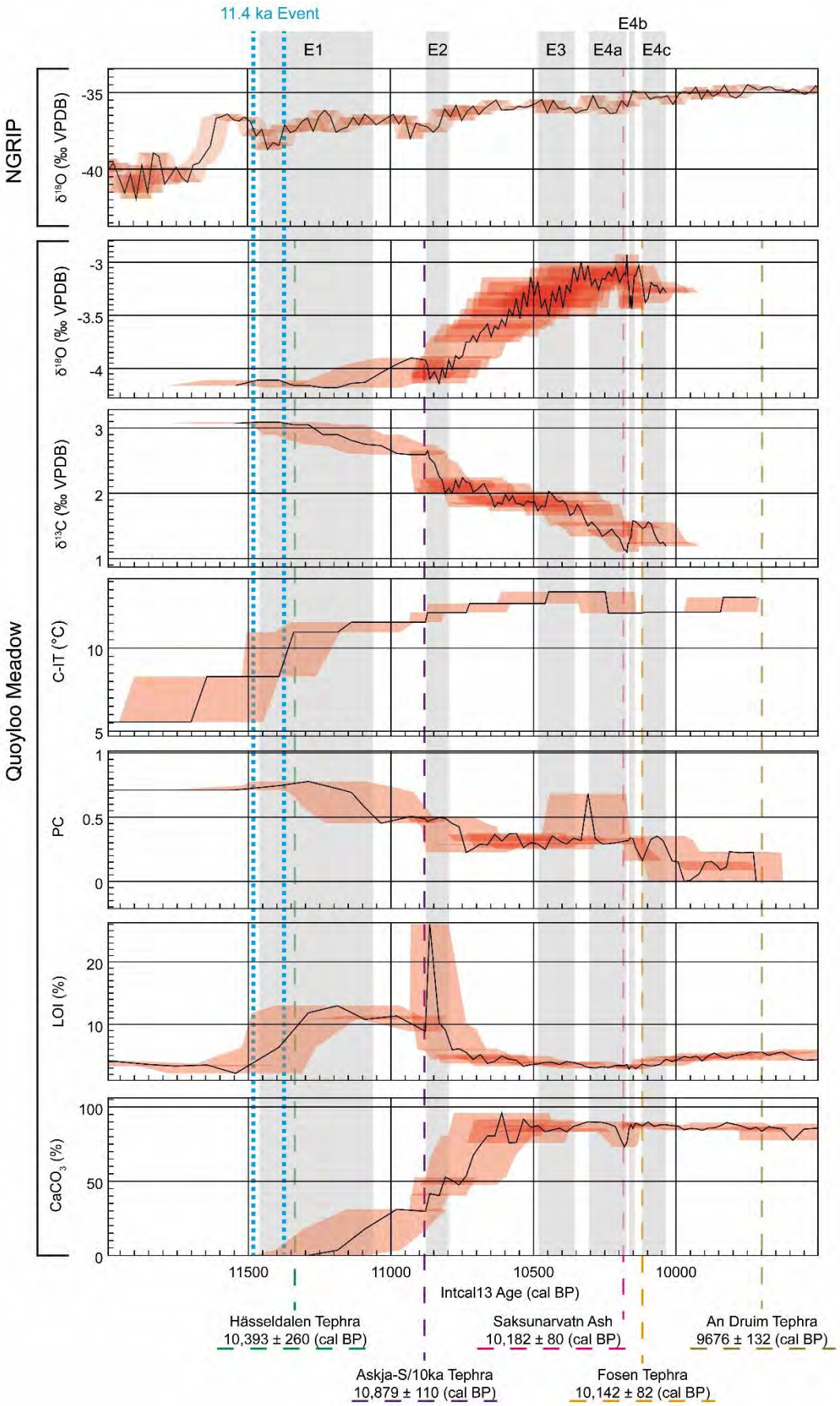

Figure 12.5 A chronological comparison between the Quoyloo Meadow event stratigraphy, and the NGRIP regional stratotype. Red error bars illustrate the chronological uncertainty of the two records. Quoyloo Meadow events are shown for illustrative purposes and do not reflect the uncertainties associated with the duration of the events. Also illustrated are key tephra identified in Quoyloo Meadow and NGRIP. NGRIP data from Rasmussen et al. (2006).

At Quoyloo Meadow a general trend of $\delta^{18}O$ enrichment can also be observed (Figure 12.5), however, the accompanying oscillatory pattern of events is not one which can be clearly recognised within the NGRIP stratotype. Quoyloo event 1, within errors, can be broadly seen to coincide with the 11.4 kyrs event. However, the multi-centennial scale uncertainty at this point in the Quoyloo Meadow chronology, prevents a more meaningful comparison at this stage. Quoyloo event 2 (ca. 10.8 kyrs) may coincide with a minor $\delta^{18}O$ depletion event in NRGIP, but this downturn has not been officially recognised by the ice core community, and hence the significance of this correlation is uncertain. Quoyloo events 3-4c seemingly have no significant comparative within the NGRIP record, although a broadly similar pattern can be observed (Figure 12.5).

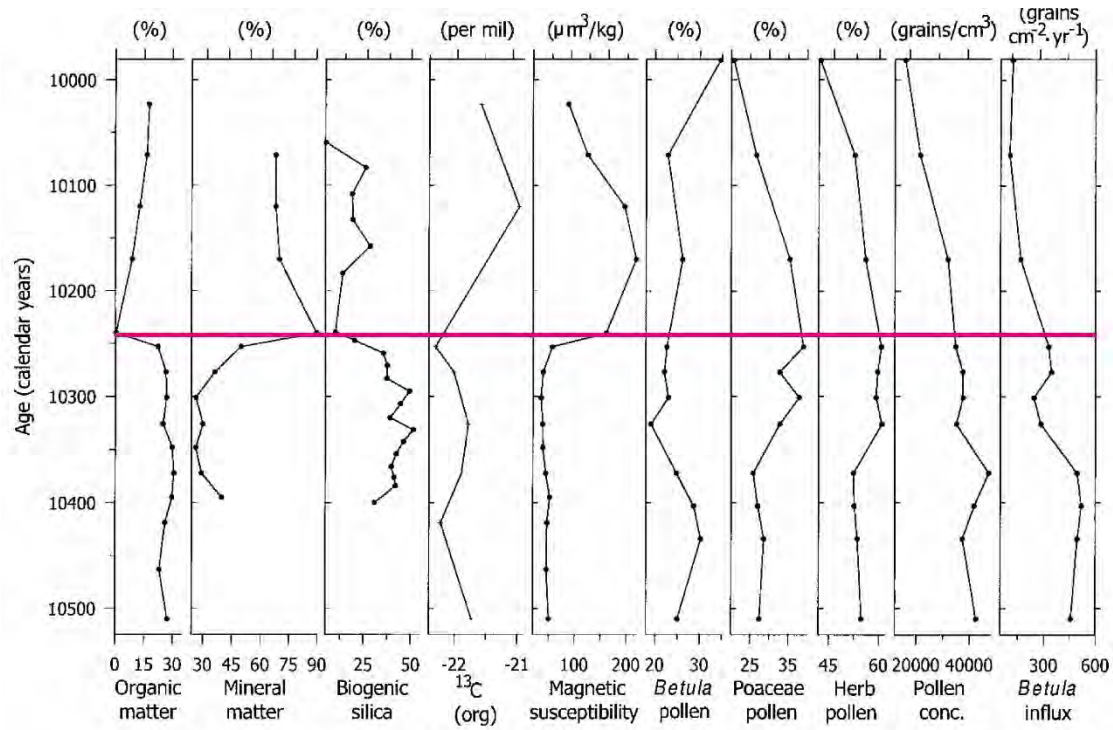

Figure 12.6 Proxy records from Lake Starvatn, Faroe Islands. The pink line denotes the position of the Saksunarvatn Ash (10,182 ± 80) which can be used to highlight the onset of climatic deterioration associated with the 10.3 ka event. Note specifically an increase in mineral matter, a decrease in biogenic silica (lake productivity) and an increase in cold climate taxa. Modified from Björck et al. (2001).

In general, the pattern of events observed at Quoyloo Meadow does not match well with Greenland. However, it should be noted that many other events are recognised around the North Atlantic periphery (Table 12.3). Many of these, like the events at Quoyloo Meadow, seemingly have no correlative within the Greenland stratotype. One of the most significant of these 'other events' is the 10.3 kyrs event (Björck et al. 2001). This oscillation has been noted to occur across the North Atlantic in various records, and according to Björck et al. (2001) is also present within the GISP and GRIP ice-core records. Why such an anomaly has yet reached further comment by the ice-core

Table 12.3 Early Holocene climatic oscillations as defined from palaeoenvironmental sequences in NW Europe and the North Atlantic periphery. Similarly aged events have been grouped together which highlights four periods of elevated variability, these are 11.0-11.5 kyrs, 10.0-10.5 kyrs, 1.0-9.5 kyrs and 8.1-8.5 kyrs.

Period (kyrs)	Event (kyrs)	Site	Onset/ca. mid-point	Termination	Duration	Proxy evidence	Key references
8.10-8.49	8.2	DYE-2; GRIP; NGRIP	8300 b2K	8140 b2k	160 ± 10 yr	$\delta^{18}O$ + accumulation rate	Rasmussen et al. 2007; Thomas et al. 2007
		DYE-2; GRIP; NGRIP	8245 b2k	8240 b2k	5 yr	very low $\delta^{18}O$ values	Rasmussen et al. 2014a
		NGRIP	8300 ± 49 b2k	8150 ± 45 b2k		$\delta^{18}O$ + Ca^{2+}	
		MD99-2251	8490 kyrs	8290 kyrs	ca. 200 yr	$\delta^{18}O$ (*Globigerina bulloides*) + *N. pachyderma s*	Ellison et al. 2006
		Haweswater	Not defined	Not defined	ca. 150 yr	$\delta^{18}O$	Marshall et al. 2007
8.50-8.99	8.5	NGRIP; GRIP; DYE-3	Not defined	Not defined	Not defined	Not defined	Rasmussen et al. 2007
		MD99-2251	ca. 8490 kyrs	Not defined	ca. 80 yr	*N. pachyderma s*	Ellison et al. 2006
	8.8	NGRIP; GRIP; DYE-3	ca. 8,800 b2k	Not defined	Not defined	Not defined	Rasmussen et al. 2007
9.00-9.49	9.3	DYE-2; GRIP; NGRIP	9350-9,310 b2k	ca. 9200 b2k	40-150 yr	$\delta^{18}O$ + accumulation rate	Rasmussen et al. 2007
		NGRIP	9350 ± 70 b2k	9240 ± 68 b2k		$\delta^{18}O$ + Ca^{2+}	Rasmussen et al. 2014a
		Haweswater	Not defined	Not defined	ca. 50 yr	$\delta^{18}O$	Marshall et al. 2007
9.50-9.99	9.7 (Erdalen)	Western Norway	ca. 9,700	Not defined	Not defined	Glacial advance, lithostratigraphy, Chironomids	Dahl et al. 2002
	9.95	DYE-2; GRIP; NGRIP	9950 b2k	9940 b2k	10 yr	$\delta^{18}O$	Rasmussen et al. 2007
10.00-10.49	10	DYE-2; GRIP; NGRIP	ca. 10,070 b2k	Not defined	ca. 100 yr	accumulation rate	Rasmussen et al. 2007
	10.0 (Erdalen)	Western Norway	10,000 cal. yrs BP	9850 cal. yrs BP	ca. 150 yr	Glacial advance, lithostratigraphy, Chironomids	Dahl et al. 2002
	10.1 (Erdalen)	Western Norway	10,100 cal. yrs BP	10,050 cal. yrs BP	ca. 50 yr	Glacial advance, lithostratigraphy, Chironomids	Dahl et al. 2002
	10.2	Holzmaar	10,450 cal. yrs BP	10,150 cal. yrs BP	ca. 300 yr	Data unavailable	Brathauer et al. 2000
	10.3	Lake Starvatn	10,350-10,300 kyrs	10,150-10,100	ca. 200 yr	Multiproxy	Bjorck et al. 2001
	10.3	Summit	ca. 10,300 cal. yrs BP	Not defined	ca. 200 yr	$\delta^{18}O$	Dansgaard et al. 1993
	IRD event 7	VM 29-191	10,400 kyrs	10,300 kyrs yr	100 yr	$\delta^{13}C$	Bond et al. 1997
10.50-10.99	10.8	Loch Inchiquin	ca. 10,800 cal. yrs BP	Not defined	Not defined	$\delta^{18}O$	Diefendorf et al. 2006
11.00-	11 (C5)	Crudale Meadow	ca. 11,000 cal. yrs BP	Not defined	Not defined	$\delta^{18}O$	Whittington et al. 2015

11.49	11.1	NGRIP; GRIP; DYE-3	ca. 11,100 b2k	Not defined	Not defined	Not defined	Rasmussen et al. 2007
	PBO?	Netherlands	ca. 11,250 cal. yrs BP				van der Plicht et al. 2004; Bos et al. 2007
	11.4 (PBO)	NGRIP; GRIP; DYE-3	ca. 11,500 b2k	ca. 11,270 b2k		$\delta^{18}O$ + accumulation rate	Rasmussen et al. 2007
		NGRIP decline in D18O	ca. 11,700 b2k	ca. 11,320 b2k		$\delta^{18}O$	Rasmussen et al. 2014a
		NGRIP 'coldest phase'	11,520 ± 97 b2k	11,400 ± 96 b2k		$\delta^{18}O$ + Ca^{2+}	Rasmussen et al. 2014a
		GRIP (GRIP chronology)	11,300 cal. yrs BP (GRIP chronology)	11,150 cal. yrs BP (GRIP chronology)	ca. 150 yr	$\delta^{18}O$	Björck et al. 1997
	Rammelbeek Phase	Netherlands	11,430 cal. yrs BP	11,350 cal. yrs BP	ca. 80 yr	Multiproxy	Bos et al. 2007
			11,450 cal BO	11,250 cal. yrs BP		Multiproxy	van der Plicht et al. 2004

community is uncertain, however, the accumulative regional and global evidence would suggest that this is a significant oscillation (Björck et al. 2001). The dating of this event has in part been assisted by the presence of the Saksunarvatn Ash (10,182 ± 80). Figure 12.6 is from Lake Starvatn on the Faroe Islands, and what can be observed shortly before the deposition of the Saksunarvatn Ash (ca. 50-100 yrs), is an increase in cold climate pollen taxa and more minerogenic styles of sedimentation (Björck et al. 2001). At Quoyloo Meadow, event 4 (4A-4C) is noted to have commenced ca. 126 years prior to the deposition of the Saksunarvatn Ash and is marked by a decline in temperatures, a shift toward cold climate taxa, and the largest $\delta^{18}O$ shift within the isotope record (Figure 12.5). This evidence is therefore interpreted as the first reliably recorded incidence of the 10.3 kyrs event in the British Isles, and one that has been facilitated by a high precision tephrochronology.

12.3.4 Quoyloo Meadow event stratigraphy: 'Wiggle matching' approach

Outlined in this section is a re-interpretation of the Quoyloo Meadow event stratigraphy if a more typical age depth model existed for the sequence. In this regard Quoyloo Meadow would resemble many palaeoenvironmental records for NW Europe, which are often beset by comparatively large multi-centennial age error uncertainties, and which also often rely on regional tuning to help explain proxy trends (e.g. Marshall et al. 2002; Brooks 2006; Marshall et al. 2007; Whittington et al. 2015). The purpose of this exercise is therefore to 1) emphasise the importance of well dated independent site chronologies; 2) re-iterate the recommendations of the 'INTIMATE approach; 3) highlight problems which might arise if these robust protocols are not adhered to; and 4) suggest means by which high resolution tephrochronologies may help to overcome these issues in other studies.

Of the climatic events identified in the early Holocene, the 8.2 kyrs event (Hammer et al. 1986; Alley and Ágústsdóttir 2005; Rohling and Pälike 2005), the 9.3 kyrs event (von Grafenstein 1999; Marshall et al. 2007; Rasmussen et al. 2007) and the 11.4 or event PBO (Björck et al. 1997; Bos et al. 2007) have received the most attention and study. These have often been used as wiggle-match tie points alongside the isotopic peak at the onset of the Holocene by studies lacking robust chronologies (e.g. Garnett et al. 2004; Ahlberg et al. 2006; Whittington et al. 2015). If this approach is applied to Quoyloo Meadow (Figure 12.7), a case could be made to assign the isotopic peak of the early Holocene to 189 cm, the PBO to 188-185 cm (isotopic Event 2), and the 9.3 kyrs event to 172-167 cm (isotopic Event 3). Isotopic Event 4a (165-159.5 cm) would have no formally recognised correlative, but an isotopic depletion at Haweswater dated

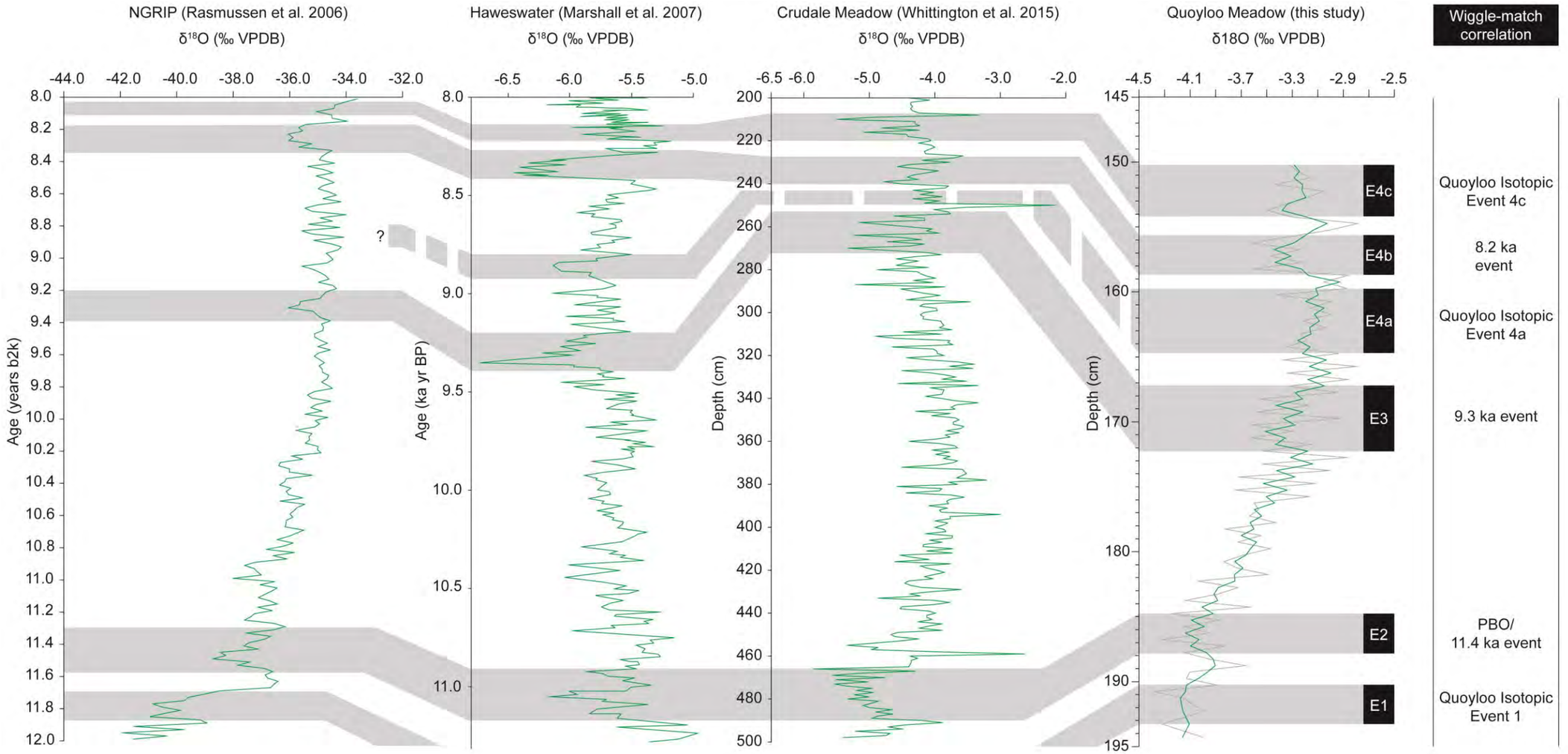

Figure 12.7 Proposed correlations for the Quoyloo Meadow event stratigraphy based on isotopic wiggle matching to local and regional records. The insert table illustrates the true age for the Quoyloo Meadow events as determined by an independent age model, and compares those with the resulting wiggle matched ages. The problems with correlating records in this manner are clearly illustrated by the age difference between the two approaches.

Event	True age ka (mid point)	Wiggle Match age ka (mid point)	Age difference (yrs)
4c	ca. 10.1	ca. 8.1	ca. 2000
4b	ca. 10.2	ca. 8.25	ca. 1950
4a	ca. 10.3	ca. 8.8	ca. 1500
3	ca. 10.4	ca. 9.3	ca. 1100
2	ca. 10.8	ca. 11.45	ca. 650
1	ca. 11.2	ca. 11.7	ca. 500

to ca. 8.8 kyrs would seem a viable match (Marshall et al. 2007). The 8.2 kyrs event could be assigned to 158.5-155 cm (isotopic Event 4b), and isotopic Event 4c (154-150 cm) like 4a, would not have a formally recognised correlative, but may link to a smaller isotopic event observed at ca. 8.1 kyrs in the Crudale Meadow and NGRIP records (Rasmussen et al 2006; Vinther et al. 2006; Whittington et al. 2015; Figure 12.7).

With a rudimentary age model, these conclusions would be somewhat justified by the manner of correlation undertaken by many other local and regional records (e.g. Whittington et al. 2015). However, as illustrated in Table 12.3 this interval is characterised by many more oscillations than are typically acknowledged, or were suggested as correlatives above. It is beyond the scope of this thesis to review all of the potential correlatives, but what is particularly evident are the uncertainties associated with these 'events'. Firstly in a temporal sense, but also in regards to the way in which the oscillation has been defined, and what proxy information has governed the definition. Errors for the most-part are not presented, and many of these studies fail to provide an age for the onset or termination, and merely state instead an approximate age of occurrence e.g. the 9.7 'Erdalen' event (Dahl et al. 2002), or 10.8 event (Diefendorf et al. 2006). This probably reflects the errors of accompanying age models, which if presented would likely be so large as to invalidate any suggestion that the discreet oscillation could be distinguished from an existing, better defined phase of climatic instability e.g. the 9.3 or PBO. Whilst this is not a suggestion that these less well documented perturbations do not exist, rather such poorly constrained events are not particularly viable for correlation.

It is perhaps this very uncertainty which drives studies to consider the larger more prominent events, as the well-defined oscillations such as the PBO, 9.3 kyrs, or 8.2 kyrs events seemingly offer more secure tie points. However, as stated at the start of the chapter, having limited chronological information when making intra-site correlations can further fuel the 'coherent-myth'. As shown in Figure 12.7 tuning to a local or regional record will likely lead to miscorrelation and the development of erroneous conclusions. What risks being developed in the context of the early Holocene is therefore 1) an over emphasis of the large scale or seemingly ubiquitous climatic events, and 2) the continuation of the temporal uncertainty characterising other early Holocene perturbations. These problems are considered below in the context of how well defined tephrochronologies may help to alleviate some of the issues.

1) Over emphasis of large scale events

The wealth of literature available for the PBO, 9.3 and 8.2 kyrs events (e.g. Björck et al. 1997; von Grafenstein 1999; Alley and Ágústsdóttir 2005), and the clear chronological/ stratigraphical context of these perturbations within the Greenland ice-core records (Rasmussen et al. 2007), make them desirable targets for other studies to identify. It has become almost 'inconvenient' to identify climatic or environmental anomalies which do not link to wider regional archives. What risks being developed therefore, is a generalisation of local event stratigraphies via the phenomena of 'reinforcement syndrome' (Blaauw 2012). Emphasis when resolving climatic records is often placed around an interval where an anticipated oscillation might reside. A recent example of this comes from Ott et al. (2016) who, using the isochronous markers of the Hässeldalen and Askja-S/10ka propose the presence of the PBO at Lake Czechowskie, based on a very minor Ti and Ca shift. The study states that without the marker horizons, this 'event' would not have been detected such is the subtleness of the chemical signal. Whilst in some respect this highlights the potential value of tephras to delineate climatic events, it also highlights the inherent expectance of finding a climatic signal where it ought to reside. At no point do Ott et al. (2016) suggest that the PBO may not be manifest or even relevant for the site, or that the otherwise insignificant Ti and Ca shifts might just be an anomaly. Further examples of reinforcement syndrome in relation to early Holocene climatic events, can be found in the few isotopic records resolved in the British Isles through this interval. In the case of Crudale Meadow (Whittington et a. 2015), a basic site chronology has been used to delineate the 9.3 and 8.2 kyrs events, despite other isotopic oscillations of a comparable magnitude occurring throughout the early Holocene record (Whittington et al. 2015; Figure 12.7). This propensity to focus on seemingly major events is also apparent at comparatively well dated sites such as Haweswater (Marshall et al. 2007; Figure 12.7), where despite the opportunity to offer reliable temporal constraints on other oscillations, discussion is driven toward the 9.3 and 8.2 kyrs events. Studies which do this, falsely elevate the significance of the event to an extent that it becomes a disproportionate point of focus.

Table 12.3 illustrates the number of differing climatic oscillations, that have been identified within early Holocene records in NW Europe and the North Atlantic periphery. As previously stated, it is evident that the early Holocene was subject to much greater levels of climatic variability and instability than many studies would allude to. It is quite probable that many of these are more regional if not local events. Hence in many instances the NGRIP regional stratotype may not be the best candidate for highlighting these revertence episodes. Thus it will be necessary for future efforts to consider this

information objectively, and consider the spatial and temporal dynamics in much the way the Lateglacial Interstadial and Younger Dryas are now being considered (e.g. Bakke et al. 2009; Lane et al. 2013). In these contexts, the isochronous properties of tephra have been fundamental in developing and shaping new ideas about the asynchronous nature of climatic transitions, and the spatial manifestation of environmental change.

2) Imprecise age constraints on early Holocene climatic events

Part of the problem with defining and correlating palaeoclimatic events of the early Holocene is: 1) the rapidity at which these are thought to have occurred; 2) the errors associated with age determinations, and, 3) the way this signal is manifest within proxy archives (Björck et al. 2001; Walker et al. 2009; Walker et al. 2012). At present many of the oscillations depicted in Table 12.3 are imprecisely dated in terrestrial settings, with many exhibiting multi-centennial errors. Thus comparing and correlating differing proxy records may be particularly misleading if response time is greater than the duration of the defined event. It is inherent that different proxies will respond at differing rates, and many of these will be dependent on a host of local feedback mechanisms, and site specific tipping points (e.g. Batterbee 2000; Wang et al. 2012). At present it is therefore difficult to determine whether proxy signals in association with 'events' at distant and separate locations, are illustrating: 1) a single synchronous event; 2) a single time-transgressive event, or; 3) several diachronous events occurring over a wide area.

Refining terrestrial ages of these events, and the proxy response time is thus essential if more meaningful and precise correlations are to be made. As demonstrated in Table 12.2 tephrochronology may be one of the most viable means to achieve this. Using well defined tephras to reduce the error estimates of these climatic perturbations has enabled at least one of the events at Quoyloo Meadow to be constrained with decadal scale accuracy i.e. event 4b. As already noted, this surpasses the precision of the GICC05 chronology in this interval, and is likely to be the best age estimate for an early Holocene climatic event recognised in a non-annually laminated record. In this regard the Saksunarvatn Ash and Fosen Tephra are a particularly useful tephra couplet, and can be further complimented by the An Druim Tephra in constraining these series of events dated around 10.2 kyrs BP. Similarly useful are the Askja-S/10ka and Hässeldalen Tephras in constraining the PBO (e.g. Davies et al. 2003; Wohlfarth et al. 2006; Ott et al. 2016). With further refinement of tephra ages, there is much scope in integrating and expanding tephrochronology as a precise method for constraining early Holocene perturbations. However, it is likely that the true advantages of tephra in this context will lie in the combination of its stratigraphic and chronological power, with ash

couplets used to define the stratigraphic position of proposed events and then chronological data used to provide chronological assessments of the events duration. In these cases an increase in the number of tephras identified in annually-laminated sequences and other well dated records is a fundamental requisite for the further application of tephrochronology in palaeoenvironmental science.

12.4 Chapter summary

This chapter has highlighted the necessity of the INTIMATE approach i.e. the development of independent age controls for the **testing** of climatic synchronicity. Warnings against wiggle-matching and tuning have been repeatedly expressed in the Quaternary literature for many years (e.g. Baillie 1991; Walker et al. 1999; Wunsch 2010; Blaauw et al. 2006; 2007; Blaauw 2012), yet this practice still remains common. This may in part reflect a misunderstanding of the problems that can arise from wiggle-matching exercises, but may also reflect a lack of viable methods to assist in testing synchronicity. In the absence of sufficient material for radiocarbon dating, there is very little prospect of developing a reliable site chronology at most sites NW Europe. As demonstrated, tephrochronology hence offers one of the best alternative methods for developing independent, high-resolution, and precise age models for palaeoenvironmental sequences. In this instance the Saksunarvatn Ash and Fosen Tephra have been invaluable in reliably constraining the 10.3 kyrs event in the British Isles for the first time. The number of tephras that have been identified across NW Europe clearly illustrates the potential for precisely linking records in this manner, but it is essential for the success of the technique that this approach is widely adopted. Poor chronologies are a particular hindrance, and unfortunately at present the errors and uncertainties associated with many records, negates the benefits of the few well resolved sequences.

Chapter 13. Conclusions

13.1 Introduction and chapter structure

In this final chapter, the main findings of this thesis are reviewed in the context of 1) key tephrostratigraphic developments; and 2) key tephrochronological developments. It is first necessary, however, to revisit the aims, and reiterate the current problems associated with distal tephra studies in NW Europe.

Primary Aim

Establish whether tephrochronology can be used to develop robust, and independent age controls on palaeoenvironmental records independent from any existing chronology, and whether the precision of these age models can be used to reliably constrain abrupt climatic oscillations of the LGIT and early Holocene.

Secondary Aims

1) Extend the Scottish tephrostratigraphic record, both in a geographic context, and hopefully also in regard to the suite of tephras that can be identified.
2) Establish whether higher resolution sampling and chemical characterisation techniques can impact on the number and chemical type of tephras identified in already studied areas.

It was noted in Chapter 2.0 that distal-tephrochronology, like many techniques used in palaeoenvironmental science, has undergone several phases of development and change. Around NW Europe, tephra studies have progressed through the earliest stages of 'inception' and 'primary growth', and has now entered a 'maturing' or consolidation era. The structure of this phase, as for any technique, is determined by the limitations and restrictions encountered during earlier intervals. For NW European tephra studies these limitations are: 1) issues of tephrostratigraphic disparity between neighbouring locales; 2) problems associated with geochemical distinguishment and repeatability of chemical signatures; 3) uncertainties with tephrostratigraphic superposition, and; 4) queries over the number of tephras identified within sites, and the level of level of stratigraphic refinement needed to identify those.

These topics shall accompany the aims and objectives as a basis for discussion in this chapter, with the final sections of this thesis considering future developments and recommendations in the field of distal tephra studies.

13.2 Tephrostratigraphic findings

- In total fifty-three intervals have been analysed across four sites with thirty-two tephra isochrons identified. Eleven tephras were recognised at Quoyloo Meadow, ten at Crudale Meadow, five at Spretta Meadow, and six at Tanera Mòr 1.

- This study has demonstrated the necessity for contiguous high resolution sampling. It has been shown that low resolution scan and resample techniques do not fully resolve tephrostratigraphic records, and that if this method is pursued it is highly likely that the number of tephras identified within a basin will be an underestimate of the total number of layers present. Crucially these findings have arisen from sites, or from sectors which have already been subjected to extensive tephrostratigraphic study. This spatial distribution and overlapping of sites henceforth discredits any suggestion that the findings of this study are purely a consequence of studying in new, or previously unexamined areas. It is very probable therefore that sites which have previously been examined in Scotland and NW Europe using standardised scan and resample techniques, will need reinvestigating in order to fully optimise site tephrostratigraphies. This will be essential if tephra disparity is to be minimised, and if more encompassing regional tephra frameworks are to be constructed in Europe.

- The results here illustrate the necessity to implement stringent and thorough protocols when selecting samples for chemical characterisation. Whilst a high resolution tephrostratigraphy may be developed, it is essential to complement this with an appropriate level of chemical refinement. A tendency to analyse primary peaks in concentration can further fuel tephrostratigraphic disparities in the same manner as low resolution refinement.

- Three visible macrotephra layers were identified during this thesis. One in association with the Vedde Ash (SPME1 681), and two in association with the Saksunarvatn Ash (QM1 160; CRUM1 380). These findings bring the total number of visible ash layers identified in the British Isles to five.

- A Borrobol-type tephra has been identified within Dimlington Stadial sediments at Tanera Mòr 1 (TM1 553, 545-546) and at Quoyloo Meadow (QM1 241). The tephra has been named the TM1 553 Tephra after the first known occurrence of

this horizon, and is indistinguishable from other Borrobol-type tephras based on major element analyses.

- A Borrobol-type tephra has been identified within late Windermere Interstadial/ early Loch Lomond Stadial deposits at Crudale Meadow (CRUM1 597) and Spretta Meadow (SPME1 701). The tephra has been named the CRUM1 597 Tephra after the first occurrence of this horizon, and is indistinguishable from other Borrobol-type tephras based on major element analyses.

- A Grímsvötn-type tephra has been identified in close association with the Askja-S/10ka Tephra at Crudale Meadow (CRUM1 496). This tephra has been named the CRUM1 496 Tephra after the first occurrence of this horizon, and is indistinguishable from other Grímsvötn-type tephras based on major element analyses.

- Further evidence for the Dimna Ash in Scotland has been provided by the identification of Katla-type shards within the Dimlington Stadial unit at Tanera Mòr 1 (TM1 553, 545-546). A tephra within the basal sediments at Crudale Meadow (CRUM1 676) has also been tentatively correlated to an intermediate fraction of the Dimna Ash. However, additional chemical analyses will be required to establish whether this correlation is valid.

- Evidence is beginning to emerge that the Penifiler Tephra and the interval in which it resides should be better considered as the Bølling-Allerød Ash Zone. Multiple chemical populations were identified within the 'Penifiler Tephra' analyses at Tanera Mòr 1, but not all of these could be correlated to known volcanic sources. These results, and others findings from sites in Britain and Europe collectively suggest this interval was an active period for volcanic provinces with the ability to generate ash clouds over Europe. Thus there is much scope in further refining this interval, and further potential for developing new tephrostratigraphic links across the continent, links which may prove more robust than the Penifiler Tephra (see section 13.4).

- The Askja-S/10ka Tephra has been identified at Quoyloo Meadow (QM1 188), Crudale Meadow (CRUM1 498), and Tanera Mòr 1 (TM1 454). These findings greatly increase the presence of this tephra in Scotland, and provide excellent chronostratigraphic links to Nordic, Irish and European tephrostratigraphies.

- The Hässeldalen Tephra has been identified in the British Isles for the first time at Quoyloo Meadow (QM1 192), and Crudale Meadow (CRUM1 543). This tephra, like the Askja-S/10ka is a crucial marker horizon for constraining early Holocene climatic perturbations like the PBO, and highlights the possibility of finding this tephra elsewhere in the British Isles.

- The Hovsdalur Tephra has been recognised in the British Isles for the first time at Quoyloo Meadow (QM1 187) and Spretta Meadow (SPME 1 622). The tephra has a limited distribution, and has previously only been identified in the Faroe Islands. Nevertheless this tephra provides an additional tephrostratigraphic marker for early Holocene sequences in Britain.

- The Hovsdalur and Hässeldalen Tephras have both been identified within the Quoyloo meadow tephrostratigraphy (QM1 187 and QM1 192 respectively). This disagrees with the suggestion made by Lind and Wastegård (2011) that the Hovsdalur may represent a poorly dated incidence of the Hässeldalen Tephra, and helps to establish the Hovsdalur as an independent marker horizon.

- The Fosen Tephra has been identified at Quoyloo Meadow (QM1 154) and Spretta Meadow (SPME1 610). This is the first time this tephra has been identified in the British Isles, and is a particularly important marker along with the Saksunarvatn Ash for marking the 10.3 kyr event.

- This thesis has presented stratigraphical, chemical and chronological data to suggest that the An Druim and Høvdarhagi Tephras should be considered the same eruptive event. Henceforth these tephras should be collectively referred to as the An Druim Tephra.

- The results from Quoyloo Meadow, Crudale Meadow, and Little Lochans highlight that carbonate-rich lacustrine sequences have the potential to preserve tephra layers of a varying composition and concentration. Furthermore the chemical characterisation of these horizons illustrates that tephras can remain chemically stable in these high pH substrates, and that dissolution of shards, at least in this instance, has been limited. This finding has particular significance for the development of high resolution palaeoclimatic records, as carbonate basins are often beset by poor chronological control, yet offer some

of the best opportunities for the development of high resolution palaeoclimate archives (Figure 12.5).

- There is an increasing problem in NW European tephrostratigraphies that concerns repeated chemical signatures and tephrostratigraphic distinction. As outlined in section 2.8.2 sedimentary superposition is one of the most crucial considerations when correlating tephra horizons. The findings of this study have partly resolved the superposition of Early Holocene age tephras in the North Atlantic margin; integrating uniquely 'British' tephras i.e. those which have exclusively been found within the British Isles such as the Ashik Tephra and the Abernethy Tephra, with their more widespread 'European' contemporaries (Figure 11.9).

- Recommendations of multi-core studies for the reliable identification of full tephra suites may be unfounded. Results from this study have shown that a greater number of tephras can be identified within single stratigraphic sequences if contiguous high resolution sampling, and chemical characterisation techniques are applied. This is of particular significance for palaeoenvironmental studies which are often restricted to single core stratigraphies.

- A key output of this project has been the development of a tephrostratigraphic framework for Scotland. However, given the hypothesised underrepresentation of tephras across Britain, this framework should be considered provisional, open to further revision, and part of a greater project designed to increase tephra connectivity across Britain and Europe as a whole. This study has identified three new tephras for the British Isles, and three previously unrecognised tephras in NW Europe. These findings have increased tephra connectivity across NW Europe by 1.25 % (Figure 10.11), and have provided new horizons by which additional connections can be made in the future.

- The findings from Little Lochans agree with previous studies, and suggests that the South Western sector of Scotland and the North Western sector of England may lie within a zone of low tephra concentration (Figure 9.7). This phenomena is likely resultant from atmospheric circulations, however, the small basin and catchment size of Little Lochans has likely exacerbated this effect. Nevertheless the findings from the site suggest that tephra horizons can be

identified in this area, and that there is much opportunity in this region to further develop tephrostratigraphic links between mainland Britain and Ireland.

13.2 Tephrochronological findings

- The development of high resolution tephrostratigraphies has facilitated the development of high precision age models derived entirely from tephrochronological information. This is one of the first occasions where this approach has been undertaken, and highlights a significant development in tephrochronological studies in NW Europe.

- The success of the tephrochronological based age models negates the need for more traditional radiocarbon dating techniques. This has particular significance for carbonate records, as these are often beset by poor chronological control derived from geological carbonate contamination of radiocarbon samples. The results here suggest that tephrochronology may be the most viable means by which secure chronologies can be developed for carbonate sequences.

- Age models of decadal-centennial scale precision were developed using Bayesian modelling techniques in Oxcal. This output is a significant development for: 1) tephrochronology in NW Europe, and; 2) the dating of Scottish lacustrine records. However, in order to maximise the chronological potential of the tephra horizons, and to hence minimise the uncertainties associated with the age models, a composite model was developed. This approach is comparatively new, but the results show much promise in further refining both chronological models and the ages of tephras in NW Europe. The ages reported in Table 11.3 should hence be regarded as the current best age estimates for these tephras. However, it is necessary to iterate that these ranges are a product of the inputted data. Dating of tephra horizons by direct methods should still be pursued, and will be essential to test the validity of modelled outputs.

- At Quoyloo Meadow, the integration of a high precision independent age-model with the $\delta^{18}O$ record allows these results to be directly compared to Greenland using an independent chronology with a precision that is comparable GICC05. This is the first incidence that a carbonate lake record from the British has been able to be compared so precisely with the Greenland strato-type.

- Between the Saksunarvatn Ash and the Fosen Tephra at Quoyloo Meadow, the age model produced exceeds the precision of the GICC05 chronology with a 2σ uncertainty of 82 years. This development highlights the significant potential of this tephra couplet to constrain the 10.3 kyr event in sedimentary sequences across NW Europe.

- The tephra couplet approach may be one of the most effective means to constrain abrupt climatic oscillation during the LGIT. This technique also has applications in the context of: 1) GI-1d, which is flanked by the Borrobol and Penifiler Tephras, and; 2) the PBO which is constrained by the Askja-S/10ka and Hässeldalen Tephras. With the discovery of new tephras in this study, it is possible that others may be found in close association with other known climatic oscillations.

13.3 Summary of findings

- Sites examined in this thesis have extended the geographical extent of the Scottish tephrostratigraphic framework.
- High resolution refinement has increased the number of tephra horizons recognised in Scotland, and provided new links to Europe.
- The number of tephras identified in previous tephrostratigraphic studies are likely to be underestimated due to low resolution and incomplete refinement.
- High resolution tephrostratigraphies have facilitated the development of independent age-depth models with a centennial-decadal uncertainty.
- Resulting age models have been able to constrain early Holocene abrupt climatic oscillations with a precision previously unmatched in Britain.

13.4 Future developments and recommendations

It is acknowledged that the contiguous high resolution sampling strategy advocated in this thesis has only been tested in the most northerly locales of the British Isles. It is necessary that a more comprehensive survey of different geographic locations be undertaken in order to test the validity of this approach. In light of this, a number of recommendations concerning the refinement of tephrostratigraphic records is presented in section 10.2.3, and readers are encouraged to refer to these in the context of this section.

Whilst success has been achieved following a contiguous 1 cm sampling strategy, it has become apparent that in some instances, even this level of refinement is inadequate to confidently assign the position of an isochron. This is particularly evident in locations where a conflation of tephras occurs e.g. Quoyloo Meadow. Higher resolution sampling at 0.5 cm or greater may help to resolve these issues, but it is essential that any such development be accompanied by an equal level of chemical characterisation. However, refinement at this level will likely be very time consuming, costly, and will also be demanding in terms of expertise and specialist equipment. It is recommended therefore, that finite study in this manner be only applied in the most exceptional circumstances where a distinction of conflated horizons will give a significant return on the time and effort invested. Alternatively, higher levels of refinement can be achieved by focussing on longer records with higher sedimentation rates. Conflation of horizons in such records should be less frequent, and in cases where they are conflated, perhaps easier to resolve.

It is recommended that stricter protocols be adopted when declaring new tephra horizons. This is a problem that is particularly evident in early Holocene sequences from NW Europe, where single site occurrences of 'new tephras' are routinely reported (e.g. Ranner et al. 2005; Pyne-O'Donnell 2007; Lind and Wastegård 2011; Lind et al. 2013). New findings should initially be referred to as a site code and depth (e.g. Matthews et al. 2011; Lane et al. 2015), and only when there is: 1) a well characterised chemical profile for the tephra (ideally tens of analyses); 2) a secure age estimate, and; 3) evidence for the horizon at two or more sites, should a formal 'name' be proposed (e.g. MacLeod et al. 2015). With the manner in which tephra studies are developing and expanding, it may be necessary to consider a process of formal ratification for newly identified horizons. Exactly how this may be undertaken, and crucially by who, is a matter open for debate, but in doing so it may help alleviate some of the already excessive and unnecessary terms for tephras in NW Europe. In light of this, it may be necessary to 'demote' certain horizons from their status as tephra horizons in NW Europe. For example the Breakish Tephra (Pyne-O'Donnell 2007), has limited chemical characterisation (4 analyses), has no reliable age estimate, and has only been identified at Loch Ashik basin B. It would seem logical that developing a standard, or checklist of attributes to test the validity and usefulness of a tephra horizon, is a necessary step in the evolution of the technique.

With this idea of a checklist for the identification of tephras, it may be prudent to consider a similar schema to quantify the robustness of tephra correlations. In section 2.8.1 it was suggested that tephra correlations must be guided by: 1) an absolute

chronology; 2) geochemical characteristics, and; 3) tephrostratigraphic superposition, and only litho- biostratigraphical or archaeological information as a last, tentative resort. Application of the latter inherently leads to circular reasoning, however, in many circumstances this process is unavoidable. Independent age controls are often difficult to resolve, chemical characterisation may only narrow potential candidates, and following standard scan and resample techniques, tephrostratigraphic superposition is often unclear. Inevitably a tephra's position in relation to bio- or lithostratigraphy does bear some influence on a tephra correlation. Whilst this should not automatically be considered as negative or detrimental, a numerical grading system may provide a means to quantify this decision, and hence enable a way in which the secureness of correlations can be compared at a wider scale. It may also help to identify those tephra which are particularly difficult to correlate to, and hence provide a focus for research groups to improve the 'correlativity' of certain tephras. A current example of this, are the issues surrounding the Penifiler Tephra. It is evident that using bio- and lithostratigraphic markers to determine the presence and isochronous position of this horizon, has resulted in a significant level of uncertainty and disparity (see section 10.3.3.2). In some circumstances the Penifiler Tephra is seen to coincide with the bio- and lithostratigraphic representation of a cold event broadly equivalent to GI-1d, and in some circumstances the tephra isochron is seen to occur after this event (Figure 10.17). These are not secure correlations, and hence this uncertainty should be highlighted as a matter of caution. Failure to address this issue now, may lead to an incidence of 'reinforcement syndrome' (Blaauw 2012), ultimately negating the tephra's isochronous potential, and subsequently devaluing tephrochronology as a key geochronological tool.

The composite age modelling approach of this thesis has shown much potential in reducing tephra age uncertainty, and improving the precision of age depth models for lacustrine sequences. However, the study has been limited to four sites. In ideal circumstances all locations bearing tephras of LGIT age would be modelled together. The development of a 'mega-composite' age model would allow the integration and consideration of all stratigraphic and chronological information when refining an isochron. Any improvement would also be automatically applied to any sequence held within the model, thus ensuring all site stratigraphic data was being compared using the same chronological parameters. At present, however, this level of modelling complexity is not widely available, and consideration must also be given to server access and model run time. Nevertheless this seems like a viable aim for the future, and one which likely emerge in time.

This study has highlighted the potential of high resolution tephrostratigraphies and the capacity of composite age models to deliver a greater insight into palaeoenvironmental change during the late Pleistocene and early Holocene. However, there is still: 1) considerable disparity concerning the distribution of tephras in NW Europe; 2) uncertainty concerning the stratigraphical and chronological integrity of some horizons, and 3) uncertainty over the age and prominence of early Holocene climatic perturbations. In reality it is unlikely that one site will resolve all of these issues, however, it may be prudent to prioritise locations which may help to address several of these concerns. As shown in this study, calcareous basins offer the potential to develop high resolution tephrostratigraphies, and they also offer some of the best opportunities in developing multi-proxy palaeoclimatic reconstructions. In Scotland these sites are relatively few, but basins such as Borrobol (Turney et al. 1997a), Lundin Tower (Whittington et al. 1996), and Whitrig Bog (Turney et al. 1997a; Mayle et al. 1997) should be considered a priority for reinvestigation. Elsewhere in the British Isles, these carbonate basins are more common, yet tephrostratigraphic studies of LGIT age are particularly sparse. It is therefore important to highlight what can be achieved with a tephrochronological approach, and encourage its integration within the wider palaeoclimatic community. Only with concerted efforts, and dedicated terrestrial, marine and ice core projects can the aforementioned tephrostratigraphic questions be addressed, and the ultimate aim of testing inter-continental climate synchronicity be reliably sought.

References

Abbott, P.M. and Davies, S.M (2012) 'Volcanism and the Greenland ice-cores: the tephra record' *Earth-Science Reviews* 115, (3) 173-191

Abel, L (2015) 'Evidence for abrupt climate change during the Early Holocene, using stable isotopes at Quoyloo Meadow, Orkney Isles, Great Britain' Unpublished BSc Thesis, University of London

Ahlberg, K., Almgren, E., Wright, H.E. and Ito, E (2001) 'Holocene stable-isotope stratigraphy at Lough Gur, County Limerick, Western Ireland' *The Holocene* 11, (3) 367-372

Albert, P (2007) 'Tephrostratigraphical investigation of Loch Etteridge: stratigraphical uncertainties' Unpublished MSc Thesis, University of London

Alley, R.B. and Ágústsdóttir, A.M (2005) 'The 8k event: cause and consequences of a major Holocene abrupt climate change' *Quaternary Science Reviews* 24, (10) 1123-1149

Alloway, B.V., Larsen, G., Lowe, D.J., Shane, P.A.R. and Westgate, J.A (2007) 'Tephrochronology' In *Encyclopedia of Quaternary Science*. Elsevier: Amsterdam, 85-114

Anderson, R., Nuhfer, E. and Dean, W.E (1984) 'Sinking of volcanic ash in uncompacted sediment in Williams Lake, Washington' *Science, New Series* 225, (4661) 505-508

Andrews, J.E (2006) 'Palaeoclimatic records from stable isotopes in riverine tufas: synthesis and review' *Earth-Science Reviews* 75, (1) 85-104

Andrews, J.T., Eberl, D.D. and Kristjansdottir, G.B (2006) 'An exploratory method to detect tephras from quantitative XRD scans: examples from Iceland and east Greenland marine sediments' *The Holocene* 16, (8) 1035-1042

Andrews, J.T., Geirsdóttir, A., Hardardóttir, J., Principato, S., Grönvold, K., Kristjansdóttir, G.B., Helgadóttir, G., Drexler, J. and Sveinbjörnsdóttir, A (2002) 'Distribution, sediment magnetism and geochemistry of the Saksunarvatn (10,180±60 cal. yr BP) tephra in marine, lake, and terrestrial sediments, northwest Iceland' *Journal of Quaternary Science* 17, (8) 731-745

Atkinson, T.C., Briffa, K.R. and Coope, G.R (1987) 'Seasonal temperatures in Britain during the past 22,000 years, reconstructed using beetle remains' *Nature* 325, 587-592

Baillie, M.G.L (1991) 'Suck-in and smear: two related chronological problems for the 90s' *Journal of theoretical archaeology* 2, 12-16

Bakke, J., Lie, Ø., Heegaard, E., Dokken, T., Haug, G.H., Birks, H.H., Dulski, P. and Nilsen, T (2009) 'Rapid oceanic and atmospheric changes during the Younger Dryas cold period' *Nature Geoscience* 2, (3) 202-205

Ballantyne, C. K (1987) 'An Teallach' In: *Wester Ross: Field Guide*. ed. by Ballantyne, C. K and Sutherland, D.G. Cambridge: Quaternary Research Association: 72-92

Ballantyne, C.K and Harris, C (1994) *The Periglaciation of Great Britain*. Cambridge: Cambridge University Press

Ballantyne, C.K (2002) 'Paraglacial geomorphology' *Quaternary Science Reviews* 21, (18) 1935-2017

Ballantyne, C.K., Hall, A.M., Phillips, W., Binnie, S. and Kubik, P.W (2007) 'Age and significance of former low-altitude corrie glaciers on Hoy, Orkney Islands' *Scottish Journal of Geology* 43, (2) 107-114

Ballantyne, C.K., Schnabel, C. and Xu, S (2009) 'Readvance of the last British–Irish ice sheet during Greenland interstade 1 (GI-1): the Wester Ross readvance, NW Scotland' *Quaternary Science Reviews* 28, (9) 783-789

Ballantyne, C.K. and Stone, J.O (2012) 'Did large ice caps persist on low ground in north-west Scotland during the Lateglacial Interstade?' *Journal of Quaternary Science* 27, (3) 297-306

Ballantyne, C.K., Rinterknecht, V. and Gheorghiu, D.M (2013) 'Deglaciation chronology of the Galloway Hills ice centre, southwest Scotland' *Journal of Quaternary Science* 28, (4) 412-420

Barton, N (2009) 'The Lateglacial or latest Palaeolithic occupation of Britain' In *The Archaeology of Britain*. ed by Hunter, J. and Ralston, I. London: Routledge: 18-52

Barton, R.N.E., Lane, C.S., Albert, P.G., White, D., Collcutt, S.N., Bouzouggar, A., Ditchfield, P., Farr, L., Oh, A., Ottolini, L. and Smith, V.C (2015) 'The role of cryptotephra in refining the chronology of Late Pleistocene human evolution and cultural change in North Africa' *Quaternary Science Reviews* 118, 151-169

Battarbee, R.W (2000) 'Palaeolimnological approaches to climate change, with special regard to the biological record' *Quaternary Science Reviews* 19, (1) 107-124

Bengtsson, L. and Enell, M (1986) 'Chemical Analysis'. In *Handbook of Holocene Palaeoecology and Palaeohydrology*. ed. by Berglund, B.E. Chichester: John Wiley & Sons Ltd: 423-451

Bennett, K.D., Boreham, S., Sharp, M.J. and Switsur, V.R (1992) 'Holocene history of environment, vegetation and human settlement on Catta Ness, Lunnasting, Shetland' *Journal of Ecology* 241-273

Bennett, K.D (1994) 'Confidence intervals for age estimates and deposition times in late-Quaternary sediment sequences' *The Holocene* 4, (4) 337-348

Bennett, K.D. and Fuller, J.L (2002) 'Determining the age of the mid-Holocene Tsuga canadensis (hemlock) decline, eastern North America' The Holocene 12, 421-429

Bennett, M. R (1991) 'Scottish "hummocky moraine" : its implications for the deglaciation of the North West Highlands during the Younger Dryas or Loch Lomond Stadial' Unpublished PhD Thesis, University of Edinburgh

Berglund, B.E., Björck, S., Lemdahl, G., Bergsten, H., Nordberg, K. and Kolstrup, E (1994) 'Late Weichselian environmental change in southern Sweden and Denmark' *Journal of Quaternary Science* 9, (2) 127-132

Bergman, J., Wastegard, S., Hammarlund, D., Wohlfarth, B. and Roberts, S.J (2004) 'Holocene tephra horizons at Klocka Bog, west-central Sweden: aspects of reproducibility in subarctic peat deposits' *Journal of Quaternary Science* 19, (3) 241-249

Bertrand, S., Daga, R., Bedert, R. and Fontijn, K (2014) 'Deposition of the 2011–2012 Cordón Caulle tephra (Chile, 40 S) in lake sediments: Implications for tephrochronology and volcanology' *Journal of Geophysical Research: Earth Surface* 119, (12) 2555-2573

Bickerdike, H.L., Evans, D.J.A., Ó Cofaigh, C. and Stokes, C.R (2016) 'The glacial geomorphology of the Loch Lomond Stadial in Britain: a map and geographic information system resource of published evidence' *Journal of Maps* 1-9

Birks, H.H (1984) 'Late-Quaternary pollen and plant macrofossil stratigraphy at Lochan an Druim, north-west Scotland.' In *Lake Sediments and Environmental History*. ed. by Haworth, E.Y. and Lund, J.W.G. Minneapolis: University of Minnesota Press

Birks, H.H., Gulliksen, S., Haflidason, H., Mangerud, J. and Possnert, G (1996) 'New radiocarbon dates for the Vedde Ash and the Saksunarvatn Ash from western Norway' *Quaternary Research* 45, (2) 119-127

Birks, H.J (1989) 'Holocene isochrone maps and patterns of tree-spreading in the British Isles' *Journal of Biogeography* 16,(6) 503-540

Birks, H.J (1989) 'Holocene isochrone maps and patterns of tree-spreading in the British Isles' *Journal of Biogeography* 503-540

Björck, S., Ingólfsson, Ó., Haflidason, H., Hallsdóttir, M., Anderson, N.J (1992) 'Lake Torfadalsvatn: a high resolution record of the North Atlantic ash zone 1 and the last glacial-interglacial environmental changes in Iceland' *Boreas* 21, 15–22

Bjorck, S., Kromer, B., Johnsen, S. and Bennike, O (1996) 'Synchronized terrestrial-atmospheric deglacial records around the North Atlantic' *Science* 274, (5290) 1155-1160

Björck, S., Rundgren, M., Ingolfsson, Ó. and Funder, S (1997) 'The Preboreal oscillation around the Nordic Seas: terrestrial and lacustrine responses' *Journal of Quaternary Science* 12, (6) 455-465

Björck, S., Walker, M.J., Cwynar, L.C., Johnsen, S., Knudsen, K.L., Lowe, J.J. and Wohlfarth, B (1998) 'An event stratigraphy for the Last Termination in the North Atlantic region based on the Greenland ice-core record: a proposal by the INTIMATE group' *Journal of Quaternary Science* 13, (4) 283-292

Björck, J. and Wastergard, S (1999) 'Climate oscillations and tephrochronology in eastern middle Sweden during the last glacial-interglacial transition' *Journal of Quaternary Science*, 14, 399-410

Björck, S., Muscheler, R., Kromer, B., Andresen, C.S., Heinemeier, J., Johnsen, S.J., Conley, D., Koç, N., Spurk, M. and Veski, S (2001) 'High-resolution analyses of an early Holocene climate event may imply decreased solar forcing as an important climate trigger' *Geology* 29, (12) 1107-1110

Björck, S., Koç, N. and Skog, G (2003) 'Consistently large marine reservoir ages in the Norwegian Sea during the Last Deglaciation' *Quaternary Science Reviews* 22, (5) 429-435

Blaauw, M. and Christen, J.A (2005) 'Radiocarbon peat chronologies and environmental change' *Applied Statistics* 54, 805-816

Blaauw, M., Christen, J.A., van der Plicht, J. and Bennett, K (2006) '21st century suck-in or smear: testing the timing of events between archives' *PAGES News* 14, (3) 15-16

Blaauw, M., Christen, J.A., Mauquoy, D., van der Plicht, J. and Bennett, K.D (2007) 'Testing the timing of radiocarbon-dated events between proxy archives' *The Holocene* 17, (2) 283-288

Blaauw, M (2010) 'Methods and code for 'classical' age-modelling of radiocarbon sequences' *Quaternary Geochronology* 5, (5) 512-518

Blaauw, M (2012) 'Out of tune: the dangers of aligning proxy archives' *Quaternary Science Reviews* 36, 38-49

Blackford J.J., Edwards K.J., Dugmore A.J., Cook G.T., Buckland P.C (1992) 'Icelandic volcanic ash and the mid-Holocene pollen decline in northern Scotland' *The Holocene* 2, (3) 260-265

Blockley, S.P., Lowe, J.J., Walker, M.J., Asioli, A., Trincardi, F., Coope, G.R. and Donahue, R.E (2004) 'Bayesian analysis of radiocarbon chronologies: examples from the European Late-glacial' *Journal of Quaternary Science* 19, (2) 159-175

Blockley, S.P.E., Pyne-O'Donnell, S.D.F., Lowe, J.J., Matthews, I.P., Stone, A., Pollard, A.M., Turney, C.S.M. and Molyneux, E.G (2005) 'A new and less destructive laboratory procedure for the physical separation of distal glass tephra shards from sediments' *Quaternary Science Reviews* 24, (16) 1952-1960

Blockley, S.P.E., Blaauw, M., Ramsey, C.B. and van der Plicht, J (2007) 'Building and testing age models for radiocarbon dates in Lateglacial and Early Holocene sediments' *Quaternary Science Reviews* 26 (15), 915-1926

Blockley, S.P., Ramsey, C.B. and Pyle, D.M (2008a) 'Improved age modelling and high-precision age estimates of late Quaternary tephras, for accurate palaeoclimate reconstruction' *Journal of Volcanology and Geothermal Research* 177 (1) 251-262

Blockley, S.P.E., Ramsey, C.B., Lane, C.S. and Lotter, A.F (2008b) 'Improved age modelling approaches as exemplified by the revised chronology for the Central European varved lake Soppensee' *Quaternary Science Reviews* 27, (1) 61-71

Blockley, S.P., Lane, C.S., Hardiman, M., Rasmussen, S.O., Seierstad, I.K., Steffensen, J.P., Svensson, A., Lotter, A.F., Turney, C.S., Ramsey, C.B. and INTIMATE Members, (2012) 'Synchronisation of palaeoenvironmental records over the last 60,000 years, and an extended INTIMATE event stratigraphy to 48,000 b2k' *Quaternary Science Reviews* 36, 2-10

Blockley, S.P., Bourne, A.J., Brauer, A., Davies, S.M., Hardiman, M., Harding, P.R., Lane, C.S., MacLeod, A., Matthews, I.P., Pyne-O'Donnell, S.D., Rasmussen, S.O, Wulf, S. and Zanchetta, G (2014) 'Tephrochronology and the extended intimate (integration of ice-core, marine and terrestrial records) event stratigraphy 8–128 ka b2k' *Quaternary Science Reviews* 106 (8)

Blockley, S.P., Edwards, K.J., Schofield, J.E., Pyne-O'Donnell, S.D., Jensen, B.J., Matthews, I.P., Cook, G.T., Wallace, K.L. and Froese, D (2015) 'First evidence of cryptotephra in palaeoenvironmental records associated with Norse occupation sites in Greenland' *Quaternary Geochronology* 27, 145-157

Blunier, T. and Brook, E.J (2001) 'Timing of millennial-scale climate change in Antarctica and Greenland during the last glacial period' *Science* 291, (5501) 109-112

Boelter, D.H (1972) ‘Water table drawdown around an open ditch in organic soils’ *Journal of Hydrology* 15, (4) 329-340

Bond, G., Broecker, W., Johnsen, S., McManus, J., Labeyrie, L., Jouzel, J., and Bonani, G (1993) ‘Correlations between climate records from North Atlantic sediments and Greenland ice’ *Nature* 365, (6442) 143-147

Bond, G., Showers, W., Cheseby, M., Lotti, R., Almasi, P., Priore, P., Cullen, H., Hajdas, I. and Bonani, G (1997) ‘A pervasive millennial-scale cycle in North Atlantic Holocene and glacial climates’ *Science* 278, (5341) 1257-1266

Bond, G.C., Showers, W., Elliot, M., Evans, M., Lotti, R., Hajdas, I., Bonani, G. and Johnson, S (1999) ‘The North Atlantic's 1-2 Kyr Climate Rhythm: Relation to Heinrich Events, Dansgaard/Oeschger Cycles and the Little Ice Age’ Mechanisms of global climate change at millennial time scales 35-58

Bond, G.C., Mandeville, C. and Hoffmann, S (2001) ‘Were rhyolitic glasses in the Vedde Ash and in the North Atlantic's Ash Zone 1 produced by the same volcanic eruption?’ *Quaternary Science Reviews* 20, (11) 1189-1199

Bondevik, S. and Mangerud, J (2002) 'A calendar age estimate of a very late Younger Dryas ice sheet maximum in western Norway' *Quaternary Science Reviews* 21, (14) 1661-1676

Bondevik S, Mangerud J, Dawson S, Dawson and A, Lohne Ø (2005) ‘Evidence for three North Sea tsunamis at the Shetland Islands between 8000 and 1500 years ago’ *Quaternary Science Reviews* 24, 1757–1775

Bonny, A.P (1978) ‘The effect of pollen recruitment processes on pollen distribution over the sediment surface of a small lake in Cumbria’ *The Journal of Ecology* 385-416

Bos, J.A., van Geel, B., van der Plicht, J. and Bohncke, S.J (2007) ‘Preboreal climate oscillations in Europe: Wiggle-match dating and synthesis of Dutch high-resolution multi-proxy records’ *Quaternary Science Reviews* 26, (15) 1927-1950

Bourne, A.J (2012) ‘The late Quaternary tephrochronology of the Adriatic region: implications for the synchronisation of marine records’ Unpublished PhD Thesis, University of London

Bourne, A.J., Albert, P.G., Matthews, I.P., Trincardi, F., Wulf, S., Asioli, A., Blockley, S.P.E., Keller, J. and Lowe, J.J (2015) ‘Tephrochronology of core PRAD 1-2 from the Adriatic Sea: insights into Italian explosive volcanism for the period 200–80 ka’ *Quaternary Science Reviews* 116, 28-43

Bourne, A.J., Cook, E., Abbott, P.M., Seierstad, I.K., Steffensen, J.P., Svensson, A., Fischer, H., Schüpbach, S. and Davies, S.M (2015) 'A tephra lattice for Greenland and a reconstruction of volcanic events spanning 25–45 ka b2k' *Quaternary Science Reviews* 118, 122-141

Bowen, D.Q., Phillips, F.M., McCabe, A.M., Knutz, P.C. and Sykes, G.A (2002) ‘New data for the last glacial maximum in Great Britain and Ireland’ *Quaternary Science Reviews* 21, (1)

Boygle, J (1999) 'Variability of tephra in lake and catchment sediments, Svínavatn, Iceland' *Global and Planetary Change* 21, 129–149

Bradbury, J.P (1996) 'Charcoal deposition and redeposition in Elk Lake, Minnesota, USA' *The Holocene* 6, (3) 339-344

Bradwell, T., Stoker, M. and Larter, R (2007) 'Geomorphological signature and flow dynamics of The Minch palaeo-ice stream, northwest Scotland' *Journal of Quaternary Science* 22, (6) 609-617

Bradwell, T., Fabel, D., Stoker, M., Mathers, H., McHargue, L. and Howe, J (2008) 'Ice caps existed throughout the Lateglacial Interstadial in northern Scotland' *Journal of Quaternary Science* 23, (5) 401-407

Bramham-Law, C.W.F., Theuerkauf, M., Lane, C.S. and Mangerud, J (2013) 'New findings regarding the Saksunarvatn Ash in Germany' *Journal of Quaternary Science* 28, (3) 248-257

Brathauer, U., Brauer, A., Negendank, J.F.W. and Zolitschka, B (2000) 'Rasche Klimaänderungen am Beginn der heutigen Warmzeit' Zweijahresbericht GeoForschungsZentrum Potsdam 1998/1999, 29-33

Brauer, A., Endres, C. and Negendank, J.F (1999) 'Lateglacial calendar year chronology based on annually laminated sediments from Lake Meerfelder Maar, Germany' *Quaternary International* 61, (1) 17-25

Brauer, A., Haug, G.H., Dulski, P., Sigman, D.M. and Negendank, J.F (2008) 'An abrupt wind shift in western Europe at the onset of the Younger Dryas cold period' *Nature Geoscience* 1, (8) 520-523

Brendryen, J., Haflidason, H. and Sejrup, H.P (2010) 'Norwegian Sea tephrostratigraphy of marine isotope stages 4 and 5: prospects and problems for tephrochronology in the North Atlantic region' *Quaternary Science Reviews* 29, (7) 847-864

Brendryen, J., Haflidason, H. and Sejrup, H.P (2011) 'Non-synchronous deposition of North Atlantic Ash Zone II in Greenland ice cores, and North Atlantic and Norwegian Sea sediments: an example of complex glacial-stage tephra transport' *Journal of Quaternary Science* 26, (7) 739-745

Bronk Ramsey, C (1995) 'Radiocarbon calibration and analysis of stratigraphy; the OxCal program' *Radiocarbon* 37, (2) 425-430

Bronk Ramsey, C (2008) 'Deposition models for chronological records' *Quaternary Science Reviews* 27, (1-2) 42-60

Bronk Ramsey, C (2009) 'Dealing with outliers and offsets in radiocarbon dating' *Radiocarbon* 51, (3) 1023-1045

Bronk Ramsey, C (2001) 'Development of the radiocarbon calibration program' *Radiocarbon* 43, 355-364

Bronk Ramsey, C., and Lee, S (2013) 'Recent and planned developments of the program OxCal' *Radiocarbon* 55, (2-3) 720-730

Bronk Ramsey, C., Housley, R.A., Lane, C.S., Smith, V.C. and Pollard, A.M (2015a) 'The RESET tephra database and associated analytical tools' Quaternary Science Reviews 118, 33-47

Bronk Ramsey, C., Albert, P.G., Blockley, S.P., Hardiman, M., Housley, R.A., Lane, C.S., Lee, S., Matthews, I.P., Smith, V.C. and Lowe, J.J (2015b) 'Improved age estimates for key Late Quaternary European tephra horizons in the RESET lattice' *Quaternary Science Reviews* 118, 18-32

Brooks, S.J (2006) 'Fossil midges (Diptera: Chironomidae) as palaeoclimatic indicators for the Eurasian region' *Quaternary Science Reviews* 25, (15) 1894-1910

Brooks, S.J. and Birks, H.J.B (2000) 'Chironomid-inferred Late-glacial air temperatures at Whitrig Bog, Southeast Scotland' *Journal of Quaternary Science* 15, (8) 759-764

Brooks, S.J., Langdon, P.G. and Heiri, O (2007) 'The identification and use of Palaearctic Chironomidae larvae in palaeoecology' *QRA Technical Guide No. 10*. London: Quaternary Research Association

Brooks, S.J., Matthews, I.P., Birks, H.H. and Birks, H.J.B (2012) 'High resolution Lateglacial and early-Holocene summer air temperature records from Scotland inferred from chironomid assemblages' *Quaternary Science Reviews* 41, 67-82

Brooks, S.J. and Langdon, P.G (2014) 'Summer temperature gradients in northwest Europe during the Lateglacial to early Holocene transition (15–8 ka BP) inferred from chironomid assemblages' *Quaternary International* 341, 80-90

Brooks, S.J., Davies, K.L., Mather, K.A., Matthews, I.P. and Lowe, J.J (2016) 'Chironomid-inferred summer temperatures for the Last Glacial–Interglacial Transition from a lake sediment sequence in Muir Park Reservoir, west-central Scotland' *Journal of Quaternary Science* 31, (3) 214-224

Bunting, M.J (1994) 'Vegetation history of Orkney, Scotland: Pollen records from two small basins in west Mainland' *New Phytologist* 128, (4) 771-792

Bunting, M.J (1996) 'Holocene Vegetation and Environment of Orkney.' In: *The Quaternary of Orkney Field Guide*. ed by: Hall, A.M. Quaternary Research Association; 20-29

Callicott, R (2013) 'Tephrostratigraphy of Eilean Fada Mor, Summer Isles' Unpublished BSc Thesis, University of London

Callicott, R (2015) 'Tephrostratigraphy of a Lateglacial sequence at the Loons, Orkney' Unpublished MSc Thesis, University of London

Candy, I., Stephens, M., Hancock, J. and Waghorne, R (2011) 'Palaeoenvironments of ancient humans in Britain: the application of oxygen and carbon isotopes to the reconstruction of Pleistocene environments' In *The Ancient Human Occupation of Britain*. ed by Ashton, N., Lewis, S.G. and Stringer, C. London: Elsevier: 23-38

Candy, I., Farry, A., Darvill, C.M., Palmer, A., Blockley, S.P.E., Matthews, I.P., MacLeod, A., Deeprose, L., Farley, N., Kearney, R. and Conneller, C (2015) 'The evolution of Palaeolake Flixton and the environmental context of Star Carr: an oxygen and carbon isotopic record of environmental change for the early Holocene' *Proceedings of the Geologists' Association* 126, (1) 60-71

Candy, I., Abrook, A., Elliot, F., Lincoln, P.C., Matthews, I.P., and Palmer (2016) 'Oxygen Isotope evidence for high magnitude, abrupt climatic events during the Late-Glacial Interstadial in northwest Europe: Analysis of a lacustrine sequence from the site of Tirinie, Scottish Highlands' *Journal of Quaternary Science* 31, (6) 607-621

Carey, S. and Sparks, R.S.J (1986) ‘Quantitative models of the fallout and dispersal of tephra from volcanic eruption columns’ *Bulletin of Volcanology* 48, (2-3) 109-125

Carrivick, J.L., Russell, A.J., Lucy Rushmer, E., Tweed, F.S., Marren, P.M., Deeming, H., and Lowe, O.J (2009) ‘Geomorphological evidence towards a de-glacial control on volcanism’ *Earth Surface Processes and Landforms* 34, (8) 1164-1178

Carter-Champion, A (2015) 'Constructing the landscape evolution of the lower Turret Bank, Glen Roy in the Last Glacial-Interglacial Transition' Unpublished MSc Thesis, University of London

Caseldine, C., Baker, A. and Barnes, W.L (1999) ‘A rapid, non-destructive scanning method for detecting distal tephra layers in peats’ *The Holocene* 9, (5) 635-638

Chambers, F.M., Daniell, J.R., Hunt, J.B., Molloy, K. and O'Connell, M (2004) ‘Tephrostratigraphy of An Loch Mor, Inis Oirr, western Ireland: implications for Holocene tephrochronology in the northeastern Atlantic region’ *The Holocene* 14, (5) 703-720

Charlesworth, J.K., (1927a) ‘I.—The Glacial Geology of the Southern Uplands of Scotland, West of Annandale and Upper Clydesdale’ *Transactions of the Royal Society of Edinburgh* 55, (1) 1-23

Charlesworth, J.K (1927b) ‘II.—The Readvance, Marginal Kame-moraine of the South of Scotland, and some Later Stages of Retreat’ *Transactions of the Royal Society of Edinburgh* 55, (1) 25-50

Charlesworth, J.K (1955) ‘XIX. —The Late-glacial History of the Highlands and Islands of Scotland’ *Transactions of the Royal Society of Edinburgh* 62, (3) 769-928

Clark, C.D., Hughes, A.L., Greenwood, S.L., Jordan, C. and Sejrup, H.P (2012) ‘Pattern and timing of retreat of the last British-Irish Ice Sheet’ *Quaternary Science Reviews* 44, 112-146

Cole, P.D., Queiroz, G., Wallenstein, N., Gaspar, J.L., Duncan, A.M. and Guest, J.E (1995) ‘An historic subplinian/phreatomagmatic eruption: the 1630 AD eruption of Furnas volcano, São Miguel, Azores’ *Journal of volcanology and geothermal research* 69, (1) 117-135

Coope, G.R., Lemdahl, G., Lowe, J.J. and Walkling, A (1998) ‘Temperature gradients in northern Europe during the last glacial–Holocene transition (14-9 14C kyr BP) interpreted from coleopteran assemblages’ *Journal of Quaternary Science* 13, (5) 419-433

Cooper, R (1999) 'Lithostratigraphy and tephrochronology of sediments spanning the time interval of the Last Glacial-Interglacial Transition at Muir Park Reservoir, Scotland and Sluggan Moss, Ireland' Unpublished MSc Thesis, University of London

Cornish, R (1981) ‘Glaciers of the Loch Lomond Stadial in the western Southern Uplands of Scotland’ *Proceedings of the Geologists' Association* 92, (2) 105-114

Coulson, J.C., Butterfield, J.E.L. and Henderson, E (1990) ‘The effect of open drainage ditches on the plant and invertebrate communities of moorland and on the decomposition of peat’ *Journal of Applied Ecology*, 549-561

Coulter, S.E., Pilcher, J.R., Hall, V.A., Plunkett, G. and Davies, S.M (2010) 'Testing the reliability of the JEOL FEGSEM 6500F electron microprobe for quantitative major element analysis of glass shards from rhyolitic tephra' *Boreas* 39, (1) 163-169

Crovisier, J.L., Advocat, T. and Dussossoy, J.L (2003) 'Nature and role of natural alteration gels formed on the surface of ancient volcanic glasses (Natural analogs of waste containment glasses)' *Journal of Nuclear Materials* 321, (1) 91-109

Dadswell, L. F (2002) 'Investigating the presence of microtephra in the Lateglacial sequence at Druim Loch, Isle of Skye, Inner Hebrides, Scotland' Unpublished BSc Thesis, University of London

Dahl, S.O., Nesje, A., Lie, Ø., Fjordheim, K. and Matthews, J.A (2002) 'Timing, equilibrium-line altitudes and climatic implications of two early-Holocene glacier readvances during the Erdalen Event at Jostedalsbreen, western Norway' *The Holocene* 12, (1) 17-25

D'Anjou, R.M., Balascio, N.L. and Bradley, R.S (2014) 'Locating cryptotephra in lake sediments using fluid imaging technology' *Journal of Paleolimnology* 52, (3) 257-264

Dansgaard, W., Johnsen, S.J., Clausen, H.B., Dahl-Jensen, D., Gundestrup, N.S., Hammer, C.U., Hvidberg, C.S., Steffensen, J.P., Sveinbjörnsdottir, A.E., Jouzel, J. and Bond, G (1993) 'Evidence for general instability of past climate from a 250-kyr ice-core record' *Nature* 364, (6434) 218-220

Darvill, C.M (2011) 'The Lateglacial at Star Carr: A Sedimentological and Stable Isotopic Investigation of Palaeoenvironmental Change in Northeast England' Unpublished MSc Thesis, University of London

Davies S.M., Turney C.S.M., and Lowe JJ (2001) 'Identification and significance of a visible, basalt-rich Vedde Ash layer in a Late-glacial sequence on the Isle of Skye, Inner Hebrides, Scotland' *Journal of Quaternary Science* 16, (2) 99-104

Davies, S.M., Branch, N.P., Lowe, J.J. and Turney, C.S (2002) 'Towards a European tephrochronological framework for Termination 1 and the Early Holocene' *Philosophical Transactions of the Royal Society of London A: Mathematical, Physical and Engineering Sciences* 360, (1793) 767-802

Davies, S.M (2003) 'Extending the known distributions of micro-tephra layers of Last Glacial–Interglacial Transition age in Europe' Unpublished PhD Thesis, University of London

Davies S.M., Wastegård, S. and Wohlfarth, B (2003) 'Extending the limits of the Borrobol Tephra to Scandinavia and detection of new early Holocene tephras' *Quaternary Research* 59, (3) 345-352

Davies, S.M., Wohlfarth, B., Wastegård, S., Andersson, M., Blockley, S. and Possnert, G (2004) 'Were there two Borrobol Tephras during the early Lateglacial period: implications for tephrochronology?' *Quaternary Science Reviews* 23, (5) 581-589

Davies, S.M., Elmquist, M., Bergman, J., Wohlfarth, B. and Hammarlund, D (2007) 'Cryptotephra sedimentation processes within two lacustrine sequences from west central Sweden' *The Holocene* 17, (3) 319-330

Davies, S.M., Larsen, G., Wastegård, S., Turney, C.S., Hall, V.A., Coyle, L. and Thordarson, T (2010) 'Widespread dispersal of Icelandic tephra: how does the Eyjafjöll

eruption of 2010 compare to past Icelandic events?' *Journal of Quaternary Science* 25, (5) 605-611

Davies, S.M., Abbott, P.M., Pearce, N.J., Wastegård, S. and Blockley, S.P (2012) 'Integrating the INTIMATE records using tephrochronology: rising to the challenge' *Quaternary Science Reviews* 36, 11-27

Davies, S. M (2015) 'Cryptotephras: the revolution in correlation and precision dating' *Journal of Quaternary Science* 30, (2) 114-130

De Vleeschouwer, F., van Vliët-Lanoé, B., Fagel, N., Richter, T. and Boës, X (2008) 'Development and application of high-resolution petrography on resin-impregnated Holocene peat columns to detect and analyse tephras, cryptotephras, and other materials' *Quaternary International* 178, (1) 54-67

Dean, W.E (1974) 'Determination of carbonate and organic matter in calcareous sediments and sedimentary rocks by loss on ignition: comparison with other methods' *Journal of Sedimentary Petrology* 44, (1) 242-248

Dearing, J.A (1986) 'Core correlation and total sediment inlux'. In *Handbook of Holocene Palaeoecology and Palaeohydrology*. ed. by Berglund, B.E. Chichester: John Wiley & Sons Ltd: 247-270

Dearing, J.A and Foster, I.D.L (1986) 'Lake sediments and palaeohydrological studies.' In *Handbook of Holocene Palaeoecology and Palaeohydrology*. ed by Berglund, B.E. Chichester: John Wiley & Sons: 67-90

Diefendorf, A.F., Patterson, W.P., Mullins, H.T., Tibert, N. and Martini, A (2006) 'Evidence for high-frequency late Glacial to mid-Holocene (16,800 to 5500 cal yr BP) climate variability from oxygen isotope values of Lough Inchiquin, Ireland' *Quaternary Research* 65, (1) 78-86

Digerfeldt, G., (1988) 'Reconstruction and regional correlation of Holocene lake-level fluctuations in Lake Bysjön, South Sweden' *Boreas* 17, (2) 165-182

Dugmore, A.J. and Newton, A.J (1992) 'Thin tephra layers in peat revealed by X-radiography' *Journal of Archaeological Science* 19, (2) 163-170

Dugmore, A.J. and Newton, A.J (1995) 'Seven tephra isochrones in Scotland' *The Holocene* 5, (3) 257-266

Dugmore, A.(1989) 'Icelandic volcanic ash in Scotland' *The Scottish Geographical Magazine* 105, (3) 168-172

Dugmore A.J., and Newton A.J (1998) 'Holocene tephra layers in the Faroe Islands' *Fróðskaparrit* 46, 191–204

Dugmore, A.J., Newton, A.J., Edwards, K.J., Larsen, G., Blackford, J.J. and Cook, G.T (1996) 'Long-distance marker horizons from small-scale eruptions: British tephra deposits from the AD 1510 eruption of Hekla, Iceland' *Journal of Quaternary Science* 11, (6) 511-516

Dugmore, A. J., Newton, A. J., Larsen, G., and Cook, G. T. (2000) 'Tephrochronology, environmental change and the norse settlement of iceland' *Environmental Archaeology* 5, 21-34

Dugmore, A.J. and Newton, A.J (2012) 'Isochrons and beyond: maximising the use of tephrochronology in geomorphology' *Jökull* 62, 39-52

Edwards, K.J. and Whittington, G (2000) 'Multiple charcoal profiles in a Scottish lake: taphonomy, fire ecology, human impact and inference' *Palaeogeography, Palaeoclimatology, Palaeoecology* 164, (1) 67-86

Eiríksson, J., Knudsen, K.L., Haflidason, H. and Henriksen, P (2000) 'Late-glacial and Holocene palaeoceanography of the North Icelandic shelf' *Journal of Quaternary Science* 15, (1) 23-42

Eiríksson, J., Larsen, G., Knudsen, K.L., Heinemeier, J. and Símonarson, L.A (2004) 'Marine reservoir age variability and water mass distribution in the Iceland Sea' *Quaternary Science Reviews* 23, (20) 2247-2268

Ellison, C.R., Chapman, M.R. and Hall, I.R (2006) 'Surface and deep ocean interactions during the cold climate event 8200 years ago' *Science* 312, (5782) 1929-1932

Enache, M.D. and Cumming, B.F (2006) 'The morphological and optical properties of volcanic glass: a tool to assess density-induced vertical migration of tephra in sediment cores' *Journal of Paleolimnology* 35, (3) 661-667

Everest, J. and Kubik, P (2006) 'The deglaciation of eastern Scotland: cosmogenic 10Be evidence for a Lateglacial stillstand' *Journal of Quaternary Science* 21, (1) 95-104

Finsinger, W., Belis, C., Blockley, S.P., Eicher, U., Leuenberger, M., Lotter, A.F. and Ammann, B (2008) 'Temporal patterns in lacustrine stable isotopes as evidence for climate change during the late glacial in the Southern European Alps' *Journal of Paleolimnology* 40, (3) 885-895

Francis, P., and Oppenheimer, C (2004) *2nd edn. Volcanoes*. Oxford: Oxford University Press

Froggatt, P.C., Gosson, G.J (1982) 'Techniques for the preparation of tephra samples for mineral or chemical analysis and radiometric dating Geology Department', Victoria University of Wellington Publication 23, 1-12

Froggatt, P.C. and Lowe, D.J (1990) 'A review of late Quaternary silicic and some other tephra formations from New Zealand: their stratigraphy, nomenclature, distribution, volume, and age' *New Zealand journal of geology and geophysics* 33, (1) 89-109

Froggatt, P.C (1992) 'Standardization of the chemical analysis of tephra deposits. Report of the ICCT working group' *Quaternary International* 13, 93-96

Gale, S. and Hoare, P (1991) *Quaternary Sediments: Petrographic methods for the study of unlithified rocks*. New York: Belhaven and Halsted Press

Garnett, E.R., Andrews, J.E., Preece, R.C. and Dennis, P.F (2004) 'Climatic change recorded by stable isotopes and trace elements in a British Holocene tufa' *Journal of Quaternary Science* 19, (3) 251-262

Gehrels, M.J., Lowe, D.J., Hazell, Z.J. and Newnham, R.M (2006) 'A continuous 5300-yr Holocene cryptotephrostratigraphic record from northern New Zealand and implications for tephrochronology and volcanic hazard assessment' *The Holocene* 16, (2) 173-187

Gehrels, M.J., Newnham, R.M., Lowe, D.J., Wynne, S., Hazell, Z.J. and Caseldine, C (2008) 'Towards rapid assay of cryptotephra in peat cores: review and evaluation of various methods' *Quaternary International* 178, (1) 68-84

Geikie, A. (1877) 'The glacial geology of Orkney and Shetland' *Nature* 16, 414-416

Geirsdóttir, Á., Miller, G.H., Axford, Y. and Ólafsdóttir, S (2009) 'Holocene and latest Pleistocene climate and glacier fluctuations in Iceland' *Quaternary Science Reviews* 28, (21) 2107-2118

Genty, D., Blamart, D., Ouahdi, R., Gilmour, M., Baker, A., Jouzel, J. and Van-Exter, S (2003) 'Precise dating of Dansgaard–Oeschger climate oscillations in western Europe from stalagmite data' *Nature* 421, (6925) 833-837

Goes, S., Spakman, W. and Bijwaard, H (1999) 'A lower mantle source for central European volcanism' *Science* 286, (5446) 1928-1931

Golledge, N.R (2007) 'An ice cap landsystem for palaeoglaciological reconstructions: characterizing the Younger Dryas in western Scotland' *Quaternary Science Reviews* 26, (1) 213-229

Golledge, N.R., Fabel, D., Everest, J.D., Freeman, S. and Binnie, S (2007) 'First cosmogenic ^{10}Be age constraint on the timing of Younger Dryas glaciation and ice cap thickness, western Scottish Highlands' *Journal of Quaternary Science* 22, (8) 785-791

Graettinger, A.H., Skilling, I., McGarvie, D. and Höskuldsson, Á (2013) 'Subaqueous basaltic magmatic explosions trigger phreatomagmatism: a case study from Askja, Iceland' *Journal of Volcanology and Geothermal Research* 264, 17-35

Granet, M., Wilson, M. and Achauer, U (1995) 'Imaging a mantle plume beneath the French Massif Central' *Earth and Planetary Science Letters* 136, (3) 281-296

Gray, J.M. and Lowe, J.J (eds) (1977) *Studies in the Scottish Lateglacial environment*. Pergamon Press: Oxford

Griffiths, S.J (2001) Late Quaternary palaeolimnology of Lake Kopais, central Greece. Unpublished PhD Thesis, University of Wales, Swansea

Griggs A.J., Davies S.M. and Abbott P.M (2014a) 'Examining the application of micromorphology and X-ray tomography within marine tephrochronology' INTIMATE Open Workshop and COST Action ES0907 Final Event Zaragoza, 15–21 June

Griggs, A.J., Davies, S.M., Abbott, P.M., Rasmussen, T.L. and Palmer, A.P (2014b) 'Optimising the use of marine tephrochronology in the North Atlantic: a detailed investigation of the Faroe Marine Ash Zones II, III and IV' *Quaternary Science Reviews* 106, 122-139

Grönvold, K., Óskarssona, N., Johnsen, S.J., Clausen, H.B., Hammer, C.U., Bond, G., and Barde, E (1995) 'Ash layers from Iceland in the Greenland GRIP ice core correlated with oceanic and land sediments' *Earth and Planetary Science Letters* 135, (1) 49-155

Grosvenor, M (2009) 'Palaeoclimatic implications of tephra at a new site within the Menteith Moraine of the Loch Lomond Readvance Glacier' *Quaternary Newsletter* 121, 61

Gudmundsdóttir, E.R., Eiríksson, J. and Larsen, G (2011) 'Identification and definition of primary and reworked tephra in Late Glacial and Holocene marine shelf sediments off North Iceland' *Journal of Quaternary Science* 26, (6) 589-602

Gudmundsdóttir, E.R., Larsen, G. and Eiríksson, J (2012) 'Tephra stratigraphy on the North Icelandic shelf: extending tephrochronology into marine sediments off North Iceland' *Boreas* 41, (4)719-734

Guðmundsson, M.T (2015) 'The Tindfjallajökull volcanic system' In Catalogue of Icelandic Volcanoes. ed. by Ilyinskaya, E., Larsen, G and Guðmundsson, M [online] Available from < http://futurevolc.vedur.is> [27 May 2016]

Haflidason, H., Eriksosn, J., and Van Kreveld, S (2000) 'The tephrochronology of Iceland and the North Atlantic region during the Middle and Late Quaternary: a review' *Journal of Quaternary Science* 15, (1) 3-22

Hajdas, I., Ivy, S.D., Beer, J., Bonani, G., Imboden, D., Lotted, A.F., Sturm, M. and Suter, M (1993) 'AMS radiocarbon dating and varve chronology of Lake Soppensee: 6000 to 12000 14C years BP' *Climate dynamics* 9, (3) 107-116

Hall, A.M. and Bent, A.J.A (1990) 'The limits of the last British ice sheet in northern Scotland and the adjacent shelf' *Quaternary Newsletter* 61, (2) 12

Hall, M. and Hayward, C (2014) 'Preparation of micro-and crypto-tephras for quantitative microbeam analysis' *Geological Society, London, Special Publications* 398, (1) 21-28

Hall, V., Pilcher, J.R., and McCormac, F.G (1993) 'Tephra dated landscape history of the north of Ireland, AD 750-1150' *New Phytologist* 125, 193-202

Hall, V.A. and Pilcher, J.R (2002) 'Late-Quaternary Icelandic tephras in Ireland and Great Britain: detection, characterization and usefulness' *The Holocene* 12, (2) 223-230

Hall, V.A. and Mauquoy, D (2005) 'Tephra-dated climate-and human-impact studies during the last 1500 years from a raised bog in central Ireland' *The Holocene* 15, (7) 1086-1093

Hammer, C.U., Clausen, H.B. and Tauber, H (1986) 'Ice-core dating of the Pleistocene/Holcene boundary applied to a calibration of the (super 14) C time scale' *Radiocarbon* 28, (2A) 284-291

Hardiman, M (2007) 'The Lateglacial sediment record in Loch Etteridge, Grampian Highlands, Scotland: tephrostratigraphy and regional tephrocorrelation' Unpublished BSc Thesis, University of London

Hardiman, M.J (2012) 'Testing and refining the chronology and correlation of Mediterranean pollen records of late Last Glacial age using tephrochronology; Unpublished PhD thesis, University of London

Harding, P.R (2013) 'Testing the potential for tephra to time glacial retreat: Tephrostratigraphic analyses of four early Holocene sequences from the Scottish Highlands' Unpublished MSc Thesis, University of London

Harms, E. and Schmincke, H.U (2000) 'Volatile composition of the phonolitic Laacher See magma (12,900 yr BP): implications for syn-eruptive degassing of S, F, Cl and H2O' Contributions to Mineralogy and Petrology 138, (1) 84-98

Hays, J.D., Imbrie, J., Shackleton, N.J (1976) 'Variations in the earth's orbit: Pacemaker of the ice ages' *Science* 194 (4270), 1121-1132

Hayward, C (2012) 'High spatial resolution electron probe microanalysis of tephras and melt inclusions without beam-induced chemical modification' *The Holocene*, 22 (1) 119-125

Heiri, O., Lotter, A.F., and Lemcke, G (2001) 'Loss on ignition as a method for estimating organic and carbonate content in sediments: reproducibility and comparability of results' *Journal of Paleolimnology* 25, 101-110

Heiri, O and Lotter, A.F (2001) 'Effects of low count sums on quantitative environmental reconstructions: an example using subfossil chironomids' *Journal of Paleolimnology* 25, 101-110

Heiri, O., Brooks, S.J., Renssen, H., Bedford, A., Hazekamp, M., Ilyashuk, B., Jeffers, E.S., Lang, B., Kirilova, E., Kuiper, S. and Millet, L (2014) 'Validation of climate model-inferred regional temperature change for late-glacial Europe' *Nature communications* 5, 1-7

Hill, A.R. and Prior, D.B (1968) 'Directions of ice movement in north-east Ireland' *Proceedings of the Royal Irish Academy. Section B: Biological, Geological, and Chemical Science* 66, (71-84)

Hjort, C., Ingólfsson, O., Norðdahl, H (1985) 'Late Quaternary geology and glacial history of Hornstrandir, northwest Iceland: a reconnaissance study' *Jökull* 35, 9-29

Horn, I., Hinton, R.W., Jackson, S.E. and Longerich, H.P (1997) 'Ultra-trace element analysis of NIST SRM 616 and 614 using laser ablation microprobe-inductively coupled plasma-mass spectrometry (LAM-ICP-MS): A comparison with secondary ion mass spectrometry (SIMS)' *Geostandards Newsletter* 21, (2) 191-203

Housley, R.A., MacLeod, A., Nalepka, D., Jurochnik, A., Masojć, M., Davies, L., Lincoln, P.C., Ramsey, C.B., Gamble, C.S. and Lowe, J.J (2013) 'Tephrostratigraphy of a Lateglacial lake sediment sequence at Węgliny, southwest Poland' *Quaternary Science Reviews* 77, 4-18

Housley, R.A. , Gamble, C.S and RESET Associates (2014) 'Examination of Late Palaeolithic archaeological sites in northern Europe for the preservation of cryptotephra layers' *Quaternary Science Reviews* 118, 142-150

Hubbard, A., Sugden, D., Dugmore, A., Norddahl, H. and Pétursson, H.G (2006) 'A modelling insight into the Icelandic Last Glacial Maximum ice sheet' *Quaternary Science Reviews* 25, (17) 2283-2296

Hughen, K.A., Eglinton, T.I., Xu, L. and Makou, M (2004) 'Abrupt tropical vegetation response to rapid climate changes' *Science* 304, (5679) 1955-1959

Hughes, A.L., Greenwood, S.L. and Clark, C.D (2011) 'Dating constraints on the last British-Irish Ice Sheet: a map and database' *Journal of Maps* 7, (1) 156-184

Hughes, A.L., Clark, C.D. and Jordan, C.J (2014) 'Flow-pattern evolution of the last British Ice Sheet' *Quaternary Science Reviews* 89, 148-168

Hughes, A.L., Gyllencreutz, R., Lohne, Ø.S., Mangerud, J. and Svendsen, J.I (2016) 'The last Eurasian ice sheets–a chronological database and time-slice reconstruction, DATED-1' *Boreas* 45, (1) 1-45

Hulme, M (2003) 'Abrupt climate change: can society cope?*' Philosophical Transactions of the Royal Society of London* 361, 2001-2021

Hunt, J.B. and Hill, P.G (1993) 'Tephra geochemistry: a discussion of some persistent analytical problems' *The Holocene* 3, (3) 271-278

Hunt, J.B. and Hill, P.G (1996) 'An inter-laboratory comparison of the electron probe microanalysis of glass geochemistry' *Quaternary International* 34, 229-241

Hunt, J.B. and Hill, P.G (2001) 'Tephrological implications of beam size—sample-size effects in electron microprobe analysis of glass shards' *Journal of Quaternary Science* 16, (2) 105-117

Imbrie, J and Imbrie, K.P (1979) *Ice Ages: Solving the Mystery*. London: Macmillan

Imbrie, J., Berger, A. and Shackleton, N.J (1993) 'Role of orbital forcing: a two-million-year perspective'. In *Global Changes in the Perspective of the Past*. ed. by Eddy, J.A and Oeschger, H. Chichester and New York: Wiley: 263-277.

Ingólfsson, O., Norðdahl, H. and Hafliðason, H (1995) 'Rapid isostatic rebound in southwestern Iceland at the end of the last glaciation' *Boreas* 24, (3) 245-259

Ingólfsson, O., Sigmarsson, O., Sigmundsson, F. and Símonarson, L (2008) 'The dynamic geology of Iceland' *Jökull*, 58 1-2

IPCC, 2007: Climate Change 2007: The Physical Science Basis. Contribution of Working Group I to the Fourth Assessment Report of the Intergovernmental Panel on Climate Change. ed. by Solomon, S., D. Qin, M. Manning, Z. Chen, M. Marquis, K.B. Averyt, M.Tignor and H.L. Miller. Cambridge University Press: Cambridge, United Kingdom and New York, NY, USA

Isarin, R.F., Renssen, H. and Vandenberghe, J (1998) 'The impact of the North Atlantic Ocean on the Younger Dryas climate in northwestern and central Europe' *Journal of Quaternary Science* 13, (5) 447-453

Isarin, R.F. and Bohncke, S.J (1999) 'Mean July temperatures during the Younger Dryas in northwestern and central Europe as inferred from climate indicator plant species' *Quaternary Research* 51, (2) 158-173

Iversen, J (1954) 'The late-glacial flora of Denmark and its relation to climate and soil' *Danmarks geologiske undersøgelse* 2, (80) 87-119

Jakobsson S.P (1979a) 'Petrology of Recent basalts of the Eastern Volcanic Zone, Iceland' *Acta Naturalia Islandica* 26, 1-103

Jakobsson S.P (1979b) 'Outline of the petrology of Iceland' *Jökull* 29, 57-73

Jakobsson, S.P., Jónnasson, K., and Sigurdsson, I.A (2008) 'The three igneous rock series of Iceland' *Jökull* 58, 117-138

Janoušek, V., Farrow, C. M. and Erban, V (2006) 'Interpretation of whole-rock geochemical data in igneous geochemistry: introducing Geochemical Data Toolkit (GCDkit)' *Journal of Petrology* 47, (6) 1255-1259

Jennings, A.E., Grönvold, K., Hilberman, R., Smith, M. and Hald, M (2002) 'High-resolution study of Icelandic tephras in the Kangerlussuaq Trough, southeast Greenland, during the last deglaciation' *Journal of Quaternary Science* 17, (8) 747-757

Jennings, A., Thordarson, T., Zalzal, K., Stoner, J., Hayward, C., Geirsdóttir, Á. and Miller, G (2014) 'Holocene tephra from Iceland and Alaska in SE Greenland shelf sediments' *Geological Society, London, Special Publications* 398, (1) 157-193

Jensen, B.J., Pyne-O'Donnell, S., Plunkett, G., Froese, D.G., Hughes, P.D., Sigl, M., McConnell, J.R., Amesbury, M.J., Blackwell, P.G., van den Bogaard, C. and Buck, C.E (2014) 'Transatlantic distribution of the Alaskan White River Ash' *Geology* 42, (10) 875-878

Jochum, K.P., Nohl, U., Herwig, K., Lammel, E., Stoll, B. and Hofmann, A.W (2005) 'GeoReM: a new geochemical database for reference materials and isotopic standards' *Geostandards and Geoanalytical Research* 29, (3) 333-338

Jóhannesdóttir, G.E., Thordarson, T., Geirsdóttir, Á. and Larsen, G (2005) 'The widespread ~10 ka Saksunarvatn tephra: a product of three large basaltic phreatoplinian eruptions.' In: *Geophysical Research Abstracts* 7, (05991) 01607-0796

Jóhansen, J. (1975) 'Pollen diagrams from the Shetland and Faroe Islands' *New Phytologist* 75, (2) 369-387

Jordan, S.C., Dürig, T., Cas, R.A.F. and Zimanowski, B (2014) 'Processes controlling the shape of ash particles: Results of statistical IPA' *Journal of Volcanology and Geothermal Research* 288, 19-27

Jordan, S.C., Le Pennec, J.L., Gurioli, L., Roche, O. and Boivin, P (2016) 'Highly explosive eruption of the monogenetic [8.6] ka BP La Vache et Lassolas scoria cone complex (Chaîne des Puys, France)' *Journal of Volcanology and Geothermal Research* In Press, Accepted Manuscript

Jouannic, G., Véronique, A., Simonnet, W., Boussuet, G., Begeot, C., and Develle, A (2015) 'Feldspar composition as an efficient tool for tephra identification: ac case study from Holocene and Lateglacial lacustrine sequences (Jura, France) identification: a case study from Holocene and Lateglacial lacustrine sequences (Jura, France) *Journal of Quaternary Science* 30, (6) 569-583

Juvigné, E.H (1982) 'Tephrostratigraphie und Reliefgenese in West- und Mitteleuropa. | [(Stratigraphy of tephra and development of relief in west and central Europe).]' *Zeitschrift fur Geomorphologie, Supplementband* 42, 195-200

Juvigné, E.H (1992) 'Distribution of widespread late glacial and Holocene tephra beds in the French Central Massif' *Quaternary international* 13, 181-185

Juvigné, É., Kozarski, S. and Nowaczyk, B (1995) 'The occurrence of Laacher See Tephra in Pomerania, NW Poland' *Boreas* 24, (3) 225-231

Juvigné, E., Bastin, B., Delibrias, G., Evin, J., Gewelt, M., Gilot, E. and Streel, M (1996) 'A comprehensive pollen-and tephra-based chronostratigraphic model for the Late Glacial and Holocene period in the French Massif Central' *Quaternary International* 34, 113-120

Kelly, T.J (2010) 'The early Holocene pollen and tephrostratigraphy at Inverlair, Glen Spean, Scottish Highlands: Testing relative chronologies' Unpublished MSc Thesis, University of London

Kelly, T.J., Hardiman, M., Lovelady, M., Lowe, J.J., Matthews, I.P. and Blockley, S.P (2016) 'Scottish early Holocene vegetation dynamics based on pollen and tephra records from Inverlair and Loch Etteridge, Inverness-shire' *Proceedings of the Geologists' Association*

Kirk, W., Godwin, H. and Charlesworth, J.K (1963) 'XI.-A Late-glacial Site at Loch Droma, Ross and Cromarty' *Transactions of the Royal Society of Edinburgh* 65, (11) 225-249

Kirkbride, M.P. and Dugmore, A.J (2005) 'Late Holocene solifluction history reconstructed using tephrochronology' *Geological Society, London, Special Publications* 242, (1) 145-155

Kitagawa, H. and van der Plicht, J (1998) 'Atmospheric radiocarbon calibration to 45,000 yr BP: Late glacial fluctuations and cosmogenic isotope production' *Science* 279, (5354) 1187-1190

Koren, J.H., Svendsen, J.I., Mangerud, J. and Furnes, H (2008) 'The Dimna Ash - a 12.8 14 Cka-old volcanic ash in Western Norway' *Quaternary Science Reviews* 27, (1) 85-94

Kristjánsdóttir, G.B., Stoner, J.S., Jennings, A.E., Andrews, J.T. and Grönvold, K (2007) 'Geochemistry of Holocene cryptotephras from the North Iceland Shelf (MD99-2269): intercalibration with radiocarbon and palaeomagnetic chronostratigraphies' *The Holocene* 17, (2) 155-176

Kuehn, S.C., Froese, D.G., Carrara, P.E., Foit, F.F., Pearce, N.J. and Rotheisler, P (2009) 'Major-and trace-element characterization, expanded distribution, and a new chronology for the latest Pleistocene Glacier Peak tephras in western North America' *Quaternary Research* 71, (2) 201-216

Kvamme, T., Mangerud, J., Furnes, H. and Ruddiman, W.F (1989) 'Geochemistry of Pleistocene ash zones in cores from the North Atlantic' *Norsk Geologisk Tidsskrift* 69, 251-272

Kwong, S (2016) 'A comparison of chironomid-inferred summer temperatures with a Lateglacial pollen record from Tanera Mor, NW Scotland' Unpublished MSc Thesis, University of London

Kylander, M.E., Lind, E.M., Wastegård, S. and Löwemark, L (2011) 'Recommendations for using XRF core scanning as a tool in tephrochronology' *The Holocene* 22, (3) 371-375

Lacasse, C., Sigurdsson, H., Jóhannesson, H., Paterne, M. and Carey, S (1995) 'Source of ash zone 1 in the North Atlantic' *Bulletin of Volcanology* 57, (1) 18-32

Lacasse, C., Carey, S. and Sigurdsson, H (1998) 'Volcanogenic sedimentation in the Iceland Basin: influence of subaerial and subglacial eruptions' *Journal of Volcanology and Geothermal Research* 83, (1) 47-73

Lacasse, C (2001) 'Influence of climate variability on the atmospheric transport of Icelandic tephra in the subpolar North Atlantic' *Global and Planetary Change* 29, (1) 31-55

Lacasse, C. and Garbe-Schönberg, C.D (2001) 'Explosive silicic volcanism in Iceland and the Jan Mayen area during the last 6Ma: sources and timing of major eruptions' *Journal of Volcanology and Geothermal Research* 107, (1) 113-147

Lane, C. S., Cullen, V. L., White, D., Bramham-Law, C. W. F., and Smith, V. C (2014) 'Cryptotephra as a dating and correlation tool in archaeology' *Journal of Archaeological Science* 42, 42-50

Lane, C.S (2004) 'Toward a lateglacial tephrostratigraphy for the North-West England: Site investigations and methodological recommendations' Unpublished MSc Thesis, University of London

Lane, C.S., Andrič, M., Cullen, V.L. and Blockley, S.P (2011a) 'The occurrence of distal Icelandic and Italian tephra in the Lateglacial of Lake Bled, Slovenia' *Quaternary Science Reviews* 30, (9) 1013-1018

Lane, C.S., Blockley, S.P.E., Ramsey, C.B. and Lotter, A.F (2011b) 'Tephrochronology and absolute centennial scale synchronisation of European and Greenland records for the last glacial to interglacial transition: a case study of Soppensee and NGRIP' *Quaternary International* 246, (1) 145-156

Lane, C.S., De Klerk, P. and Cullen, V.L (2012a) 'A tephrochronology for the Lateglacial palynological record of the Endinger Bruch (Vorpommern, north-east Germany)' *Journal of Quaternary Science* 27, (2) 141-149

Lane, C.S., Blockley, S.P.E., Mangerud, J., Smith, V.C., Lohne, Ø., Tomlinson, E.L., Matthews, I.P. and Lotter, A.F (2012b) 'Was the 12.1ka Icelandic Vedde Ash one of a kind?' *Quaternary Science Reviews* 33, 87-99

Lane, C.S., Blockley, S.P.E., Lotter, A.F., Finsinger, W., Filippi, M.L., and Matthews, I.P (2012c) 'A regional tephrostratigraphic framework for central and southern European climate archives during the Last Glacial to Interglacial transition: Comparisons north and south of the Alps' *Quaternary Science Reviews* 36, 50-58

Lane, C.S., Brauer, A., Blockley, S.P. and Dulski, P (2013) 'Volcanic ash reveals time-transgressive abrupt climate change during the Younger Dryas' *Geology* 41, (12) 1251-1254

Lane, C.S., Cullen, V.L., White, D., Bramham-Law, C.W.F. and Smith, V.C (2014) 'Cryptotephra as a dating and correlation tool in archaeology' *Journal of Archaeological Science* 42, 42-50

Lane, C.S., Brauer, A., Martín-Puertas, C., Blockley, S.P., Smith, V.C. and Tomlinson, E.L (2015) 'The Late Quaternary tephrostratigraphy of annually laminated sediments from Meerfelder Maar, Germany' *Quaternary Science Reviews* 122, 192-206

Lang, B., Brooks, S.J., Bedford, A., Jones, R.T., Birks, H.J.B. and Marshall, J.D (2010) 'Regional consistency in Lateglacial chironomid-inferred temperatures from five sites in north-west England' *Quaternary Science Reviews* 29, (13) 1528-1538

Langdon, P.G. and Barber, K.E (2004) 'Snapshots in time: precise correlations of peat-based proxy climate records in Scotland using mid-Holocene tephras' *The Holocene* 14, (1) 21-33

Larsen, G., and Eríksson, J (2008) 'Holocene tephra archives and tephrochronology in Iceland – a brief overview' *Jökull* 58, 229-250

Larsen, G., and Eríksson, J (2013) 'Volcanism in Iceland' In: *Holocene tephrochronology applications in South Iceland, Field Guide and Road Log*, Larsen, G., and Eríksson, J (eds). Quaternary Research Association; 13-26

Larsen, G., Eiríksson, J., Knudsen, K.L. and Heinemeier, J (2002) 'Correlation of late Holocene terrestrial and marine tephra markers, north Iceland: implications for reservoir age changes' *Polar Research* 21, (2) 283-290

Larsen, G., Newton, A.J., Dugmore, A.J. and Vilmundardóttir, E.G (2001) 'Geochemistry, dispersal, volumes and chronology of Holocene silicic tephra layers from the Katla volcanic system, Iceland' *Journal of Quaternary Science* 16, (2) 119-132

Larsen J.J (2013) 'Lateglacial and Holocene tephrostratigraphy in Denmark Volcanic ash in a palaeoenvironmental context' Unpublished PhD Thesis, University of Copenhagen

Larsen J.J. and Noe-Nygaard, N (2013) 'Lateglacial and early Holocene tephrostratigraphy and sedimentology of the Store Slotseng basin, SW Denmark: A multi-proxy study' *Boreas* 43, (2) 349-361

Lawson, I.T., Swindles, G.T., Plunkett, G. and Greenberg, D (2012) 'The spatial distribution of Holocene cryptotephras in north-west Europe since 7 ka: implications for understanding ash fall events from Icelandic eruptions' *Quaternary Science Reviews* 41, 57-66

Le Bas, M.J., Le Maitre, R.W., Streckeisen, A. and Zanettin, B (1986) 'A chemical classification of volcanic rocks based on the total alkali-silica diagram' *Journal of petrology* 27, (3) 745-750

Leahy, K (1997) 'Discrimination of reworked pyroclastics from primary tephra-fall tuffs: a case study using kimberlites of Fort a la Corne, Saskatchewan, Canada' *Bulletin of Volcanology* 59, (1) 65-71

LeGrande, A.N., Schmidt, G.A., Shindell, D.T., Field, C.V., Miller, R.L., Koch, D.M., Faluvegi, G. and Hoffmann, G (2006) 'Consistent simulations of multiple proxy responses to an abrupt climate change event' *Proceedings of the National Academy of Sciences of the United States of America* 103, (4) 837-842

Leng, M.J. and Marshall, J.D (2004) 'Palaeoclimate interpretation of stable isotope data from lake sediment archives' *Quaternary Science Reviews* 23, (7) 811-831

Lilja, C., Lind, E.M., Morén, B. and Wastegård, S (2013) 'A Lateglacial–early Holocene tephrochronology for SW Sweden' *Boreas* 42, (3) 544-554

Lincoln, P.C (2011) 'Tephrostratigraphic and Taphonomic study from Pulpit Hill, Western Scotland' Unpublished MSc Thesis, University of London

Lind, E.M. and Wastegård, S (2011) 'Tephra horizons contemporary with short early Holocene climate fluctuations: new results from the Faroe Islands' *Quaternary International* 246, (1) 157-167

Lind, E.M., Wastegård, S., and Larsen, J.J (2013) 'A Late Younger Dryas-Early Holocene tephrostratigraphy for Fosen, Central Norway' *Journal of Quaternary Science* 28, (8) 803-811

Lind, E.W., Lilja, C., Wastegård, S. and Pearce, N (2016) 'Revisiting the Borrobol Tephra' Boreas, in press

Lisiecki, L.E. and Raymo, M.E (2005) 'A Pliocene-Pleistocene stack of 57 globally distributed benthic δ18O records' *Paleoceanography* 20, (1) 1-17

Lohne, Ø.S., Mangerud, J. and Birks, H.H (2013) 'Precise 14C ages of the Vedde and Saksunarvatn ashes and the Younger Dryas boundaries from western Norway and their comparison with the Greenland Ice Core (GICC05) chronology' *Journal of Quaternary Science* 28, (5) 490-500

Lohne Ø.S., Mangerud J. and Birks H.H (2014) 'IntCal13 calibrated ages of the Vedde and Saksunarvatn ashes and the Younger Dryas boundaries from Kråkenes, western Norway' *Journal of Quaternary Science* 29, (5) 506-507

Long, D., Bent, A., Harland, R., Gregory, D.M., Graham, D.K. and Morton, A.C (1986) 'Late Quaternary palaeontology, sedimentology and geochemistry of a vibrocore from the Witch Ground Basin, central North Sea' *Marine Geology* 73, 109-123

Long, D. and Morton, A.C (1987) 'An ash fall within the Loch Lomond stadial' *Journal of Quaternary Science* 2, 97-101

Lowe, D.J., Hogg, A.G. and Hendy, C.H (1980) 'Detection of thin tephra deposits in peat and organic lake sediments by rapid X-radiography and X-ray fluorescence techniques'. In *Proceedings of Tephra Workshop*, 30th June-1st July, Victoria University of Wellington,

Lowe, D.J (1988) 'Stratigraphy, age, composition, and correlation of late Quaternary tephras interbedded with organic sediments in Waikato lakes, North Island, New Zealand' New Zealand journal of geology and geophysics 31, (2) 125-165

Lowe, D.J. and Hunt, J.B (2001) 'A summary of terminology used in tephra-related studies' *Les Dossiers de l'Archaéo-Logis* 1, 17-22

Lowe, D.J., Newnham, R.M., McFadgen, B.G. and Higham, T.F (2000) 'Tephras and New Zealand archaeology' *Journal of Archaeological Science* 27, (10) 859-870

Lowe, D.J., Shane, P.A., Alloway, B.V. and Newnham, R.M (2008) 'Fingerprints and age models for widespread New Zealand tephra marker beds erupted since 30,000 years ago: a framework for NZ-INTIMATE' *Quaternary Science Reviews* 27, (1) 95-126

Lowe, D.J (2011) 'Tephrochronology and its application: a review' *Quaternary Geochronology* 6, (2) 107-153

Lowe, D.J (2016) 'Connecting, synchronising, and dating with tephras: principles and applications of tephrochronology in Quaternary research' In: *Measuring Change and Reconstructing Past Environments*. GNS Science, New Zealand 1-31

Lowe, J.J., and Turney, C.S.M (1997) 'Vedde ash layer discovered in a small lake basin on the Scottish mainland' *Journal of the Geological Society* 154, (4) 605-612

Lowe, J.J., Birks, H.H., Brooks, S.J., Coope, G.R., Harkness, D.D., Mayle, F.E., Sheldrick, C., Turney, C.S.M. and Walker, M.J.C (1999) 'The chronology of palaeoenvironmental changes during the Last Glacial-Holocene transition: towards an event stratigraphy for the British Isles' *Journal of the Geological Society* 156, (2) 397-410

Lowe, J.J (2001) ‘Abrupt climatic changes in Europe during the last glacial–interglacial transition: the potential for testing hypotheses on the synchroneity of climatic events using tephrochronology’ Global and Planetary Change 30, (1) 73-84

Lowe, J.J. and Hoek, W.Z (2001) ‘Inter-regional correlation of palaeoclimatic records for the Last Glacial Interglacial Transition: a protocol for improved precision recommended by the INTIMATE project group’ *Quaternary Science Reviews* 20, 1175-1187

Lowe, J.J and Roberts, S.J (2003) ‘Muir Park Reservoir’. In: *The Quaternary of the Western Highland Boundary*. ed. by Evans, D.J.A. Quaternary Research Association: 117-124

Lowe, J.J., Walker, M.J.C., Scott, E.M., Harkness, D.D., Bryant, C.L. and Davies, S.M (2004) ‘A coherent high-precision radiocarbon chronology for the Late-glacial sequence at Sluggan Bog, Co. Antrim, Northern Ireland’ *Journal of Quaternary Science* 19, (2) 147-158

Lowe, J.J., Rasmussen, S.O., Björck, S., Hoek, W.Z., Steffensen, J.P., Walker, M.J. and Yu, Z.C (2008a) ‘Synchronisation of palaeoenvironmental events in the North Atlantic region during the Last Termination: a revised protocol recommended by the INTIMATE group’ *Quaternary Science Reviews* 27, (1) 6-17

Lowe, J., Albert, P., Hardiman, M., MacLeod, A., Blockley, S., and Pyne-O’Donnell, S (2008b) 'Tephrostratigraphical investigations of the basal sediment sequence at Loch Etteridge'. In: *The Quaternary of Glen Roy and Vicinity Field Guide*. ed. by Palmer, A.P., Lowe, J.J., Rose, J. Quaternary Research Association: 60-65

Lowe, J., Barton, N., Blockley, S., Ramsey, C.B., Cullen, V.L., Davies, W., Gamble, C., Grant, K., Hardiman, M., Housley, R. and Lane, C.S., Lee, S., Lewis, M., MacLeod, A., Menzies, M., Müller, W., Pollard, M., Price, C., Roberts, A.P., Rohling, E.L., Satow, C., Smith, V.C., Stringer, C.B., Tomlinson, E.L., White, D., Albert, P., Arienzo, I., Barker, G., Borić, D., Carandenre, A., Civetta, L., Ferrier, C., Guadelli, J., Karkanas, P., Koumouzelis, M., Müller, U.C., Orsi, G., Pross, J., Rosi, M., Shalamanov-Korobar, S., Sirakov, N. and Tzedakis, P.C (2012) ‘Volcanic ash layers illuminate the resilience of Neanderthals and early modern humans to natural hazards’ *Proceedings of the National Academy of Sciences* 109, (34) 13532-13537

Lowe, J.J. and Walker, M.J (2015) 3rd edn. *Reconstructing Quaternary Environments*. London: Routledge

Lowe, J.J., Ramsey, C.B., Housley, R.A., Lane, C.S., Tomlinson, E.L., RESET Team. and RESET Associates (2015) ‘The RESET project: constructing a European tephra lattice for refined synchronisation of environmental and archaeological events during the last c. 100 ka’ *Quaternary Science Reviews* 118, 1-17

Lowe, J, Pyne-O'Donnell, S.D.F & Timms, R 2016, 'Tephra layers on Skye dating to the Lateglacial-Early Holocene interval and their wider context'. in *The Quaternary of Skye: Field Guide. Quaternary Research Association*. ed. by Ballantyne, C. and Lowe J. Quaternary Research Association, London:157-183

Mackay, H., Hughes, P.D., Jensen, B.J., Langdon, P.G., Pyne-O'Donnell, S.D., Plunkett, G., Froese, D.G., Coulter, S. and Gardner, J.E (2016) ‘A mid to late Holocene cryptotephra framework from eastern North America’ *Quaternary Science Reviews* 132, 101-113

Mackie, E.A., Davies, S.M., Turney, C.S., Dobbyn, K., Lowe, J.J. and Hill, P.G (2002) 'The use of magnetic separation techniques to detect basaltic microtephra in last glacial-interglacial transition (LGIT; 15–10 ka cal. BP) sediment sequences in Scotland' *Scottish Journal of Geology* 38, (1) 21-30

Mackie, E.A.V (2000) 'Identification and extraction of basaltic tephra layers from Scottish Lateglacial (14-9,000 years B.P.) deposits' Unpublished MSc thesis, University of London

Maclachlan A (2014) 'A tephrochronology investigation of Straloch Loch, Scotland' Unpublished MSc Thesis, University of London

MacLeod, A (2008) 'Tephrostratigraphy of the Loch Laggan East lake sequence.' In: The Quaternary of Glen Roy and Vicinity Field Guide. ed by: Palmer AP, Lowe JJ, Rose J. Quaternary Research Association; 83-91

MacLeod, A. and Davies, S.M (2016) 'Caution in cryptotephra correlation: resolving Lateglacial chemical controversies at Sluggan Bog, Northern Ireland' *Journal of Quaternary Science* 31, (4) 406-415

MacLeod, A., Matthews, I.P., Lowe, J.J., Palmer, A.P. and Albert, P.G (2015) 'A second tephra isochron for the Younger Dryas period in northern Europe: The Abernethy Tephra' *Quaternary Geochronology* 28, 1-11

Magny, M (2004) 'Holocene climate variability as reflected by mid-European lake-level fluctuations and its probable impact on prehistoric human settlements' *Quaternary international* 113, (1) 65-79

Mangerud, J., Andersen, S.T., Bergland, B.E., and Donner, J.J (1974) 'Quaternary stratigraphy of Norden, a proposal for terminology and classification' *Boreas* 3, 109-128

Mangerud, J., Lie, S. E., Furnes, H., Kristiansen, I. L., and Lømo, L (1984) 'A Younger Dryas ash bed in western Norway, and its possible correlations with tephra in cores from the Norwegian Sea and the North Atlantic' *Quaternary Research* 21, 85-104

Mangerud, J., Furnes, H. and Jóhansen, J (1986) 'A 9000-year-old ash bed on the Faroe Islands' *Quaternary Research* 26, (2) 262-265

Marshall, J.D., Jones, R.T., Crowley, S.F., Oldfield, F., Nash, S. and Bedford, A (2002) 'A high resolution late-glacial isotopic record from Hawes Water, northwest England: Climatic oscillations: Calibration and comparison of palaeotemperature proxies' *Palaeogeography, Palaeoclimatology, Palaeoecology* 185, (1) 25-40

Marshall, J.D., Lang, B., Crowley, S.F., Weedon, G.P., van Calsteren, P., Fisher, E.H., Holme, R., Holmes, J.A., Jones, R.T., Bedford, A. and Brooks, S.J (2007) 'Terrestrial impact of abrupt changes in the North Atlantic thermohaline circulation: Early Holocene, UK' *Geology* 35, (7) 639-642

Maslin, M.A. and Ridgwell, A.J (2005) 'Mid-Pleistocene revolution and the 'eccentricity myth'' *Geological Society, London, Special Publications* 247, (1) 19-34

Matthews, I. P (2002) 'Factors affecting the variability of distribution of Vedde Ash shards, Loch Ashik, Skye' Unpublished BSc Thesis, University of London

Matthews, I.P (2008) 'The potential of tephrostratigraphy in the investigation of wetland archaeological records' Unpublished PhD Thesis, University of London

Matthews, I.P., Birks, H.H., Bourne, A.J., Brooks, S.J., Lowe, J.J., MacLeod, A. and Pyne-O'Donnell, S.D.F (2011) 'New age estimates and climatostratigraphic correlations for the Borrobol and Penifiler Tephras: evidence from Abernethy Forest, Scotland' *Journal of Quaternary Science* 26, (3) 247-252

Matthews, I.P., Trincardi, F., Lowe, J.J., Bourne, A.J., MacLeod, A., Abbott, P.M., Andersen, N., Asioli, A., Blockley, S.P.E., Lane, C.S., Oh, Y.A., Satow, C.S., Staff, R.A. and Wulf, S (2015) 'Developing a robust tephrochronological framework for Late Quaternary marine records in the Southern Adriatic Sea: new data from core station SA03-11' *Quaternary Science Reviews* 118, 84-104

Mayewski, P.A., Rohling, E.E., Stager, J.C., Karlén, W., Maasch, K.A., Meeker, L.D., Meyerson, E.A., Gasse, F., van Kreveld, S., Holmgren, K. and Lee-Thorp, J (2004) 'Holocene climate variability' *Quaternary research* 62, (3) 243-255

Mayfield, R (2015) 'A multiproxy approach to evaluating deglaciation at Rannoch Moor, Scotland' Unpublished MSc Thesis, University of London

Mayle, F.E., Lowe, J.J. and Sheldrick, C (1997) 'The Late Devensian Lateglacial palaeoenvironmental record from Whitrig Bog, SE Scotland. 1. Lithostratigraphy, geochemistry and palaeobotany' *Boreas*, 26, (4) 279-295

Merkt, J., Müller, H., Knabe, W., Müller, P., Weiser, T (1993) 'The early Holocene Saksunarvatn tephra found in lake sediments in NW Germany' Boreas 22, (2) 93-100

Miallier, D., Michon, L., Evin, J., Pilleyre, T., Sanzelle, S., & Vernet, G (2004) 'Volcans de la chaine des Puys (Massif central, France) : point sur la chronologie Vasset-Kilian-Pariou-Chopine' *Comptes Rendus Geosciences* 336, (15) 1345-1353

Mithen, S., Wicks, K., Pirie, A., Riede, F., Lane, C., Banerjea, R., Cullen, V., Gittins, M. and Pankhurst, N (2015) 'A Lateglacial archaeological site in the far north-west of Europe at Rubha Port an t-Seilich, Isle of Islay, western Scotland: Ahrensburgian-style artefacts, absolute dating and geoarchaeology' *Journal of Quaternary Science* 30, (5) 396-416

Moar, N.T (1969a) 'Two pollen diagrams from the Mainland, Orkney Islands' *New Phytologist* 68, (1) 201-208

Moar, N.T (1969b) 'Late Weichselian and Flandrian pollen diagrams from south-west Scotland' *New Phytologist* 68, (2) 433-467

Moore, R.B (1990) 'Volcanic geology and eruption frequency, São Miguel, Azores' *Bulletin of Volcanology* 52, (8) 602-614

Morgan, G.B., VI, London, D (1996) 'Optimizing the electron microprobe analysis of hydrous alkali aluminosilicate glasses' *American Mineralogist* 81, 1176-1185

Morishita, T., Ishida, Y., Arai, S. and Shirasaka, M (2005) 'Determination of Multiple Trace Element Compositions in Thin (> 30 μm) Layers of NIST SRM 614 and 616 Using Laser Ablation-Inductively Coupled Plasma-Mass Spectrometry (LA-ICP-MS)' *Geostandards and Geoanalytical Research* 29, (1) 107-122

Mortensen, A.K., Bigler, M., Grönvold, K., Steffensen, J.P. and Johnsen, S.J (2005) 'Volcanic ash layers from the Last Glacial Termination in the NGRIP ice core' *Journal of Quaternary Science* 20, (3) 209-219

Mykura, W., Flinn, D., and May, F (1976) British regional geology: Orkney and Shetland.

Neave, D.A., Maclennan, J., Thordarson, T. and Hartley, M.E (2015) 'The evolution and storage of primitive melts in the Eastern Volcanic Zone of Iceland: the 10 ka Grímsvötn tephra series (i.e. the Saksunarvatn ash)' *Contributions to Mineralogy and Petrology* 170, (2) 1-23

Nesje, A., Bakke, J., Brooks, S.J., Kaufman, D.S., Kihlberg, E., Trachsel, M., D'Andrea, W.J. and Matthews, J.A (2014) 'Late glacial and Holocene environmental changes inferred from sediments in Lake Myklevatnet, Nordfjord, western Norway' *Vegetation history and archaeobotany* 23, (3) 229-248

Nesse W (2000) *Introduction to Optical Mineralogy*. New York: Oxford University Press: 442

Norðdahl, H., Ingólfsson, Ó., Pétursson, H.G. and Hallsdóttir, M (2008) 'Late Weichselian and Holocene environmental history of Iceland' *Jökull* 58, 343-364

Nowaczyk (2001) 'Logging of Magnetic Susceptibility' In *Tracking Environmental Change Using Lake Sediments. Volume 1; Basin Analysis, Coring and Chronological Techniques*. ed. by Smol, J.P., Birks, J.B., and Last, W.M. Dordrecht, The Netherlands: Kluwer Academic Publishers: 155-170

Nowell, D.A., Jones, M.C. and Pyle, D.M (2006) 'Episodic Quaternary Volcanism in France and Germany' *Journal of Quaternary Science* 21, (6) 645-675

Óladóttir, B.A., Larsen, G., Thordarson, T. and Sigmarsson, O (2005) 'The Katla volcano S-Iceland: Holocene tephra stratigraphy and eruption frequency' Jökull 55, 53-74

Ott, F., Wulf, S., Serb, J., Słowiński, M., Obremska, M., Tjallingii, R., Błaszkiewicz, M. and Brauer, A (2016) 'Constraining the time span between the Early Holocene Hässeldalen and Askja-S Tephras through varve counting in the Lake Czechowskie sediment record, Poland' *Journal of Quaternary Science* 31, (2) 103-113

Palmer, A.P., Rose, J., Lowe, J.J. and MacLeod, A (2010) 'Annually resolved events of Younger Dryas glaciation in Lochaber (Glen Roy and Glen Spean), Western Scottish Highlands' *Journal of Quaternary Science* 25, (4) 581-596

Palmer, A.P., Matthews, I.P., Candy, I., Blockley, S.P.E., MacLeod, A., Darvill, C.M., Milner, N., Conneller, C. and Taylor, B (2015) 'The evolution of Palaeolake Flixton and the environmental context of Star Carr, NE. Yorkshire: stratigraphy and sedimentology of the Last Glacial-Interglacial Transition (LGIT) lacustrine sequences' *Proceedings of the Geologists' Association* 126, (1) 50-59

Park, R.G., Stewart, A.D. and Wright, D.T (2002) 'The Hebridean terrane' In *The geology of Scotland*. ed. by Trewin, N.H. London: Geological Society of London: 45-80

Parruzot, B., Jollivet, P., Rébiscoul, D. and Gin, S (2015) 'Long-term alteration of basaltic glass: Mechanisms and rates' *Geochimica et Cosmochimica Acta* 154, 28-48

Payne R, Blackford J (2006) 'Microwave digestion and the geochemical stability of tephra' *Quaternary Newsletter* 106, 24–33

Payne, R. and Gehrels, M (2010) 'The formation of tephra layers in peatlands: an experimental approach' *Catena* 81, (1) 12-23

Peach, B.N. and Horne, J (1880) ‘The glaciation of the Orkney Islands’ Quarterly *Journal of the Geological Society* 36, (1-4) 648-663

Peacock, J.D and Everest, J.D (2010) ‘Pre-Late Devensian high-arctic marine deposits in SW Scotland’ *Scottish Journal of Geology* 46, (1) 89-92

Pearce, N.J., Denton, J.S., Perkins, W.T., Westgate, J.A. and Alloway, B.V (2007) ‘Correlation and characterisation of individual glass shards from tephra deposits using trace element laser ablation ICP-MS analyses: current status and future potential’ *Journal of Quaternary Science* 22, (7) 721-736

Pearce, N.J., Perkins, W.T., Westgate, J.A. and Wade, S.C (2011) ‘Trace-element microanalysis by LA-ICP-MS: the quest for comprehensive chemical characterisation of single, sub-10 μm volcanic glass shards’ *Quaternary International* 246, (1) 57-81

Pearce, N.J., Abbott, P.M. and Martin-Jones, C (2014) 'Microbeam methods for the analysis of glass in fine-grained tephra deposits: a SMART perspective on current and future trends' *Geological Society, London, Special Publications* 398, (1) 29-46

Peccerillo, A. and Taylor, S.R (1976) ‘Geochemistry of Eocene calc-alkaline volcanic rocks from the Kastamonu area, northern Turkey’ *Contributions to mineralogy and petrology* 58, (1) 63-81

Pennington, W., Tutin, T.G., Haworth, E.Y., Bonny, A.P. and Lishman, J.P (1972) ‘Lake sediments in northern Scotland’ *Philosophical Transactions of the Royal Society of London B: Biological Sciences* 264, (861) 191-294

Pennington W. (1977) ‘Lake sediments and the Lateglacial environment in Northern Scotland’ In: *Studies in the Scottish Lateglacial Environment*. ed. by Gray J.M and Lowe J.J. Oxford: Pergamon: 119-143

Pennington, W (1979) ‘The origin of pollen in lake sediments: an enclosed lake compared with one receiving inflow streams’ *New Phytologist* 83, (1) 189-213

Persson C. (1971) Tephrochronological investigation of peat deposits in Scandinavia and on the Faroe Islands. Geological Survey of Sweden: C 656

Phillips, W.M., Hall, A.M., Ballantyne, C.K., Binnie, S., Kubik, P.W. and Freeman, S (2008) ‘Extent of the last ice sheet in northern Scotland tested with cosmogenic 10Be exposure ages’ *Journal of Quaternary Science* 23, (2) 101-107

Pilcher J.R and Hall V.A (1992) ‘Towards a tephrochronology for the Holocene of the north of Ireland’ *The Holocene* 2, 255-259

Pilcher, J.R., Hall, V.A. and McCormac, F.G (1995) ‘Dates of Holocene Icelandic volcanic eruptions from tephra layers in Irish peats’ *The Holocene* 5, (1) pp.103-110

Pilcher, J. R., Hall, V. A. and McCormac, F. G. (1996) ‘An outline tephrochronology for the Holocene of the north of Ireland’ *Journal of Quaternary Science* 11, (6) 485-494

Pilcher, J., Bradley, R.S., Francus, P. and Anderson, L (2005) 'A Holocene tephra record from the Lofoten Islands, Arctic Norway' *Boreas* 34, (2) 136-156

Pilcher, J.R and Hall, V.A (1996) ‘Tephrochronological studies in northern England’ *The Holocene* 6, (1) 100-105

Pollard, A.M., Blockley, S.P.E. and Ward, K.R (2003) 'Chemical alteration of tephra in the depositional environment: theoretical stability modelling' *Journal of Quaternary Science* 18, (5) 385-394

Pollard, A.M., Blockley, S.P.E. and Lane, C.S (2006) 'Some numerical considerations in the geochemical analysis of distal microtephra' *Applied Geochemistry* 21, (10) 1692-1714

Pyne-O'Donnell, S.D.F (2005) 'The factors affecting the distribution and preservation of microtephra particles in Lateglacial and early Holocene lake sediments' Unpublished PhD Thesis, University of London

Pyne-O'Donnell, S.D.F (2007) 'Three new distal tephras in sediments spanning the Last Glacial-Interglacial Transition in Scotland' *Journal of Quaternary Science* 22, (6) 559-570

Pyne-O'Donnell, S.D.F., Blockley, S.P.E., Turney, C.S.M. and Lowe, J.J., (2008) 'Distal volcanic ash layers in the Lateglacial Interstadial (GI-1): problems of stratigraphic discrimination' *Quaternary Science Reviews* 27, (1) 72-84

Pyne-O'Donnell, S (2011) 'The taphonomy of Last Glacial–Interglacial Transition (LGIT) distal volcanic ash in small Scottish lakes' *Boreas* 40, 131-145

Rae, D.A (1976) 'Aspects of Glaciation in Orkney' Unpublished PhD Thesis, University of Liverpool

Ranner, P.H (2005) 'Lateglacial and early Holocene environmental changes along the Northwest European continental margin' Unpublished PhD Thesis, Durham University

Ranner, P.H., Allen, J.R.M., and Huntley, B (2005) 'A new early Holocene cryptotephra from northwest Scotland' *Journal of Quaternary Science* 20, (3) 201-208

Rasmussen, S.O., Abbott, P.M., Blunier, T., Bourne, A.J., Brook, E., Buchardt, S.L., Buizert, C., Chappellaz, J., Clausen, H.B., Cook, E. and Dahl-Jensen, D (2013) 'A first chronology for the North Greenland Eemian Ice Drilling (NEEM) ice core' *Climate of the Past* 9, (6) 2713-2730

Rasmussen, S.O., Andersen, K.K., Svensson, A.M., Steffensen, J.P., Vinther, B.M., Clausen, H.B., Siggaard-Andersen, M.L., Johnsen, S.J., Larsen, L.B., Dahl-Jensen, D., Bigler, M., Röthlisberger, R., Fischer, H., Goto-Azuma, K., Hansson, M.E., Ruth, U (2006) 'A new Greenland ice core chronology for the last glacial termination' *Journal of Geophysical Research D: Atmospheres* 111, (6) D06102

Rasmussen, S.O., Vinther, B.M., Clausen, H.B. and Andersen, K.K (2007) 'Early Holocene climate oscillations recorded in three Greenland ice cores' *Quaternary Science Reviews* 26, (15) 1907-1914

Rasmussen, S.O., Bigler, M., Blockley, S.P., Blunier, T., Buchardt, S.L., Clausen, H.B., Cvijanovic, I., Dahl-Jensen, D., Johnsen, S.J., Fischer, H., Gkinis, V., Guillevic, M., Hoek, W.Z., Lowe, J.J., Pedro, J.B., Popp, T., Seierstad, I.K., Steffensen, J.P., Svensson, A.M., Vallelonga, P., Vinther, B.M., Walker, M.J.C., Wheatley, J.J. and Winsrtup, M (2014) 'A stratigraphic framework for abrupt climatic changes during the Last Glacial period based on three synchronized Greenland ice-core records: refining and extending the INTIMATE event stratigraphy' *Quaternary Science Reviews* 106, 14-28

Rasmussen, S.O., Birks, H.H., Blockley, S.P., Brauer, A., Hajdas, I., Hoek, W.Z., Lowe, J.J., Moreno, A., Renssen, H., Roche, D.M., Svensson, A.M., Valdes, P. and Walker, M.J.C (2014b) 'Dating, synthesis, and interpretation of palaeoclimatic records of the Last Glacial cycle and model-data integration: advances by the INTIMATE (INTegration of Ice-core, MArine and TErrestrial records) COST Action ES0907' *Quaternary Science Reviews* 106, 1-13

Rebiscoul, D., Van der Lee, A., Rieutord, F., Né, F., Spalla, O., El-Mansouri, A., Frugier, P., Ayral, A. and Gin, S (2004) 'Morphological evolution of alteration layers formed during nuclear glass alteration: new evidence of a gel as a diffusive barrier' *Journal of Nuclear Materials* 326, (1) 9-18

Reed, S.J.B (2005) 2nd edn. Electron microprobe analysis and scanning electron microscopy in geology. Cambridge: Cambridge University Press

Reilly, E (2006) 'Geochemical analysis of tephra samples from late Holocene small hollow and mor humus deposits in Killarney National Park, Co. Kerry, southwest Ireland' *Quaternary Newsletter* 109, 42-45

Reilly, E and Mitchell, F.J (2014) 'Establishing chronologies for woodland small hollow and mor humus deposits using tephrochronology and radiocarbon dating' *The Holocene*, 1-12

Reimer, P.J., Baillie, M.G., Bard, E., Bayliss, A., Beck, J.W., Bertrand, C.J., Blackwell, P.G., Buck, C.E., Burr, G.S., Cutler, K.B. and Damon, P.E (2004) 'IntCal04 terrestrial radiocarbon age calibration, 0-26 cal kyr BP' *Radiocarbon* 46, (3) 1029-1058

Reimer, P.J., Baillie, M.G., Bard, E., Bayliss, A., Beck, J.W., Blackwell, P.G., Bronk, R.C., Buck, C.E., Burr, G.S., Edwards, R.L. and Friedrich, M (2009) 'IntCal09 and Marine09 radiocarbon age calibration curves, 0-50,000 years cal BP' *Radiocarbon* 51, (4) 1111-1150

Reimer, P.J., Bard, E., Bayliss, A., Beck, J.W., Blackwell, P.G., Ramsey, C.B., Buck, C.E., Cheng, H., Edwards, R.L., Friedrich, M., Grootes, P.M., Guilderson, TP., Haflidason, H., Hajdas, I., Hatté, C., Heaton, T.J., Hoffmann, D.L., Hogg, A.G., Hughen, K.A., Kaiser, K.F., Kromer, B., Manning, S.W., Niu, M., Reimer, R.W., Richards, D.A., Scott, E.M., Southon, J.R., Staff, R.A., Turney, C.S.M. and van der Plicht, J (2013) 'IntCal13 and Marine13 radiocarbon age calibration curves 0–50,000 years cal BP' *Radiocarbon* 55, (4) 1869-1887

Riede, F. and Edinborough, K (2012) 'Bayesian radiocarbon models for the cultural transition during the Allerød in southern Scandinavia' *Journal of Archaeological Science* 39, (3) 744-756

Riede, F. and Thastrup, M.D (2013) 'Tephra, tephrochronology and archaeology–a (re-) view from northern Europe' *Heritage Science* 1, (15) 1-17

Roberts, D.O (1999) 'The use of microtephra horizons as time synchronous markers in the Last Glacial–Holocene Transition: a palaeoenvironmental study from the Isle of Mull, Inner Hebrides, Scotland' Unpublished MSc. Thesis, University of London

Roberts, S.J (1997) 'The spatial and geochemical characteristics of Lateglacial tephra deposits of Scotland and Northern England' Unpublished MSc Thesis, University of London

Roberts, S.J., Turney, C.C.M. and Lowe, J. (1998) 'Icelandic Tephra in Late-glacial Sediments of Scotland (14 - 9,000 14C BP)' *Fróðskaparrit* 46, 335-339

Robinson, M. and Ballantyne, C.K (1979) ‘Evidence for a glacial readvance pre-dating the Loch Lomond Advance in Wester Ross’ *Scottish Journal of Geology* 15, (4) 271-277

Rohling, E.J. and Pälike, H (2005) ‘Centennial-scale climate cooling with a sudden cold event around 8,200 years ago’ *Nature* 434, (7036) 975-979

Roland, T.P., Mackay, H. and Hughes, P.D.M (2015) 'Tephra analysis in ombrotrophic peatlands: a geochemical comparison of acid digestion and density separation techniques' *Journal of Quaternary Science* 30, (1) 3-8

Rollinson, H (1993) *Using geochemical data: evaluation, presentation, interpretation*. London: Pearson Education Ltd

Rose, N.L., Golding, P.N.E. and Battarbee, R.W (1996) 'Selective concentration and enumeration of tephra shards from lake sediment cores' *The Holocene* 6, (2) 243-246

Ruddiman, W.F. and Glover, L.K (1972) ‘Vertical mixing of ice-rafted volcanic ash in North Atlantic sediments’ *Geological Society of America Bulletin* 83, (9) 2817-2836

Ruddiman, W.F. and McIntyre, A (1981) ‘The North Atlantic Ocean during the last deglaciation’ *Palaeogeography, Palaeoclimatology, Palaeoecology* 35, 145-214

Ruddiman, W.F., Raymo, M.E., and McIntyre, A (1986) ‘Matuyama 41,000-year cycles: North Atlantic Ocean and northern hemisphere ice sheets’ *Earth and Planetary Science Letters* 80, (1-2) 117-129

Ruddiman, W. F., and Raymo, M. E (1988) ‘Northern Hemisphere Climate Regimes During the Past 3 Ma: Possible Tectonic Connections’ *Philosophical Transactions of the Royal Society of London. Series B, Biological Sciences* 318, (1191) 411-429

Salt, K.E. and Evans, D.J (2004) ‘Superimposed subglacially streamlined landforms of southwest Scotland’ *The Scottish Geographical Magazine* 120, (1-2) 133-147

Sejrup, H.P., Haflidason, H., Aarseth, I., King, E., Forsberg, C.F., Long, D. and Rokoengen, K (1994) ‘Late Weichselian glaciation history of the northern North Sea’ *Boreas* 23, (1)1-13

Sejrup, H.P., Hjelstuen, B.O., Nygård, A., Haflidason, H. and Mardal, I (2015) ‘Late Devensian ice-marginal features in the central North Sea–processes and chronology’ *Boreas* 44, (1) 1-13

Sejrup, H.P., Clark, C.D. and Hjelstuen, B.O (2016) ‘Rapid ice sheet retreat triggered by ice stream debuttressing: Evidence from the North Sea’ *Geology* 44, (5) 355-358

Shane, P (2000) ‘Tephrochronology: a New Zealand case study’ *Earth-Science Reviews* 49, (1) 223-259

Shaw, C.S. and Woodland, A.B (2012) ‘The role of magma mixing in the petrogenesis of mafic alkaline lavas, Rockeskyllerkopf Volcanic Complex, West Eifel, Germany’ *Bulletin of Volcanology* 74, (2) 359-376

Shennan, I. and Horton, B (2002) ‘Holocene land-and sea-level changes in Great Britain’ *Journal of Quaternary Science* 17, (5-6) 511-526

Siegenthaler, U., and Eicher, U (1986) 'Stable oxygen and carbon isotope analyses'. In *Handbook of Holocene Palaeoecology and Palaeohydrology*. ed. by Berglund, B.E. Chichester: John Wiley & Sons Ltd: 407-422

Sigmundsson, F., Pinel, V., Lund, B., Albino, F., Pagli, C., Geirsson, H., and Sturkell, E (2010) 'Climate effects on volcanism: Influence on magmatic systems of loading and unloading from ice mass variations, with examples from Iceland' *Philosophical Transactions of the Royal Society A: Mathematical, Physical and Engineering Sciences* 368 (1919) 2519-2534

Sigurdsson, H (1990) 'Assessment of the atmospheric impact of volcanic eruptions' *Geological Society of America Special Papers* 247, 99-110

Sigurdsson, H. (1982) 'Utbreidslaíslenskra gjóskulaga á botni Atlanthafs. [Distribution of Icelandic Tephra Layers on the Atlantic Ocean Floor]'. In *Eldur er í nordri*. ed. by Thorarinsdóttir, H., Oskarsson, O. H., Steinthorsson, S. & Einarsson, T: Sögufélag, Reykjavík (in Icelandic)119–127.

Sigvaldason, G.E (2002) 'Volcanic and tectonic processes coinciding with glaciation and crustal rebound: an early Holocene rhyolitic eruption in the Dyngjufjöll volcanic centre and the formation of the Askja caldera, north Iceland' *Bulletin of Volcanology* 64, (3-4) 192-205

Simpson, G.L and Birks, H.J.B (2012) 'Statistical Learning in Palaeolimnology.' In *Tracking Environmental Change Using Lake Sediments Volume 5: Data Handling and Numerical Techniques*. ed. by Birks, H.J.B, Lotter, A.F., Juggins, S. and Smol, J.P. Heidelberg: Springer 249-327

Sissons, J.B (1974) 'The Quaternary in Scotland: a review' *Scottish Journal of Geology* 10, (4) 311-337

Sissons, J.B (1977) 'The Loch Lomond Readvance in the Northern Mainland of Scotland' In: *Studies in the Scottish Lateglacial Environment*. ed. by Gray J.M and Lowe J.J. Oxford: Pergamon: 45-59

Slater, L., Jull, M., McKenzie, D. and Gronvöld, K (1998) 'Deglaciation effects on mantle melting under Iceland: results from the northern volcanic zone' *Earth and Planetary Science Letters* 164, (1) 151-164

Smith, V.C., Isaia, R. and Pearce, N.J.G (2011) 'Tephrostratigraphy and glass compositions of post-15 kyr Campi Flegrei eruptions: implications for eruption history and chronostratigraphic markers' *Quaternary Science Reviews* 30, (25) 3638-3660

Søndergaard, M. K. B (2005) 'Lateglacial and Holocene palaeoclimatic fluctuations on the North Icelandic shelf – foraminiferal analysis, BOREAS Tephra stratigraphy on the North Icelandic shelf 733 sedimentology and tephrochronology of core MD992275' Unpublished PhD Thesis, University of Aarhus

Sparks, R.S.J (1986) 'The dimensions and dynamics of volcanic eruption columns' *Bulletin of Volcanology* 48, (1) 3-15

Spray, J.G., and Rae, D.A (1995) 'Quantitative electron-microprobe analysis of alkali silicate glasses: a review and user guide' *Canadian Mineralogist* 33, 323-323

Steffensen, J.P., Andersen, K.K., Bigler, M., Clausen, H.B., Dahl-Jensen, D., Fischer, H., Goto-Azuma, K., Hansson, M., Johnsen, S.J., Jouzel, J. and Masson-Delmotte, V

(2008) ‘High-resolution Greenland ice core data show abrupt climate change happens in few years’ *Science* 321, (5889) 680-684

Stevenson, J.A., Loughlin, S., Rae, C., Thordarson, T., Milodowski, A.E., Gilbert, J.S., Harangi, S., Lukács, R., Højgaard, B., Árting, U., Pyne-O'Donnell, S., MacLeod, A., Whitney, B. and Cassidy, M (2012) ‘Distal deposition of tephra from the Eyjafjallajökull 2010 summit eruption’ *Journal of Geophysical Research: Solid Earth* (1978–2012), 117 (B9)

Stevenson, J.A., Loughlin, S.C., Font, A., Fuller, G.W., MacLeod, A., Oliver, I.W., Jackson, B., Horwell, C.J., Thordarson, T. and Dawson, I (2013) ‘UK monitoring and deposition of tephra from the May 2011 eruption of Grímsvötn, Iceland’ *Journal of Applied Volcanology* 2, (1) 1-17

Stevenson, J.A., Millington, S.C., Beckett, F.M., Swindles, G.T. and Thordarson, T (2015) ‘Big grains go far: understanding the discrepancy between tephrochronology and satellite infrared measurements of volcanic ash’ *Atmospheric Measurement Techniques* 8, (5) 2069-2091

Stoker, M.S., Leslie, A.B., Scott, W.D., Briden, J.C., Hine, N.M., Harland, R., Wilkinson, I.P., Evans, D. and Ardus, D.A (1994) ‘A record of late Cenozoic stratigraphy, sedimentation and climate change from the Hebrides Slope, NE Atlantic Ocean’ *Journal of the Geological Society* 151, (2) 235-249

Stoker, M. and Bradwell, T (2005) ‘The Minch palaeo-ice stream, NW sector of the British–Irish Ice Sheet’ *Journal of the Geological Society* 162, (3) 425-428

Stoker, M.S., Bradwell, T., Howe, J.A., Wilkinson, I.P. and McIntyre, K (2009) ‘Lateglacial ice-cap dynamics in NW Scotland: evidence from the fjords of the Summer Isles region’ *Quaternary Science Reviews* 28, (27) 3161-3184

Stocker, L.N.S (2014) ‘Utilising Palynology and Tephrochronology to assess the onset of the Holocene and its potential timing from Kingshouse 2, Rannoch Moor, NW Scotland’ Unpublished MSc Thesis, University of London

Stone, P (1995) *Geology of the Rhins of Galloway district*. British Geological Survey: Stationery Office Books (TSO)

Streeter, R. and Dugmore, A (2014) ‘Late-Holocene land surface change in a coupled social–ecological system, southern Iceland: a cross-scale tephrochronology approach’ *Quaternary Science Reviews* 86, 99-114

Sutherland, D.G (1984) ‘The Quaternary deposits and landforms of Scotland and the neighbouring shelves: a review’ *Quaternary Science Reviews* 3, (2) 157-254

Sutherland, D.G (1991) ‘The glaciation of the Shetland and Orkney Islands.’ In: *Glacial Deposits in Great Britain and Ireland*. ed by Ehlers, J., Gibbard, P.L. & Rose, J. Rotterdam: Balkema:121–127

Swindles, G.T., Lawson, I.T., Matthews, I.P., Blaauw, M., Daley, T.J., Charman, D.J., Roland, T.P., Plunkett, G., Schettler, G., Gearey, B.R. and Turner, T.E (2013) ‘Centennial-scale climate change in Ireland during the Holocene’ *Earth-Science Reviews* 126, 300-320

Swindles, G.T., Lawson, I.T., Savov, I.P., Connor, C.B. and Plunkett, G (2011) ‘A 7000 yr perspective on volcanic ash clouds affecting northern Europe’ *Geology* 39, (9) 887-890

Taddeucci, J., Scarlato, P., Montanaro, C., Cimarelli, C., Del Bello, E., Freda, C., Andronico, D., Gudmundsson, M.T. and Dingwell, D.B (2011) 'Aggregation-dominated ash settling from the Eyjafjallajökull volcanic cloud illuminated by field and laboratory high-speed imaging' *Geology* 39, (9) 891-894

Tallantire, P.A (2002) 'The early-Holocene spread of hazel (Corylus avellana L.) in Europe north and west of the Alps: an ecological hypothesis' *The Holocene* 12, (1) 81-96

Taylor, K.C., Lamorey, G. and Doyle, G., Alley, R.B., Grootes, P.M., Mayewski, P.A., White, J.W.C. and Barlow, L.K (1993) 'The 'flickering switch' of Late Pleistocene climate change' *Nature* 361, (6411) 432-436

Telford, R.J., Heegaard, E. and Birks, H.J.B (2004) 'All age–depth models are wrong: but how badly?' *Quaternary Science Reviews* 23, (1) 1-5

Thomas, E.R., Wolff, E.W., Mulvaney, R., Steffensen, J.P., Johnsen, S.J., Arrowsmith, C., White, J.W., Vaughn, B. and Popp, T (2007) 'The 8.2 ka event from Greenland ice cores' *Quaternary Science Reviews* 26, (1) 70-81

Þórarinsson, S (1944) 'Tefrokronologiska studier pa Island' Geografiska Annaler 26, 1-217

Thorarinsson, S., and Sæmundsson, K (1979) 'Volcanic activity in historical time'. *Jökull* 29, 29–32

Thordarson, T., and Larsen, G (2007) 'Volcanism in Iceland in historical time: Volcano types, eruption styles and eruptive history' *Journal of Geodynamics* 43, 118-152

Thordarson, T., and Höskuldsson, Á (2008) 'Postglacial volcanism in Iceland' *Jökull* 58, 197-228

Thordarson T (2014) 'The widespread ~10 ka Saksunarvatn tephra is not a product single eruption' American Geophysical Union, Fall Meeting 2014, abstract #V24B-04

Thornalley, D.J., McCave, I.N. and Elderfield, H (2011) 'Tephra in deglacial ocean sediments south of Iceland: Stratigraphy, geochemistry and oceanic reservoir ages' *Journal of Quaternary Science* 26, (2) 190-198

Timms, R.G.O., Matthews, I.P., Palmer, A.P., Candy, I. and Abel, L (2016) 'A high-resolution tephrostratigraphy from Quoyloo Meadow, Orkney, Scotland: Implications for the tephrostratigraphy of NW Europe during the Last Glacial-Interglacial Transition' Quaternary Geochronology

Tipping, R., Verrill, L., Bradley, M., Housley, R. and Saville, A (2016) 'Chapter 6: The Landscape context of Scotland's first open-air Late Upper Palaeolithic archaeological site'. In: *Prehistory without Borders: The Prehistoric Archaeology of the Tyne-Forth Region*. ed. by Tipping, R., Fowler, C. and Crellin, R. Oxford: Oxbow Books

Tomlinson, E.L., Thordarson, T., Müller, W., Thirlwall, M. and Menzies, M.A (2010) 'Microanalysis of tephra by LA-ICP-MS—strategies, advantages and limitations assessed using the Thorsmörk Ignimbrite (Southern Iceland)' *Chemical Geology* 279, (3) 73-89

Tomlinson, E.L., Thordarson, T., Lane, C.S., Smith, V.C., Manning, C.J., Müller, W. and Menzies, M.A (2012a) 'Petrogenesis of the Sólheimar ignimbrite (Katla, Iceland): Implications for tephrostratigraphy' *Geochimica et Cosmochimica Acta* 86, 318-337

Tomlinson, E.L., Arienzo, I., Civetta, L., Wulf, S., Smith, V.C., Hardiman, M., Lane, C.S., Carandente, A., Orsi, G., Rosi, M. and Müller, W (2012b) 'Geochemistry of the Phlegraean Fields (Italy) proximal sources for major Mediterranean tephras: implications for the dispersal of Plinian and co-ignimbritic components of explosive eruptions' *Geochimica et Cosmochimica Acta* 93, 102-128

Trewin, N.H. (ed.) (2002) *The geology of Scotland. London*: Geological Society of London

Troels-Smith, J (1955) 'Characterisation of unconsolidated sediments' Danmarks Geologiske Undersoegelse 4, 1-73

Tryon, C.A., Roach, N.T. and Logan, M.A.V (2008) 'The Middle Stone Age of the northern Kenyan Rift: age and context of new archaeological sites from the Kapedo Tuffs' *Journal of Human Evolution* 55, (4) 652-664

Turner, L (2016) 'A lateglacial interstadial chironomid inferred temperature record from the site of Tirinie, Scotland' Unpublished MSc Thesis, University of London

Turney, C.S., Harkness, D.D. and Lowe, J.J (1997) 'Rapid Communication: The use of microtephra horizons to correlate Late-glacial lake sediment successions in Scotland' *Journal of Quaternary Science* 12, (6) 525-531

Turney, C.S.M (1998a) 'Isotope stratigraphy and tephrochronology of the Last Glacial–Interglacial Transition (14–9 ka 14CBP) in the British Isles' Unpublished PhD Thesis, University of London

Turney, C.S.M (1998b) 'Extraction of rhyolitic component of Vedde microtephra from minerogenic lake sediments' *Journal of Paleolimnology* 19, (2) 199-206

Turney, C.S., Lowe, J.J., Davies, S.M., Hall, V., Lowe, D.J., Wastegård, S., Hoek, W.Z. and Alloway, B (2004) 'Tephrochronology of Last Termination sequences in Europe: a protocol for improved analytical precision and robust correlation procedures (a joint SCOTAV–INTIMATE proposal)' Journal of Quaternary Science 19, (2) 111-120

Turney C.S.M., Van Den Burg, K., Wastegård, S., Davies, S.M., Whitehouse, N.J., Pilcher, J.R. and Callaghan, C (2006) 'North European last glacial–interglacial transition (LGIT; 15–9 ka) tephrochronology: extended limits and new events' *Journal of Quaternary Science* 21, (4) 335-345

Valentine, H (2015) 'Constraining the timing of deglaciation on Priest Island, Summer Isles using tephrostratigraphy' Unpublished MSc Thesis, University of London

van den Bogaard, P., and Schmincke, H.U (1985) 'Laacher See Tephra: A widespread isochronous late Quaternary tephra layer in central and northern Europe' *Geological Society of America Bulletin* 96, (12) 1554-1571

van den Bogaard, C., Dörfler, W., Sandgren, P. and Schmincke, H.U (1994) 'Correlating the Holocene records: Icelandic tephra found in Schleswig-Holstein (northern Germany)' *Naturwissenschaften* 81, (12) 554-556

van den Bogaard, P (1995) '40 Ar/39 Ar ages of sanidine phenocrysts from Laacher See Tephra (12,900 yr BP): Chronostratigraphic and petrological significance' *Earth and Planetary Science Letters* 133, (1) 163-174

van den Bogaard, C. and Schmincke, H.U (2002) 'Linking the North Atlantic to central Europe: a high-resolution Holocene tephrochronological record from northern Germany' *Journal of Quaternary Science* 17, (1) 3-20

van der Plicht, J., Van Geel, B., Bohncke, S.J.P., Bos, J.A.A., Blaauw, M., Speranza, A.O.M., Muscheler, R. and Björck, S (2004) 'The Preboreal climate reversal and a subsequent solar-forced climate shift' *Journal of Quaternary Science* 19, (3) 263-269

Van Vliet-Lanoë, B., Guðmundsson, Å., Guillou, H., Duncan, R.A., Genty, D., Ghaleb, B., Gouy, S., Récourt, P. and Scaillet, S (2007) 'Limited glaciation and very early deglaciation in central Iceland: implications for climate change' *Comptes Rendus Geoscience* 339, (1) 1-12

Vannière, B., Bossuet, G., Walter-Simonnet, A.V., Ruffaldi, P., Adatte, T., Rossy, M. and Magny, M (2004) 'High-resolution record of environmental changes and tephrochronological markers of the Last Glacial–Holocene transition at Lake Lautrey (Jura, France)' *Journal of Quaternary Science* 19, (8) 797-808

Vellinga, M and Wood, R.A (2002) 'Global climatic impacts of a collapse of the Atlantic Thernohaline circulation' *Climatic Change* 54, 251-267

Vellinga, M. and Wood, R.A (2008) 'Impacts of the thermohaline circulation shutdown in the twenty-first century' *Climatic Change* 91, 43-63

Vernet, G., Raynal, J.P., Fain, J., Miallier, D., Montret, M., Pilleyre, T. and Sanzelle, S (1998) 'Tephrostratigraphy of the last 160ka in western Limagne (France)' *Quaternary International* 47, 139-146

Vernet, Gerard, & Raynal, J (2000) 'Un cadre tephrostratigraphique reactualise pour la prehistoire tardiglaciaire et holocene de Limagne (Massif central, France)' Comptes Rendus de l'Academie de Sciences - Serie IIa: Sciences de la Terre et des Planetes 330, (6) 399-405

Vinther, B.M., Clausen, H.B., Johnsen, S.J., Rasmussen, S.O., Andersen, K.K., Buchardt, S.L., Dahl-Jensen, D., Seierstad, I.K., Siggaard-Andersen, M.L., Steffensen, J.P. and Svensson, A (2006) 'A synchronized dating of three Greenland ice cores throughout the Holocene' *Journal of Geophysical Research: Atmospheres* 111, (D13)

von Grafenstein, U., Erlenkeuser, H., Brauer, A., Jouzel, J. and Johnsen, S.J (1999) 'A mid-European decadal isotope-climate record from 15,500 to 5000 years BP' *Science* 284, (5420) 1654-1657

Waagstein R, Jóhansen J (1968) 'Tre vulkanske askelage fra Færø' *Meddelelser fra Dansk Geol Foren* 18, 257–264

Walker, M.J.C (1984) 'Pollen analysis and Quaternary research in Scotland' *Quaternary Science Reviews* 3, (4) 369-404

Walker, M.J.C (1995) 'Climatic changes in Europe during the last glacial/interglacial transition' Quaternary International 28, 63-76

Walker, M.J.C., Björck, S., Lowe, J.J., Cwynar, L.C., Johnsen, S., Knudsen, K.L. and Wohlfarth, B (1999) 'Isotopic 'events' in the GRIP ice core: a stratotype for the Late Pleistocene' *Quaternary Science Reviews* 18, (10) 1143-1150

Walker, M.J.C., Bryant, C., Coope, G.R., Harkness, D.D., Lowe, J.J. and Scott, E.M (2001) 'Towards a radiocarbon chronology of the Late-Glacial: sample selection strategies' *Radiocarbon* 43, (2B) 1007-1019

Walker, M.J.C (2004) 'A Lateglacial pollen record from Hallsenna Moor, near Seascale, Cumbria, NW England, with evidence for arid conditions during the Loch Lomond (Younger Dryas) Stadial and early Holocene' *Proceedings of the Yorkshire Geological and Polytechnic Society* 55, (1) 33-42)

Walker, M., Johnsen, S., Rasmussen, S.O., Popp, T., Steffensen, J.P., Gibbard, P., Hoek, W., Lowe, J., Andrews, J., Björck, S. and Cwynar, L.C (2009) 'Formal definition and dating of the GSSP (Global Stratotype Section and Point) for the base of the Holocene using the Greenland NGRIP ice core, and selected auxiliary records' *Journal of Quaternary Science* 24, (1) 3-17

Walker, M.J., Berkelhammer, M., Björck, S., Cwynar, L.C., Fisher, D.A., Long, A.J., Lowe, J.J., Newnham, R.M., Rasmussen, S.O. and Weiss, H (2012) 'Formal subdivision of the Holocene Series/Epoch: a Discussion Paper by a Working Group of INTIMATE (Integration of ice-core, marine and terrestrial records) and the Subcommission on Quaternary Stratigraphy (International Commission on Stratigraphy)' *Journal of Quaternary Science* 27, (7) 649-659

Walkley, A. and Black, I.A (1934) 'An examination of the Degtjareff method for determining soil organic matter, and a proposed modification of the chromic acid titration method' *Soil Science* 37, 29-38

Wang, R., Dearing, J.A., Langdon, P.G., Zhang, E., Yang, X., Dakos, V. and Scheffer, M (2012) 'Flickering gives early warning signals of a critical transition to a eutrophic lake state' *Nature* 492, (7429) 419-422

Wanner, H., Solomina, O., Grosjean, M., Ritz, S.P. and Jetel, M (2011) 'Structure and origin of Holocene cold events' *Quaternary Science Reviews* 30, (21) 3109-3123

Wastegård, S., Turney, C.S.M., Lowe, J.J., and Roberts, S.J (2000a) 'New discoveries of the Vedde Ash in southern Sweden and Scotland' *Boreas* (29) 72-78

Wastegård, S., Wohlfarth, B., Subetto, D.A. and Sapelko, T.V (2000b) 'Extending the known distribution of the Younger Dryas Vedde Ash into northwestern Russia' *Journal of Quaternary Science* 15, (6) 581-586

Wastegård, S (2002) 'Early to middle Holocene silicic tephra horizons from the Katla volcanic system, Iceland: new results from the Faroe Islands' *Journal of Quaternary Science* 17, (8) 723-730

Wastegård, S. (2005) 'Late quaternary tephrochronology of Sweden: a review' *Quaternary International* 130, (1) 49-62

Wastegård, S., Rasmussen, T.L., Kuijpers, A., Nielsen, T. and van Weering, T.C.E. (2006). 'Composition and origin of ash zones from marine isotope stages 3 and 2 in the north atlantic' *Quaternary Science Reviews* 25, (17-18) 2409-2419

Wastegård, S. and Davies, S.M (2009) 'An overview of distal tephrochronology in northern Europe during the last 1000 years' *Journal of Quaternary Science* 24, (5) 500-512

Watson, E.J., Swindles, G.T., Lawson, I.T. and Savov, I.P (2015) 'Spatial variability of tephra and carbon accumulation in a Holocene peatland' *Quaternary Science Reviews* 124, 248-264

Watson, J.E., Brooks, S.J., Whitehouse, N.J., Reimer, P.J., Birks, H.J.B. and Turney, C (2010) 'Chironomid-inferred late-glacial summer air temperatures from Lough Nadourcan, Co. Donegal, Ireland' *Journal of Quaternary Science* 25, (8) 1200-1210

Whittington, G., Fallick, A.E and Edwards, K.J (1996) 'Stable oxygen isotope and pollen records from eastern Scotland and a consideration of Late-glacial and early Holocene climate change for Europe' *Journal of Quaternary Science* 11, (4) 327-340

Whittington, G., Edwards, K.J., Zanchetta, G., Keen, D.H., Bunting, M.J., Fallick, A.E. and Bryant, C.L (2015) 'Lateglacial and early Holocene climates of the Atlantic margins of Europe: Stable isotope, mollusc and pollen records from Orkney, Scotland' *Quaternary Science Reviews* 122, 112-130

Wilson, G.V., Edwards, W., Knox, J., Jones, R.C.B., and Stephens, J.V (1935) 'The geology of the Orkneys' *Memoir of the Geological Survey of Scotland*

Wohlfarth, B., Blaauw, M., Davies, S.M., Andersson, M., Wastegard, S., Hormes, A. and Possnert, G (2006) 'Constraining the age of Lateglacial and early Holocene pollen zones and tephra horizons in southern Sweden with Bayesian probability methods' *Journal of Quaternary Science* 21, (4) 321-334

Wolff-Boenisch, D., Gislason, S.R., Oelkers, E.H. and Putnis, C.V (2004) 'The dissolution rates of natural glasses as a function of their composition at pH 4 and 10.6, and temperatures from 25 to 74 C' *Geochimica et Cosmochimica Acta* 68, (23) 4843-4858

Woodcock P (2003) 'Amplifying the dequence of Lateglacial environmental change in Wales' Unpublished MSc, University of London

Wulf, S., Kraml, M., Brauer, A., Keller, J. and Negendank, J.F (2004) 'Tephrochronology of the 100ka lacustrine sediment record of Lago Grande di Monticchio (southern Italy)' *Quaternary International* 122, (1) 7-30

Wulf, S., Kraml, M. and Keller, J (2008) 'Towards a detailed distal tephrostratigraphy in the Central Mediterranean: the last 20,000 yrs record of Lago Grande di Monticchio' *Journal of Volcanology and Geothermal Research* 177, (1) 118-132

Wulf, S., Keller, J., Paterne, M., Mingram, J., Lauterbach, S., Opitz, S., Sottili, G., Giaccio, B., Albert, P.G., Satow, C. and Tomlinson, E.L (2012) 'The 100–133 ka record of Italian explosive volcanism and revised tephrochronology of Lago Grande di Monticchio' *Quaternary Science Reviews* 58, 104-123

Wulf, S., Dräger, N., Ott, F., Serb, J., Appelt, O., Guðmundsdóttir, E., van den Bogaard, C., Słowiński, M., Błaszkiewicz, M. and Brauer, A (2016) 'Holocene tephrostratigraphy of varved sediment records from Lakes Tiefer See (NE Germany) and Czechowskie (N Poland)' *Quaternary Science Reviews* 132, 1-14

Wunsch, C (2006) 'Abrupt climate change: An alternative view' *Quaternary Research* 65, (2) 191-203

Yew, C.H. and Taylor, P.A (1994) 'A thermodynamic theory of dynamic fragmentation' *International journal of impact engineering* 15, (4) 385-394

Zachos, J., Pagani, H., Sloan, L., Thomas, E., and Billups, K (2001) ‘Trends, rhythms, and aberrations in global climate 65 Ma to present’ *Science* 292, (5517) 686-693

Zanchetta, G., Sulpizio, R., Roberts, N., Cioni, R., Eastwood, W.J., Siani, G., Caron, B., Paterne, M. and Santacroce, R (2011) ‘Tephrostratigraphy, chronology and climatic events of the Mediterranean basin during the Holocene: an overview’ *The Holocene* 21, (1) 33-52

Zawalna-Geer, A., Lindsay, J.M., Davies, S., Augustinus, P. and Davies, S (2016) ‘Extracting a primary Holocene crytoptephra record from Pupuke maar sediments, Auckland, New Zealand’ *Journal of Quaternary Science*

Zielinski, G.A., Mayewski, P.A., Meeker, L.D., Grönvold, K., Germani, M.S., Whitlow, S., Twickler, M.S., and Taylor, K (1997) 'Volcanic aerosol records and tephrochronology of the Summit, Greenland, ice cores' *Journal of Geophysical Research* 102, (26) 625–26,640

Zimanowski, B., Wohletz, K., Dellino, P. and Büttner, R (2003) ‘The volcanic ash problem’ *Journal of Volcanology and Geothermal Research* 122, (1) 1-5

Zolitschka, B., Negendank, J.F.W. and Lottermoser, B.G (1995) ‘Sedimentological proof and dating of the early Holocene volcanic eruption of Ulmener Maar (Vulkaneifel, Germany)’ *Geologische Rundschau* 84, (1) 213-219

Appendices (on disc)

Appendix A - Stub codes

Appendix B - Geochemistry and geochemical references

Appendix C - Age models

Appendix D - Quoyloo Meadow data

Appendix E - Crudale Meadow data

Appendix F - Spretta Meadow data

Appendix G - Tanera Mòr data

Appendix H - Little Lochans

Appendix I - Additional palaeoenvironmental data

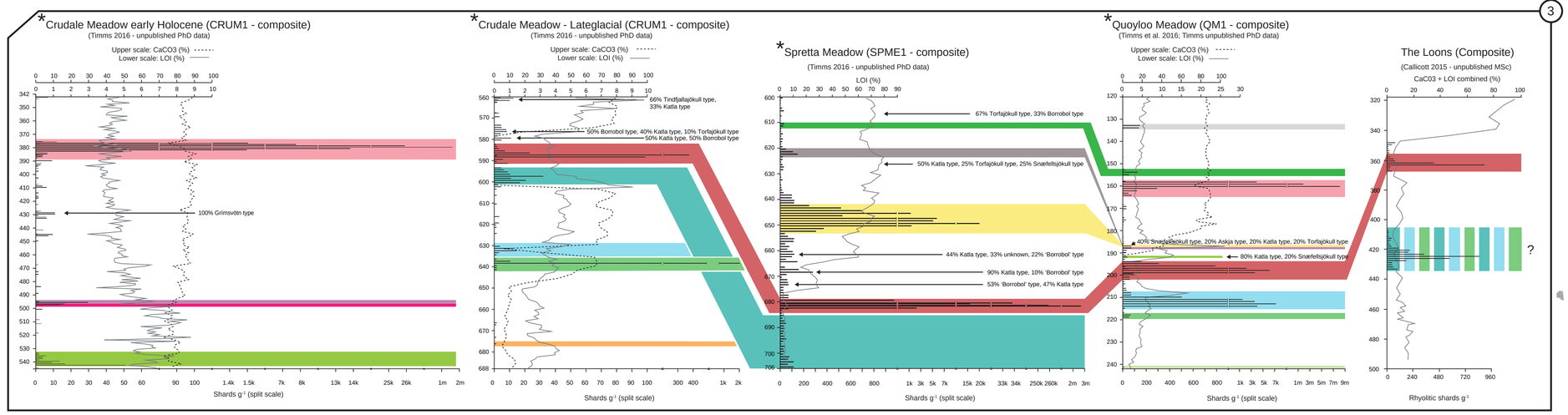

Figure 10.8
Revised Scottish Tephrostratigraphic Framework. Solid colour bars denote a correlation based on geochemical means, whilst dashed coloured bars represent a correlation made on stratigraphic superposition. Where multiple cores from the same location have been studied, only the most representative tephrostratigraphies are shown.